The Stability of New Generation Intravenous Lipid Emulsions

Helen Mary King

A thesis submitted to Cardiff University in accordance with the conditions governing candidates for the degree of Philosophiæ Doctor

The School of Pharmacy and Pharmaceutical Sciences,

Cardiff University

January 2019

DECLARATIONS

STATEMENT 1 This thesis is being submitted in partial fulfilment of the requirements for the degree of PhD

Signed _____ (Helen King)   Date 28th Jan 2019

STATEMENT 2 This work has not been submitted in substance for any other degree or award at this or any other university or place of learning, nor is it being submitted concurrently for any other degree or award (outside of any formal collaboration agreement between the University and a partner organisation)

Signed _____(Helen King)   Date 28th Jan 2019

STATEMENT 3 I hereby give consent for my thesis, if accepted, to be available in the University's Open Access repository (or, where approved, to be available in the University's library and for inter-library loan), and for the title and summary to be made available to outside organisations, subject to the expiry of a University-approved bar on access if applicable.

Signed _____(Helen King)   Date 28th Jan 2019

DECLARATION This thesis is the result of my own independent work, except where otherwise stated, and the views expressed are my own. Other sources are acknowledged by explicit references. The thesis has not been edited by a third party beyond what is permitted by Cardiff University's Use of Third Party Editors by Research Degree Students Procedure.

Signed _____(Helen King)   Date 28th Jan 2019

WORD COUNT: 65,815

ACKNOWLEDGEMENTS

Firstly, I would like to thank my supervisor's Dr Allan Cosslett, Dr Chris Thomas and Dr Rebecca Price-Davies for guiding me through this project, offering support throughout the three years, welcoming me into the laboratory and enabling me to develop as a researcher and complete a piece of work that I am proud to present.

To Emma Jones, lab technician but more importantly friend, thanks for putting up with me through three years of strife and struggle, you've made it a fun and enjoyable experience even in the darkest of PhD hours!

I would like to thank Fresenius Kabi for the supply of the lipid emulsions used within this work.

To Jennifer King and Neelufer Kazi, you are my rocks and my world, thank you for the endless love, support and proof reading I would never have been able to fulfil my dream of completing this research without you.

Finally, I dedicate this thesis and the last three years of work to my late father Norman King who always pushed me to achieve my dreams. I finished it Dad, this one's for you x

SUMMARY

Intravenous lipid emulsions (IVLE's) form a staple part of parenteral nutrition (PN). PN provides life sustaining support where gastrointestinal nutrition is inadequate due to disease or prematurity. Whilst the physical stability of IVLE's is relatively well known and quantified, chemical stability is an area where little testing has occurred.

Lipids are susceptible to breakdown through free radical attack leading to lipid peroxidation, a cyclical process resulting in the production of primary and secondary toxic lipid peroxidation products. This thesis presents the development and validation of a method for measurement of peroxidation and triglyceride (TAG) breakdown occurring within two intravenous lipid emulsions.

The high-performance liquid chromatography (HPLC) method developed uses in-line ultra-violet (UV) and charged aerosol detection (CAD) to monitor the six main TAGs in Intralipid® emulsion and 10 TAGs in SMOFlipid® and detects the toxic secondary peroxidation products 4-Hydroxynonenal (HNE) and Hydroxyundecenal (HUE). The assay was validated in line and employed to test the chemical stability the established lipid emulsion (Intralipid®) and a newer lipid emulsion (SMOFlipid®).

Both lipids were subject to up to 84 days storage within 50 ml syringes, 250 ml PN bags and 50 ml glass vials at room and fridge temperatures. The effect of light exposure was tested using light protected and non-light protected samples of each lipid. Results within each chapter detail the extensive levels of TAG losses observed within each container and the detection of secondary peroxidation products. Fridge temperature limited TAG loss and peroxidation in all containers, however secondary peroxidation products were detected. Both SMOFlipid® and Intralipid® gave in excess of 30 % losses in TAGs over 84 days storage. HNE, HUE and a triglyceride remnant were all recorded in SMOFlipid® and Intralipid® syringes (both temperatures) and small volume PN bags at room temperature. Light protection within this study showed no significant difference vs non-light protection.

The results obtained from the work within this thesis are of vital importance when considering the safety of lipid emulsions for intravenous nutrition. This work provides an initial data set on the levels of peroxidation occurring within two commercially available in-use lipid emulsions and highlights the necessity for the stability and storage limits of these emulsions to be re-assessed.

LIST OF ABBERVIATIONS

PN	Parenteral Nutrition
AIO	All-in-one
HPN	Home Parenteral Nutrition
IVLE	Intravenous Lipid Emulsion
EFA	Essential Fatty Acid
PUFA	Poly Unsaturated Fatty Acid
IFALD	Intestinal Failure Associated Liver Disease
PNALD	Parenteral Nutrition Associated Liver Disease
MCT	Medium Chain Triglyceride
USP	United States Pharmacopeia
ROS	Reactive Oxygen Species
MDA	Malondialdehyde
HNE	4-Hydroxynonenal
HUE	Hydroxyundecenal
TBARS	Thiobarbituric acid reactive substance
FOX	Ferrous oxidation-xylenol orange
BHT	Butylated hydroxytoluene
HPLC	High-Performance Liquid Chromatography
TBA	Thiobarbituric Acid
UV	Ultra Violet
CAD	Charged Aerosol Detection
RP-HPLC	Reversed-Phase High-Performance Liquid Chromatography
NARP	Non-Aqueous Reversed Phase
BuOH	Butanol
IPA	Isopropanol
ACN	Acetonitrile
ML	Multi-layered

Contents

List of Tables

List of Figures.

Chapter 1

Introduction

1.1. Parenteral Nutrition

1.1.1 History and development of parenteral nutrition

Parenteral Nutrition (PN) has since the late 1960's, been a vital method of delivering essential nutrition to patients who are unable to meet their daily nutritional requirements orally (Dudrick 2009). Early advances in PN saw the development of simple mixtures of glucose as a source of energy, fibrin hydrolysate to provide amino acids and nitrogen, and combinations of trace elements, electrolytes and vitamins added in quantities dependent upon the daily blood results of the patient (Dudrick 2003). Such infusions were initially administered peripherally via peripheral vein cannulation. The large volume of fluids given, often several litres to control tonicity, resulted in phlebitis and collapse of cannulated peripheral veins and loss of intra venous (IV) access to the patient. The high glucose content of early PN also provided ideal environments for bacterial growth and subsequent infections (Hamilton et al. 2006).

Whilst limited early trials proved to be relatively successful, early PN mixtures proved inadequate in providing a total nutrition source to the patient. Patients who were solely dependent on PN for nutrition developed essential fatty acid deficiencies due to the lack of a lipid component to the PN formulation. Fat soluble vitamins were also lacking in such patients intake causing deficiencies in Vitamin K, D, A and E (Barr et al. 1981). To overcome such deficiencies, intravenous lipid emulsions (IVLEs) were introduced as part of the PN regimen, initially as cottonseed oil emulsion which was quickly withdrawn due to the development of fat overload syndrome causing severe anaphylaxis and an immune mediated allergic response (Hamilton et al. 2006). Subsequent research and development led to the use of soybean oil as an aqueous emulsion, marketed and still in use today as Intralipid® (other brands also available). This IVLE has become a staple to PN, allowing in some circumstances for the entire nutritional needs of a patient to be met intravenously. IVLE's have also enabled the addition of fat-soluble vitamins to PN preventing deficiencies from occurring.

Venous access has moved in accordance with medical advances, addressing the problems of venous collapse and the limited volume tolerances of peripheral lines. From the first instance of central venous access being used in a neonatal infant reliant upon PN due to near total bowel resection (Dudrick 2003), central access has become a staple in the delivery of PN, especially within the secondary care

setting where acutely ill patients, commonly within an intensive care setting, are reliant on PN and require central access for the delivery of drugs and analysis of biochemical status. Within the home PN setting, where patients are reliant on PN for nutrition due to chronic conditions, venous access is achieved usually through peripherally inserted central catheters (PICC line). These lines reduce the risk of infection with appropriate aseptic training given to the patients and carers, allowing long term patients on stable regimens of PN to receive their PN in a home care setting (Pittiruti et al. 2009). Peripheral venous access is still used for the delivery of PN, but is usually only employed when low volume, short term therapy is required within an acute setting.

1.1.2   PN indications

Dependence on PN as a nutritional source is the result of many different chronic and acute medical conditions. PN is indicated when there is an overarching diagnosis of the inadequacy of the gastrointestinal (GI) tract to meet the daily nutritional needs of the patient. Within an acute secondary care setting, indication for PN is most commonly due to surgical trauma or resection of the bowel, bowel rest post GI surgery (fistulae removal, cancer resection), or due to trauma causing GI malfunction. Typically acute indications for PN lead to short term use averaging 7-10 days in length allowing GI recovery and eventual reversion to enteral feeding and nutritional support (Gibson 2012).

Home PN (HPN) as a result of chronic intestinal failure (IF) is required over long-term periods and is often the sole form of nutrition in patients. In 2011, the number of HPN patients within the UK was 523 (Smith et al. 2011), a number that has continually risen per annum to 1360 in 2015 (Smith and Naghibi 2016) All HPN patients have IF due to a variety of conditions, the most common being inflammatory bowel diseases and bowel ischemia leading to surgical bowel resection and subsequent short bowel syndrome. Malabsorption conditions and cancer are also indicators for long term HPN (Smith et al. 2011).

Neonatal patients are a cohort where the delivery of PN can be required due to insufficiency of the GI tract due to prematurity. Such patients have very unique nutritional requirements, discussed in the following sections, resulting in PN being separated into lipid and aqueous portions.

1.1.3 PN formulations and components

Nutritional requirements and therefore regimen requirements in PN will be unique to the patient and regular biochemical monitoring is necessary to allow adjustments to a patients PN regimen to be made to maintain adequate requirements. The stability of a patient's condition will govern the frequency of monitoring required and subsequently if the patient is able to continue to receive HPN. It is worth noting that although a chronic patient on HPN may be stable in the disease status requiring PN, acute illness, infection and inflammation will change their nutritional requirements rapidly. As such, patients and carers are educated in how to recognise the signs and symptoms in changes in their condition/acute illnesses and how to seek medical assistance to have their PN regimen reviewed and altered if necessary. Inflammation and the resultant oxidative stress that is placed on the body in incidences of acute infection, trauma or disease alter how the body deals with nutrition. This includes a patient's insulin response to glucose, fat utilisation and breakdown at a cellular level and nitrogen (amino acid) requirements (Beisel 1975).

Modern PN typically consists of an all-in-one (AIO) mixture of the components outlined in table 1.1.

Table 1.1 Components of PN and nutritional requirements.

Nutrient Group	PN formulation and requirement.
Carbohydrates	Glucose solution – source of calories.
Proteins	Amino acid solution – provides essential and non-essential amino acids and nitrogen source.
Water	Water for injection – maintains tonicity of PN and hydration of patient.
Fats	Lipid emulsion – see below (page 8).
Vitamins	Fat and water soluble multivitamins – prevent vitamin deficiencies and subsequent disease development.
Trace elements	Micronutrients as essential elements (zinc, selenium, iron etc.) – essential within the body in complexation with enzymes and bioactive pathways.
Electrolytes	Inc. sodium, magnesium, calcium etc. – essential nutrients to maintain a wide variety of physiological functions including muscle contraction.

PN as described in table 1.1 is given as an AIO mixture commonly in two to three litres total of fluid. When patients are purely reliant on PN for their nutritional needs, this fluid volume is typically given every day. Patients with some enteral feeding will receive PN to top-up enteral nutrition, commonly 2-3 times a week. Patient specific requirements can often alter this total volume. For example, in fluid restricted patients due to renal failure, typically low volume, high calorific regimens are employed. AIO mixtures offer a complete nutritional source to the patient but have inherent risks associated with them. Such mixtures often contain upwards of 50

different components, each potentially having an effect on the others. As such AIO PN is inherently unstable and liable to physically break down. Development of PN into an AIO mixture has enabled these components to be tested in varying concentrations and stability parameters to be established. As such there are limits on the volumes and ratios of each component that can be added to an AIO mixture to ensure its physical stability.

The uniqueness of the situation of trying to prescribe a 'set' regimen to an individual patient calls for the use of component volumes in PN that sometimes fall outside of the known ranges of stability for AIO mixtures. In such cases the lipid component of PN is often delivered separately from the aqueous portion, allowing for concentrations of components to be increased where necessary. This is often done in cases where high levels of calcium are required. Calcium in the presence of phosphorous is liable to cause complexation and the subsequent precipitation of calcium phosphate. This is a particular problem in PN regimens that require high levels of calcium due to either metabolic bone disease in adults or simply in order to meet the nutritional requirements of neonatal patients to support bone growth and development (Machmon et al. 1990). Lipid emulsions are cream/white in colour and as such can obscure visualisation of precipitation within PN. To overcome this problem and allow for further separation of certain PN components to maintain stability, the lipid portion of PN is separated from the aqueous portion and stored in two separate containers. These are then given concomitantly through separate lines that join at a Y-junction at the point of cannulation. This enables regimens to be altered to meet patient needs whilst maintaining the physical stability of PN and allowing visualisation to confirm stability to occur. Infusion times are also maintained by running both aqueous and lipid portions together.

1.2 Intravenous lipid emulsions

All lipid emulsions in use within PN are oil-in-water emulsions with an average fat globule diameter of 0.5 microns (Eriksson 2001). The development of IVLEs for utilization as a nutritional source aims to reflect the natural metabolism and elimination of chylomicrons. Lipid utilization, distribution and storage through the body is complex and dependent on many factors, of which the type of lipid and its formulation to an IVLE becomes the controlling factor when lipid nutrition is delivered solely via the intravenous route. Emulsified lipid droplets are produced to

0.5 µm diameter to mimic the dimensions of naturally occurring chylomicrons which transport absorbed fats formed by enterocytes of the GI tract.

PN lipid emulsions broadly contain an aqueous base, a proportion of appropriate oil formed into droplets through emulsification with phospholipids and glycerin to achieve an isotonic emulsion.

1.2.1 Phospholipids/emulsifiers

Phospholipids used within currently available lipid emulsions are extracted from egg yolk, acting as anionic emulsifying agents (Driscoll et al. 2008). These form a layer surrounding the oil droplets, creating a net negative charge across the surface of the lipid droplets. This repulsive charge forms the key to emulsion stability and helps prevents droplets from flocculating which can lead to coalescence and eventual cracking (breakdown) of the emulsion into its oil and water components.

Within IVLEs, egg yolk phospholipids account for around 1.2% of the lipid emulsion (Tashiro et al. 1992; Kabi 2009). Although only accounting for 1.2%, the phospholipids are provided in excess to ensure full coverage of all oil droplets present. Excess phospholipids form sub 80nm liposomes which are of little nutrient use. Through the development of lipids for PN, the emulsifier limit has been formed of around 1.2%, a value that was initially much higher. The production of larger numbers of liposomes from an increased excess of emulsifier has proven to have detrimental effects. Infused liposomes can have two negative impacts on lipid metabolism. Initially liposomes reduce lipolysis of artificial chylomicrons from infused oil. Secondly they interact with cholesterol present within the blood, forming complexes known as Lipoprotein X, a harmful substance that mimics low density lipoproteins and results in hypercholesterolemia and the mis-management of free fatty acids (Calder et al. 2015; Waitzberg et al. 2015).
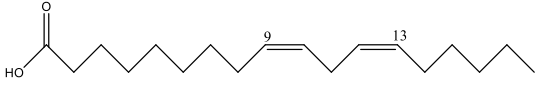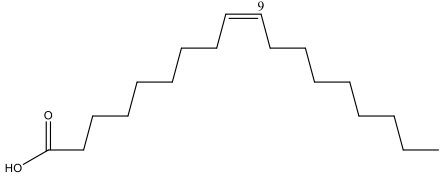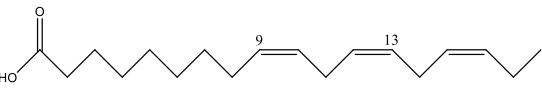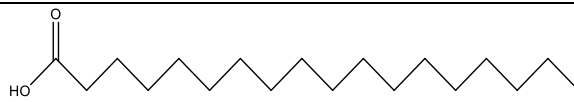
Table 1.2 Components of Intralipid® 20% emulsifiers. R-groups represent different fatty acids in IVLE. R_1 and R_2 denote fatty acid chains.

Phospholipid	Chemical structure	% component of Intralipid® 20% (Wabel 1998)
Phosphatidylcholine	R_1 ... O^- ... O—P—O ... N^+ ; R_2 ; O	87.1
Phosphatidylethanolamine	R_1 ... OH ... O—P—O ... NH_2 ; R_2 ; O	7.8
Lyso-phosphatidylcholine	R_1 ... O^- ... O—P—O ... N^+ ; HO ; O	2.5
Lyso-phosphatidylethanolamine	R_1 ... OH ... O—P—O ... NH_2 ; HO ; O	2.5

1.2.2 Fatty acids

The fatty acids that form the oil proportion of IVLE's varies and is dependent on the type of oil used to form the emulsion. Traditional lipid emulsions were formed of soybean oil which is predominately comprised of the omega 6 long chain polyunsaturated fatty acids (PUFA's) shown in table 1.3.

Table 1.3 Fatty acid components of Intralipid emulsion for injection (Wabel 1998)

Fatty acid (FA)	Structure	Formula	% in Intralipid emulsion	Type of Fatty acid
Linoleic acid		$C_{18}H_{32}O_2$	44-62	Omega 6 PUFA
Oleic acid		$C_{18}H_{34}O_2$	19-30	Monounsaturated FA
α-Linolenic acid		$C_{18}H_{30}O_2$	4-11	Omega 3 PUFA
Palmitic acid		$C_{16}H_{32}O_2$	7-14	Saturated FA
Stearic acid		$C_{18}H_{36}O_2$	1.4-5.5	Saturated FA

The highest proportion fatty acid seen in soybean oil is that of Linoleic acid ($C_{18}H_{32}O_2$). Linoleic and α-linolenic acid are considered the only two true essential fatty acids (EFA). This is due to the fact that humans lack Δ12 and Δ15 desaturases and therefore cannot synthesize either of these fatty acids (Calder et al. 2015). When these EFA's are removed from a patients' nutrition, metabolism of available oleic acid is increased leading to the production of Mead acid. This is used as a marker for the diagnosis of EFA deficiency which, where present, can cause skin rashes, lack of growth and can prove fatal (Barr et al. 1981; Hamilton et al. 2006). Long chain fatty acids have been traditionally used very effectively in PN for a prolonged period of time, preventing EFA deficiency from occurring. There are however limitations to their use and they have been proven to have detrimental effects to the body through prolonged use. In order to understand the mechanisms behind these unwanted side effects it is important to look at the initial metabolism pathway of long chain PUFA's including the EFA's linoleic and α-linolenic acid as shown in figure 1.1.
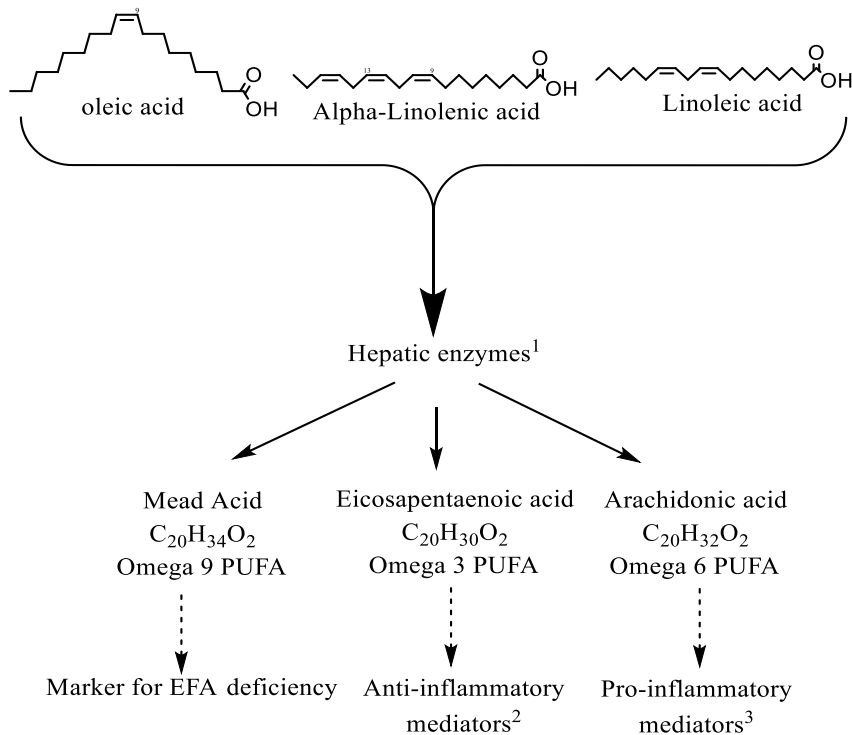
1. *Hepatic enzymes produce desaturation and elongation of carbon chain.*
2. *Eicosapentaenoic acid converted to docosahexaenoic acid then further broken down to prostaglandin 3, leukotriene 5 and thromboxane 3.*
3. *Pro-inflammatory mediators prostaglandin 2, leukotriene 4, thromboxane 2* (Hamilton et al. 2006)

Figure 1.1 Initial metabolism of PUFA's present in Soybean emulsion.

Linoleic acid in soybean oil emulsions has been proven to have implications in the inflammatory pathways of the body. Production of pro-inflammatory mediators due to excess metabolism of linoleic acid has been associated with impaired lymphocyte function, limiting the body's ability to deal with infection. The production of leukotriene 4 and prostaglandin 2, inflammatory mediators, also serve to increase inflammation within an already stressed system that is an acutely ill patient on PN (Wischmeyer 2015). Soybean oil as a plant derived oil also contains phytosterols, a substance that when infused over a prolonged period of time has been shown to cause intestinal failure-associated liver disease (IFALD) (previously known as parenteral nutrition associated liver disease (PNALD)) (Gura et al. 2005; Gura et al. 2006). IFALD is a particular problem within neonatal patients who require PN from birth due to prematurity. Burrin et al. (2014) reported that in neonatal infants receiving soybean based PN for at least 2 months there is up to a 50% incidence of INFALD or a graduation of cholestatic liver dysfunction, that ultimately if not treated, leads to total liver failure and the requirement for liver transplantation. This statistic is further supported by Paltrinieri et al. (2016) who reported an incidence of IFALD of between 40-60% in neonates within a London trust hospital.

1.2.3 New intravenous lipid emulsions

Within the above association of IFALD, the omega 6 PUFAs and phytosterols has been one of the driving factors in the development of new IVLEs where soybean oil is either replaced or complimented by different oils. Olive oil, coconut oil derived medium chain triglycerides and fish oils have all been formulated into PN emulsions. Each of these oils provides different fatty acid combinations to that of the omega 6 FA's in soybean oil as seen in table 1.4.

*Table 1.4 Proportions of lipid in new IVLE's: *Medium chain triglycerides. (1) Fresenius Kabi, (2) Baxter Healthcare, (3) B Braun. (Burrin et al. 2014)*

Intravenous Lipid Emulsion	% Proportion of oil component & source			
	Soybean	Olive	Fish	MCT's*
Intralipid[1]	100			
SMOFlipid[1]	30	25	15	30
Omegaven[1]			100	
Clinoleic[2]	20	80		
Lipofundin[3]	50			50
Lipoplus[3]	40		10	50

The introduction of newer formulations of IVLE's has aimed to reduce incidences of IFALD, improve patients' lipid tolerance and more closely mimic the body's naturally occurring processes of lipid metabolism. With reference to Figure 1.1, fish oil provides both EPA and DHA and therefore promotes the production of anti-inflammatory products. Omegaven® (100% fish oil) is licensed for use as a component of lipid PN due to its lack of EFA's, but has been used off license as a sole lipid agent to treat neonatal PNALD (Gura et al. 2006).

SMOFlipid® contains a mixture of soybean, olive, fish oil and MCTs (see table 1.4). The reduction in omega 6 PUFAs coupled with the addition of anti-inflammatory omega 3 PUFAs from fish oils aims to reduce the inflammatory response to lipid PN by providing a more adequate ratio of omega 6 and omega 3 PUFAs (Waitzberg et al. 2015). Olive oil, high in omega 9 FAs was introduced post studies into the 'Mediterranean diet', that showed reduced levels of atherosclerosis and liver disease (Sala-Vila et al. 2007; Waitzberg et al. 2015). MCTs are metabolized faster than longer chain PUFAs and provide a rapid energy release. This reduces liver

accumulation of fatty acids and, as they are unsaturated and of short carbon chains, are resistant to oxidation (Hippalgaonkar et al. 2010). SMOFlipid® also contains a higher proportion of vitamin E which is postulated to act as an antioxidant preventing peroxidation of PUFAs. Whilst a marked reduction in pro-inflammatory omega 6 PUFAs provides beneficial effects to the patient, SMOFlipid® still contains appreciable levels of phytosterols and therefore still has a potential link to IFALD processes. Data from Burrin et al. (2014) indicates however that the reduction in phytosterols in SMOFlipid® reduces the development of IFALD in an animal model and hypothesises that phytosterols may be the causative component of IFALD.

1.3 Stability of IVLE's

1.3.1   Physical stability

Physical stability of IVLEs is well quantified and dependent on a raft of internal and external factors. In PN where IVLEs are incorporated into AIO mixtures, each component of the PN will have stabilizing or destabilizing effects on the lipid emulsion:

- Amino acids: provide a buffering capacity to PN. Large volumes of amino acid solutions buffer against the pH changes caused by additions of other components (Hardy and Puzovic 2009).

- Glucose: Used as a rapid energy source. High concentration, low volumes provides an energy source as the low pH of glucose is a destabilizing factor for lipid emulsions. Glucose in high concentrations can interact with lecithin in IVLEs and lead to discoloration of PN mixtures, obscuring changes in physical stability (Hippalgaonkar et al. 2010).

- Electrolytes – Whilst added in small volumes as a necessity within AIO PN, electrolytes can interfere with the zeta potential and surface charges of oil droplets leading to emulsion destabilization (Hippalgaonkar et al. 2010). Electrolytes within standard PN mixtures include potassium, sodium, magnesium, calcium and phosphate. Potassium and sodium as monovalent ions are relatively stable within PN. Divalent ions, in particular calcium, are liable to form precipitates with phosphate. The factors affecting precipitation of calcium phosphate occurring are

multiple. pH of a PN mixture is critical in controlling the equilibrium for the three possible phosphate states than occur within a mixture. Tribasic phosphate is uncommon within PN due to its requirement for high pH. Mono and dibasic phosphate can readily occur within PN, the most problematic being dibasic phosphate as it readily combines with free calcium ions and forms a relatively insoluble precipitate. The concentration of amino acids present and the glucose concentration will govern the final pH of the PN mixture and therefore will contribute to buffering pH and preventing calcium phosphate precipitation from occurring. Other factors including temperature, calcium concentration, calcium formulation and concentration of magnesium will all also have an effect on calcium phosphate precipitation (Allwood and Kearney 1998).

- Vitamins – Vitamin E (fat soluble) acts as an scavenger for free radicals, limiting but not preventing the peroxidation and subsequent breakdown of PUFA's contributing to the chemical stability of PN (Steger and Mühlebach 1998; Grand et al. 2011). Vitamin C (water soluble) in itself is not a destabilizing factor of PN. It is however rapidly oxidized and broken down into oxalic and threonic acid, both acidic and can therefore reduce the pH of AIO PN, destabilizing lipid emulsions. Riboflavin (water soluble) acts within PN as a photosensitizer therefore promoting the production of reactive oxygen species which can cause peroxidation (Ferguson et al. 2014).

- Trace elements – Including chromium, selenium, copper, iron, zinc, manganese, iodine, fluorine and in certain PN mixtures molybdenum. The majority of these trace elements are relatively stable within standard PN mixtures. Of note however, the following trace elements can cause stability issues within PN:
  - Iron – Ferric (Fe^{3+}) ions are not stable in lipid PN as they can reduce the zeta potential charge on the surface of the lipid globules thereby destabilizing the lipid emulsion. Iron has also been implicated in the lipid peroxidation of IVLE's though data suggests that light protection of PN can reduce this (Grand et al. 2011).
  - Chromium – Is considered stable unless is in the presence of metal chelating agents which can lead to precipitation occurring.

- Zinc – Stable in PN mixtures but is known to bind to certain amino acids within PN mixtures affecting its bioavailability. Is also present in materials and consumables used during compounding and as such research has suggested that patients can receive higher doses than prescribed (Hardy et al. 2009).

The separation of PN into lipid and aqueous portions as described above is employed when high concentrations of electrolytes or trace elements is required as described for neonatal PN above.

External destabilizing factors of PN include temperature, oxygen and light. High temperatures are known to promote the peroxidation and chemical breakdown of PUFA's as well as cause physical destabilization of lipid emulsions (Steger and Mühlebach 1997). Oxygen permeation of susceptible PN containers leads to chemical and physical instability. Oxygen can promote ascorbic acid breakdown leading to lower pH conditions and destabilization of emulsions. Peroxidation of lipids is also catalyzed by the presence of oxygen (Gonyon et al. 2013; Ozcan and Ogun 2015).

1.3.1.1 Physical stability testing

The physical stability of IVLE's in their constituent parts (licensed) and when mixed as AIO PN (unlicensed) is well categorized. Multiple methods exist and are well used to categorize physical attributes of lipid emulsions used in PN and therefore are used as a measure of PN stability. Physical stability of PN is assessed mainly through the quantification of particle size distribution. This aims to identify particles of large size, typically >5µm (Calder et al. 2015). Whilst the British Pharmacopeia doesn't specifically currently contain any monographs pertaining to the globule size distribution of IVLE's, manufactures tend to follow the United States Pharmacopeia monographs (USP). Testing methods for lipid globule size and particle size distribution laid out in USP monograph 729 enable accurate and quantifiable monitoring of the physical stability of IVLE's (United States Pharmacopeia and National Formulary (USP38 - NF 33) 2016b). When used in AIO PN mixtures or when licensed lipid emulsions are used with additions of fat soluble vitamins their stability limits will be altered due to the factors discussed previously. USP 729 methods are then used to monitor for lipid degradation and to quantify usable stability parameters and storage limits. Common physical stability testing regimes

use PN bags under fridge storage up to 84 days to give data on extended storage periods.

1.3.2   Chemical stability

Unlike the relatively well quantified parameters of IVLE's and subsequent PN's physical stability, their chemical stability has been only limitedly explored and quantified. Chemical parameters such as pH, concentrations of trace elements and electrolytes have all been successfully monitored but always with relation to their effect on the physical stability of AIO PN. Vitamin concentrations have been explored and shown to chemically alter and breakdown during PN storage and administration, again leading to emulsion destabilization and vitamin loss (Nonneman et al. 2002; Ferguson et al. 2014). With specific regards to the chemical stability of IVLEs it has been proven that lipids break down under the influence of both internal and external factors (Hardy and Puzovic 2009). This breakdown primarily is due to lipid peroxidation. Whilst the process of lipid peroxidation has been well studied, little has been done to quantify peroxidation levels within PN and the subsequent differing amounts of lipids that are infused to the patient post peroxidation during storage. This gap in knowledge in the area of chemical stability of IVLE's is addressed within this work and forms the basis of the research aims and objectives set out overleaf.

1.4 Lipid peroxidation

1.4.1   Principles

The principles of lipid peroxidation can broadly be split into endogenous and exogenous processes. Endogenous stages of peroxidation concern the enzymatic breakdown of lipids within the metabolism pathways in the body. Whilst this is a naturally occurring process within the body, as this work is focusing on peroxidation occurring in PN before administration, only exogenous processes will be considered here.

Lipid peroxidation is the process by which PUFA's present in PN lipid emulsions are degraded by a self-propagating chain reaction initiated by a reactive oxygen species (ROS) or other free radical (Mühlebach and Steger 1998; Kamal-Eldin 2003). This reaction also takes place naturally during many pathways in the body, but a healthy, non-stressed human deals effectively with this. However, within a chronic or acutely unwell patient where endogenous ROS levels will already have stretched the bodies coping and detoxification mechanisms to their limit, this can cause a potentially catastrophic problem when peroxidation products are then administered within PN to the patient. Therefore, quantifying the levels of peroxidation occurring in PN and IVLE's is of vital importance and the focus of this work.

Peroxidation can be broadly broken down into three areas, initiation, propagation and termination.

1.4.1.1 Initiation

The initiation of lipid peroxidation relies upon the creation of a ROS or free radical that can then go on to abstract a hydrogen from a PUFA. Essentially a free radical is any atom that has an unpaired electron and can exist as a single entity, therefore having the ability to gain an electron, usually in the form of a hydrogen atom (unpaired electron) (Halliwell and Chirico 1993). The availability of oxygen within a PN system is a crucial factor with regards to the initiation step of lipid peroxidation when ROS are considered as the initiating radical. Oxygen levels are limited in the components of PN by their preparation in oxygen free environment during bulk manufacture. However, during the manufacture of PN it is almost inevitable that a small amount of oxygen will be introduced to the PN bag. Whilst as much air as

possible is standardly removed from PN bags at the end of the compounding process, small volumes remain, as does oxygen within the giving sets connected to PN bags upon administration.

Transition metals such as iron (present in standard PN mixtures) promote the formation of hydroxyl radicals (OH$\cdot$) through the Fenton reaction (Fe^{2+} + H$_2$O$_2$ -> Fe^{3+} + OH$\cdot$ + OH$^-$). Hydroxyl radicals are one of the most reactive free radical species (Sodergren 2000; Kamal-Eldin 2003). Transition metals also have a role in the production of (OH$\cdot$) radicals from oxygen. Oxygen can accept an electron creating a free radical, either a superoxide anion (O$_2^-$) or a peroxide ion (2O$_2^-$). Peroxide ions, at physiological pH and pH present within a PN lipid emulsion, rapidly protonate forming hydrogen peroxide (H$_2$O$_2$). Hydrogen peroxide and superoxide are strong oxidising agents and in the presence of transitional metals create hydroxyl radicals (OH$\cdot$).

Light exposure also plays a role in free radical generation within IVLE's. Known as photo-oxidation, UV exposure from ambient light sources can lead to electron rearrangement and creation of a singlet oxygen molecule (O$_2^1$). Though not a true free radical with respect to the initiation step of peroxidation, singlet oxygen interacts directly with lipid molecules creating lipid peroxides. This bypasses the initiation step of abstraction of a hydrogen atom from the lipid. As such it is a catalyst for both the initiation and propagation processes (Halliwell and Chirico 1993; Kamal-Eldin and Min 2008). Singlet oxygen can also be produced when certain compounds, including riboflavin (component of AIO PN) are exposed to light. Such compounds absorb light, enter a higher electron excitation state and then transfer this energy to oxygen thereby creating singlet oxygen molecule which can then react with PUFA's.

$$\text{LIPID}\text{———}\text{H} \; + \; \text{OH}^{\bullet} \; \longrightarrow \; \text{H}_2\text{0} \; + \; \text{LIPID}^{\bullet}$$
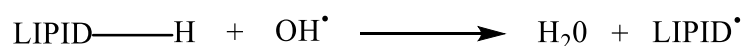
Figure 1.2 Initiation scheme for peroxidation through abstraction of a hydrogen from a lipid creating a lipid radical.

Within IVLE's, the susceptibility of the lipid to peroxidation is centred on the presence of double carbon bonds i.e. the level of unsaturation of the fatty acid. A double bond within a chain of carbons weakens the C-H bond on the adjacent carbon from the double bond due to electron delocalisation through the double bond. This makes abstraction of a hydrogen atom from said carbon easier (Kamal-

Eldin 2003). The more double bonds within a PUFA, the more likely peroxidation is to occur. Hence why of the lipids present in IVLE's linoleic acid with two double bonds is the most susceptible to peroxidation.

Once a hydrogen has been removed from a lipid molecule, the lipid radical is unstable and undergoes a molecular rearrangement to stabilise the system. This leads to the formation primarily of a conjugated diene (molecule where two double bonds within a carbon chain are separated by a single carbon bond, allowing delocalisation of electrons to occur, stabilizing the system) as shown in figure 1.3.

Lipid radicals are themselves reactive and therefore readily combine with oxygen present in a PN system to form a peroxyl radical (ROO·).

lipid radical

conjugated diene radical

or

9

+O$_2$

13

O
O
9

lipid peroxyl radical

or

O
O
13
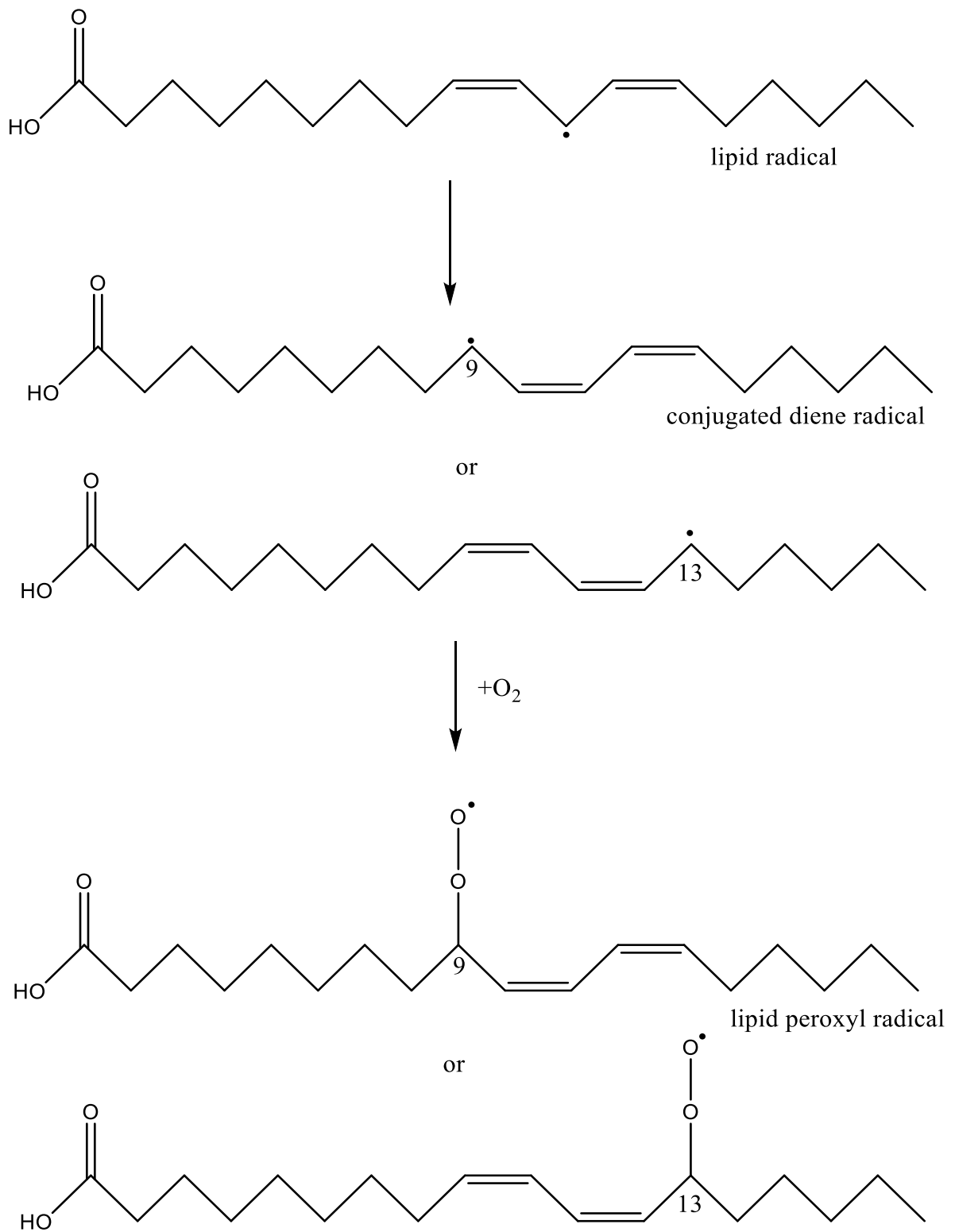
Figure 1.3 Molecular rearrangement of linoleic acid radical and subsequent reaction with oxygen to yield peroxyl radicals.

Lipid peroxidation is a self-propagating process. The production of a lipid peroxyl radical in the initiation steps means that this radical itself is then able to interact with other PUFA's, abstracting a hydrogen from an adjacent PUFA, thereby creating another lipid peroxyl radical and a lipid hydroperoxide (Repetto et al. 2012). Lipid hydroperoxides are always the first products of lipid peroxidation.

$$\text{LIPID} - \text{O} - \text{O}^\bullet \ + \ \text{LIPID} \longrightarrow \text{LIPID} - \text{O} - \text{OH} \ + \ \text{LIPID}^\bullet$$
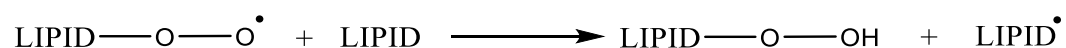
Figure 1.4 Propagation step of peroxidation. Lipid peroxyl radical is able to abstract a hydrogen from another PUFA, creating a lipid hydroperoxide and another lipid radical.

This process of lipid radical production, rearrangement to a conjugated diene, reaction with oxygen to form a peroxyl radical and then subsequent further lipid radical production continues until either a termination reaction occurs, or the availability of oxygen becomes a limiting factor.

Transition metals can abstract the oxygen and hydrogen atoms from a lipid hydroperoxide, forming a lipid radical and re-initiating the process of peroxidation. Hence within PN, the presence of transition metals has an effect on the levels of peroxidation seen (Repetto et al. 2012).

1.4.1.3 Termination

The process of lipid peroxidation has several ways in which it can be terminated. The principle of termination of peroxidation is when either two lipid radicals come into contact with each other, or when a lipid radical comes into contact with an anti-oxidant molecule. Two lipid radicals have the ability to bond together and form a stable lipid dimer molecule or form two lipid hydroperoxides. The presence of anti-oxidant molecules within PN such as α-tocopherol (vitamin E) or riboflavin has a definitive effect on limiting the level of lipid peroxidation that occurs (Lavoie et al. 1997; Steger and Mühlebach 1998). Lipid hydroperoxides can also be rearranged to form cyclic endoperoxides, particularly those from PUFA's such as Arachidonic acid (Leray 2016).

$$\text{LIPID}-\text{O}-\text{O}^{\bullet} \quad + \quad \text{LIPID}-\text{O}-\text{O}^{\bullet} \quad \longrightarrow \quad \text{LIPID}-\text{O}-\text{O}-\text{LIPID} \; + \; \text{O}_2$$

$$\text{LIPID}^{\bullet} \quad + \quad \text{LIPID}^{\bullet} \quad \longrightarrow \quad \text{LIPID}-\text{LIPID}$$

$$\text{LIPID}-\text{O}-\text{O}^{\bullet} \quad + \quad \begin{array}{c}\text{Free radical scavenger}\\ \text{(Anti-oxidant)}\end{array} \quad \longrightarrow \quad \text{LIPID}-\text{O}-\text{OH}$$

Figure 1.5 - Pathways for termination of lipid peroxidation.

1.4.2 Lipid peroxidation products

The initial products of PUFA peroxidation are always mono-hydroperoxides. The number of positionally different hydroperoxides that can be formed from a PUFA can broadly be defined using the formula 2n-2 where n stands for the number of double bonds within a PUFA (Esterbauer 1993). Using linoleic acid as an example, this PUFA has the formula 18:2 (2 double bonds) and therefore if capable of forming 2 different hydroperoxides, hence the greater degree of unsaturation of the PUFA, the greater the number of possible hydroperoxides. Eicosapentaenoic acid (EPA) found in fish oil PN is 20:6 in structure and therefore can create 10 different hydroperoxides upon peroxidation.

The position along the carbon chain of the PUFA where the hydroperoxide forms is dependent on the position of the double bonds within the PUFA. As shown in figure 1.3, peroxidation of linoleic acid results in C13 and C9 hydroperoxides. This is correct for the case of peroxidation due to auto-oxidation, or free radical initiated peroxidation. However, when looking at photo-oxidation of PUFA's by light exposure and the creation of singlet oxygen molecules, the carbon centres of 12 and 13 are targeted by singlet oxygen, therefore creating different hydroperoxides. It has been proven however that the vast majority of hydroperoxides generated when auto-oxidation and photo-oxidation are simultaneous will be those of C13 and C9 hydroperoxides in the case of linoleic acid, i.e. auto-oxidation is the dominant peroxidation pathway (Mlakar and Spiteller 1996).

Primary hydroperoxides are relatively stable in isolation, but in the presence of transitional metals, vitamins, an acidic pH or increased temperatures rapidly degrade to secondary products of peroxidation. Within an AIO PN system or within a lipid emulsion with fat soluble vitamins the rate of degradation of primary hydroperoxides will make measurement of them inaccurate in quantifying levels of

peroxidation. Hydroperoxides always rapidly undergo secondary and tertiary reactions to form a multitude of peroxidation products including reactive aldehydes, complex lipid endoperoxides and larger lipid structures. These products are formed in a variety of different ways, many of which are not fully understood. The main principles of these secondary and tertiary reactions are explained below. For the purposes of this body of work, the formation of the reactive aldehydes will be focused on and therefore are explained due to their inherent toxicity and risk they pose to the patient.

- Chain-breaking reactions: Involves splitting of the carbon backbone of the PUFA chain, creating two smaller molecules, one from the methyl end of the PUFA and the other from the acyl end which is often still attached to a phospholipid molecule. The type of methyl molecule created will always be a volatile aldehyde. Which aldehyde is formed is dependent on the type of PUFA the parent molecule is.

  Omega 6 PUFA's, as shown with linoleic acid in figure 1.6, will always form several possible aldehydes the most reactive being 4-hydroxynonenal (HNE) whereas omega 3 PUFA's will form 4-hydroxyhexanal (HHE) (Esterbauer 1993).
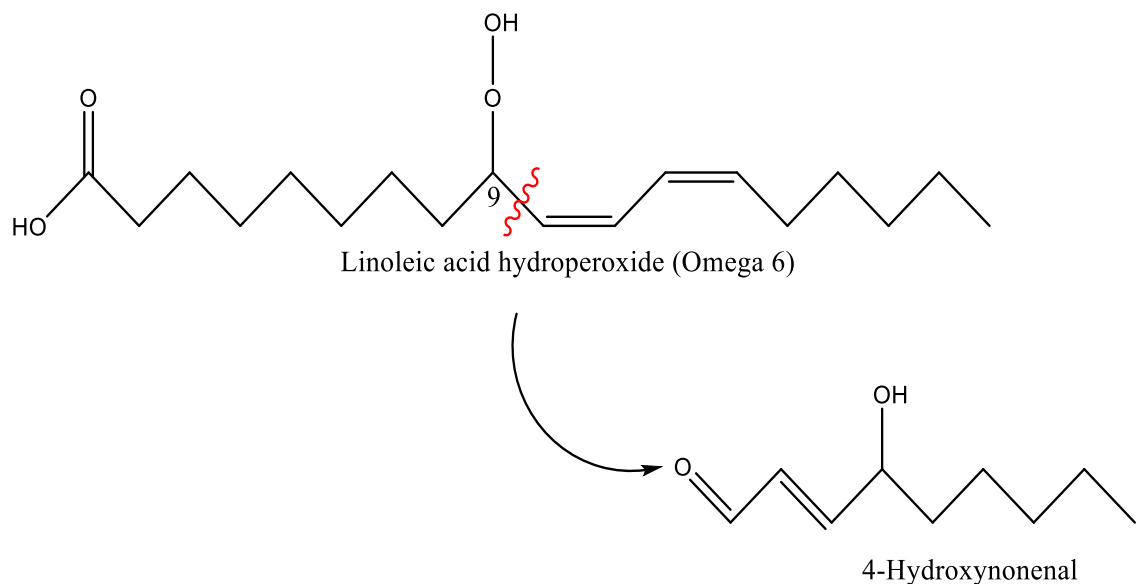
Figure 1.6 Production of 4-Hydroxynonenal from omega 6 fatty acids (Schneider et al. 2008).

22

- Formation of cyclic hydroperoxides is a complex process involving the rearrangement of PUFA's to form endoperoxides. These subsequently then further break down into smaller molecules including the aldehyde malondialdehyde (MDA) (Schaur et al. 2015).
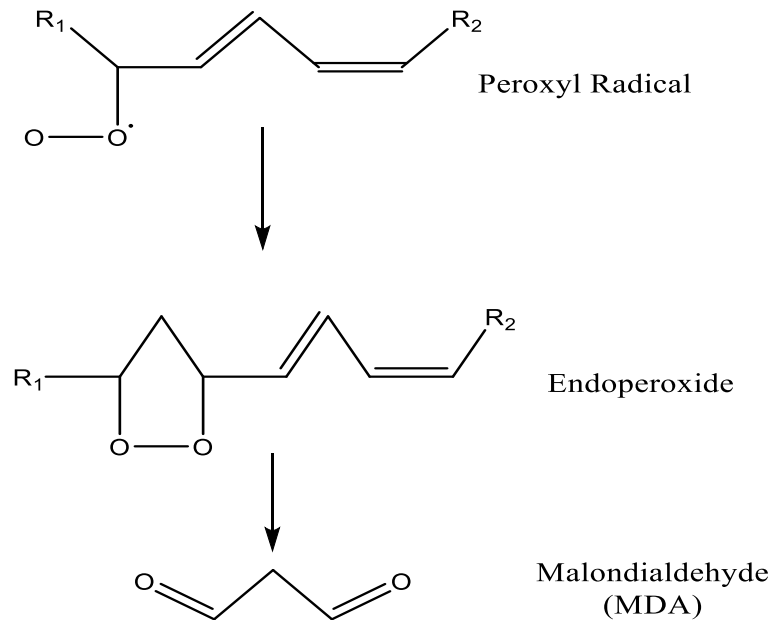
Figure 1.7 Production of MDA from unsaturated fatty acids.

Whilst numerous other secondary and tertiary products are formed, their processes of formation and their biological activity within the body are not well understood and therefore will be excluded from this body of work.

With regards to the production of secondary and tertiary products from the peroxidation of PN lipids, as described above these are due to either auto-oxidation or photo-oxidation. This to a certain extent limits the number of end products created, as within the body many tertiary products created are a result of the metabolism of primary hydroperoxides through enzymatic actions. This limits the number of peroxidation products possible *in vitro* within PN systems due to the lack of any enzymatic processes. The numerous other components within PN such as amino acids etc. will however interact with volatile peroxidation end products. This interaction will form adducts of aldehydes with amino acids etc. and numerous products with unknown biological significance. Therefore, quantification of peroxidation is a complex area as discussed below.

1.5 Peroxidation testing

Currently in the release criteria within the available pharmacopeia monographs for IVLE's there are no limitations on the level of peroxidation present. We hypothesise that this is however an area that requires quantifying due to the potential toxicity of the products produced from peroxidation.

Lipid peroxidation has been quantified in a variety of ways. Each type of testing has its own limitations and merits. With regards to PN, the main testing methods are reviewed in the following text.

1.5.1 Peroxide value

Peroxide value is to date the only specified test for peroxidation within the United States Pharmacopeia (USP). Whilst existing within the USP monograph for fats and fixed oils, this test is based on the reaction between peroxides and iodine which is then titrated against sodium thiosulfate. This gives a peroxide value, defined as the amount of peroxide oxygen per 1 kg of fat or oil. The limit for fats and fixed oils is set as 5 nM (United States Pharmacopeia and National Formulary (USP38 - NF 33) 2016a). Whilst used effectively to quantify overall peroxide levels within fats and fixed oils, this method needs an adaptation step for use within PN. Due to the other components within PN AIO mixtures that can interact with iodine, a lipid extraction step is required prior to testing peroxide value (Steger and Mühlebach 1998; Muhlebach 2015). Peroxide value testing, whilst relatively quick and low cost, has questionable specificity as a test for lipid peroxidation. It is known that hydrogen peroxide present will also reduce iodine, thereby giving a false positive reading for peroxidation (Halliwell and Chirico 1993).

1.5.2 Thiobarbituric Acid Reactive Substances Test (TBARS)

TBARS is the most commonly used test for peroxidation. The sample is heated with thiobarbituric acid at a low pH and the intensity of the resulting pink adduct is quantified by measuring its absorbance at 532 nm or through the use of fluorescence at 553nm (Halliwell and Chirico 1993; Marrow 2010). Whilst the TBARS assay is one of the quickest, cheapest and easiest test available for defining peroxidation levels within a system, it has marked limitations, proven by results from its use as a testing mechanism for peroxidation within PN solutions (Picaud et al.

2004; Grand et al. 2011). Looking at the testing procedure itself, the heating step within the method is problematic when considering peroxidation. Heat is a known catalyst for the breakdown of primary hydroperoxides and therefore secondary and tertiary products can be created providing a false result.

The TBARS assay has been used within the testing of PN and IVLE's for peroxidation (Pitkanen et al. 1991; Basu et al. 1999b; Sala-Vila et al. 2007) but due to the fact that other aldehydes and amino acids can also interact with TBA (Sodergren 2000; Shintani 2013), the assay is largely disregarded when looking at peroxidation within PN.

1.5.3   Ferrous oxidation in xylenol orange assay (FOX)

The FOX assay exists as a bench top low cost assay for the measurement of lipid hydroperoxides, the primary products within the peroxidation process. The test works on the bases of oxidation of Fe^{2+} ions to Fe^{3+} ions by hydroperoxides. Then the subsequent reaction of Fe^{3+} ions with xylenol orange to form a coloured complex read by its UV absorbance at 560nm (Sodergren 2000). The initial FOX assay, known as FOX-I, was developed for quantification of aqueous peroxides. This was then modified with addition of butlylated hydroxytoluene (BHT) and methanol for the measurement of lipid hydroperoxides (FOX-II assay). The sensitivity of FOX-II is approximately five times lower than that of FOX-I (Nourooz-Zadeh et al. 1995). The FOX-II assay has been further developed where methanol was replaced with n-propanol to enable full dispersion of lipid emulsions to occur (FOX-III).

The issues of using FOX-III for the quantification of lipid peroxidation in PN lipids revolves around those similar to that of the TBARS assay. Many substances can interfere with the results of the FOX-III assay including ascorbate, included in multivitamin preparations used within PN mixtures (Karen and Winterbourn 2001). It has also been established that if lipids and lipid peroxides are not extracted from the aqueous portion of PN prior to quantification, any hydrogen peroxides present not due to lipid peroxidation will give false readings. Silvers et al. (2001) confirmed this by comparing the effect of multivitamin addition to lipid infant PN through the use of the FOX-III assay with an added initial lipid extraction method against a high performance liquid chromatography (HPLC). Their results concluded that in AIO PN mixtures the FOX-III assay gave values of peroxidation approximately double to that of the HPLC quantification method confirming that substances other than peroxides interfere with the FOX assay. Further work comparing all three versions of the FOX

assay in PN testing was carried out by Karen & Winterbourn (2001). Their conclusions discounted the use of the FOX assay for testing peroxidation levels in lipid PN mixtures due to interactions with multivitamins and aqueous hydroperoxides.

The measurement of lipid hydroperoxides by any method is limited by the stability of such primary products of peroxidation. Primary hydroperoxides are rapidly degraded into secondary and tertiary products, making any method quantifying primary peroxidation products questionable as an effective assay for assessing overall peroxidation within a system.

1.5.4 Existing high-performance liquid chromatography methods

The lack of sensitivity of the TBARS assay has been addressed by the adaptation of the assay through use of HPLC to increase the accuracy of the measurement of MDA production due to peroxidation. The TBARS assay is carried out as above, creating a TBA-MDA adduct which is then subjected to HPLC (Marrow 2010). Whilst HPLC can increase the accuracy of quantifying the levels of TBA adducts present, this system does not remove the inherent inaccuracies of the TBARS test itself neither does it address the issues of substances other than malondialdehyde reacting with TBA to form adducts, although these will be separated and may be identifiable by HPLC.

HPLC has been employed in the testing of MDA within lipid PN through derivatisation of MDA with diaminonaphthalene. The derivatised MDA forms a distinct peak at 311 nm under UV detection and this method has been used to quantify the levels of MDA within neonatal lipid PN solutions (Steghens et al. 2001; Picaud et al. 2004).

With regards to measuring the total aldehyde load of a sample as a measure of peroxidation, HPLC methods with UV detection and fluorescence detection have been developed, again through derivatisation of reactive aldehydes (Lovell 2003). Both detection procedures have been used to quantify aldehydes within lipid system, but there have been no published reports of their use within PN systems. The measurement of total aldehyde content as a measure of peroxidation is a contentious issue especially when considering the multiple components present within a PN AIO system. It is unlikely, without an extraction procedure employed prior to HPLC analysis, that a measure of total aldehyde content could be achieved.

Aldehydes will also be present that will not be a result of lipid peroxidation and therefore may give anomalous results.

Chemiluminescence is a relatively well exploited technique for the HPLC measurement of lipid hydroperoxides. Yamamoto & Ames (1987) developed the technique for identification of lipid hydroperoxides and hydrogen peroxide. The technique has been modified using methanol lipid extraction followed by HPLC separation, post column reaction with isoluminol and fluorometer detection and employed by Helbock et al. (1993) for the testing of peroxidation in neonatal lipid emulsions. Whilst the assay appears to give a sensitive tool for the detection of lipid hydroperoxides, Yamamoto & Ames (1987) noted that the presence of antioxidants within the sample could interfere with the result through interaction and removal of lipid hydroperoxides prior to HPLC separation. Whilst the assay appears effective, with regards to the testing of PN lipids, it again detects the primary lipid peroxidation products, which can rapidly degrade to further products as discussed above making the rate of the assay a limiting factor.

HPLC with UV detection has been used as a direct testing method for the identification and quantification of HNE and MDA. The assay for both MDA and HNE uses standard conditions for reversed phase HPLC (RP-HPLC) and provides effective separation using a C-18 column (Esterbauer and Zollern 1989; Emerit et al. 1991; Karatas et al. 2002). Neither method requires a lipid extraction method to be employed, reducing lab testing time and increasing reproducibility. Neither testing method has been employed within the lipid PN testing of peroxidation. The direct analysis of MDA through RP-HPLC would require a sample clean up step with regards to the removal of amino acids from the sample, as MDA interacts with free amino acids, which would be problematic with regards to PN solutions. The rationale for the decision to focus on the identification and quantification of HNE or MDA is discussed below in the form of a review of their known toxicities within the body.

1.6 Review of the biological actions of 4-hydroxynonenal and Malondialdehyde

HNE and MDA are two of the most studied products of peroxidation with regards to their respective actions within the body. Both are known to be toxic and have been linked to a variety of different pathophysiological disease processes.

Esterbauer (1993) provided an extensive review paper on the cytotoxicity's of lipid peroxidation products, mainly focusing on HNE and MDA research work. Looking at HNE, the paper reviews research that suggests HNE is highly toxic to cells. It establishes concentrations of HNE required to produce different effects, outlined in table 1.5.

Table 1.5 Effects of HNE on mammalian cells - adapted from Esterbauer 1993.

HNE concentration	Effects
>100 µM	Cell lyses occurs
1-50 µM	Inhibition of protein and DNA synthesis and cell proliferation.
<1 µM	Genotoxic to lymphocytes, disturbances in gap junction signalling, phospholipase C stimulation.

The review also looks at the work performed on lipid hydroperoxide toxicities, and MDA toxicity, establishing that MDA is generally considered to be less toxic than HNE. MDA levels have however been quantified to be significantly increased in incidences of atherosclerosis, cardiovascular disease (CVD) and myocardial infarctions (MI).

The role of HNE in the mechanisms of cancer has been extensively studied and is reviewed by Zhong & Yin (2015). The interactions between HNE with DNA, mitochondria and proteins are discussed within this paper. This suggests several complex mechanisms by which HNE may be involved in the proliferation and spread of cancer cells through the body. Csala et al. (2015) and Hauck & Bernlohr (2016) further reviewed the cytotoxic nature of HNE within the body, including its involvement in cell signalling, proliferation, apoptosis. HNE's effects on the pathogenesis of several diseases including Huntington's disease, other neurodegenerative conditions, cancer and cardiovascular diseases are also considered. Schaur et al. (2015) is a large body of work on the production, metabolism and actions of endogenous HNE in the body. Conclusions from the work include the important finding that the concentration of HNE is a key factor in the modulation of its effect on the body. When present in lower concentrations, the bodies' detoxification systems can deal with HNE. At higher concentrations HNE often forms adducts with proteins and enzymes, thereby altering signalling

pathways, receptor sites and cellular processes, leading to alterations in cell growth, development and death. This establishes again the relationship between HNE and many pathophysiological disease states.

Adams et al. (1999) paper looked at the effects of MDA and HNE on plant cell proliferation and development, concluding, in support of Esterbauer (1993) that MDA is less toxic than HNE, in this case towards embryonic plant cells.

Basu et al. (1999a) specifically commented upon the levels of MDA present within neonatal PN and the resulting effects within the body. The results showed that PN administration to both stable and acutely unwell critical neonatal patients resulted in an increase in free radicals within the body measured by the presence of MDA.

The cytotoxicity of linoleate hydroperoxide (a pre-cursor to HNE) within rats was summarized by Cutler & Schneider (1974) whose work found that said hydroperoxides increased numbers of mammary and pituitary tumours thereby concluding that hydroperoxides were both cytotoxic and mutagenic.

1.7 Conclusions and review of research aims and objectives

The above review encompasses the biological effects of both HNE and MDA. Whilst both have been studied extensively, emphasis has been placed upon HNE rather than MDA. This is due to the toxicity of HNE being far greater than MDA at concentrations that are likely to be found within cells of the body. With regards to lipid peroxidation in IVLE's the only papers found bore relevance to the quantification of MDA through the use of the TBARs assay and HPLC as discussed above.

When considering the objectives of this work, the goal is to identify the level of lipid peroxidation occurring within lipid PN formulations. The merits and limitations of the current available assays are discussed above and conclude that there currently isn't an appropriate assay available to accurately and reproducibly measure the peroxidation occurring in such formulations. Likewise, when considering the products of peroxidation, the multiple different compounds formed means that it would be impossible to develop an assay to quantify all these products. Therefore, it was decided to look specifically for the presence of HNE within PN solutions. It has been hypothesised that HNE is one of the most toxic breakdown products of peroxidation and as such will serve as a marker for the level of peroxidation occurring within lipid emulsions.

As HNE levels can only be viewed as a marker for lipid peroxidation occurring within lipids, it was decided that a complementary assay should also be developed to look at the amount of lipids that are lost in the process of peroxidation within PN solutions. Developing an assay that would quantify the amount of triglycerides (TAGs) that are initially within a PN solution and then comparing this to PN subjected to differing storage conditions will show the amount of TAGs that have been lost through their breakdown. This will also act as a comparison, aiming to equate the amount of lipids lost with the level of HNE produced through peroxidation.

The availability of HPLC instruments within the research laboratory, along with the merits of direct analysis of HNE as discussed above will focus this research on the development of an assay that will directly quantify the level of HNE within lipid PN solutions through the use of reverse phase HPLC with UV detection.

Concurrently with the above assay and through the use of HPLC coupled with a charged aerosol detector (CAD) (see chapter 2 for details) an assay will be developed to accurately quantify the amount of TAGs present within each lipid emulsion. This CAD allows the direct quantification of lipids without the need for derivatisation.

Once assay development has been achieved, IVLE's will be tested in a variety of differing conditions. This aims to establish the chemical stability of new and established IVLE's with regards to the levels of lipid peroxidation occurring and the level of toxic HNE produced *in vitro* before administration to the patient.

1.8 Research aims and objectives

1.8.1 Research aim

Explore how different storage conditions and containers affect the level of lipid peroxidation occurring within both gold standard and new generation intravenous lipid emulsions (IVLEs).

1.8.2 Research objectives

- Development and validation of an accurate and repeatable assay to quantify peroxidation levels to ensure stability of PN products and to provide a quality assurance testing method for peroxidation values in PN.

- To quantify the level of lipid peroxidation occurring within IVLEs during *in vitro* storage before administration to the patient: Whilst the process of peroxidation itself has been extensively studied, little is known with regards to its detrimental effects on lipid emulsions found in parenteral nutrition (PN) particularly when considering the stability of PN emulsions *in vitro*.

- To quantify levels of chemical stability of new IVLEs: Intravenous lipid emulsions form a staple part of parenteral nutrition (PN). The limited stability testing that has been carried out with the newer emulsions indicates that the fatty acid compositions of the oils will afford differing levels of stability to PN.

- Stability testing of small volume PN in infusion bags: Specifically, with regards to neonatal PN, current clinical practise is to use a syringe as a storage device for the lipid proportion. Local PN providers are considering a move from a syringe to storage in an infusion bag and therefore stability testing of small volume lipid PN in infusion bags is required to establish safe shelf lives.

Chapter 2

Method Development

2.1 HPLC principles

HPLC separates compounds within a sample by passing them through a chromatographic column at high pressure. Normal phase HPLC uses a polar stationary phase column and a non-polar mobile phase whilst reverse phase HPLC uses a non-polar stationary phase and a polar mobile phase. Depending on an individual compound's chemical characteristics it will partition between the mobile phase and the stationary phase of the column at a different rate, thereby separating multiple compounds within the sample (Hamilton and Hamilton 1992). When considering lipid chromatography, the selection of chromatography conditions is dependent on a) the composition of the lipid being analysed and b) the type of separations that are required. Different column choices can be employed depending on whether lipids need to be separated simply by class (phospholipids, mono, di and triglycerides etc.), if inter-class separation is required i.e. TAGs based on their partition number, or if further separations are required for example distinguishing between triglycerides with the same fatty acid chains but at different sn1, 2 and 3 positions. Typically when distinguishing between classes of lipids using HPLC, normal phase HPLC is employed, using a stationary phase such as silica or cyanopropyl and organic mobile phases (Lin and McKeon 2005), mimicking the TLC (thin layer chromatography) conditions from which lipid analysis via HPLC has developed.

Reverse phase HPLC (RP-HPLC) employs a stationary phase formed of carbon of a specific chain length bonded to an inert basement substrate, commonly silica and has developed to become the staple mode of HPLC for inter-class lipid analysis. RP-HPLC is typically more robust than normal phase due to the stability of the stationary phases, resulting in satisfactory repeatable assay development (Synder et al. 1997). RP-HPLC mobile phases commonly employ an organic phase and an aqueous phase, providing a balance that when developed correctly, will elute molecules from the hydrophobic stationary phase by producing an environment for small molecules, often with mixed hydrophobic and hydrophilic properties to partition into, thus creating separations. The issue however, when considering lipid analysis by RP-HPLC is the presence of water within the mobile phase. Lipids are highly hydrophobic molecules and therefore when presented with a mobile phase with a degree of aqueous phase within it, will simply partition onto the carbon hydrophobic stationary phase and thus will not be eluted from the column, leading to

undetectable signals, column blockages and high pressures. To circumvent this issue, all organic mobile phases can be employed, eliminating water and therefore creating a hydrophobic mobile phase, allowing partition from the stationary phase to the mobile phase to occur which, when optimised effectively, will achieve desired separations (Sewell 1992; Lin et al. 1997).

2.2   Non-aqueous Reversed Phase (NARP) HPLC

2.2.1   NARP introduction

Using non-aqueous mobile phases with a carbon stationary phase allows the effective separation and elution of hydrophobic molecules. Effective separations under such circumstances are dependent on multiple factors, the most influential being stationary phase chain length and choice of organic mobile phases.

The principles of NARP HPLC have been employed successfully for the separation and quantification of lipids, including TAGs which form the staple component of all lipid emulsions used for parenteral nutrition. NARP has been used to separate TAGs within oils by multiple researchers (Swe et al. 1996; Lísa et al. 2007; Hmida et al. 2015). Byrdwell et al. (1996) successfully separated TAGs present within soybean oil, the primary oil found within the PN lipid formulation Intralipid[®] and within newer lipid emulsion formulations (SMOFlipid[®] etc.). Lisa et al. (2007) successfully separated 19 triglycerides using an C18 stationary phase with a mobile phase gradient comprised of Acetonitrile (ACN), Isopropanol (IPA) and hexane, with a charged aerosol detector.

2.2.2   Mobile phases

Choice of organic solvents employed within NARP varies depending on the formulation being assessed. NARP requires the use of a weak solvent, commonly acetonitrile (Hmida et al. 2015) and a strong solvent. With regards to NARP where a carbon non-polar stationary phase is employed, the difference in strength of organic solvents used is the governing factor on elution of compounds. Said strength of solvent is inversely proportional to the polarity index of the organic solvent. The lower the polarity index of the organic solvent, the stronger it's eluting strength due to its ability to interact with the non-polar components of lipid molecules, counteracting the lipids attraction to the non-polar stationary phase. Conversely,

when considering the phospholipids present within an emulsion their more polar nature results in them being eluted slower by lower polarity or strong solvents and faster by more polar weaker solvents. Therefore, the choice of organic solvents used is crucial to the separation of a lipid emulsion. Solvent choice however is limited depending on the type of detector employed. When considering UV detection, certain solvents cannot be employed at low wavelength detection as they will be detected and produce an unstable baseline (Synder et al. 1997). With regards to charged aerosol detection (CAD), the choice of organic solvents is unlimited as CAD detection will be unaffected due to the volatility of the solvents.

Hmida et al. (2015) established a solvent strength scale for organic solvents in NARP HPLC conditions when looking at the separation of nine different seed oils at varying temperatures. The work showed that all combinations of iso-eluotropic organic mobile phases used could be employed for the separation of TAGs from oils. A combination of Acetonitrile (ACN) /Isopropanol (IPA) sits in the middle of the scale produced within this work (represented in table 2.1), making it a good starting point for assay development with respect to separations of TAGs within lipid emulsions. Both IPA and ACN are applicable to UV analysis across the majority of wavelengths.

Table 2.1 – Data summarised from Hmida et al. (2015) *showing effectiveness of strong solvents with Acetonitrile in detection of triglyceride peaks within oils.*

	BuOH 26% | ACN	AcMe 50 % | ACN	AcOEt 34 % | ACN	IPA 34 % | ACN
Oil	**Number of peaks identified**			
Tamanu	20	16	17	18
Soya	19	14	16	18
Pistachio	16	13	15	16
Olive	17	14	16	16
Black currant stone	24	23	23	24
Tung	24	11	23	23
Pine nut	15	14	15	14
Pomegranate	21	15	20	17
Babassu	17	15	16	16
Rank	**1st**	**4th**	**3rd**	**2nd**

2.2.3   Column choice

The standard choice of stationary phase for RP-HPLC is a carbon column (C18) with an 18-carbon chain length. Carbon stationary phase columns are formulated with C18 organosilanes covalently bonded onto an inert silica base. The structure

created and the three-dimensional positioning of the C18 chains and therefore their availability to interact with sample components is governed by the basement particle size and shape. Optimum column efficiency is achieved by maximising the C18 to basement silica particle ratio. Over packing of basement particles will cause steric hinderances to interacting molecules and the potential for unreacted silica to interact with sample molecules, whilst over bonding of C18 chains will alter pore size of the column, limiting the proportion of each C18 chain available for interaction (Synder et al. 1997; Scientific 2011). Certain columns undergo a process known as end-capping where any silica support molecule that is not bonded to C18 chains is reacted with a small silane such as di or trimethylchlorosilane to produce an inert base, preventing solute molecules from interacting with the silica base and altering the column properties (Synder et al. 1997; Scientific 2003). Carbon chain length of the stationary phase will change the retention time of sample molecules. Sample retention in reverse phase increases with increasing carbon chain length of the stationary phase. C18 chains fall within the middle of the chain lengths available as stationary phases, making such a length a good starting point for method development. C18 columns have also been used in multiple methods for the effective separation of lipids and fatty acids (Lísa et al. 2007; Makahleh et al. 2010; Gonyon et al. 2013).

When considering lipid chromatography in NARP mode, the carbon chain length of the sample TAGs will have a governing factor on the separations achieved. Chain length establishes the 'strength' of the hydrophobic environment achieved by the column, thereby directly affecting the retention or k of compounds. TAGs are broadly structured as seen in figure 2.1, where each R group corresponds to a specific fatty acid of varying chain length and level of saturation.
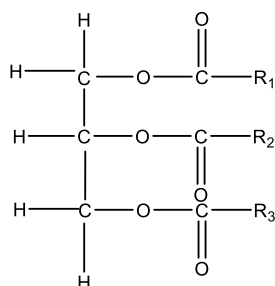
Figure 2.1 General chemical structure of triglycerides. R_1, R_2 and R_3 represent fatty acid chains conferring varying levels of saturation.

The chain length of each R group will initially govern the interaction between the C18 chains of the stationary phase and the R group fatty acid. The greater the chain length of each R group, the greater the level of interaction with the C18 chains, increasing the retention time of the TAG on the column. Therefore, higher chain length TAGs will elute later than TAGs with lower chain lengths. There is however exceptions to this guide as the level of unsaturation present in each R group and mobile phase choice will alter retention times of TAGs of similar components. Broadly speaking the partition number or elution order of each TAG can be estimated using the formula shown in figure 2.3 i.e., can be used to estimate TAG elution order of triglycerides with the same lengths of fatty acid chains but differing levels of saturation. The greater the level of unsaturation, the lower the partition number expected. As assay development will initially be employed to look at the triglycerides present within Intralipid® 20%, this is important when considering the elution order of TAGs as Intralipid® has high levels of fatty acids with multiple levels of unsaturation within their chains.

$$PN = CN - 2DB$$

Figure 2.2 - Elution order equation, PN = partition number, CN = carbon number, DB = number of double bonds.

Due to the levels of fatty acids within Intralipid® 20% as seen in table 2.2 the triglycerides formed will potentially vary by a single level of unsaturation and as such the assay developed will need to distinguish between such TAGs. Therefore, column choice as explained above is of vital importance in providing sufficient carbon chain length and density to facilitate such separations.

Table 2.2 – Fatty acid composition of Intralipid® 20%.

Fatty acid component	Average % in Intralipid® 20%	Amount in 50mg of Intralipid® (mg)
linoleic acid (18:2)	51	5.1
oleic acid (18:1)	24.5	2.45
palmitic acid (16:0)	10.5	1.05
α-linolenic acid (18:3)	7.5	0.75
stearic acid (18:0)	3.45	0.345

2.3   HPLC detector choice

The required assay needs to facilitate the rapid detection of TAGs within lipid emulsions and the presence of the secondary aldehydic peroxidation product 4-Hydroxynonenal. Due to the chemical structures and properties of each of these molecules, simultaneous detection of both proves to be a challenge.

Triglycerides are relatively bulky large molecules, with relatively high boiling points, but lacking the desired chromophores that would enable them to be detected effectively through UV detection. Existing methods for TAG detection using HPLC often require extensive sample preparation, extraction and/or argentation to produce molecules that can be detected through UV detection. The assay being developed is designed for use as a relatively simple assay to monitor the stability of lipid emulsions over storage before delivery to the patient and therefore expensive and extensive sample preparation is unsuitable. This makes UV detection of TAGs unsuitable for the assay and as such a different mode of detection is required. Charged aerosol detection (discussed further in section 2.5) provides a means to detect TAGs and larger non-volatile molecules without a chromophore without the need for complex sample preparation or any form of derivatisation (Moreau 2009; Gamache 2018). The CAD can be utilised in-line with a UV detector to facilitate the detection of TAGs and simultaneous detection of 4-Hydroxynonenal (HNE).

 HNE is a relatively short chain (C9) secondary aldehyde that is too volatile in nature to be detected by the CAD. HNE however, can be successfully detected as free HNE without derivatisation using UV detection (Emerit et al. 1991; Esterbauer et al. 1991). Whilst this detection method is somewhat dated, the detection of free HNE has been utilised less since the period where initial HNE discovery was undertaken due to the move to quantify HNE within complex biological systems. The study of HNE presence within cellular components requires complex extractions of HNE to occur and result in HNE that is often complexed with other cellular components such as proteins. As such derivatisation techniques for the detection of HNE has become the recent focus on HNE detection (Ligor et al. 2015; Sousa et al. 2017). Within this assay development the focus is on the detection of HNE within a relatively simple matrix with regards to its number of components and the lack of potential molecules for free HNE to complex too. Therefore, the direct detection of free HNE by UV detection is appropriate for assay development.

2.4 Initial method development split – CAD and UV

CAD and UV detection are inherently very different detection techniques and as such initial assay development for each needs to be approached individually. The aim of the CAD detection section of the assay is to develop a repeatable assay to monitor the potential loss of TAGs within each lipid emulsion. The UV detector will aim to detect HNE occurring through the peroxidation and breakdown of the lipids within each emulsion. As such, initial assay development for TAGs will use the desired lipid emulsion whereas for initial HNE method development an HNE standard will be used as the levels of HNE produced from the lipid emulsions tested is, as yet, unknown. Whilst optimally the assay conditions developed to achieve this need to be the same for each section of the assay (i.e. for TAGs and HNE) and the detectors will be placed in-line with each other, initially assay development will be split into different sections. Once initial development is completed and conditions for the detection of HNE within the tested lipid emulsion has been achieved then the assay conditions and detectors will be combined. This will further develop a set of final assay conditions with in line UV and CAD detection.

2.5 HPLC-CAD method development

2.5.1 CAD principles

The CAD works on the principle of transferring positive charge, from a positively charged nitrogen gas source, to compounds in the eluent from the HPLC column. The larger the mass of the compound, the more charge the compound can hold and therefore the larger the detection peak seen. The schematic below in figure 2.3 taken from Plante et al. (2013) explains the principles of the detector:

1. Liquid eluent enters from HPLC system
2. Pneumatic nebulization occurs
3. Small droplets enter drying tube
4. Large droplets exit to drain
5. Dried particles enter mixing chamber
6. Gas stream passes over corona needle
7. Charged gas collides with particles and charge is transferred
8. High mobility species are removed
9. Charge is measured by a highly sensitive electrometer
10. Signal transferred to chromatographic software

Figure 2.3 CAD process of detection

2.5.1.2 Nebulisation

The pneumatic nebulisation process involves the process of nebulising the eluent from the column and drying it to leave an aerosolised residue which then gains a positive charge. This process somewhat governs the choices of mobile phases acceptable by the CAD. Organic phases are volatile in nature so will be 'dried off' with the evaporation process making them compatible with the CAD and achieving good constant baselines and minimal noise. Mobile phases should however be as pure as possible as non-organic contaminants will be dried and passed onto the detection process, disrupting the baseline. Therefore LC-MS grade solvents were used throughout (Plante et al. 2011; Gamache 2018). The use of non-organic buffers typically used in reversed phase chromatography is not ideal in CAD detection as, like non-volatile impurities, these will reach the detector of the CAD and as such can disrupt CAD response and baseline noise. This limits the mobile phase choice for method development.

2.5.1.3 Aerosol charging

Analyte particles in the CAD are charged via a unipolar diffusion charging technique (Gamache 2018). This is where the aerosolised compounds are exposed to ions of a single charge; in the CAD's case positively charge ions are used. The nitrogen entering the CAD passes over a corona needle which transfers a positive charge to the nitrogen ions. The positive charging of the nitrogen source briefly works by producing a nonuniform electrostatic field across the tip of a corona needle and an orifice plate. Electrons produced are of high enough velocity that when they collide with the nitrogen, they knock off electrons from the nitrogen, creating positively charged ions. These positive nitrogen ions then collide with the dried analyte compounds and on the basis of Brownian motion and positive charge is transferred to the analyte. The size of the analyte present is directly proportional to the amount of charge that is transferred from the positively charged nitrogen source.

2.5.1.4 CAD response curves

The CAD is a non-linear detector and as such calibration curves and validation of methods should take this into consideration. Typically, with a linear detector calibration curves are plotted of response vs. concentration and linear regression lines plotted to define the R^2 value of the desired peak. With the CAD however, due to the non-linear response over a range of concentrations typically plotted to form a calibration curve, the regression line plotted needs to be adjusted to allow for this non-linear response. Typically a second-order polynomial (quadratic) function is applied to the regression curves to obtain an accurate fit and therefore this fit will be used during the assay validation process (Crafts et al. 2011; Ilko et al. 2014; Gamache 2018).

2.5.1.5 Gradient vs. isocratic elution in CAD detection

Gradient elution is commonly used within reversed phase chromatography to enhance separations achieved between molecules. There are however issues that gradient elution raises with CAD detection. Changing a mobile phase composition entering the CAD will result in a change in baseline observed on the chromatogram. Organic phases are evaporated by the CAD as explained above; however, changing the proportion of organic phase will have an effect on its evaporation from the

CAD's drying tube and alter the drying speeds of the analyte molecules, resulting in baseline drift during gradient elution. Ideally isocratic mobile phase programs should therefore be used for CAD methods. If a gradient is necessary, a secondary HPLC pump can be employed to provide a reverse gradient to the CAD at the point of entry to the detector. This permits a gradient elution to be run through the chromatographic column, but an isocratic phase adjustment to be made at the point of entry to the CAD, achieving a stable non-drifting baseline (Lísa et al. 2007).

2.5.2   Non-volatiles and semi-volatiles

Due to the nebulization process, the detector is only able to analyse non-volatile or semi-volatile substances. Volatile substances along with organic mobile phases will be evaporated during the nebulization process and removed via the waste exhaust. Typically, the CAD can analyse any non-volatile substance with a boiling point >400°C and any semi-volatile (300-400°C), although with semi-volatile compounds detector response and sensitivity can be reduced (Gamache 2018). This therefore renders the CAD inadequate to detect HNE due to the volatile nature of the short chain aldehyde and thus the requirement for UV-CAD inline detection.

2.5.3   Method development and optimisation

2.5.3.2   Initial Method

Upon consultation of the literature with regards to emulsion separation and quantification through NARP, a manuscript of particular interest has been written by Gonyon et al. (Gonyon et al. 2013). This research effectively used NARP HPLC with a mobile phase of ACN/IPA and a C18 column to look at the effect of container materials on a PN mixture. Whilst the data is centred on looking for extractable and leachables from EVA versus glass containers, the lipid residues post emptying of the containers were analysed successfully through NARP HPLC coupled with a charged aerosol detector (CAD). The lipid emulsion used in this particular PN formulation was ClinOleic® 20 %, an emulsion of soybean and olive oils. This thesis will focus on Intralipid®, the most established and most commonly used lipid emulsion within the United Kingdom for PN formulations. Gonyon et al.'s research provides an initial set of chromatographic conditions from which method development can commence. The aim is to achieve chromatographic separation of the TAGs and phospholipids present within Intralipid® 20%. Upon achieving

adequate separations, the method will be used to quantify the amount of selected TAGs present at time point zero versus the amount of TAGs after storage for a period of time under specified conditions.

Gonyon et al. (2013)'s method was used as a basis for the detection of TAGs within Intralipid® 20% and was employed in the following way during initial method development:

- C-18 column 150 mm x 3 mm, 5 µm particle size

- Mobile phase: IPA:ACN 60:40

- CAD nebuliser temperature: 50°C

- Column temperature: 25°C

- Auto sampler temperature: 20°C

- Flow rate: 750 µl/min

- Injection Volume 20 µl

- Intralipid® serially diluted in IPA to 1000 µg/ml and 100 µg/ml samples.

All injections were repeated in triplicate to ensure reproducibility. Method development for the CAD assay was carried out on an Ultimate 3000 HPLC system and a Corona Charged Aerosol Detector (Thermo Scientific, West Palm Beach, United States). All reagents were HPLC grade (Fisher Scientific). Intralipid® 20% was obtained from Fresenius Kabi and once opened stored in the fridge at 2-8°C for a maximum of two weeks before replacement.

The chromatograms (figures 2.4 and 2.5) show that concentrations of Intralipid® below 1000 µg/ml are insufficient for lipid detection due to the lack of discernible peaks at 100 µg/ml. The lack of resolution between peaks was identified as an issue and therefore the governing factors over effective resolution were researched.
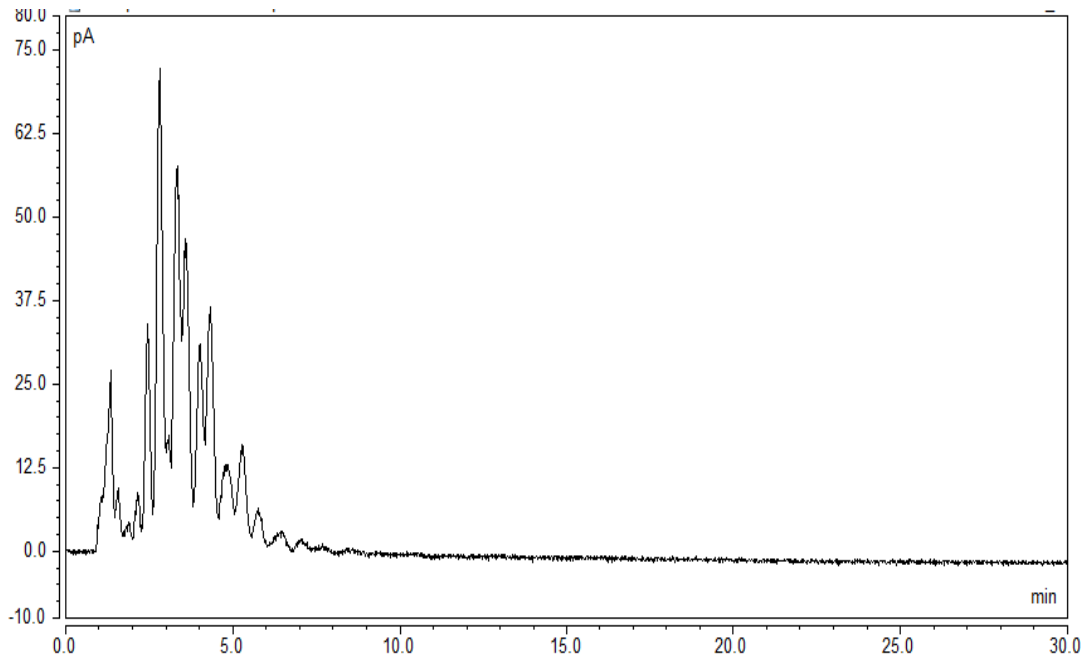
Figure 2.4 NARP-HPLC with CAD detection of Intralipid 1000 µg/ml. C-18 column, mobile phase IPA:ACN 60:40
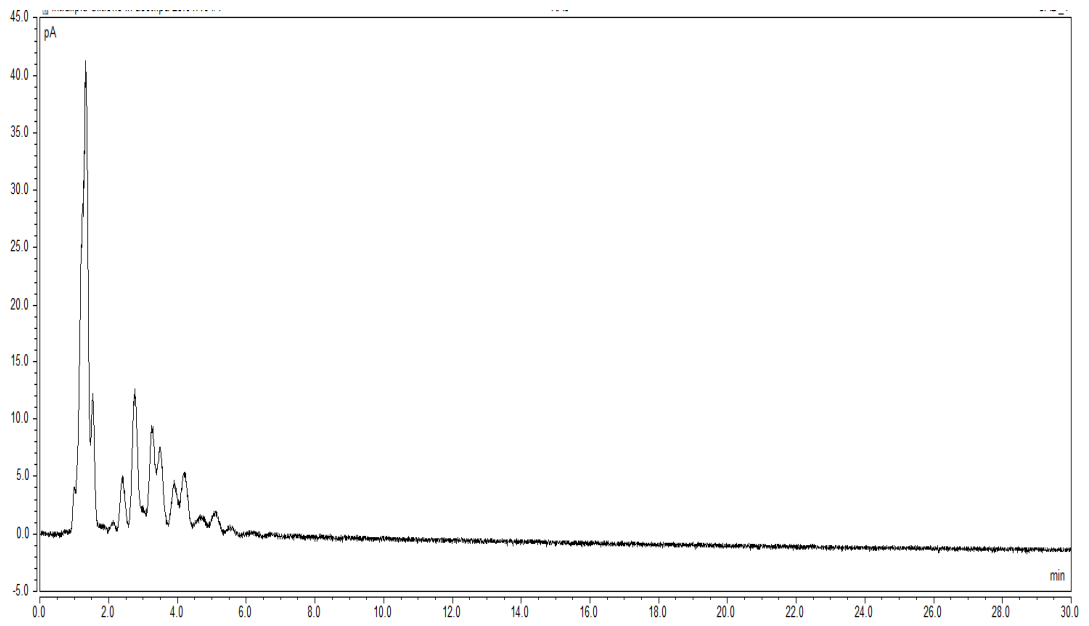
Figure 2.5 NARP-HPLC with Intralipid 100 µg/ml. C-18 column, mobile phase IPA:ACN 60:40.

44

Principally, the longer the column, the more C-18 chains present within the stationary phase, therefore the greater the availability for lipid interaction/bonding to occur, slowing the elution of the components from the column. This relates to the resolution equation shown in figure 2.6, which indicates the governing factors in chromatographic resolution achieved from a particular column.

$$R = \frac{1}{4}\left(\sqrt{N}\right) x \frac{k}{k+1} \, x \, (\alpha - 1)$$

(efficiency)   (retention)   (selectivity)

Figure 2.6 Resolution expressed as a combination of three factors, efficiency, retention and selectivity. N = theoretical plate number, α = separation factor, k = average retention factor for two specified bands. (Synder et al. 1997)

When looking at the resolution achieved from a particular column, the factors within the equation above can be considered individually. k and α are parameters that are primarily determined by the factors that govern the partitioning of a compound from mobile to stationary phases. These controllable factors include column stationary phase composition, mobile phase composition and temperature. Changes in all the above factors can be easily achieved and therefore these factors can be used to achieve method optimisation.

The theoretical plate number of a column and therefore its efficiency is related to the column dimensions and particle size. The larger the plate number (N) the more efficient the column. Plate number is directly proportional to the length of the column (mm) and inversely proportional to the particle size (µm). With regards to chromatography columns, particle size refers to the spherical diameter of the basement supports used to attach the stationary phase and pack the column.

Therefore, generally speaking, the longer the column and the smaller the particle size, the more efficient the column. Selectivity of the stationary phase, as seen in figure 2.6 is the most powerful factor affecting retention. From these theoretical factors, and with reference to the method of Gonyon et. al., (Gonyon et al. 2013) a C-18 250mm x 3mm column with a 3µm particle size was purchased (Acclaim 120, Thermo Scientific) and substituted into the assay instead of the 150 mm /5 µm column with the aim to optimise the selectivity of the stationary phase prior to optimisation of mobile phase, column temperature etc.

Upon running the same chromatographic conditions as above with the new 250 mm C-18 column, the chromatogram seen in figure 2.7 was achieved. Intralipid® concentrations of 1000 µg/ml, 2000 µg/ml and 4000 µg/ml were run in triplicate under the above conditions to establish the optimum concentration of Intralipid with which to continue assay development. The concentration of 1000µg/ml gave a detection level with clear peaks and was chosen as appropriate for further use within assay development.
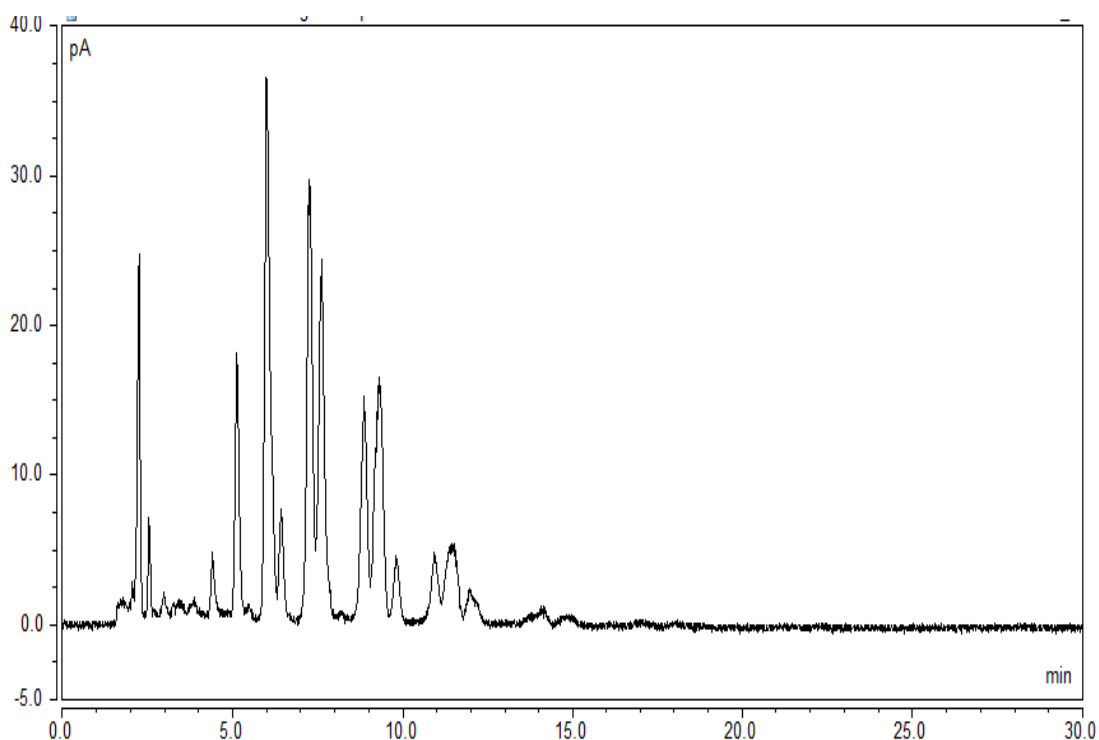
Figure 2.7 Initial assay conditions run on C-18 250 mm x 3 mm column. Intralipid® 20 % at 1000 µg/ml.

2.5.3.4 Column temperature optimisation

Once the C-18 250 mm x 3 mm column was established as the column to be used for initial method development and with regards to the resolution equation (figure 2.6), controllable factors including mobile phase composition and column temperature can be varied to optimise separations. As the mobile phase composition of 60 % IPA / 40 % ACN had been used effectively for the separation of Clinoleic® (Gonyon et al. 2013), it should be able to be used to create adequate separations of Intralipid®. Therefore, at this stage mobile phase composition was held at 60:40 IPA:ACN.

Column temperature control is critical to controlling resolution between eluting compounds within HPLC. Altering column temperature is a simple tool in regulating separations from a column and therefore the next focus of assay development. Until relatively recently column temperature optimisation was not an area used for assay optimisation due to the lack of availability of column thermostats. With regards to resolution theory, increasing temperature by 1°C can decrease k by between 1 and 2 %, thereby reducing resolution between peaks (Synder et al. 1997). Using the chromatographic conditions stated below, the temperature of the column was varied

47

in a systematic fashion as displayed in table 2.3. Initially temperature was increased from the 25°C to a maximum of 45°C to prove the above theory was relevant for these chromatographic conditions. After this column temperature was reduced to enhance resolutions. Each was run in triplicate and the results of the separations noted.

- C-18 column 250 mm x 3 mm, 3 µm particle size
- Mobile phase: IPA: ACN 60:40
- CAD nebuliser temperature: 50°C
- Auto sampler temperature: 20°C
- Flow rate: 750 µl/min

- Injection Volume 10 µl
- Intralipid 1000 µg/ml in IPA

Table 2.3 Temperature variations employed in assay development

Assay Number	Column temperature (°C)	Chromatogram observations
1	25	Initial assay
2	35	Worse than 25°C – split peaks
3	45	Completely unresolved chromatogram
4	20	Longer retention times but better peak resolution than 25°C.
5	15	Longer retention times but better peak resolution than 20°C.
6	10	Longer retention times but better peak resolution than 15°C

As shown in figure 2.8 peak resolution is improved with reducing temperatures. As temperature increases, k (average retention factor) is decreased, thereby reducing retention times. As the initial chromatogram obtained under 25°C conditions did not obtain adequate resolutions, the temperature was lowered through 20°C to 10°C to improve it. A temperature change of 20°C showed the most significant change from the chromatogram separation at 25°C and therefore 20°C was used for continuing assay development.
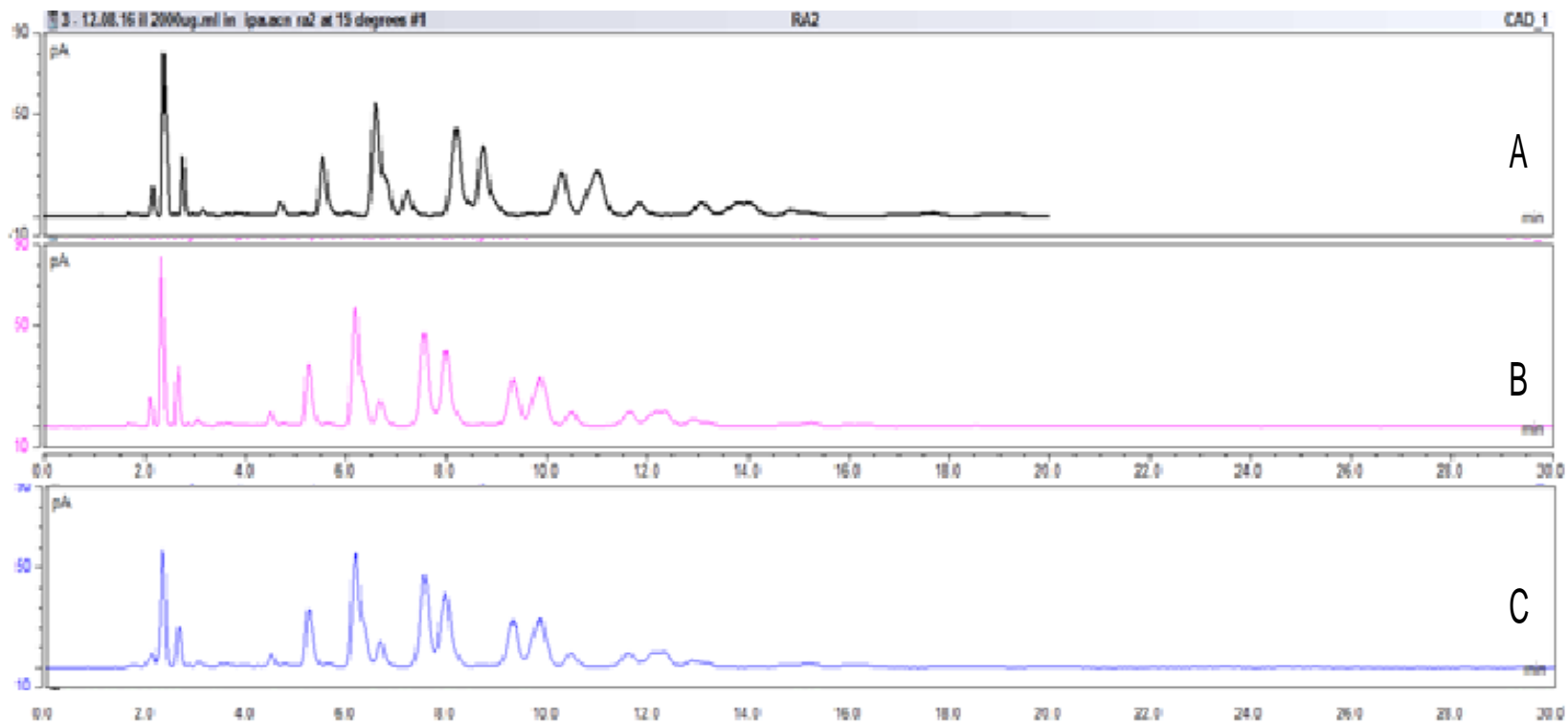
Figure 2.8 Comparison of effects of temperature on HPLC analysis of Intralipid. 6a = 15°C, 6b = 20°C, 6c = 25°C

Whist the composition of Intralipid® is referenced as individual fatty acids (Eriksson 2001) as shown in table 2.2, these will be formulated as TAGs within lipid globules surrounded by phospholipids ensuring a disperse oil within a continuous aqueous phase. Therefore, when looking at the separations and identifications of compounds through the HPLC assay peaks detected will be TAGs containing different combinations of fatty acids and the two phospholipids used within Intralipid® as emulsifiers.

Both phospholipids and the TAGs present have similar general structures (figure 2.9), the main difference being the replacement of one of the three fatty acid chains with either the choline or ethanolamine ester of phosphoric acid in the case of the phospholipids (Eriksson 2001).
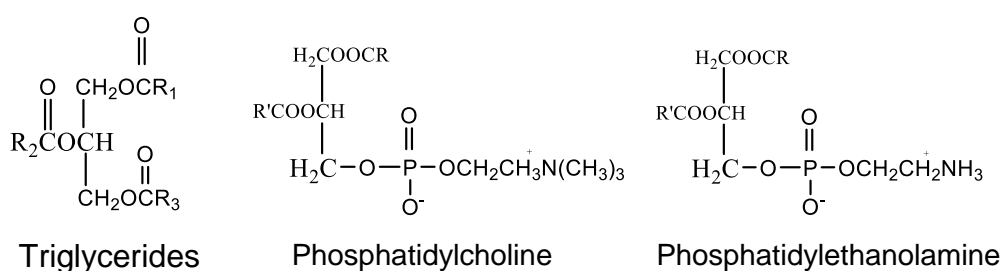
Figure 2.9 General structures of triglycerides and phospholipids present within Intralipid® 20%. R groups denote position of fatty acid chains (Eriksson 2001)

Due to the nature of the mobile phase currently being used (IPA:ACN 60:40), the strength of the IPA will pull TAGs from the column before phospholipids. IPA is a strong organic solvent in respect to NARP because it has a low polarity index. Therefore, TAGs that are hydrophobic will be eluted before hydrophilic phospholipids.

To confirm that IPA was the driving force behind elution from the column, a gradient elution was performed over 60 minutes from 80% IPA to 40% IPA. The increased runtime was due to the need to reduce the flow rate from 0.75 ml/min to 0.6 ml/min due to the increased percentage of IPA present. IPA has a much higher viscosity (2.04 mPA s) than ACN (0.369 mPA s) (Chromacademy 1999) and therefore will create an increased pressure within the column. The reduction in flow rate allows for this pressure to be maintained at an acceptable level.

As predicted, the increase in IPA % through the run resulted in all components eluting off the column within the first 10 minutes, resulting in a poor chromatogram with no resolution between peaks. At this point with the IPA % being established as a critical factor in elution and better resolutions and separation being required, the gradient was reversed to reduce the initial IPA %. Whilst this required an extended run time due to the slower elution of compounds, slowing the elution of compounds from the column with a slow gradient change increasing the IPA % over time was designed to improve separations. The gradient in table 2.4 shows the mobile phase changes through the assay. Flow rate was maintained at 0.6 ml/min and the run time was set at 60 minutes to allow for complete elution of all compounds. The last 10 minutes of the run was a reverse gradient to allow for re-equilibration of the column back to the initial conditions for subsequent runs.

Table 2.4 Gradient composition

Time (minutes	IPA %	ACN %
0	20	80
40	60	40
50	60	40
55	20	80

Initially at 20°C, the gradient was repeated with lowering temperatures as previously investigated for the isocratic runs to try and improve separations. The optimum run that was achieved from this was using the gradient as set out in table 2.4 at a column temperature of 5°C with the auto sampler temperature being introduced as a further temperature control, set at 8°C to hold the samples at a low temperature. The reduction in temperature, whilst increasing the pressure due to the increasing viscosity of the mobile phases at lower temperature, was not sufficient to warrant a further flow rate reduction at this stage and therefore the flow rate was maintained at 0.6 ml/min. The run time was extended to 70 minutes to ensure column cleaning and re-equilibration between runs. The resulting chromatogram is shown in figure 2.10.
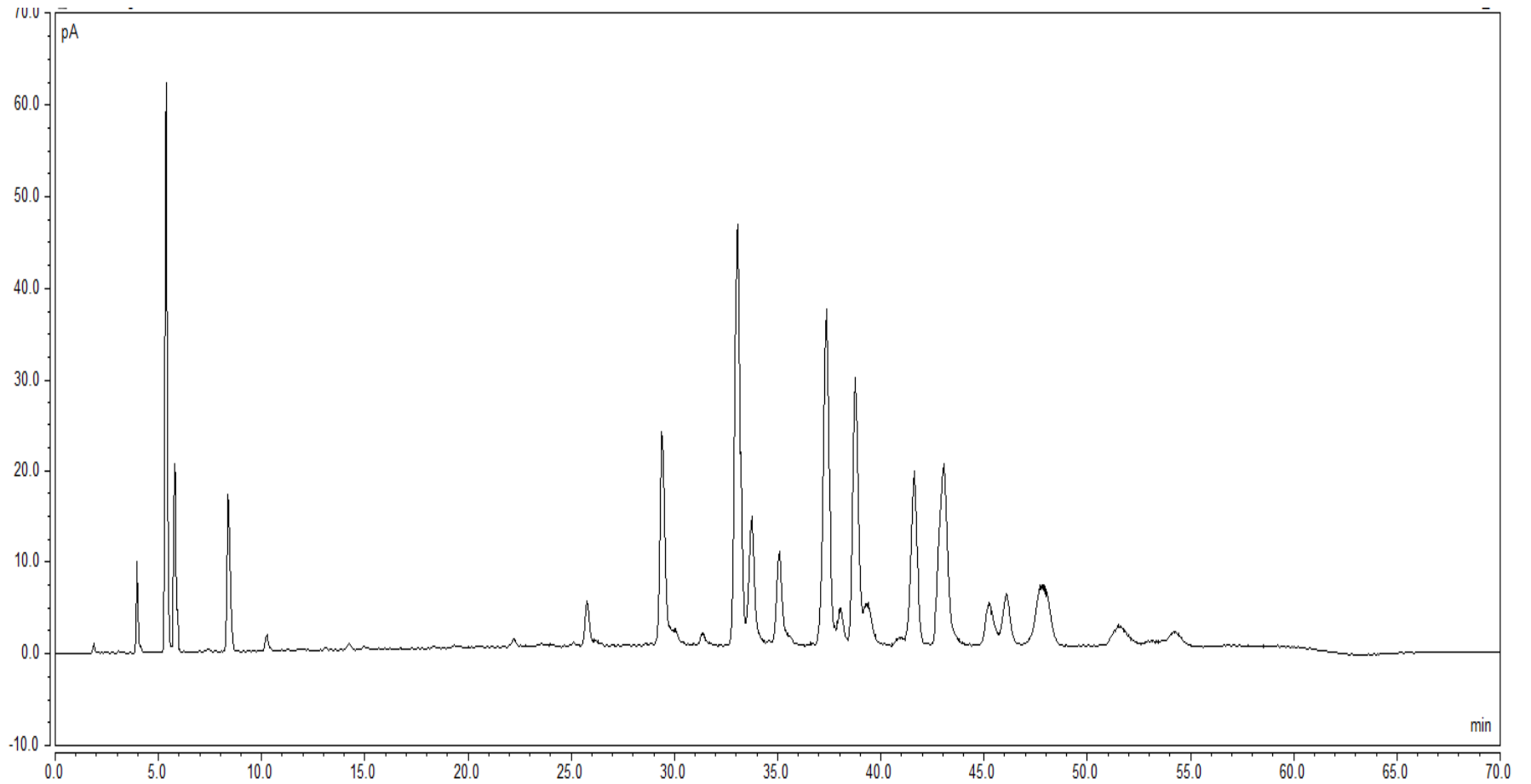
Figure 2.10 HPLC of Intralipid® 20% using gradient elution detailed in table 2.4 of IPA: ACN.

From the chromatogram in figure 2.10, the first four main peaks eluting from the column were of interest as their retention times were significantly different from the other components. To identify if these peaks were due to contamination of the sample, the assay was re-run with samples of blank mobile phase and IPA and ACN individually. All samples gave the same initial peak pattern (figure 2.10), proving that the four peaks observed from 0 – 10 minutes were due to some form of contaminates.

At this point all solvents were replaced, the column was cleaned using a column cleaning protocol and the CAD was cleaned by running low flow rate methanol: water over 12 hours. Due to the highly sensitive nature of the CAD and its ability to detect small levels of contamination, the HPLC vials and septa being used were also changed from amber vials with separate screw caps and rubber septa to clear vials with pre-fabricated caps (PTFE) (Thermo Scientific). Rubber septa are well known to be potential sources of contamination of chromatography samples (Pereira et al. 2000). To further reduce the possibility of contamination from mobile phases and to ensure low baseline noise LCMS grade solvents IPA and ACN (Fisher Chemical) were purchased and used for subsequent assay development. Post aforementioned cleaning, samples of blank mobile phase were run through the assay conditions as above to confirm the removal of contamination. Baseline was achieved for all blank runs. From this new Intralipid® 20% was prepared in IPA (1000µg/ml) and the assay was run using the gradient run conditions as per table 2.4 Column temperature was maintained at 5°C and auto sampler temperature at 8°C.
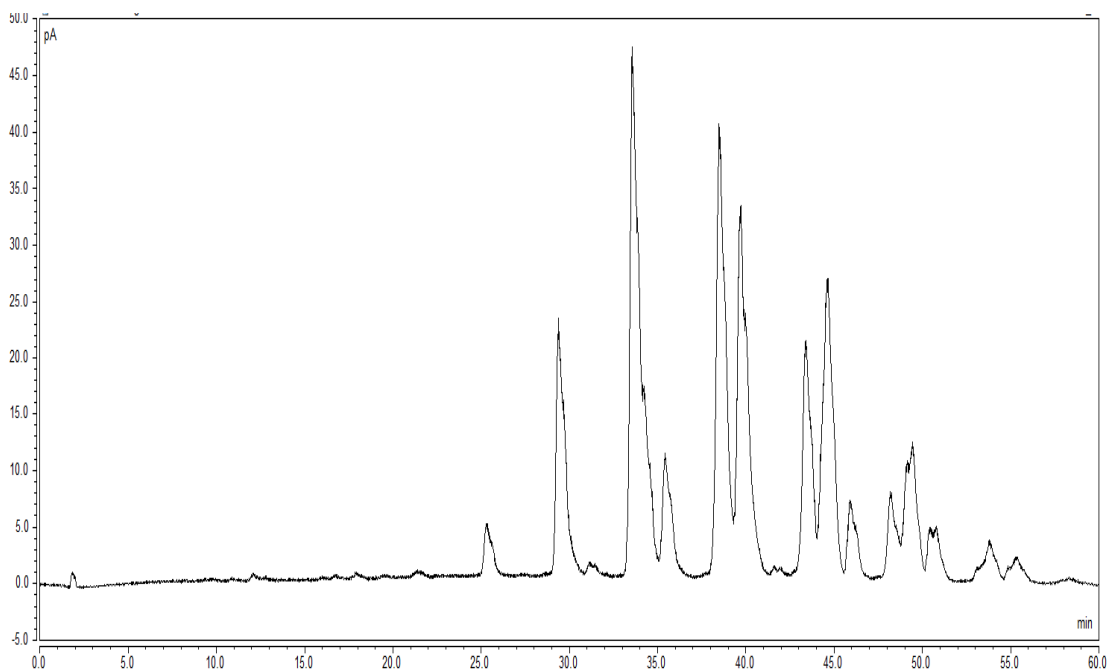
Figure 2.11 HPLC analysis of Intralipid® 20% using gradient elution post column clean and using LCMS grade solvents, column temperature 5⁰C, flow rate 0.6ml/min.

As shown in figure 2.11 the initial 25 minutes of the gradient show no peak elution now that the contamination peaks had been successfully removed from the sample/assay. At approximately 25 minutes the IPA % present was estimated to be 50 %. Due to the fact that the initial isocratic runs contained 60 % IPA but at a higher flow rate and higher temperature, an isocratic run of 60 % IPA: 40 % ACN at 5°C with a flow rate of 0.5 ml/min was used. If possible, an isocratic run would be beneficial versus a gradient run due to the aim to combine this assay at a later stage in development with a HPLC-UV assay for the detection of HNE within samples. The above isocratic run within 60:40 IPA: ACN gave a relatively well resolved series of peaks; however significant peak splitting was observed. After further investigation through injection of a caffeine standard which gave a split peak, this was identified to be due to column stationary phase breakdown and therefore a new column was required.

2.5.3.6 Column stationary phase choice

It is well known that within NARP chromatography a C-18 stationary phase can be utilised for the separation of TAG molecules under a variety of chromatographic conditions (Lin et al. 1997; Schönherr et al. 2009; Gonyon et al. 2013; Hmida et al.

54

2015). Most of this work has been the identification of TAGs present within an oil as opposed to an emulsion. As the body of this work is focused on the quantification of key TAGs within lipid emulsions, the ability to separate TAGs from phospholipids is an essential requirement. Liu et al. (2014) showed effective separation of both TAGs and phospholipids using a C-30 stationary phase. The increase in chain length of the stationary phase will increase the interactions occurring from the fatty acid chains within TAGs and phospholipids. Whilst this may increase the retention times observed versus a C-18 column, the increased interactions should increase the selectivity of the assay, allowing for the separation of TAGs and phospholipids to occur. With reference to resolution theory (figure 2.6), changing the stationary phase of the column will affect α and k and potentially also the theoretical plate number of the column, therefore having a potentially large effect on resolution (Synder et al. 1997). Elution order again will be based initially on the partition number of fatty acids within phospholipids, however the hydrophilic nature of the phospholipid head group will govern its elution time. The availability of a C-30 250 mm x 3 mm column with a 3 μm particle size allowed for a direct method transfer to occur from a C-18 stationary phase to a C-30 phase and a comparison on the optimum stationary phase to use for further assay development to be made. As the length, diameter and pore size of the C-30 column is the same as the C-18 column the theoretical plate number will remain constant.

Isocratic runs of 60:40 IPA: ACN were carried out using the C-30 and new C-18 column with the following conditions:

- C-30 column 250 mm x 3 mm 3 μm particle size or C-18 column 250 mm x 3 mm 3 μm particle size.

- Mobile phase: IPA: ACN 60:40

- CAD nebuliser temperature: 50°C

- Auto sampler temperature: 8°C

- Column temperature: 5°C

- Flow rate: 0.30 μl/min

- Injection Volume 10 μl
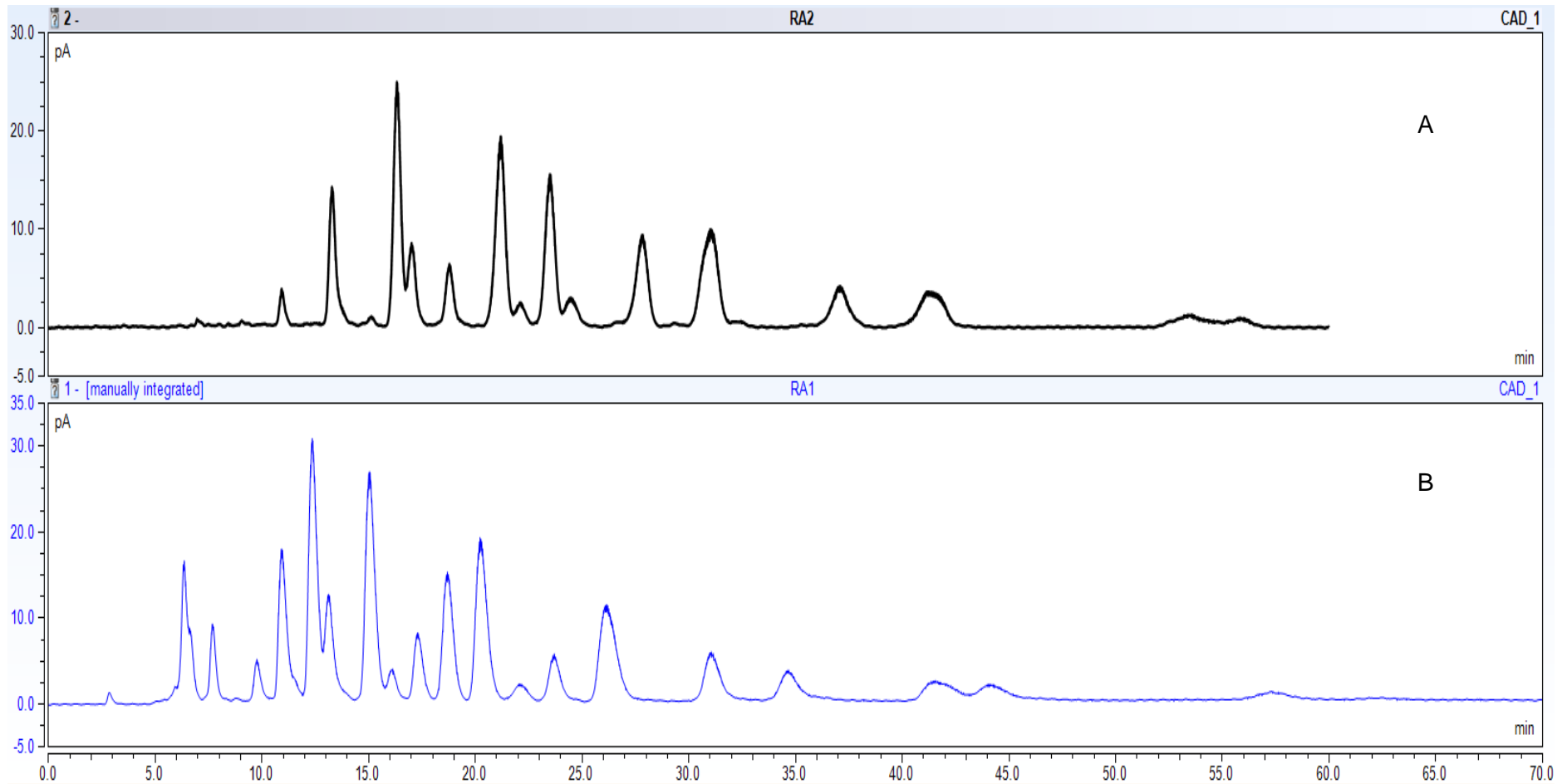
Figure 2.12 HPLC analysis of Intralipid® 20% using A - C-18 column and B - C-30 column.

As observed in figure 2.12 the C-30 column chromatogram under identical conditions to the C-18 column showed superior separations of the Intralipid® emulsion. Increased numbers of clear peaks are identifiable and resolution (R_s) between peaks is adequate for quantification. An R_s of over 1.5 (as calculated using the equations shown in figure 2.44) between peaks from 14 minutes onwards suggested definite baseline resolution between them. It is worth noting the drop in flow rate further to 0.3 ml/min at this stage was due to a column pressure increase due to the addition of a C30 guard column to increase column lifespan and protect the column from damage. At this stage the development of the CAD assay was at an appropriate stage to combine with the UV assay for the detection of HNE. This process is detailed in section 2.8 after the following UV method development.

2.6   HPLC-UV method development

2.6.1   Principles of UV detection

UV detection works on the principles of measuring the absorption of monochromatic light in the UV spectrum against a reference beam of light and comparing this to calculate sample absorbance and therefore concentration. Light from the lamp is directed through a flow cell and impinges on a diode that reads the light intensity. Light is also directed to the reference diode to allow a comparison in intensity to be calculated (Synder et al. 1997). The optical path that UV light takes through a detector is briefly as follows: Polychromatic light is formed from a tungsten or deuterium lamp and focused onto the entrance of a monochromator which selectively transmits the desired wavelength(s) through an exit slit. This then reflects of a series of mirrors to the reference diode and through the sample flow cell to the sample diode for detection. The wavelength of measurement i.e. the specific wavelength desired is selected using the data system and a grating mounted on a turntable within the detector. Figure 2.13 shows this process in further detail.
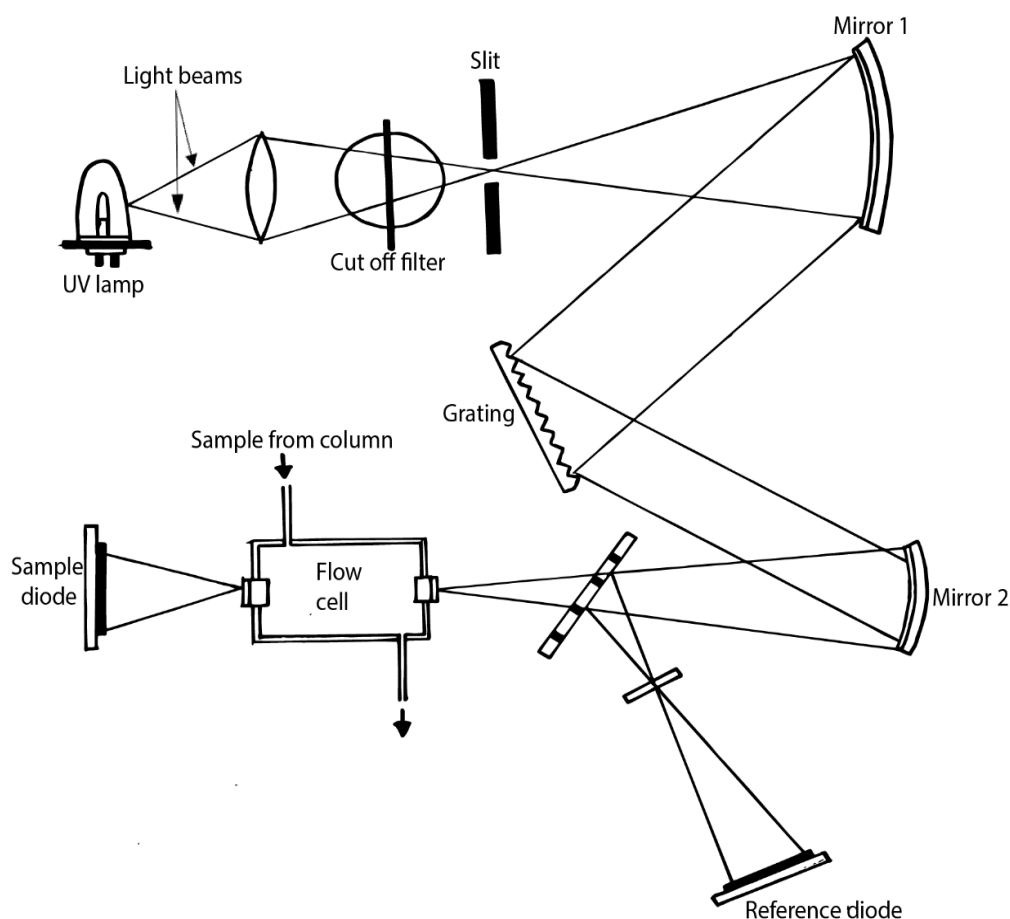
Figure 2.13 Expanded diagram of the UV detector and pathway of light.

Analyte concentration in UV detection is calculated using absorption (A) (calculated from sample and reference diode intensity readings) and Beer-Lambert's Law (figure 2.14)

$$A = C \varepsilon L_{fc}$$

Figure 2.14 Beer-Lamberts Law. A = Absorption, ε = molar absorption coefficient ($dm^3 mol^{-1} cm^{-1}$), L = flow cell length (cm), C = analyte concentration ($mol\ dm^{-3}$).

UV detection relies upon the sample molecule possessing a chromophore e.g. structures with double bonds or conjugated systems that can absorb UV light and enter a higher excitation state at a specific wavelength. This is where there is an inherent problem with the UV detection of TAGs. Triglycerides possess no chromophores above ≈ 190 nm i.e. double carbon-carbon bonds in polyunsaturated fatty acid chains (Plattner 1989). The vast majority of organic mobile phases used within HPLC identical to the TAGs have carbon-carbon bonds as their structure.

Therefore, organic phases will also have a UV absorbance under 200 nm, creating a baseline level of absorbance that will negate any absorbance from the sample TAGs and as such making them unable to be detected via UV absorption. HNE however has a strong UV absorbance based from its UV spectra (figure 2.15) at 222 nm making it easily detectable with UV detection.
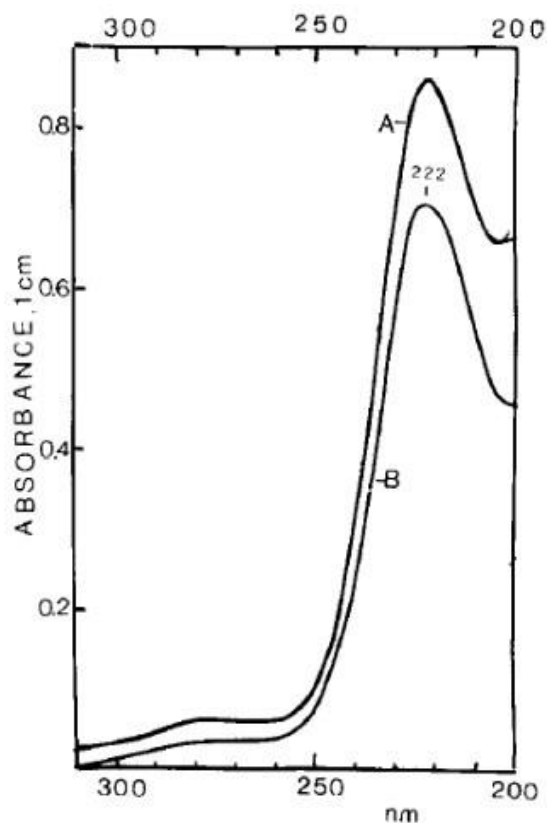
Figure 2.15 UV spectrum of HNE. (A) biogenic 4-HNE isolated from the experimental sample by high-pressure liquid chromatography. (B) synthetic 4-HNE. Solvent: acetonitrile/water (1:1 v/v) taken from Benedetti et al. (1980).

2.6.2 Initial HNE UV method

There are several existing papers documenting the UV detection of free HNE within a variety of samples and different matrices. These are discussed below and provide a base from which assay development can be initiated. The key differences between the existing assays as described vs. the desired assay are the sample matrix. The aim is to detect HNE within IVLE's, so emulsion properties will influence assay development.

Esterbauer and Zollern (1989) were considered the pioneers for the detection and classification of HNE as a substance. Their direct detection method uses an ODS

(C-18) column with an isocratic mobile phase of acetonitrile: water 40:60 at a flow rate of 1ml/min. UV detection was set at 220nm. The method was able to detect HNE with a limit of detection of around 2 pmole. The method is used to detect HNE within cellular fractions and uses an initial sample clean up step to remove these subcellular fractions, a step that can be excluded in the analysis of IVLEs in PN due to the *in vitro* nature of the samples.

Laing et al. (1985) used a similar HPLC method and compared this with derivatised HNE and free HNE detected with gas chromatography (GC) and flame ionisation detection. The HPLC method was found to be around one order of magnitude more sensitive than the GC method. The RP-HPLC was carried out on a C-18 column with acetonitrile: water 40:60 or methanol: water 65:35 as the mobile phase. Flow rate was 1 ml/min and the absorbance set at 220 nm with an injection volume of 20 µl. Standard calibration curves were created from 0.1µM to 500 µM concentrations.

Benedetti et al. (1986) used a similar method using a C-18 column with a mobile phase of acetonitrile: water 50:50 at a flow rate of 1 ml/min. This method was used to detect HNE in liver cell fractions in the form of free HNE and in parallel a derivatisation method of identification of HNE with DNPH. Both assays gave repeatable and accurate results of HNE in liver cells.

The above papers provide a set of assay conditions that can be used as a base for initial assay development. All employ a water: acetonitrile mobile phase system with a flow rate of 1ml/min. A C-18 column was chosen for initial assay development due to both its proven ability to separate HNE as described above but also with mind to its ability to separate TAGs efficiently.

2.6.2.2 Initial Method

The work was carried out on a Spectra system (Thermo Scientific, West Palm Beach, United States). Reference standards of 4-HNE were obtained from Santa Cruz Biotechnology (Dallas, Texas) and were supplied under dry ice storage (-70℃) in ethanol. Standards were supplied at a concentration of 10 mg/ml (1 mg/100µl). An OmniSpher 5 C18 150 x 3 mm, 5µm particle size (Varian, Palo Alto, USA) column was chosen for initial method development. Reagents (acetonitrile, propan-2-ol (IPA), methanol, water and ethanol) were all HPLC grade (Fisher Chemical).

Initial method used was as follows for the identification of HNE from standard reference:

- C-18 column 150 mm x 3 mm, particle size 5 μm
- Mobile phase: Acetonitrile: water 40:60
- Injection Volume: 20 μl
- Flow rate: 1 ml/min
- UV wavelength: 222 nm
- Run time: 20 mins

HNE sample: 12.5μl of standard (1mg/100μl) diluted in 250μl of ethanol.
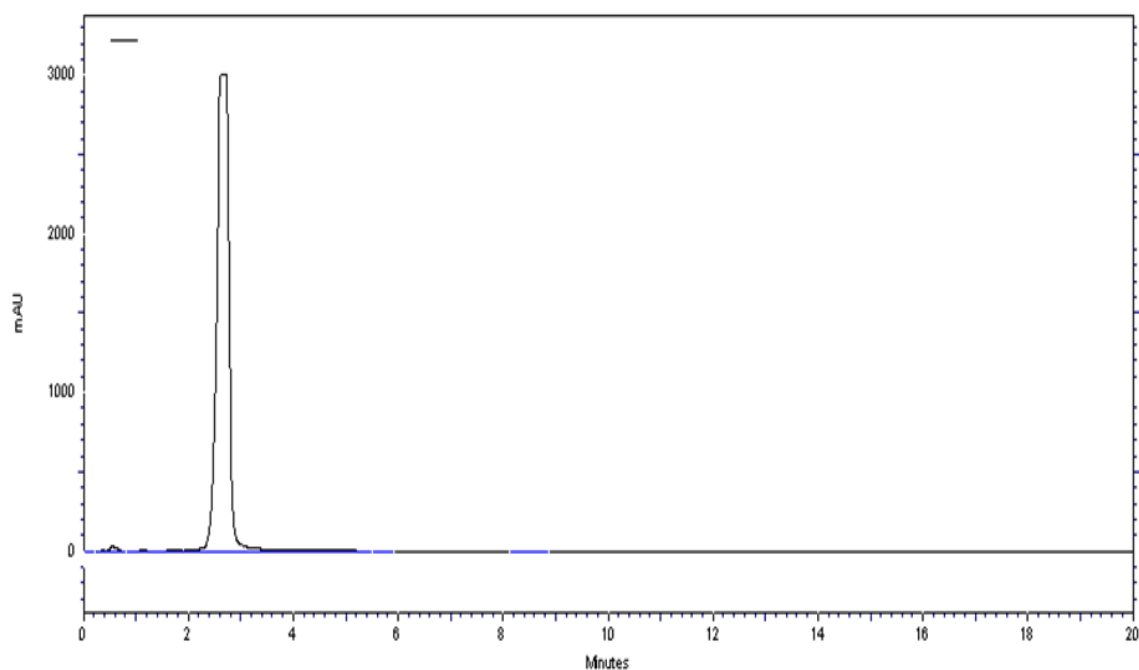
Figure 2.16 HPLC of HNE standard, mobile phase acetonitrile: water 40:60. The flattening of the peak is due to the concentration of HNE standard being too high.

2.7   Method development and optimisation

2.7.1   HNE standard concentration

The initial run detailed above proved that HNE was easily detectable using the above assay through RP-HPLC and UV detection.

This method was then adjusted to look at a sample of Intralipid® 20%. From the literature search detailed above with regards to the method development with the CAD for Intralipid® 20%, the use of NARP chromatography was chosen for the

analysis of lipids. Whilst the lipids themselves within Intralipid® are not the subject of the UV section of the assay for the detection of HNE, they still need to be effectively eluted from the stationary phase and the combination of both assays is the aim. Therefore, a change of mobile phase from acetonitrile: water to acetonitrile: IPA was undertaken to allow effective elution of the Intralipid® from the column.

Initially a sample of HNE standard was run through the HPLC system under the following conditions to ensure the detection of HNE was still effective with a changed mobile phase:

- C-18 column 150 mm x 3 mm, 5 µm particle size
- Flow rate: 0.75 ml/min
- Injection Volume: 20 µl
- Mobile phase: IPA: Acetonitrile 60:40
- UV wavelength: 222 nm
- HNE standard 6.25 µl in 250 µl (halved concentration due to previous cut out of detection due to high concentration
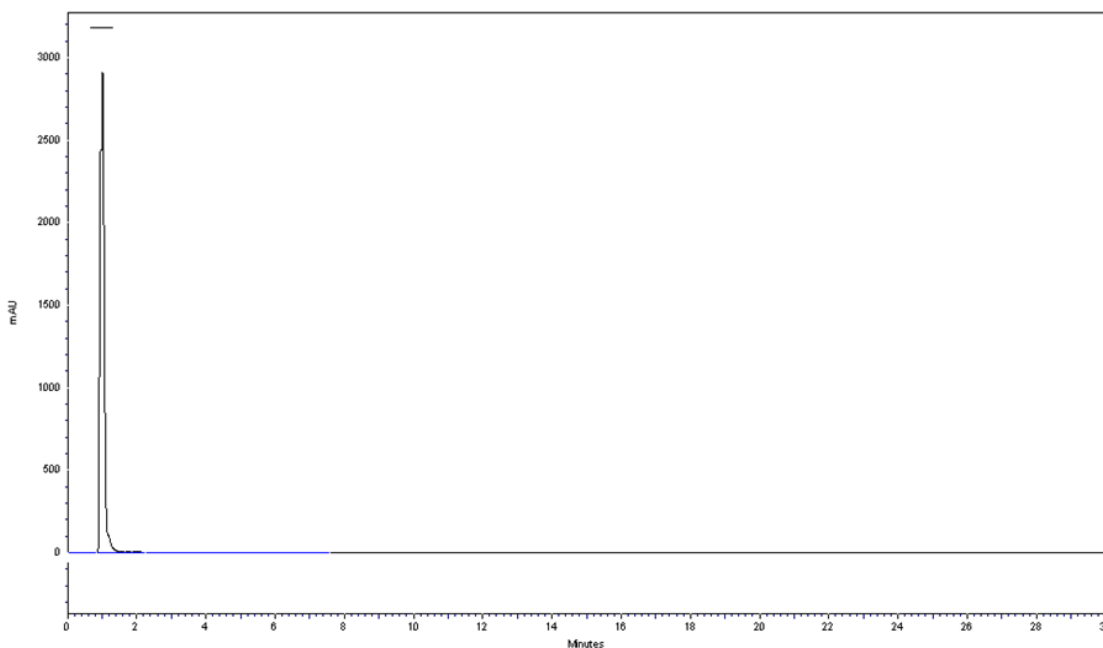
Figure 2.17 HNE standard (6.25 µl in 250 µl ethanol), mobile phase IPA: acetonitrile 60:40.

Whilst this mobile phase clearly moved the elution time of HNE from around 2.5 minutes to around 1 minute, the peak was still easily identifiable. Whist within the solvent front this is appropriate for this stage of development.

This same method was then used as a basis for the introduction of Intralipid® 20 % to the sample, spiked with HNE standard.

Sample preparation involved the creation of an HNE stock solution through the addition of 12.5 µl of HNE to 500 µl of ethanol. 125 µl of this was then added to 125µl of Intralipid® 20% giving a concentration of 83.3 µM (3.125 µl HNE in 250 µl). Samples were prepared in amber glass vials (National Scientific) with fixed 250 µl glass inserts to allow for the testing of small volumes.
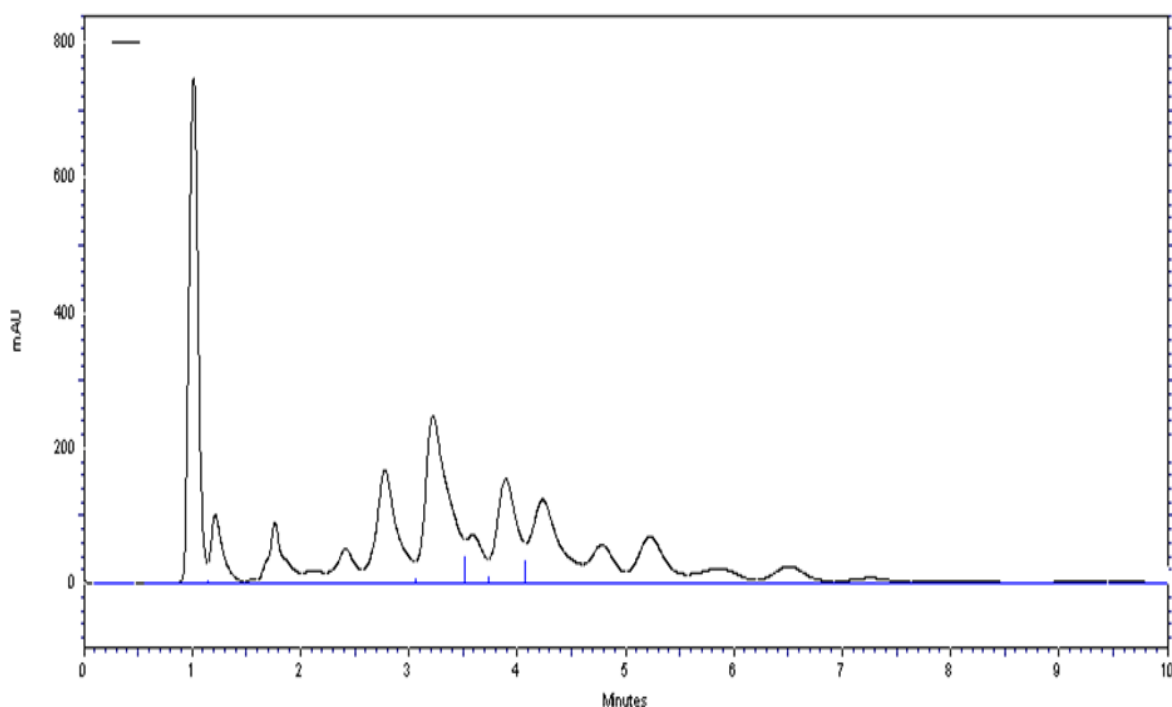
Figure 2.18 RP-HPLC of HNE in Intralipid®. Mobile phase IPA:ACN 60:40.

The large peak at 1 minute is the HNE standard with subsequent peaks being attributed to the triglycerides and phospholipids present in the Intralipid® sample. Whilst these peaks are not well defined, nor do they achieve baseline resolution, for the purposes of the UV assay this is not important as these lipids will not be quantified through UV detection. The peak co-eluting with the HNE standard is the issue that further work aimed to separate as baseline resolution needs to be achieved to allow quantification of HNE to occur. The HNE created in the peroxidation of lipids will be at a much lower concentration than the standard used

within this section of the assay and therefore baseline separation of all other components from the HNE peak is vital.

2.7.2 Mobile phase optimisation

Mobile phase composition in NARP chromatography is all organic and as such the polarities of the organic components is a governing factor on the elution times of compounds.

Alteration of mobile phase composition was trialled using the following scheme (table 2.5). All trials were run in triplicate. The run time was reduced to 10 minutes per run as indicated by the above assay time (figure 2.18). Injection volume was also reduced to 10 µl to increase the number of runs possible from each sample and preserve stocks of HNE standard.

Table 2.5 Mobile phase changes in NARP-HPLC of Intralipid® with HNE standard.

Mobile phase composition	Effect on assay result
IPA: Acetonitrile 70:30	No appreciable changes to chromatogram.
IPA: Acetonitrile 50:50	All components eluted later except HNE and co-eluting molecule.
IPA: Acetonitrile 30:70	Loss of chromatogram, indistinguishable peaks.
IPA: Acetonitrile 90:10	Components eluted earlier on chromatogram.

The polarity factor of IPA is 3.9 and of acetonitrile is 5.8 (as reference water has a polarity factor of 10.2) (Christie 2003). The relative closeness in polarity between the two mobile phases being used may account for the lack of movement in the chromatogram upon alteration of the percentage composition of the mobile phase.

The lack of movement of the co-eluting peak along with the HNE standard in response to mobile phase alteration resulted in reverting to the initial mobile phase of IPA: acetonitrile 60:40 as this gave the optimal chromatogram.

2.7.3 Column change

At this stage, as assay development was running in parallel to that of the HPLC-CAD assay, the column change in the CAD assay to a C-30 column (section 2.5.3.6) prompted the same column to be tried for the HNE assay. From this point

forward, assay development for the HNE-UV assay was transferred to the Ultimate 3000 HPLC system as used for the HPLC-CAD assay, with the Spectra UV detector being added to the system in-line with the CAD detector. The UV detector is placed before the CAD as the CAD detector is destructive in nature. This set-up allows the assays once optimised to be combined and run as one assay.

Initially with the new C-30 column HNE and Intralipid® were run with the optimised CAD assay conditions. Figure 2.19 shows both HNE and Intralipid® 20% chromatogram run with the new C-30 column, achieving a superior separation between the HNE and initial Intralipid® peaks.

Optimised CAD assay conditions were:

- C-30 column 250 mm x 3 mm 3 µm particle size

- Mobile phase: IPA:ACN 60:40

- Auto sampler temperature: 8°C

- Column temperature: 5°C

- Flow rate: 0.30 µl/min

- Injection Volume 10 µl

- Samples of Intralipid® 20% were prepared at 1000 µg/ml in IPA.
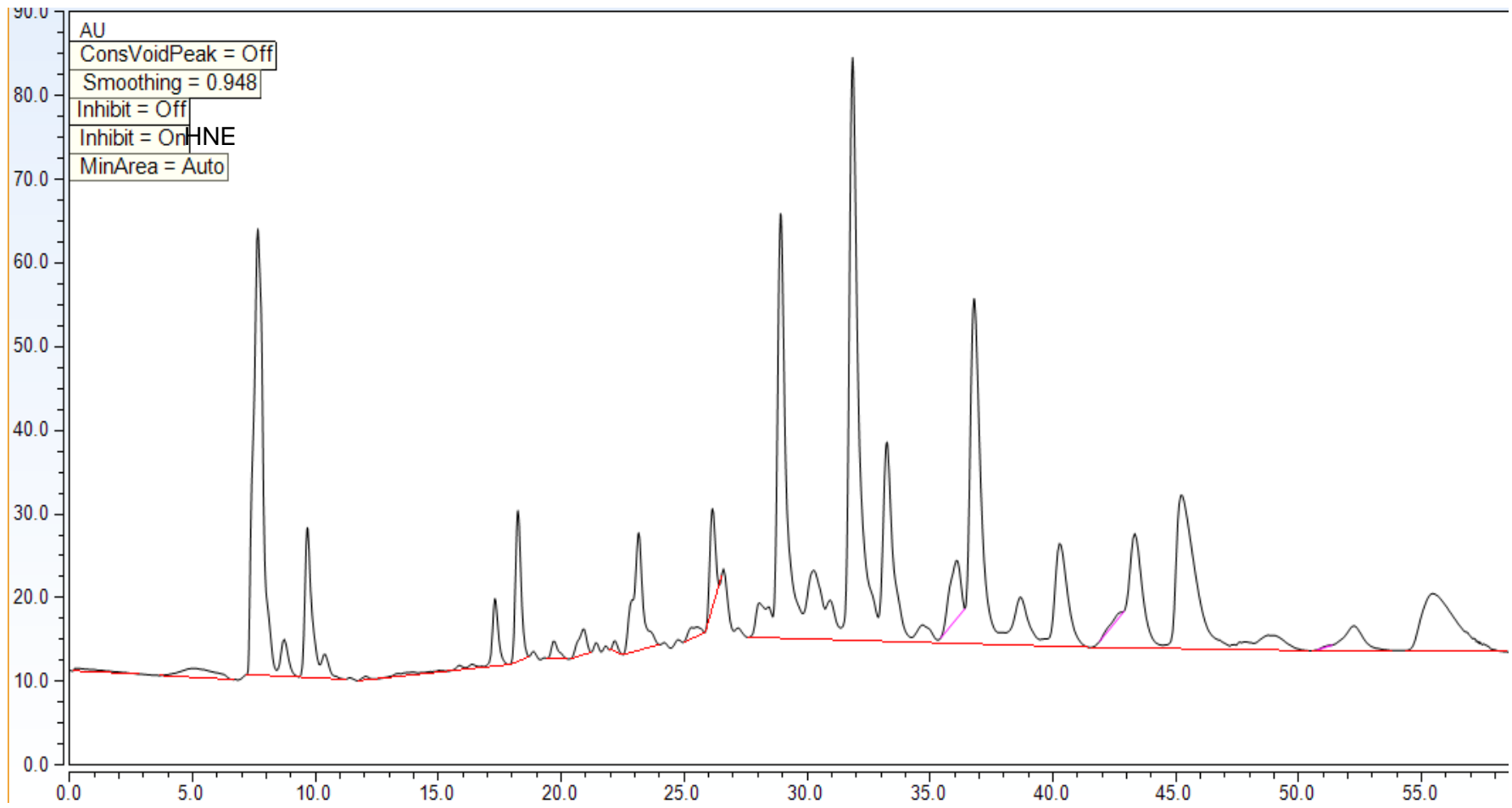
Figure 2.19 UV chromatogram of HNE in Intralipid® 20% showing good separation between Intralipid peaks and HNE standard.

At this stage the HNE assay is sufficient for validation of the assay to occur, however combination of the UV and CAD assays was the aim and therefore the next stage in assay development.

2.8   Combination of CAD and UV assays.

Both the CAD assay of TAGs and the UV assay of HNE were now at an appropriate stage that they could be combined to run simultaneously. Therefore, the assay conditions of each were matched and the UV detector placed in-line with the CAD detector. Sample preparation was also changed at this stage to simplify the system with a view to making the assay as accessible as possible for future stability testing. Until this point the Intralipid® 20 % has been diluted in IPA to a concentration of 1000 µg/ml and an injection volume of 10 µl used. It was noted however as the run time has now increased to 90 minutes that the IPA diluting the Intralipid® in the sample preparation was resulting in oil separation over time whilst samples are standing prior to use. Therefore, to overcome this, samples were changed to neat Intralipid® with no dilution to maintain stable emulsions during extended testing times. To compensate for this 100 % concentrated sample, injection volume was reduced from 10 µl to 1 µl, maintaining adequate responses by the detectors and achieving repeatable responses through the HPLC system.

2.9   Final assay conditions

Using the combined in line detectors as described above, the following assay conditions were used to form the completed assay:

- C-30 column 250 mm x 3 mm 3 µm particle size

- Mobile phase: IPA: ACN 60:40

- CAD nebuliser temperature: 50°C

- Auto sampler temperature: 8°C

- Column temperature: 5°C

- Flow rate: 0.20 µl/min

- Injection Volume 1 µl

The above conditions gave the chromatograms as seen in figures 2.20 and 2.21. Figure 2.20 Shows the UV chromatogram of Intralipid® spiked with 6 µg/ml of HNE clearly showing the separation of HNE from the less well defined Intralipid® peaks.

Figure 2.21 Shows the combined CAD and UV traces of Intralipid® with spiked HNE standard, showing that the CAD trace provides quantifiable peaks of the TAGs within the emulsion.
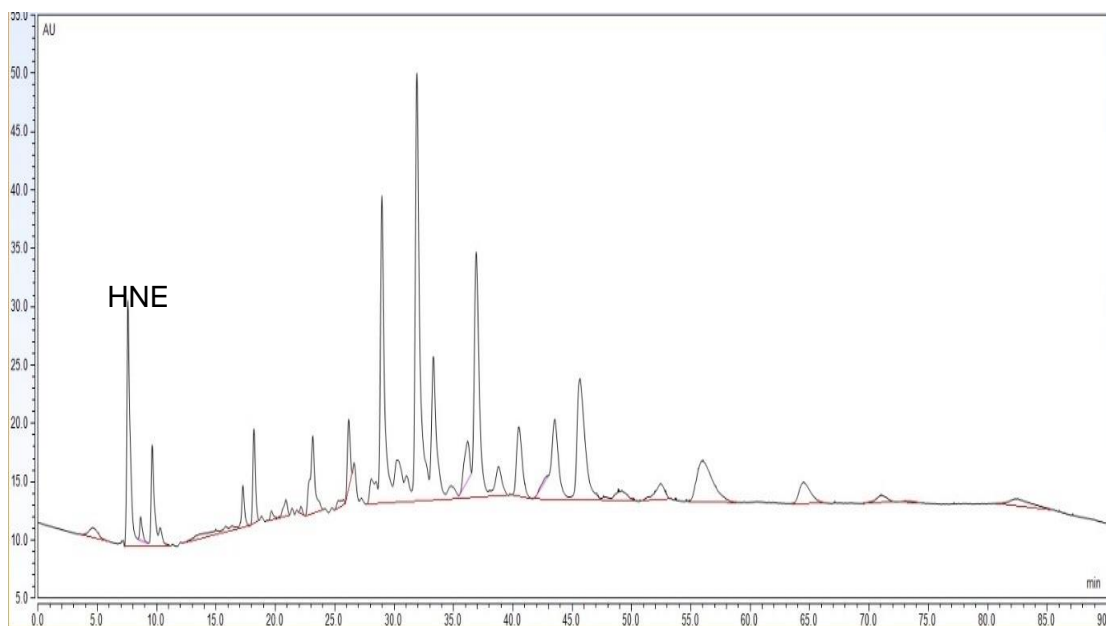
Figure 2.20 HPLC-UV chromatogram using final assay conditions. HNE clearly separated from other less defined Intralipid® peaks.
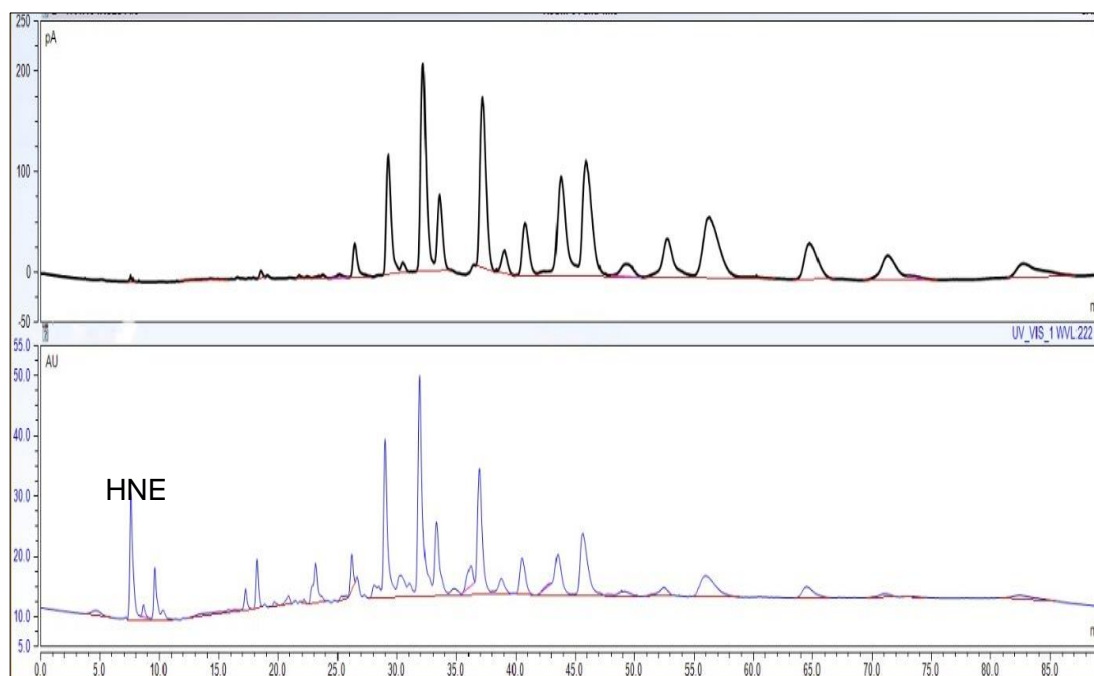
Figure 2.21 HPLC-UV-CAD chromatograms of final assay conditions. A – HPLC-CAD chromatogram of Intralipid® 20 %. B – HPLC-UV chromatogram of Intralipid® 20 % with added 6 µg HNE standard.

At this stage in assay development, whilst the HNE peak has been confirmed by the addition of a standard of HNE to the emulsion, the aim is also to monitor the changes in the levels of TAGs present. The peaks of the HPLC-CAD chromatogram as yet remain unidentified and as such identification of these peaks formed the next stage in assay development for Intralipid®.

2.10 SMOFlipid® chromatogram and peak selection

Current method development had now succeeded in creating an assay capable of separating TAGs and HNE in Intralipid® samples and so the assay conditions were used to run another lipid emulsion used within parenteral nutrition. As discussed in the introduction (section 1.2.3) SMOFlipid® 20% is a newer generation intravenous lipid emulsion containing a mixture of soybean, olive and fish oils with added chemically synthesised medium chain saturated triglycerides. Percentage composition of SMOFlipid® is described in table 2.6.

Table 2.6 Fatty acid composition of SMOFlipid®

Fatty acid	Carbon number: double bond	SMOFlipid® 20 %
Oleic acid	C18:1	23-35%
Linoleic acid	C18:2	14-25%
Caprylic acid	C8:0	13-24%
Palmitic acid	C16:0	7-12%
Capric acid	C10:0	5-15%
Stearic acid	C18:0	1.5-4%
α-linolenic acid	C18:3	1.5-3.5%
EPA	C20:5	1-3.5%
DHA	C22:6	1-3.5%

From these % combinations of fatty acids formulated as TAGs it was predicted that the chromatogram for SMOFlipid® would differ from that of Intralipid®. The presence of soybean oil in both emulsions however was predicted to produce an identical predictive peak pattern within both chromatograms. To ensure that the above assay conditions achieved adequate separations for SMOFlipid® the emulsion was run and gave the chromatograms seen in figure 2.22 The same sample but spiked with HNE is shown in figure 2.23.
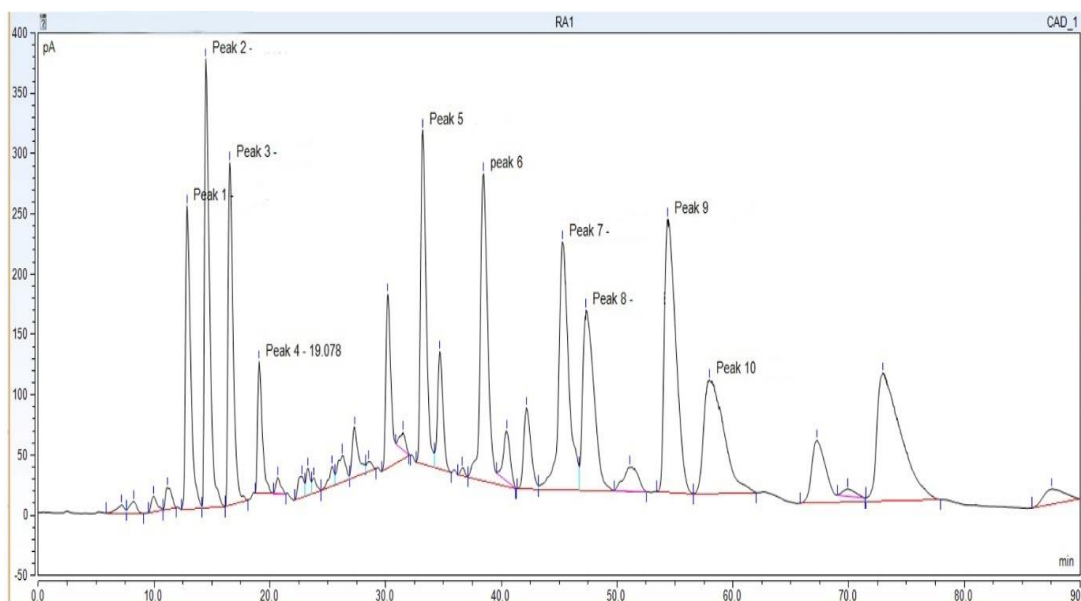
Figure 2.22 HPLC-CAD chromatogram of SMOFlipid® 20 %.
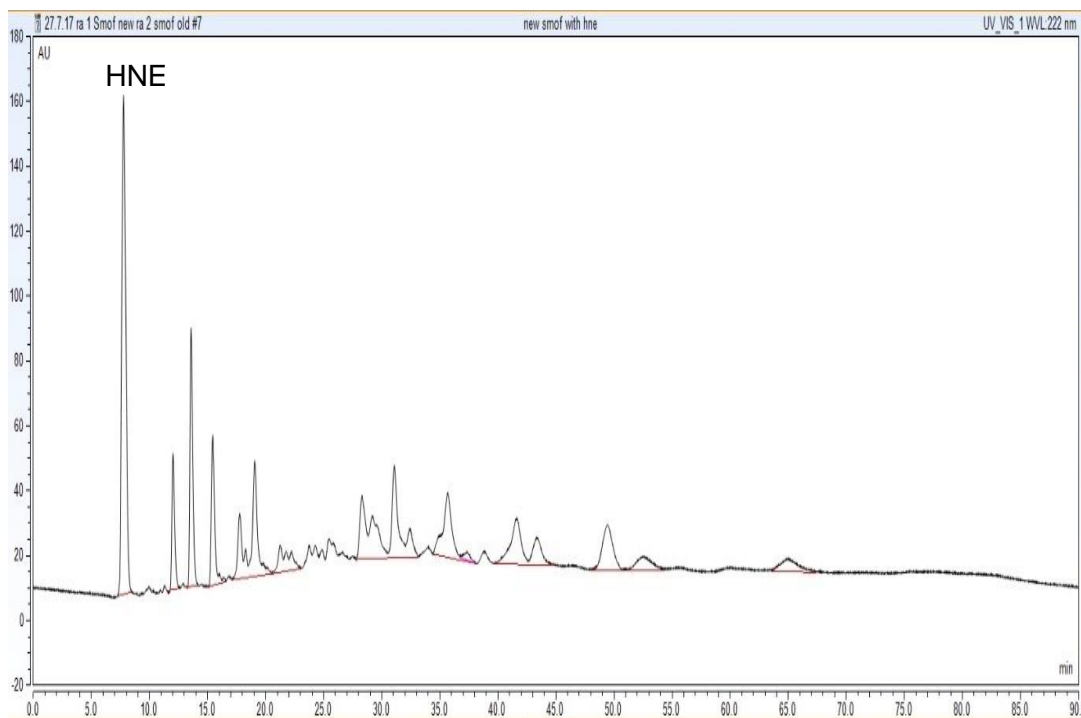
Figure 2.23 HPLC-UV chromatogram of SMOFlipid® with added HNE standard.

As seen in the above figures the assay achieved adequate separations for SMOFlipid® and HNE. The peaks within the CAD chromatogram show the greater number of TAGs present compared to the Intralipid® chromatogram (figure 2.21) as predicted due to the increased number of oils present within SMOFlipid®. The peak pattern as seen in the overlaid chromatograms in figure 2.24 show the peaks within the SMOFlipid® chromatogram that are attributed to the soybean oil present within Intralipid® giving a distinct peak pattern with peaks 5 to 10 in figure 2.24 matching peaks 1 to 6 in figure 2.21.
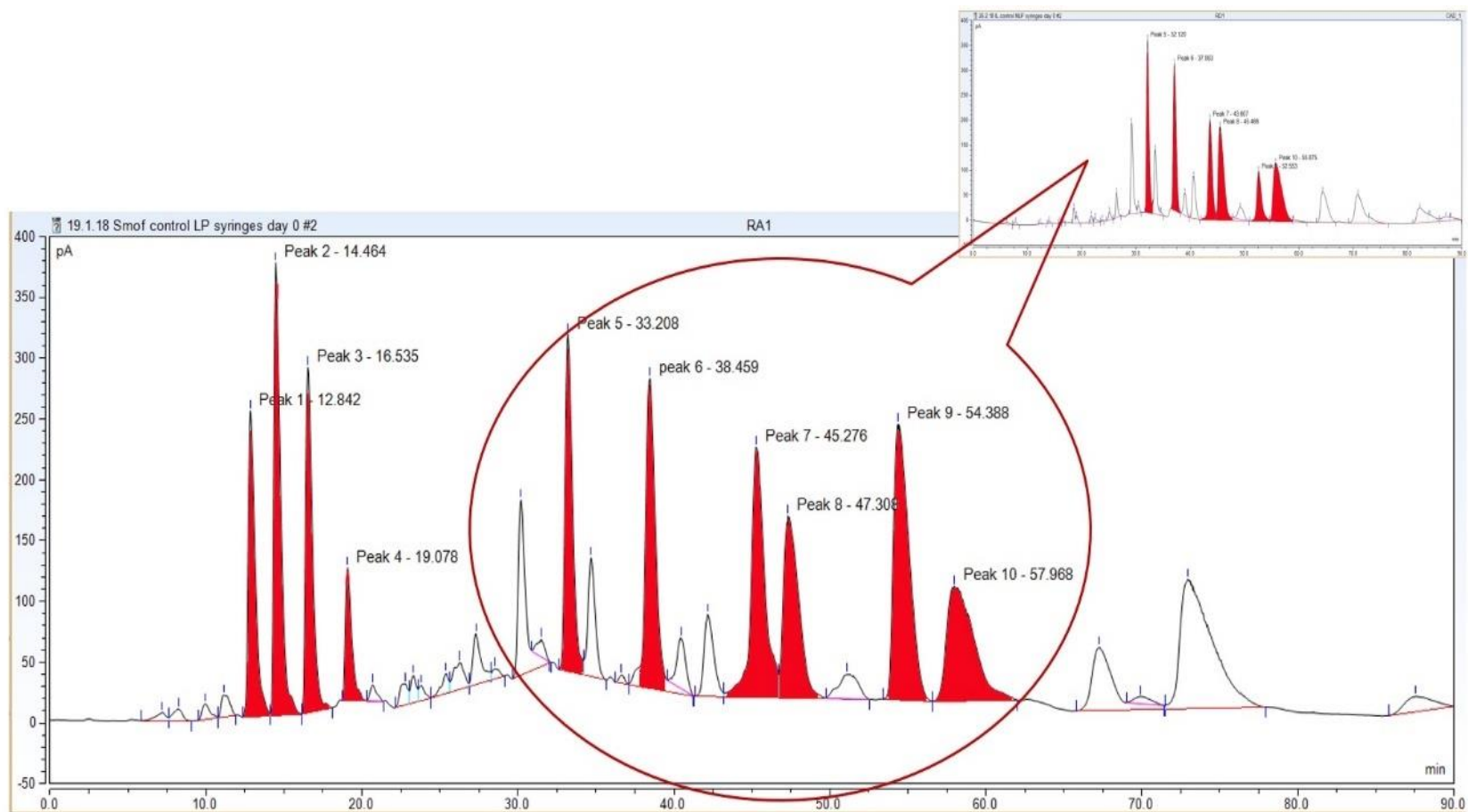
Figure 2.24 HPLC-CAD chromatogram of SMOFlipid® showing the identical peaks attributed to the soy bean oil present in the Intralipid® chromatogram insert.

As seen in figure 2.24 the ten major peaks within SMOFlipid® were selected for identification. Following the theoretical partition number equation as explained in section 2.2.3 (figure 2.2) the initial peaks seen in the SMOFlipid® chromatogram were predicted to be attributed to the shorter chain saturated medium chain TAGs present from the chemically synthesised medium chain fatty acids (C8 to C10 carbon numbers). These peaks were therefore labelled 1 to 4 and selected for identification. The other 6 major peaks within the chromatogram matched the Intralipid® trace and were therefore attributed to soybean oil and the TAGs with the highest % fatty acids according to table 2.6. These peaks were labelled 5 to 10 and selected for identification.

2.11 Triglyceride identification

The presence of a mixture of fatty acids in the form of TAGs and phospholipids present in the lipid solutions means that peak identification using fatty acid standards is not possible. As there are five fatty acids present (table 1.3) within soybean oil that forms Intralipid®, the possible combinations created in the formation of TAGs are too numerous (~125) to be able to take the approach of acquiring standard TAGs and trying to identify peaks using these standards. As the formulation in question is an emulsion, using TAG standards that are formulated as an oil will also result in a different chromatogram to that seen from Intralipid emulsion, making the traditional approach of using standards to spike peaks for identification unusable in this assay. As the purpose of the assay is to monitor the lipid emulsion being tested for peroxidation and subsequent TAG breakdown and loss, the identification of the main primary TAGs present within each emulsion is necessary. These can then be used as markers to monitor the losses of TAG occurring during peroxidation and storage.

The combination of fatty acids within Intralipid® and SMOFlipid® when formulated into TAGs will produce numerous different TAGs as represented by the peaks seen within the HPLC-CAD chromatograms. It is predicted that peroxidation and breakdown of the fatty acid chains present within the TAGs will produce two main effects to the chromatogram being observed. Firstly, a loss of peak size should be observed as specified TAG concentrations are lost/altered by their changing chemical structure and carbon numbers. As the CAD signal observed is one of charge that is directly proportional to the mass of the analyte present, peak area loss will directly represent the loss of a specific TAG mass. Secondly, the presence

73

of new peaks within the chromatogram would be expected to be observed. The breakdown products of peroxidation from the hydroxyl end of the fatty acid chain, in several forms, including reactive aldehydes and longer fragments will also be detected. It is worth noting here that these peaks will be limited in their presence in the CAD chromatogram due to the volatile nature of the aldehydes created. Shorter chain aldehydes such as HNE and hydroxyhexanal (HHE) will not be detected by this part of the assay employing the CAD as a detector as they are too volatile and are completely lost during the nebulisation process. Longer chain fragments from TAGs and the fatty acids now remaining as effectively different TAG 'remnants' should however be effectively detected by the CAD resulting in new peaks being observed in the chromatogram.

As it is not practical to identify all the TAGs present, it was decided that initial identification of the six clear and substantial peaks within the Intralipid® chromatogram should occur. Peaks chosen for identification are shown as peaks 1, 2, 3, 4, 5 and 6 in figure 2.25. Within the SMOFlipid® chromatogram 10 main peaks were selected for analysis as seen in figure 2.24.
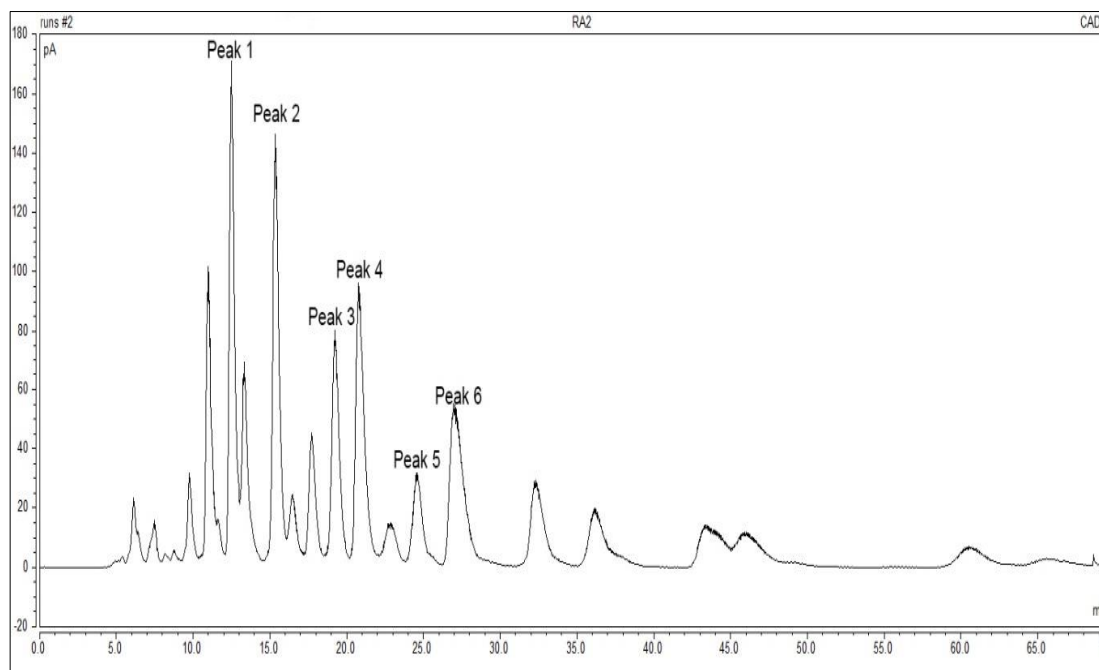
Figure 2.25 HPLC of Intralipid® 20%. Peaks 1 to 6 identified as peaks to be collected. Typical pre-collection run chromatogram.

2.12 Mass spectrometry

2.12.1 Mass spectrometry introduction

Eluent collected from the six major peaks in Intralipid® and the ten major peaks in SMOFlipid® were subjected to mass spectrometry (MS) to identify their mass/charge (m/z) ratio and therefore the potential TAGs responsible for each peak.

Electrospray Ionisation (ESI) MS has been used effectively to analyse TAGs in a variety of edible oils and seeds (List et al. 2000; Li et al. 2014). The fundamentals of ESI involve the introduction of a continuous stream of sample solution into a capillary tube which is at a high (2-6 Kv) voltage. This produces highly charged (either positive or negative depending on the mode) droplets. The addition of a nebulising gas (usually nitrogen) and high temperatures leads to the evaporation of the solvent from these charged droplets. Droplet diameter reduces, and surface charge increases to a point where ions within the droplet have sufficient kinetic energy to be ejected into a gaseous phase. These charged ions are sampled via a skimmer and accelerated into the mass analyser being used (Ho et al. 2003). Due to the 'soft' nature of ESI as the sample is ionised by the addition (+ve) or abstraction (-ve) of a proton with little surplus energy remaining, molecules analysed via this method are more likely to remain intact and be identified as such in the spectrum obtained.

Molecules up to a size of approximately 1200 Daltons give rise to singly charged protonated / de-protonated ions ($M-H^+$ or $M-H^-$). Commonly where sodium ions are present within mobile phases due to minute contamination or background ions present, $M-Na^+$ ions will also be detected in positive modes (Christie 2003). With respect to positive or negative modes of ionisation, this relates to the charge that is applied to the tip of the capillary tube and therefore the charge transferred to the analyte. If the sample contains functional groups that are easily protonated, positive mode should be selected. Conversely samples containing groups that readily lose protons should be scanned in negative mode. As seen in figure 2.1 the general structure of all TAGs results in the carboxylic acid groups of the fatty acids present being unavailable for deprotonation due to their bonds with glycerol. Therefore, negative mode will be ineffective in scanning for TAGs and positive mode should be used. Mobile phases comprised of Methanol (MeOH) with 0.1% Formic acid and water with 0.1% Formic acid was selected for analysis of the fragments collected. Formic acid is added into mobile phase at a low concentration to enhance

protonation of samples in positive mode (Waters 2018). Samples collected from the HPLC-CAD assay were in IPA/ACN 60/40 making them compatible for analysis.

Time of flight (TOF) analysers are relatively simple mass analysers used within mass spectrometry. TOF analysers are comprised of a flight tube under vacuum with no electric fields. Ions collected post ESI are accelerated by an electric field and delivered to the TOF analyser. Ions proceed to 'drift' through the flight tube via the kinetic energy obtained from the potential energy of the electric field employed for acceleration. The specific kinetic energy that the ion obtains related to the equation in figure 16 that gives the mass/charge (m/z) ratio for the compound.

$$\frac{m}{z} = (2t^2K)/L^2$$

Figure 2.26 – t = drift time, L= drift length, m = mass, K = kinetic energy of ion, z = number of charges on ion.

If the electric field applied is constant, the kinetic energy each ion will obtain will again be constant. Therefore, the velocity of each ion will be dependent on its mass/charge ratio i.e. the size of the ion. The smaller the ion, the larger the velocity and the shorter the time of flight recorded by the detector at the end of the flight tube and conversely the larger the ion the lower the velocity. Time of flight is recorded for each ion passing through the analyser and is initially plotted as abundance of ion vs time. This can be calibrated and re-plotted as m/z vs intensity to give the typical mass spectrum observed.

2.12.2 Mass Spectrometry experimental method

The use of mass spectroscopy was employed to obtain a mass/charge ratio for each of the labelled peaks, with the aim to identify the TAG responsible for each selected peak. Fragments from the HPLC-CAD were collected at the respective time points for each peak to be identified. The chromatogram observed in figure 2.27 shows a typical collection run where peaks 1, 2 and 3 of Intralipid® were collected through collection of the eluent from the column at the point of entry to the CAD detector. As the CAD detection process is a destructive one, fragments had to be collected pre-entry to the detector. Each pre-collection run was carried out in duplicate, allowing for the times of the peaks 1 to 6 of Intralipid® and 1 to 10 of SMOFlipid® to be identified from the chromatograms present, accounting for inter-day variability. Subsequent runs were then carried out per the example in figure 2.27. And the fragments collected and stored in amber HPLC vials at 2-8°C until analysis with mass spectroscopy.
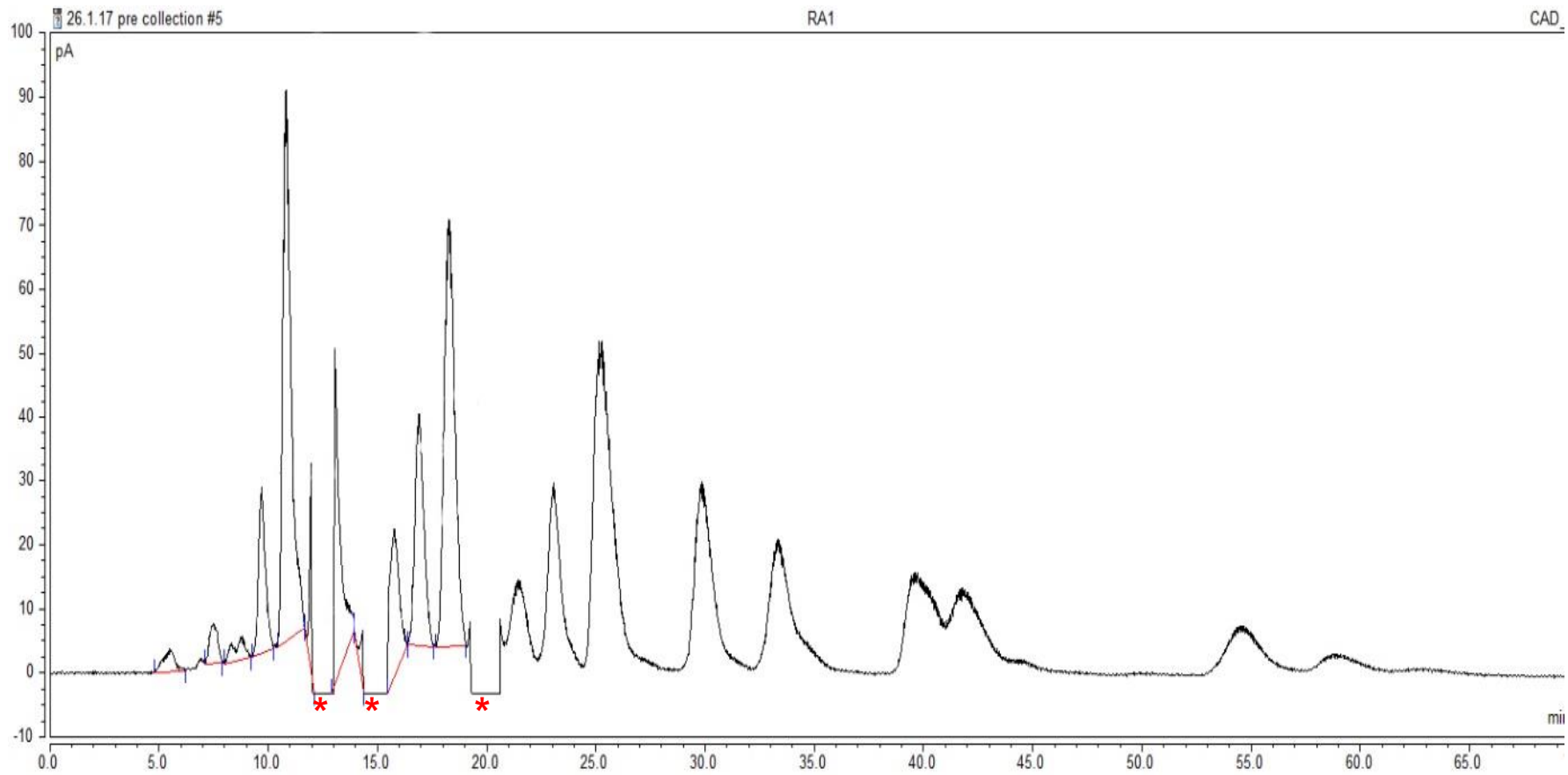
Figure 2.27 Collection run of selected peaks 1, 2 and 3. Red * and gaps identify where fragments eluted from the column have been collected.

All fragments were analysed using an Agilent 1100 series auto-sampler (Agilent Technologies, Santa Clara USA) and a Bruker MicroTOF (Bruker Daltonics, Massachusetts, USA) in positive mode with ESI of samples. ESI-MS spectra were obtained for all fractions using the source parameters:

- Capillary voltage: 4500 V
- End Plate offset: -500 V
- Nebuliser pressure (N_2): 0.4 Bar
- Dry Gas (N_2): 4 L/min
- Dry heater: 200ºC

Collected fragments from HPLC-CAD analysis were labelled with respective fraction number (1 to 6 and 1 to 10). Each fraction for MS analysis was collected in triplicate. Sample volume for MS was optimised to 30µL to achieve an acceptable response defined as above 6000 intensity (see figure 2.28). Each sample was directly injected into the analyser using MeOH (+0.1% Formic acid) and H_2O (+0.1% Formic acid) 90%:10% as mobile phase at a flow rate of 1ml/min. Each run was 3 minutes. Spectra for each peak obtained was recorded and analysed. Figure 2.28 shows a typical mass spectrum report generated for each sample analysed.
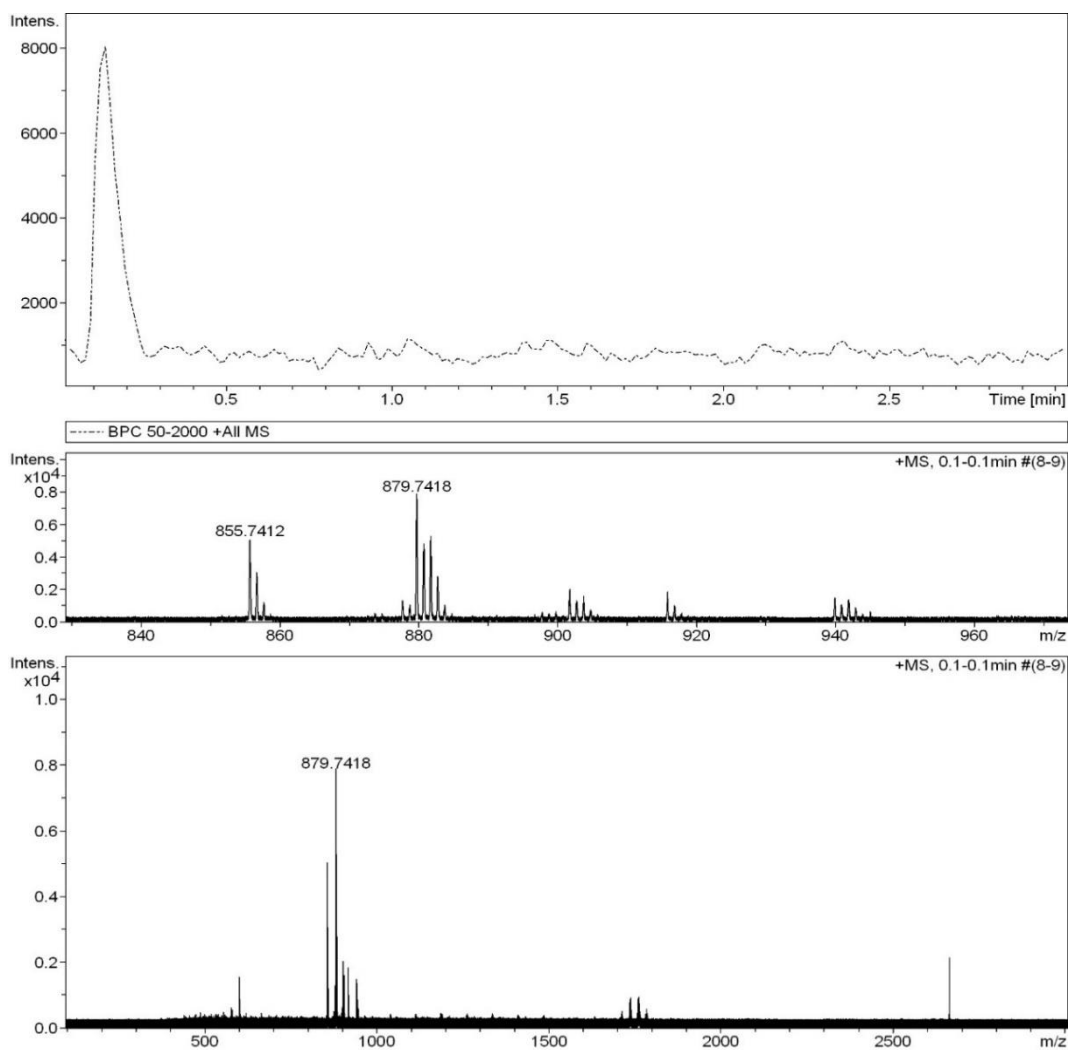
Figure 2.28 ESI-MicroTOF mass spectra report for fraction corresponding to peak 1 in HPLC-CAD chromatogram of Intralipid®.

2.12.2.1 Intralipid® mass spectrometry results and triglyceride identification.

As reported in figure 2.29 to 2.34 the mass spectra for peaks 1 to 6 in Intralipid® 20 % give clear m/z data. Table 2.7 reports the m/z data of multiple runs for each peak.
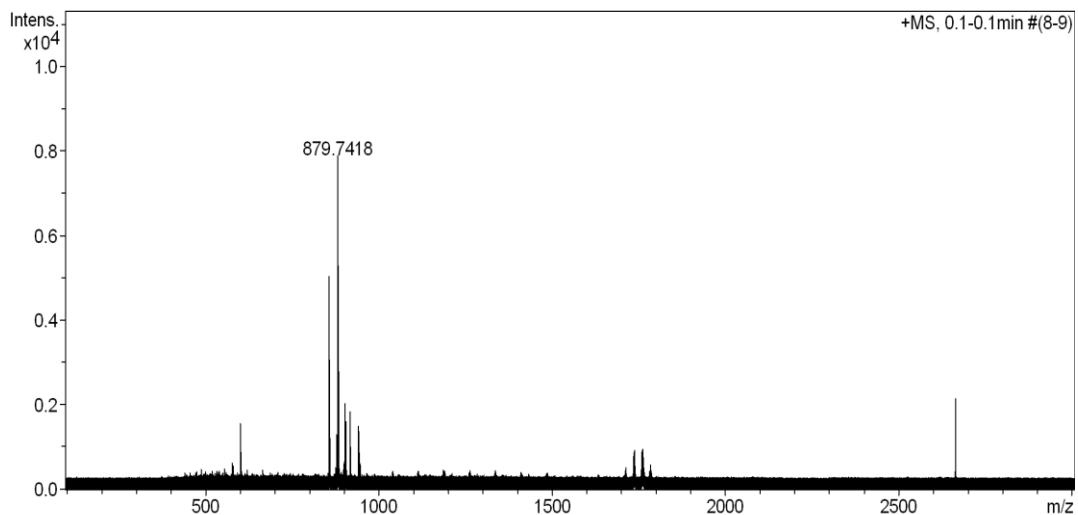
Figure 2.29 Intralipid® Peak 1 mass spectrum.
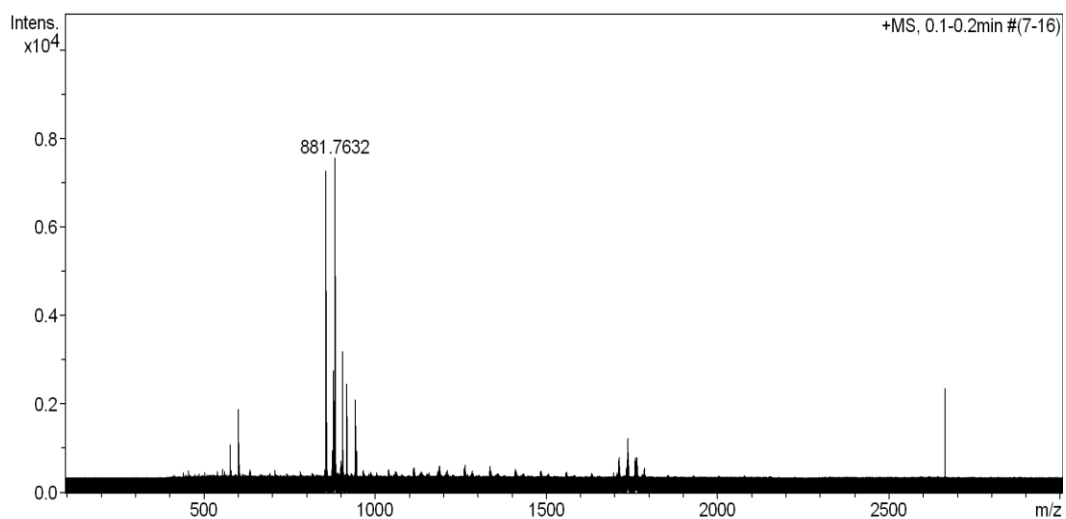
Figure 2.30 Intralipid® Peak 2 mass spectrum.
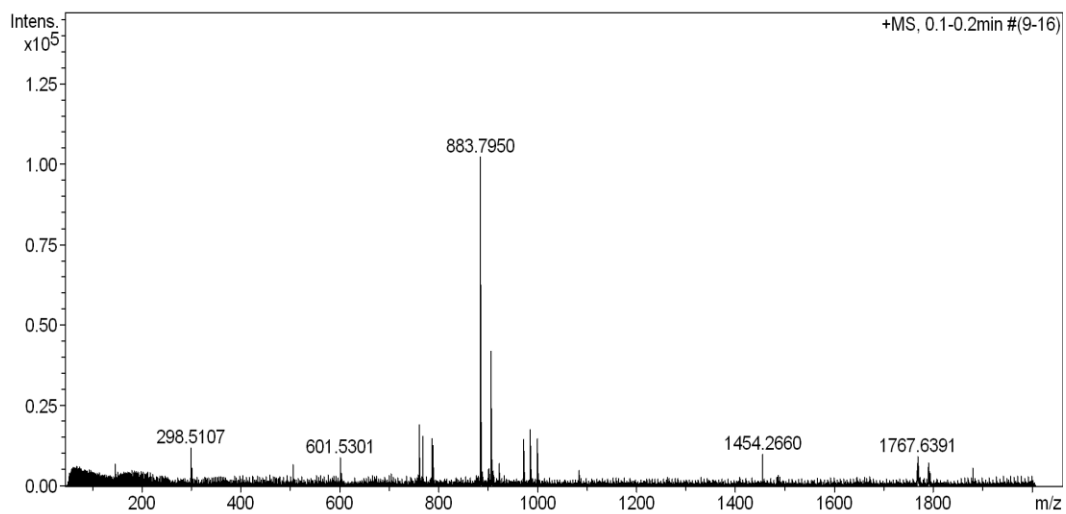
Figure 2.31 Intralipid® Peak 3 mass spectrum.
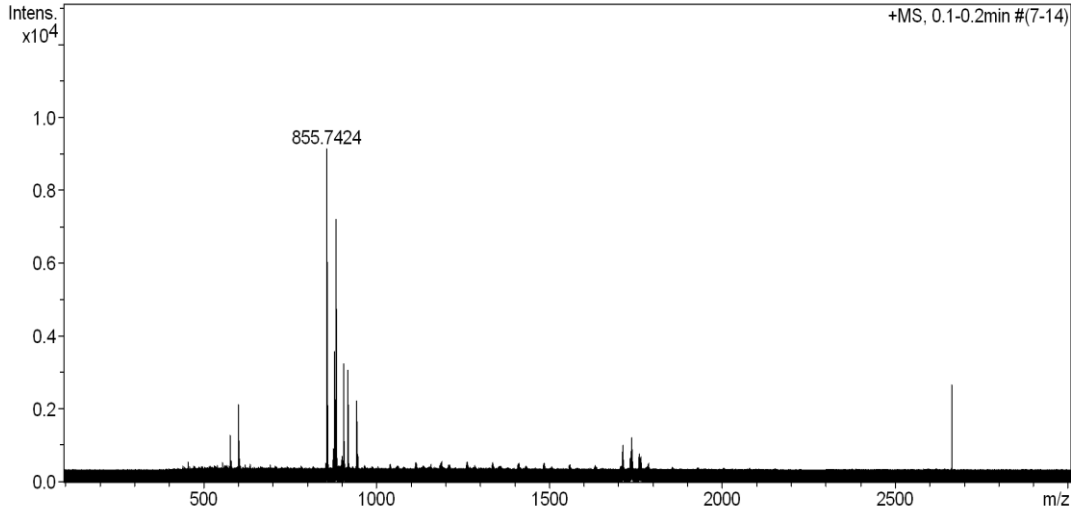
Figure 2.32 Intralipid® Peak 4 mass spectrum
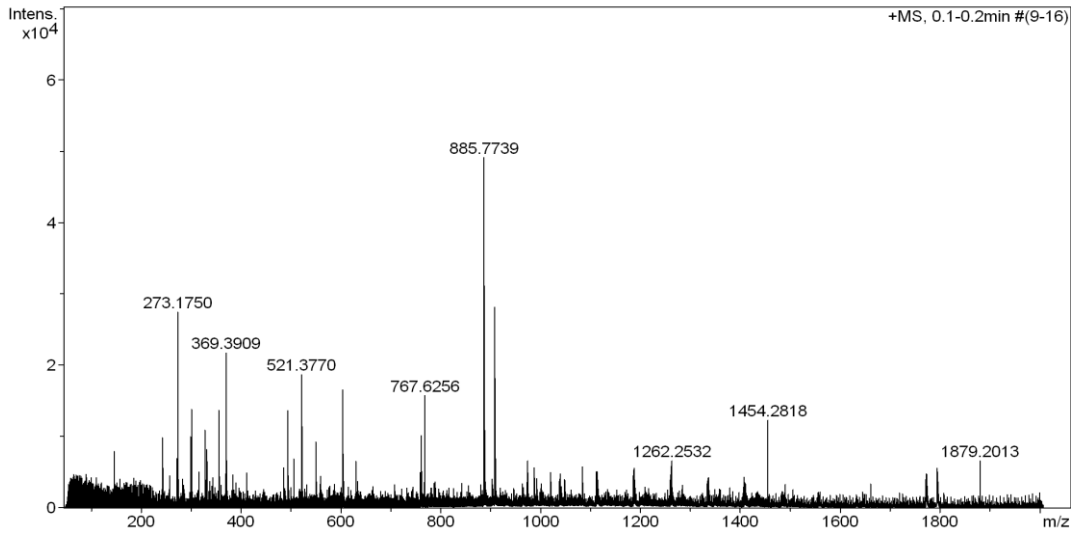
Figure 2.33 Intralipid® Peak 5 mass spectrum.
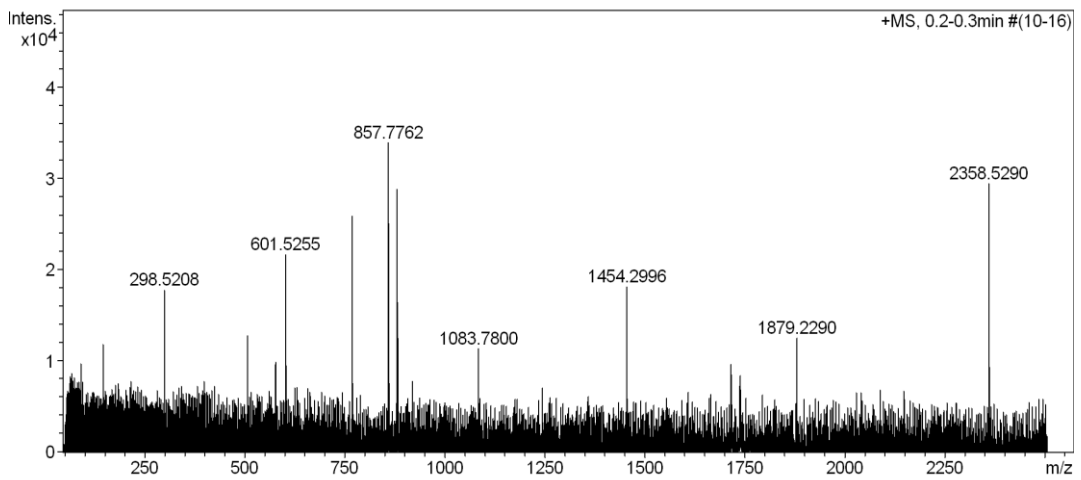
Figure 2.34 Intralipid® Peak 6 mass spectrum.

81

Table 2.7 Mass spectra data for Intralipid® 20 % Peaks 1 to 6. Data in bold represent the main peaks in each repetition and match the predicted TAG data as shown in table 2.8. Data in blue represents [M+Na]⁺ or [2M+H]⁺ peaks also seen in spectra.

	Rep 1	Rep 2	Rep 3	Rep 4	Rep 5
Peak 1	**879.7488**	**879.7428**	**879.7418**	**879.7425**	
		901.7294	855.7412	855.7435	
		855.7424		901.7338	
				599.4886	
Peak 2	**881.7588**	**881.7632**	**881.7615**	**881.7397**	**881.7578**
		855.7414	903.7508	855.7364	903.7478
			855.7375	903.7301	
				599.4911	
				1762.487	
Peak 3	883.8	**883.805**	883.795		
Peak 4	**881.7596**	855.7356	855.7424	855.7414	**881.761**
	855.7405	881.7595	881.7585	881.7601	855.748
	903.748			903.7437	
peak 5	**855.7744**	**855.77**	**855.77**		
	603.5195	355.28	767.64		
	369.38				
peak 6	**879.792**	**879.773**	**857.756**		
	857.7762	857.756	879.442		

From this data the aim of the mass spectrometry was to identify the TAGs responsible for each peak. As per table 1.3 Intralipid® 20% contains 5 fatty acids, linoleic acid (L), oleic acid (O), palmitic acid (P), linolenic acid (Ln) and stearic acid (S). Using the online RCM lipid analysis tool (Murphy 2017) and the LipidMAPS Mass spectrometry peak predictor (Fahy et al. 2007) the average m/z ratios were analysed to identify the possible TAGs present. Table 2.8 displays the possible TAGs that can be attributed to each peak and the occurrence of either the [M+H]⁺ or [M+Na]⁺ ion in each chromatogram.

Table 2.8 Predicted TAGS from spectra data using the RCM lipid analysis tool (Murphy 2017) and the LIPIDMAPS peak predictor (Fahy et al. 2007).

Peak 1	Ion	Predicted m/z		Peak 4	Ion	Predicted m/z
C18:2/18:2/18:2	[M+H]+	879.744		**C18:2/18:2/16:0**	[M+H]+	855.744
	[M+Na]+	901.7259		**C18:1/18:3/16:0**	[M+H]+	855.7439
C18:3/18:2/18:1	[M+Na]+	879.7434		**Peak 5**		
	[M+Na]+	901.258			[M+H]+	885.7908
C18:3/18:3/18:0	[M+Na]+	879.7439		**C18:1/C18:1/C18:1**	[M+Na]+	907.7727
	[M+Na]+	901.7258			2[M+Na]+	1792.5557
Peak 2					[M+H]+	885.7908
C18:2/18:3/18:0	[M+H]+	881.7596		**C18:2/C18:1/C18:0**	[M+Na]+	907.7727
	[M+Na]+	903.7415			2[M+Na]+	1792.5557
	2[M+H]+	1762.5036			[M+H]+	885.7908
C18:3/18:1/18:1	[M+H]+	881.7595		**C18:0/C18:0/C18:3**	[M+Na]+	907.7727
	[M+Na]+	903.7414			2[M+Na]+	1792.5557
C18:2/18:2/18:1	[M+H]+	881.7596				
	[M+Na]+	903.7415		**Peak 6**		
Peak 3				**C18:3/18:0/16:0**	[M+H]+	857.75
C18:2/C18:2/C18:0	[M+H]+	883.78			[M+Na]+	879.75
C18:3/C18:1/C18:0	[M+H]+	883.7863		**C18:1/C18:2/C16:0**	[M+H]+	857.75
C18:1/C18:1/C18:2	[M+H]+	883.7862			[M+Na]+	879.75

As seen in table 2.8 from the mass spectrometry data for each of the peaks 1 to 6 in Intralipid® can be attributed to 2 or 3 TAGs. The mass spectrometry equipment used as detailed above was only sensitive to the level as shown and as such was incapable of looking at distinguishing between TAGs of the same m/z through identifying the fragments of each TAG. If a non-ion trap system was available, TAGs of the same overall m/z can be identified by looking for the loss of each individual fatty acid chain and calculating the remaining fragments m/z (Christie 2003). As such the fatty acid combination in each TAG can be identified. This was as discussed not possible due to the low sensitivity of the mass spectroscopy equipment available.

As an alternative method to enable the prediction of the highest probability TAG attributed to each peak, work by Li et al. (2014) looked in detail at the composition of soy-bean oil, the oil used in Intralipid®, and the TAGs present and the percentage occurrence of each of them within the oil. Figure 2.35 adapted from this work displays the percentage occurrence of each of the TAGs present within the oil. From this data and from the data displayed in table 1.3 showing the percentages of each

fatty acid present within Intralipid®, with the mass spectroscopy data acquired, a reliable prediction was made to attribute an individual TAG to each of the peaks 1 to 6 collected.
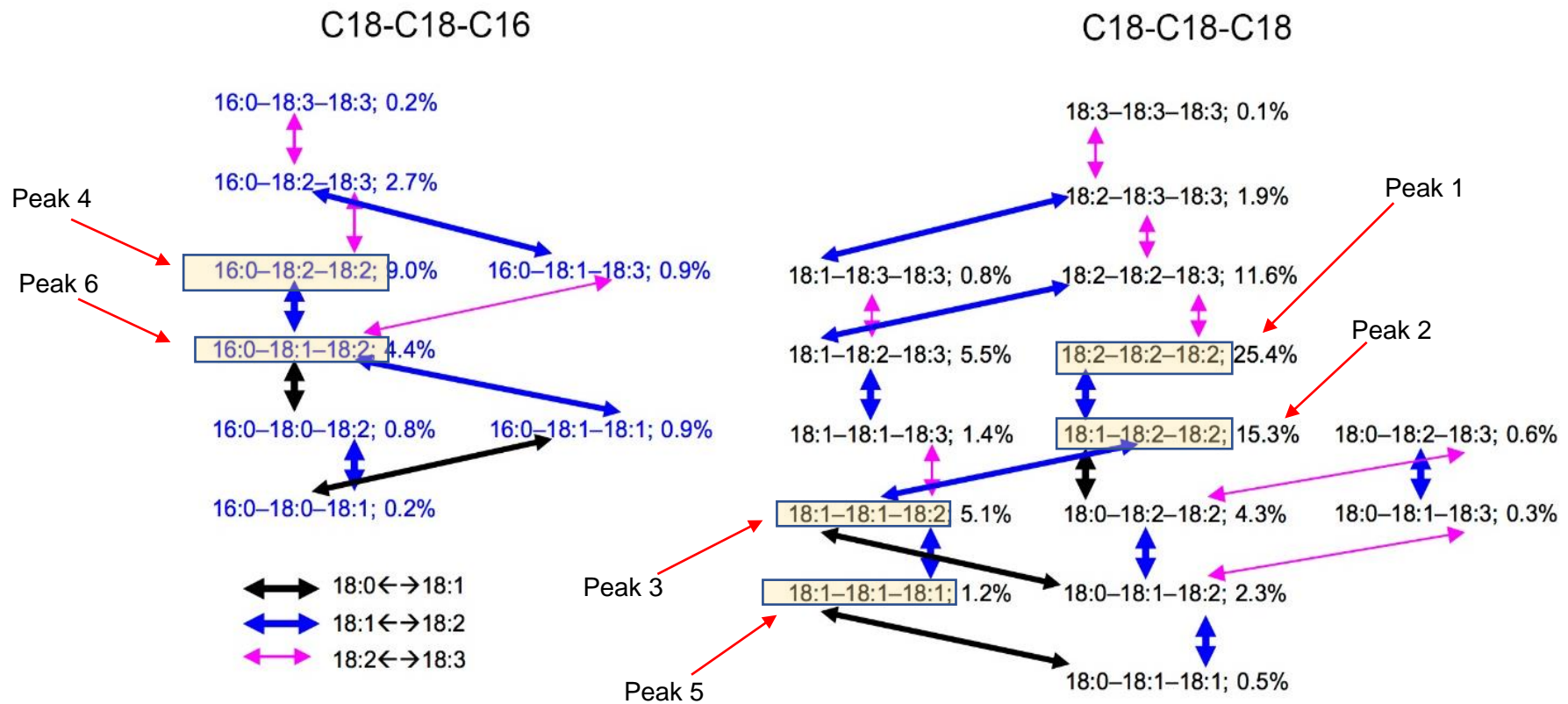
Figure 2.35 Adapted from Lin et al. 2014. Percentage occurrences of TAGs formed in soybean seed oil from two acyl chains (C18 and C16). Each arrow denotes a change in saturation by one double bond Yellow highlighted TAG's and red notations indicate the TAGs with the highest probability of being responsible for the peaks analysed in the HPLC-CAD assay of Intralipid®.

From this data the six peaks collected and analysed within the HPLC-CAD chromatogram of Intralipid® can be attributed to the TAGs within figure 2.35 with a high degree of probability. With regards to the elution order of the TAGs, as predicted by the partition number equation (figure 2.2), the TAG elution order that the mass spectrometry data indicated matches the predicted elution order with reference to carbon bond number and level of unsaturation. As the assay was designed to monitor the main TAGs within such a lipid emulsion and monitor their breakdown and subsequent loss of peak area during storage, the level of probability achieved is satisfactory to establish that the main TAGs present will indeed be monitored by the assay. It is worth noting however that as this is only a prediction of the TAG responsible for each peak, albeit with a high level of probability, the other TAGs shown in table 2.8 for each peak may also form a component of the corresponding peak shown within the HPLC-CAD chromatogram. This however does not present a problem when looking at the potential peroxidation and breakdown of these TAGs as the peaks being monitored form the bulk of the Intralipid® TAGs observed and as such a sufficient level of monitoring to indicate stability of each TAG through storage.

2.12.3 SMOFlipid® mass spectrometry and triglyceride identification

As shown in detail in figure 2.36 peaks 5 to 10 of SMOFlipid and peaks 1 to 6 of Intralipid have the same elution times and chromatographic shapes. Mass spectrometry of each of these peaks in SMOFlipid® was done to confirm their identical m/z data to that of Intralipid®. Table 2.9 shows the mass spectrometry data from peaks 5 to 10 of SMOFlipid. When compared to table 2.8 showing the mass spectrometry data from peaks 1 to 6 of Intralipid® this confirmed the identical TAGs present and that peaks 5 to 10 of SMOFlipid® are indeed attributed to that of soybean oil.
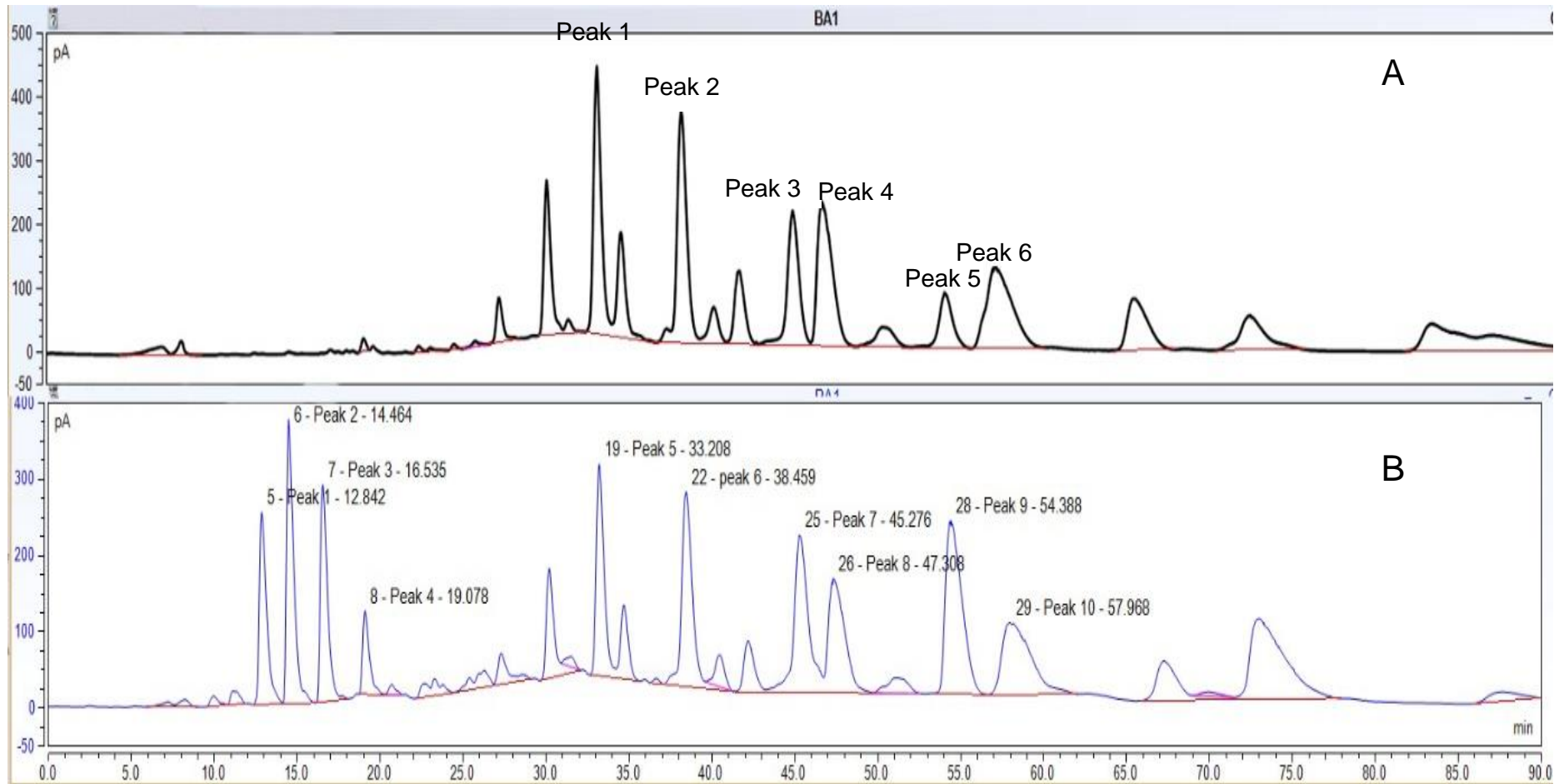
Figure 2.36 A = HPLC-CAD chromatogram of Intralipid®. B = HPLC-CAD chromatogram of SMOFlipid®. Peak 5 to 10 on the SMOFlipid® chromatogram showing the same elution times and peak pattern as Intralipid®.

Table 2.9 Mass spectrometry data for SMOFlipid® peaks 5 to 10.

Peak number	M/z data	Predicted TAG attributed to peak.
5	879.75 [M+H]+ 901.73 [M+Na]+	TG (18:2/18:2/18:2)
6	881.76 [M+H]+ 903.75 [M+Na]+	TG (18:2/18:2/18:1)
7	883.775 [M+H]+	TG (18:1/18:1/18:2)
8	855.74 [M+H]+	TG (18:2/18:2/16:0)
9	855.78 [M+H]+ 907.76 [M+Na]+	TG (18:1/18:1/18:1)
10	857.75 [M+H]+ 879.75 [M+Na]+	TG (18:2/18:1/16:0)

It is significant however, that when comparing the overlaid HPLC-CAD chromatograms of Intralipid and SMOFlipid as seen in figure 2.37 the peak areas observed are different.
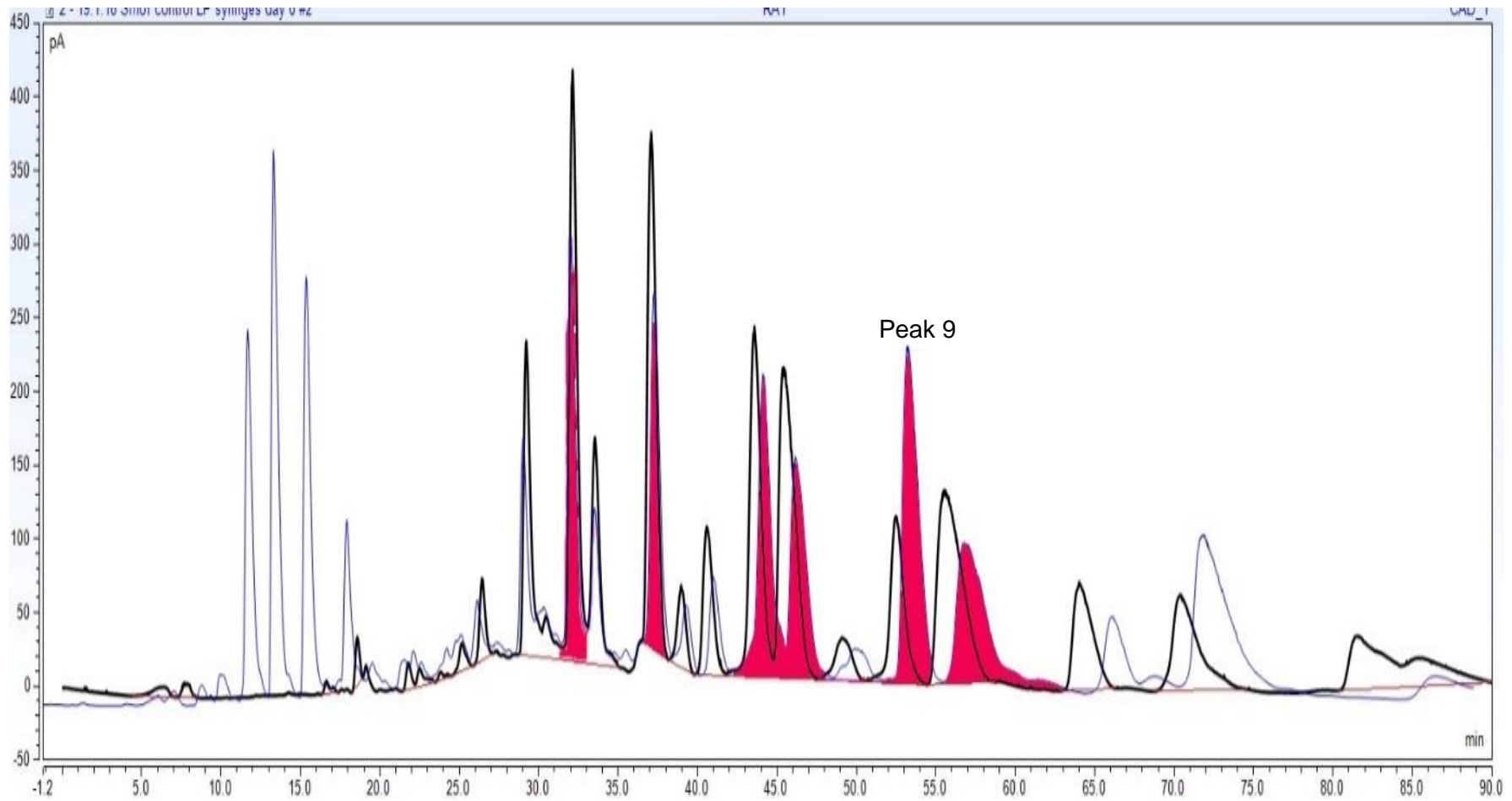
Figure 2.37 Overlaid chromatograms of SMOFlipid® (blue trace) and Intralipid® (black trace). Peaks 5 to 10 of SMOFlipid® are highlighted in red to show the differences in peak size relative to the same Intralipid® peaks.

With regards to the percentage composition of fatty acids in SMOFlipid® vs Intralipid® as shown in table 2.10 the higher % of oleic acid (18:1) is due to the presence of oleic acid in both soybean oil and olive oil found in SMOFlipid®. When looking specifically at the peaks highlighted in figure 2.37 peak 9 is significantly higher in SMOFlipid® than Intralipid®. Looking at the mass spectrometry data for this peak the TAG option attributed to this peak for Intralipid® was 18:2/18:1/18:0 due to its higher occurrence in soysbean oil than TAG 18:1/18:1/18:1. The chromatographic data for SMOFlipid® and the summary of product characteristics (SPmC) for this lipid showed an increase in oleic acid (18:1) and a reduction in linoleic acid (18:2) concentration when compared to Intralipid®. This therefore was used to predict peak 9 of the SMOFlipid® chromatogram to predominately be due to the TAG 18:1/18:1/18:1. This also confirmed that it is probable that whist both the TAGs present with the same m/z data are attributing to the single chromatographic peak seen within the lipid, the predominant TAG responsible for each peak can accurately be predicted. This is sufficient as for Intralipid® to monitor the level of peroxidation and breakdown occurring within the main TAGs with the lipid.

Table 2.10 Fatty acid compositions of SMOFlipid® and Intralipid® as taken from their respective product summary of product characteristics data.

Fatty acid	Carbon number: double bond	SMOFlipid® 20 %	Intralipid® 20 %
Oleic acid	C18:1	23-35%	19-30%
Linoleic acid	C18:2	14-25%	44-62%
Caprylic acid	C8:0	13-24%	-
Palmitic acid	C16:0	7-12%	7-14%
Capric acid	C10:0	5-15%	-
Stearic acid	C18:0	1.5-4%	1.4-5.5%
α-linolenic acid	C18:3	1.5-3.5%	4-11%
EPA	C20:5	1-3.5%	-
DHA	C22:6	1-3.5%	-

With respect to peaks 1 to 4 of the HPLC-CAD chromatogram of SMOFlipid® it was predicted using partition number that the early eluting peaks would be attributed to TAGs containing fatty acids of lower carbon numbers. In the composition of SMOFlipid, such TAGs would be comprised of the unsaturated medium chain fatty acids capric acid (C10) and caprylic acid (C8) sourced from the chemically synthesised coconut oil component of the lipid emulsion. To confirm this and to identify each individual peak 1 to 4, fragments from HPLC elution were collected and subjected to mass spectrometry under the same conditions as above.

Mass spectra for each are displayed in figures 2.38 to 2.41. The mass/charge m/z data was again analysed using the RCM lipid analysis tool (Murphy 2017) and the LIPIDMAPS peak predictor (Fahy et al. 2007). Due to the unsaturated nature of the medium chain triglycerides present only one TAG could be attributed to each of the peaks 1 to 4 of SMOFlipid®, providing a positive identification of these peaks within the chromatogram as shown in table 2.11.
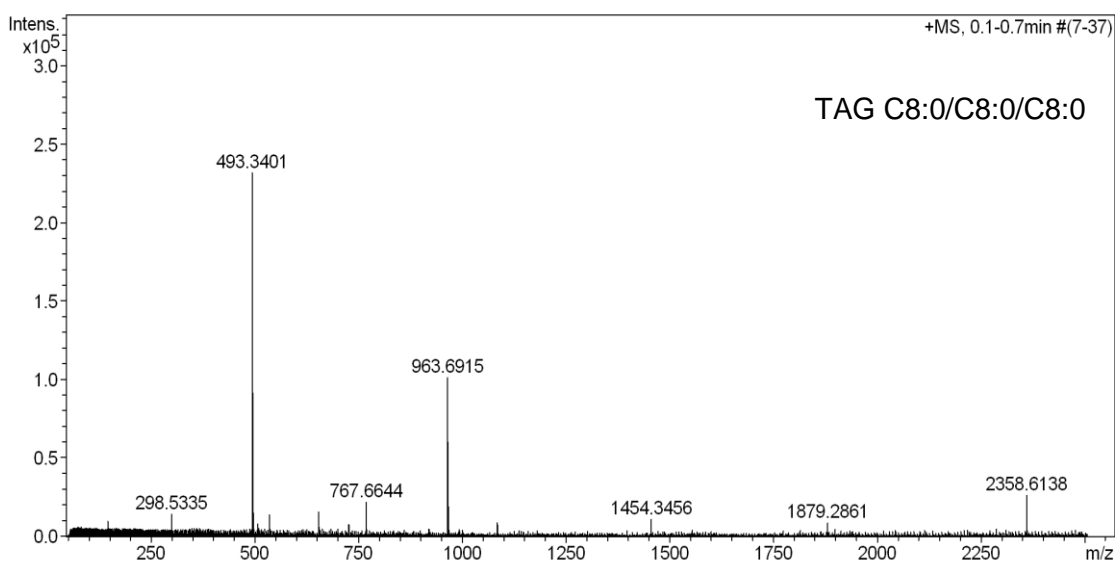
Figure 2.38 Mass spectra of Peak 1 SMOFlipid®.

91
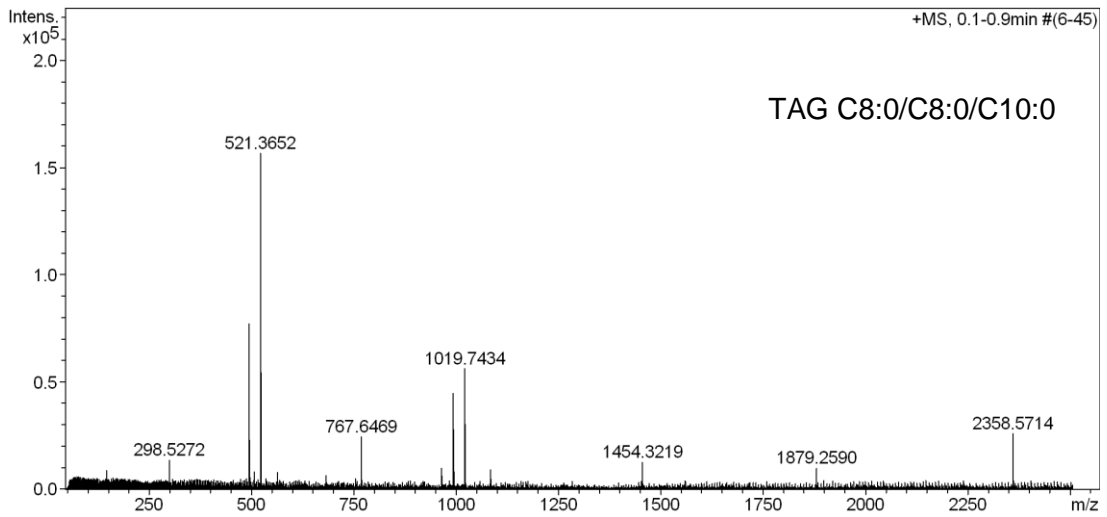
Figure 2.39 Mass spectra of Peak 2 SMOFlipid®.
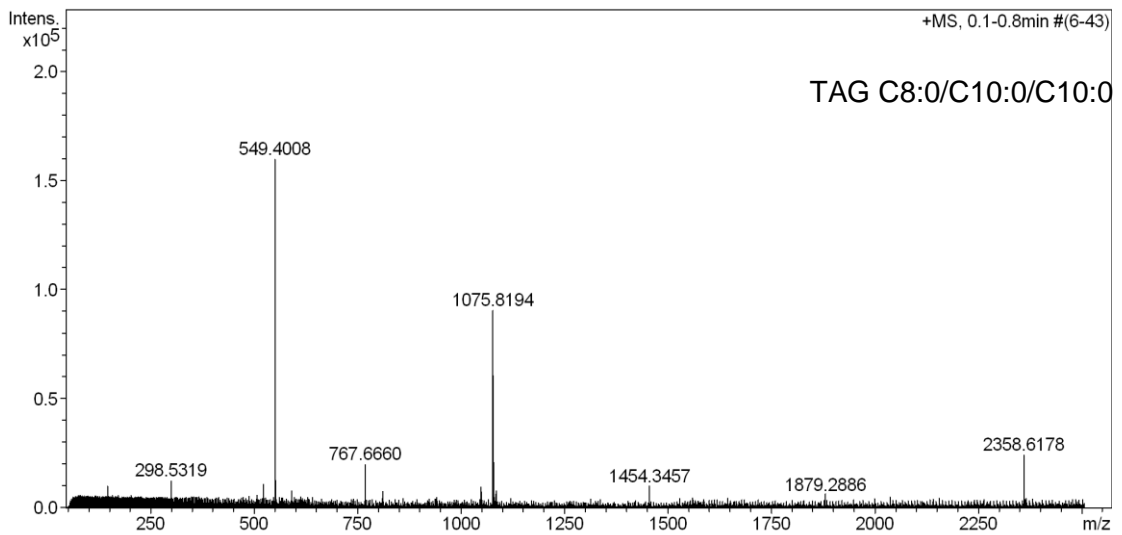
Figure 2.40 Mass spectra Peak 3 SMOFlipid®.
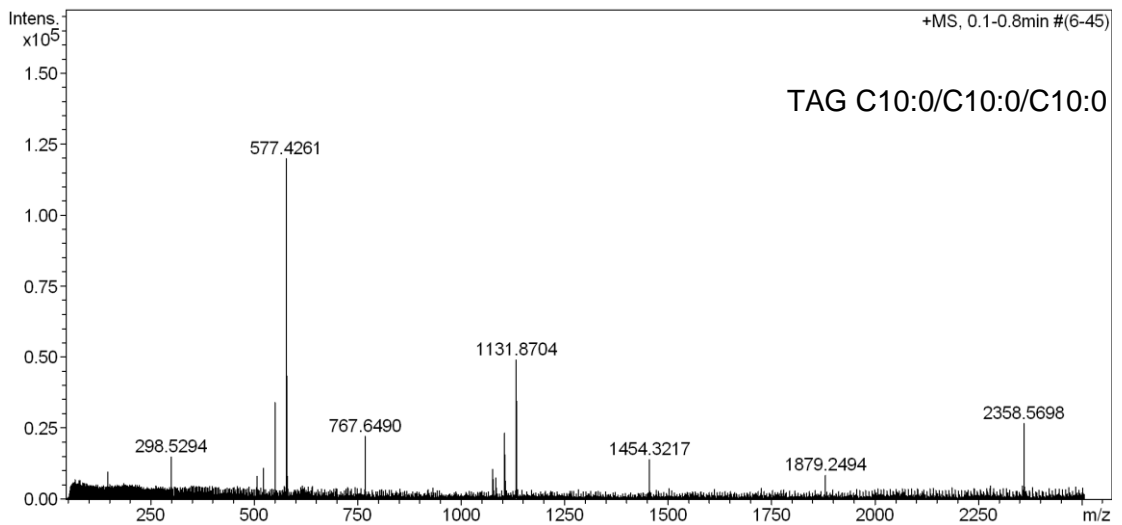
Figure 2.41 Mass spectra Peak 4 SMOFlipid®.

92

Table 2.11 Mass spectra data for Peaks 1 to 4 of SMOFlipid with identified TAG for each peak.

Peak	TAG attributed	M/z theoretical data		M/z experimental data
Peak 1	**C8:0/C8:0/C8:0**	[M+Na]$^+$	493.35	**493.3448**
		2[M+Na]$^+$	963.71	**963.7065**
Peak 2	**C8:0/C8:0/C10:0**	[M+Na]$^+$	521.38	**521.3652**
		[2M+Na]$^+$	1019.77	**1019.7476**
Peak 3	**C8:0/C10:0/C10:0**	[M+Na]$^+$	549.41	**549.3985**
		[2M+Na]$^+$	1075.83	**1075.8214**
Peak 4	**C10:0/C10:0/C10:0**	[M+Na]$^+$	577.44	**577.4292**
		[2M+Na]$^+$	1131.89	**1131.8862**

The mass spectra for peaks 1 to 4 of SMOFlipid® gave data that only showed the sodium adduct of each TAG. Both the spectra data for all Intralipid® peaks and peaks 5 to 10 of SMOFlipid® showed both the sodium adduct of each TAG and the molecular [M+H]$^+$ ion. The presence of sodium within the mass spectrometry data was due to trace sodium contamination of the mobile phases used within the system. The next phase of development was the validation of the HPLC-UV-CAD assay for both Intralipid®, SMOFlipid® and HNE.

2.13 Assay validation

Assay validation for this assay is an integral part of method development and ensures that the assay developed for both Intralipid®, SMOFlipid® and the detection of the breakdown product HNE is accurate, repeatable and reliable for use as an effective tool in monitoring the stability of such lipid emulsions.

2.13.1 International conference on harmonisation.

The International Council for Harmonisation of Technical Requirements for pharmaceuticals for Human Use (ICH) is a body that was formed in 1990 to co-ordinate the process of pharmaceutical product registration across the different world-wide regulatory bodies. The aim of the ICH is to ensure the same regulatory standards are met throughout the registration process of every pharmaceutical products across the world regardless of the location and regulatory body responsible for the registration procedures (Harmonisation 2018). As such the ICH has released a series of technical documents that are designed for use during the

validation procedures and registration procedures of pharmaceutical products to ensure testing of such products is comparable in every registration. Whilst this body of work is aimed at developing a stability indicating assay for lipid emulsions and as such will not be used for product registration, the ICH guidelines for assay validation provide an in-depth testing regime that was used as a guide for this assay validation.

The ICH guideline 'Validation of analytical procedures Q2R1' (Q2R1) (Shabir 2004; ICH 2005) is the technical document that was produced by the ICH to facilitate assay validation of testing procedures used for product registration. This document will be adapted and used as a guide for this stability indicating HPLC assay. Each section of the assay (HPLC-UV assay of HNE and HPLC-CAD assay of TAGs) will be validated separately due to their differing requirements for validation.

2.13.2 HPLC-UV of HNE assay validation

2.13.2.1 Linearity

Linearity of a method is a measure the accuracy of detector response to a range of concentrations of a particular compound. This is vital to determine for a stability indicating assay as HNE is a degradation compound of the lipid emulsions being tested and as such the concentration of HNE is expected to change during storage as it is produced by peroxidation of the fatty acids within the TAGs of the lipid emulsion. Therefore, the change in peak area needs to accurately represent the concentration change of HNE during testing. The ICH guidelines state that a minimum of five different concentrations should be tested across a representative range of HNE concentrations that will likely be found during degradation of the lipid emulsions. This is an area that is difficult to quantify before testing has occurred due to the fact that it is unknown how much HNE is likely to be produced within a stability study. In an aim to overcome this issue and give a guide for the concentrations that should be used for the linearity calculations for the assay, degraded Intralipid® 20 % that was held in a 50 ml oxygen permeable syringe (BD Plastipak, Beckton Dickinson, SA), at room temperature with no light protection for 90 days was run through the developed assay and the level of HNE calculated against a standard run of HNE at 6 µg/ml. Figure 2.42 Shows the degraded Intralipid® sample HPLC-UV chromatogram.

94
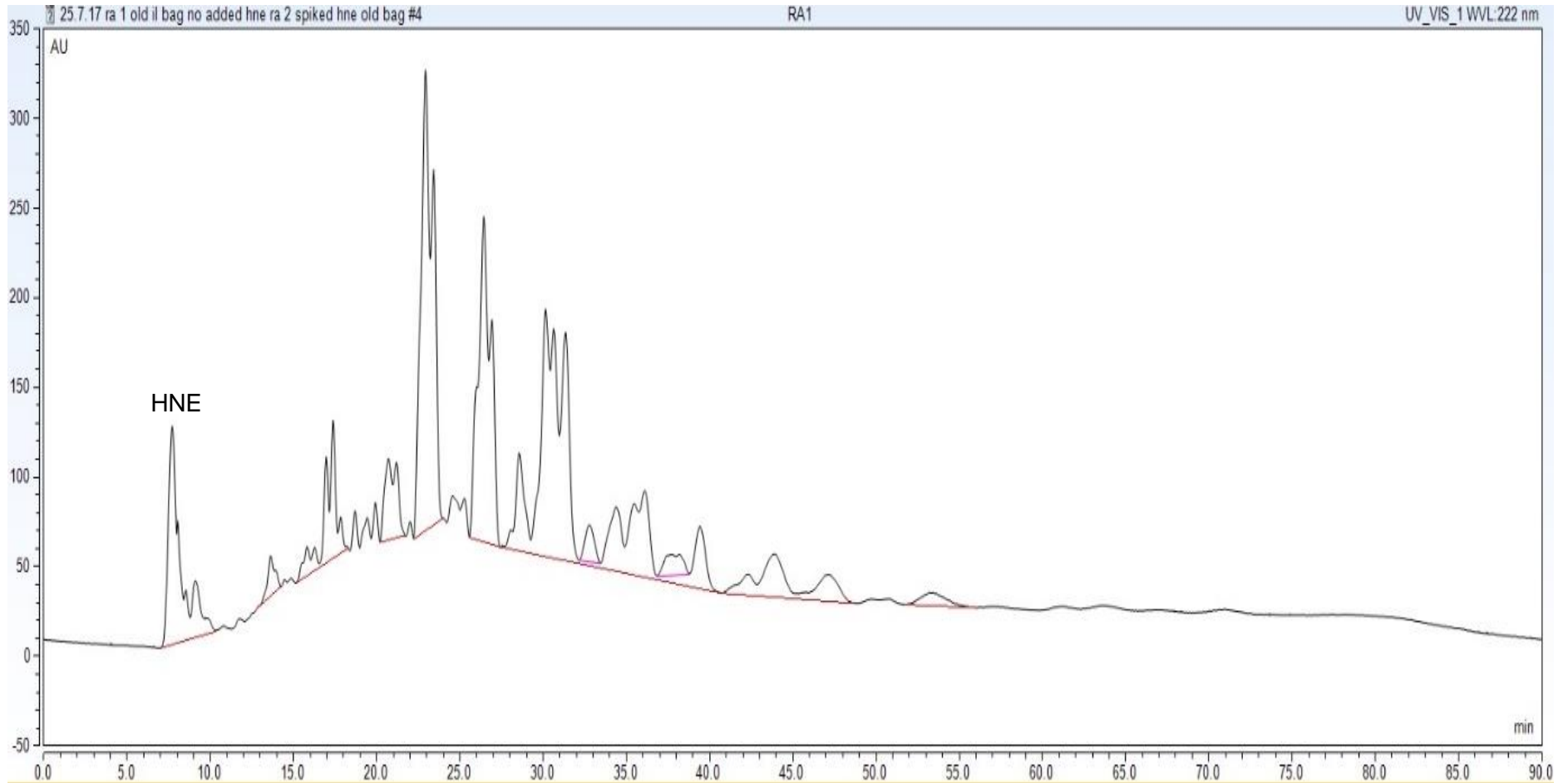
Figure 2.42 Old Intralipid® degraded over 90 days at room temperature with no light protection in a 50 ml syringe.

From this the peak area of HNE in degraded Intralipid® was averaged (triplicate runs) and gave 149.476 AU. HNE standard 12 µg in 2 ml new Intralipid® gave an average peak area of 29.436. From this is was calculated as an estimate that the maximum concentration of HNE likely to be created through the stability studies would be around 60.93 µg in 2ml of Intralipid®. This amount was therefore used as the 100% concentration for the production of calibration curves for HNE. Five concentrations of 12.5, 25, 50, 75 and 100% of estimated HNE production were calculated and 2 mls of IPA with addition of HNE standards were created as per table 2.12. As the stock solution of HNE was at a concentration of 1mg/100µl, 20 µg of this stock was diluted in 180µl of IPA to give a concentration of 1µg/µl. From this, required volumes of this diluted stock were added to each vial as per table 2.12. IPA was used instead of Intralipid® for HNE calibration runs to ensure clean peaks were observed for the HNE standards. The elution time and peak size was comparable to HNE in Intralipid®, confirming that substituting IPA for Intralipid® was acceptable for HNE calibration.

Table 2.12 Calibration concentrations for HNE.

Calibration Concentration	HNE amount (µg)	HNE concentration (µM)	IPA volume (ml)
100%	64	204.83	1.946
75%	48	153.62	1.962
50%	32	102.51	1.978
25%	16	51.21	1.984
12.5%	8	25.62	1.992

All concentrations were run in triplicate and calibration curves of peak area (absorbance) and concentration were calculated with standard deviation error bars. Figure 2.43 shows the calibration curve created for HNE. As the UV is a linear detector a linear regression line was added to the graph. Linearity is expressed as a value of R^2 which is how well the data points plotted fit the linear regression line. Usually an R^2 value of greater than 0.999 is acceptable however, this limit is less for impurities (0.98) (Shabir 2004). As HNE being monitored is a degradation product of the lipid emulsions being tested a level above 0.99 was deemed to be acceptable. The calibration graph plotted gave an R^2 value of 0.9972 showing an acceptable

level of linearity across all concentrations predicted to be seen through assay use in stability testing.
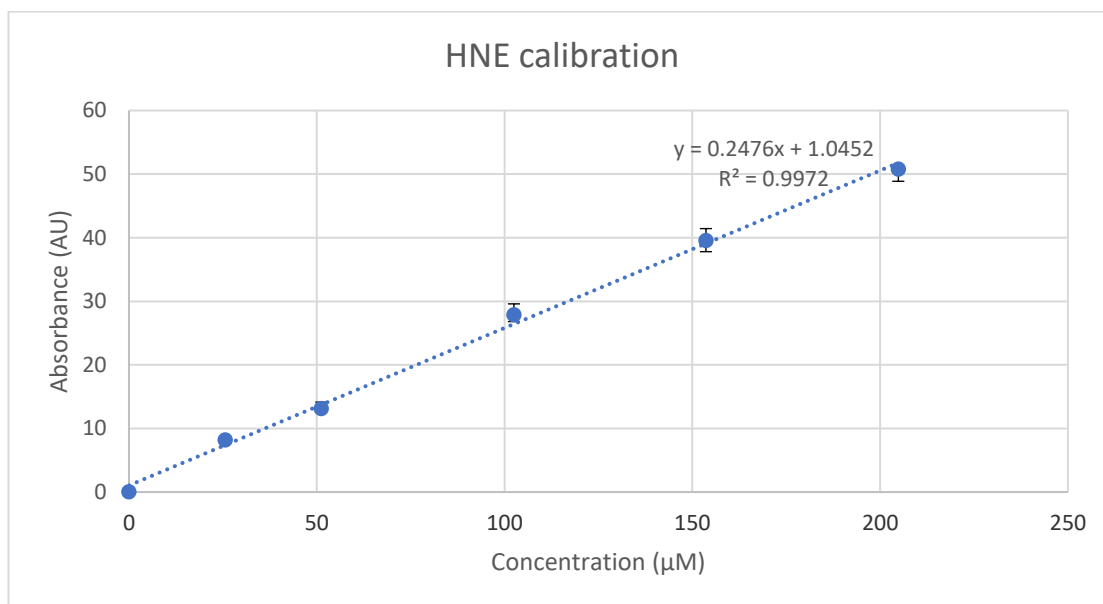
Figure 2.43 Calibration plot for HNE in IPA.

Accuracy of a method is defined as the closeness of agreement between the value which is accepted as a true value and the value recorded during the test procedure (ICH 2005). Acceptable values lie between 80 % and 120 % (Synder et al. 1997). As shown in table 2.13 the accuracy of the assay across five concentrations of HNE all lie within 84.35 to 117.5 % showing an acceptable level of accuracy for the method.

Precision is a measure of how reproducible results from a method are and is measured in a variety of ways according to the ICH guidelines. Precision is expressed as relative standard deviation (RSD), the lower the RSD achieved the better. No set limits exist, and RSD levels will vary depending on the detector chosen.

ICH guidelines state that repeatability, intermediate precision and reproducibility are all ways of measuring the precision of a particular method (ICH 2005). Repeatability also termed intra-day repeatability is calculated as the RSD of multiple runs of the sample over a short period of time one after the next. Intermediate precision is a measure of inter-day repeatability where injections are carried out using the same

concentrations over different days and different weeks to measure repeatability during different days and therefore different laboratory environmental conditions. Intra-day repeatability was carried out in triplicate runs of each concentration used for calibration curve creation and inter-day repeatability was carried out on separate days on different weeks giving an n of 6 runs (Synder et al. 1997; Shabir 2004). Data in table 2.13 shows the RSD results for each of the concentrations. All RSDs fall under 7.5% showing an acceptable level of repeatability. Reproducibility is a measure of precision between different laboratories and as such was not tested due to lack of availability of equipment in a different laboratory for testing. Whilst the assay being developed is a stability assessing one that ideally will be used to test lipid emulsion stability during development and when testing different parenteral nutrition regimes, for the purpose of this body of work all stability testing will be carried out in the same laboratory as assay development and validation and as such reproducibility was not tested.

Table 2.13 Accuracy and Precision values for HNE assay validation.

| HNE concentration (µM) | Precision | | Accuracy |
	RSD_1 (%) (n=3)	RSD_2 (%) (n=6)	(%)
25.6	7.33	1.05	117.50
51.21	3.07	1.70	84.35
102.51	7.19	3.76	96.90
153.62	5.40	4.37	90.14
204.83	5.53	3.75	97.39

2.13.2.3 Resolution

Resolution is defined as the level of baseline resolution or separation between two peaks within a chromatogram (Synder et al. 1997). The better the resolution the superior the integration of each peak and therefore the more accurate the data recorded. Whilst resolution as a measure is not within the ICH Q2R1 technical document, it is a good indicator of the ability of an assay to accurately quantify specific peaks within a chromatogram. Resolution was measure for the HNE peak against the next eluting peak from Intralipid® and SMOFlipid® calculated using Chromeleon (Thermo Scientific) chromatography software. The resolution equation used is detailed in figure 2.44.

$$R_s = \frac{1.18\,(T_2 - T_1)}{(W50_1 + W50_2)}$$

Figure 2.44 Resolution equation based on the European Pharmacopeia method. T_1 and T_2 = retention times of two adjacent peaks, $W50_1$ and $W50_2$ = width of adjacent peaks at 50% of peak height.

A resolution of over 1.5 is optimal and shows definite baseline resolution between eluting peaks. Figures 2.45 and 2.46 shows the chromatograms of HNE standard added to Intralipid® and SMOFlipid® to enable resolution to be calculated. As shown the resolution for HNE in both lipids is well above the 1.5 minimum for baseline resolution.
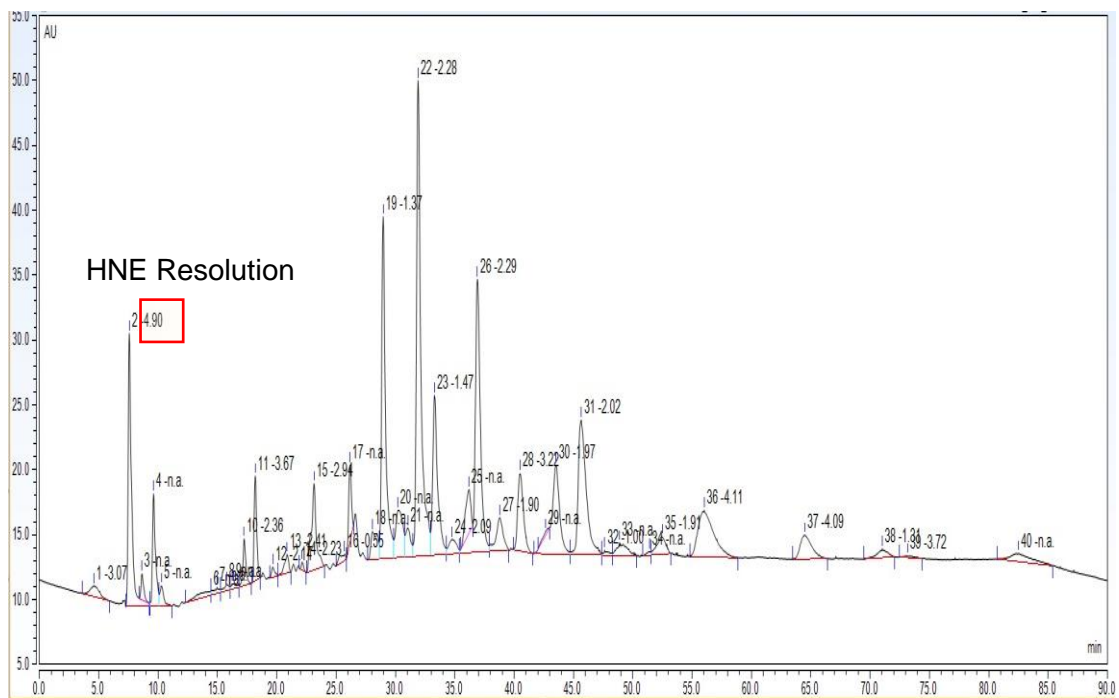
Figure 2.45 HPLC chromatogram of HNE in Intralipid® with Chromeleon calculated resolution for each peak.
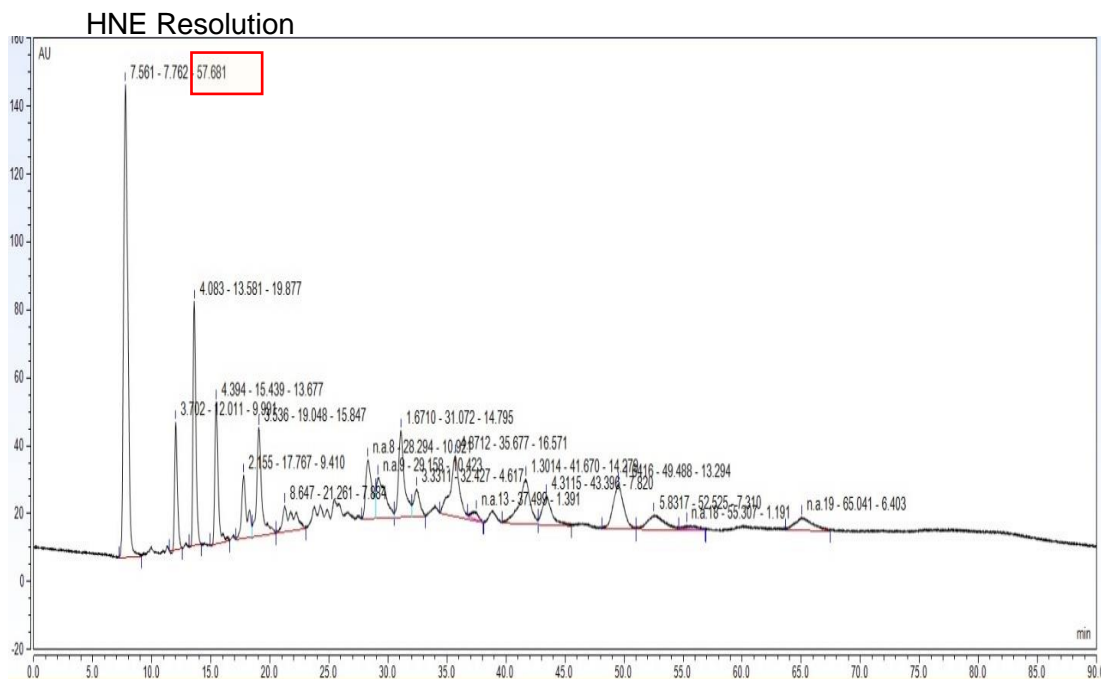
Figure 2.46 HPLC chromatogram of HNE in SMOFlipid® with Chromeleon calculated resolution for HNE peak.

2.13.2.4 Limits of detection and quantification

Limit of detection (LOD) is recognised as the smallest amount of analyte that can be detected from the baseline of the chromatogram. Limit of Quantification (LOQ) is the smallest amount of sample that can be quantified with a repeatable and reproducible level of accuracy. There are multiple methods available for calculating both LODs and LOQs that are recognised as acceptable by the ICH. Using signal to noise ratio is one way of determining each with a signal to noise ratio of 3 and 10 being calculated as the LOD and LOQ respectively. From the calibration chromatograms for HNE using this signal to noise method LOD was calculated as 3.123 µM and LOQ as 8.974 µM. As a comparison both LODs and LOQs were calculated from the linear regression plot (figure 2.43) using the standard deviation from triplicate runs from each calibration concentration (table 2.13). These figures were calculated using the equation shown in figure 2.47 and gave a LOD of 2.958 µM and an LOQ of 8.765 µM.

$$LOD = \frac{3.3\sigma}{S} \qquad\qquad LOQ = \frac{10\sigma}{S}$$

Figure 2.47 Limit of detection and Limit of Quantification equations based on response and shape of calibration plot.

For the best results possible, the higher LOD and LOQ from the signal to noise baseline calculations were therefore used.

As per the ICH guidelines on assay validation (ICH 2005) it is typical for degradation studies of a sample to be carried out to ensure upon degradation that no degradation products interfere with the peak being analysed. This is important as this is a stability indicating assay, but as HNE is a degradation product itself and the method has been developed to separate this from any eluting TAG peaks that will be studied, a degradation study per say has not been carried out for the HNE portion of the assay. As shown from the chromatogram in figure 2.42 degraded Intralipid® showing the production of HNE was run through the final method and clearly separated the degradation products from the TAGs. It is also worth noting that the only peak being monitored by the UV detector within the assay is that of HNE and therefore as this peak showed good resolution from TAGs, it is sufficient to validate the assay for HNE.

2.13.3 Triglyceride HPLC-CAD validation

2.13.3.1 Intralipid® validation

2.13.3.1.1 Linearity

The CAD detector is a non-linear detector and therefore calibration curves created are subjected to a second order polynomial regression line fit. SPC data for both IVLEs provides ranges of concentrations for each fatty acid present. This prevents the individual concentrations of specific triglycerides from being calculated due to the variability of fatty acid concentrations in each IVLE. Individual triglyceride standards cannot be used as internal standards due to the formulation properties of the emulsion. Therefore, to overcome these issues concentrations of 12.5, 25, 50, 75 and 100 % v/v of each IVLE diluted with water were created to enable calibration curves to be created. Figures 2.48 to 2.53 show the calibration curves for each of the six peaks selected within Intralipid®.
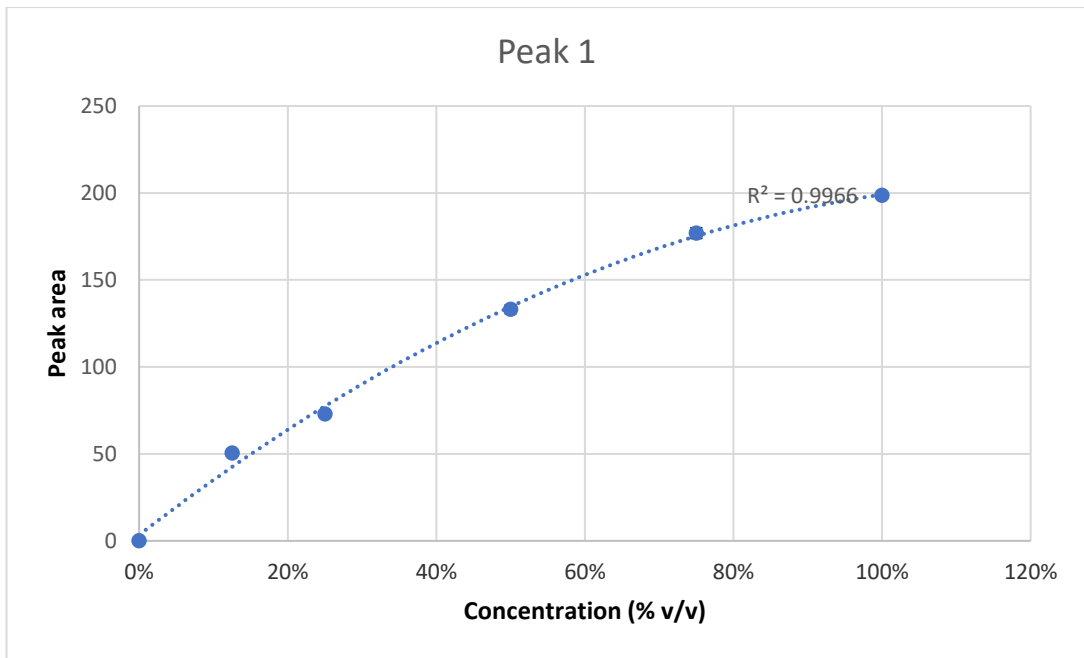
Figure 2.48 Calibration plot for Intralipid® Peak 1.
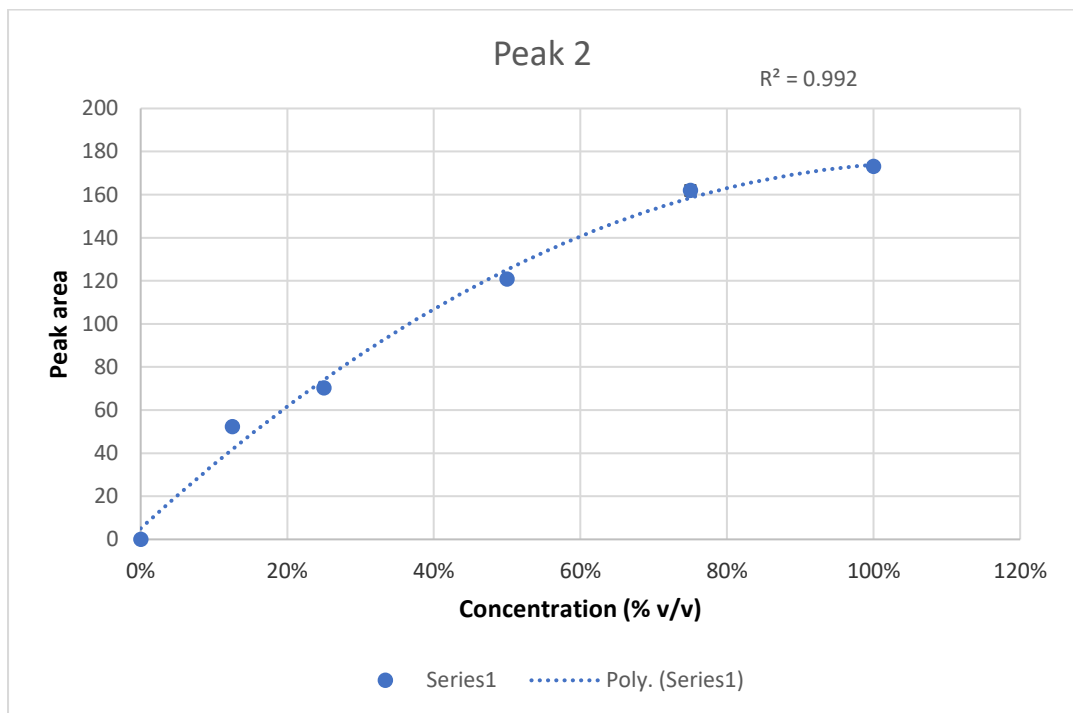
Figure 2.49 Calibration plot for Intralipid® Peak 2.
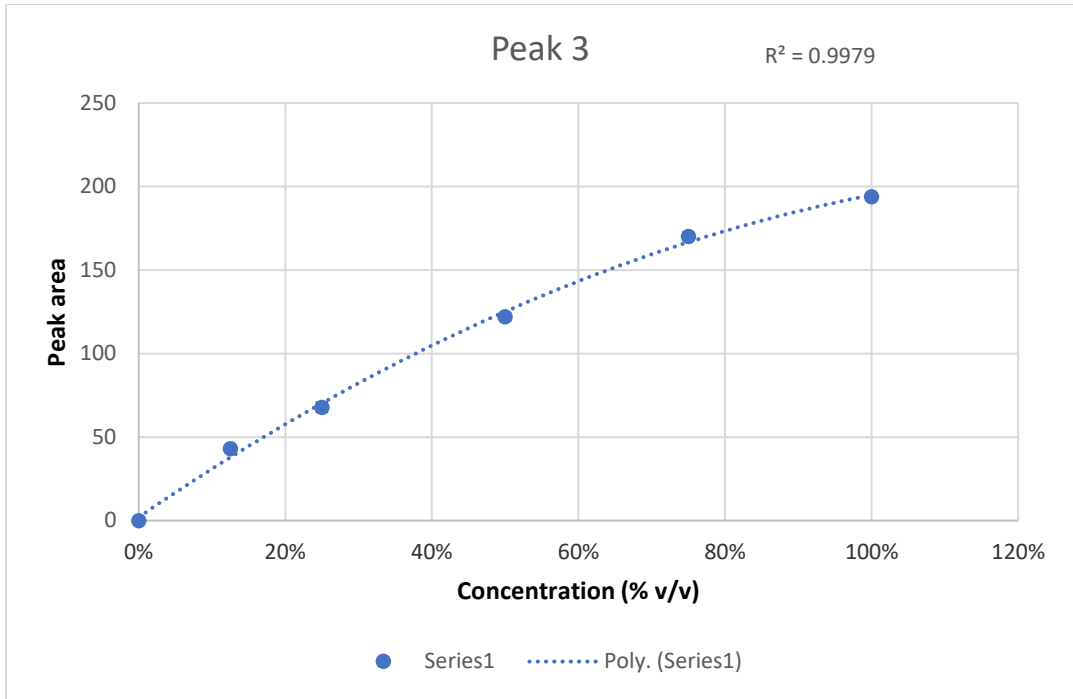
Figure 2.50 Calibration Plot for Intralipid® Peak 3.
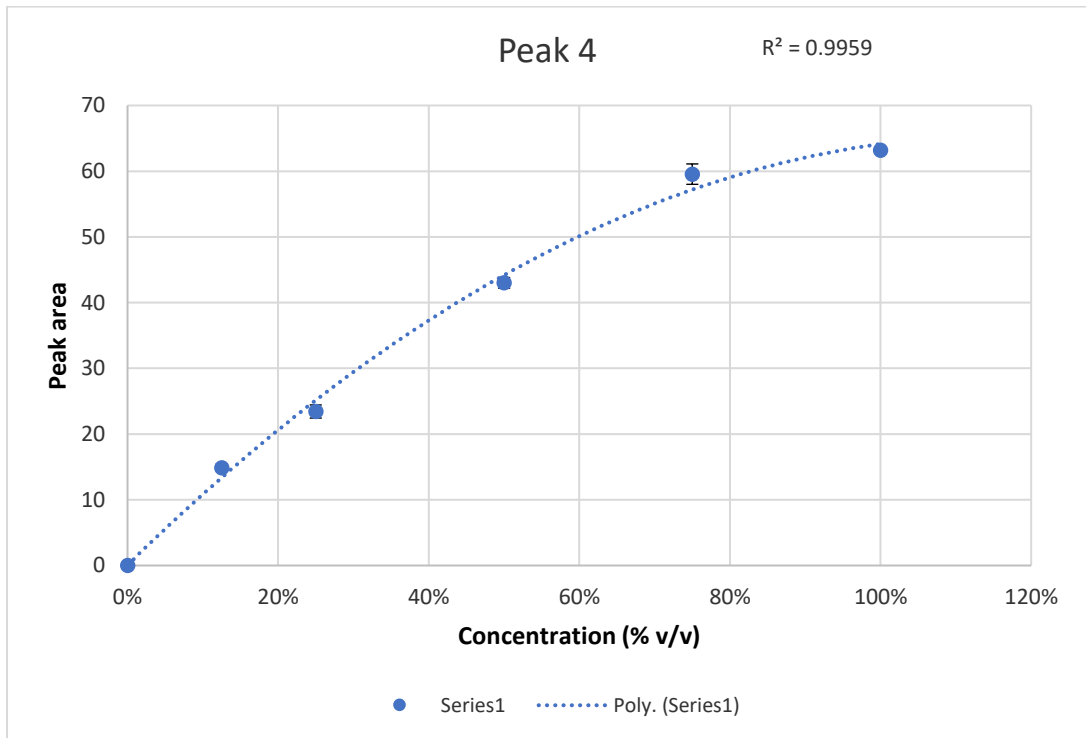
Figure 2.51 Calibration plot for Intralipid® Peak 4.
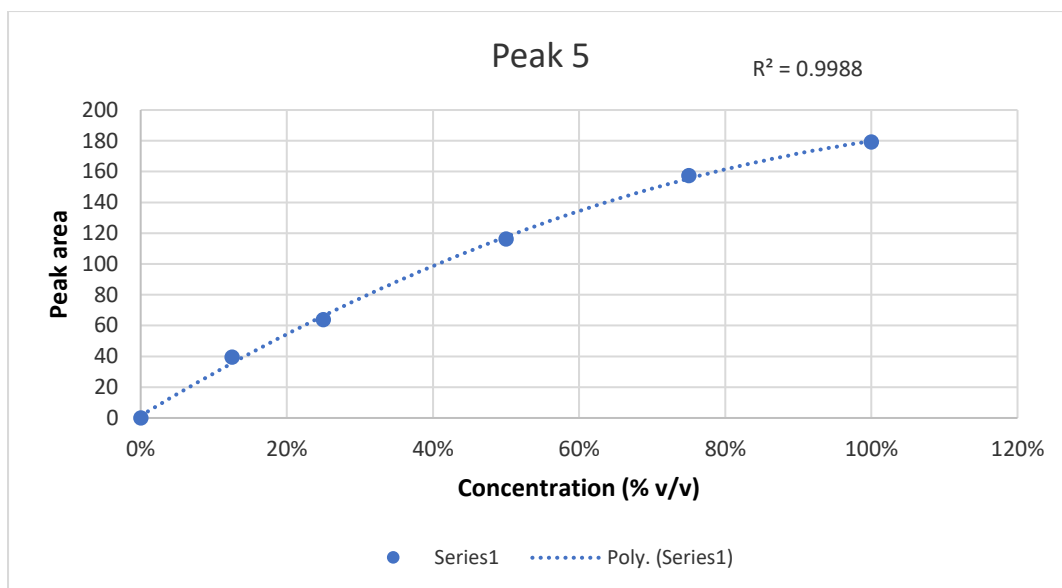
Figure 2.52 Calibration plot for Intralipid® Peak 5.
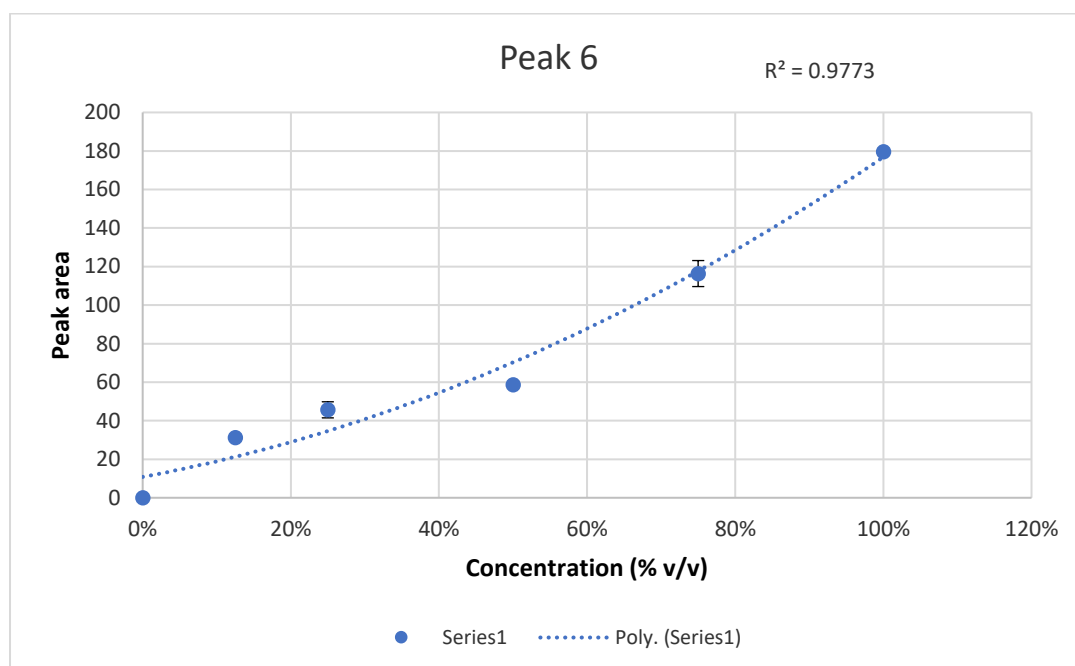
Figure 2.53 Calibration plot for Intralipid® Peak 6.

As summarised in table 2.14 The R^2 values for all of the six peaks validated gave values of above 0.99 with the exception of peak 6 which gave an R^2 value of 0.9773. Whilst this is less than the optimal 0.99 value, as the assay is not being used for product registration and all other peaks are within the optimal 0.99 value it was decided that this level of 0.977 was acceptable for one TAG peak within the chromatogram.

Table 2.14 Calibration linearity summary for all selected Intralipid® peaks.

	Peak number	R^2
Intralipid® 20 %	1	0.996
	2	0.992
	3	0.997
	4	0.995
	5	0.998
	6	0.977

2.13.3.1.2 Precision and accuracy

Precision both inter and intra-day were tested for all six peaks in the same way as for HNE (2.12.2.2). Table 2.15 shows the precision results for each of the six peaks within Intralipid®.

Table 2.15 Precision results for Intralipid®.

Intralipid® peak number	Precision	
	Intra-day (RSD %) n = 3	Inter-day (RSD %) n = 6
1	1.689	1.931
2	3.679	1.567
3	2.079	4.534
4	5.209	4.225
5	0.566	3.812
6	3.879	6.337

The RSD precision results show a maximum RSD of 6.337 with most of the results within a maximum RSD of 5 %. The CAD detector factory testing shows an ideal RSD of around 2 %, however, multiple assays have shown that precision RSD up to a limit of 5 % is acceptable (Crafts et al. 2011). Therefore, the results from the peaks for Intralipid® were considered to be acceptable.

As shown in table 1.3 the SPC data for Intralipid® is given as a percentage range of each fatty acid present. Therefore, as such both the amounts of each TAG created

from these fatty acids and the ultimate concentration of each TAG present cannot be accurately calculated. If considering oils rather than emulsions, normal practise would be to spike each TAG with a known amount of standard to ascertain the concentration of each TAG present. This however is not possible for this analyte due to the nature of the emulsion being tested. As discussed earlier in this chapter, spiking an emulsion with a TAG standard will not produce the same elution peak as the TAG within the emulsion. Therefore, in this case accuracy of the assay cannot be calculated. However, as all other validation parameters were tested successfully this was deemed as acceptable for this assay as the aim of the assay is to monitor the changes and loss of particular TAGs during storage. This data will not be able to be shown in terms of molarity concentration change of each TAG but will be presented as a percentage loss against a control reference standard of new lipid.

2.13.3.1.3 Limits of Detection and Quantification

When considering the validation of the CAD section of the assay for the quantification of TAGs, LOD and LOQ cannot be calculated due to the limited information given in each of the IVLE's SPC. As discussed above, amounts are given as a range of concentrations of individual fatty acids. Due to this, exact concentrations of each triglyceride attributed to each selected peak cannot be calculated, preventing LOD and LOQ from being calculated as a molarity. However, LOD and LOQ can be expressed as a percentage concentration from a neat standard (100 %) of IVLE. For Intralipid® 20 %, the LOD and LOQ for the smallest measured peak (peak 6) were 0.64 % and 2.32 % respectively. For the purposes of the use of the assay, such LOD's and LOQ's are sufficient validation as, during storage before delivery to the patient, the amount of TAGs lost will be no more than 50 % as shown through the testing of a 90-day sample of Intralipid®.

2.13.3.1.4 Resolution

Resolution for each of the six peaks was calculated using Chromeleon software using the formula described in figure 2.44. Figure 2.54 shows the resolution calculated for each Intralipid peak. All peaks gave a resolution above 1.5 except peak 3 where the resolution was 1.20, however due to the number of peaks being analysed and the complexity of the sample present this was deemed as acceptable.

It would not be possible to optimise the method further to increase the resolution of one particular peak without disrupting all other peaks within the chromatogram.
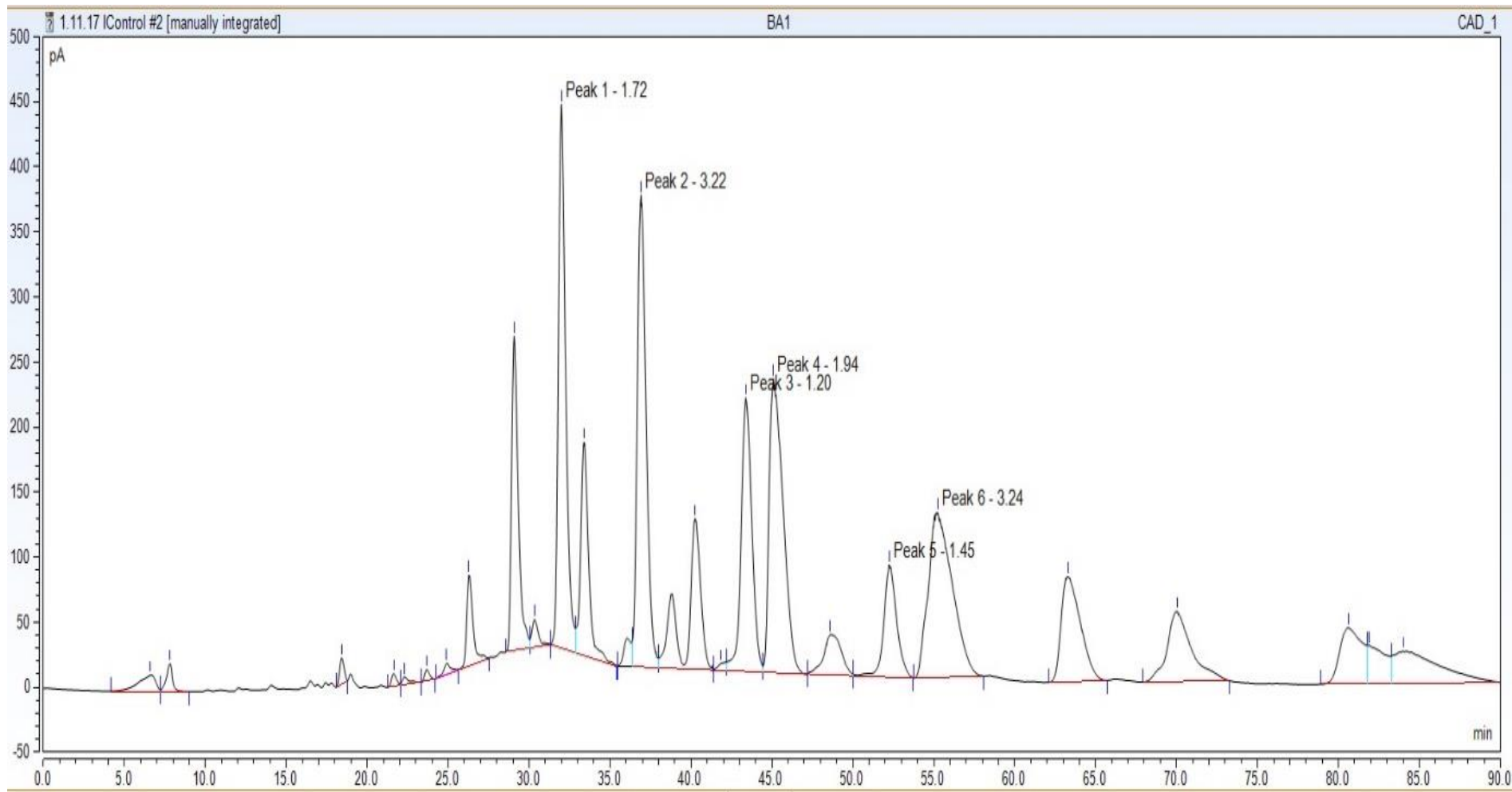
Figure 2.54 Chromatogram of Intralipid® showing the calculated resolution of each peak.

2.13.3.1.5 Degradation

To simulate the effects of degradation, Intralipid® was subjected to 90 days storage at room temperature in a non-light protected oxygen permeable syringe. The HPLC-CAD chromatogram of this degraded sample is shown in figure 2.55. The chromatogram clearly shows that the degradation products made do not interfere with the six selected peaks for calibration and monitoring.
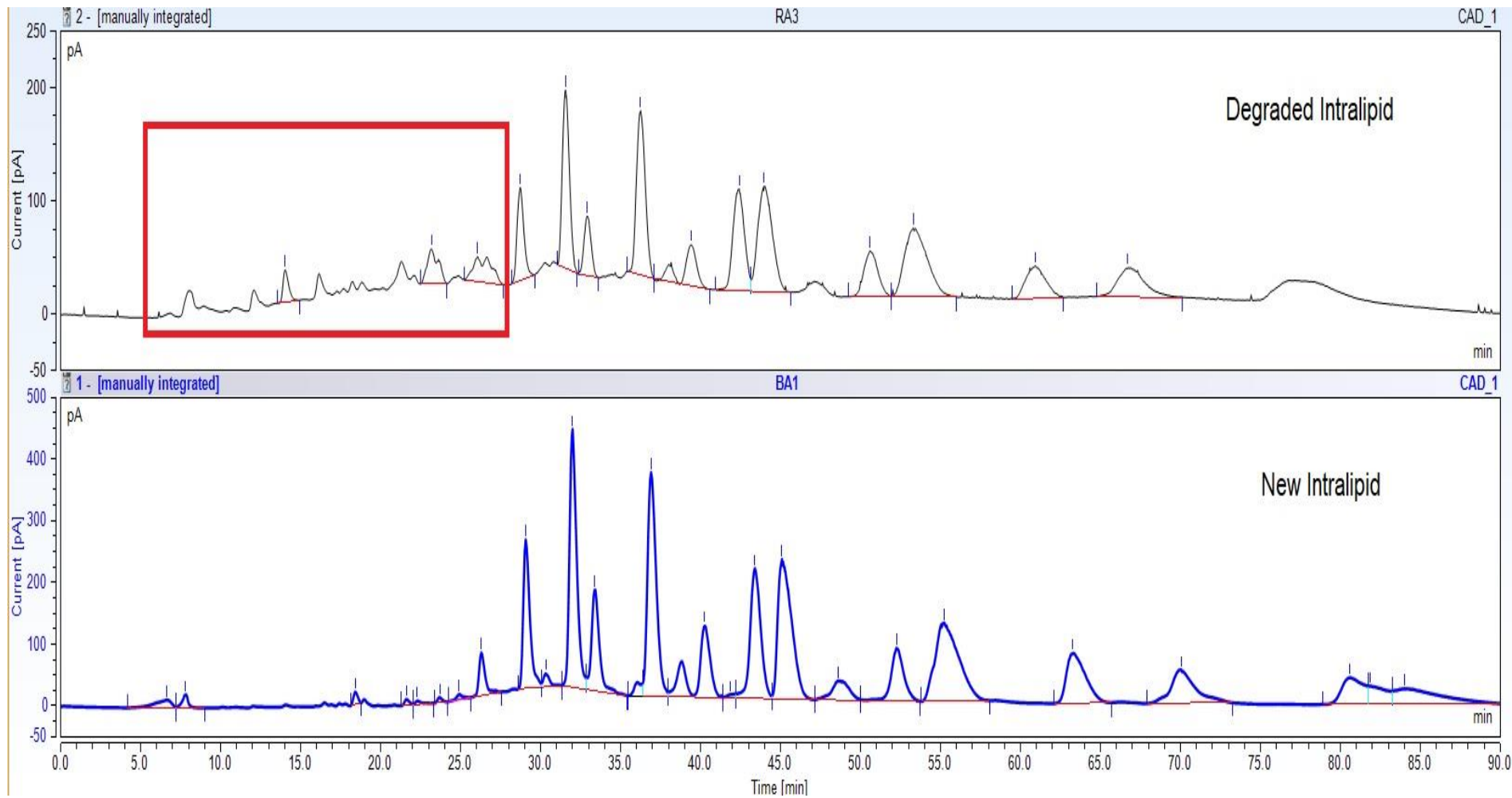
Figure 2.55 HPLC-CAD chromatograms of new and degraded Intralipid®. Primary degradation products highlighted in red.

2.13.4 SMOFlipid® validation

2.13.4.1 Calibration curves

As per Intralipid®, SMOFlipid® 20 % was tested and calibration curves for each of the ten selected peaks created as shown in figures 2.56 to 2.65 with standard deviation error bars. All results were in triplicate for each concentration. R^2 values are summarised for each peak in table 2.16.
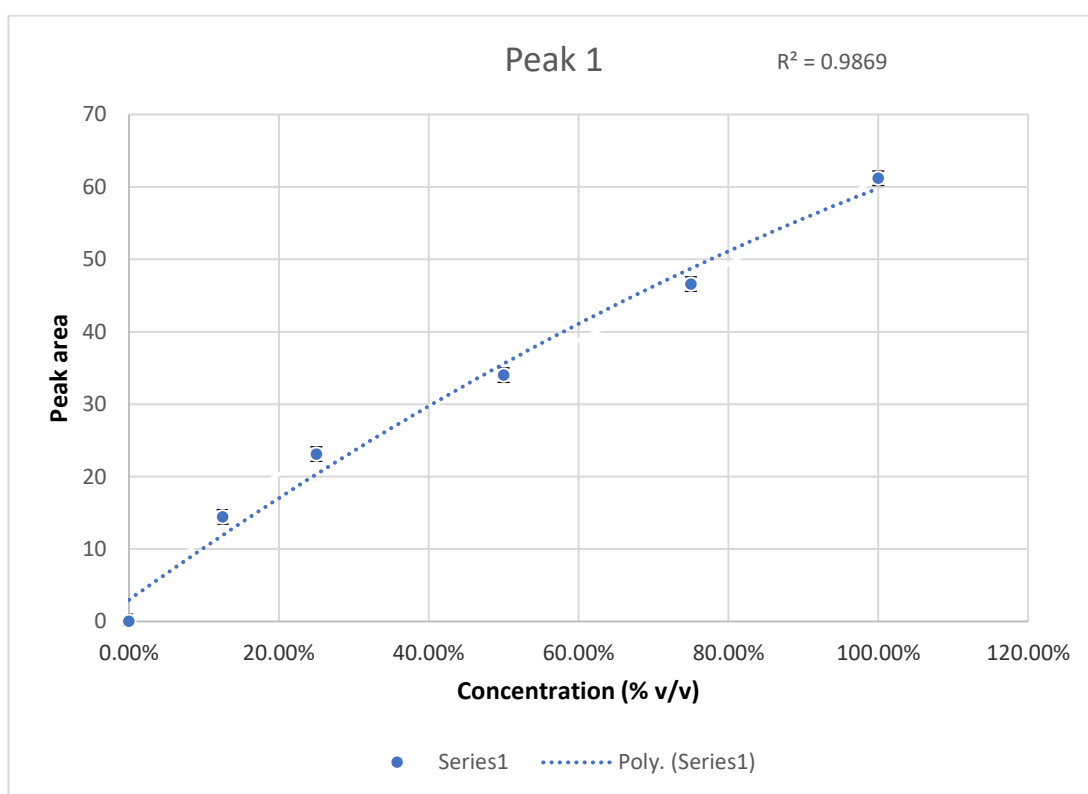
Figure 2.56 Calibration plot for SMOFlipid® Peak 1.
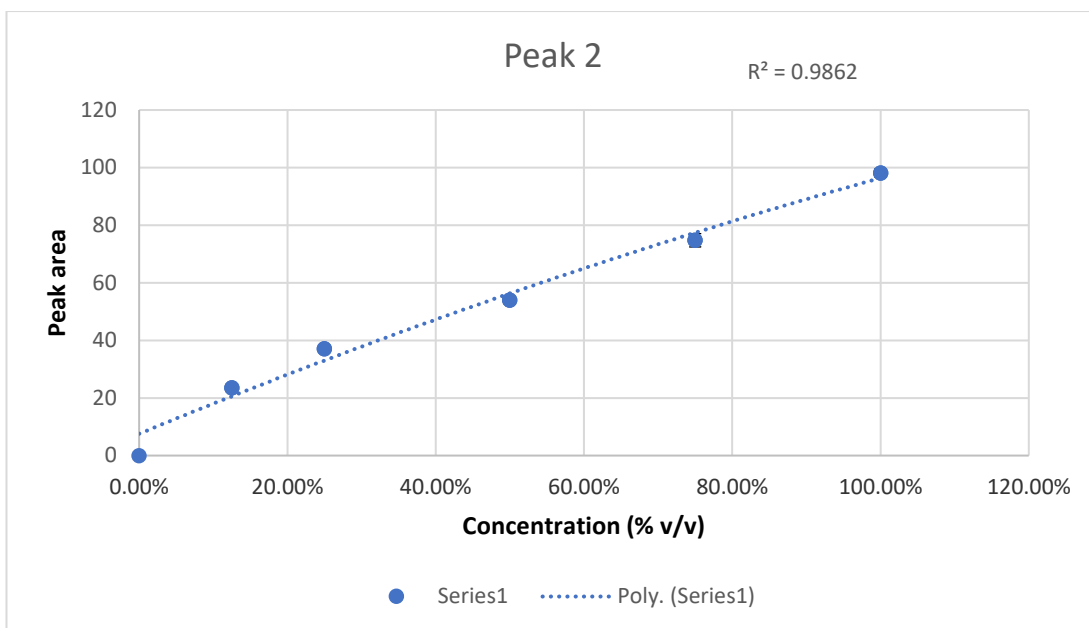
Figure 2.57 Calibration plot for SMOFlipid® Peak 2.
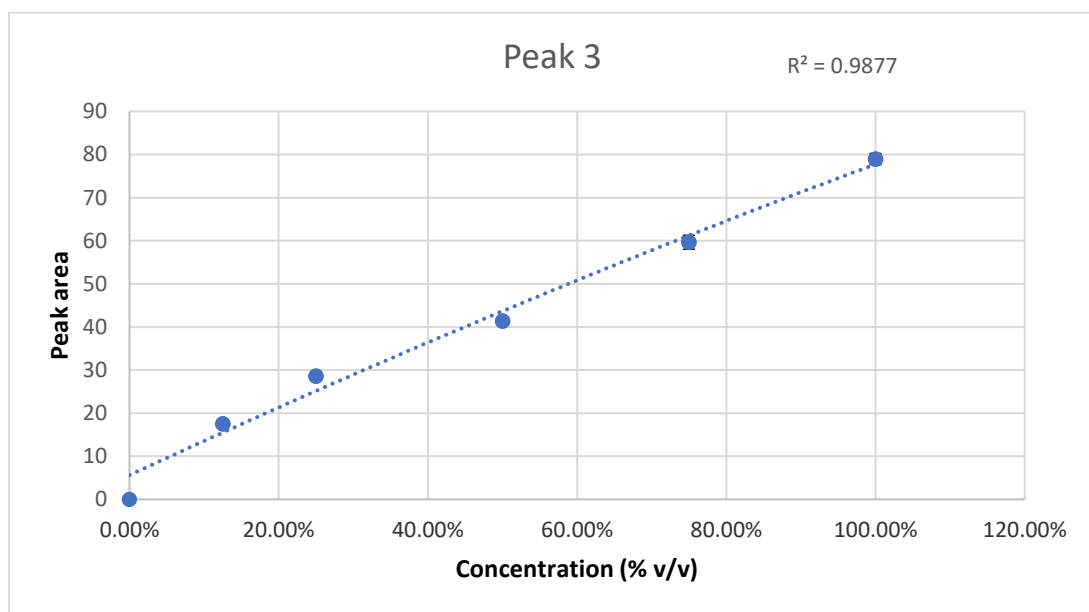
Figure 2.58 Calibration plot for SMOFlipid® Peak 3.
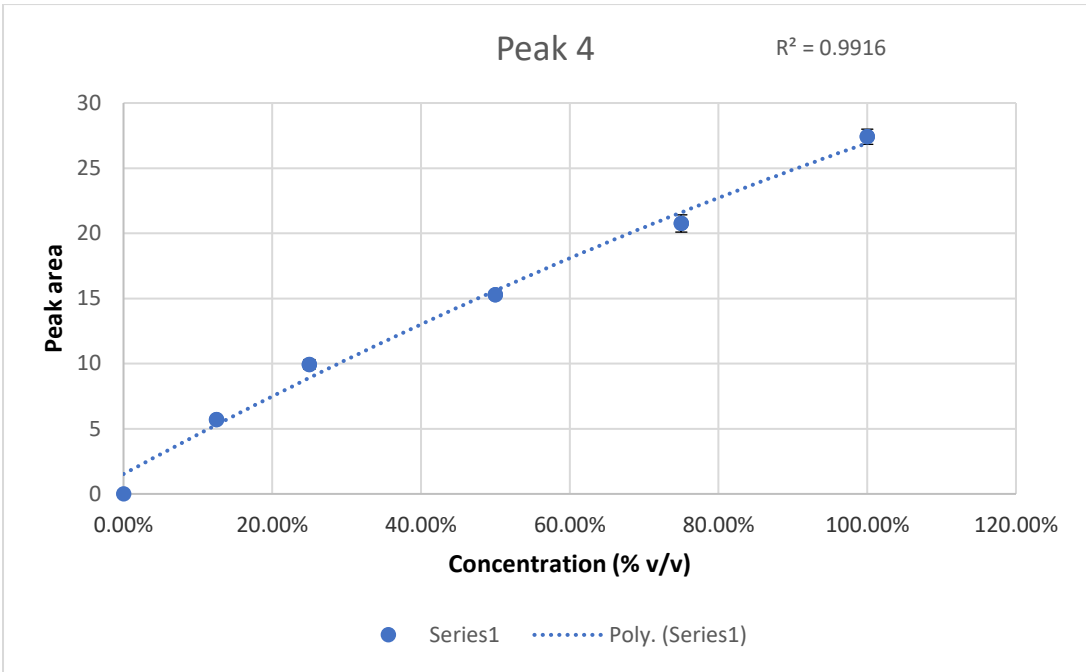
Figure 2.59 Calibration plot for SMOFlipid® Peak 4.
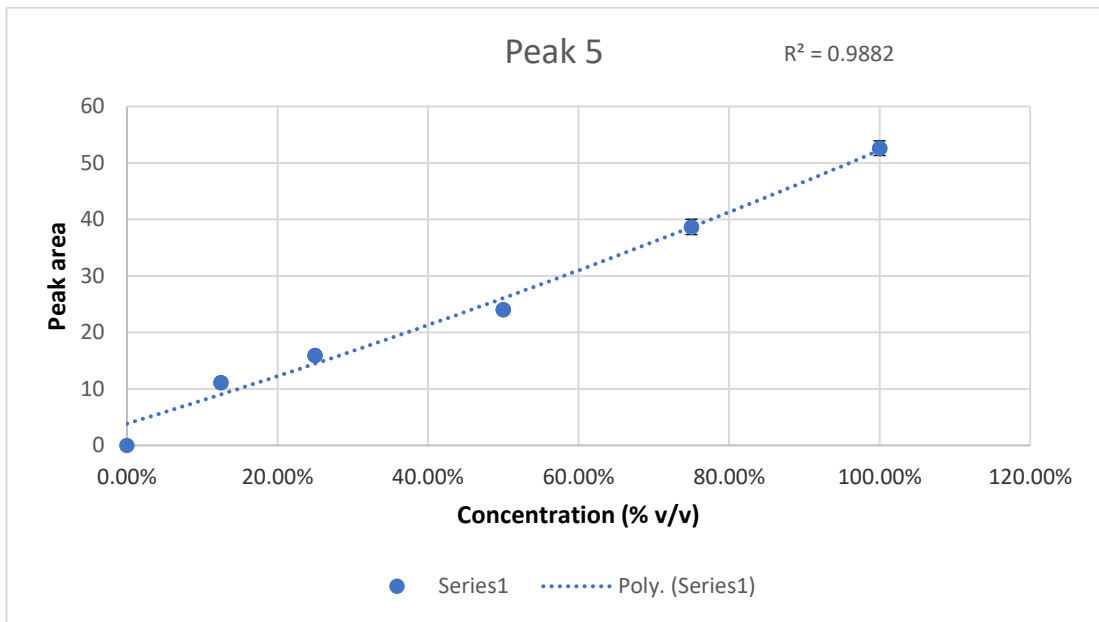
Figure 2.60 Calibration plot for SMOFlipid® Peak 5.
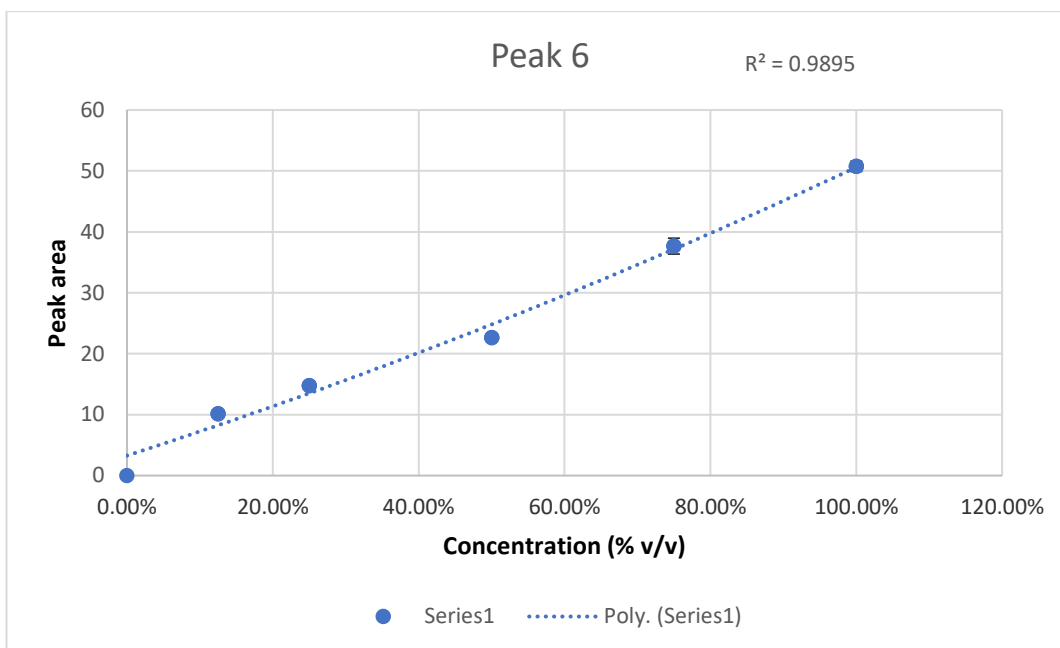
Figure 2.61 Calibration plot for SMOFlipid® Peak 6.
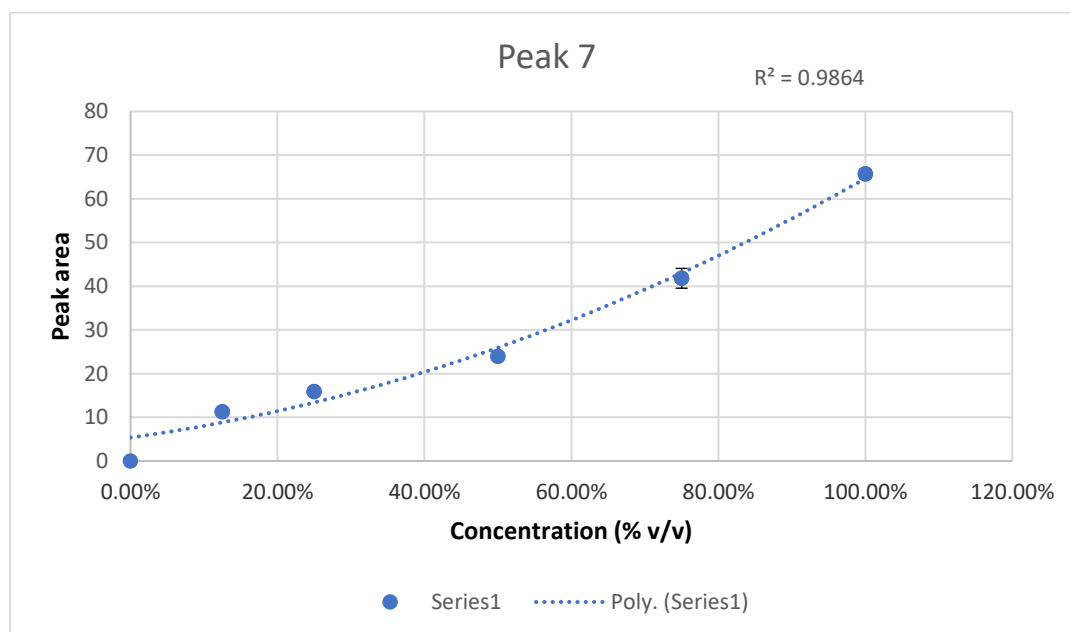
Figure 2.62 Calibration plot for SMOFlipid® Peak 7.
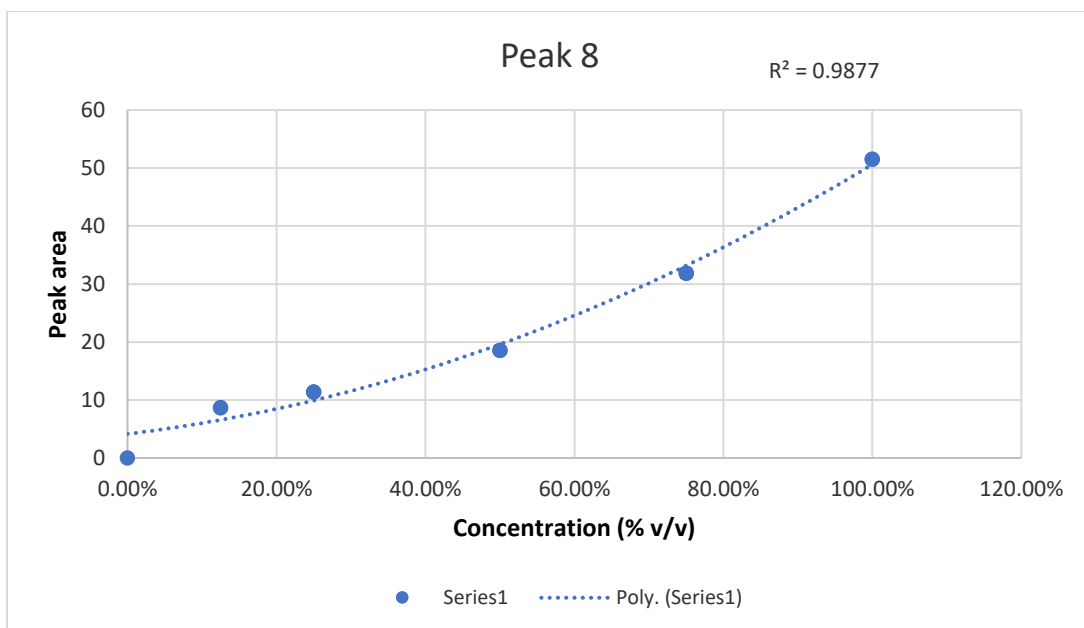
Figure 2.63 Calibration plot for SMOFlipid® Peak 8.
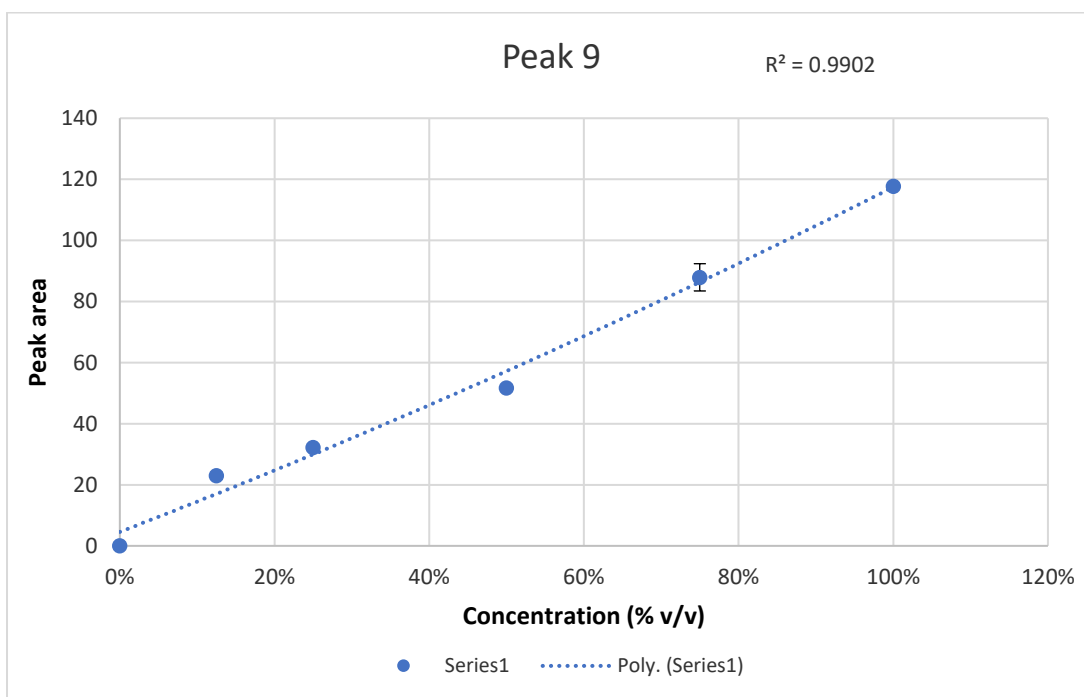
Figure 2.64 Calibration plot for SMOFlipid® Peak 9.
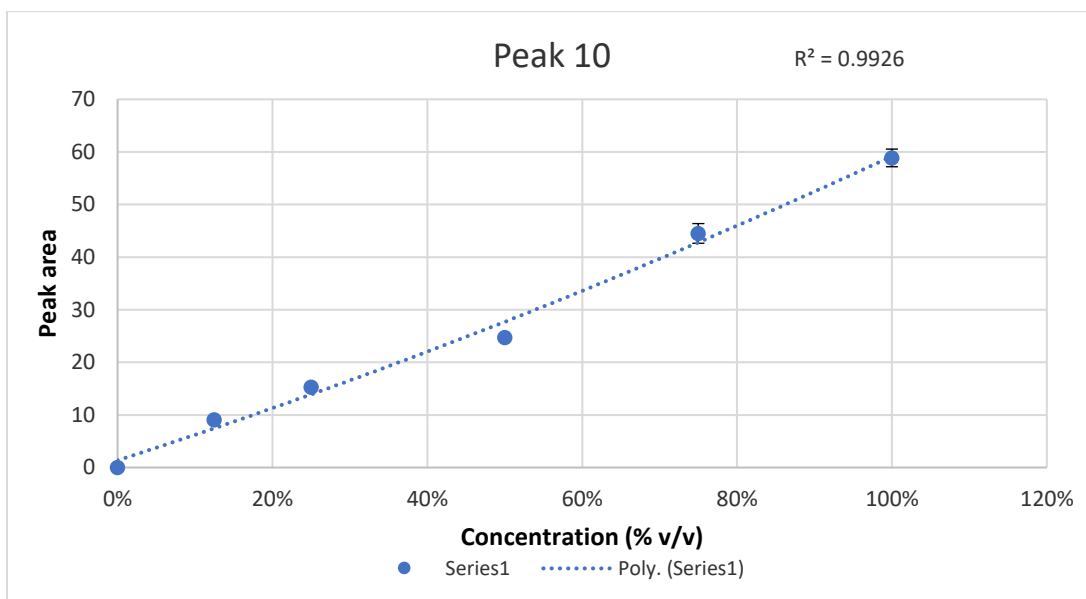
Figure 2.65 Calibration plot for SMOFlipid® Peak 10.

Table 2.16 SMOFlipid® Calibration curve results summary.

SMOFlipid® peak number	R^2 coefficient
1	0.9869
2	0.9862
3	0.9877
4	0.9916
5	0.9882
6	0.9895
7	0.9864
8	0.9877
9	0.9902
10	0.9926

All the calibration coefficients calculated were above 0.98 which is deemed acceptable for an assay where there are 10 or more peaks present (Synder et al. 1997).

2.13.4.2 Precision and accuracy

As discussed in section 12.2.3.1.2 for Intralipid®, SMOFlipid's SPC gives the percentage composition of each fatty acid present as a range. Therefore, as discussed for Intralipid® SMOFlipid® accuracy cannot be calculated in terms of % recovery of each peak. The stability data gathered during the following studies on

SMOFlipid® will like Intralipid® be presented as a % loss of peak area in comparison to a new sample of lipid taken on each testing day.

Precision of each of the ten selected peaks within SMOFlipid® was calculated with inter and intra-day repeatability. Each of the relative standard deviations for each peak are displayed in table 2.17 the maximum value recorded gave a RSD of 5.158, well within the acceptable levels for the CAD detector(Crafts et al. 2011).

Table 2.17 Inter and intraday repeatability results for SMOFlipid®.

SMOFlipid® peak number	Precision	
	Intra-day (RSD %) (n=3)	Inter-day (RSD %) (n=6)
1	0.831	3.740
2	0.618	2.597
3	0.498	2.258
4	2.319	1.614
5	0.863	2.048
6	0.342	2.384
7	1.652	5.158
8	0.055	3.544
9	0.373	2.607
10	2.855	4.745

2.13.4.3 Limits of detection and quantification

LOD and LOQ for SMOFlipid® were again calculated as a percentage of the peak area of a 100% sample due to the inability to calculate a molarity concentration. SMOFlipid® 20 % produced LOD and LOQs of 1.57 % and 5.57 % for the smallest peak quantified. This again is acceptable levels as the maximal degradation over storage will be less than 60% loss of each peak area.

2.13.4.4 Resolution

Calculated using the European Pharmacopeia method and Chromeleon software, the resolutions for each of the ten peaks of SMOFlipid are shown in figure 2.55 and show that peaks 1 to 4, 5, 6, 8 and 10 all have a resolution well above 1.5 showing a good level of resolution between peaks. Peaks 7 and 9 have resolutions of 1.13 and 1.32 respectively and whist not ideal, with regards to CAD assays and for example Gonyon's (Gonyon et al. 2013) work with lipid emulsions and the CAD, the acceptable level of resolution that can be accurately quantified through this form of detection is lower than is seen in other types of detectors. As such the two resolutions for peaks 7 and 9 along with their proven repeatability RSDs are acceptable.
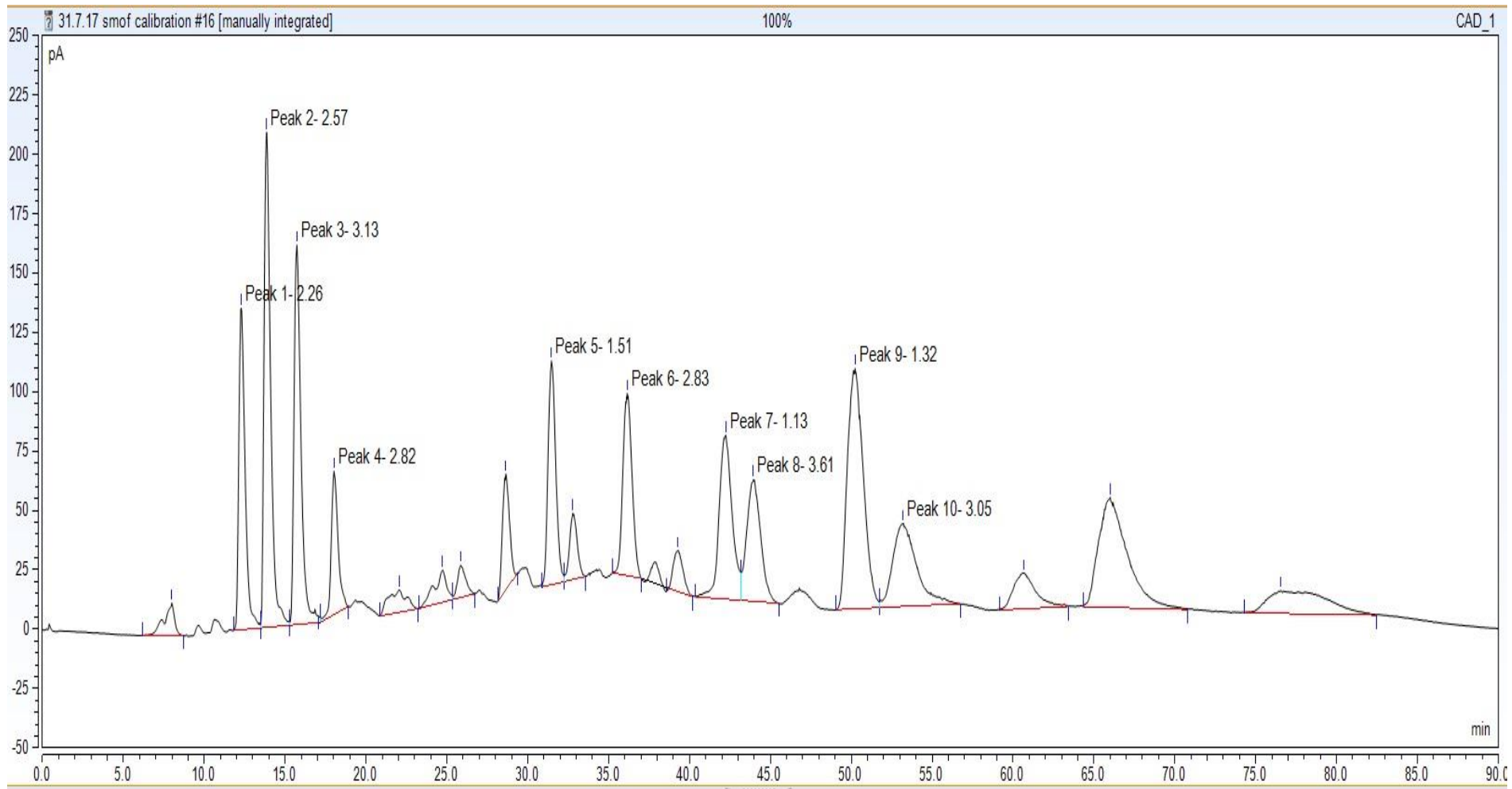
Figure 2.66 HPLC-CAD chromatogram pf SMOFlipid® showing calculated resolutions for each peak.

2.13.4.5 Degradation

As per Intralipid® validation, a 90-day sample of SMOFlipid® held at room temperature in an oxygen permeable syringe with no light protection was used to show the degradation peaks seen through the CAD detection. Figure 2.67 shows the chromatogram of this degraded SMOFlipid® in comparison to a new sample of the same lipid. One of the advantages of the CAD is that only semi or non-volatile analytes will be detected by the CAD and as such many of the degradation products of triglyceride breakdown will be evaporated by the higher temperature of the CAD detector and as such will not be detected. This is also one of the reasons why the CAD assay is coupled with a UV assay to detect these semi and volatile products of TAG breakdown. As figure 2.67 shows the degradation peaks do not elute near any of the ten peaks being monitored for SMOFlipid®.
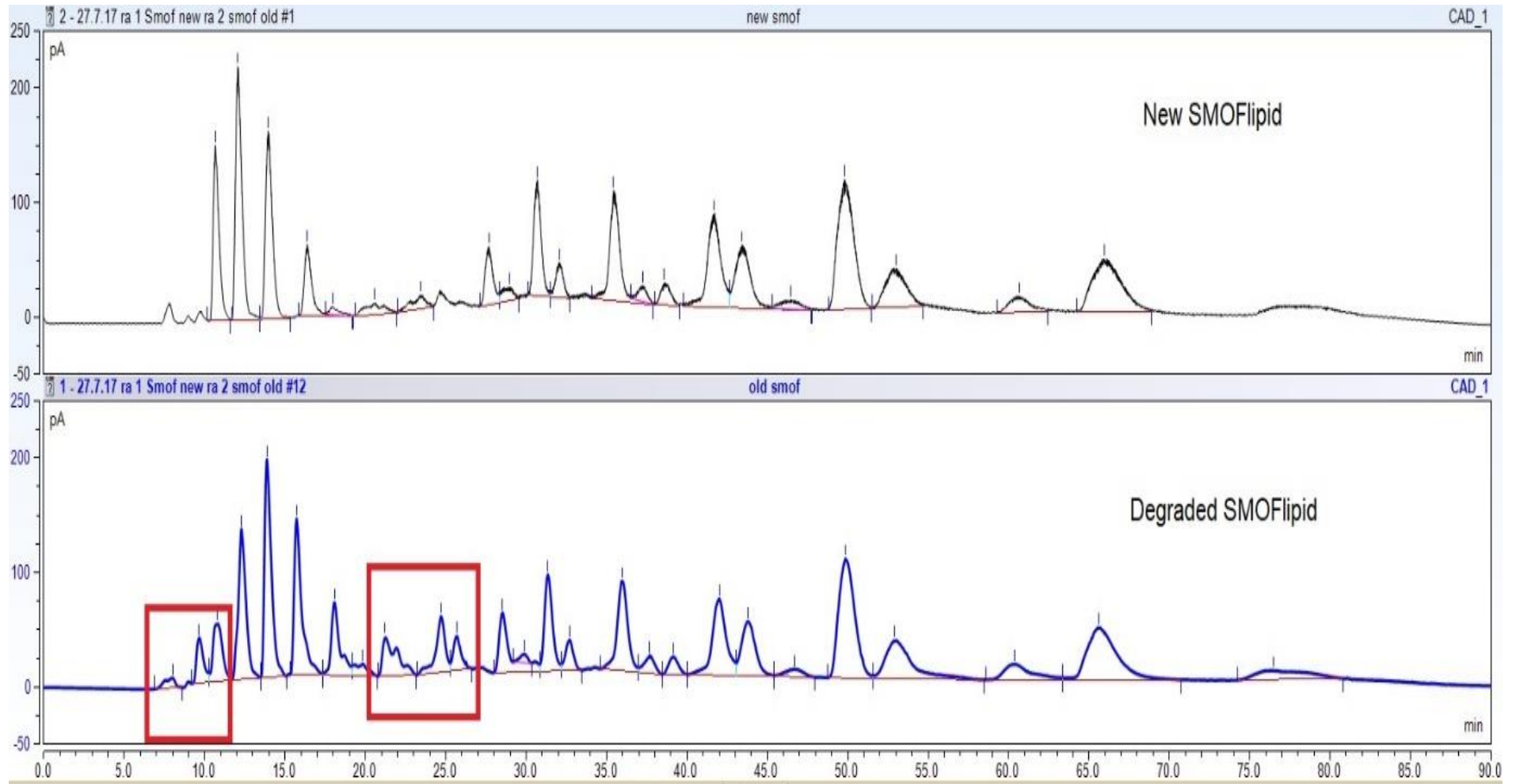
Figure 2.67 HPLC-CAD chromatograms of new and degraded SMOFlipid®. Red boxes indicate degradation peaks seen.

2.14 Assay validation conclusions

The above assay validation procedure, led by the ICH guidelines (ICH 2005) supports the creation of a repeatable and accurate assay for the detection of HNE via UV detection and the monitoring of six and ten peaks within Intralipid® and SMOFlipid® respectively using CAD detection. This shows that the results obtained through using this assay for the stability testing of both lipids are reliable and repeatable with a high level of confidence.

2.15 Method development conclusions

The aim of this project is to quantify and monitor the changes within different IVLE's during storage under a variety of conditions. The assay developed and validated enabled this to be undertaken as shown in the following work. The production of the toxic secondary peroxidation product HNE along with the changes in TAG composition can be accurately and repeatedly monitored allowing an analysis of storage parameters for such lipids to take place. The combination of the UV and CAD to monitor such parameters and the assay conditions achieved are novel and as such the following body of work is novel and will give detailed stability data for IVLEs used within parenteral nutrition. It is also of note that the assay developed could be used theoretically for the testing of a wide variety of lipid emulsions across many different industries and sectors. As such the method was submitted accepted and published in Clinical Nutrition ESPEN as a method paper as shown in appendix 1.

Chapter 3

Intralipid® Light Protected Syringes, Bags and Vials

3.1 Introduction to stability testing of Intralipid®

The remaining chapters of this thesis aim to utilise the assay developed in chapter 2 to test a range of storage conditions for both the traditional lipid emulsion Intralipid® and the newer generation IVLE SMOFlipid®. The assay has been validated for monitoring TAGs within both lipid emulsions and the detection of the peroxidation product HNE. This chapter offers an introduction to the stability testing regimes and protocols that will be followed for all succeeding chapters for each emulsion under different storage conditions. This chapter also provides detailed descriptions of the container types being tested, the theory behind each container material and the principles of light and non-light protection. Each testing regime follows the same plan as detailed in section 3.4 which, in part, is laid out to match and complement the existing testing protocol used within the laboratory for the physical stability testing of both PN and IVLE's.

3.2 Containers

3.2.1   50 ml Syringes

BD 50 ml oxygen permeable plastic syringes were filled with 50 ml of each IVLE test emulsion. BD Plastipak® syringes (Beckton Dickenson) figure 3.1 were chosen for testing for several reasons. Syringes in principle were tested due to their use within the delivery of neonatal PN. Due to neonates' unique requirements for differing levels of nutrients within PN cf. adult PN, neonatal PN is susceptible to precipitation particularly of the calcium portion of PN due to its complexation with phosphates present (Maruyama et al. 2018) . Such precipitation poses a risk to blockage of capillaries within neonatal circulation and such is contraindicated in the delivery of PN. Therefore, PN needs to be closely monitored for the occurrence of precipitation through turbidity testing and microscopy, physical stability tests that are routinely carried out when stability data is generated for a specific PN regime. IVLE's used within neonatal PN are emulsions and are consequently a white to off-white colour which when mixed together with the aqueous portion of PN will obscure visualisation of any precipitation occurring. To circumvent this issue neonatal PN is separated into aqueous and lipid portions.

Figure 3.1 BD Plastipak® 50ml syringes used for lipid storage and delivery.

Currently the lipid portion of neonatal PN is stored in 50 ml plastic syringes formed of polycarbonate with a polypropylene barrel and a latex free elastomer stopper. The barrel is lubricated using a medical grade silicone oil (BD Medical 2015). Such syringes are acceptable and licensed as such for "general purpose injection and aspiration of fluids from vials, ampoules and parts of the body below the surface of the skin. Perfusion syringes, 50ml syringes, are designed for short term use in syringe pumps (active IIa devices) for the administration of pharmaceuticals" (BD Medical 2015) and are currently employed as containers for the storage and delivery of lipid PN. However, as described above, such syringes are optimally used for the delivery of pharmaceuticals and not the storage of them. Storage within syringes is not ideal due to the oxygen permeability of the materials used and the innate risk of oxygen ingress into the contents of the syringe due to the moving parts involved. The presence of lubricants within syringes also poses another issue when considering storing lipids as these oils and the plastics can cause extractables and leachables to enter the stored lipid. Recent work (Driscoll et al. 2007a; Dorival-García et al. 2017) has focused on the extractables and leachables of syringes and concludes that a move away from the storage of lipids within syringes is desired. With regards to oxygen permeability and therefore the potential for lipid peroxidation and breakdown to occur this was the area of focus for the project and the subsequent stability testing of lipids within syringes was designed to test the storage limits with regards to peroxidation and lipid breakdown.

3.2.2   Small volume PN bags

Standard adult PN where lipid and aqueous portions of PN are mixed together are stored in multi-layer (ML) bags comprised of ethyl-vinyl alcohol-polyvinylidine combinations or ethyl-vinyl acetate (EVA) single layer large volume PN bags. When comparing the two bags and their effect on the stability of PN Balet et al. (2004) studied the effects on each type of bag on four different lipid emulsions (Intralipid®

124

included) with respect to peroxidation and tocopherol content. Whilst peroxidation was measured through the FOX analysis method which, as discussed in section 1.6.3, often leads to overestimations of peroxidation, when compared under the same method, peroxidation was more prevalent within EVA bags than multilayer PN bags. With regards to neonatal PN, as discussed above, current practise is the storage of lipids within syringes for delivery to the patient. The issues raised with syringes as storage containers are discussed above and there is a drive to move the lipid proportion of neonatal PN from syringe storage into small volume PN bags typically 250 ml or less to minimise surface area. Typically, 50 ml of lipid is prescribed per neonate and as such PN bag size should be as small as possible to match this volume. Reducing the PN bag size as much as possible will limit the amount of lipid exposed to light by reducing the surface area of lipid exposed to the surfaces of the PN bag. Small volume PN bags were chosen as a container to be tested to give a comparative data set to lipid storage in syringes providing essential stability data to investigate the hypothesis that syringes will cause a greater level of degradation within the lipid than PN bags. Small multi-layer PN bags of 250 ml volume (Baxa) as shown in figure 3.1 were chosen for analysis.

Figure 3.2 Baxa ExactaMIx® Multilayer 250ml PN bag used for small volume lipid storage.

The evidence of multi-layer bags preventing peroxidation vs. EVA bags influenced the choice of bag for testing as eradicating peroxidation occurrence within neonatal PN is essential due to the potentially harmful effects peroxidation products would have on an already oxidatively stressed premature patient.   ML bags are impermeable to oxygen and have a protective effect against oxygen ingress and oxygen initiated and propagated lipid peroxidation (Balet et al. 2004). These ML bags were used for testing to provide a comparison against oxygen permeable syringes and therefore the type of peroxidation occurring during storage of IVLE's prior to delivery.

3.2.3   50ml glass vials

Whilst glass vials are not typically used for the storage and delivery of formulated PN to patients, many of the individual components of PN are stored in glass for long term stability. SMOFlipid® until early 2018 was stored in glass vials until formulation into PN per individual patient requirements. Intralipid® is stored in overwrapped bags formed of a multilayer polymer film. The overwrap provides protection against oxygen ingress during long term storage and each container has an oxygen sensor which indicates the presence of oxygen inside the overwrap through a colour change. Glass vials are impermeable to oxygen and theoretically will protect against oxidative peroxidation though this is dependent on the internal space of the vial being filled with oxygen free lipid and an oxygen free headspace. There is a further issue with EVA bags where though relatively inert, Gonyon et al. (Gonyon et al. 2013) showed that leachables from EVA potentially appeared within a parenteral nutrition lipid emulsion and that triglycerides had a higher association and uptake by EVA vs glass containers. As such, traditionally glass was used for lipid storage over EVA containers. Glass vials do however have certain disadvantages compared to EVA containers primarily being that the removal of any gaseous phase from EVA containers is easier than glass vials reducing the probability of oxygen initiated/propagated peroxidation. Due to the use of both glass vials and EVA bags for the storage of IVLE's 50ml glass vials as shown in figure 3.3 were chosen for analysis to provide a standard from which syringe and ML bag storage could be compared.

Figure 3.3 50 ml glass vial with rubber septum and metal clasp filled with 50 ml lipid emulsion.

Vials chosen were small volumes of 50 ml to match the small lipid volumes being tested within bags and syringes. The main aim of glass vial testing was to create and maintain an oxygen free environment from which lipid stability testing could occur providing an insight into the amount of oxygen dependant peroxidation occurring vs other potential peroxidation processes as discussed in section 1.5.1. To achieve an oxygen free lipid and an oxygen free headspace within each glass vials, 50 ml of each lipid was placed into a glass vial under atmospheric conditions due to the lack of availability of an oxygen free preparation area, and then nitrogen was bubbled through the lipid and headspace to remove any oxygen present. To validate this procedure and ensure a complete oxygen free environment was created, a model 9500 dissolved oxygen meter (Jenway, Staffordshire, UK) was used to create a protocol from which each vial tested was subjected to. The meter was calibrated as per its standard operating procedure (SOP). 50 ml of lipid was placed within a sterilised (heat autoclaved) glass vial and sealed with a rubber septum and metal clasp. Nitrogen was then bubbled through the lipid and headspace at a constant regulator pressure of 2000 psi through a 19G BD (Beckton Dickenson) needle and vented through another 21G BD needle as shown in figure 3.4. Nitrogen flow was maintained in increments of 2 minutes and at each time point dissolved oxygen was measured. Each result was performed in triplicate to ensure validity of results. It was found that 10 minutes of Nitrogen flow created a 0% dissolved oxygen reading within each lipid. To ensure the headspace present within each vial was also oxygen free, each vial was vented with nitrogen for a further 2

minutes each time. Each vial tested underwent this sterilisation and oxygen removal process.

Figure 3.4 50 ml glass vial with 50 ml Lipid emulsion showing oxygen removal procedure through nitrogen flushing.

3.3 Light protection principles and relevance

3.3.1   Relevance

The relevance of protecting PN from light exposure is well established and extensive studies have been carried out on the effect of light exposure on vitamin stability and degradation. Studies by Allwood and Ferguson et al. (2000; 2014) clearly demonstrate the liability of riboflavin and further water-soluble vitamins found within PN to light exposure induced degradation. Miloudi et al. (2012) studied the effects of different lipid emulsions on the generation of peroxides and HNE, comparing a lipids makeup as a possible strategy for preventing peroxidation vs. light protecting PN when considering all-in-one PN solutions and hypothesising that certain lipid formulations may provide a protective effect against peroxidation by preventing the breakdown of pro-oxidant vitamins. With regards to lipid stability and peroxidation within PN lipids, the presence of ascorbate within multivitamin preparations used within all-in-one PN has been shown by Silvers et al. (2001) to have a protective effect on peroxidation of lipids through its anti-oxidant pathways and free-radical scavenging functions. When considering lipid alone however, or

with the presence of fat soluble vitamins only as in the case of lipid separated PN delivery to neonatal patients, vitamin E is the only available free-radical scavenger within certain lipid emulsions (SMOFlipid®). The lack of effective free-radical scavengers within lipid emulsions heightens the need for light protection against photo-oxidative or light induced peroxidation.

When considering the effectiveness of light protecting PN in neonatal patients a meta-analysis by Chessex et al. (2015) showed around a 50 % decrease in mortality of neonates receiving light protected PN vs. non-light protected PN. This finding is of great significance when considering the necessity of light protection. The reduction in mortality in two of the four studies reviewed was linked to a similar reduction in bronco-pulmonary dysplasia (BPD) a fatal condition that is associated potentially with the delivery of peroxidised lipids (Chessex et al. 2007). Recent work by Lavoie et al. (2018) compared Intralipid® and SMOFlipid® both light and non-light protected and the development of hypo-alveolarization (linked with BPD) in guinea pigs. The principle findings of the study support the use of light protection within PN lipid emulsions but indicate that the newer SMOFlipid® lipid emulsion may have a greater pro-oxidant effect and increase hypo-alveolarization. This research is particularly interesting as SMOFlipid® contains added tocopherols as free-radical scavengers principally designed to reduce peroxidation whereas Intralipid® does not, indicating that tocopherols as anti-oxidants within lipid emulsions may not be as effective as previously thought, therefore placing further significance to the light protection of lipid emulsions in PN.

3.3.2   Principles

The principles of light protection revolve around the covering of the PN container (bag or syringe) with or without added coverage of the infusion lines from the container to the patient by a suitable material that will prevent light penetration, thus protecting the contained lipid emulsion from light exposure. The physical characteristics of the covering used will define the level and type of light able to penetrate to the lipid. Studies by Laborie et al. (1999) compared the effectiveness of plastic coverings of different colours (orange, yellow, black and clear) in protecting PN solutions from peroxidation. The study concluded that in PN with a lipid component present, protection with black covering reduced the peroxide value by up to two thirds. Results were however calculated using the FOX II method which is reported to give an over estimation of peroxides present, however all PN tested was subjected to the same testing method so the differences in peroxides present will be

comparable. The necessity for the protection of the delivery infusion lines with the same coloured protection to prevent peroxides forming is highlighted by the study.

In a clinical setting whilst black covering of PN is optimal for protecting against peroxidation there are issues with such a covering being used. During infusion to the patient it is vital that clinical staff can observe the infusion being delivered, the container (bag/syringe) for signs of physical instability and the infusion line for air bubbles which need to be eliminated before reaching the patient. Many infusion lines contain an in-line filter typically 5 µm or smaller to prevent any particulates present from being infused into the patient. This need to observe the infusion makes covering them with black plastic not possible. Therefore, with reference to the studies above different colour plastics are used for infusion coverage. Red, orange and brown semi-transparent coverages are routinely employed for the protection against peroxidation within a clinical setting, all providing differing degrees of light protection. It is not always routine to protect the infusion lining in a clinical setting despite the above evidence clearly showing the optimal prevention of peroxidation includes the protection of the infusion lines.

For the purposes of the following studies, the aim was to compare peroxidation occurring within syringes, bags and vials of lipids with and without light protection. Infusion lines will not be studied due to the variability of lines used and the aim of the study being to establish the chemical stability of lipids after formulation into PN before delivery to the patient and not during infusion. To create a complete level of light protection that guaranteed no light penetration would occur, aluminium foil was chosen as the cover for each container. Foil negates the issues with plastic covers and the partial control of different light wavelengths penetrating through the cover. To ensure each bag, vial and syringe was fully protected as shown in figure 3.5 foil was used to cover the entirety of each container including the sampling ports during storage, with ports being uncovered only when sampling took place or nitrogen top-up was carried out in the vial samples.

Figure 3.5 Light protected 50 ml glass vial, 50 ml syringe and 250 ml multi-layer PN bag covered with aluminium foil.

3.4 Testing protocol

The following testing protocol and schedule was employed for all subsequent testing of all lipids in all conditions. The time frame for testing was set to reflect the physical stability protocols currently used within the laboratory for developing stability limits for PN regimes for adults and neonatal patients. Initial stability information assimilated for the first week is important due to the fact that the clear majority of neonatal PN is made and delivered within 24 hours to 7 days. Adult PN regimes are however often delivered to home PN patients and as such extended stability is favourable to allow patients to have convenient home delivery of PN. Therefore, physical stability testing regimes up to 90 days are used within the laboratory and reflected in the following studies for chemical stability. Whilst the testing was undertaken in small volume lipids, this extended time frame will give an introductory data set for the potential chemical stability of lipids over an extended period. The studies are with lipid alone and do not consider the addition of either fat-soluble vitamins or other components of all-in one PN where aqueous and lipid phases are combined. Theoretically lipid emulsions alone should provide chemical stability data on the most stable form of the lipid emulsions and therefore provides a good starting point for forming chemical stability data on PN lipids.

Initial testing at days 0, 1, 2, 5 and 7 was undertaken to provide detailed changes over the initial 7-day storage after formulation. After this testing was carried out on days 14, 28, 56 and 84 providing extended storage data and matching the physical stability testing regimes. Temperature was controlled in all samples and designated at either fridge storage temperature (2 to 8°C) or room temperatures (22 to 24°C). Light protection was achieved as described above through complete wrapping with aluminium foil (figure 3.5). All samples were prepared in triplicate to achieve statistically significant results. Samples were prepared in a laminar air flow cabinet (BioQuell, Andover UK) using aseptic technique and marked with relevant identifiers and date. BD 50 ml syringes and 19G BD needles were used to manufacture each lipid syringe, bag or vial, batch numbers of all items used were recorded for posterity. A control bag of lipid kept as per supply from the manufacturer was used as a control sample for each day of testing to ensure HPLC method reproducibility. Each control samples chromatogram was monitored for peak areas of selected peaks and the relative standard deviation from the day zero sample to ensure the method being used was consistent over a prolonged period of testing.

Six samples of each lipid (Intralipid$^{®}$ or SMOFlipid$^{®}$) were prepared for each container type (bags, syringes or vials), all light protected with aluminium foil. The vial samples were subjected to oxygen removal with nitrogen gas as described above in section 3.2.3. Three samples of each container were designated for fridge storage, mimicking the normal storage temperature for formulated PN prior to infusion to the patient. The other samples were held at room temperature between 22 and 24°C for the entirety of the study to create a comparator to fridge temperature and investigate the effects of temperature on peroxidation levels.

On every designated testing day each container was sprayed with 70 % IPA and placed into the laminar airflow cabinet where 1 ml of lipid was removed from each sample using BD syringes and needles and placed into an autosampler HPLC vial. Such vials were formed of amber glass to ensure light protection was achieved and sealed to prevent further oxygen ingress. Vials were held in the HPLC autosampler as per method at 8°C to achieve an optimal environment at which to hold the sample to prevent further peroxidation from occurring during testing.

All samples were labelled according to their container, lipid, temperature of storage and repetition number. Due to the testing time of 90 minutes per run and each sample being tested in triplicate, the testing schedule was divided into different days. Intralipid$^{®}$ fridge and room temperature syringes were formulated and tested

on one day, fridge and room bags on another and fridge and room vials on another. Testing of each container set was scheduled to allow all days of testing to be completed without overlap to another containers schedule.

Each sample was subjected to the final HPLC method as detailed in Chapter 2, with a blank 30-minute compressed run between samples to ensure column cleaning and re-equilibration. For Intralipid® samples the identified 6 TAG peaks were monitored through recording of peak area from the CAD chromatogram of each sample for each testing day. The UV chromatogram of each sample was monitored for the development of HNE or other unidentified peaks produced from peroxidation and breakdown of the lipid during storage.

Results were recorded as peak area for each replicate and analysed using Microsoft excel software where averages, standard deviations (SD) and relative standard deviations (RSD) were calculated. RSD was used to monitor the level of precision for the method and ensure the identification of any potentially erroneous results. For the CAD chromatograms of Intralipid® and SMOFlipid® an acceptable level of RSD was set to be lower than 12%. As discussed in the method development of this work, factory settings from Thermo Scientific state the RSD for the CAD should ideally lie under 5 % (Crafts et al. 2011), however when considering CAD use as a detector for identification and monitoring of components within an emulsion formulation, RSD's of up to 12% have been validated as acceptable (Fox et al. 2013; Márquez-Sillero et al. 2013).

3.5 Intralipid® light protected syringe results

Results were recorded for all days of testing as per protocol as peak area and integrated using Chromeleon software (7.2, Thermo Scientific). For the CAD chromatogram each of the six TAG peaks were recorded and a % loss in peak area calculated from the day 0 readings. All were performed in triplicate as described above and RSD's monitored for each sample and the control sample used throughout testing. The % loss for each peak is shown below in figures 3.7 to 3.12. Both room temperature and fridge temperature results are indicated on all graphs. SD error bars are present on all data points.

As shown in the graphs the amount of triglyceride loss occurring increases with storage time at both fridge and room temperature to a maximal 35 % as seen for peaks 2 and 4 at room temperature. Maintaining storage at fridge temperature reduced and delayed the amount of TAG loss of all peaks but significantly for peaks

2,3,4 and 6, however a substantial amount of TAG loss still occurred for all monitored peaks. TAG results are discussed further in section 3.8.

The amount of HNE produced is presented in figure 3.13 with standard deviation error bars on all results. Chromatograms of day 0 and day 84 Intralipid® syringes stored at both fridge and room temperatures for both CAD and UV detection are shown in figures 3.14 and 3.15 with day 0 chromatograms for reference.

The maximum peak area seen for HNE at room temperature was 3.537 AU (n=3) and for fridge temperature was 3.1206 AU (n=3). Using the equation from the calibration plot (figure 3.6) the concentration of HNE present was calculated to be a maximum of 10.209 µM HNE in room temperature syringes whilst fridge temperature storage yielded 8.38 µM HNE. The fridge level of HNE is under the LOQ of 8.974 µM and is therefore not considered to be quantifiable. However, the chromatogram and presence of HNE is still of relevance and shows the production above the level of detection (LOD) within syringes at fridge temperature.
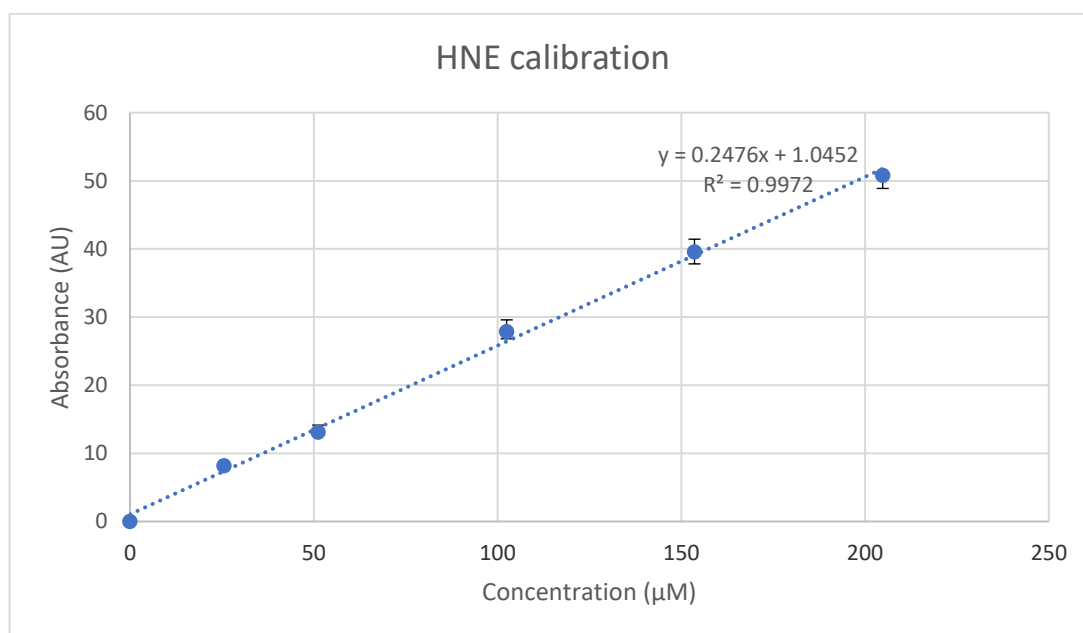
Figure 3.6 HNE calibration graph with linear regression equation used to calculate concentrations of HNE present within tested samples.

Figure 3.16 shows the day 0 and day 84 room temperature syringe chromatograms overlaid. These figures show how the loss of TAGs affect the chromatogram peak area (see y axis scales on figure) and the identification of highlighted new peaks (figure 3.16) A and B attributed to degradation/peroxidation products discussed further in section 3.8.

Figure 3.7 HPLC-CAD results for peak 1 (C18:2/18:2/18:2) triglyceride of Intralipid® 20 % stored in light protected 50 ml syringes. Percentage loss of peak shown calculated from day 0 data. Room (Red) and Fridge (Blue) results shown with standard deviation error bars on all points.

Figure 3.8 HPLC-CAD results for peak 2 (C18:2/18:2/18:1) triglyceride of Intralipid® 20 % stored in light protected 50 ml syringes. Percentage loss of peak shown calculated from day 0 data. Room (Red) and Fridge (Blue) results shown with standard deviation error bars on all points.

Figure 3.9 HPLC-CAD results for peak 3 (C18:2/18:1/18:1) triglyceride of Intralipid® 20 % stored in light protected 50 ml syringes. Percentage loss of peak shown calculated from day 0 data. Room (Red) and Fridge (Blue) results shown with standard deviation error bars on all points.

Figure 3.10 HPLC-CAD results for peak 4 (C18:2/18:2/16:0) triglyceride of Intralipid® 20 % stored in light protected 50 ml syringes. Percentage loss of peak shown calculated from day 0 data. Room (Red) and Fridge (Blue) results shown with standard deviation error bars on all points.

136

Figure 3.11 HPLC-CAD results for peak 5 (C18:2/18:1/18:0) triglyceride of Intralipid® 20 % stored in light protected 50 ml syringes. Percentage loss of peak shown calculated from day 0 data. Room (Red) and Fridge (Blue) results shown with standard deviation error bars on all points.

Figure 3.12 HPLC-CAD results for peak 6 (C18:2/18:1/16:0) triglyceride of Intralipid® 20 % stored in light protected 50 ml syringes. Percentage loss of peak shown calculated from day 0 data. Room (Red) and Fridge (Blue) results shown with standard deviation error bars on all points.

137
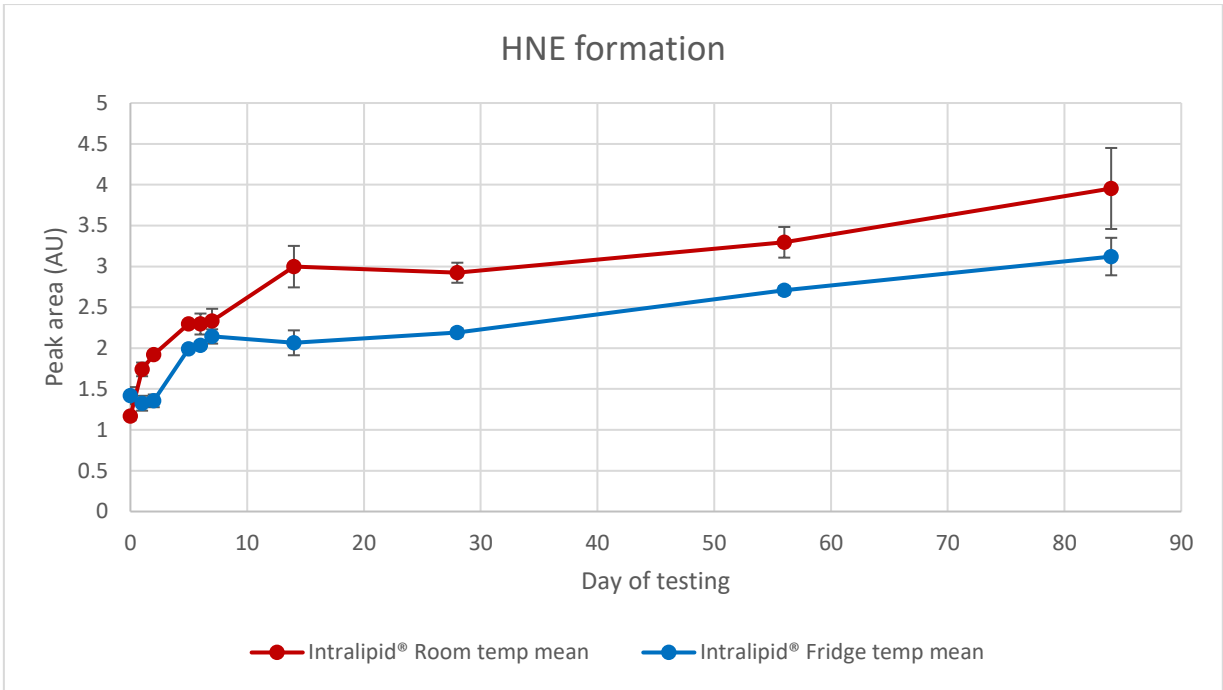
Figure 3.13 HPLC-UV data showing the production of 4-Hydroxynonenal in Intralipid® 20 % over 84-day storage and both room (red) and fridge (blue) temperatures in 50 ml syringes.
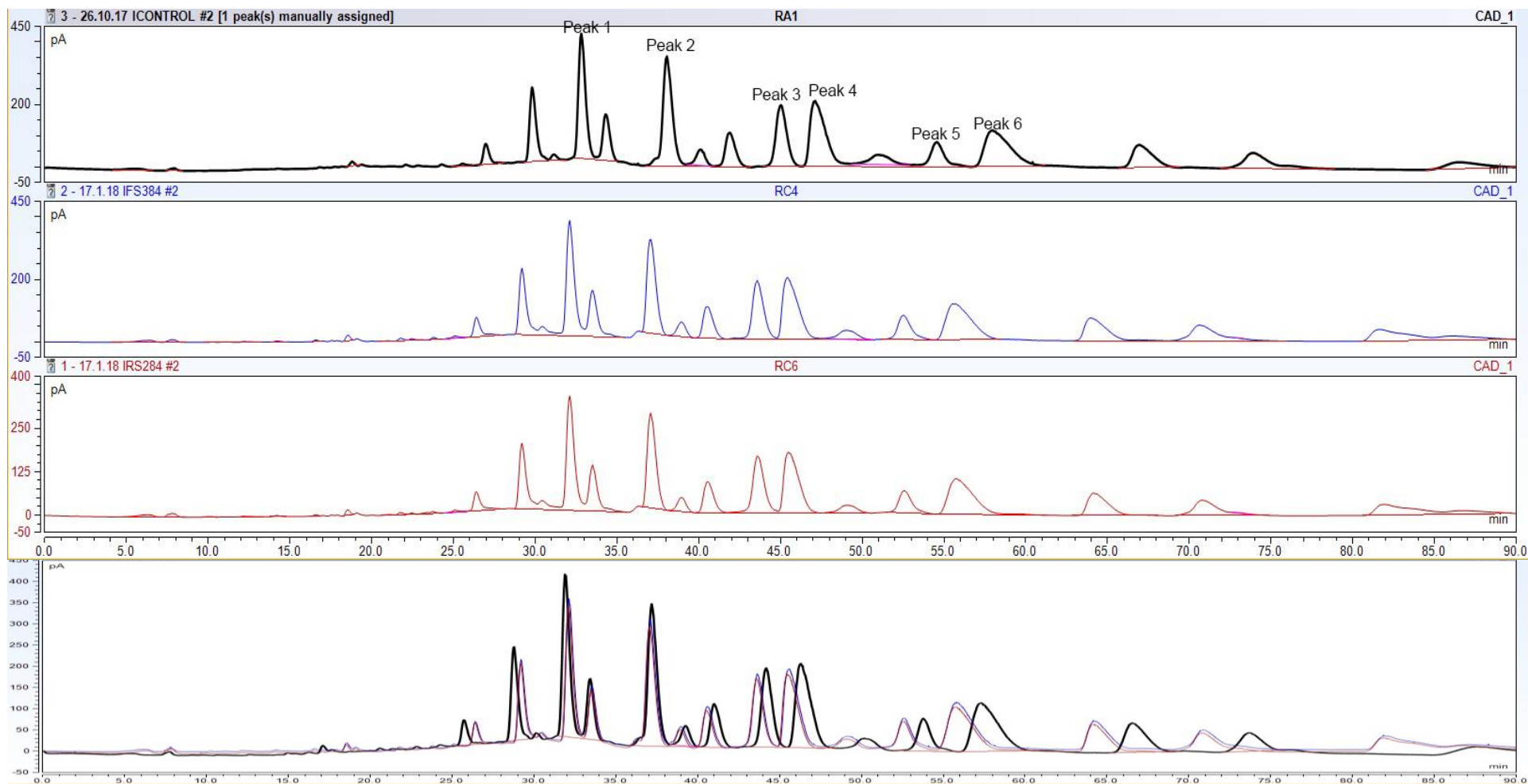
Figure 3.14 HPLC-CAD chromatograms of Intralipid® 20% stored in 50 ml syringes. Day 0 control (black), day 84 fridge temperature (blue trace) and day 84 room temperature (red trace). The y-axis of each chromatogram gives an indication of peak height and the corresponding drop in peak area seen in the 84 day chromatograms. Overlaid chromatogram shows changes in peaks in comparison to control.
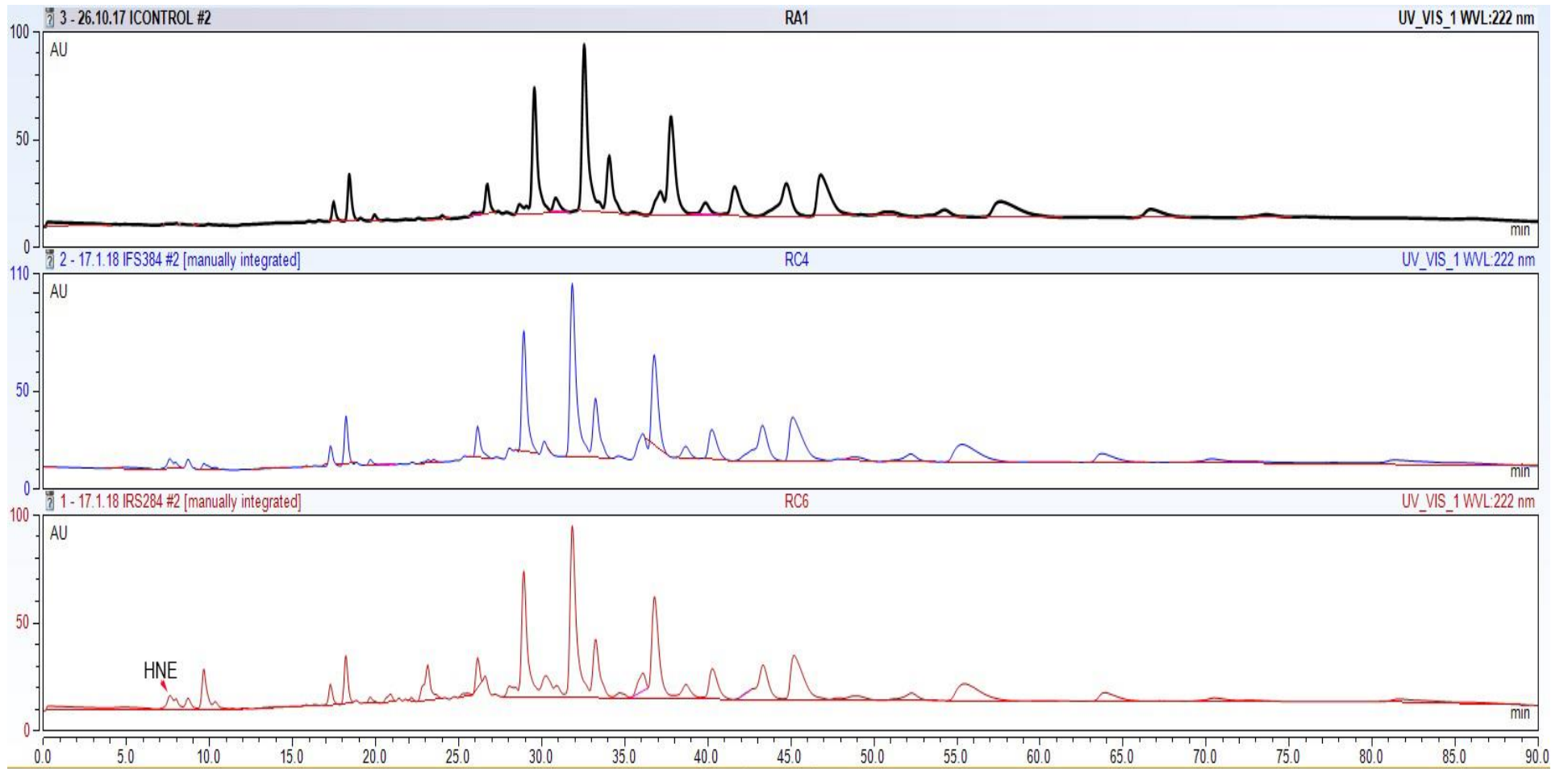
Figure 3.15 HPLC-UV chromatograms of Intralipid® 20% stored in 50 ml syringes. Day 0 chromatogram (black trace), day 84 fridge temperature syringes (blue trace) and day 84 room temperature syringes (red trace). The production of HNE in both fridge and room temperature syringes can be seen and is indicated on the chromatogram.

140
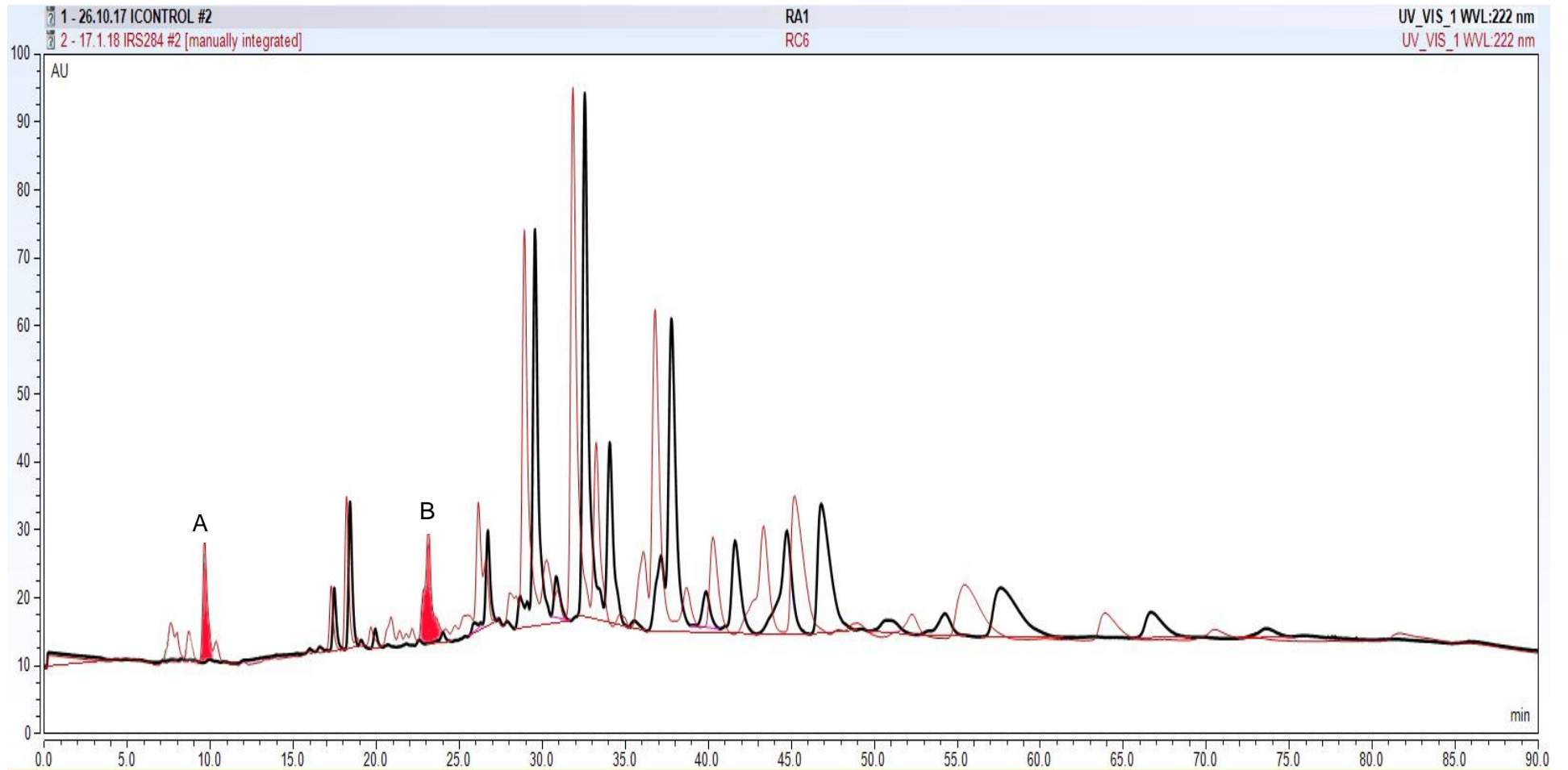
Figure 3.16 Overlaid HPLC-UV chromatograms of day 0 (black trace) and day 84 room temperature (red trace) Intralipid® 20 % stored in 50 ml syringes. Peaks on the 84 day chromatogram highlighted in red show unknown degradation products A and B discussed in section 3.8.

3.6 Intralipid® light protected PN bag results

As per testing protocol 250 ml Baxa EVA multi-layer PN bags were filled with 50 ml Intralipid® 20 %, light protected with aluminium foil and stored at room and fridge temperature. At each point of testing 1 ml of lipid was removed and tested. All possible air was removed from each PN bag at all testing points. A control sample in its original packaging was tested at each time point to ensure method precision. All results were performed in triplicate and standard deviations and relative standard deviations calculated for each point. Raw data is shown in appendix 2 and the following figures 3.17 to 3.22 show the data for all six TAGs monitored as a % loss from their day 0 amount.

PN bags which are impermeable to oxygen produced a maximal % TAG loss of around 30 % at room temperature at the end of 84 days of storage. Temperature of storage had less of an effect on TAG loss. All peaks showed a significant loss of triglycerides throughout storage and this is further discussed in section 3.8.

HNE was not produced in quantifiable concentrations during storage in light protected PN bags. The limit of quantification (LOQ) as discussed in chapter 2 (section 2.12.2.4) was 8.974 µM which would give a peak area of 3.267 (calculated from the linear regression equation used for HNE calibration in Intralipid®). The largest area integrated in the HPLC-UV PN bag chromatograms was 1.670, thus making the level of HNE present un-quantifiable. However, the identification of another degradation/peroxidation product as highlighted in figure 3.25 is of interest. This product has the same elution time as peak B produced during the storage of Intralipid in 50 ml syringes at room temperature (figure 3.16) and further identification was undertaken as discussed in section 3.8.

Figures 3.23 and 3.24 show the CAD and UV chromatograms of fridge and room temperature storage of Intralipid® at day 0 as a control and at day 84. The loss of TAGs can be visualised by the change in y-axis scale giving an indication of the change in peak size occurring.

Figure 3.17 HPLC-CAD results for peak 1 (C18:2/18:2/18:2) triglyceride of 50 ml Intralipid® 20 % stored in 250ml light protected PN bags. Percentage loss of peak shown calculated from day 0 data. Room (Red) and Fridge (Blue) results shown with standard deviation error bars on all points.

Figure 3.18 HPLC-CAD results for peak 2 (C18:2/18:2/18:1) triglyceride of 50ml Intralipid® 20 % stored in light protected 250 ml PN bags. Percentage loss of peak shown calculated from day 0 data. Room (Red) and Fridge (Blue) results shown with standard deviation error bars on all points.

Figure 3.19 HPLC-CAD results for peak 3 (C18:2/18:1/18:1) triglyceride of 50 ml Intralipid® 20 % stored in light protected 250 ml PN bags. Percentage loss of peak shown calculated from day 0 data. Room (Red) and Fridge (Blue) results shown with standard deviation error bars on all points.

Figure 3.20 HPLC-CAD results for peak 4 (C18:2/18:2/16:0) triglyceride of 50 ml Intralipid® 20 % stored in light protected 250 ml PN bags. Percentage loss of peak shown calculated from day 0 data. Room (Red) and Fridge (Blue) results shown with standard deviation error bars on all points.

Figure 3.21 HPLC-CAD results for peak 5 (C18:2/18:1/18:0) triglyceride of 50 ml Intralipid® 20 % stored in light protected 250 ml PN bags. Percentage loss of peak shown calculated from day 0 data. Room (Red) and Fridge (Blue) results shown with standard deviation error bars on all points.

Figure 3.22 HPLC-CAD results for peak 6 (C18:2/18:1/16:0) triglyceride of 50 ml Intralipid® 20 % stored in light protected 250 ml PN bags. Percentage loss of peak shown calculated from day 0 data. Room (Red) and Fridge (Blue) results shown with standard deviation error bars on all points.
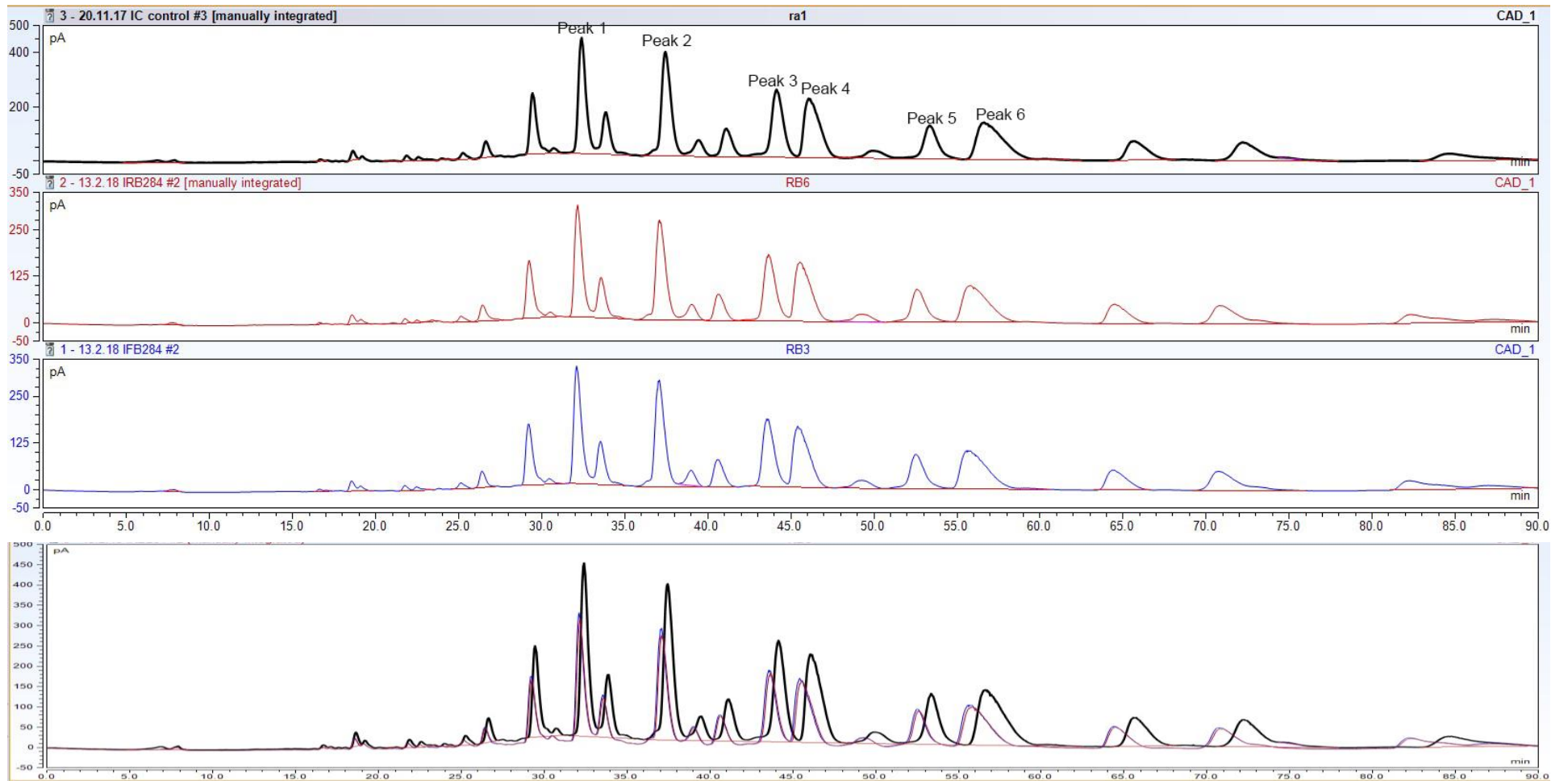
Figure 3.23 HPLC-CAD chromatograms of 50 ml Intralipid® 20% stored in 250 ml PN bags. Day 0 control (black), day 84 room temperature chromatogram (red trace) and day 84 fridge temperature (blue trace). The y-axis of each chromatogram gives an indication of peak height and the corresponding drop in peak area seen in the 84 day chromatograms. Overlaid chromatogram shows changes in peaks in comparison to control.

146
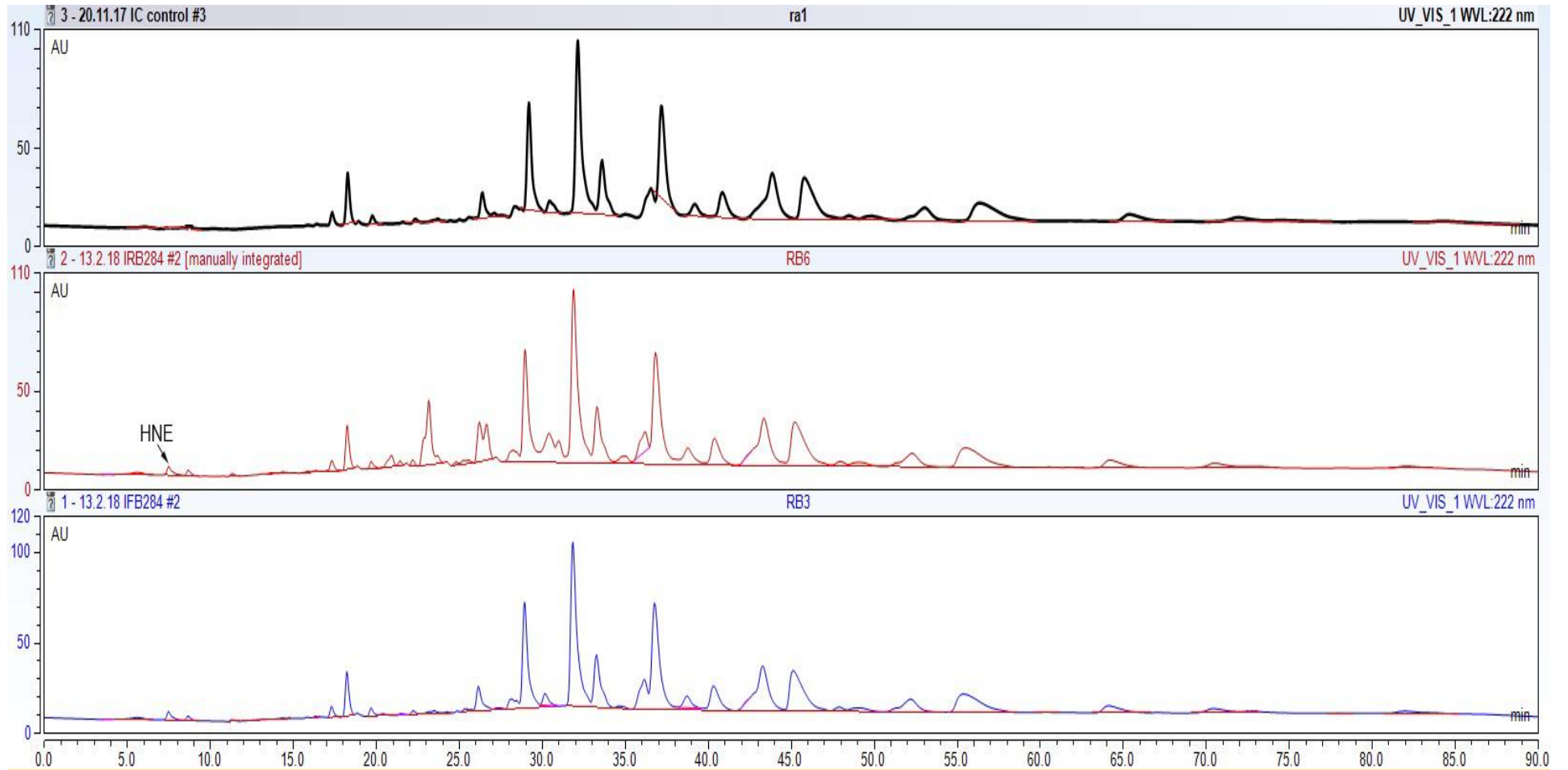
Figure 3.24 HPLC-UV chromatograms of 50 ml Intralipid® 20% stored in 250 ml PN bags. Day 0 chromatogram (black trace), day 84 fridge temperature bags (blue trace) and day 84 room temperature syringes (red trace). The production of HNE in both fridge and room temperature syringes can be seen and is indicated on the chromatogram but was below the limit of quantification.
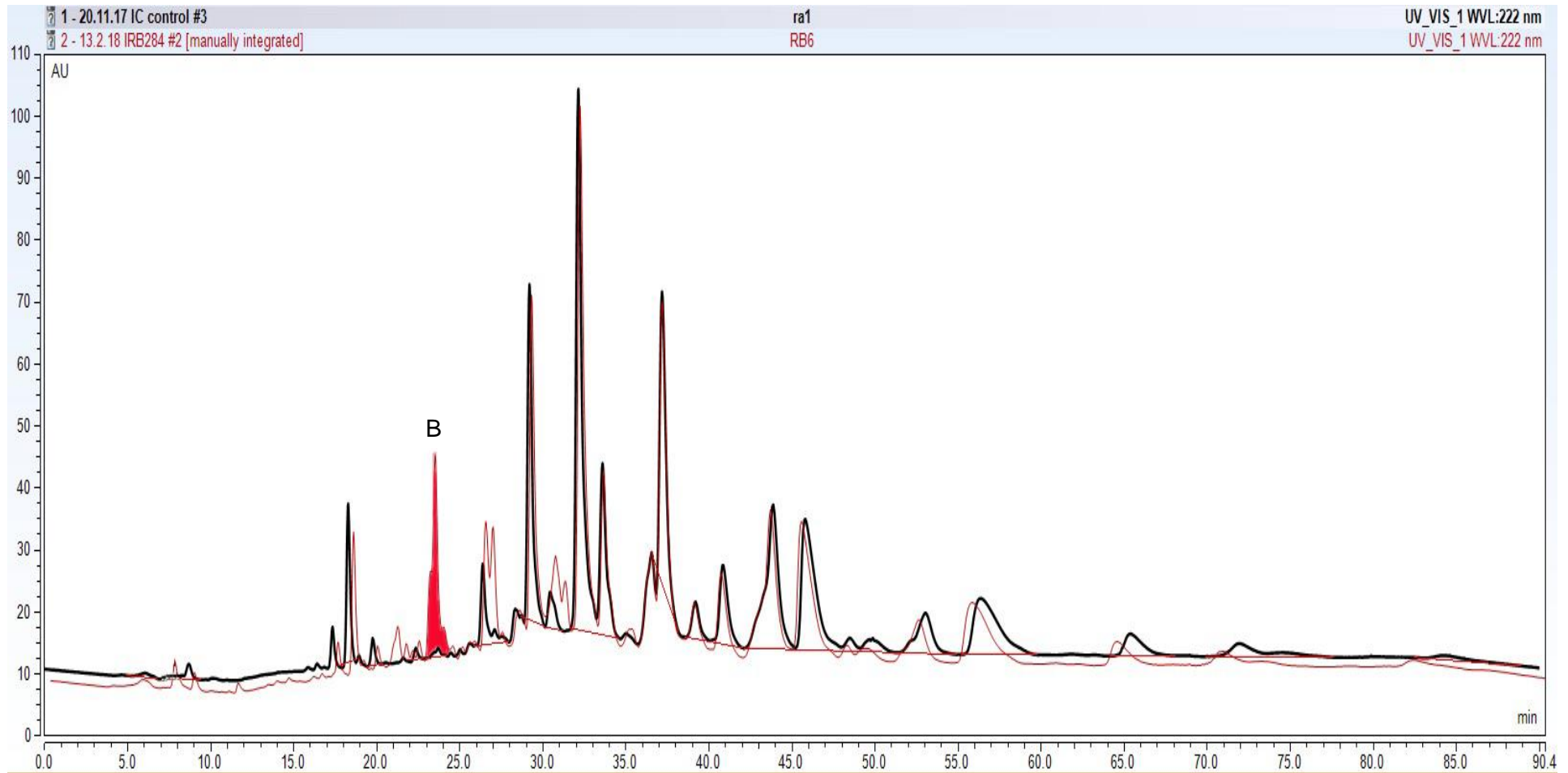
Figure 3.25 Overlaid HPLC-UV chromatograms of day 0 (black trace) and day 84 room temperature (red trace) Intralipid® 20 % stored in 250 ml PN bags. Peak on the 84 day chromatogram highlighted in red show unknown degradation product B discussed in section 3.8.

3.7 Intralipid® light protected vials results

As per protocol glass vials were filled with 50 ml Intralipid® and sealed with metal crimps. Oxygen was removed from the lipid and headspace using nitrogen as described in section 3.2.3. At each testing point 1 ml of lipid was removed from the vial and placed into autosampler vials for testing.

Each of the graphs in figures 3.26 to 3.31 Show the TAG loss that occurred for each selected peak/triglyceride. The maximum peak loss observed was for vials stored at room temperature were peak 3 triglyceride which lost 22.58% over 84 days storage. Fridge storage in vials was much more successful in preventing TAG loss from occurring with a maximum of less than 10 % loss occurring with all monitored triglycerides.

The incidence of TAG loss itself however, within an oxygen free environment, is of considerable interest. As no new peaks were produced during storage that were visualised at 222 nm UV or through CAD detection, peroxidation that was oxygen or temperature dependant would seem unlikely. This would potentially indicate either a different mechanism of TAG loss occurring or that the secondary peroxidation products produced were not able to be visualised at the 222 nm wavelength or through the CAD. Whilst the UV detector used could not wavelength scan during a method, a specific wavelength of 222 nm had to be used as the primary aim was to identify HNE occurring. If postulating that peroxidation was still occurring due to the TAG losses seen, oxygen ingress into the system must then be considered. Whilst every effort was taken to maintain an oxygen free environment throughout storage, samples at each testing point were taken via syringe and needle under oxygen. This potentially introduced a small amount of oxygen into each vial, initiating the peroxidation process and causing the TAG losses observed. To overcome this for the testing reported in glass vials in subsequent chapters a further step within the testing protocol was introduced. At each testing point, after 1 ml of lipid was removed, each glass vial was flushed with nitrogen again in the same process as described in the testing procedure (section 3.4) and thus maintaining an oxygen free environment throughout the testing process.

No visible peroxidation products including HNE were produced through storage at either room or fridge temperatures as shown in figures 3.33 and 3.34.

The lack of TAG loss occurring during the initial 7 days of testing would indicate a lack of peroxidation and a successful maintenance of an oxygen free environment.

When considering the fridge temperature results for all TAGs, day 28 testing results produced a data set that was 10 to 15 % over what was expected in relation to day 7, 14, 56 and 84 result trends. Therefore, this day's data set was identified as an outlier and excluded from further analysis. The cause of the anomalous result was unknown but could have been due to a change in lab temperature, mobile phase contamination or column contamination though contamination is unlikely due to the control sample for the day 28 results and the room temperature results being within RSD limitations and following the trend of all other results. Mobile phases were changed, and the column cleaned for further reassurance. Lab temperature fluctuations were limited as much as possible and all further analysis fell within expected ranges.
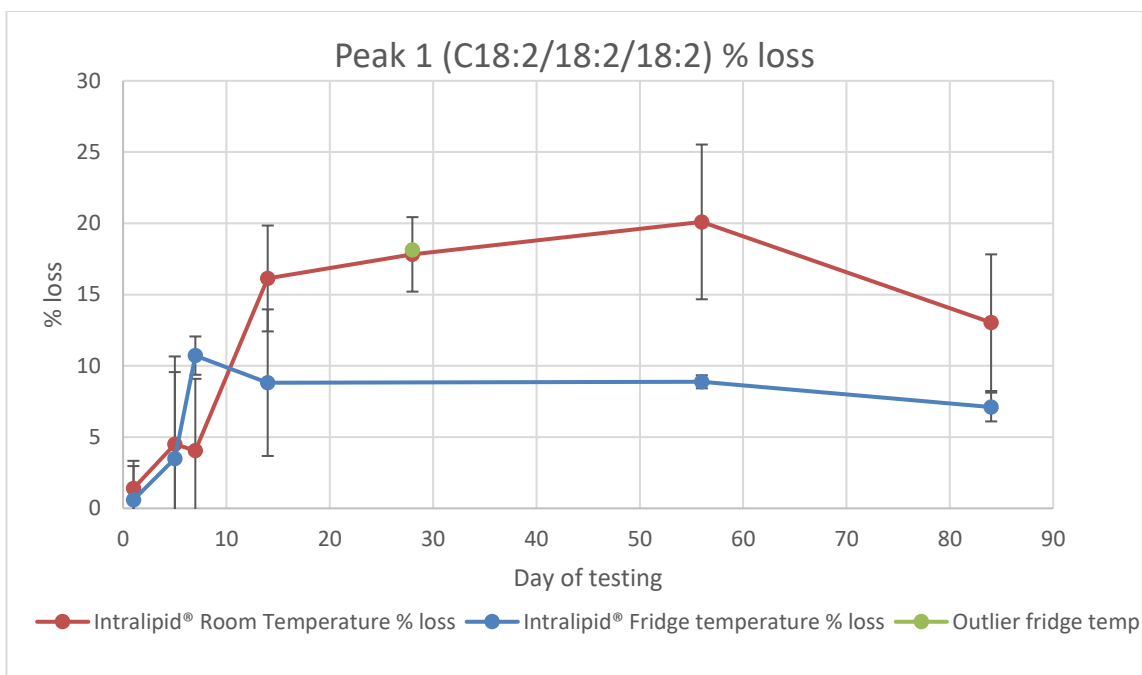
Figure 3.26 HPLC-CAD results for peak 1 (C18:2/18:2/18:2) triglyceride of Intralipid® 20 % stored in 50ml light protected glass vials. Percentage loss of peak shown calculated from day 0 data. Room (Red) and Fridge (Blue) results shown with standard deviation error bars on all points. Outlier identified in fridge temperature results and indicated on graph.
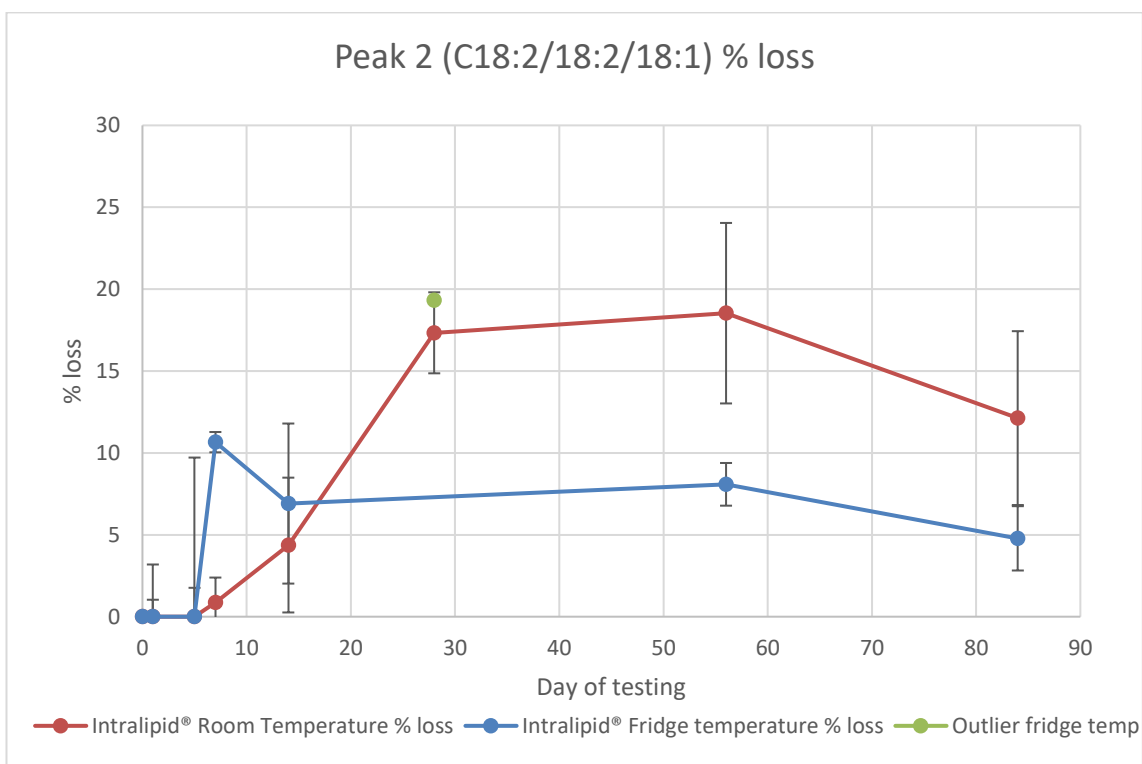
Figure 3.27 HPLC-CAD results for peak 2 (C18:2/18:2/18:1) triglyceride of Intralipid® 20 % stored in light protected 50 ml glass vials. Percentage loss of peak shown calculated from day 0 data. Room (Red) and Fridge (Blue) results shown with standard deviation error bars on all points. Outlier of day 28 fridge temperature result shown on graph but excluded from analysis.
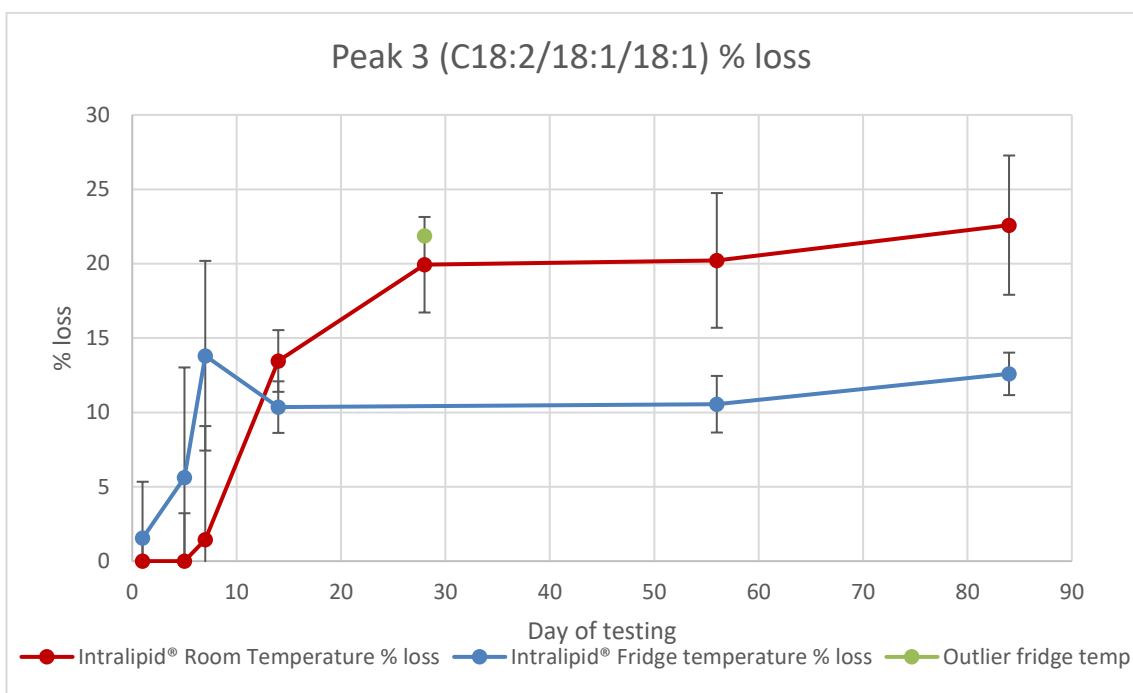
Figure 3.28 HPLC-CAD results for peak 3 (C18:2/18:1/18:1) triglyceride of Intralipid® 20 % stored in light protected 50 ml glass vials. Percentage loss of peak shown calculated from day 0 data. Room (Red) and Fridge (Blue) results shown with standard deviation error bars on all points. Outlier of day 28 fridge temperature result shown on graph but excluded from analysis.
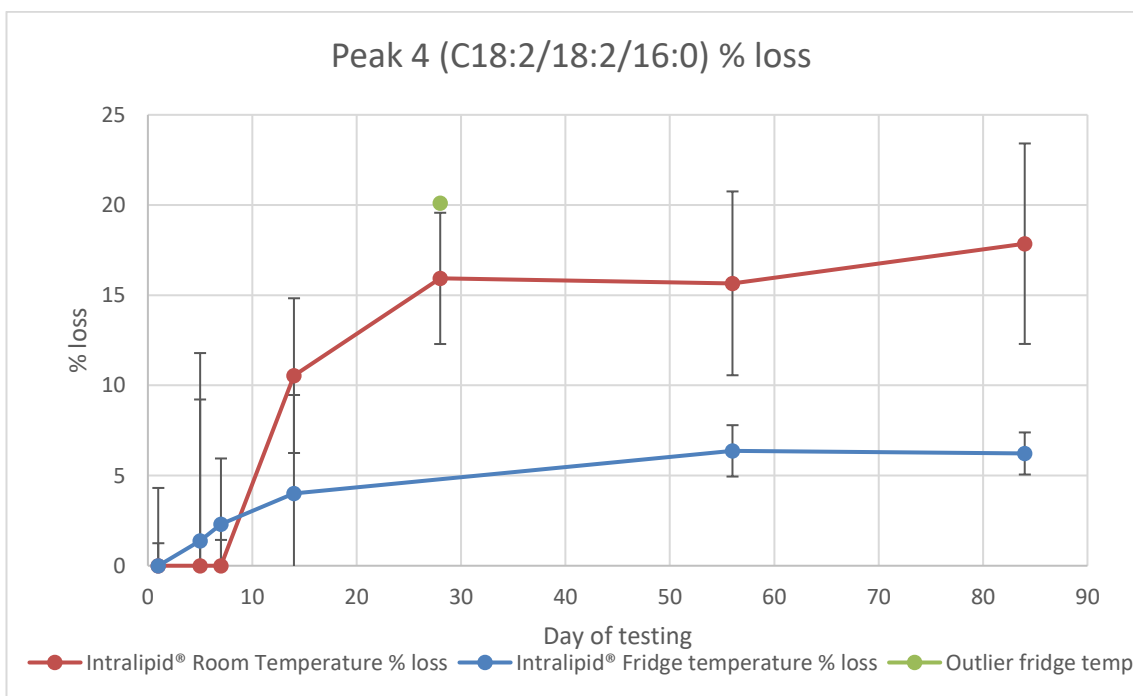
Figure 3.29 HPLC-CAD results for peak 4 (C18:2/18:2/16:0) triglyceride of Intralipid® 20 % stored in light protected 50 ml glass vials. Percentage loss of peak shown calculated from day 0 data. Room (Red) and Fridge (Blue) results shown with standard deviation error bars on all points. Outlier of day 28 fridge temperature result shown on graph but excluded from analysis.
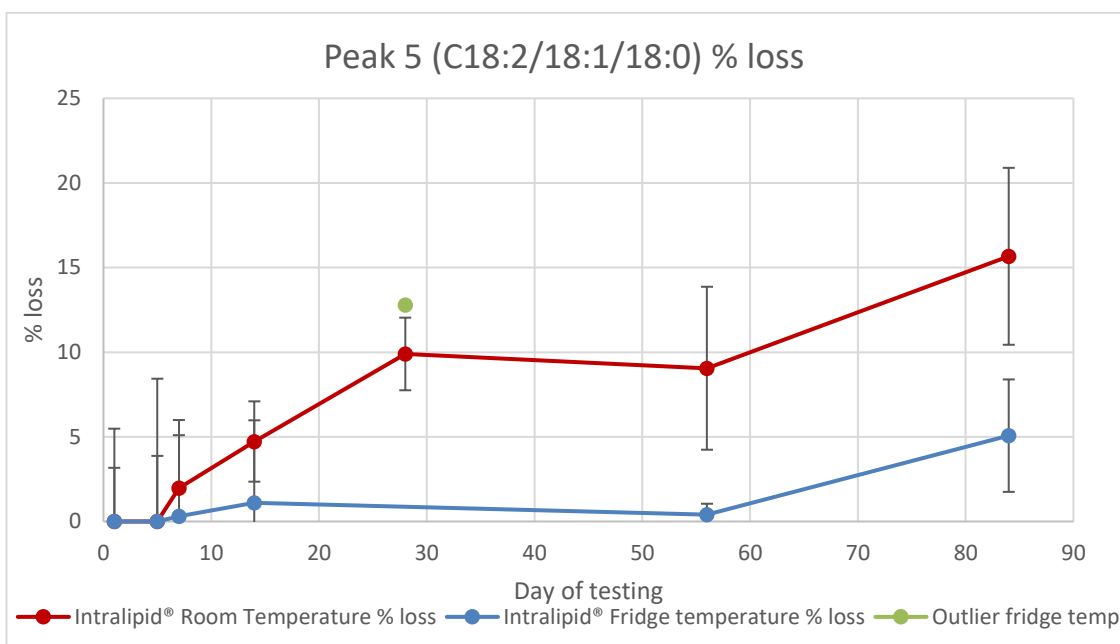
Figure 3.30 HPLC-CAD results for peak 5 (C18:2/18:1/18:0) triglyceride of Intralipid® 20 % stored in light protected 50 ml glass vials. Percentage loss of peak shown calculated from day 0 data. Room (Red) and Fridge (Blue) results shown with standard deviation error bars on all points. Outlier of day 28 fridge temperature result shown on graph but excluded from analysis.
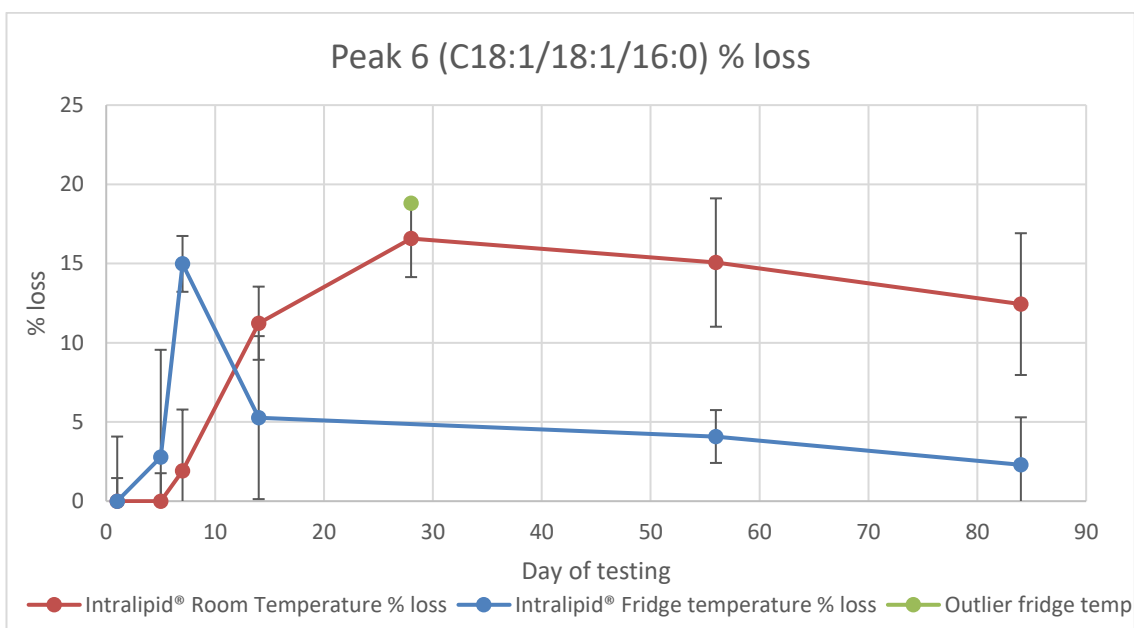
Figure 3.31 HPLC-CAD results for peak 6 (C18:2/18:1/16:0) triglyceride of Intralipid® 20 % stored in light protected 50 ml glass vials. Percentage loss of peak shown calculated from day 0 data. Room (Red) and Fridge (Blue) results shown with standard deviation error bars on all points. Outlier of day 28 fridge temperature result shown on graph but excluded from analysis.
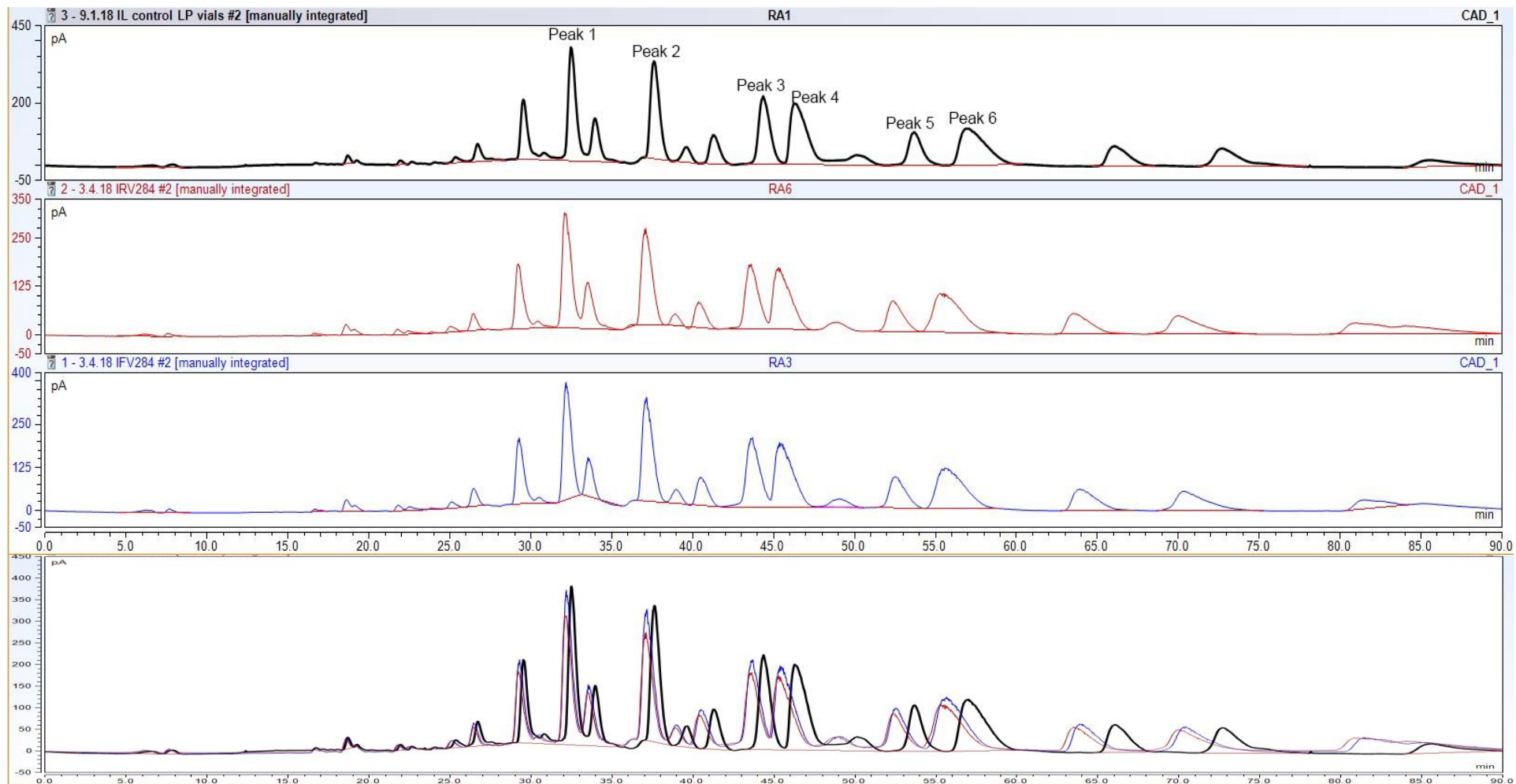
Figure 3.32 HPLC-CAD chromatograms of Intralipid® 20% stored in 50 ml glass vials. Day 0 control (black), day 84 room temperature chromatogram (red trace) and day 84 fridge temperature (blue trace). The y-axis of each chromatogram gives an indication of peak height and the corresponding drop in peak area seen in the 84 day chromatograms. Overlaid chromatogram shows changes in peaks in comparison to control.

154
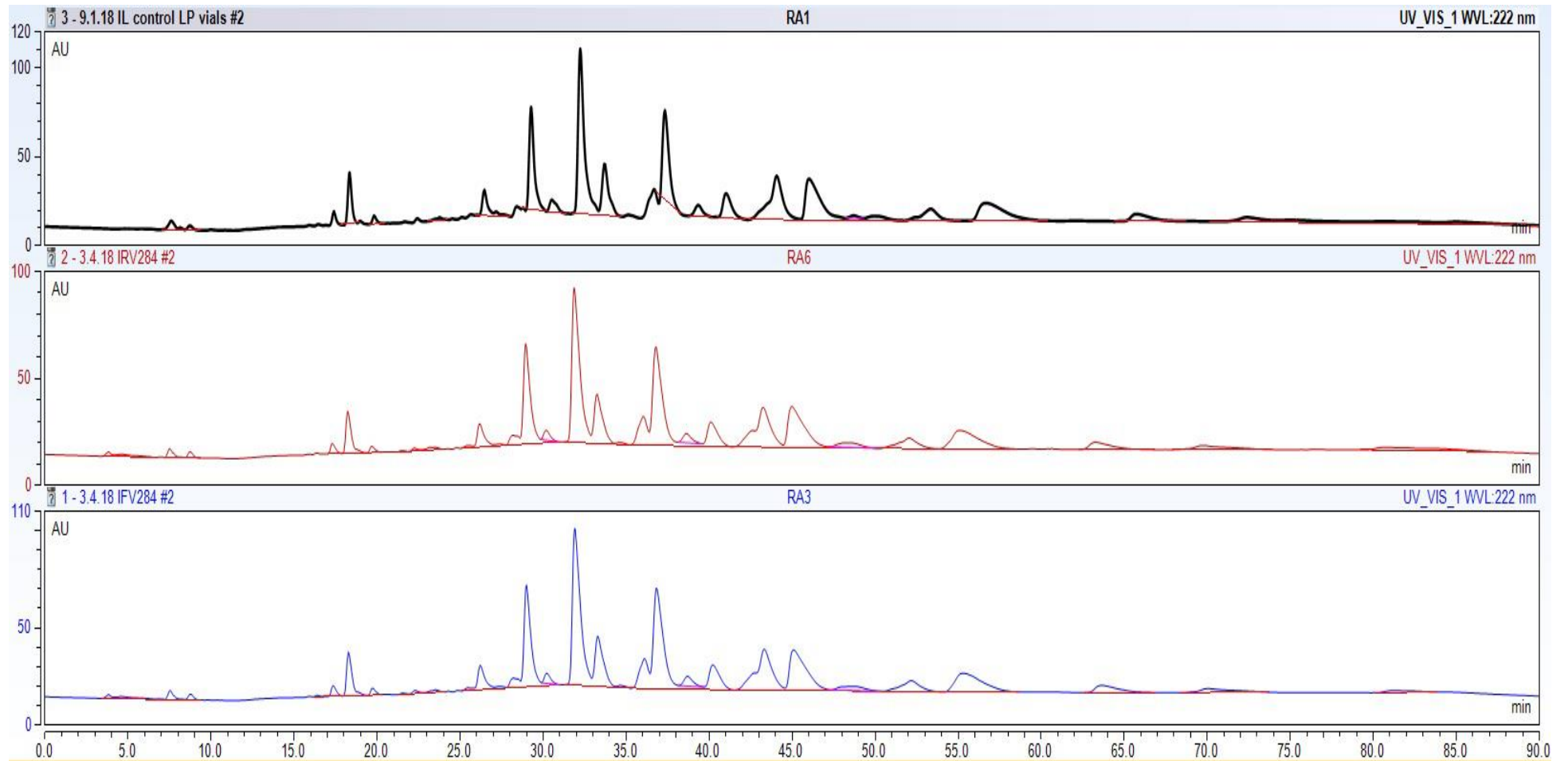
Figure 3.33 HPLC-UV chromatograms of Intralipid® 20% stored in 50 ml glass vials. Day 0 chromatogram (black trace), day 84 room temperature syringes (red trace) and day 84 fridge temperature syringes (blue trace). The lack of production of new peaks indicates a lack of degradation products.
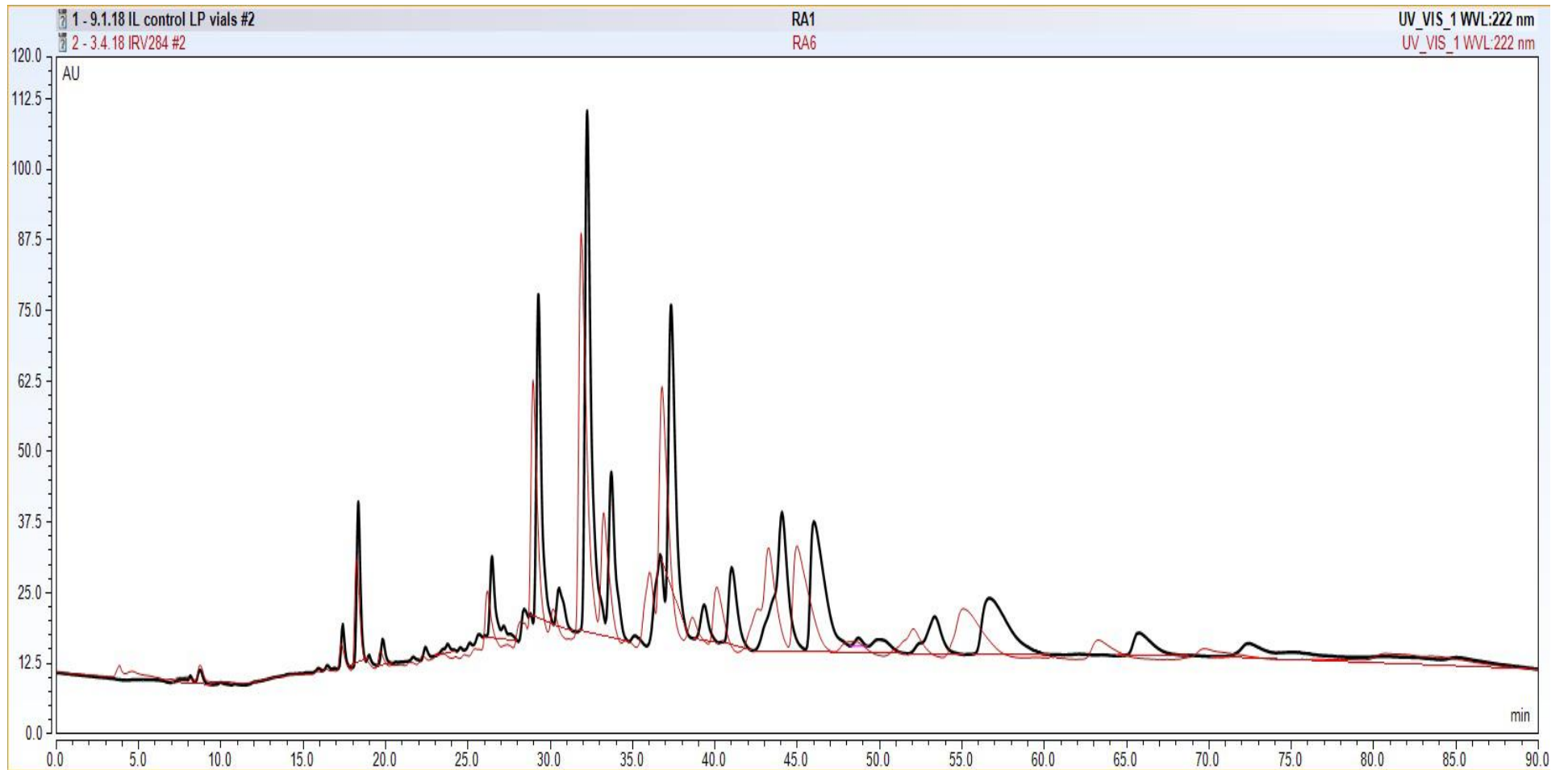
Figure 3.34 Overlaid HPLC-UV chromatograms. Day 0 (back trace) and day 84 room temperature (red trace) Intralipid® stored in 50 ml glass vials. The presence of no new peaks indicates a lack of degradation/peroxidation products seen at this specific wavelength (222 nm).

3.8 Discussion of Intralipid® light-protected results

3.8.1 Triglyceride loss

Triglyceride losses occurred in all containers tested under light protected conditions. The level of loss occurring however was different in each container and temperature dependant. All % loss differences between containers and temperatures at 84 days were statistically significant ($P<0.05$) tested by ANOVA analysis using SPSS (IBM version 25) and summarised in table 3.1(see appendix 3 for data) and checked with Excel. As shown in figure 3.35 at 84 days testing room temperature syringes produced the maximum level of triglyceride loss for all monitored triglycerides except peak 5 (C18:2/18:1/18:0) where room temperature PN bags produced a maximal level of loss. When considering peroxidation, any TAG with a double bond is susceptible to peroxidation and breakdown, which is substantiated by the results seen, as double bond fatty acids are present in all TAGs monitored within Intralipid®. The higher number of double bonds present the greater the predicted extent of peroxidation and breakdown and as such peak 1 (C18:2/18:2/18:2) would be predicted to undergo the greatest amount of peroxidation. In contradiction to this however, the result with the greatest level of TAG loss was peak 2 (C18:2/18:2/18:1) in room temperature syringes yielding a maximal loss of over 35 %. The level of triglyceride loss observed in peak 1 was however the most constant between syringes and PN bags and independent of temperature at which each container was held. This suggests that TAG 1 as predicted was the most likely to peroxidise regardless of temperature of storage.

Whilst syringes are permeable and PN bags are impermeable to oxygen, both showed significant peroxidation and TAG loss. In comparison to this, glass vials filled under nitrogen showed significantly less peroxidation and as stated above (section 3.7) the peroxidation that did occur was postulated to be due to these vials being testing under oxygen and as such a small level of oxygen ingress to the system, initiating peroxidation and the loss observed. The results indicate the necessity of oxygen for initiation of TAG loss, supporting the hypothesis that TAG losses seen are due to peroxidation of the lipids as oxygen is the limiting factor in peroxidation initiation (see intro section 1.5). The amount of oxygen needed to produce the significant levels of TAG losses seen is however minimal, as indicated by the PN bags and syringe results. PN bags when formulated under atmospheric conditions have the maximum amount of air possible removed at the end of the

production process, however a small amount (visibly less than the area of a 50 pence piece) is deemed acceptable in current clinical manufacturing. The results obtained indicate that this small level of oxygen and the potential for dissolved oxygen to be present within the lipid are enough to initiate peroxidation of the TAGs monitored and produce a level of loss similar to syringes.

When considering the effect of temperature on the level of peroxidation and TAG loss occurring, at day 84 after substantial storage time temperature had little effect on the level of TAG loss and peroxidation in PN bags. There was a statistically significant difference ($P<0.05$ ANOVA with post hoc Tukey HSD analysis) in the level of peroxidation within peak 1 (C18:2/18:2/18:2) TAG in vials stored at room and fridge temperatures at day 84 however syringe and bag data were not proven to be statistically significant between different temperatures. Table 3.1 summaries the significant results observed at day 84 between all container types at both temperatures. This would indicate that over a prolonged storage time temperature is less of a governing factor on the amount of peroxidation occurring. It is known however that temperature effects the rate of peroxidation occurring (Seppanen and Saari Csallany 2002; Yuan et al. 2018), with higher temperatures acting as a catalyst for peroxidation. To investigate this, results of the initial 7 days of testing were plotted as shown in figure 3.36. Syringe data showed that temperature had a significant effect within the first 7 days of testing with triglyceride loss being higher at room temperatures vs fridge temperatures. This follows the predicted pattern that fridge temperatures delay/reduce the rate at which peroxidation occurs. PN bag results show little differences between fridge and room temperatures for all triglycerides within the first seven days. This would indicate that the potential differences within syringe peroxidation are due to temperature affecting the physical characteristics of syringes and therefore the level of oxygen ingress occurring. As PN bags are impermeable to oxygen, the presence of any oxygen at the end of manufacturing will initiate peroxidation and results indicate that temperature of storage has little effect on the rate of this occurring. With regards to the glass vial results at 7 days, levels of triglyceride loss at fridge temperature far exceed that at room temperature. Whilst this result is the opposite of what was predicted in respect to temperature, as discussed in section 3.7 this could have been due to oxygen ingress due to sampling under atmospheric conditions. As such, the effect of temperature on glass vials will be compared further in subsequent chapters where oxygen was removed after each testing point.
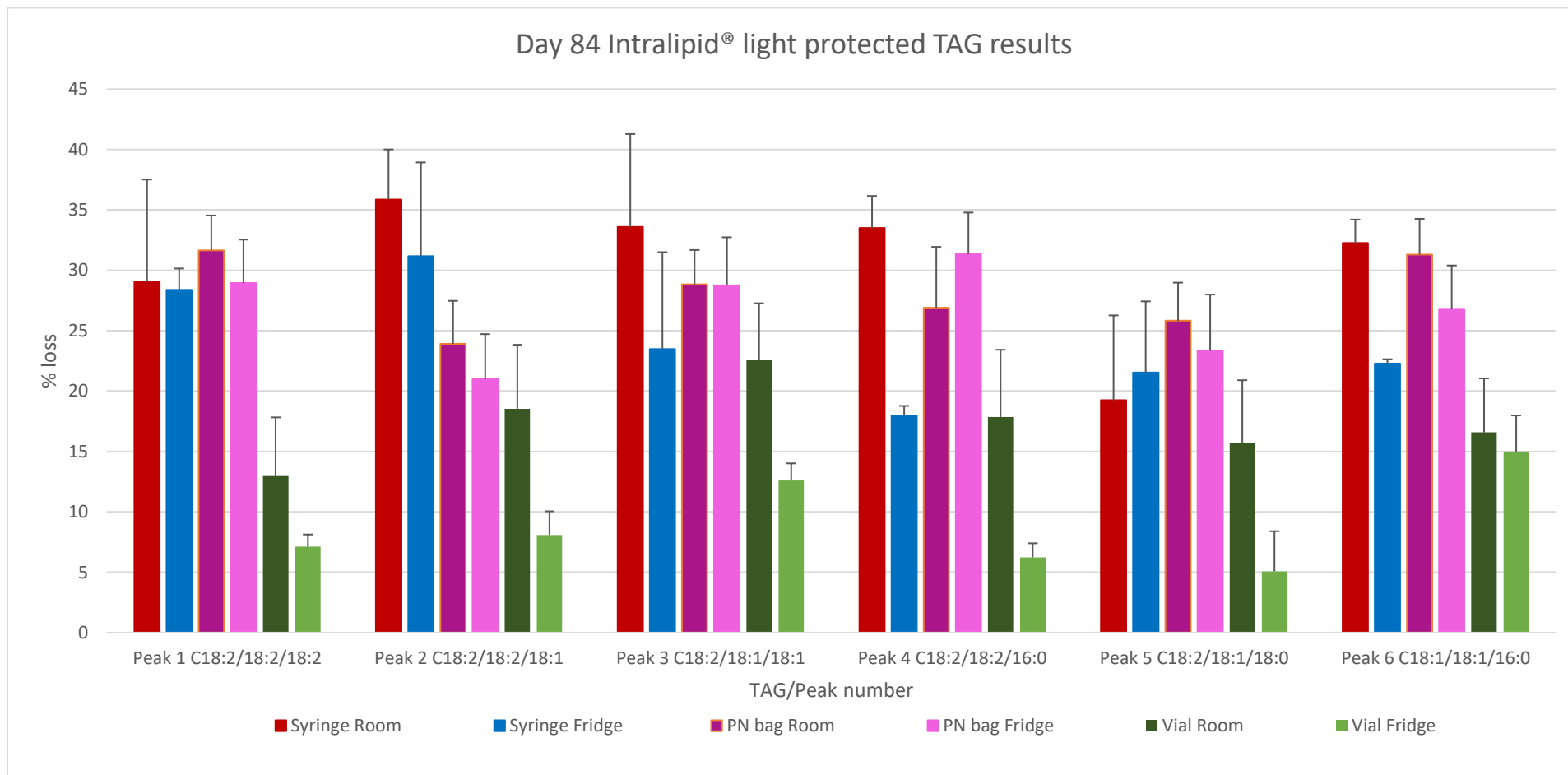
Figure 3.35 Triglyceride loss at 84 days storage for Intralipid® stored in syringes, PN bags and glass vials.

Table 3.1 Light protected Intralipid in all containers at all temperatures for each of the six peaks monitored. * indicates significant differences between results as calculated through ANOVA analysis with post hock Tukey analysis between each container type. (significant defined as $P<0.05$).

Peak 1	Room syringe	Room Bag	Room Vial	Fridge Syringe	Fridge Bag	Fridge Vial
Room Syringe	▨		*			*
Room Bag		▨	*			*
Room Vial	*	*	▨	*	*	
Fridge Syringe			*	▨		*
Fridge Bag					▨	*
Fridge Vial	*	*	*	*	*	▨

Peak 4	Room syringe	Room Bag	Room Vial	Fridge Syringe	Fridge Bag	Fridge Vial
Room Syringe	▨		*	*		*
Room Bag		▨		*		*
Room Vial	*		▨			*
Fridge Syringe	*			▨	*	
Fridge Bag					▨	*
Fridge Vial	*	*	*		*	▨

Peak 2	Room syringe	Room Bag	Room Vial	Fridge Syringe	Fridge Bag	Fridge Vial
Room Syringe	▨		*			*
Room Bag		▨				*
Room Vial	*		▨	*		
Fridge Syringe			*	▨		*
Fridge Bag					▨	*
Fridge Vial	*	*		*	*	▨

Peak 5	Room syringe	Room Bag	Room Vial	Fridge Syringe	Fridge Bag	Fridge Vial
Room Syringe	▨					*
Room Bag		▨	*			*
Room Vial		*	▨			*
Fridge Syringe				▨		*
Fridge Bag					▨	*
Fridge Vial	*	*	*	*	*	▨

Peak 3	Room syringe	Room Bag	Room Vial	Fridge Syringe	Fridge Bag	Fridge Vial
Room Syringe	▨					*
Room Bag		▨				*
Room Vial			▨			
Fridge Syringe				▨		
Fridge Bag					▨	*
Fridge Vial	*	*			*	▨

Peak 6	Room syringe	Room Bag	Room Vial	Fridge Syringe	Fridge Bag	Fridge Vial
Room Syringe	▨		*			*
Room Bag		▨	*			*
Room Vial	*	*	▨		*	
Fridge Syringe				▨		*
Fridge Bag			*		▨	*
Fridge Vial	*	*		*	*	▨

Figure 3.36 Triglyceride loss after 7 days of storage of Intralipid® in syringes, PN bags and glass vials.

3.8.2   HNE production

HNE production was observed within syringes stored at both fridge and room temperatures and minimally in room temperature PN bags. Room temperature syringes created a maximum of 10.209 µM HNE whilst fridge temperature storage yielded 8.38 µM HNE however this result was under the LOQ for the method. Both fridge PN bags and all glass vials showed no detectable HNE creation despite a level of TAG loss in PN bags similar to that within syringes. This result is interesting as it is apparent that peroxidation is still occurring within PN bags due to the TAG losses seen and the production of other peroxidation products (discussed in section 3.8.3). It can be postulated that potentially the products being created through the peroxidation process are either different within PN bags to syringes, or the rate of terminal peroxidation is different, i.e. less of the secondary product HNE is being made and greater amounts of primary peroxidation products are present. The presence of water within the emulsion could also permit hydrolysis reactions to occur, cleaving fatty acids from the glycerol backbone and causing TAG losses to be observed. Whilst the method was developed to specifically look for HNE present within samples, other peroxidation products were seen within the UV chromatogram and identified as discussed in 3.8.3. The method is limited however to UV detection at 222 nm wavelength and therefore other peroxidation products that would be detected with different wavelengths may be present within samples but undetectable due to the fixed wavelength of the equipment used.

The amount of HNE present within syringes is however of clinical significance, particularly with regards to the delivery of lipids to neonatal patients. As discussed in section 1.7 HNE at a concentration of less than 1 µM is shown to be genotoxic to cells (Esterbauer 1993). Delivery of lipids to paediatric patients is currently given through storage in 50 ml syringes and as such the production of HNE in both room and fridge temperatures is important. With respect to HNE alone, the move of lipids from syringes to PN bags for light protected Intralipid® would be beneficial to eliminate HNE production.

3.8.3 Degradation products 'A' and 'B'

The production of further degradation products as shown in figures 3.16 and 3.25 (UV chromatograms of PN bags and syringes at room temperature above in results section) labelled A and B are of interest and whilst the assay is not validated enable a concentration of these products to be calculated, their presence is important and as such investigated further. As discussed above, the UV chromatograms produced were from a wavelength of 222 nm as the detector used was at a fixed wavelength only. Both Intralipid® in room temperature syringes and PN bags formed a new peak through the course of testing labelled peak 'B' on chromatograms. Syringes stored at room temperature produced a further peak 'A' product.

Peak 'A' elutes early in the chromatogram of syringes at room temperature, near the HNE peak and therefore it was predicted that this peak was a secondary aldehydic product of peroxidation similar to HNE. Peak B elutes later in the chromatogram and was predicted to be the triglyceride 'remnant' i.e. the shorter TAG left after cleavage of secondary peroxidation products from the fatty acids present. To confirm these predictions eluate from the HPLC was collected at each of the time peaks corresponding to peaks A and B from multiple runs of the day 84 room temperature syringes and peak B from the day 84 room temperature PN bags. These fragments were then subjected to mass spectrometry analysis as per section 2.11.2. Peak B was detected in positive mode as per method, whilst peak 'A' was only detectable in negative mode, however all other parameters remained as defined in section 2.11.2. Figures 3.37 and 3.38 show the mass spectrum obtained for each peak. Table 3.2 Summarises the results from each peak.
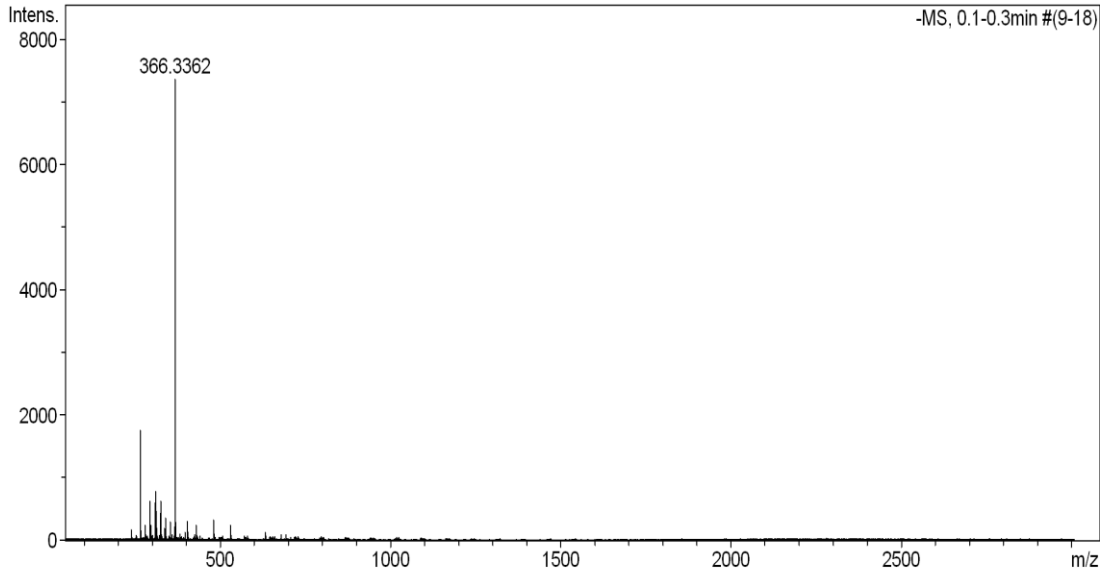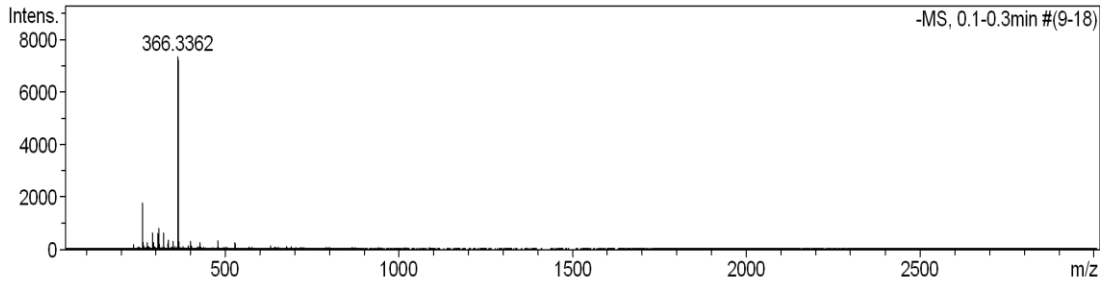
Figure 3.37 Mass spectrum for Peak 'A' in room temperature Intralipid® light protected syringes at day 84.
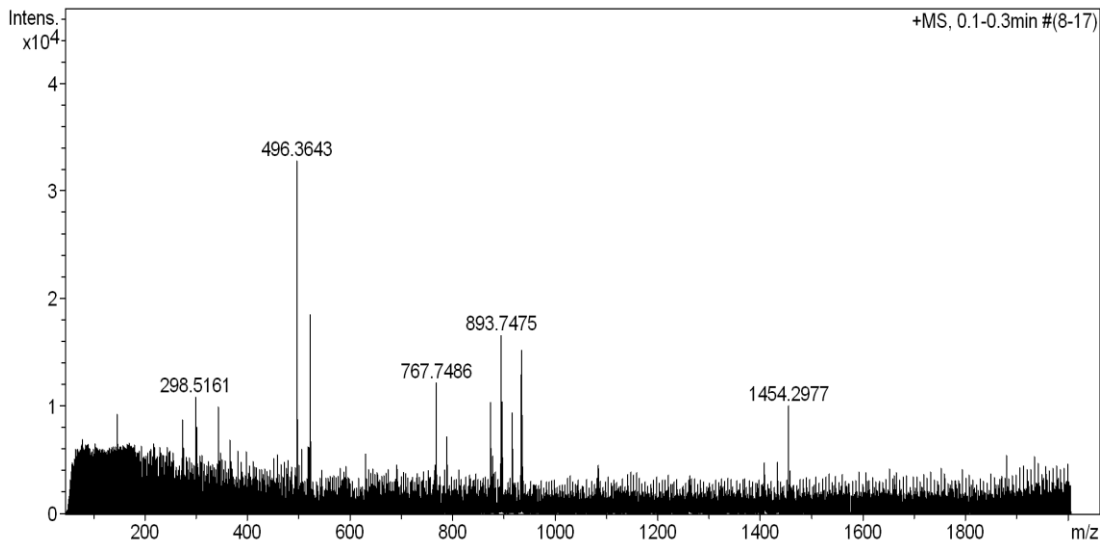
Figure 3.38 Mass spectrum for peak 'B' in Intralipid® light protected syringes. PN bags peak 'B' gave the same m/z data.

164

Peak reference	Storage container	Storage Temperature	Average m/z data (n=3)
A	Syringe	Room	366.34 (-ve mode)
B	Syringe	Room	496.40 (+ve mode)
B	PN bag	Room	496.34 (+ve mode)
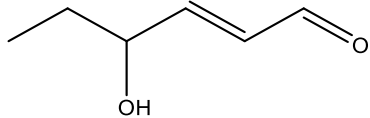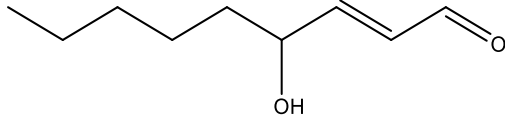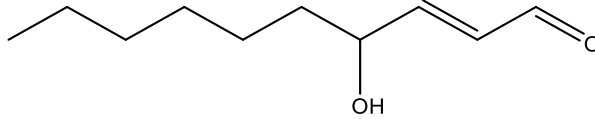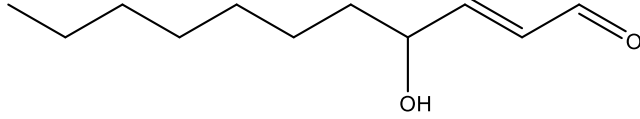
3.8.3.1 Peak A

Mass spectrometry data showed peak A to have a m/z ratio of 366.34 in negative mode. With respect to its elution position in the chromatogram of Intralipid® syringes at room temperature, peak A elutes close to HNE. Whilst HNE was selected as the secondary peroxidation product to be monitored due to its known toxicity, it was predicted that many other primary and secondary peroxidation products would also be produced. The presence of multiple fatty acids with multiple levels of unsaturation within Intralipid® chemically predicts the production of several secondary products of differing carbon chain length. Table 3.2 Shows the calculated theoretical m/z for secondary aldehydic products of increasing chain length. The table includes only products that can be formed form linoleic, linolenic or oleic acids as these are the only fatty acids present within the TAGs in Intralipid® that are liable to peroxidation.

As shown in table 3.3 the mass spectrometry data for peak A in room temperature syringes gave an average m/z of 366.30 which matches the theoretical data for 4-hydroxyundec-2-enal (HUE). HUE is a secondary aldehyde formed from the peroxidation of oleic acid (Loidl-Stahlhofen et al. 1995). Whilst little studied in comparison to HNE, HUE confers a level of toxicity greater than that of the smaller C6 aldehyde Hydroxyhexenal (HHE) formed from linolenic acid (18:3) when considering DNA damage (Eckl et al. 1993) and therefore is of clinical significance. Whilst the concentration of HUE produced in the 84 days syringes cannot be quantified by the assay, the peak area observed approximately 3 times greater than the quantified peak of HNE (figure 3.16), indicating that the HUE present is at a concentration higher than that of HNE, however each of these aldehydes will have a different absorption level at 222 nm and therefore the concentration of HUE cannot accurately be gauged from comparison with HNE alone.

Looking into the rate of production of peak A/HUE within Intralipid® room temperature syringes, peak area was monitored through the 84 days of testing. Figure 3.39 represents the formation of this peak within room temperature syringes. The data shows a relatively steady rate of HUE (peak A) production across the 84-day testing period indicating a steady rate of oleic acid peroxidation occurring. Of the triglycerides identified and monitored peaks 2,3,5 and 6 contain at least one oleic acid within its corresponding triglyceride and all show a substantial loss over storage, theoretically allowing a production of HUE to occur through peroxidation.

Table 3.3 Potential secondary peroxidation products from linoleic (18:2), linolenic (18:3) and oleic acids (18:1).

Name	Carbon number	Structure	Mass spectrometry predicted data		
			m/z	[M-H]⁻	[2M-H]⁻
4-hydroxyhex-2-enal (HHE)	C6		114.07	113.07	227.14
4-hydroxynon-2-enal (HNE)	C9		156.12	155.12	311.24
4-hydroxydec-2-enal (HDE)	C10		170.13	169.13	339.26
4-hydroxyundec-2-enal (HUE)	C11		185.15	184.15	366.30
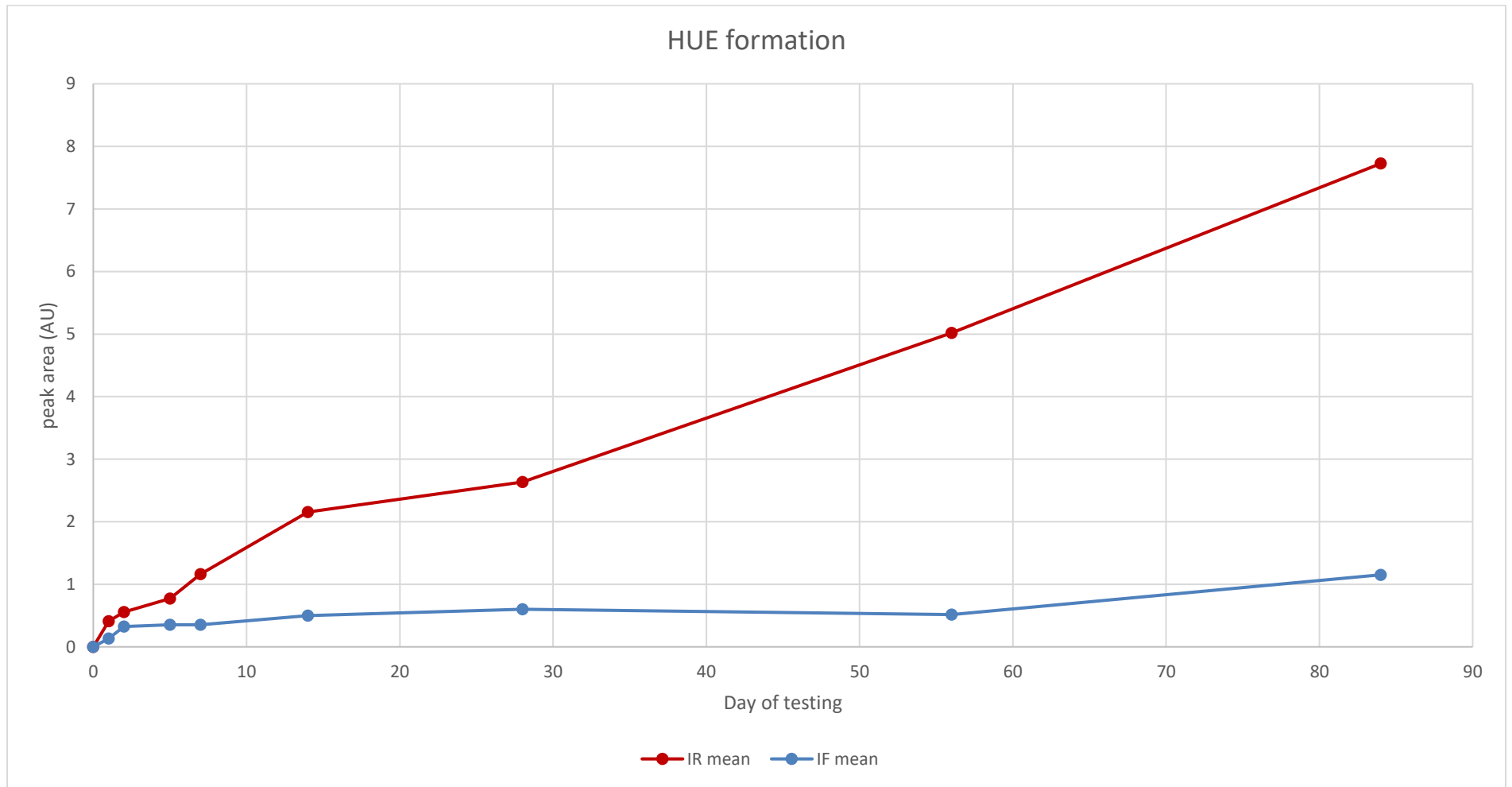
Figure 3.39 Formation of HUE (Peak A) in 50 ml Intralipid® syringes at room (red) and fridge (blue) temperatures.

As shown in table 3.2 and figure 3.38 the mass spectrometry data from peak B in both room temperature syringes and PN bags show the production of a peak with a m/z of 496.35. The prediction for this peak was that it could potentially be the remains of a triglyceride after the fatty acids within the TAG had peroxidised and cleaved, leaving a smaller chained TAG 'remnant'. When considering the peaks monitored, peak 3, (C18:1/18:1/18:2) contains two oleic acid fatty acids and one linoleic acid. At the end of 84 days of storage in syringes this TAG lost over 30 % at room temperature and over 20 % at fridge temperature. Chemically, the peroxidation of this TAG as shown schematically in figure 3.40 could theoretically peroxidise to form 2 molecules of HUE and 1 molecule of HNE per TAG. This peroxidation pathway would leave the TAG 'remnant' as shown in figure 3.40 which has a molecular weight of 495.35 and a predicted $[M+H]^+$ of 496. This matches the results seen from peak B and as such confirms the likelihood that B is a remnant of Peak 3 triglyceride and its peroxidation.

The rate of TAG remnant production, whilst not quantifiable through the assay, was plotted as shown in figure 3.41 for room temperature syringes and room temperature bags. Both show a production of this TAG remnant, suggesting peroxidation of peak 3, however room temperature bags did not show an apparent production of HUE. This suggests therefore, that peak B may not only be attributed to a TAG remnant from peak 3 but potentially from more than one compound with the same m/z, caused through the peroxidation and cleavage of other fatty acids present within the numerous TAGs present. For the purposes of this work, further identification was not achieved due to the limited fractionation capacity of the mass spectrometry and that the main aims of the project were to monitor the TAG loss and HNE production as validated in the method, within PN lipids. The clinical relevance of the peak B is important as it indicates peroxidation and TAG breakdown is occurring in the Intralipid® bag and syringe samples tested at room temperature.

C18:1/18:1/18:2 (OLEIC/OLEIC/LINOLEIC)

+H_2O

13' HYDROPEROXIDE

OLEIC RADICALS

+OH·

HUE

HUE

+

+

HNE

Teiglyceride 'remnant'
m/z: 495.35
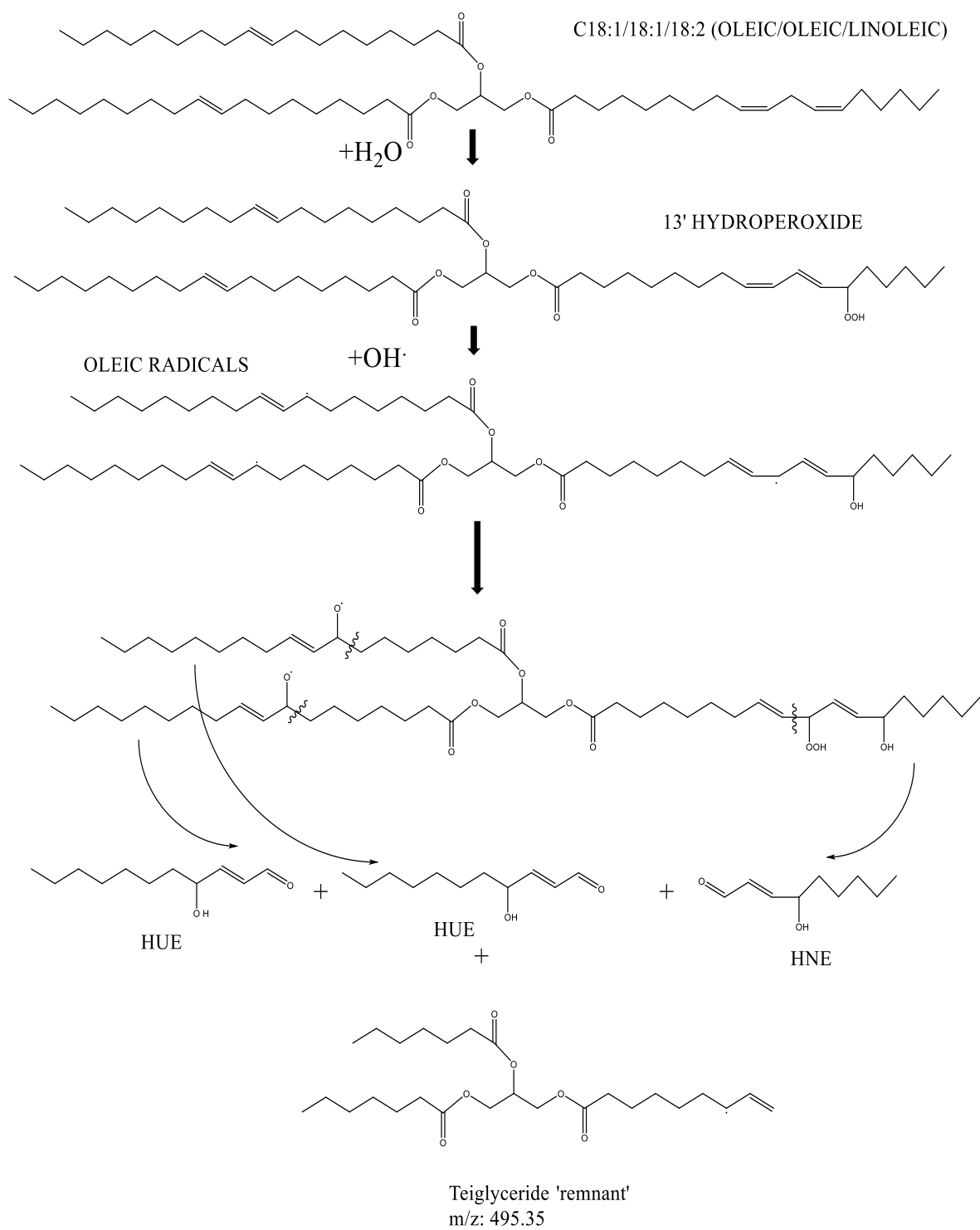
Figure 3.40 Predicted chemical schematic of the production of HUE and HNE and Tag remnant from Peak 3 TAG in Intralipid®
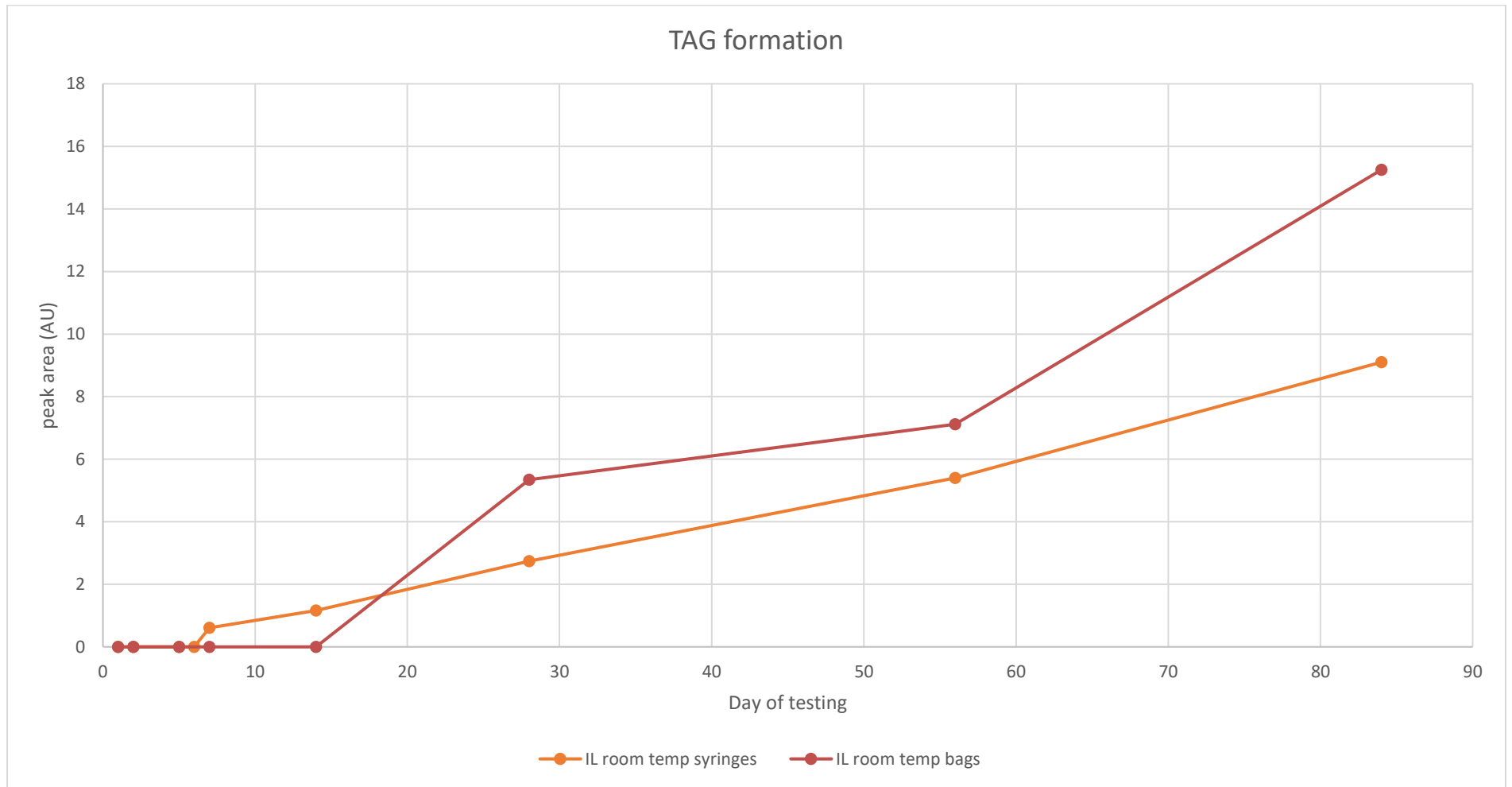
Figure 3.41 HPLC-UV results of TAG remnant/peak B formation in Intralipid® room temperature syringes and bags.

Chapter 4

Intralipid® Non-light Protected Syringes, Bags and Vials

4.1. Introduction to non-light protected testing

Light induced lipid peroxidation or photo-oxidation as discussed in section 1.5.1 (introduction section 1.5) provides a secondary pathway for the initiation of peroxidation within lipid emulsions. As discussed in chapter 3 in light protected testing, the level of oxygen present within the storage system is critical to the peroxidation process. This is equally true for non-light protected lipid emulsions as the propagation of the peroxidation process is oxygen dependant (Halliwell and Chirico 1993).

4.1.1. Light radical formation

The formation of a reactive oxygen species (ROS), commonly a peroxyl radical, due to light exposure provides the radical required for the initiation of peroxidation (Mühlebach and Steger 1998; Hardy and Puzovic 2009). Light exposure in the presence of oxygen can further lead to the creation of singlet oxygen ($^1O_2$). Whilst not a 'true radical', the formation of two negatively charged electrons within the same orbital creates an unstable species with high reactivity. Singlet oxygen is commonly formed in the presence of a photo-sensitizer such as riboflavin in the case of milk peroxidation, however evidence postulates that its production may result as a degradation product of lipid peroxides (Van Dyck 2010; Leray 2016). Therefore, this chapter looks at non-light protected Intralipid® in the same containers and conditions as outlined in testing protocol in section 3.4 minus the light protective foil. The work aimed to create a dataset that acts as a comparator to light protected data, giving an indication on whether photooxidation could occur and if the rate and extent of peroxidation seen differed from light protected containers.

4.2. Light control

To create a set of comparative data to that collected in chapter 3, the same testing protocol was carried out for non-light protected lipid syringes, ML bags and glass vials. Intralipid® samples were prepared as per section 3.4 and held at both fridge and room temperature. The variable factor tested was light exposure and therefore light exposure was controlled throughout storage. For fridge temperatures light exposure was limited due to the nature of the storage within a refrigerator, however containers were exposed to ambient light during testing and placed on separate fridge shelves to maximise available light exposure. The lack of a light control

mechanism for fridge storage temperatures was a factor that could not be altered within this testing however introduction of a light source within a refrigerator would enable light exposure to be further controlled.

4.2.1. Stability chamber light and temperature control

For room temperature, storage containers were placed in a stability chamber (Sanyo/Weiss Gallenkamp model PSC062). This enabled control over temperature, humidity and light exposure. Temperature was set at 22 $^\circ$C throughout storage to match the average temperature of the room data in chapter 3. Humidity was controlled at 60 % throughout storage to match the testing protocols used for physical stability within the laboratory. The primary purpose of the stability chamber was to enable control over the type and extent of light exposure samples would be subject to. Cool white visible strip lights are used within the chamber to emit a light that falls within the ICH Q1B guidelines for pharma-light sources for stability testing (Harmonisation 1996). As per the chamber's manual, light emission was validated and monitored using lux sensors to ensure uniformity of emitted light. Intensity of light was set to level 5/10 as per manual to mimic exposure to natural daylight (with UV exposure) (Weiss Gallenkamp 2006). Samples were placed on shelves within the stability chamber ensuring that equal distances between placement of samples was achieved.

4.3. Testing schedule

An identical testing protocol was followed as per section 3.4. To summarise, 50 ml of Intralipid® was placed in 50 ml syringes, 50 ml ML PN bags and 50 ml glass vials, the latter being purged with nitrogen after formulation. Six samples of each lipid in each container were produced, 3 held at room temperature as discussed above and 3 at fridge temperature. All samples were tested in triplicate using the HPLC method set out in chapter 2 at days 0, 1, 2, 7, 14, 28, 56 and 84. The following results sections detail the data collected from all samples that were exposed to light throughout storage. The control sample used for each day of testing was a lipid in its original container that was light protected with foil to prevent possible peroxidation and ensure a control set of data.

4.4. Intralipid® non-light protected syringe results

As discussed in section 3.5 all data was analysed using Chromeleon software (Thermo Scientific) with each six TAG peaks monitored through CAD detection as a % loss in peak area. HNE production is presented in figure 4.7 ± standard deviation, however as shown in the 84-day chromatograms in figure 4.11 HNE detection was minimal and below the validated limit of quantification. All RSD's were monitored for all peaks and controls throughout testing to ensure data was precise and reproducible. As shown in appendix 2 all RSD's were <12 which were acceptable (as discussed in section 3.4).

TAG loss exceeded 40 % for peaks 3 to 6 at both fridge and room temperatures as shown in figures 4.1 to 4.6. Raw data for all results is shown in appendix 2. Peaks 1 and 2 showed a maximal loss of 35 and 30 % respectively. As shown in figures 4.1 and 4.2 temperature had a statistically significant effect on TAG loss for peaks 1 (C18:2/18:2/18:2) and 2 (C18:2/18:2/18:1), but little effect on the level of TAG loss for all other peaks monitored. TAG results are discussed further in section 4.7.

As postulated in section 3.8.3 two degradation products were visualised and identified in the light protected testing results. Peak 'A' being identified potentially was HUE and peak 'B' as a triglyceride remnant due to the peroxidation of peak 3. In the non-light protected results as shown in figures 4.8 and 4.9 both products are identified. HUE (peak 'A') was detected in both fridge and room temperatures. The triglyceride remnant (peak 'B') was produced and detected in room temperature Intralipid® syringes but undetectable in fridge storage. Both products are discussed further in section 4.7.

Figure 4.1 HPLC-CAD results for peak 1 (C18:2/18:2/18:2) triglyceride of Intralipid® 20 % stored in non-light protected 50 ml syringes. Percentage loss of peak shown calculated from day 0 data. Room (Red) and Fridge (Blue) results shown with standard deviation error bars on all points

Figure 4.2 HPLC-CAD results for peak 2 (C18:2/18:2/18:1) triglyceride of Intralipid® 20 % stored in non-light protected 50 ml syringes. Percentage loss of peak shown calculated from day 0 data. Room (Red) and Fridge (Blue) results shown with standard deviation error bars on all points.

Figure 4.3 HPLC-CAD results for peak 3 (C18:2/18:1/18:1) triglyceride of Intralipid® 20 % stored in non-light protected 50 ml syringes. Percentage loss of peak shown calculated from day 0 data. Room (Red) and Fridge (Blue) results shown with standard deviation error bars on all points.

Figure 4.4 HPLC-CAD results for peak 4 (C18:2/18:2/16:0) triglyceride of Intralipid® 20 % stored in non-light protected 50 ml syringes. Percentage loss of peak shown calculated from day 0 data. Room (Red) and Fridge (Blue) results shown with standard deviation error bars on all points.

Figure 4.5 HPLC-CAD results for peak 5 (C18:2/18:1/18:0) triglyceride of Intralipid® 20 % stored in non-light protected 50 ml syringes. Percentage loss of peak shown calculated from day 0 data. Room (Red) and Fridge (Blue) results shown with standard deviation error bars on all points.

Figure 4.6 HPLC-CAD results for peak 6 (C18:2/18:1/16:0) triglyceride of Intralipid® 20 % stored in non-light protected 50 ml syringes. Percentage loss of peak shown calculated from day 0 data. Room (Red) and Fridge (Blue) results shown with standard deviation error bars on all points

Figure 4.7 HPLC-UV data showing the production of 4-Hydroxynonenal in Intralipid® 20 % over 84-day storage and both room (red) and fridge (blue) temperatures in 50 ml syringes.
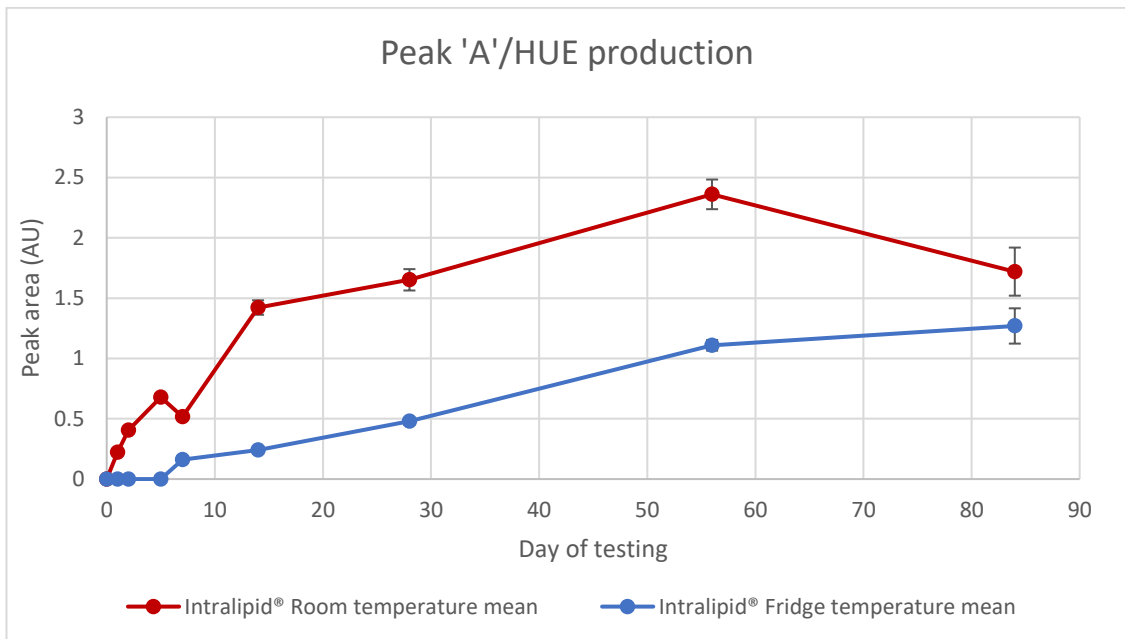
Figure 4.8 HPLC-UV data showing the formation of HUE (Peak A) in non-light protected 50 ml Intralipid® syringes at room (red) and fridge (blue) temperatures.
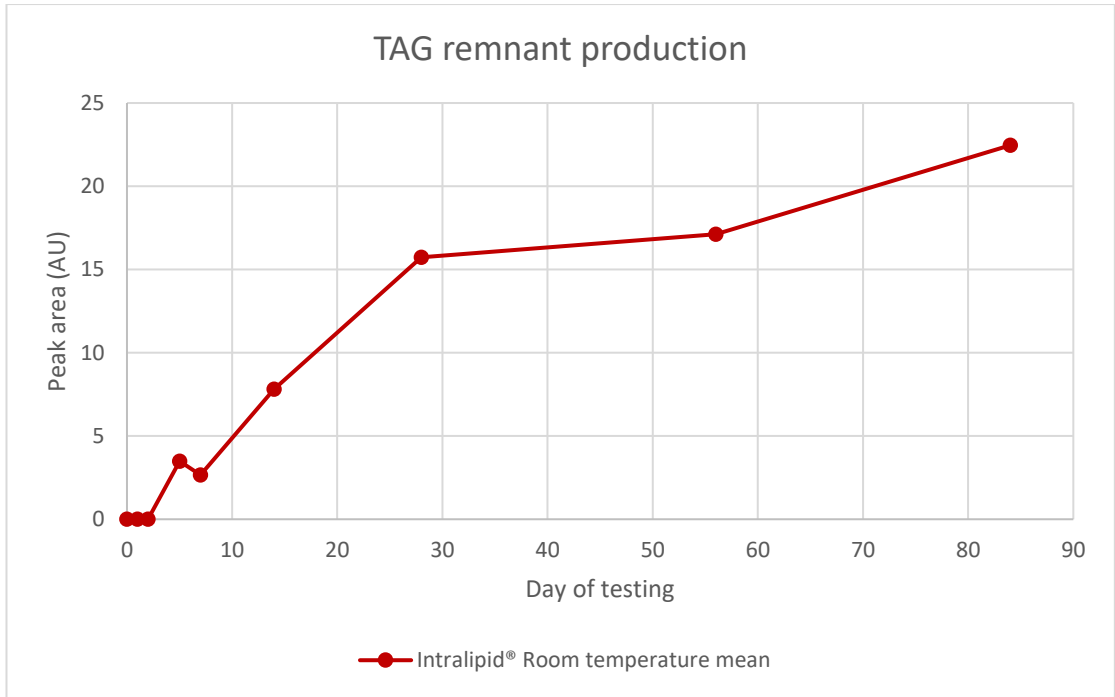
Figure 4.9 HPLC-UV data showing the production of the TAG remnant/peak B in non-light protected 50 ml Intralipid® syringes at room temperature.

Figure 4.10 HPLC-CAD chromatograms of Intralipid® 20% stored in non-light protected 50 ml syringes. Day 0 control (black), day 84 fridge temperature (blue trace) and day 84 room temperature (red trace). The y-axis of each chromatogram gives an indication of peak height and the corresponding drop in peak area seen in the 84 day chromatograms. Overlaid chromatogram shows changes in peaks in comparison to control.

Figure 4.11 HPLC-UV chromatograms of Intralipid® 20% stored in 50 ml syringes. Day 0 chromatogram (black trace), day 84 fridge temperature syringes (blue trace) and day 84 room temperature syringes (red trace). The production of HNE, HUE and the TAG remnant can be seen in room temperature syringes as indicated on the chromatogram.

Figure 4.12 Overlaid HPLC-UV chromatograms of day 0 (black trace) and day 84 room temperature (red trace) Intralipid® 20 % stored in non-light protected 50 ml syringes. Peaks on the 84 day chromatogram highlighted in red show HUE and the TAG remnant formation.

4.5. Intralipid® non-light protected bag results

As per testing protocol 250 ml Baxa EVA multi-layer PN bags were filled with 50 ml Intralipid® 20 % and stored at room and fridge temperature with exposure to light. Room temperature samples were held in the stability chamber as described in section 4.2.1 to control light exposure levels and temperature. At each point of testing 1 ml of lipid was removed and tested. All possible air was removed from each PN bag at all testing points. A control sample in its original packaging was tested at each time point to ensure method precision. All results were performed in triplicate and standard deviations and relative standard deviations calculated for each point. Raw data is shown in appendix 2 and the following figures 4.13 to 4.18 show the data for all six TAGs monitored as a % loss from their day 0 amount.

The data collected when analysed showed RSD's of the day 84 control samples to be >12 which, as detailed in chapter 2 was considered an unacceptable level of variation for the CAD detector. Therefore, whilst the following figures show the plotted day 84 results, all day 84 results were marked as outliers and excluded from the analysis in section 4.7. The high RSD's in the samples occurred across all day 84 samples tested for the ML PN bags and was attributed to an increased ambient temperature within the testing laboratory (hottest day of the year). The HPLC system was cleaned using a standard organic protocol and testing of subsequent samples was carried out only when the ambient temperature within the laboratory had reduced. All RSD's for the next set of samples run fell within acceptable levels.

At day 56, all TAGs monitored showed a maximal loss of ~20 %. All TAGs other than peak 3 (C18:2/18:1/18:1) showed a significantly higher level of loss at room temperatures than at fridge temperatures.

No quantifiable levels of HNE were observed throughout both fridge and room temperature storage. HUE as identified in section 3.8.3 was detected as shown in figure 4.19 in PN bags stored at room temperature. Fridge storage inhibited the production of HUE.

The TAG remnant/ peak B as discussed in section 3.8.3 was identified in room temperature PN bags as shown in figure 4.20. Fridge storage inhibited its formation, suggesting that the peroxidation processes monitored were minimal in PN bags stored at fridge temperatures. Results are discussed further in context with all results within the chapter in section 4.7.
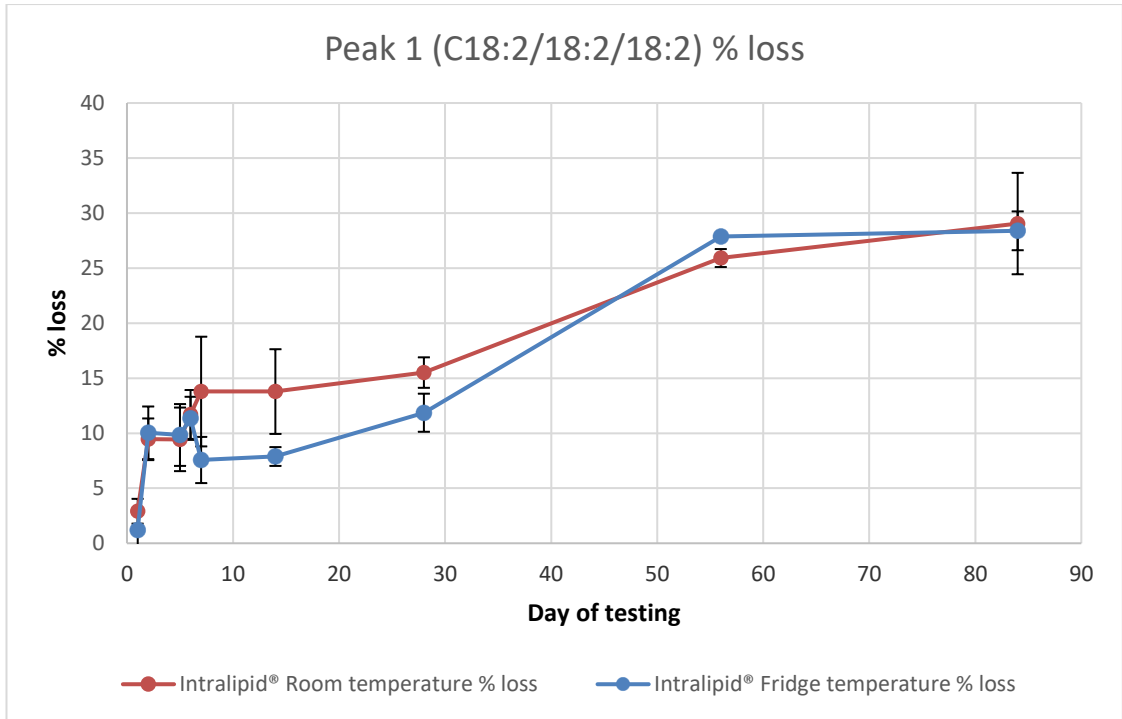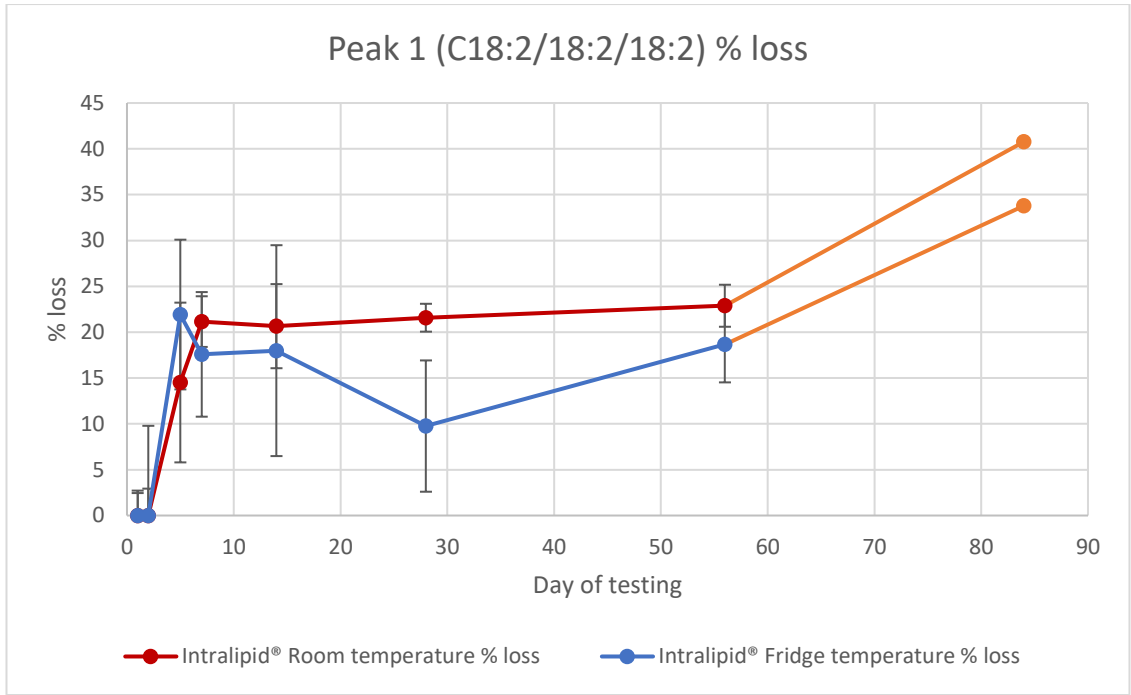
Figure 4.13 HPLC-CAD results for peak 1 (C18:2/18:2/18:2) triglyceride of 50 ml Intralipid® 20 % stored in 250ml non-light protected PN bags. Percentage loss of peak shown calculated from day 0 data. Room (Red) and Fridge (Blue) results shown with standard deviation error bars on all points. Orange points denotes day 84 results identified as anomalous.
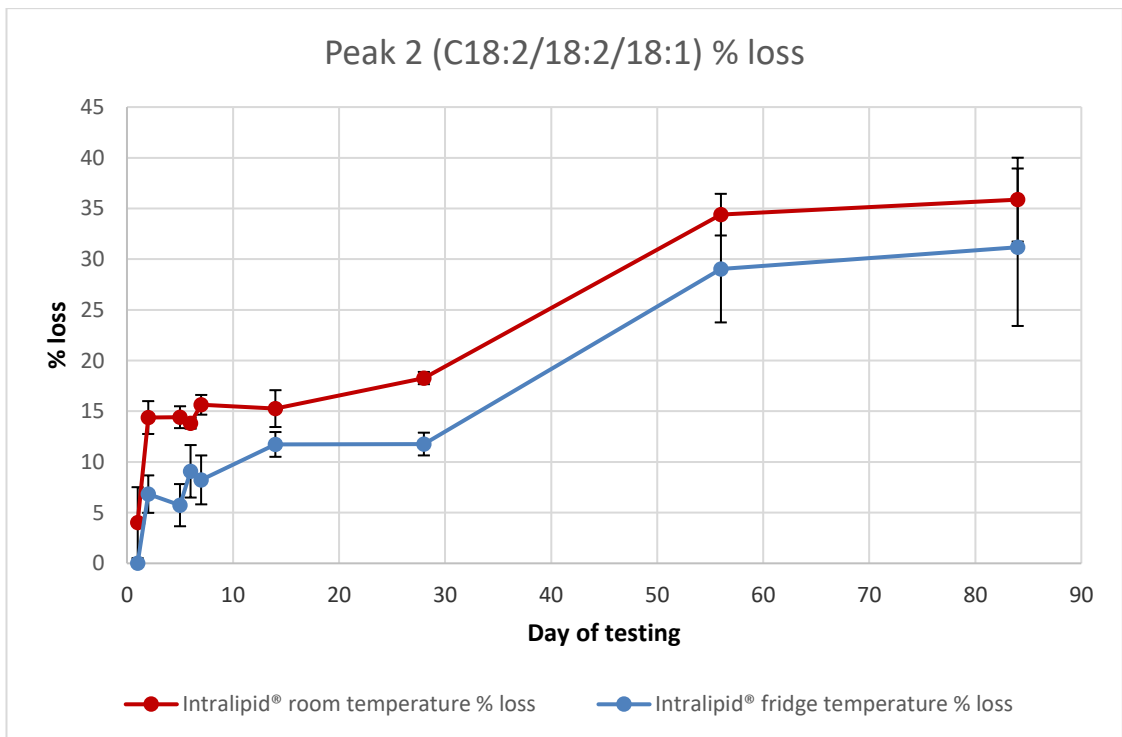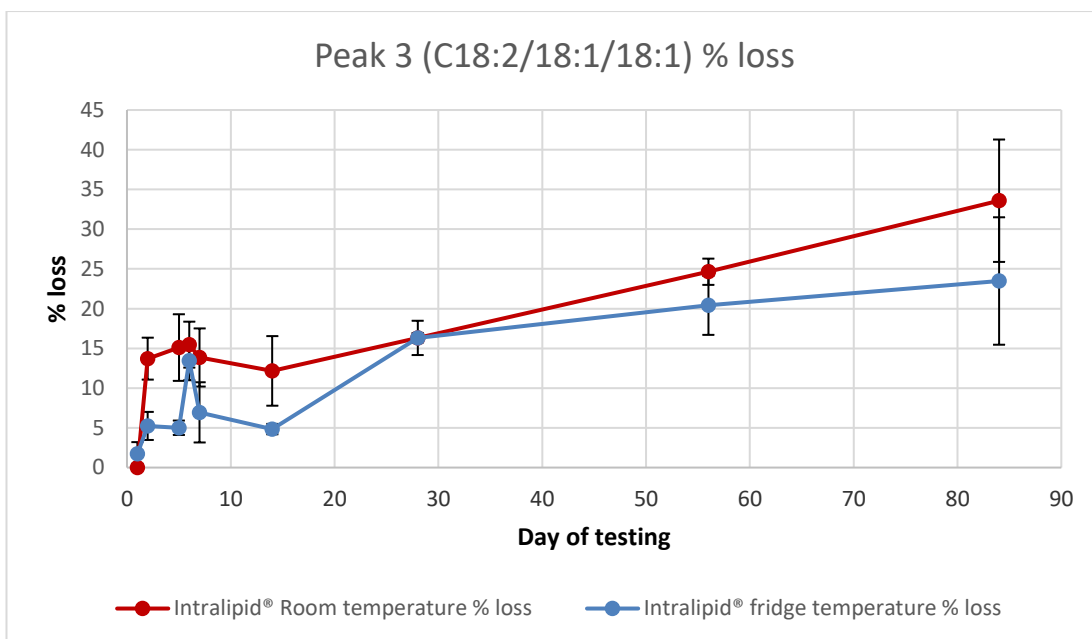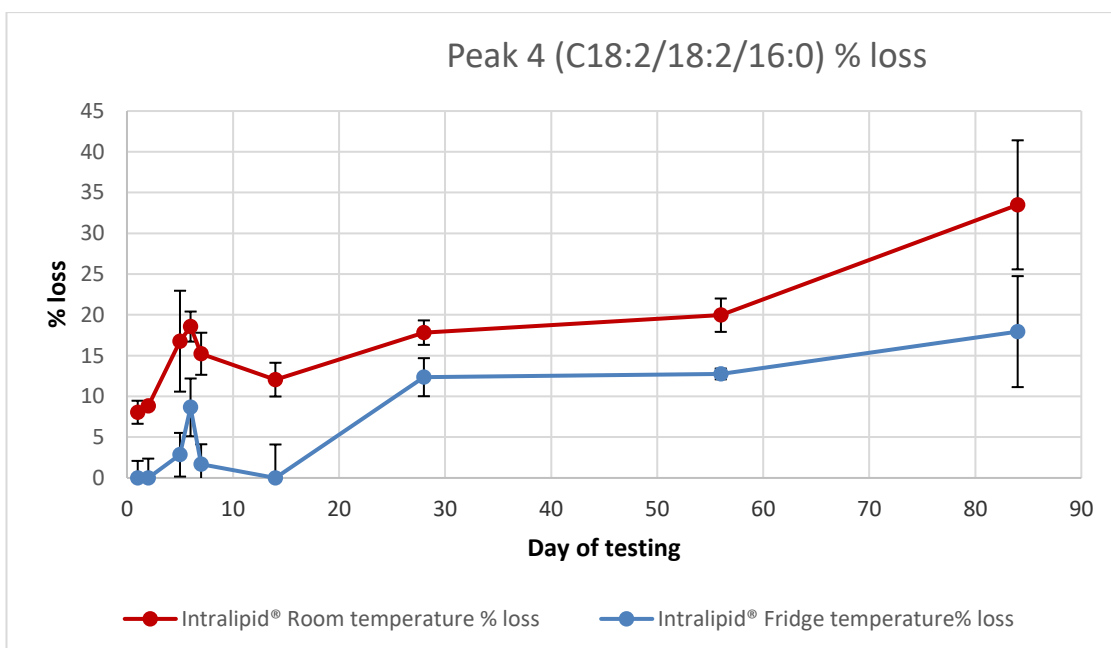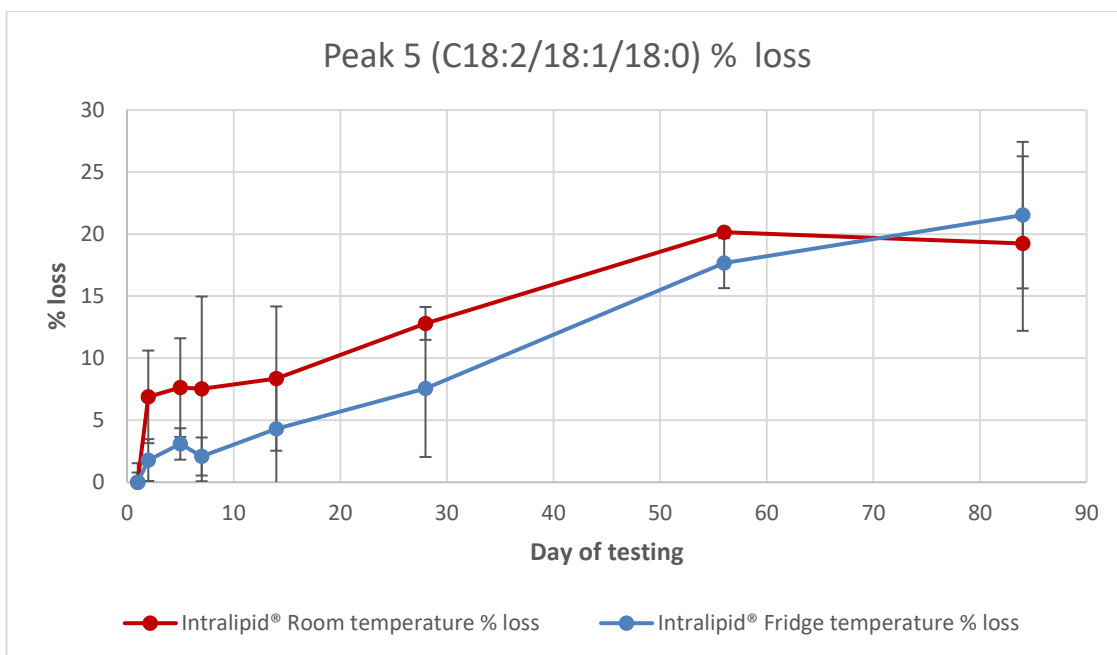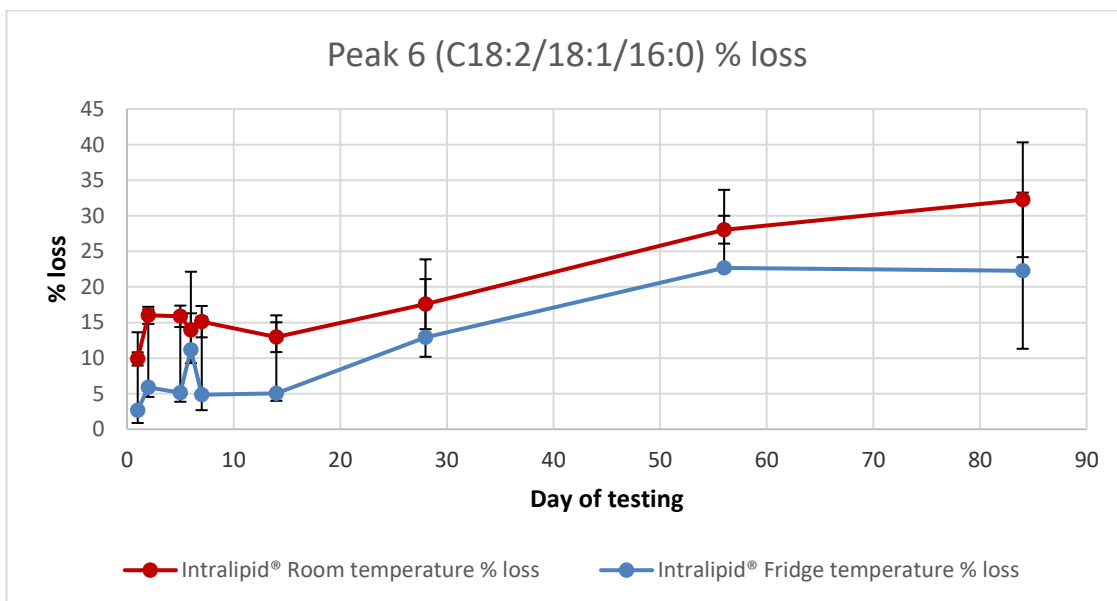

Figure 4.14 HPLC-CAD results for peak 2 (C18:2/18:2/18:1) triglyceride of 50ml Intralipid® 20 % stored in light protected 250 ml PN bags. Percentage loss of peak shown calculated from day 0 data. Room (Red) and Fridge (Blue) results shown with standard deviation error bars on all points. Orange points denotes day 84 results identified as anomalous.

Figure 4.15 HPLC-CAD results for peak 3 (C18:2/18:1/18:1) triglyceride of 50 ml Intralipid® 20 % stored in light protected 250 ml PN bags. Percentage loss of peak shown calculated from day 0 data. Room (Red) and Fridge (Blue) results shown with standard deviation error bars on all points. Orange points denotes day 84 results identified as anomalous.

Figure 4.16 HPLC-CAD results for peak 4 (C18:2/18:2/16:0) triglyceride of 50 ml Intralipid® 20 % stored in light protected 250 ml PN bags. Percentage loss of peak shown calculated from day 0 data. Room (Red) and Fridge (Blue) results shown with standard deviation error bars on all points. Orange points denotes day 84 results identified as anomalous.

Figure 4.17 HPLC-CAD results for peak 5 (C18:2/18:1/18:0) triglyceride of 50 ml Intralipid® 20 % stored in light protected 250 ml PN bags. Percentage loss of peak shown calculated from day 0 data. Room (Red) and Fridge (Blue) results shown with standard deviation error bars on all points. Orange points denotes day 84 results identified as anomalous.

Figure 4.18 HPLC-CAD results for peak 6 (C18:2/18:1/16:0) triglyceride of 50 ml Intralipid® 20 % stored in light protected 250 ml PN bags. Percentage loss of peak shown calculated from day 0 data. Room (Red) and Fridge (Blue) results shown with standard deviation error bars on all points. Orange points denotes day 84 results identified as anomalous.
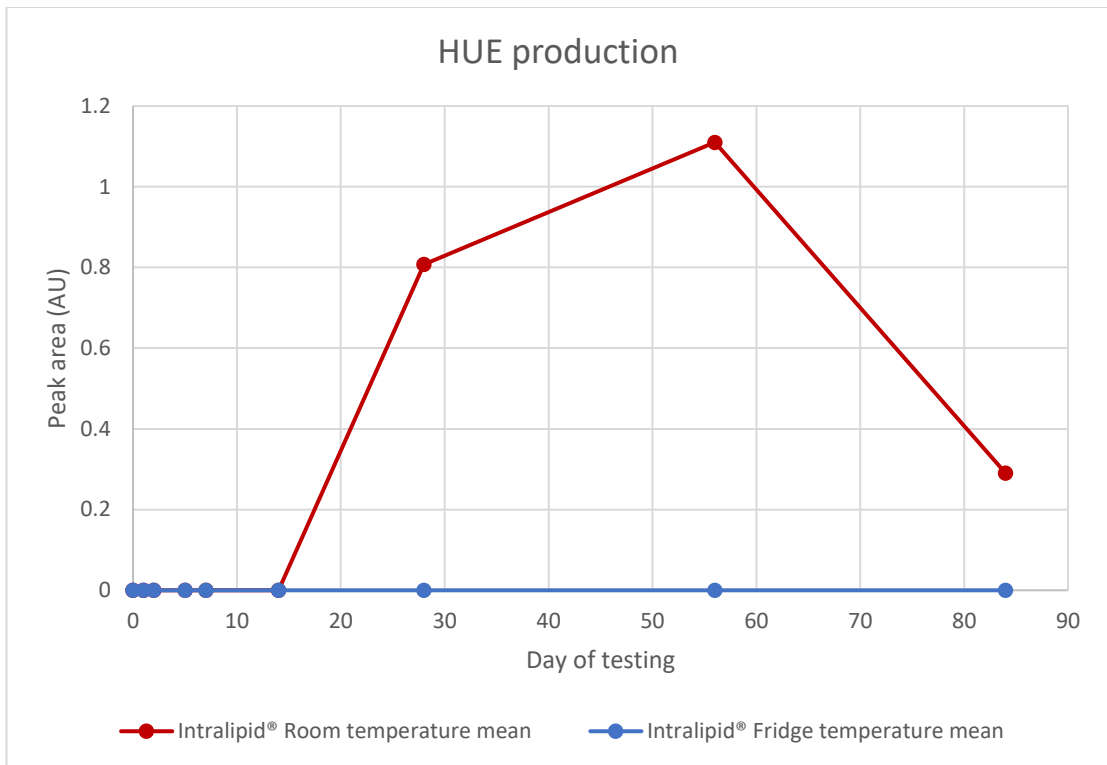
Figure 4.19 HPLC-UV results for 250ml ML PN bags exposed to light. Red indicates formation of HUE in Room temperature bags, blue indicates lack of HUE in fridge temperature bags over 84 days.
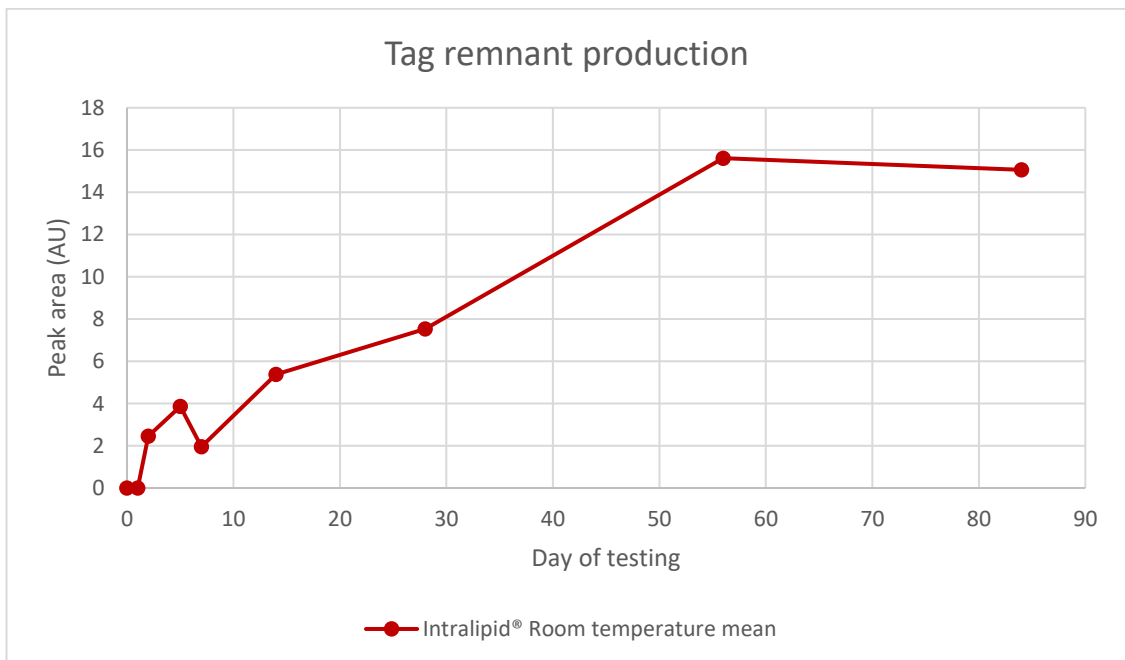
Figure 4.20 HPLC-UV result showing the production in peak area of the TAG remnant/peak B in PN bags at room temperature.

Figure 4.21 HPLC-CAD chromatograms of 50 ml Intralipid® 20% stored in 250 ml PN bags. Day 0 control (black), day 84 fridge temperature chromatogram (blue trace) and day 84 room temperature (red trace). The y-axis of each chromatogram gives an indication of peak height and the corresponding drop in peak area seen in the 84 day chromatograms. Overlaid chromatogram shows changes in peaks in comparison to control.

Figure 4.22 HPLC-UV chromatograms of 50 ml Intralipid® 20% stored in 250 ml light exposed PN bags. Day 0 chromatogram (black trace), day 84 fridge temperature bags (blue trace) and day 84 room temperature syringes (red trace). The production of HUE and the TAG remnant in room temperature bags can be seen and is indicated on the chromatogram.

Figure 4.23 Overlaid HPLC-UV chromatograms of day 0 (black trace) and day 84 room temperature (red trace) Intralipid® 20 % stored in 250 ml light exposed PN bags. Peaks on the 84 day chromatogram highlighted in red show HUE and TAG remnant production.

191

4.6. Intralipid® non-light protected vial results

As per protocol, glass vials were filled with 50 ml Intralipid® and sealed with metal crimps. Oxygen was removed from the lipid and headspace using nitrogen as described in section 3.2.3. At each testing point 1 ml of lipid was removed from the vial and placed into autosampler vials for testing. All vials were left exposed to light with room temperature samples placed in a stability chamber to control light intensity and temperature.

All peaks/TAGs monitored showed minimal (less than 15 %) loss over 84-day storage at both temperatures except peak 2 (TAG C18:2/18:2/18:1) which showed ~40% loss at day 84 in both fridge and room temperatures. The RSD's of the control sample used each day fell above acceptable levels for all peaks at day 84 of testing which was attributed to high laboratory temperatures on day 84. When considering up to day 56 results, all peaks/TAGs showed a less than 15% loss. TAG loss was inhibited in all samples until day 28. Figures 4.24 to 4.29 show the HPLC-CAD results for each peak expressed as a % loss of peak area from day 0. All raw data is recorded in appendix 2.

No HNE, HUE or TAG remnant was recorded in any of the samples across the 84-day testing period (figures 4.30 to 4.32). This indicates a lack of peroxidation occurring within all samples. The lack of TAG loss until day 56 in all samples indicates that the method of oxygen replacement with nitrogen at all testing points was successful until this point in preventing identifiable peroxidation from occurring. The increase in TAG loss at day 84 could be due to an ingress of oxygen into the system and the initiation of peroxidation occurring after day 56, however the increased values and RSD's of the control samples at day 84 correspond to the increased % loss seen in all samples. This indicates that the day 84 results may not be precise and as such are excluded from further analysis. The high laboratory temperatures on day 84 testing could have contributed to the increased RSD's and TAG loss rather than oxygen ingress.

The lack of identifiable peroxidation products within Intralipid® vials exposed to light suggests that effective removal of oxygen inhibits the initiation of peroxidation. This indicates that the peroxidation processes occurring within Intralipid® samples are oxygen dependant as shown in chapter 1 (section 1.5). Results are further discussed in comparison with PN bags and syringes in section 4.7.
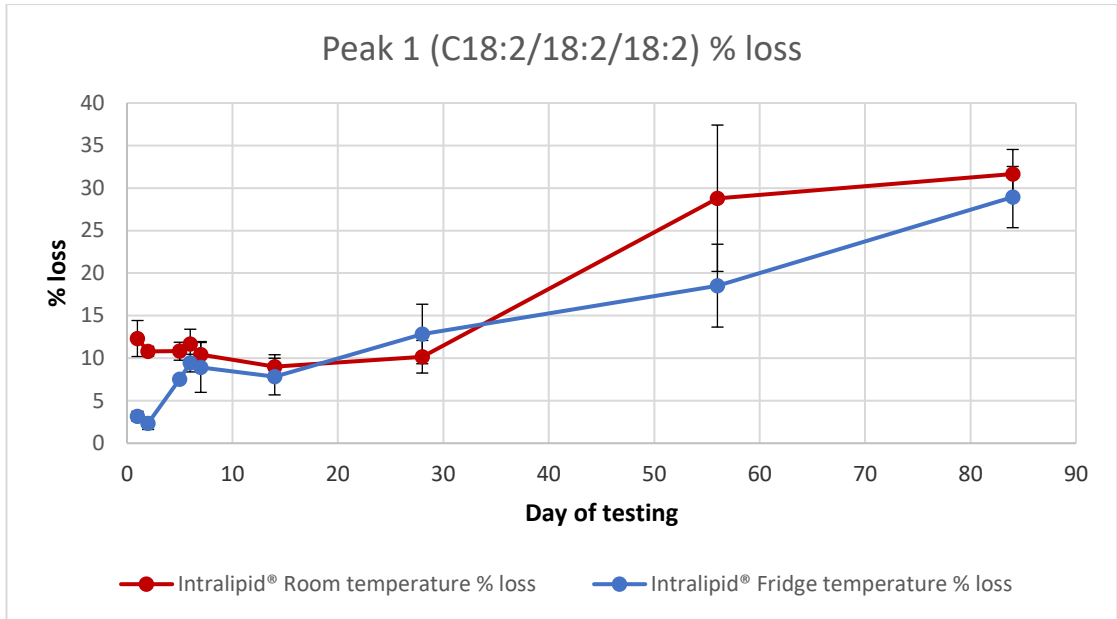
Figure 4.24 HPLC-CAD results for peak 1 (C18:2/18:2/18:2) triglyceride of Intralipid® 20 % stored in 50ml non-light protected glass vials. Percentage loss of peak shown calculated from day 0 data. Room (Red) and Fridge (Blue) res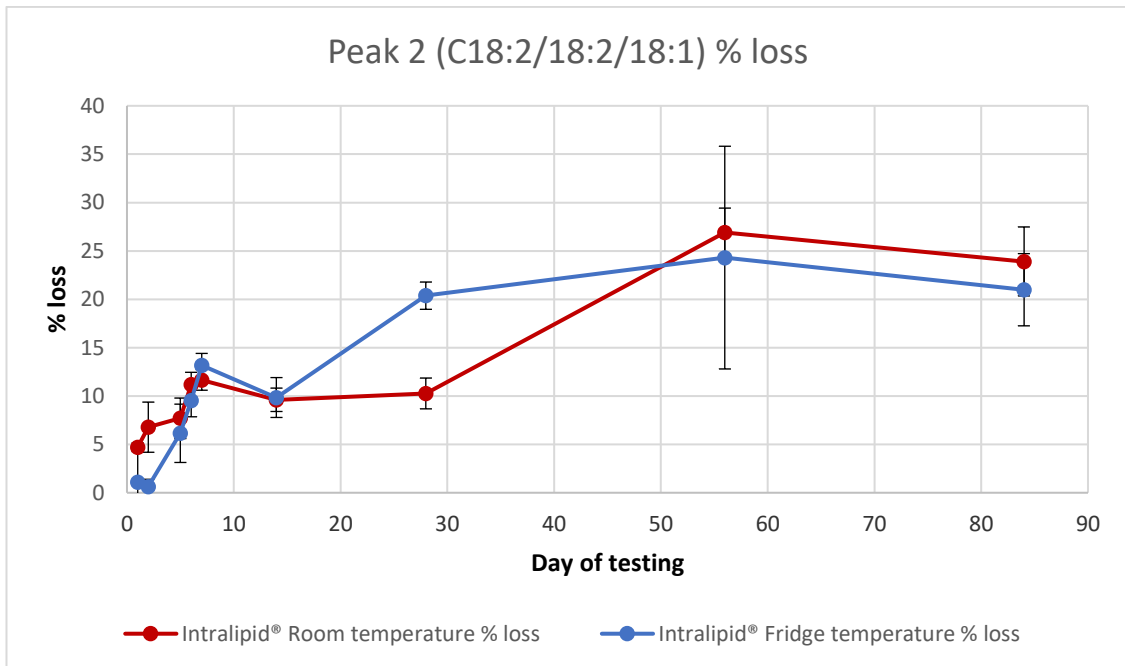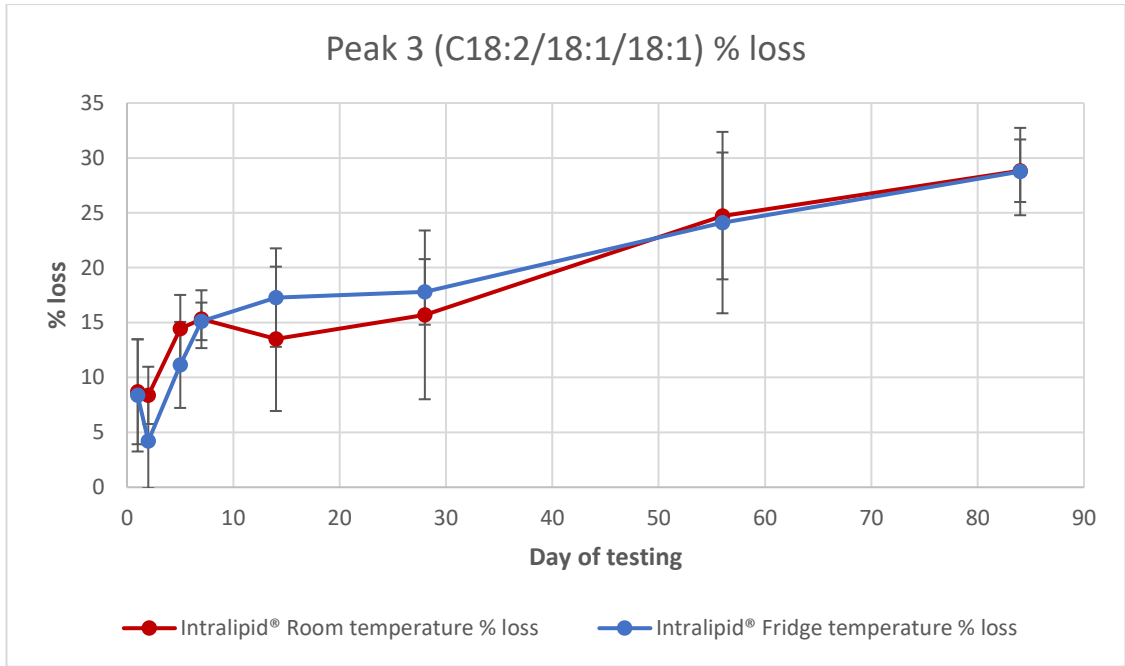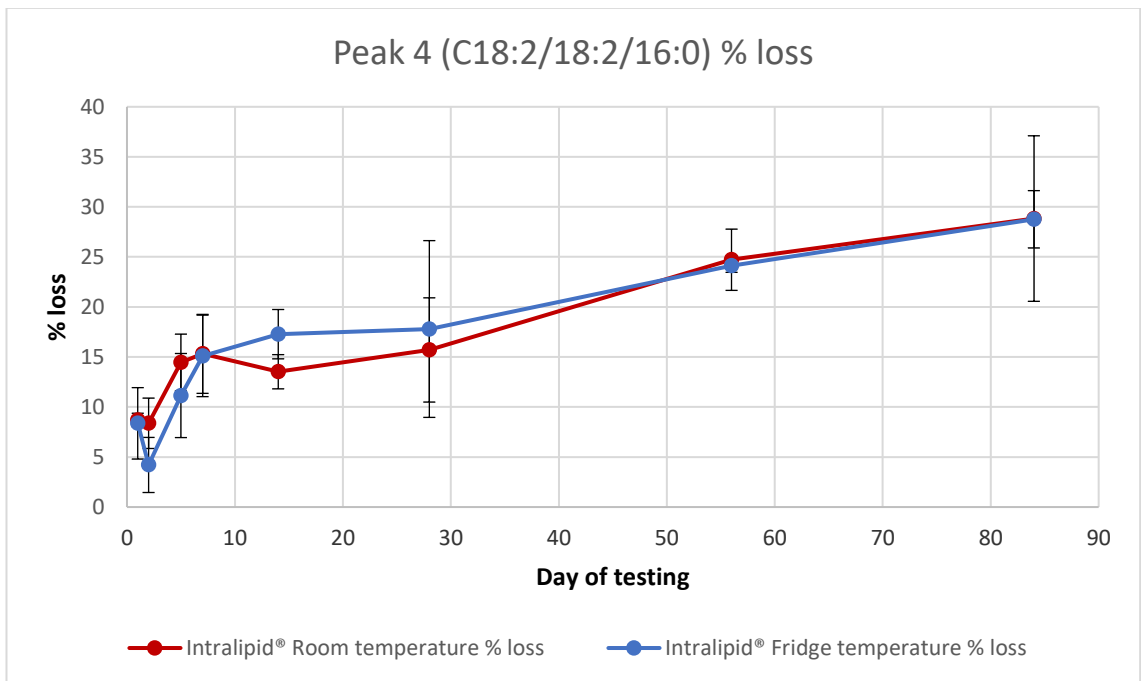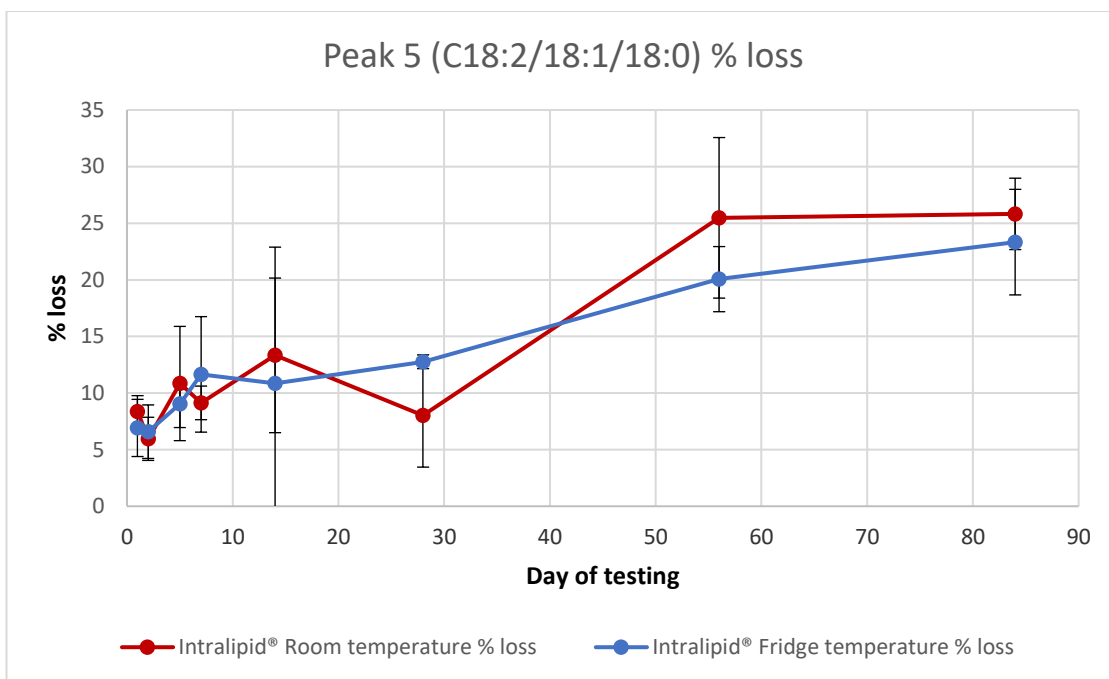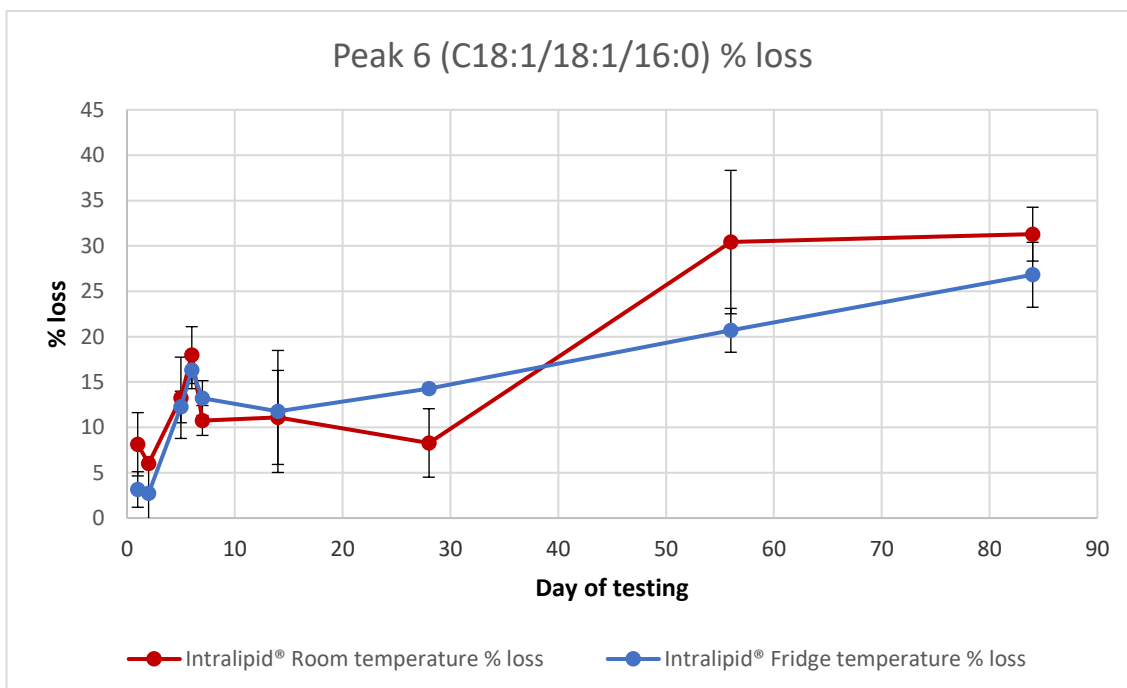ults shown with standard deviation error bars on all points. Day 84 results highlighted in orange and excluded from further analysis due to high RSD's.

Figure 4.25 HPLC-CAD results for peak 2 (C18:2/18:2/18:1) triglyceride of Intralipid® 20 % stored in non-light protected 50 ml glass vials. Percentage loss of peak shown calculated from day 0 data. Room (Red) and Fridge (Blue) results shown with standard deviation error bars on all points. Day 84 results highlighted in orange and excluded from further analysis due to high RSD's.

193

Figure 4.26 HPLC-CAD results for peak 3 (C18:2/18:1/18:1) triglyceride of Intralipid® 20 % stored in non-light protected 50 ml glass vials. Percentage loss of peak shown calculated from day 0 data. Room (Red) and Fridge (Blue) results shown with standard deviation error bars on all points. Day 84 results highlighted in orange and excluded from further analysis due to high RSD's.

Figure 4.27 HPLC-CAD results for peak 4 (C18:2/18:2/16:0) triglyceride of Intralipid® 20 % stored in non-light protected 50 ml glass vials. Percentage loss of peak shown calculated from day 0 data. Room (Red) and Fridge (Blue) results shown with standard deviation error bars on all points. Day 84 results highlighted in orange and excluded from further analysis due to high RSD's.

Figure 4.28 HPLC-CAD results for peak 5 (C18:2/18:1/18:0) triglyceride of Intralipid® 20 % stored in non-light protected 50 ml glass vials. Percentage loss of peak shown calculated from day 0 data. Room (Red) and Fridge (Blue) results shown with standard deviation error bars on all points. Day 84 results highlighted in orange and excluded from further analysis due to high RSD's.

Figure 4.29 HPLC-CAD results for peak 6 (C18:2/18:1/16:0) triglyceride of Intralipid® 20 % stored in non-light protected 50 ml glass vials. Percentage loss of peak shown calculated from day 0 data. Room (Red) and Fridge (Blue) results shown with standard deviation error bars on all points. Day 84 results highlighted in orange and excluded from further analysis due to high RSD's.

Figure 4.30 HPLC-CAD chromatograms of Intralipid® 20% stored in 50 ml glass vials. Day 0 control (black), day 84 fridge temperature chromatogram (blue trace) and day 84 room temperature (red trace). Overlaid chromatogram shows changes in peaks in comparison to control.

Figure 4.31 HPLC-UV chromatograms of Intralipid® 20% stored in 50 ml glass vials. Day 0 chromatogram (black trace), day 84 fridge temperature syringes (blue trace) and day 84 room temperature syringes (red trace). The lack of production of new peaks indicates a lack of degradation products.

197

Figure 4.32 Overlaid HPLC-UV chromatograms. Day 0 (back trace) and day 84 room temperature (red trace) Intralipid® stored in 50 ml glass vials. The presence of no new peaks indicates a lack of degradation/peroxidation products seen at this specific wavelength (222 nm).

4.7. Discussion of Intralipid® non-light protected results.

4.7.1. Triglyceride loss

Both syringes and PN bags under all temperatures showed significant TAG losses. Table 4.1 indicates the statistically significant results between different container types at different temperatures as tested by ANOVA analysis using SPSS (appendix 3). Syringe results were analysed up to 84 days, however both PN bag and glass vial results were only analysed up to 56 days due to increased RSD's of the control sample tested on day 84. Therefore, when considering all container types collectively, only the results up to and including day 56 are analysed.

Figure 4.34 shows the % loss of each monitored TAG after 56 days of storage. All results gave a maximal loss of under 30 %. When considering the level of peroxidation occurring in each TAG monitored, a higher level of unsaturation should be predictive of an increased level of peroxidation. However, for the non-light protected results at day 56, the highest level of TAG loss observed was for peak 4 (C18:2/18:2/16:0) in syringes at room temperature. If analysed collectively across all containers Peak 3 (C18:2/18:1/18:1) as shown in figure 4.34 creates the most consistent % loss of around 20 %. Both peaks contain multiple levels of unsaturation.

With regards to the initiation of peroxidation, the higher the level of unsaturation present, the greater the likelihood of a lipid free radical being created. The presence of multiple double bonds within a fatty acid enables the stabilisation of a free radical via electron delocalisation through the double bonds, increasing the probability of extraction of a hydrogen by a ROS or photo-oxidation and the initiation of peroxidation. Peroxidation is therefore initiated easier in polyunsaturated than mono-saturated fatty acids (Porter et al. 1995). It can be predicted because of this that the TAGs monitored with higher levels unsaturated fatty acids should have an increased rate of peroxidation.

Figure 4.33 shows the results of all containers at 7 days of storage. The highest levels of % loss occur in Peak 3 (C18:1/18:1/18:2) and 4 (C18:2/18:2/16:0) in PN bags at both temperatures. Both TAGs contain multiple linoleic acids which would be predicted to peroxidise first due to its higher level of unsaturation. Following Portor et al's (1995) finding of lower bond dissociation energy requirements for the initiation of peroxidation within linoleic acid vs, oleic acid, it could be predicted that

peak 1 (C18:2/18:2/18:2) should have the highest rate of peroxidation. However as shown in figure 4.33 peaks 3 and 4 have higher initial rate of peroxidation observed by % loss at 7 days. It is of note that when considering the oxidation of fatty acids within emulsions as opposed to pure oils, work by Khanum, R and Thevanayagam, H (Khanum and Thevanayagam 2017) suggests that the presence of oleic acid within an emulsion increases the amount of lipid hydroperoxides (transient primary peroxidation products) produced by over 5 % vs polyunsaturated emulsions alone. The rate of peroxidation within the emulsion was unaffected suggesting that fatty acid composition of TAGs within an emulsion was a minor influence on the rate of peroxidation and other factors such as temperature were predicted to be rate limiting. When considering the total level of peroxidation as indicated by % TAG loss across all containers at 56 days, peak 3 shows the highest average % loss. Peak 3 (C18:2/18:1/18:1) contains linoleic acid, predicted to peroxidise first due to its multiple double bonds, and oleic acid, a mono-saturate which requires more energy to extract a hydrogen and form a lipid radical. If we consider Khanum and Thevanayaham's (Khanum and Thevanayagam 2017) work and extrapolate it as a predictor to the level of peroxidation occurrence in Intralipid®, peak 3 (C18:2/18:1/18:1) would be indicated to peroxidise to the highest degree as shown in figures 4.33 and 4.34.
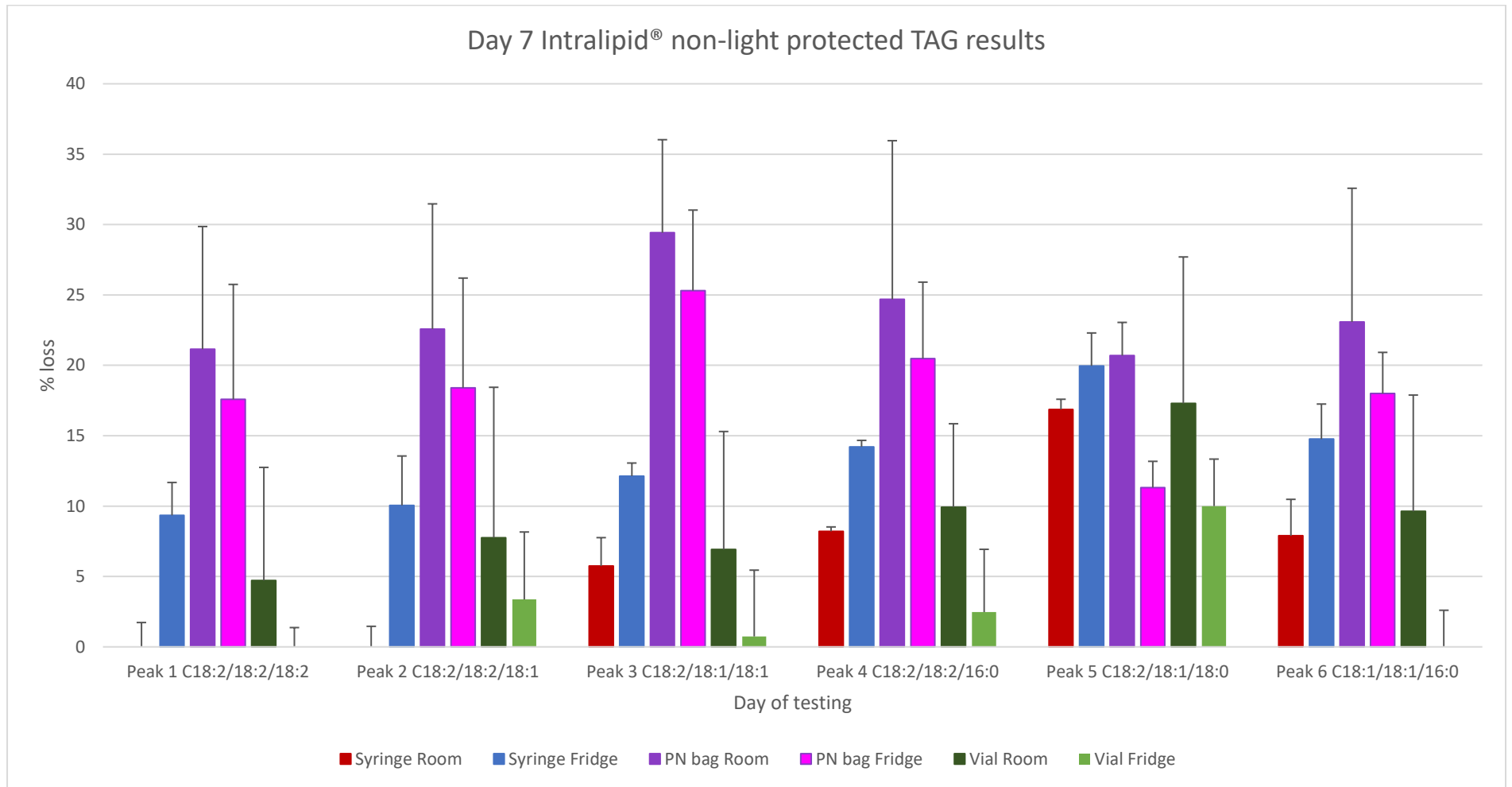
Figure 4.33 Triglyceride loss after 7 days of storage of Intralipid® in syringes, PN bags and glass vials

Figure 4.34 Triglyceride loss at 56 days storage for Intralipid® stored in syringes, PN bags and glass vials.

Table 4.1 Non-light protected Intralipid® in all containers at all temperatures for each of the six peaks monitored. * indicates significant differences between results as calculated through ANOVA analysis with post hock Tukey analysis between each container type. (significant defined as $P<0.05$).

Peak 1

Peak 1	Room syringe	Room Bag	Room Vial	Fridge Syringe	Fridge Bag	Fridge Vial
Room Syringe	▨	*				*
Room Bag	*	▨	*	*		
Room Vial		*	▨			*
Fridge Syringe		*		▨	*	*
Fridge Bag				*	▨	*
Fridge Vial	*		*	*	*	▨

Peak 2

Peak 2	Room syringe	Room Bag	Room Vial	Fridge Syringe	Fridge Bag	Fridge Vial
Room Syringe	▨		*	*		
Room Bag		▨			*	
Room Vial	*		▨		*	
Fridge Syringe	*			▨	*	*
Fridge Bag		*	*	*	▨	*
Fridge Vial				*	*	▨

Peak 3

Peak 3	Room syringe	Room Bag	Room Vial	Fridge Syringe	Fridge Bag	Fridge Vial
Room Syringe	▨	*				*
Room Bag	*	▨	*	*		
Room Vial		*	▨			*
Fridge Syringe		*		▨		*
Fridge Bag					▨	*
Fridge Vial	*		*	*	*	▨

Peak 4

Peak 4	Room syringe	Room Bag	Room Vial	Fridge Syringe	Fridge Bag	Fridge Vial
Room Syringe	▨	*				*
Room Bag	*	▨	*	*	*	
Room Vial		*	▨			*
Fridge Syringe		*		▨		*
Fridge Bag		*			▨	*
Fridge Vial	*		*	*	*	▨

Peak 5

Peak 5	Room syringe	Room Bag	Room Vial	Fridge Syringe	Fridge Bag	Fridge Vial
Room Syringe	▨	*	*			*
Room Bag	*	▨	*	*	*	
Room Vial	*	*	▨			*
Fridge Syringe		*		▨		*
Fridge Bag		*			▨	*
Fridge Vial	*		*	*	*	▨

Peak 6

Peak 6	Room syringe	Room Bag	Room Vial	Fridge Syringe	Fridge Bag	Fridge Vial
Room Syringe	▨	*		*		*
Room Bag	*	▨	*	*	*	
Room Vial		*	▨			*
Fridge Syringe	*	*		▨	*	*
Fridge Bag		*		*	▨	*
Fridge Vial	*		*	*	*	▨

The presence of oxygen is a key factor in the initiation of peroxidation as discussed in section 1.5.1 (chapter 1). When considering the level of TAG loss shown in the day 7 results (figure 4.33) multi-layer PN bags which are oxygen impermeable show significantly greater TAG loss than syringes. As discussed in section 3.8.1 with light protected Intralipid® testing whilst PN bags are impermeable to oxygen and syringes permit a level of oxygen ingress, initial presence of atmospheric oxygen will be higher in PN bags. This is due to the manufacturing process which leaves a small amount of air in the PN bag after formulation. All air is initially removed from syringes, with air ingress occurring over a prolonged period of storage. BD syringes are formed of propylene barrels and plungers and latex free elastomer stoppers (BD Medical 2015). Whilst the materials themselves are impermeable to oxygen, the movable nature of the barrel and plunger permits a level of oxygen ingress during storage. As such whilst initial 7-day results (figure 4.33) show low levels of TAG loss in syringes, loss at 56 days is maximal in syringes compared to PN bags. It is postulated that peroxidation in PN bags is therefore initially rapid due to the presence of a limited volume of atmospheric air but limited by the impermeable nature of the multi-layer bags, hence when oxygen supplies are exhausted, peroxidation rate reduces. Conversely in syringes little air is present within the syringe initially, causing a reduced rate of peroxidation, however over the storage time, air ingress initiates peroxidation and ultimately results in a higher % TAG loss occurring. The importance of oxygen is further substantiated by the relatively minimal % TAG loss observed in the non-light protected glass vials filled under nitrogen.

4.7.1.2. Temperature effect on TAG loss

Temperature had a significant effect on the level of TAG loss in syringes, but little effect on loss in PN bags or glass vials. There was a statistically significant difference between temperature of storage ($P < 0.05$ ANOVA with post hoc Tukey HSD analysis) in the level of TAG loss and therefore peroxidation within peak 1 in vials, peak 2 in syringes and bags, peak 3 in vials, peak 4 in bags and vials, peak 5 in bags and vials and peak 6 in all containers. Table 4.1 Summaries these results indicating statistical significance. The results indicate that in non-light protected

containers, temperature has a significant effect on TAG loss and the level of peroxidation occurring after prolonged storage periods (56 days). It is hypothesised that room temperature storage would cause a higher level of peroxidation or TAG loss as increased temperatures increase the number of collisions occurring between molecules thereby increasing the rate at which peroxidation occurs (Seppanen and Saari Csallany 2002; Yuan et al. 2018). To investigate this day 7 TAG loss results for all non-light protected containers were analysed and shown in figure 4.33 Peroxidation levels indicated by % TAG loss for non-light protected syringes at day 7 were significantly greater in fridge temperatures than room temperature storage (10-20% vs 0 to 10% TAG loss). Therefore, a raised temperature of storage with regards to the initiation of peroxidation in syringes has little effect. When considering PN bag results at 7 days, room temperature bags did have a greater % TAG loss for peaks 1 to 4 and peak 6, suggesting that the rate of initial peroxidation in PN bags may be affected by raised temperatures. Glass vials with oxygen excluded through nitrogen addition provided an interesting comparator between temperatures. Oxygen removed vials were designed as a control to provide a comparator to the level of oxygen dependant mechanisms of peroxidation occurring vs other lipid breakdown. Whilst the % TAG loss in the glass vials was minimal throughout storage, at 7 days temperature influenced TAG loss with all peaks showing a greater loss at room temperature than fridge temperature.

From the results above with regards to oxygen presence and temperature of storage, the presence of oxygen is shown to be a vital factor in the initiation and rate of peroxidation occurring, with PN bags with oxygen present at day 0 having a greater rate of TAG loss than syringes and vials. When considering temperature, the results indicate that lipid stored at room temperature in the presence of oxygen show the highest level of TAG loss and therefore indicates the highest level of peroxidation.

4.7.1.3. Light exposure and TAG loss

The data within this chapter as discussed in section 4.1 is designed to create a comparative data set for Intralipid® stored in syringes, bags and vials between light exposed and light protected containers discussed in chapter 3. As such, results between chapters and the analysis of the effect of light on the levels of TAG loss and peroxidation occurring can be found in chapter 7.

4.7.2. Peroxidation products formation

4.7.2.1. HNE formation

As shown by figure 4.11 and 4.12 HNE was only detected in room temperature non-light protected syringes. Whilst figure 4.12 shows the production of a HNE peak under HPLC-UV conditions, the amount of HNE present is below the limit of quantification. Therefore, whilst the data was recorded and plotted in figure 4.7 the levels cannot be deemed reliable. All other containers at all temperatures shown no detectable HNE production throughout storage. This suggests that the peroxidation occurring in the lipid (indicated by significant TAG losses) is not forming HNE as a secondary product. The peroxidation pathways as described in chapter 1 (section 1.5.1) shows the formation of many primary and secondary peroxidation products from TAG breakdown. The products formed as indicated by TAG losses could be other secondary products (see HUE and TAG remnant formation below) or primary hydroperoxides.

The secondary aldehyde produced is dependent on the position of the double bonds within a TAGs fatty acids and the positional isomers created. Extensive work has been undertaken by multiple researchers into the primary hydroperoxides created through the different positional isomers formed upon hydrogen extraction and initial lipid radical formation (Porter et al. 1980; Schneider et al. 2001; Porter 2013). From this work we can postulate that the peroxidation processes occurring in light exposed Intralipid® could theoretically be creating secondary products other than HNE. The TAG losses within specific peaks as discussed above indicate the greatest levels of peroxidation occurred in peak 3 (C18:2/18:1/18:1). Theoretically this TAG could only make HNE from the linoleic acid fatty acid chain with potentially different aldehydes being produced dependant on which double bond is targeted during peroxidation. Light exposure and therefore the potential for photo-oxidation processes to occur could also lead to the production of different secondary products other than HNE. As shown below, both HUE and the TAG remnant from peak 3 (C18:2/18:1/18:1) are identified in all containers that show significant TAG losses (PN bags and syringes). As the UV detector used throughout the studies was set at 222nm, there is potential that other peroxidation products may be being formed and simply not detected at this specific wavelength. Such small products would also be volatile in nature and therefore not detected by the CAD detector.

HUE was detected in room temperature PN bags, room temperature syringes and to a lesser extent fridge temperature syringes as shown in figures 4.8 and 4.19. All peak areas detected were relatively small (~2 Pa). This peak was not validated with the assay due to its unexpected formation upon testing and therefore a limit of detection in terms of a concentration of HUE present cannot be established. With regards to peak height however a LOD can be established using the signal to noise ratio of the chromatogram. A signal to noise ratio >3 is sufficient as a LOD (Synder et al. 1997). As such, the level of HUE detected in syringes and PN bags produced a signal to noise ratio >3 for all chromatograms, therefore establishing that HUE is detectable through UV. The concentration of HUE present cannot be calculated however due to the lack of a HUE standard for validation. The comparison between light and non-light exposed containers with regards to HUE production is discussed further in chapter 7. Room temperature syringes within this non-light protected dataset produced the highest level of HUE. Temperature of storage influenced the production of HUE, thought to be produced from the peroxidation of oleic acid as discussed in chapter 3. The greatest level of TAG loss seen in room temperature syringes was peak 5 (C18:2/18:1/18:0) and peak 3 (C18:2/18:1/18:1) (figure 4.34), both containing oleic acid and therefore predicted to create HUE through the peroxidation process.

4.7.2.3. TAG remnant formation

Peak 'B' or the triglyceride remnant identified in chapter 3 through mass spectrometry was detected in room temperature syringes and room temperature PN bags exposed to light throughout storage (figures 4.9 and 4.20). Whilst again unquantifiable in terms of concentration due to the lack of validation of the peak, all peaks observed at all time points were above a LOD established from a signal to noise ratio of >3. Room temperature syringes produced the highest recorded levels of this TAG remnant which as discussed in chapter 3 could be formed from the peroxidation of the peak 3 TAG. The presence of this TAG remnant, the production of HUE and the % TAG losses seen can be used to confirm the occurrence of lipid *peroxidation* in syringes and PN bags. Further analysis of the TAG remnant formation in light exposed and light protected containers of Intralipid® is discussed in chapter

Chapter 5

SMOFlipid® Light Protected Syringes, Bags and Vials

5.1. Introduction to stability testing SMOFlipid®

Both the chapters 5 and 6 utilise the method developed in chapter 2 to test the newer intravenous lipid emulsion SMOFlipid® under a variety of storage containers and conditions. As per previous chapters containers tested were 50 ml syringes, 250 ml multilayer (ML) PN bags and 50 ml glass vials as described in detail in section 3.2. Assay validation is described in chapter 2 enables 10 TAGs to be monitored in SMOFlipid® and the occurrence of HNE. These TAGs as identified through mass spectrometry (section 2.12 chapter 2) are summarised in table 5.1 and shown in figure 5.1 in a standard SMOFlipid® chromatogram.

Table 5.1 TAG Peaks identified, validated and monitored during the stability testing of SMOFlipid®

Peak number	TAG identified
1	C8:0/8:0/8:0
2	C8:0/8:0/10:0
3	C8:0/10:0/10:0
4	C10:0/10:0/10:0
5	C18:2/18:2/18:2
6	C18:2/18:2/18:1
7	C18:1/18:1/18:2
8	C18:2/18:2/16:0
9	C18:1/18:1/18:1
10	C18:2/18:1/16:0

The initial 4 peaks monitored in SMOFlipid® contain relatively short chain saturated fatty acids which when considered as individual fatty acids are resistant to peroxidation (Manuel-y-Keenoy et al. 2016; Khanum and Thevanayagam 2017). Therefore, they will be used as a comparator to the TAG losses observed in peaks 5 to 10 where levels of unsaturation are present.
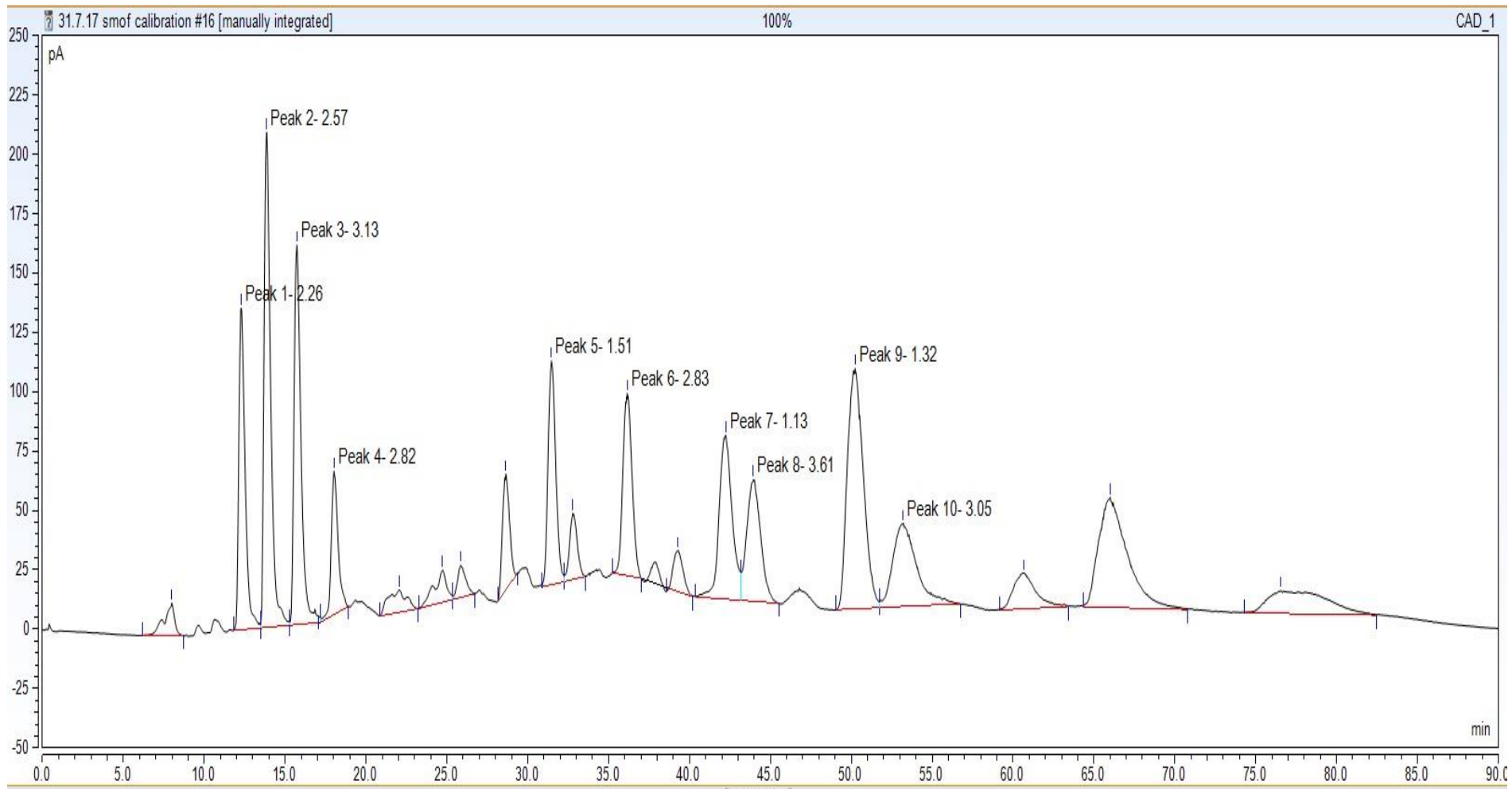
Figure 5.1 HPLC-CAD chromatogram of SMOFlipid® showing the 10 peaks monitored during the following stability testing.

5.2. SMOFlipid® components vs. Intralipid®

The fatty acid composition of SMOFlipid® is governed by the oils which make up the emulsion formulation as shown in table 5.2 Unlike Intralipid® where soybean oil is the singular component oil of the emulsion, SMOFlipid® contains a mixture of oils (discussed in detail in chapter 1, section 1.2). The combination of oils (soybean, olive, fish and synthesised saturated medium chain triglycerides (MCT's)) produces the increased numbers of TAGs visualised in the SMOFlipid® chromatogram (figure 5.1). The 10 TAGs monitored for SMOFlipid® are formed from the soybean oil, olive oil and MCT components of the emulsion. Olive oil contains the same fatty acids as soybean oil but in different proportions. Oleic acid (C18:1) is the prominent fatty acid in olive oil. This is reflected in the proportions of fatty acids seen in each lipid emulsion as shown in table 5.2 As such, the proportions of TAGs/ peaks 5 to 10 in SMOFlipid® will be different to Intralipid®.

Table 5.2 Fatty acid composition and proportions within SMOFlipid® and Intralipid®. Data extracted from SmPCs for each lipid.

Fatty acid	Carbon number: double bond	SMOFlipid®° 20 %	Intralipid® 20 %
Oleic acid	C18:1	23-35%	19-30%
Linoleic acid	C18:2	14-25%	44-62%
Caprylic acid	C8:0	13-24%	-
Palmitic acid	C16:0	7-12%	7-14%
Capric acid	C10:0	5-15%	-
Stearic acid	C18:0	1.5-4%	1.4-5.5%
α-linolenic acid	C18:3	1.5-3.5%	4-11%
EPA	C20:5	1-3.5%	-
DHA	C22:6	1-3.5%	-

Figure 5.2 shows the chromatograms of the same volumes of SMOFlipid® and Intralipid® overlaid indicating the differences in peak size and therefore proportions of TAGs 5 to 10 in each emulsion.
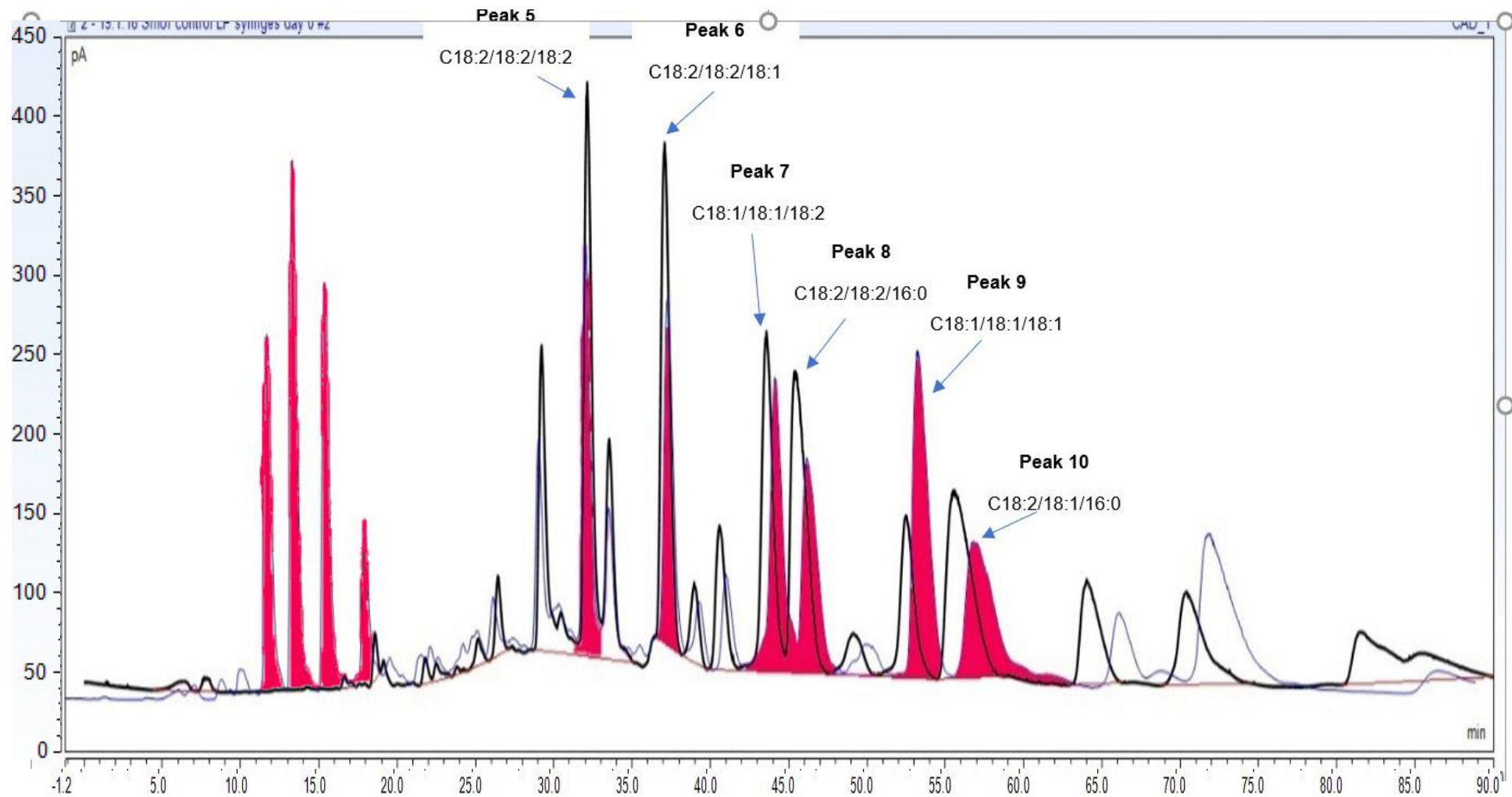
Figure 5.2 HPLC-CAD chromatograms of Intralipid® (white peaks) and SMOFlipid® (red peaks) showing the differences in TAG proportions for peaks 5 to 10.

As predicted by the components of each lipid, peak 9 (C18:1/18:1/18:1) is larger in SMOFlipid® than in Intralipid® as oleic acid is the prominent fatty acid in olive oil. Through comparing the differences in TAG amounts in SMOFlipid® vs. Intralipid® we can predict that the levels of potential peroxidation and therefore TAG losses will be different in each lipid. When considering the olive oil and soybean oil proportions alone, the extent of peroxidation would be postulated to be less in SMOFlipid® than Intralipid® due to the increased levels of saturated and monounsaturated fatty acids present, reducing the ease of peroxidation.

It is of note however that whilst not monitored through the assay due to the small quantities present, SMOFlipid® also contains two fatty acids from fish oil (EPA and DHA), both long chain and highly unsaturated. These are therefore particularly prone to peroxidation and have the potential to initiate the process, creating highly reactive lipid radicals which could subsequently abstract hydrogens from TAGs with lower levels of unsaturation (those found within the olive oil and soybean oil portions of the emulsion), leading hypothetically to higher levels of peroxidation in SMOFlipid® than would be expected in olive oil and soybean oil alone.

5.2.1. Vitamin E

To counteract the potentially pro-oxidant nature of the introduction of fish oils into the emulsion and to reduce the level of peroxidation occurring, SMOFlipid® emulsion contains added α-tocopherol (vitamin E) at a concentration of between 16.3 to 22.5 mg per 100 ml (Kabi 2018). The effectiveness of vitamin E as an anti-oxidant and free-radical scavenger has been questioned in recent research and many contradictory papers exist. With specific regards to vitamin E supplementation in lipid emulsions, recent work has focused on the levels of vitamin E within blood samples of patient receiving PN, concluding that vitamin E addition positively increased level within blood, thus reducing *in vivo* oxidation (Wu et al. 1999; Nonneman et al. 2002). It is worth noting however that supplementation with high levels of vitamin E when considering the use of vitamin E as an anti-oxidant *in vitro* has been shown to increase overall mortality rates (Miller et al. 2005).

Conversely to the multiple works that deal with the *in vivo* effects of vitamin E supplementation, less work has considered the *in vitro* anti-oxidant nature of tocopherols with relation to the extent of lipid peroxidation during storage. Skouroliakou et al. (2012) monitored the levels of peroxidation and vitamin E content in all-in-one PN containing SMOFlipid®. Whilst the determination of

peroxidation was completed via the FOX assay which as discussed in chapter 1 (section 1.6.3) can overestimate the level of peroxides present, they concluded that whilst vitamin E levels remained chemically stable over 24 hours lipid peroxidation was the limiting factor on chemical stability. When considering the anti-oxidant capacity of vitamin E on reducing lipid peroxidation, its mechanism of action involves its conjugation with a lipid radical, eliminating the radical and creating a tocopherol-lipid complex. Yamauchi (1997) provides a detailed description of this process as shown in figure 5.3 When applied to the lipid peroxidation occurring in SMOFlipid® as seen in the Skouroliakou et al study, it can be postulated that if the vitamin E present is working as an anti-oxidant, its measured levels should decrease through storage. However, levels remained static over >24hours, suggesting that potentially the level of effectiveness of the addition of vitamin E should be questioned. It is worth noting however when considering this study in relation to the work presented here, 24 hours is a short storage time compared to the 84 days studied in this work. Hoff and Michaelson's review (2009) also found studies where the levels of primary hydroperoxides were unaffected by the presence of vitamin E in lipid emulsions stored in light-protected syringes, again postulating that vitamin E may not be effective in preventing *in vitro* peroxidation occurring.
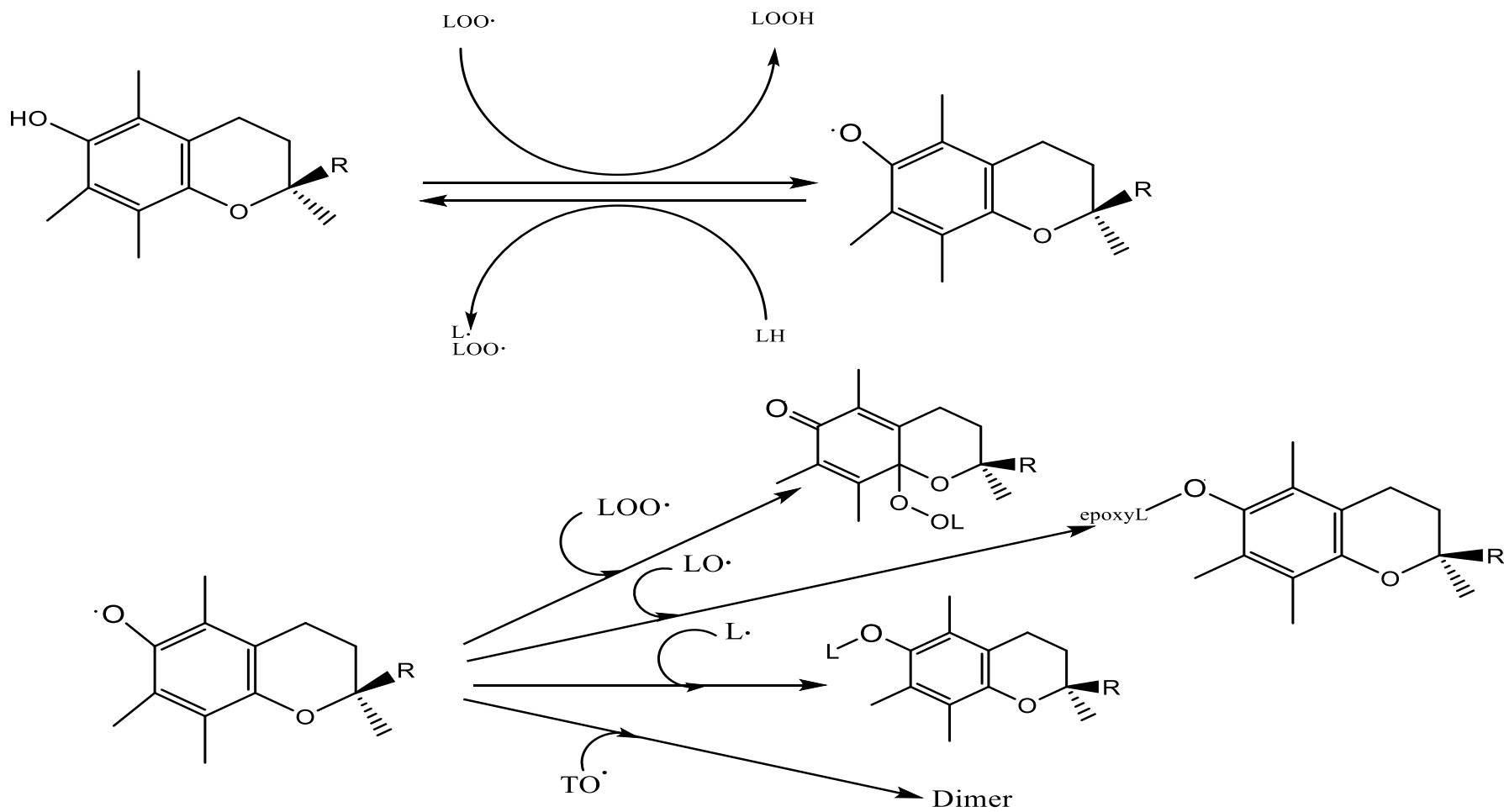
Figure 5.3 Adapted from Yamauchi, R (1997), the proposed mechanism of tocopherol (vitamin E) anti-oxidant capacity. LH, polyunsaturated lip radical; LOOH, lipid hydroperoxide; LOO• lipid-peroxyl radical; TO•, α-tocopheroxyl.

5.3. Testing protocol and schedule.

To facilitate comparisons to be made between SMOFlipid® stability testing and the Intralipid® testing seen in chapters 3 and 4, the same testing protocols and schedule as laid out in chapter 3 (section 3.4) will be used for SMOFlipid® testing.

To summarise, 10 identified TAG peaks were monitored for SMOFlipid® emulsion. 50 ml of lipid was placed in 50 ml syringes, 250 ml ML PN bags and 50 ml glass vials (with nitrogen replacement or air). All containers were light protected using aluminium foil throughout storage. 6 of each container type were formulated, 3 stored at fridge temperature (2-8°C) and 3 stored at room temperature (22°C). Testing was carried out at days 0, 1, 2, 5, 7, 14, 28, 56 and 84 as per lab protocols for physical stability testing. At each testing point, 1ml of lipid was removed under aseptic conditions and placed in an amber HPLC vial for testing. For glass vials, at each testing time point nitrogen was flowed through the lipid and headspace after removal of lipid for testing to maintain the oxygen free environment.

Each sample was subjected to HPLC as per chapter 2 with the 10 validated TAGs monitored during storage through CAD detection, the production of HNE through UV detection and the production of HUE and the TAG remnant products found and identified during the testing of Intralipid® (section 3.8.3). Control samples of new SMOFlipid® held in its original container were tested at each time point and RSD's of all control samples monitored. Data was excluded if RSD's fell above the acceptable range of <12 (section 3.4). Results for each container type are shown in the following sections.

5.4. SMOFlipid® light protected syringe results

Chromatogram results for each day of testing were integrated using Chromeleon (Thermo Scientific) and peak area reported (raw data for all results within chapter shown in appendix 2). For HPLC-CAD results for each of the 10 monitored triglycerides data is presented as a % loss from day 0 with room and fridge temperature results indicated on each graph. Standard deviation error bars are present on all results.

As shown in figures 5.4 to 5.13 maximal % TAG loss was recorded in peak 6, 9 and 10 at 25 % over 84 days. All TAG peaks monitored showed little loss (< 20 %) up to 56 days of testing with a rapid rise in loss detected from day 56 onwards. Temperature had little effect on stability, with fridge temperature samples showing

greater loss than room temperature samples across all TAGs but the difference not being statistically significant (section 5.7). Results for all monitored TAGs are discussed further in section 5.7.

Minimal HNE was produced throughout 84 days of storage at both temperatures. Figure 5.14 shows HNE results with standard error bars. The amount of HNE produced a maximal peak area of 3.41 (AU). This area using the calibration equation shown in figure 3.6 (section3.5) ($y = 0.2476x + 1.0452$) equates to a concentration of 1.889 µM. As discussed in chapter 2, the limit of quantification for the assay of HNE is 8.974 µM. As such the levels of HNE recorded are so minimal that they are not reliably quantifiable through the assay.

Despite little HNE being recorded, room temperature syringes showed the production of HUE from day 14 onwards which positively correlated to the production of the TAG remnant from day 28 onwards as shown in figures 5.15 and 5.16. Fridge temperature syringes showed no TAG remnant but a small amount of HUE from day 56 onwards. All light protected syringe results are discussed further in section 5.7.

Figure 5.4 HPLC-CAD results for peak 1 (C8:0/8:0/8:0) triglyceride of SMOFlipid® 20 % stored in light protected 50 ml syringes. Percentage loss of peak shown calculated from day 0 data. Room (Red) and Fridge (Blue) results shown with standard deviation error bars on all points.
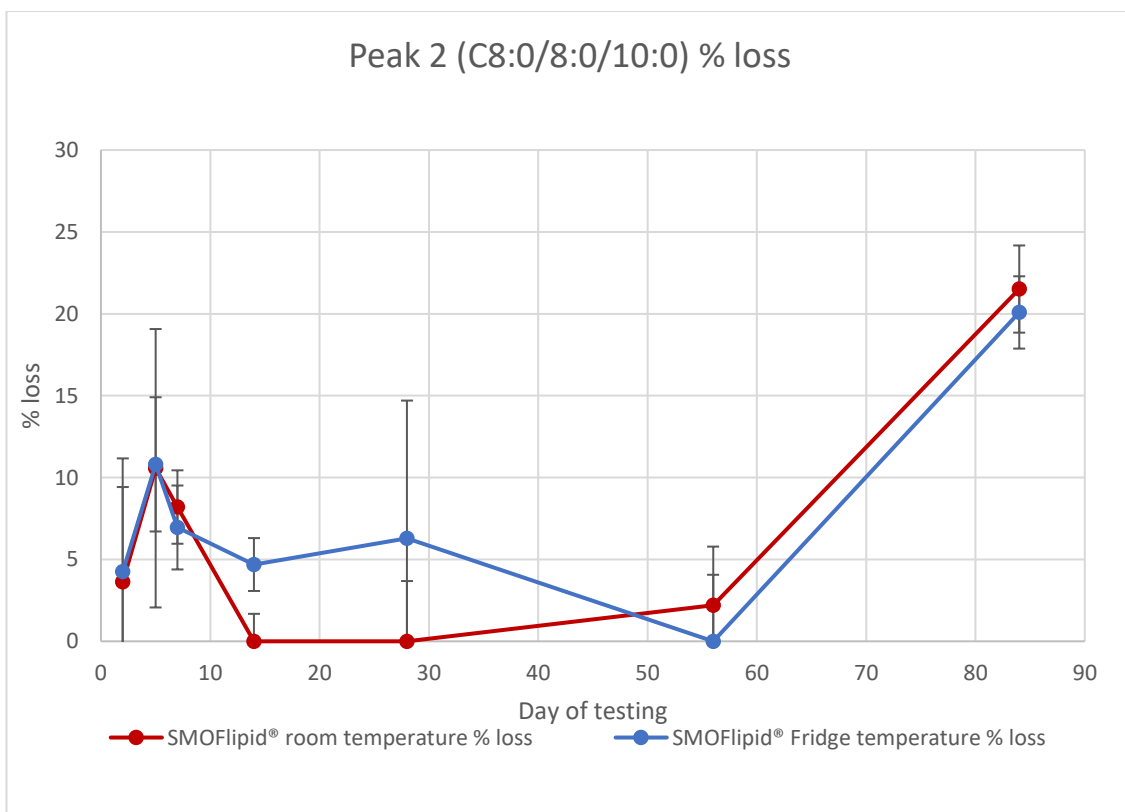
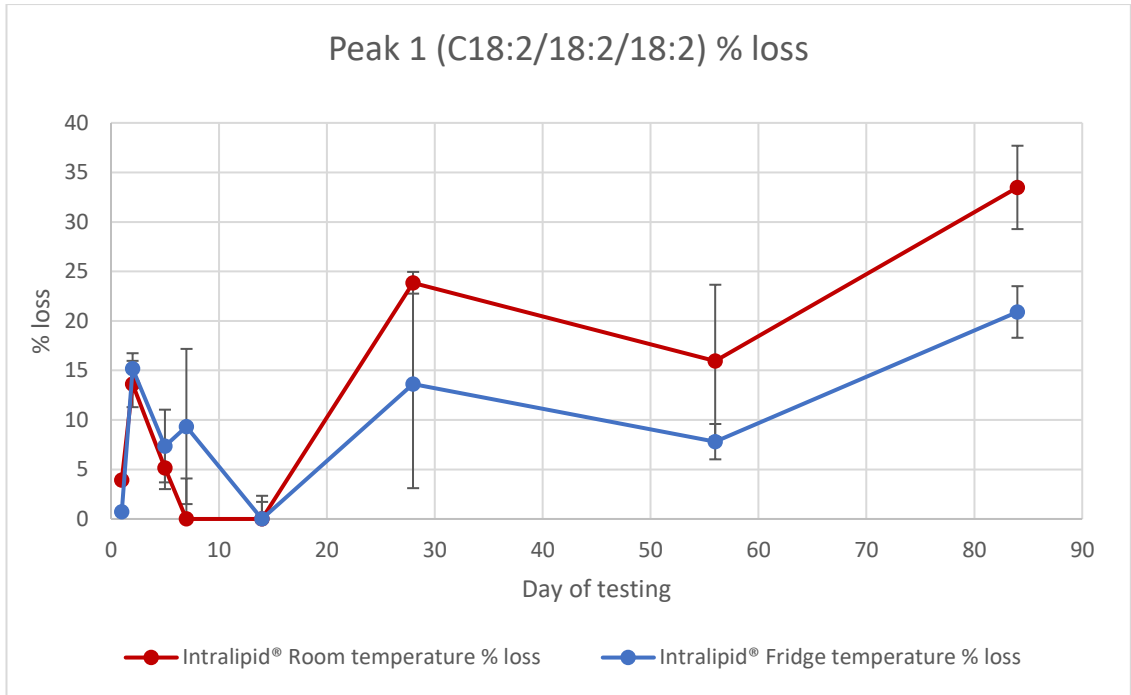*Figure 5.5 HPLC-CAD results for peak 2 (C8:0/8:0/10:0) triglyceride of SMOFlipid® 20 % stored in light protected 50 ml syringes. Percentage loss of peak shown calculated from day 0 data. Room (Red) and Fridge (Blue) results shown with standard deviation error bars on all points.*

218
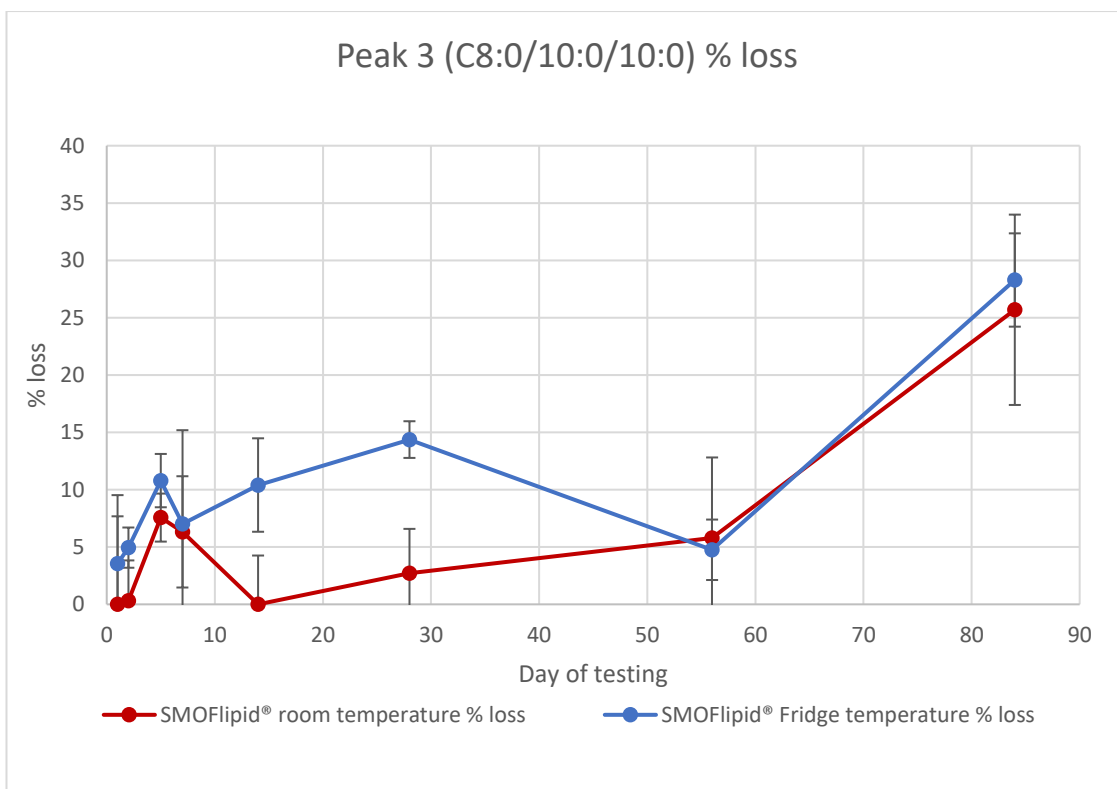
Figure 5.6 HPLC-CAD results for peak 3 (C8:0/10:0/10:0) triglyceride of SMOFlipid® 20 % stored in light protected 50 ml syringes. Percentage loss of peak shown calculated from day 0 data. Room (Red) and Fridge (Blue) results shown with standard deviation error bars on all points.
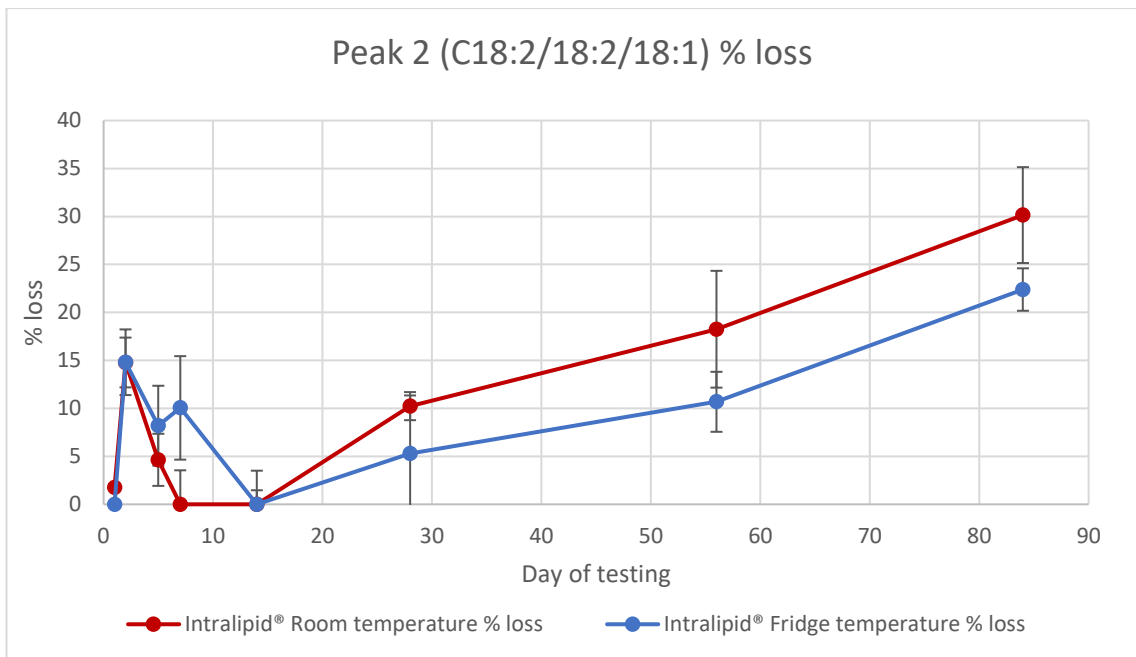

Figure 5.7 HPLC-CAD results for peak 4 (C10:0/10:0/10:0) triglyceride of SMOFlipid® 20 % stored in light protected 50 ml syringes. Percentage loss of peak shown calculated from day 0 data. Room (Red) and Fridge (Blue) results shown with standard deviation error bars on all points.
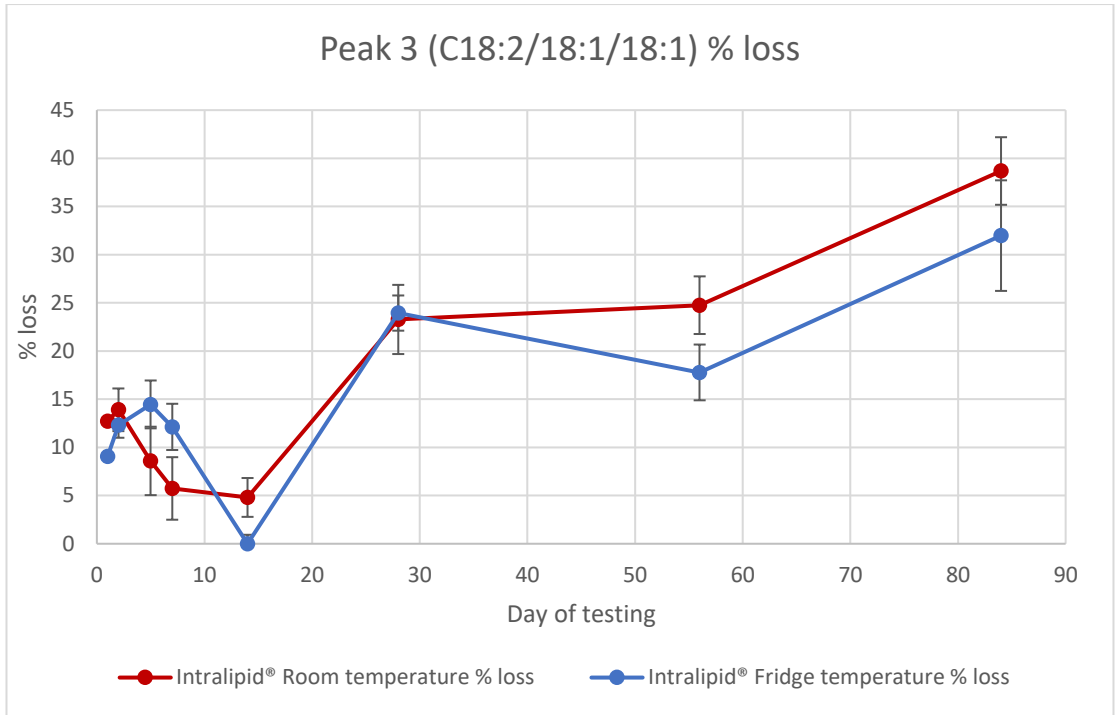
Figure 5.8 HPLC-CAD results for peak 5 (C18:2/18:2/18:2) triglyceride of SMOFlipid® 20 % stored in light protected 50 ml syringes. Percentage loss of peak shown calculated from day 0 data. Room (Red) and Fridge (Blue) results shown with standard deviation error bars on all points.

Figure 5.9 HPLC-CAD results for peak 6 (C18:2/18:2/18:1) triglyceride of SMOFlipid® 20 % stored in light protected 50 ml syringes. Percentage loss of peak shown calculated from day 0 data. Room (Red) and Fridge (Blue) results shown with standard deviation error bars on all points.
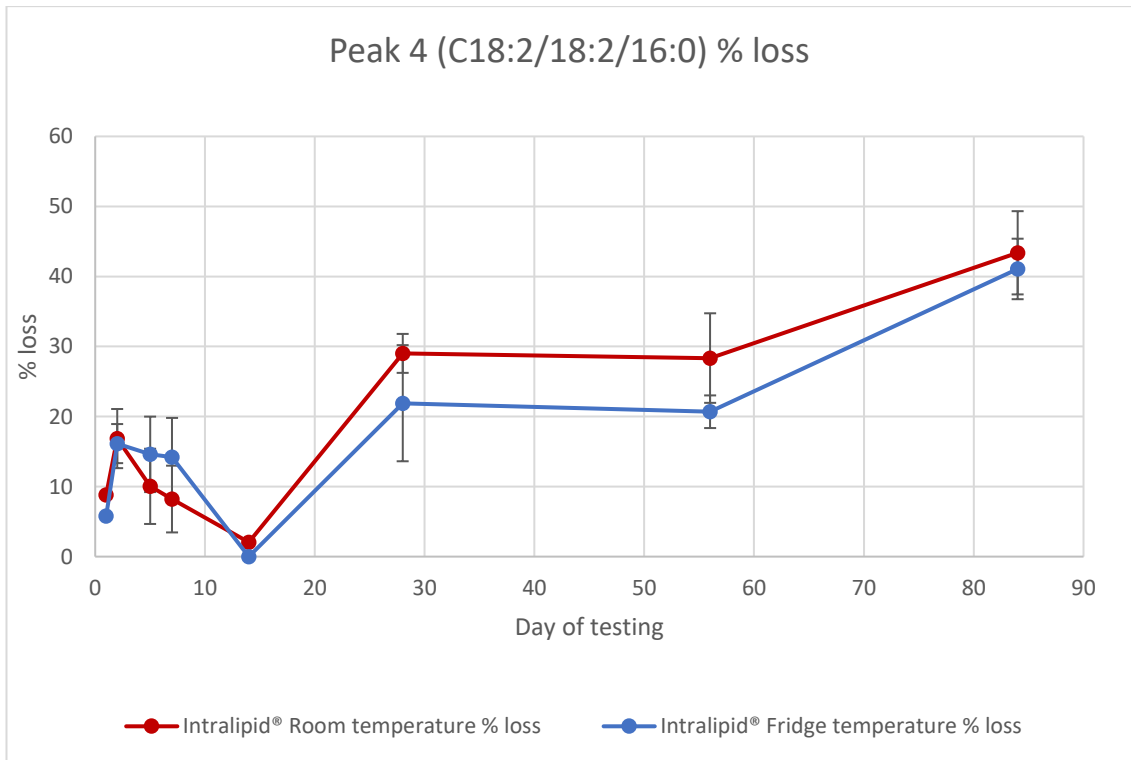
Figure 5.10 HPLC-CAD results for peak 7 (C18:2/18:1/18:1) triglyceride of SMOFlipid® 20 % stored in light protected 50 ml syringes. Percentage loss of peak shown calculated from day 0 data. Room (Red) and Fridge (Blue) results shown with standard deviation error bars on all points.
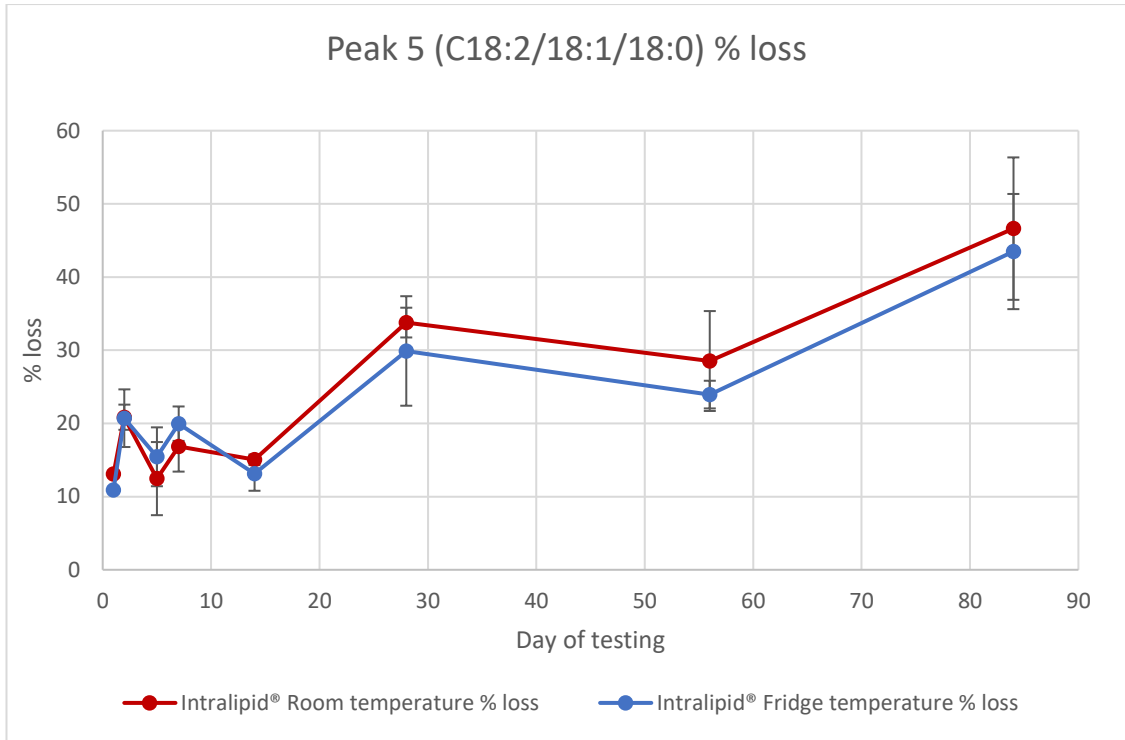

Figure 5.11 HPLC-CAD results for peak 8 (C18:2/18:2/16:0) triglyceride of SMOFlipid® 20 % stored in light protected 50 ml syringes. Percentage loss of peak shown calculated from day 0 data. Room (Red) and Fridge (Blue) results shown with standard deviation error bars on all points.

Figure 5.12 HPLC-CAD results for peak 9 (C18:2/18:1/18:0) triglyceride of SMOFlipid® 20 % stored in light protected 50 ml syringes. Percentage loss of peak shown calculated from day 0 data. Room (Red) and Fridge (Blue) results shown with standard deviation error bars on all points.
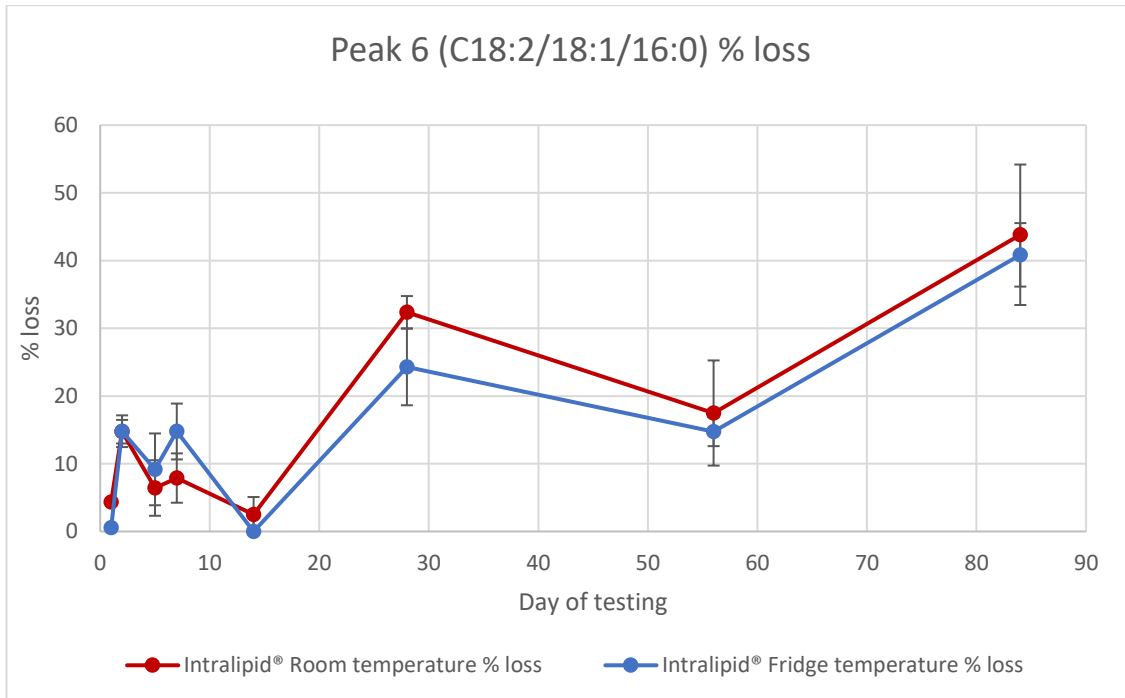

Figure 5.13 HPLC-CAD results for peak 10 (C18:2/18:1/16:0) triglyceride of SMOFlipid® 20 % stored in light protected 50 ml syringes. Percentage loss of peak shown calculated from day 0 data. Room (Red) and Fridge (Blue) results shown with standard deviation error bars on all points.
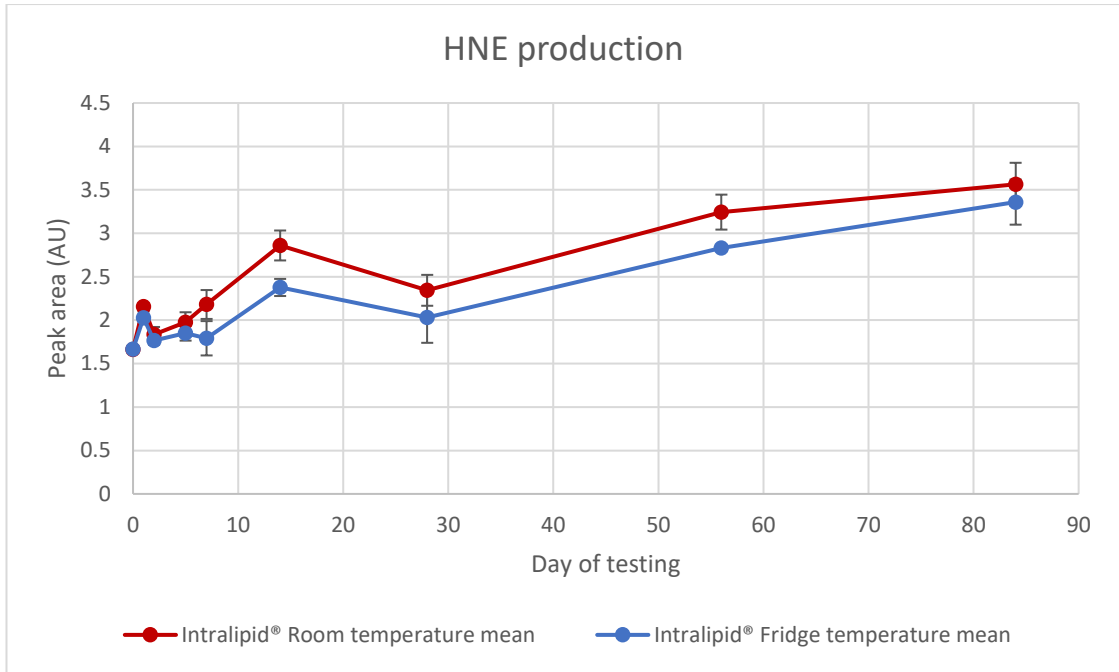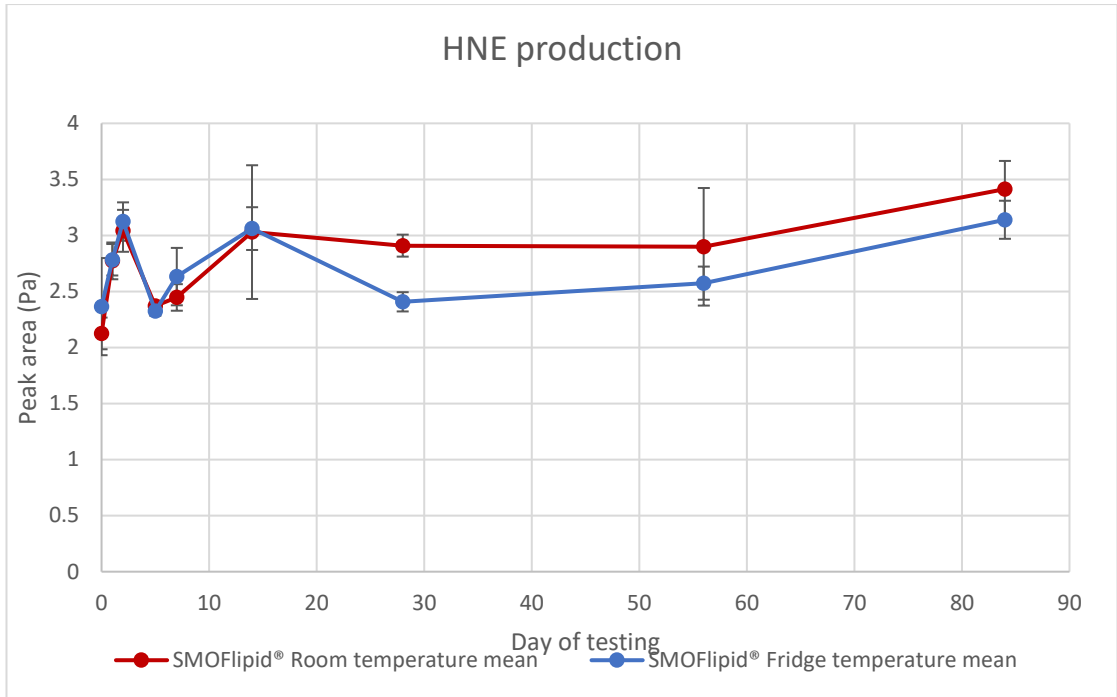
Figure 5.14 HPLC-UV data showing the minimal production of 4-Hydroxynonenal in SMOFlipid® 20 % over 84-day storage and both room (red) and fridge (blue) temperatures in 50 ml syringes.
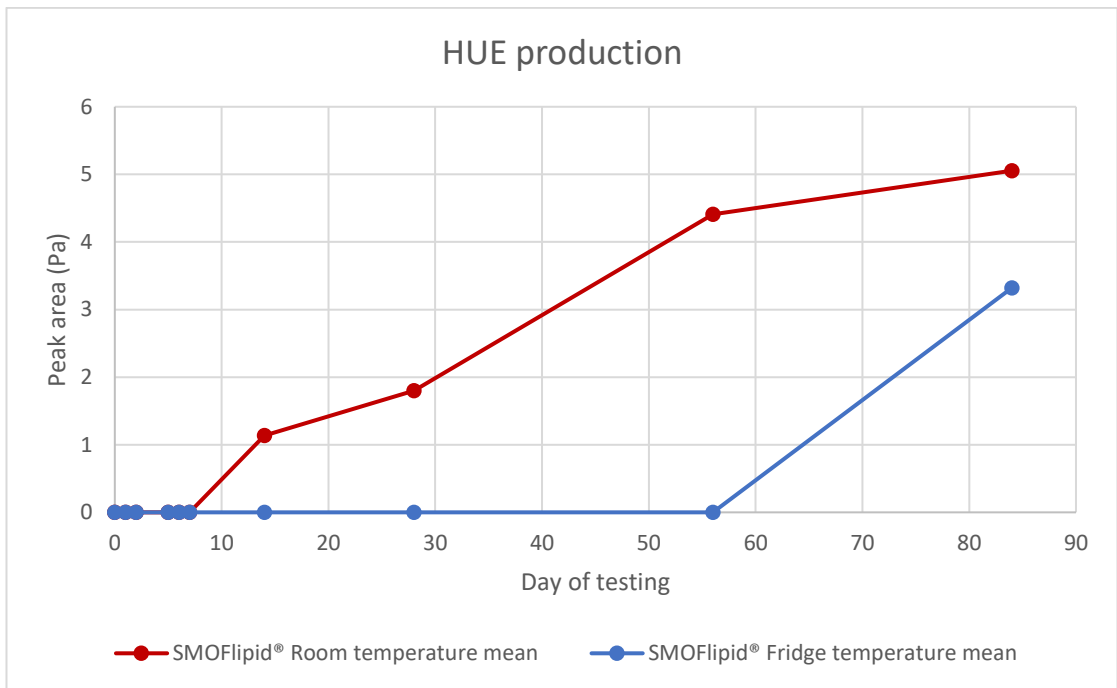

Figure 5.15 HUE production in 50 ml SMOFlipid® light protected syringes over 84 days of storage. Room temperature (red trace) and fridge temperature (blue trace).
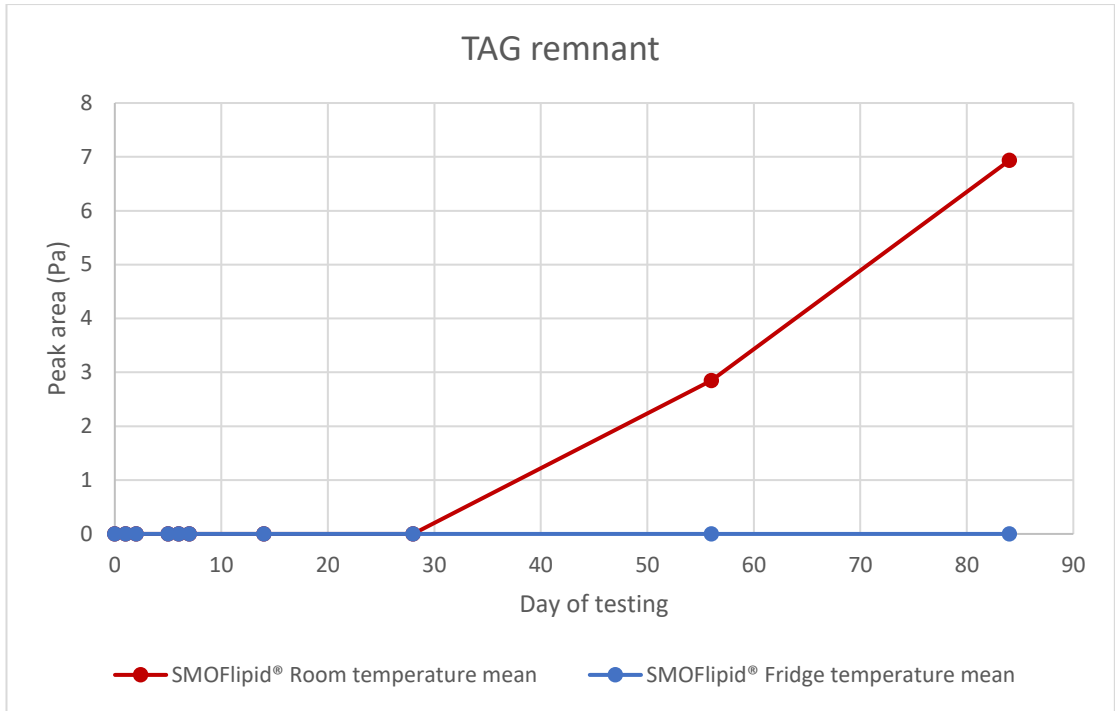
Figure 5.16 HPLC-UV of TAG remnant production in 50 ml SMOFlipid® light protected syringes over 84 days storage. Room temperature (red trace) showing production from day 28, no fridge temperature production (blue trace).
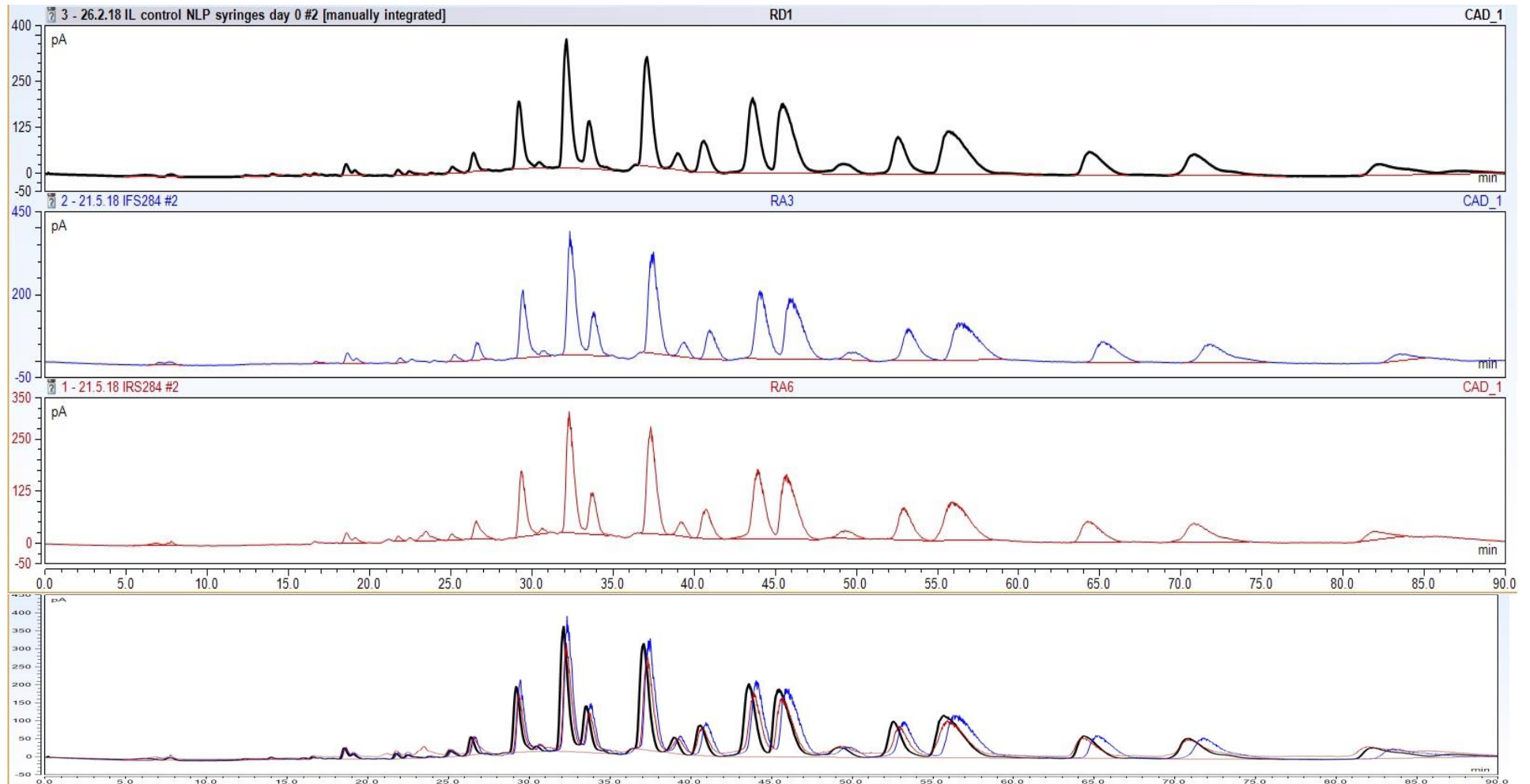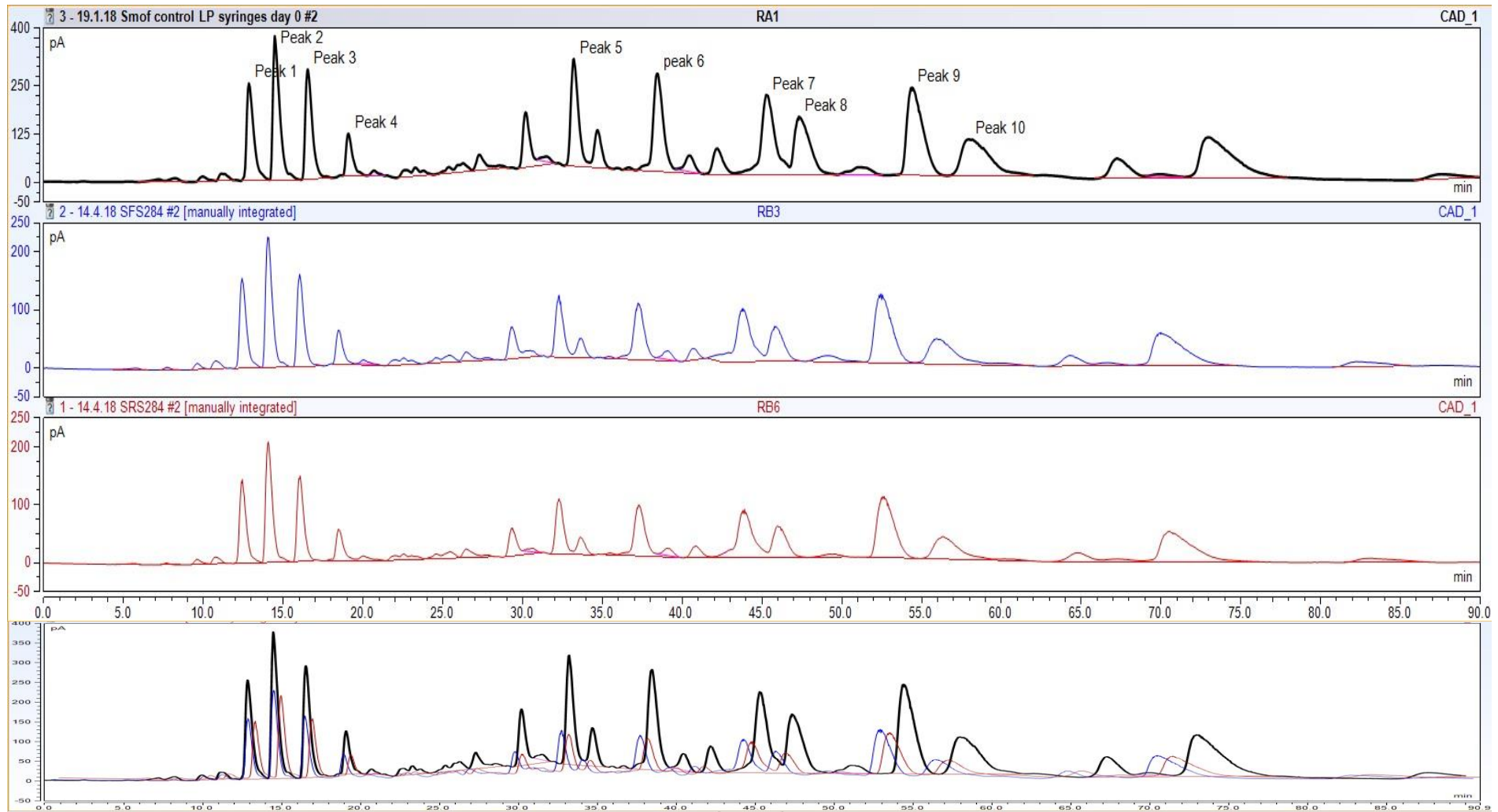
Figure 5.17 HPLC-CAD chromatograms of SMOFlipid® 20% stored in 50 ml syringes. Day 0 control (black), day 84 fridge temperature (blue trace) and day 84 room temperature (red trace). Overlaid chromatogram shows changes in peaks in comparison to control.
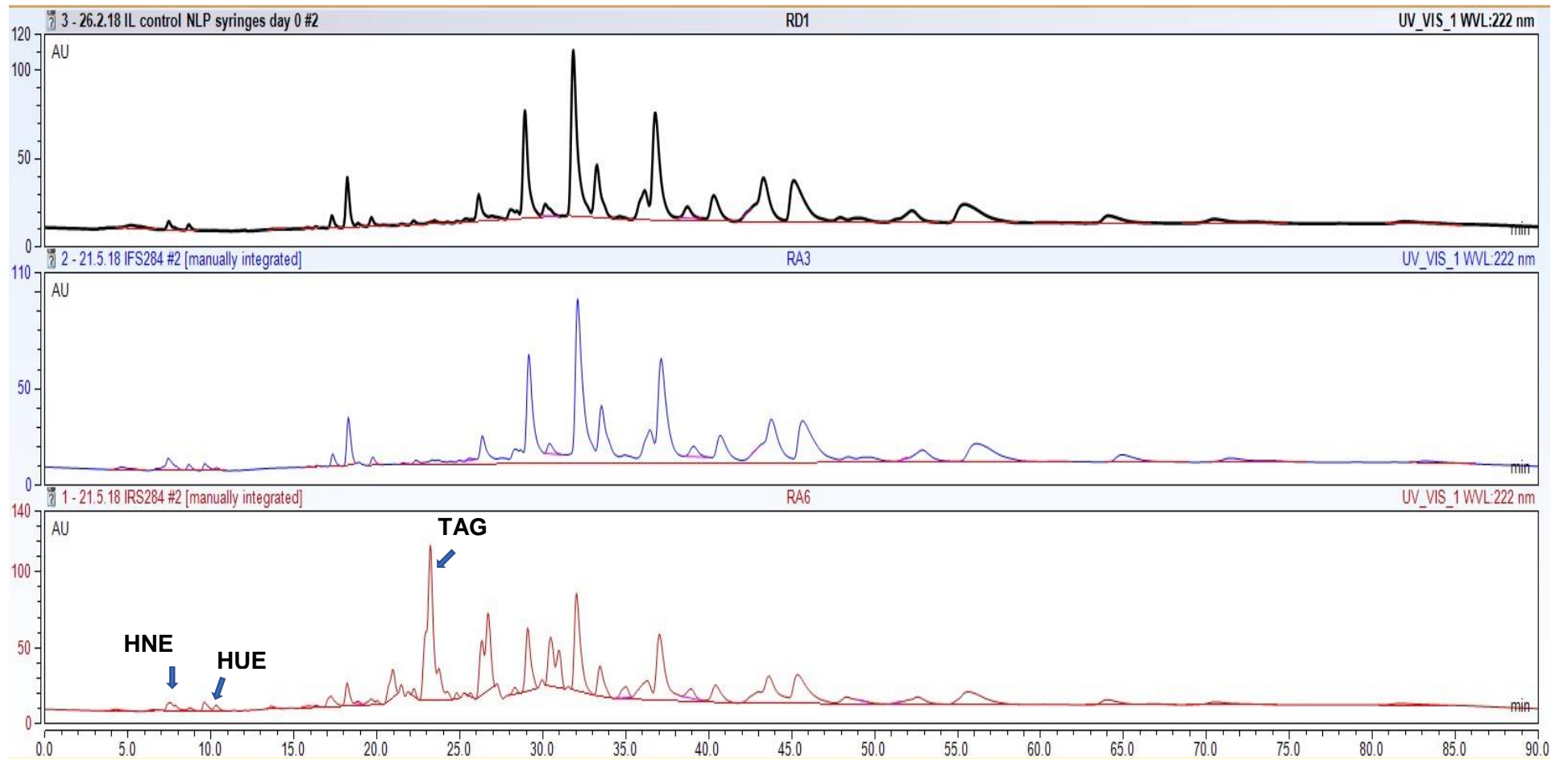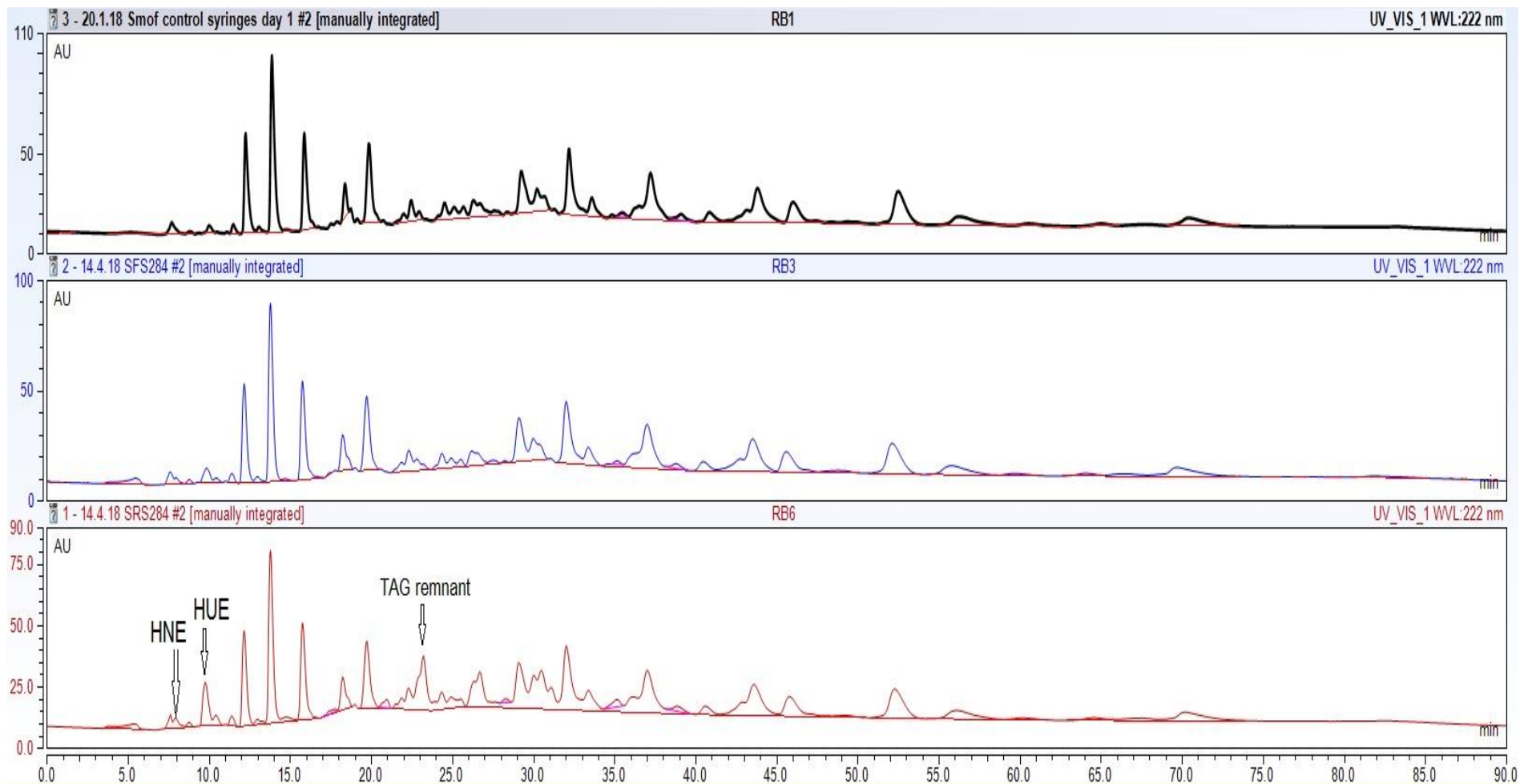
Figure 5.18 HPLC-UV chromatograms of SMOFlipid® 20% stored in 50 ml syringes. Day 0 chromatogram (black trace), day 84 fridge temperature syringes (blue trace) and day 84 room temperature syringes (red trace). The production of HNE, HUE and TAG remnant in room temperature syringes can be seen and is indicated on the chromatogram.
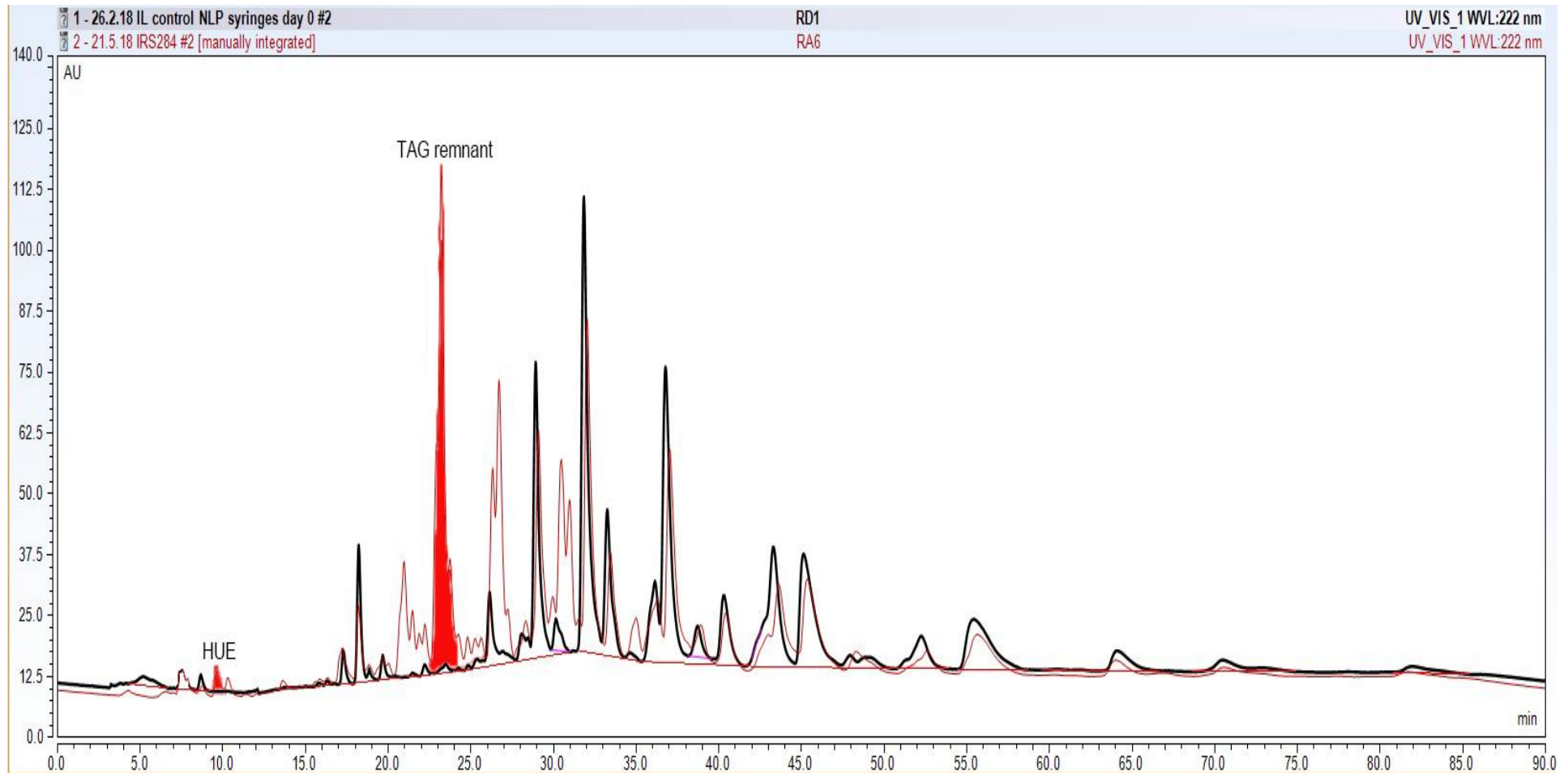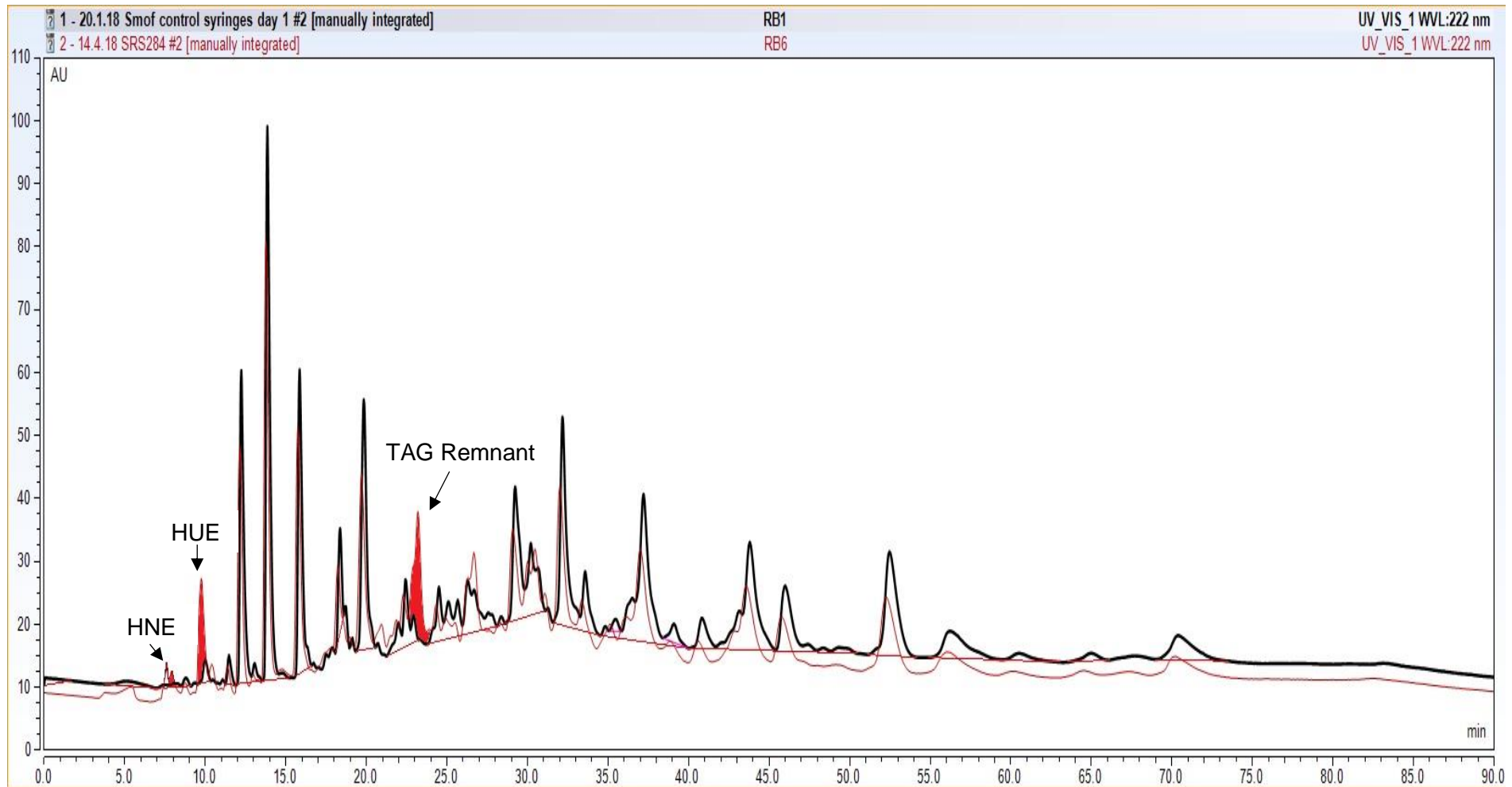
Figure 5.19 Overlaid HPLC-UV chromatograms of day 0 (black trace) and day 84 room temperature (red trace) SMOFlipid® 20 % stored in 50 ml syringes. Peaks on the 84 day chromatogram highlighted in red show HNE, HUE and TAG remnant.

227

5.5. SMOFlipid® light-protected PN bag results

Following the testing protocol laid out in section 3.4, 250ml Baxa multi-layer PN bags were filled with 50 ml SMOFlipid® and all possible air removed. All containers were covered with aluminium foil to protect from light. At each testing point 1ml of lipid was removed and all air removed from the PN bag. A control sample of SMOFlipid® in its original packaging was testing at each time point to ensure precision was maintained. All results were performed in triplicate and standard deviation and relative standard deviation calculated. Any result with a control sample RSD of >12 was excluded from further analysis as per method precision limits set out in section 3.5.

Figures 5.20 to 5.29 show the % losses recorded for each of the 10 TAGs monitored. Raw data is recorded in appendix 2. All data is recorded and shown graphically up to day 84, however the control samples RSD's fell outside the acceptable range (>12) on day 84. Therefore, day 84 results are indicated on graphs in orange and excluded from further analysis in section 5.7. Day 84 testing was performed with raised laboratory temperatures which could have accounted for the variation in precision observed in the results. Figure 5.31 shows the stacked chromatograms of day 56 SMOFlipid® in PN bags stored and room and fridge temperature and a control sample, indicating the % loss in peak area observed through a change in peak area and height.

PN bags produced a maximal % loss of over 40 % in both room and fridge temperature samples. Greatest loss was observed in peaks 8, 9 and 10 corresponding to TAGs containing largely C18:2 (linoleic) and C18:1 (oleic) fatty acids with minimal C18:0 (stearic) and C16:0 (palmitic) fatty acids. Room temperature losses were greater than fridge temperature for all peaks, but statistically significant differences were observed in peaks 1, 6 and 9 (see section 5.7 for further analysis).

No detectable HNE or HUE was recorded in any PN bags over 84 days of storage at either temperature, however TAG remnant production was observed in room temperature PN bags from day 14 onwards as shown in figure 5.30. This suggests that the apparent peroxidation observed through significant TAG losses could be through processes different to those observed previously in this work. As such potentially different secondary peroxidation products could be created which are undetectable by the UV assay as it has a fixed wavelength of 222 nm. Potential

pathways of peroxidation and the TAG losses observed are discussed further in section 5.7.

Figure 5.20 HPLC-CAD results for peak 1 (C8:0/8:0/8:0) triglyceride of SMOFlipid® 20 % stored in light protected 250 ml PN bags. Percentage loss of peak shown calculated from day 0 data. Room (Red) and Fridge (Blue) results shown with standard deviation error bars on all points. Orange data from day 84 excluded from further analysis due to high RSD.

Figure 5.21 HPLC-CAD results for peak 2 (C8:0/8:0/10:0) triglyceride of SMOFlipid® 20 % stored in light protected 250 ml PN bags. Percentage loss of peak shown calculated from day 0 data. Room (Red) and Fridge (Blue) results shown with standard deviation error bars on all points. Orange data from day 84 excluded from further analysis due to high RSD.
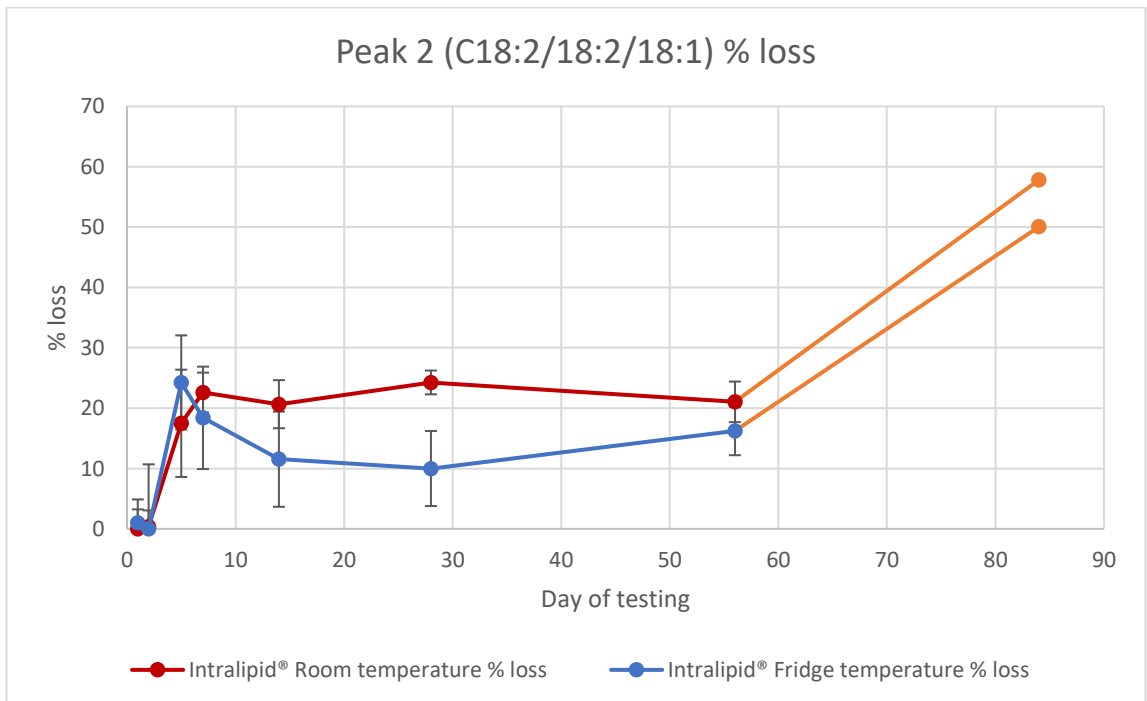
Figure 5.22 HPLC-CAD results for peak 3 (C8:0/10:0/10:0) triglyceride of SMOFlipid® 20 % stored in light protected 250 ml PN bags. Percentage loss of peak shown calculated from day 0 data. Room (Red) and Fridge (Blue) results shown with standard deviation error bars on all points. Orange data from day 84 excluded from further analysis due to high RSD.
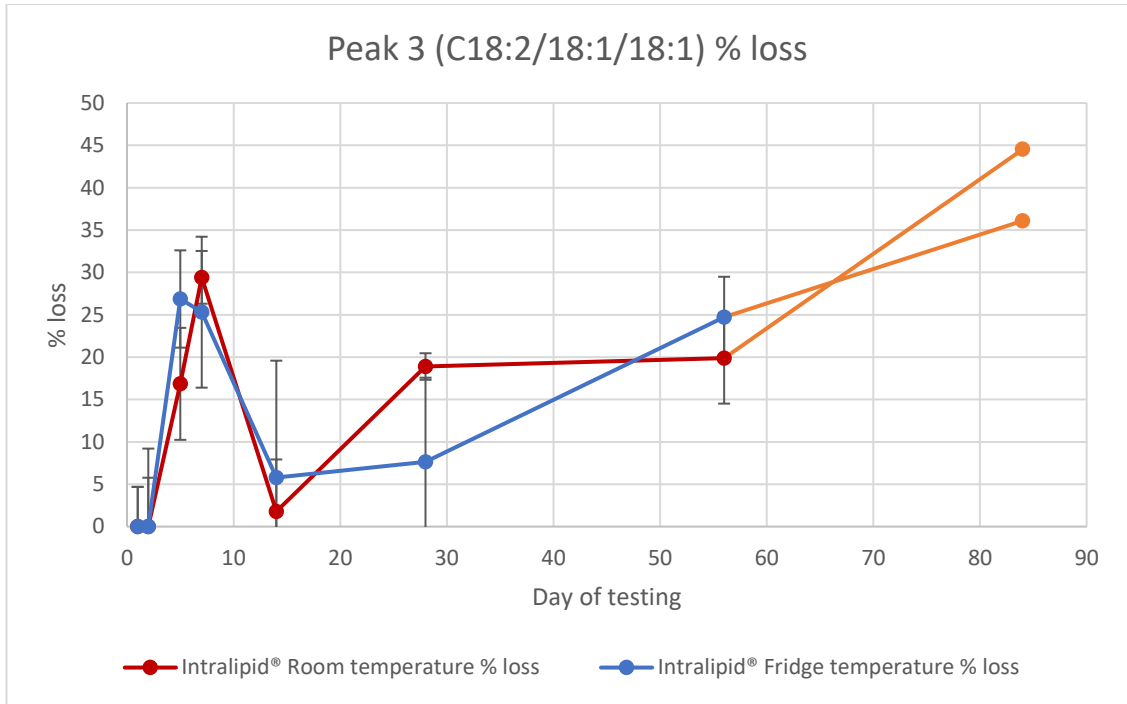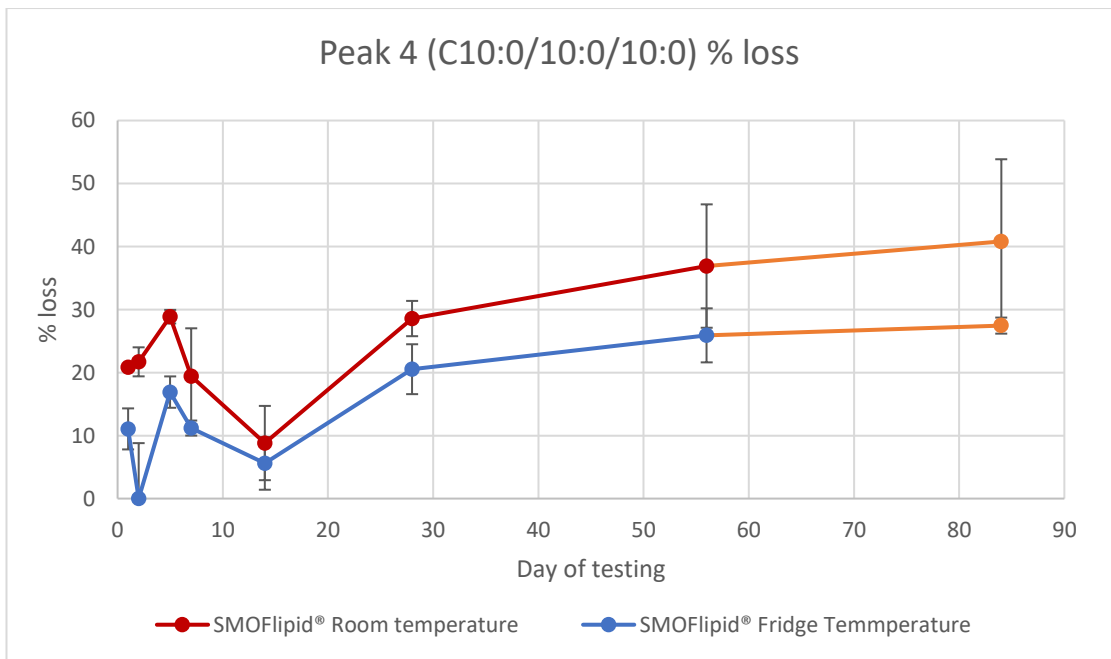

Figure 5.23 HPLC-CAD results for peak 4 (C10:0/10:0/10:0) triglyceride of 50 ml SMOFlipid® 20 % stored in light protected 250 ml PN bags. Percentage loss of peak shown calculated from day 0 data. Room (Red) and Fridge (Blue) results shown with standard deviation error bars on all points. Orange data from day 84 excluded from further analysis due to high RSD.

Figure 5.24 HPLC-CAD results for peak 5 (C18:2/18:2/18:2) triglyceride of 50 ml SMOFlipid® 20 % stored in 250ml light protected PN bags. Percentage loss of peak shown calculated from day 0 data. Room (Red) and Fridge (Blue) results shown with standard deviation error bars on all points. Orange data from day 84 excluded from further analysis due to high RSD.
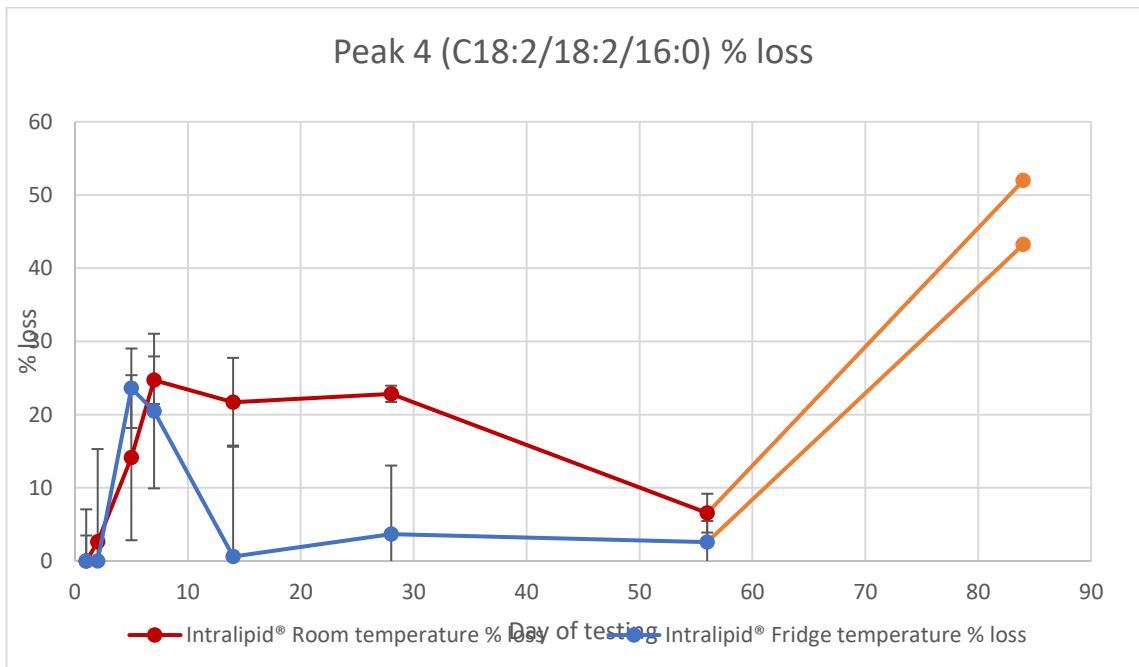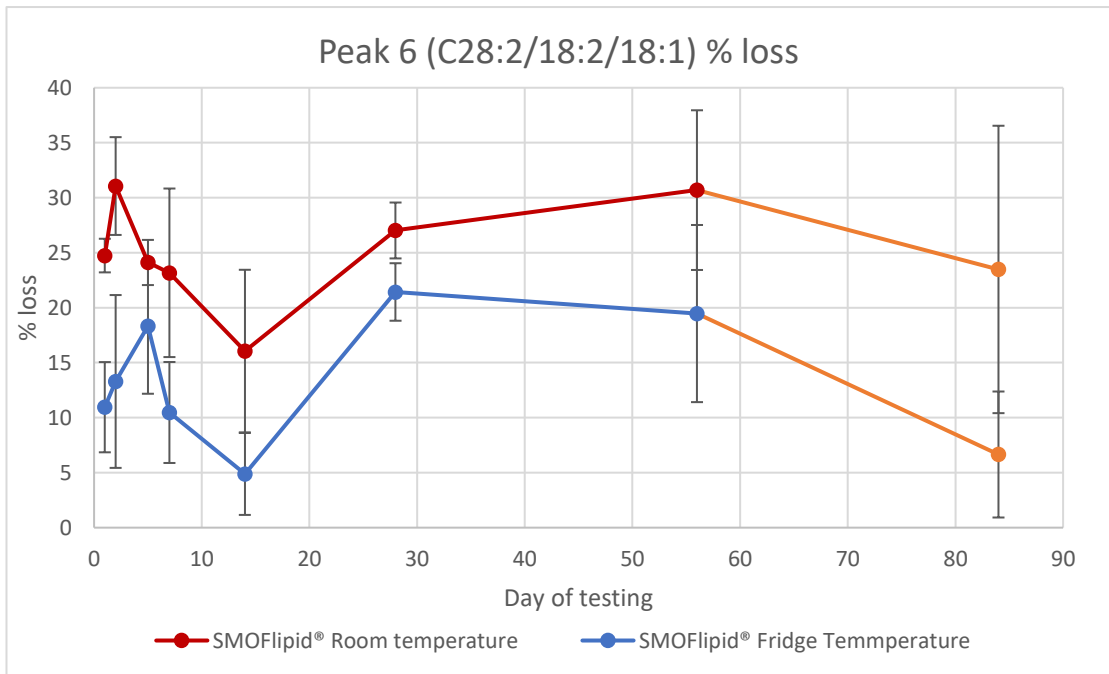

Figure 5.25 HPLC-CAD results for peak 6 (C18:2/18:2/18:1) triglyceride of 50ml SMOFlipid® 20 % stored in light protected 250 ml PN bags. Percentage loss of peak shown calculated from day 0 data. Room (Red) and Fridge (Blue) results shown with standard deviation error bars on all points.
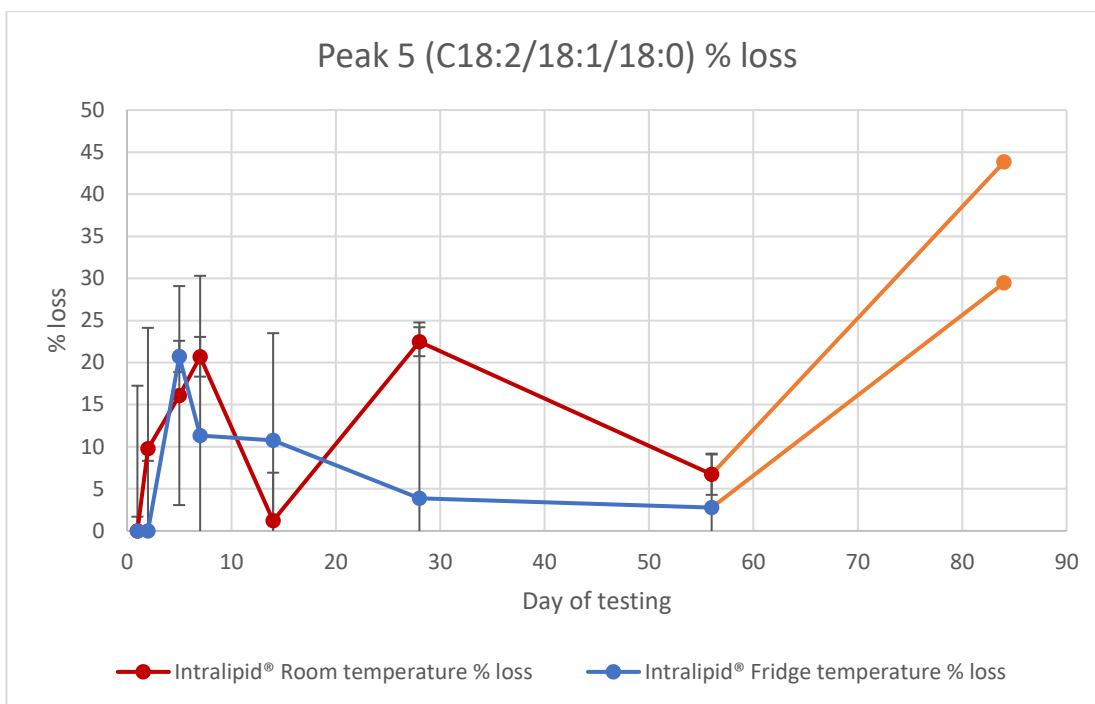
Figure 5.26 HPLC-CAD results for peak 7 (C18:2/18:1/18:1) triglyceride of 50 ml SMOFlipid® 20 % stored in light protected 250 ml PN bags. Percentage loss of peak shown calculated from day 0 data. Room (Red) and Fridge (Blue) results shown with standard deviation error bars on all points. Orange data from day 84 excluded from further analysis due to high RSD.
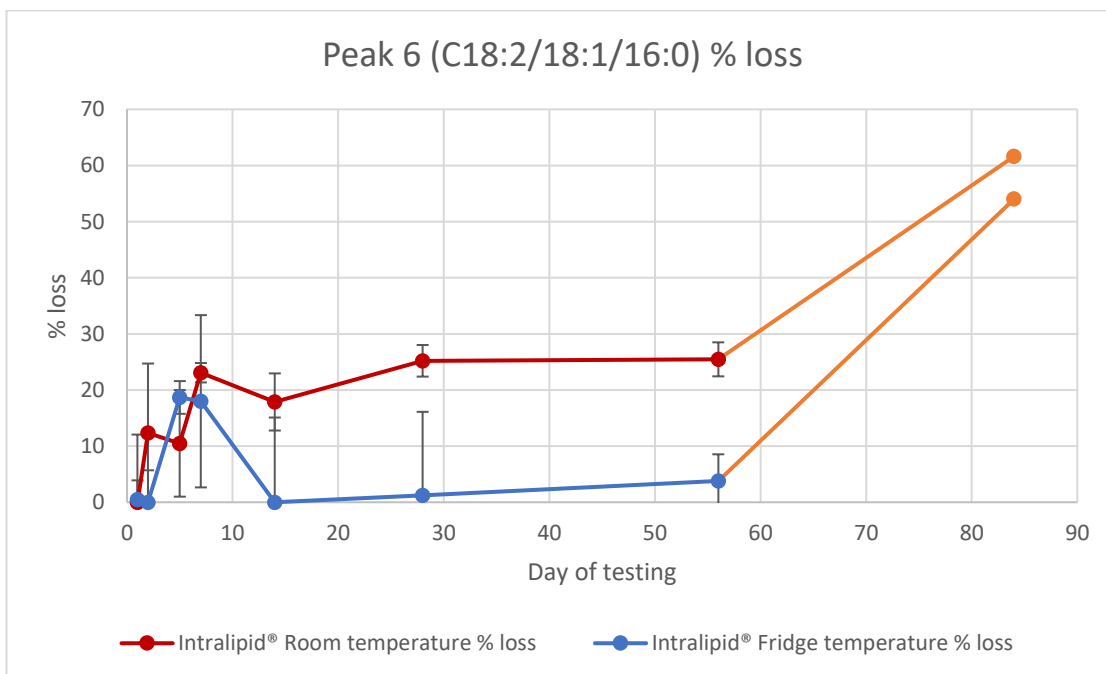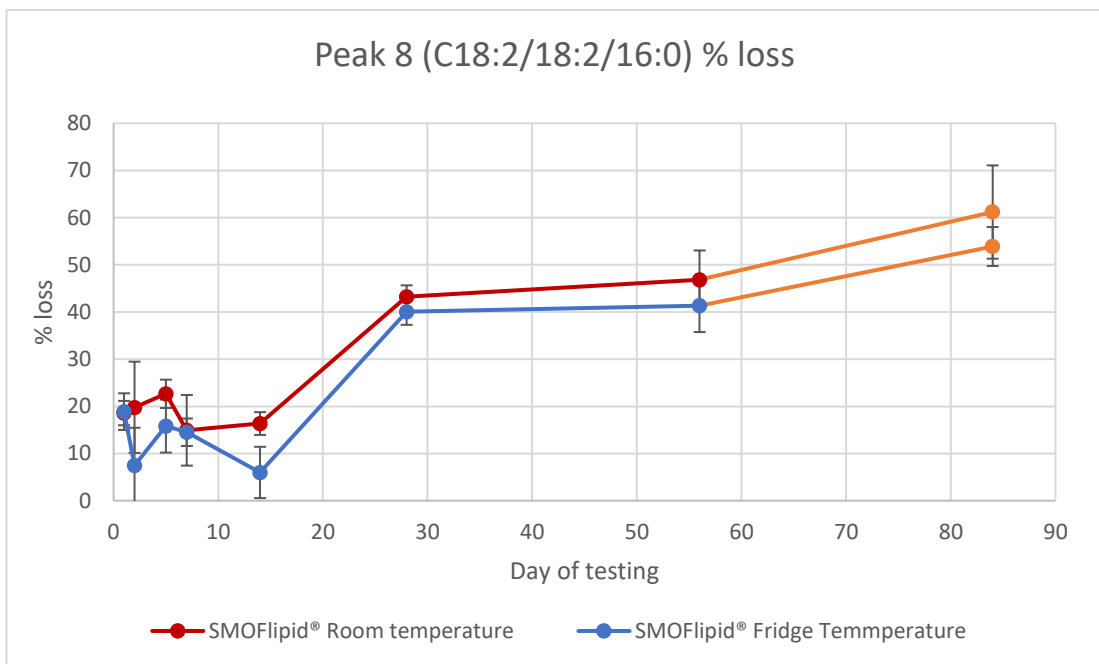

Figure 5.27 HPLC-CAD results for peak 8 (C18:2/18:2/16:0) triglyceride of 50 ml SMOFlipid® 20 % stored in light protected 250 ml PN bags. Percentage loss of peak shown calculated from day 0 data. Room (Red) and Fridge (Blue) results shown with standard deviation error bars on all points. Orange data from day 84 excluded from further analysis due to high RSD.

Figure 5.28 HPLC-CAD results for peak 9 (C18:2/18:1/18:0) triglyceride of 50 ml SMOFlipid® 20 % stored in light protected 250 ml PN bags. Percentage loss of peak shown calculated from day 0 data. Room (Red) and Fridge (Blue) results shown with standard deviation error bars on all points. Orange data from day 84 excluded from further analysis due to high RSD.

Figure 5.29 HPLC-CAD results for peak 10 (C18:2/18:1/16:0) triglyceride of 50 ml SMOFlipid® 20 % stored in light protected 250 ml PN bags. Percentage loss of peak shown calculated from day 0 data. Room (Red) and Fridge (Blue) results shown with standard deviation error bars on all points.
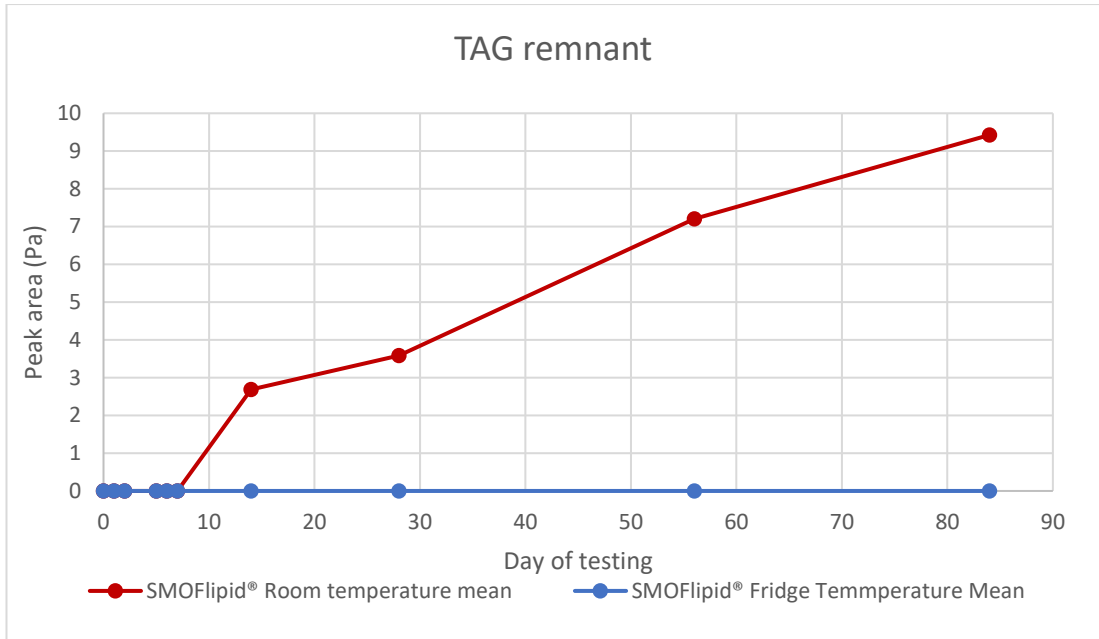
Figure 5.30 HPLC-UV of TAG remnant production in 50 ml SMOFlipid® light protected 250 ml PN bags over 84 days storage. Room temperature (red trace) showing production from day 28, no fridge temperature production (blue trace).
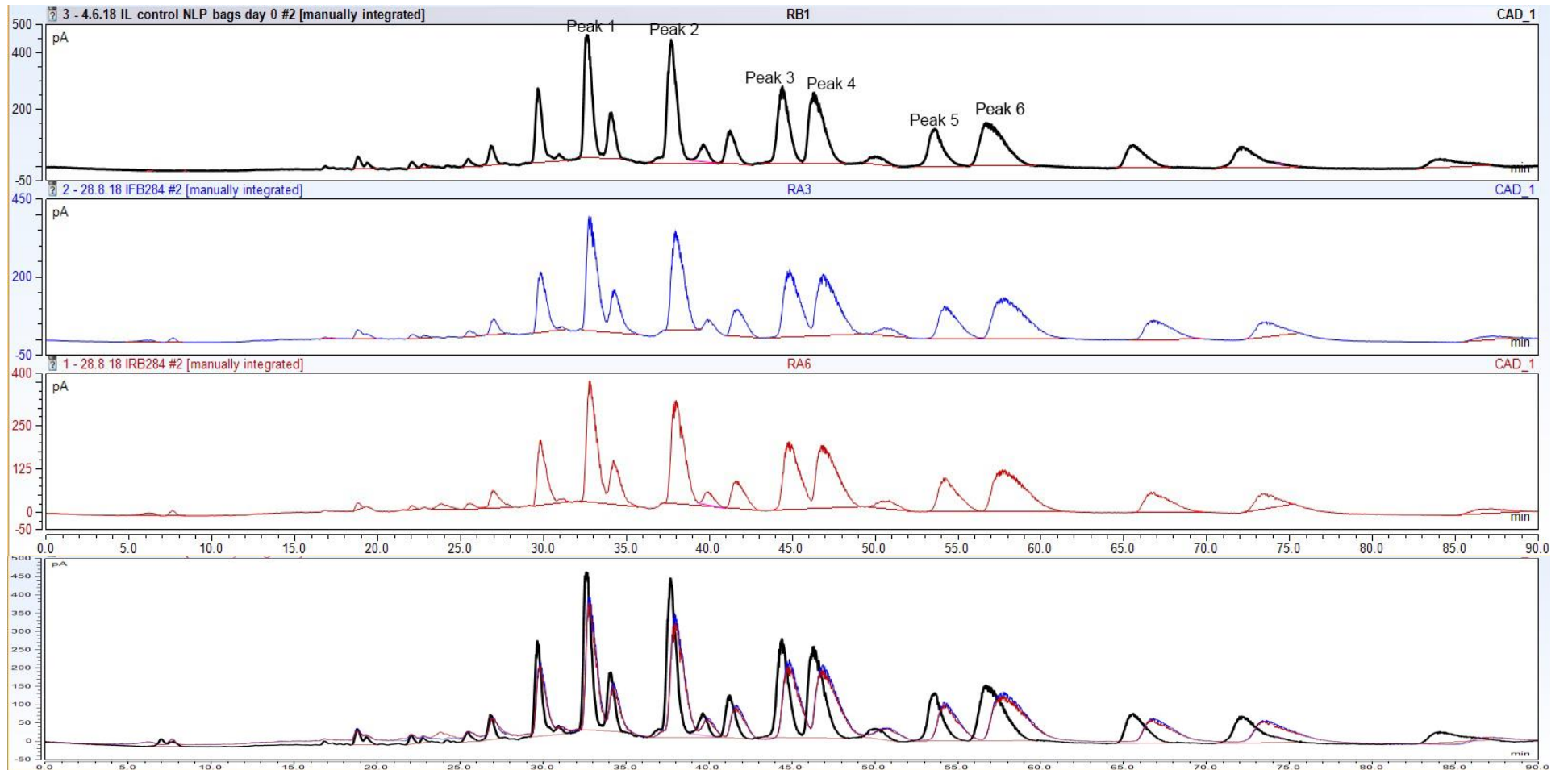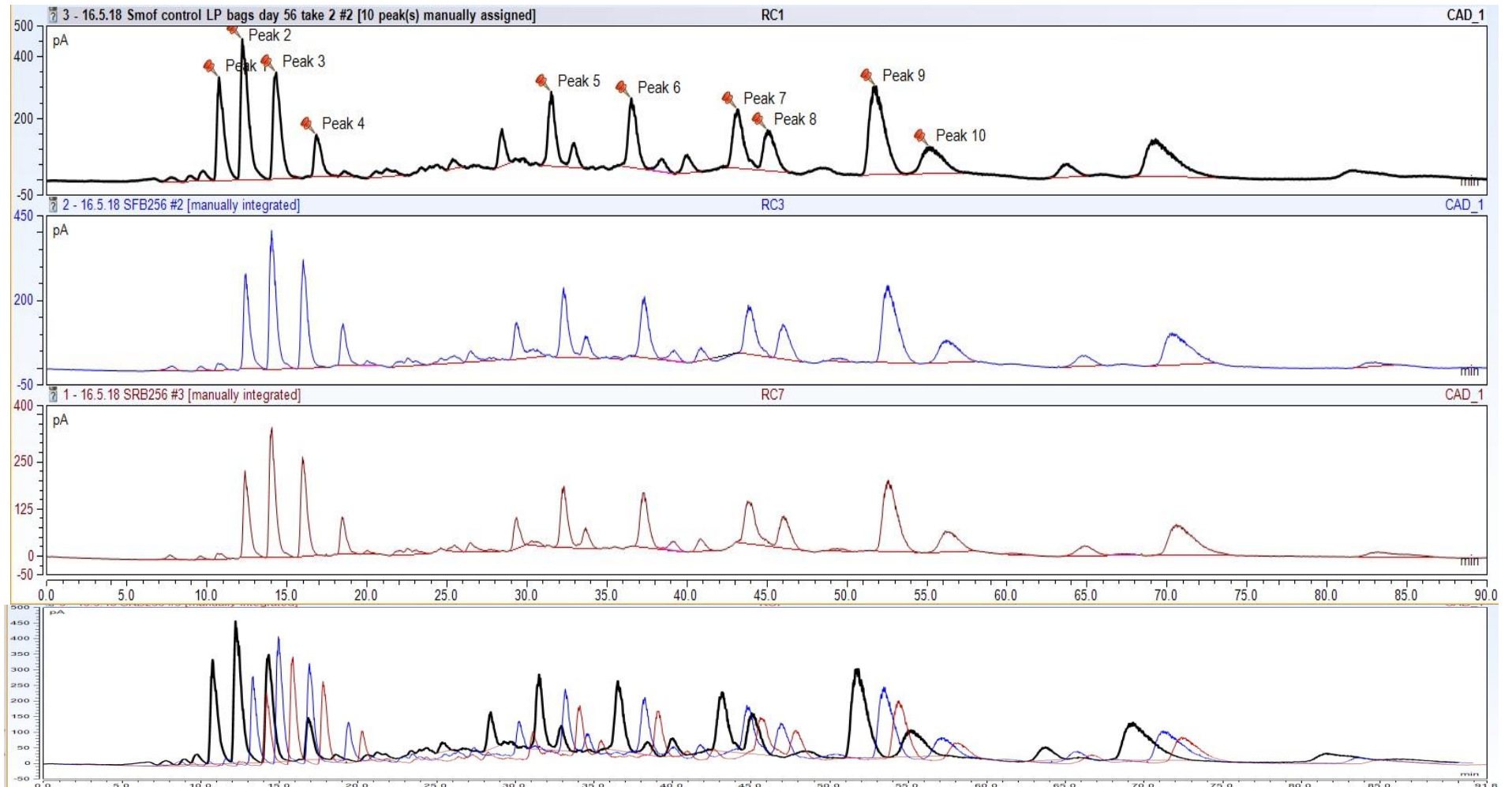
Figure 5.31 HPLC-CAD chromatograms of 50 ml SMOFlipid® 20% stored in 250 ml PN bags. Day 0 control (black), day 84 fridge temperature chromatogram (blue trace) and day 84 room temperature (red trace). Overlaid chromatogram with signal time offset shows changes in peaks in comparison to control.
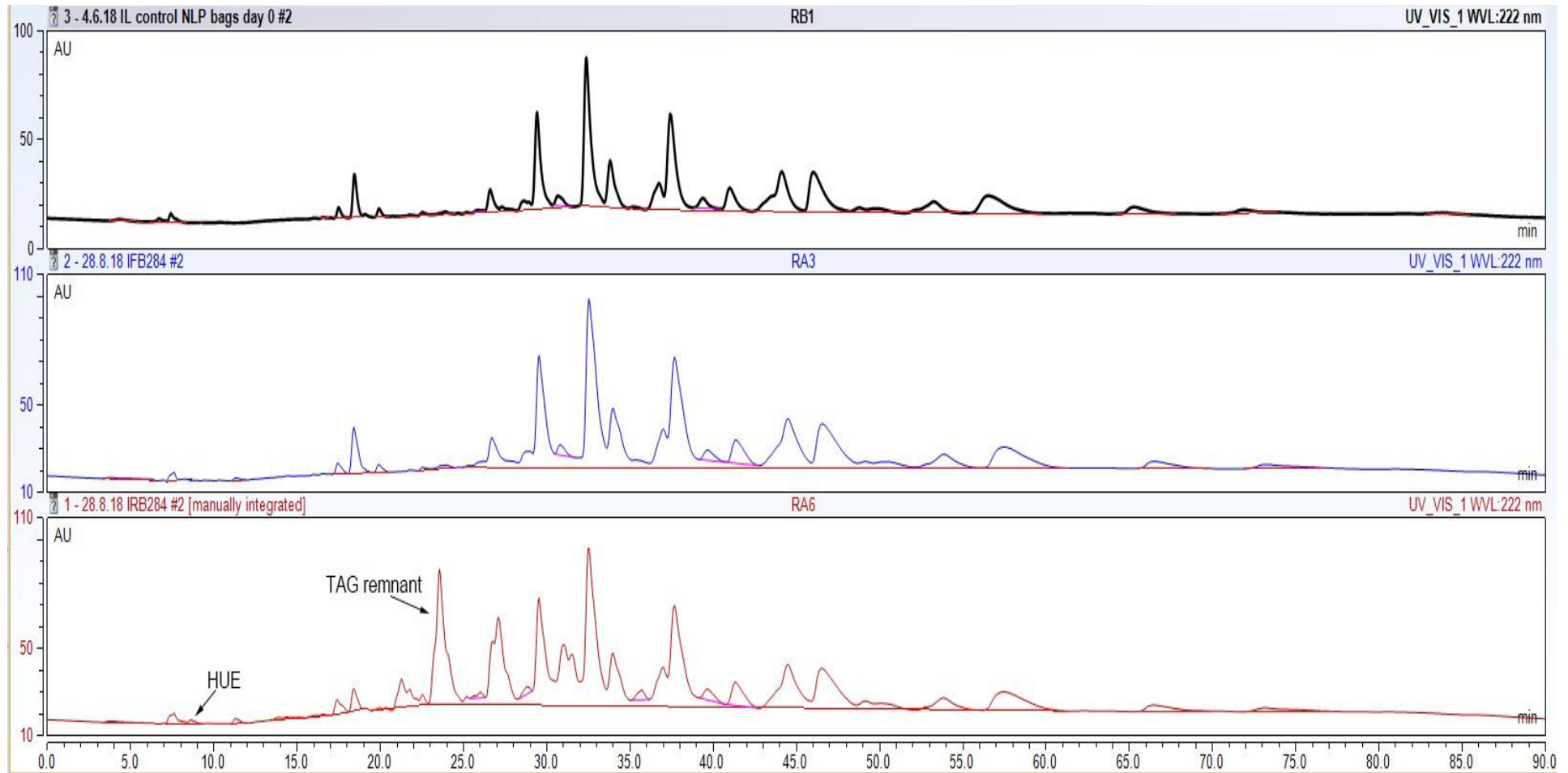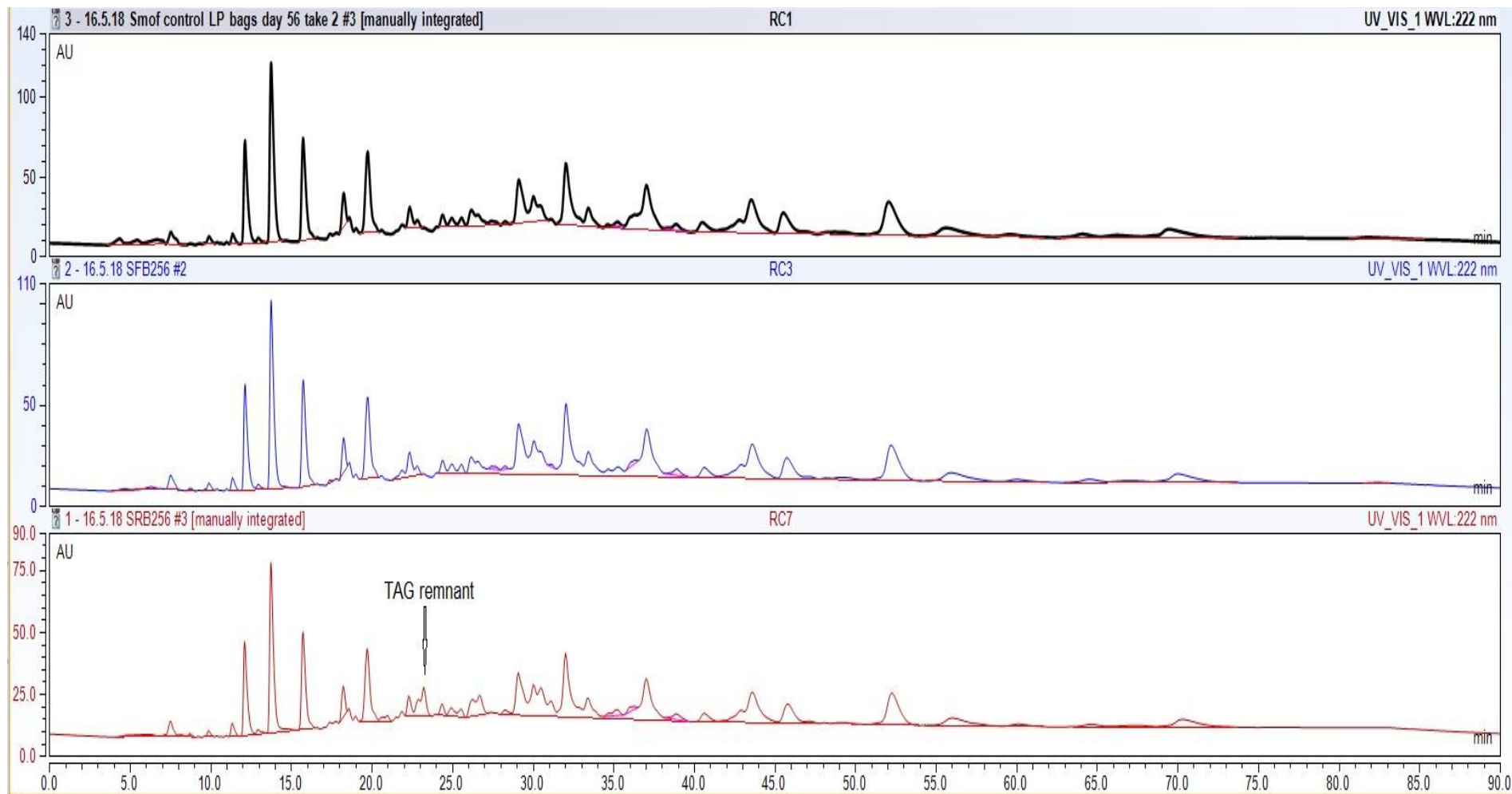
Figure 5.32 HPLC-UV chromatograms of 50 ml SMOFlipid® 20% stored in 250 ml PN bags. Day 0 chromatogram (black trace), day 84 fridge temperature bags (blue trace) and day 84 room temperature syringes (red trace). TAG remnant production is indicated in room temperature PN bags.
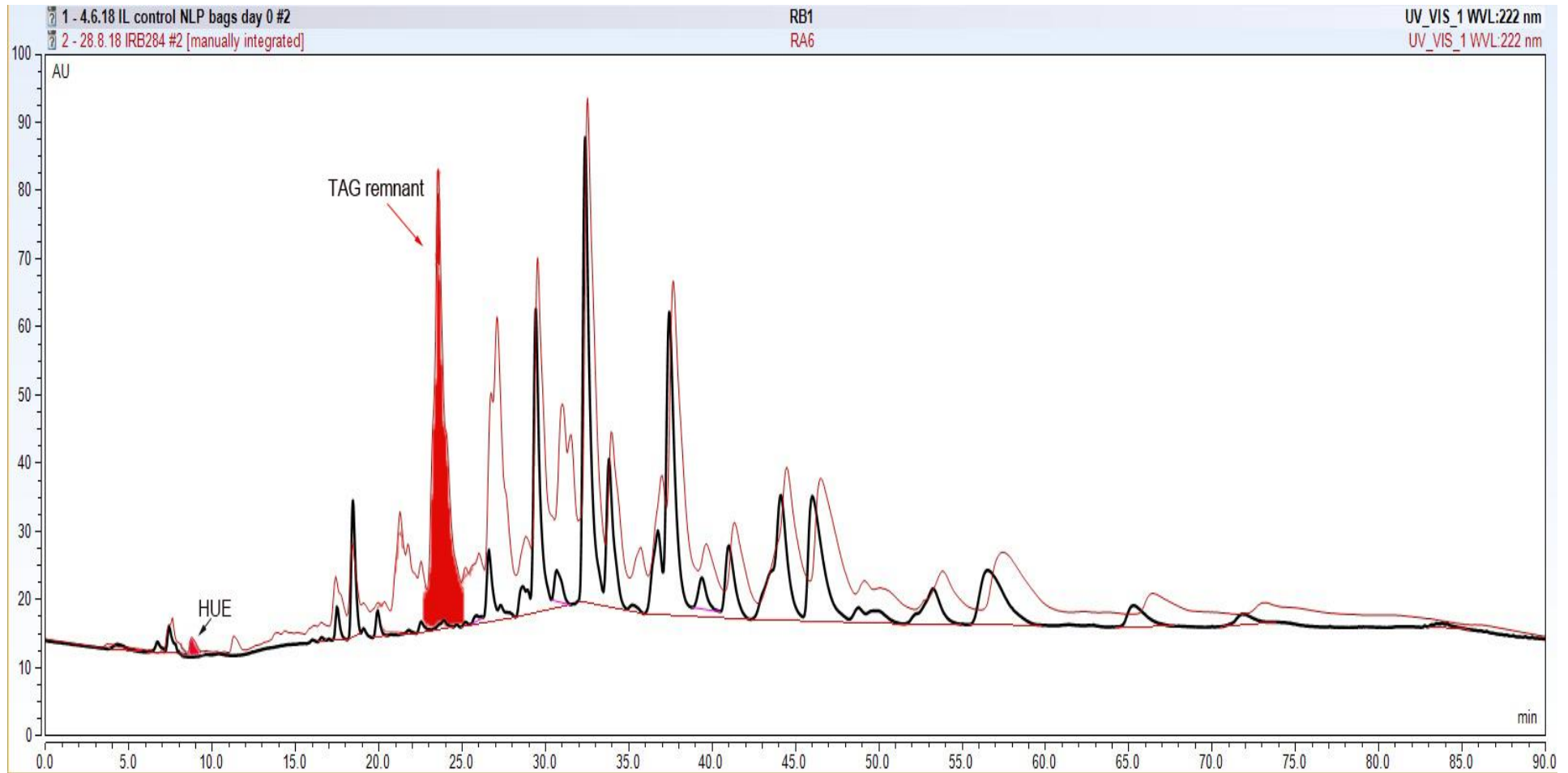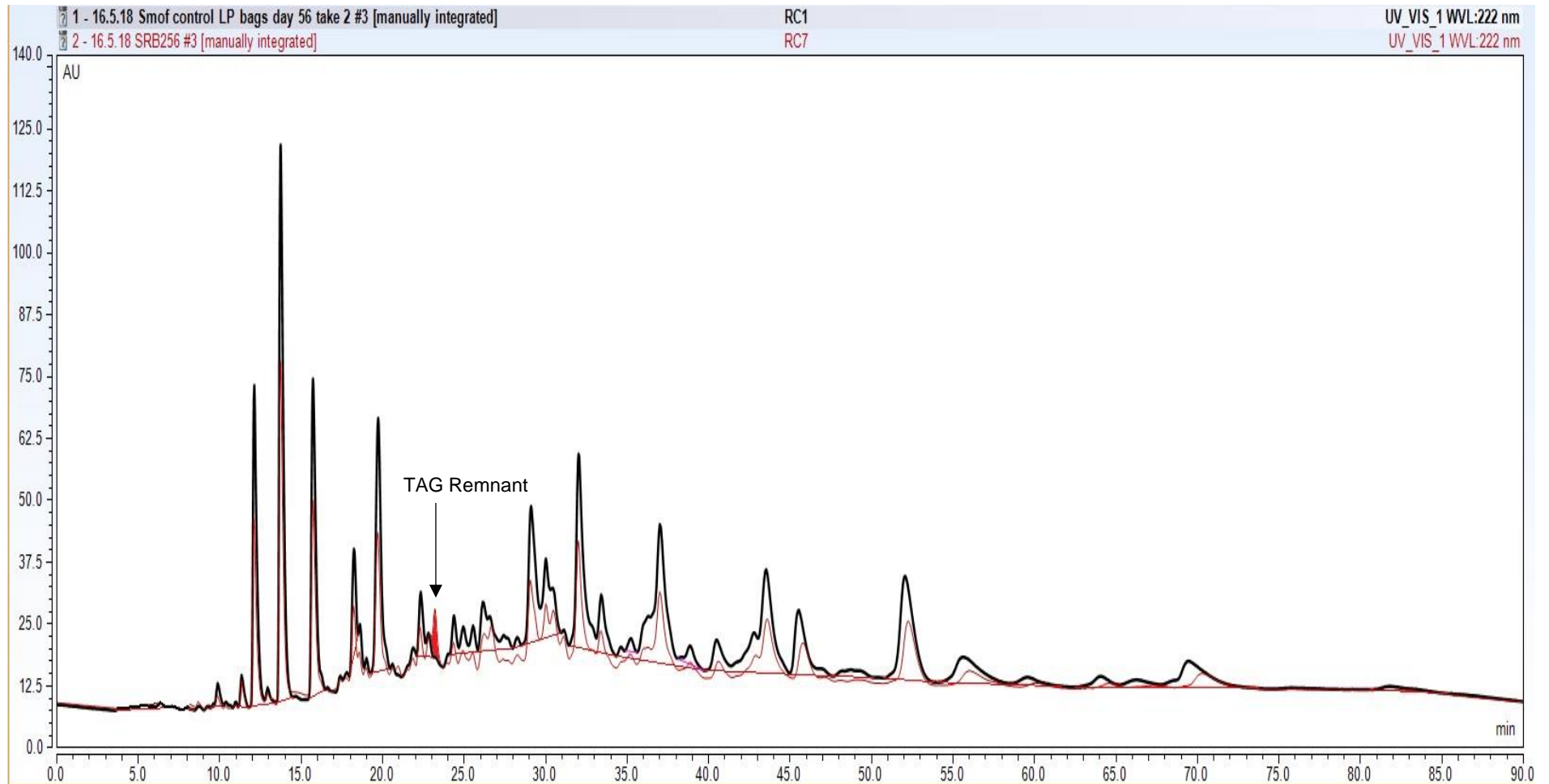
Figure 5.33 Overlaid HPLC-UV chromatograms of day 0 (black trace) and day 84 room temperature (red trace) SMOFlipid® 20 % stored in 250 ml PN bags. Peak on the 84-day chromatogram highlighted in red shows the TAG remnant produced.

5.6. SMOFlipid® light protected glass vial results

50 ml of SMOFlipid® was sealed in 50 ml glass vials as per testing protocol in section 3.4. Atmospheric air was removed through nitrogen purging as discussed in chapter 3.2.3. Air was purged again with nitrogen at each testing point after removal of lipid. All vials were protected from light with aluminium foil wraps. All results are recorded in triplicate and standard deviations and relative standard deviation calculated. All chromatograms were integrated, and peak areas calculated and recorded. TAG losses are shown as % loss from a day 0 standard. At each time point to ensure method precision a control sample of new SMOFlipid® was tested and its RSD monitored for acceptability (<12) (Fox et al. 2013; Márquez-Sillero et al. 2013).

Figures 5.34 to 5.43 show the TAG losses for all monitored peaks. Chromatograms seen in figures 5.44 and 5.45 indicate the day 84 TAG losses observed and the lack of secondary peroxidation products. All vials indicated minimal TAG losses through the initial 28 days of testing. However, beyond this time point TAG losses increased to a maximum of 35 % in room temperature vials and ~ 20 % at fridge temperature. Temperature had a significant effect on TAG loss (statistically different for peaks 4,6,8,9 and 10, see section 5.7). Peroxidation and therefore TAG loss was minimised until day 28 which can be explained by the successful removal of air and therefore oxygen from the system by nitrogen purging. This prevents the initiation of oxygen-dependant peroxidation from occurring. Light protection also inhibits photo-oxidation from initiating the peroxidation process. The rise in TAG loss at day 28 could be due to oxygen ingress through repeated sampling through the rubber vial tops, creating a passage for air to leak into the system during prolonged storage.

No HNE, HUE or TAG remnant were detected throughout the 84-day storage period at both temperatures, suggesting that minimal peroxidation was occurring. Whilst TAG losses were observed from day 28 onwards, the lack of detectable secondary peroxidation products could suggest that peroxidation is still within the initiation and propagation phases, that the products formed from day 28 onwards are the initial primary lipid hydroperoxides not detected through the assay, or that different secondary products are formed and not detected. Both the lack of products and the TAG losses are discussed further in section 5.7.
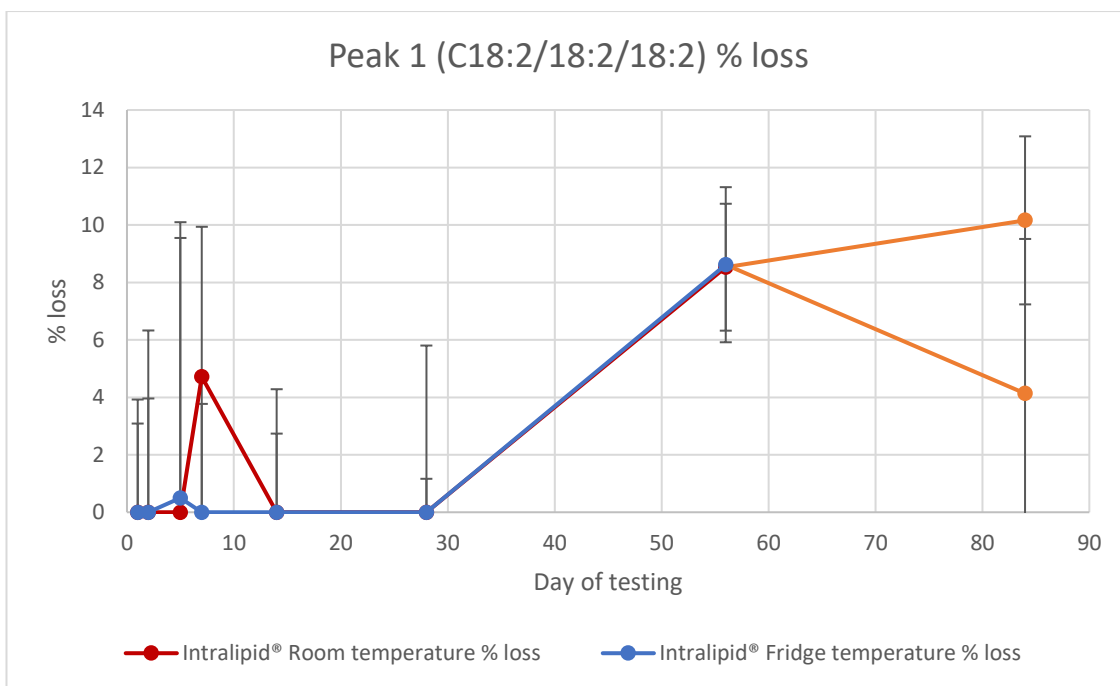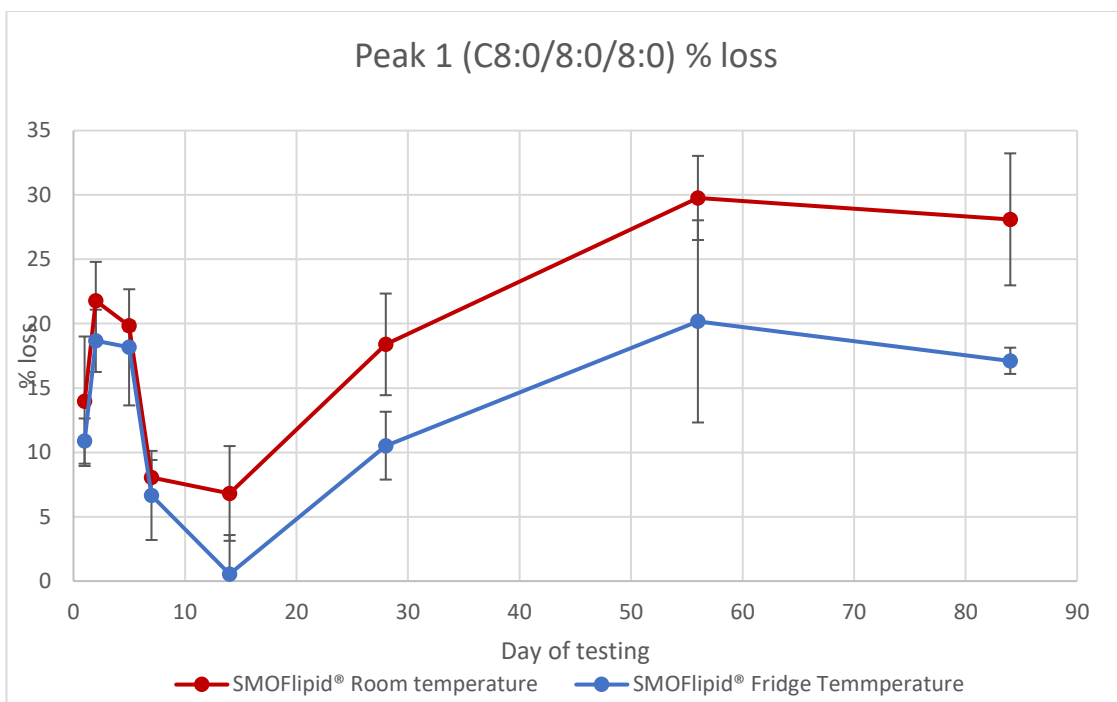
Figure 5.34 HPLC-CAD results for peak 1 (C8:0/8:0/8:0) triglyceride of SMOFlipid® 20 % stored in 50ml light protected glass vials. Percentage loss of peak shown calculated from day 0 data. Room (Red) and Fridge (Blue) results shown with standard deviation error bars on all points.
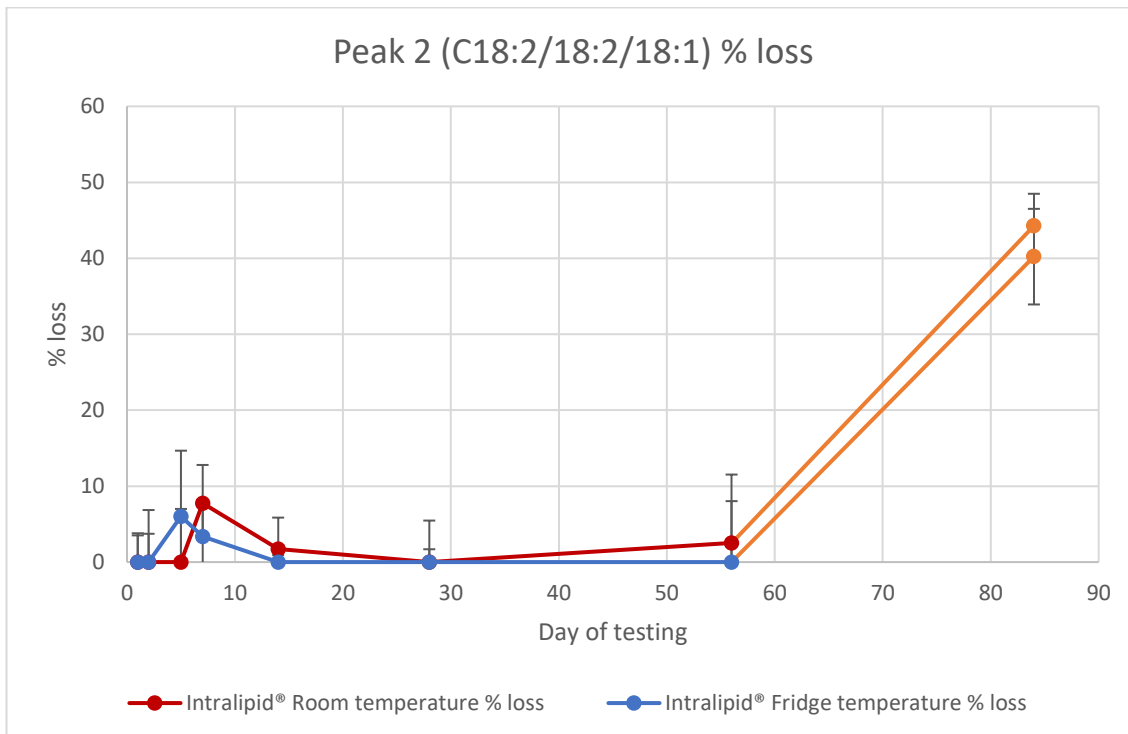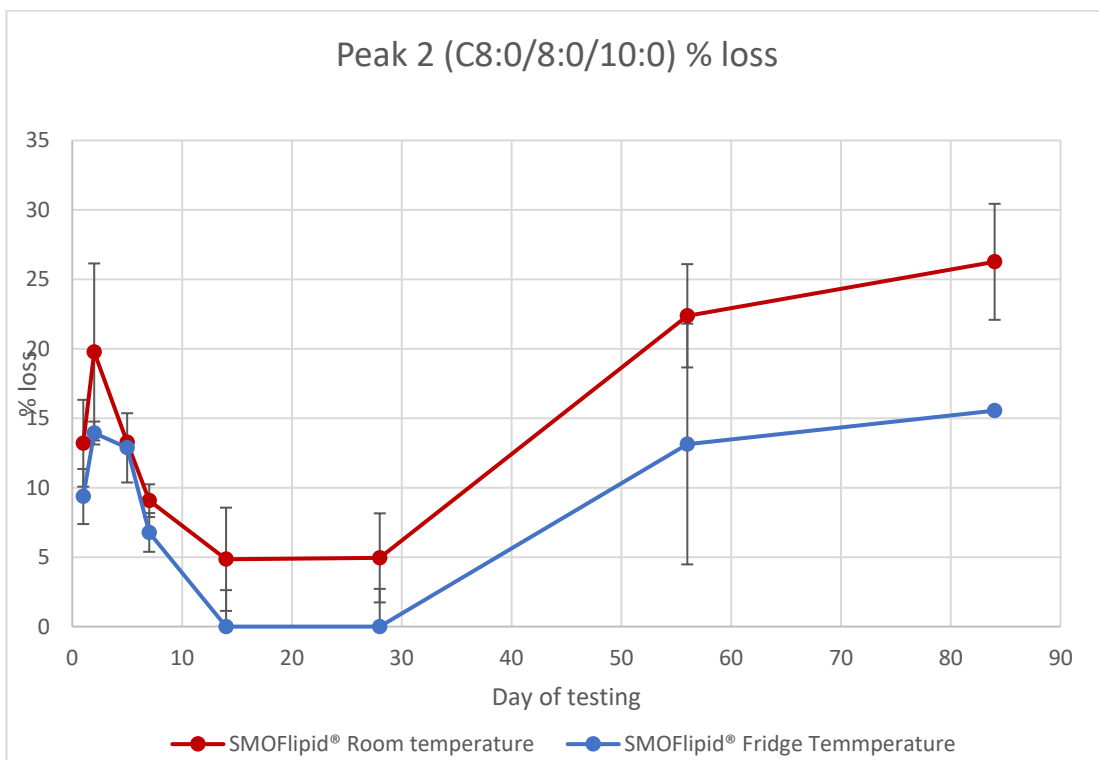

Figure 5.35 HPLC-CAD results for peak 2 (C8:0/8:0/10:0) triglyceride of SMOFlipid® 20 % stored in light protected 50 ml glass vials. Percentage loss of peak shown calculated from day 0 data. Room (Red) and Fridge (Blue) results shown with standard deviation error bars on all points.
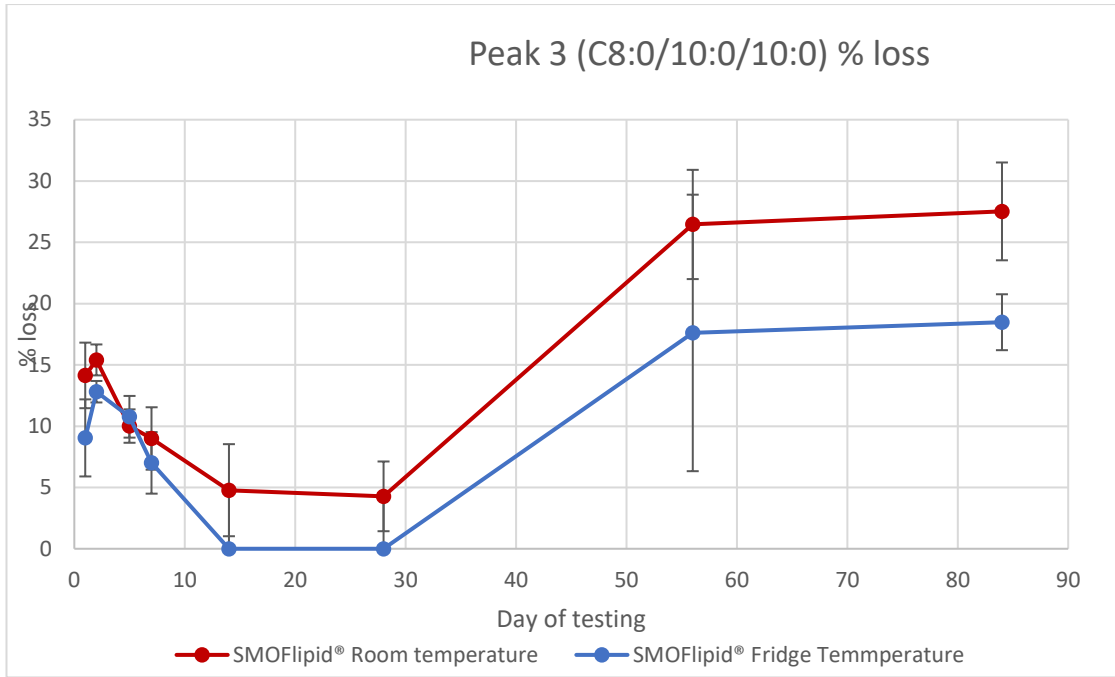
Figure 5.36 HPLC-CAD results for peak 3 (C8:0/10:0/10:0) triglyceride of SMOFlipid® 20 % stored in 50ml light protected glass vials. Percentage loss of peak shown calculated from day 0 data. Room (Red) and Fridge (Blue) results shown with standard deviation error bars on all points.
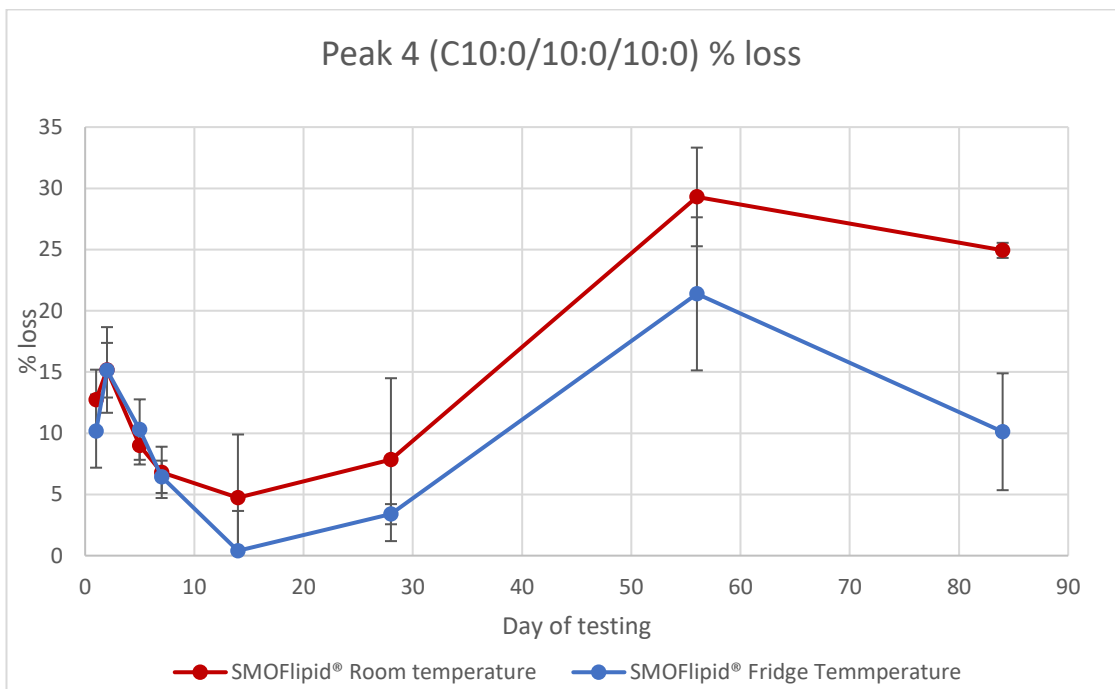
Figure 5.37 HPLC-CAD results for peak 4 (C10:0/10:0/10:0) triglyceride of SMOFlipid® 20 % stored in 50ml light protected glass vials. Percentage loss of peak shown calculated from day 0 data. Room (Red) and Fridge (Blue) results shown with standard deviation error bars on all points.
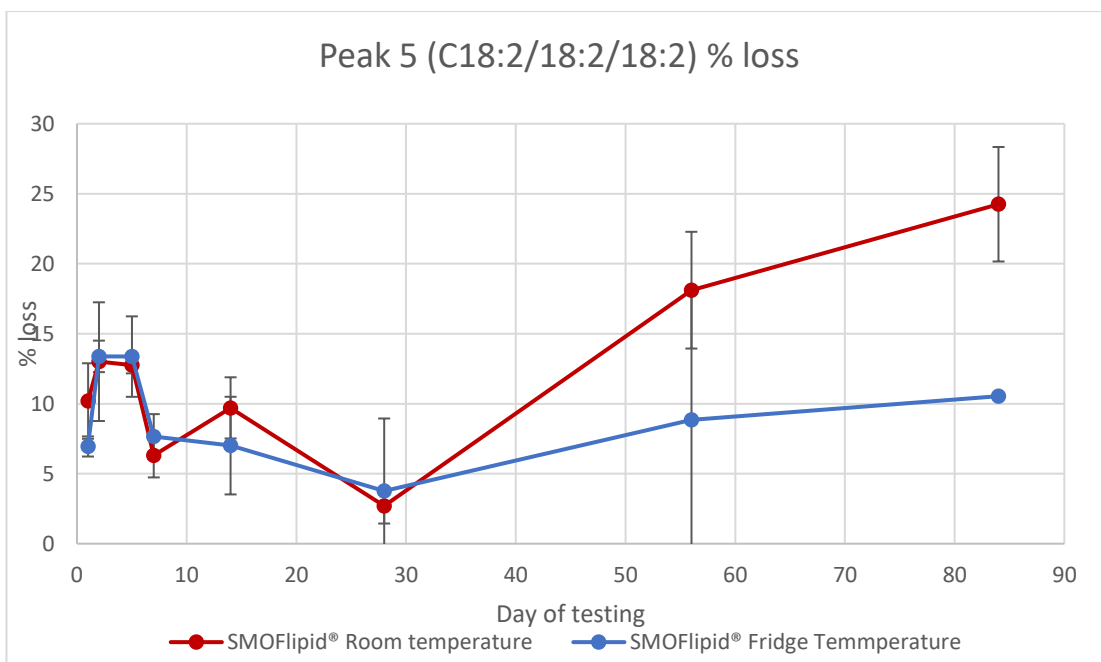
Figure 5.38 HPLC-CAD results for peak 5 (C18:2/18:2/18:2) triglyceride of SMOFlipid® 20 % stored in 50ml light protected glass vials. Percentage loss of peak shown calculated from day 0 data. Room (Red) and Fridge (Blue) results shown with standard deviation error bars on all points.
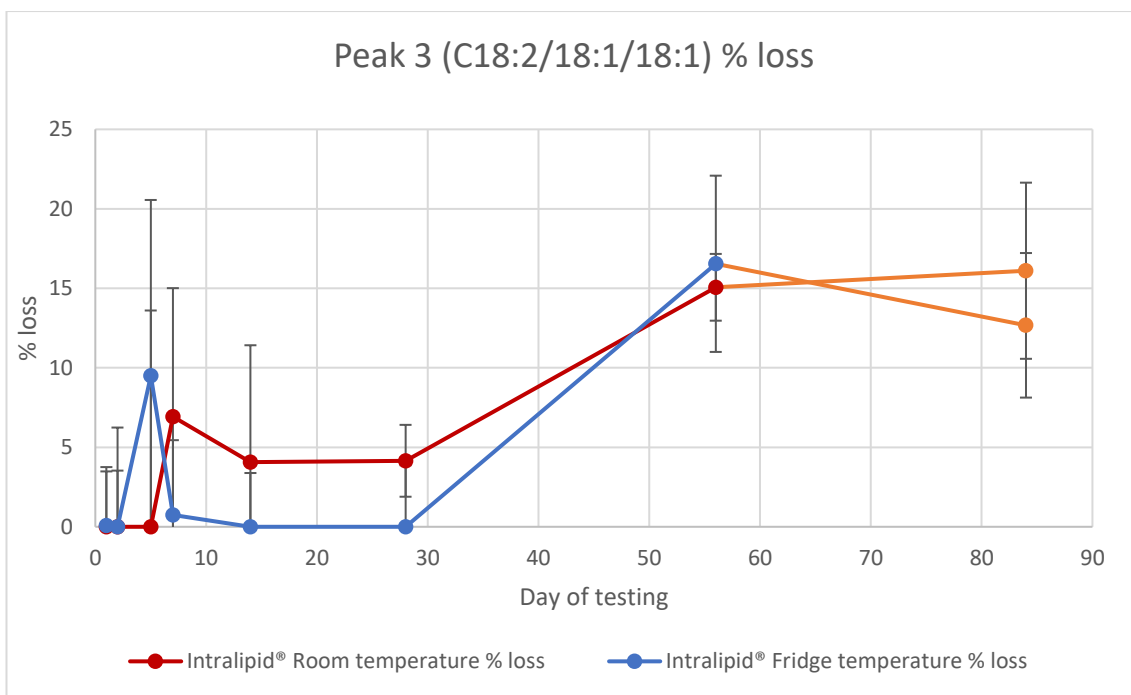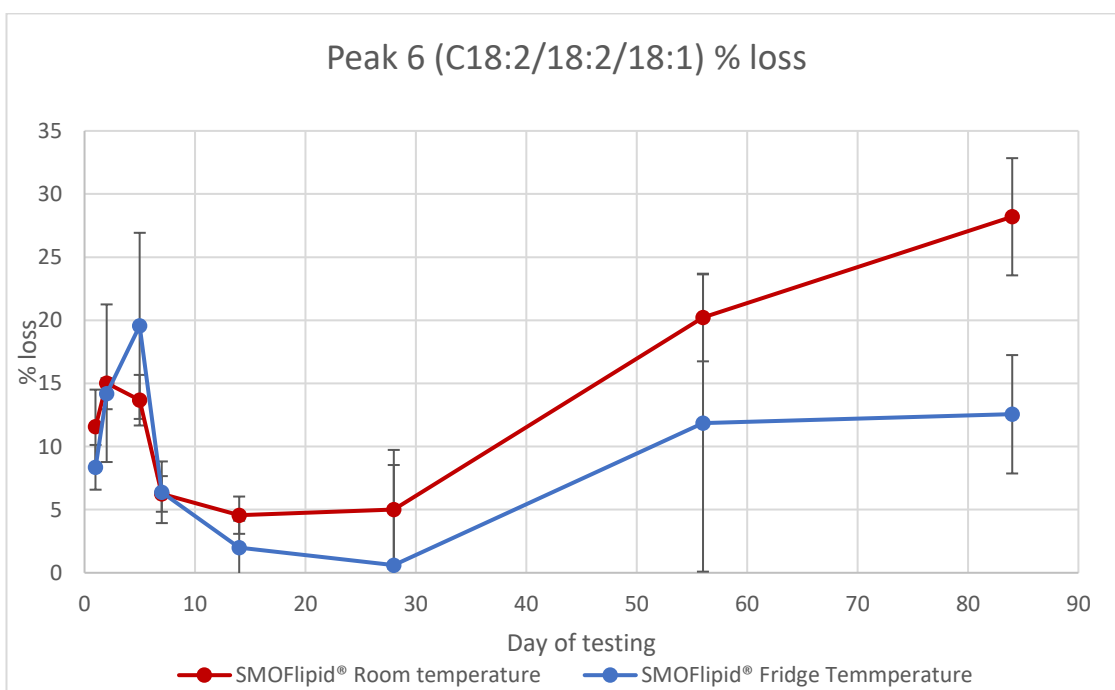

Figure 5.39 HPLC-CAD results for peak 6 (C18:2/18:2/18:1) triglyceride of SMOFlipid® 20 % stored in light protected 50 ml glass vials. Percentage loss of peak shown calculated from day 0 data. Room (Red) and Fridge (Blue) results shown with standard deviation error bars on all points.
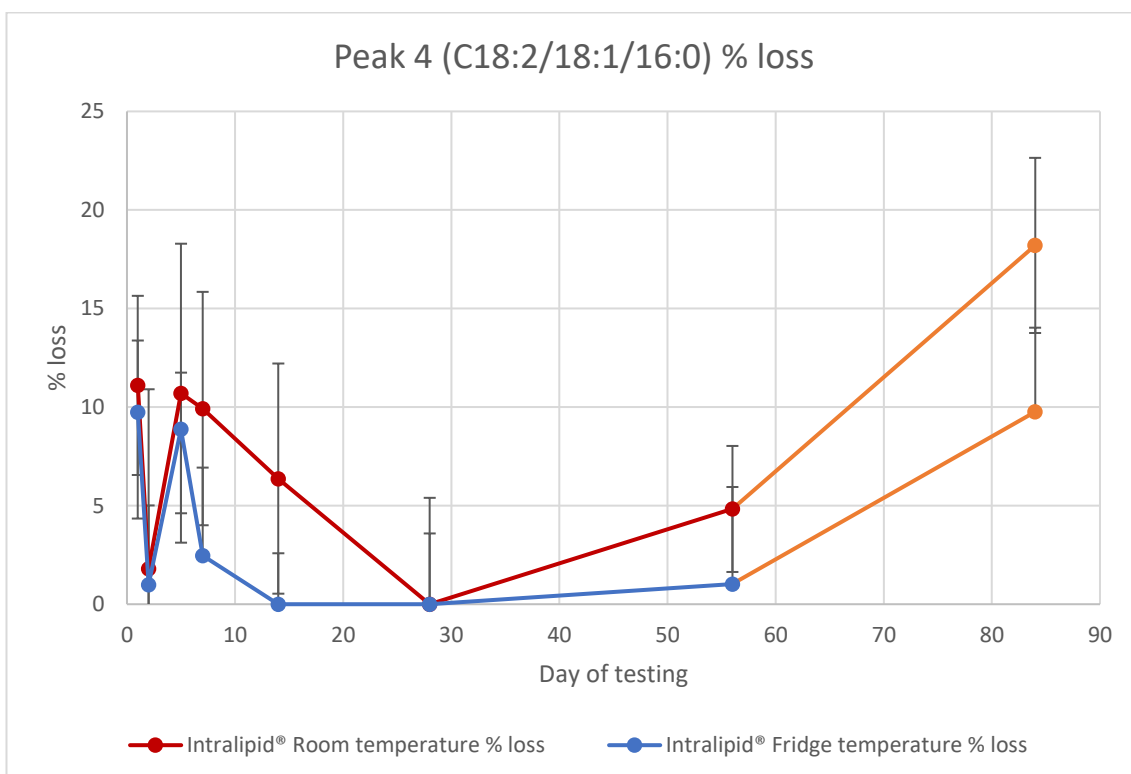
241
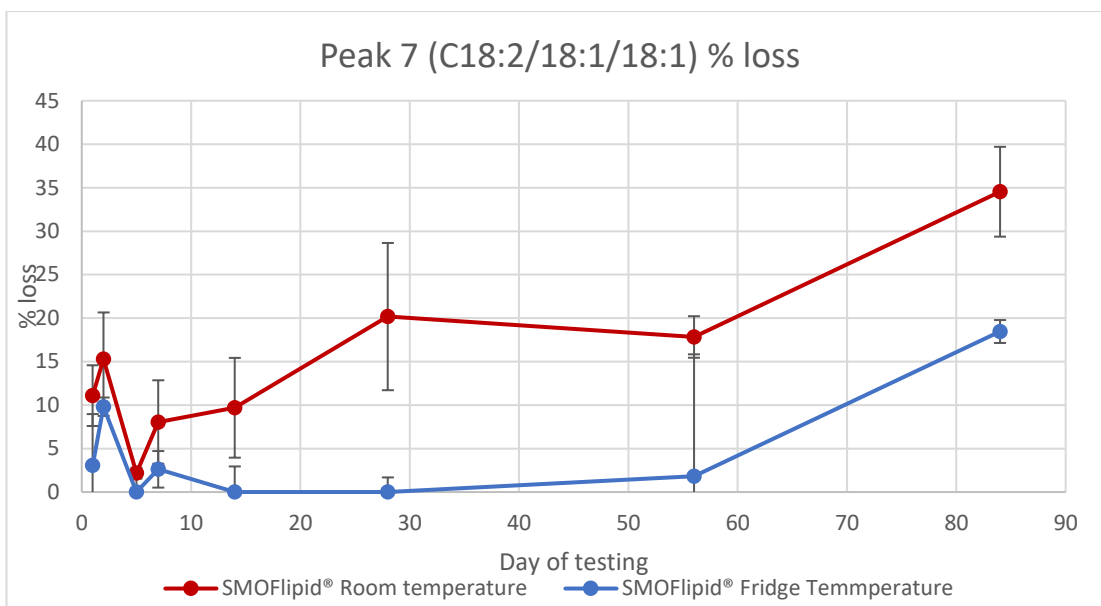
Figure 5.40 HPLC-CAD results for peak 7 (C18:2/18:1/18:1) triglyceride of SMOFlipid® 20 % stored in light protected 50 ml glass vials. Percentage loss of peak shown calculated from day 0 data. Room (Red) and Fridge (Blue) results shown with standard deviation error bars on all points.
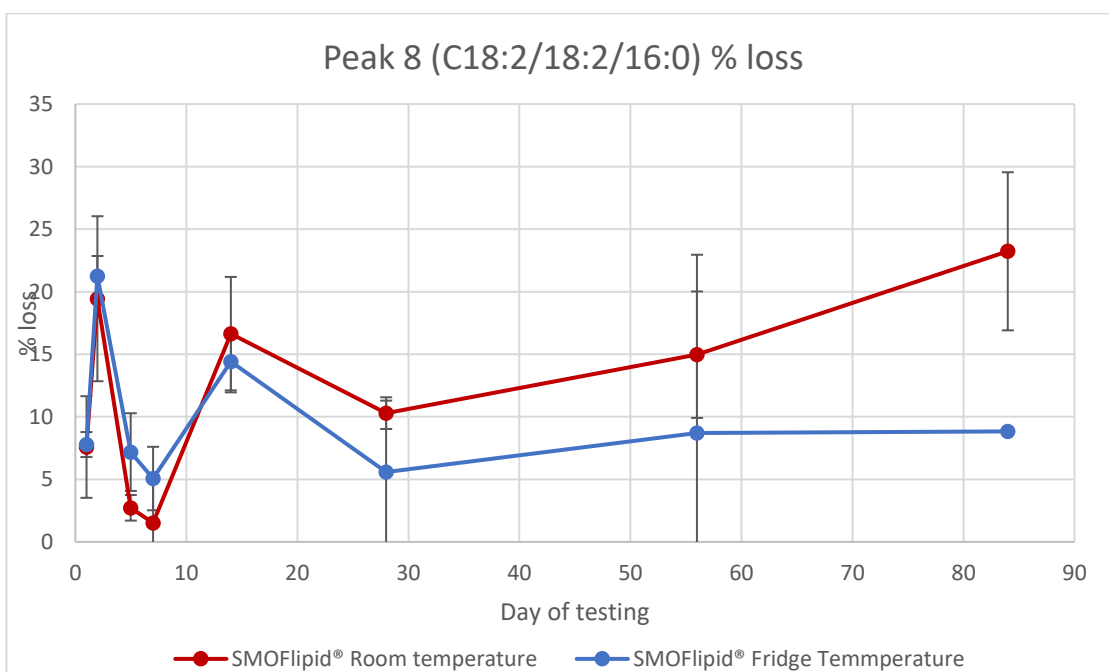
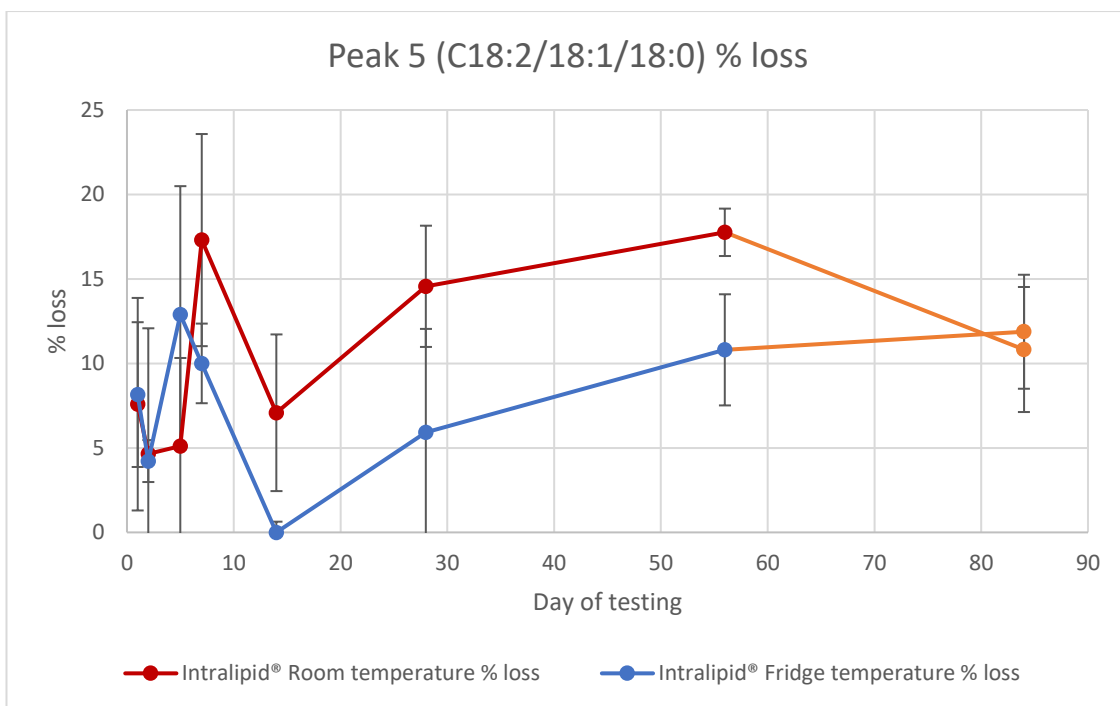*Figure 5.41 HPLC-CAD results for peak 8 (C18:2/18:2/16:0) triglyceride of SMOFlipid® 20 % stored in light protected 50 ml glass vials. Percentage loss of peak shown calculated from day 0 data. Room (Red) and Fridge (Blue) results shown with standard deviation error bars on all points.*
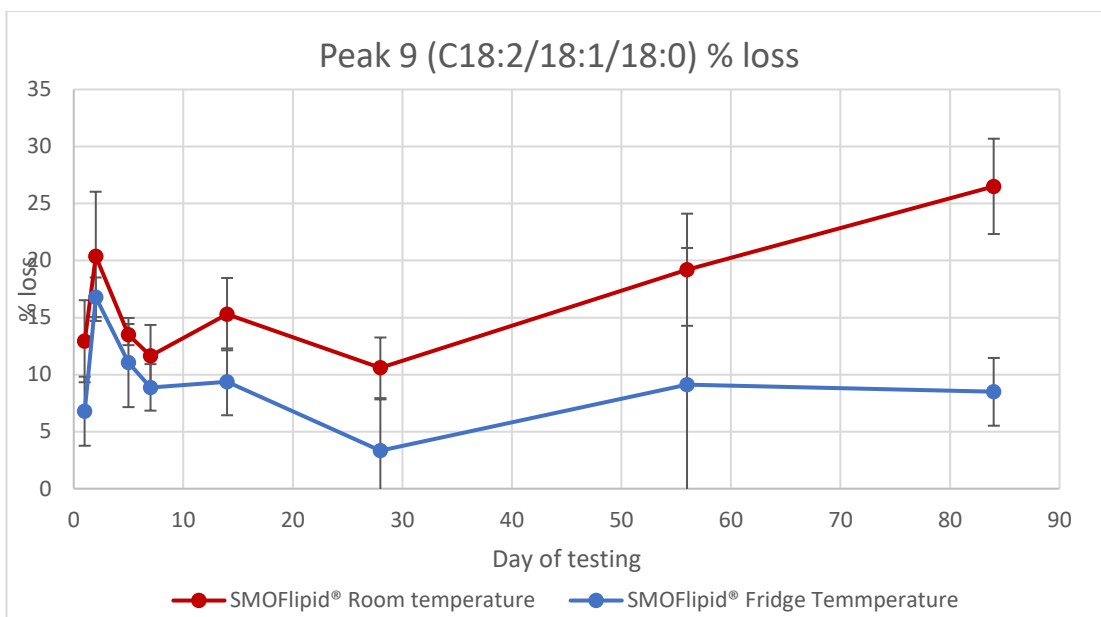
Figure 5.42 HPLC-CAD results for peak 9 (C18:2/18:1/18:0) triglyceride of SMOFlipid® 20 % stored in light protected 50 ml glass vials. Percentage loss of peak shown calculated from day 0 data. Room (Red) and Fridge (Blue) results shown with standard deviation error bars on all points.
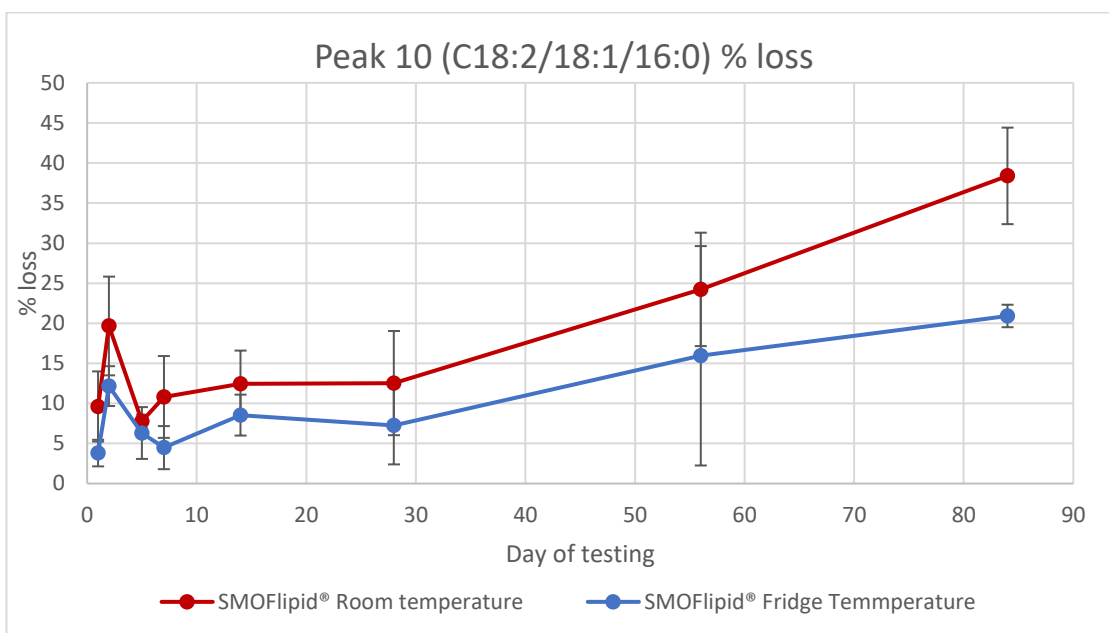
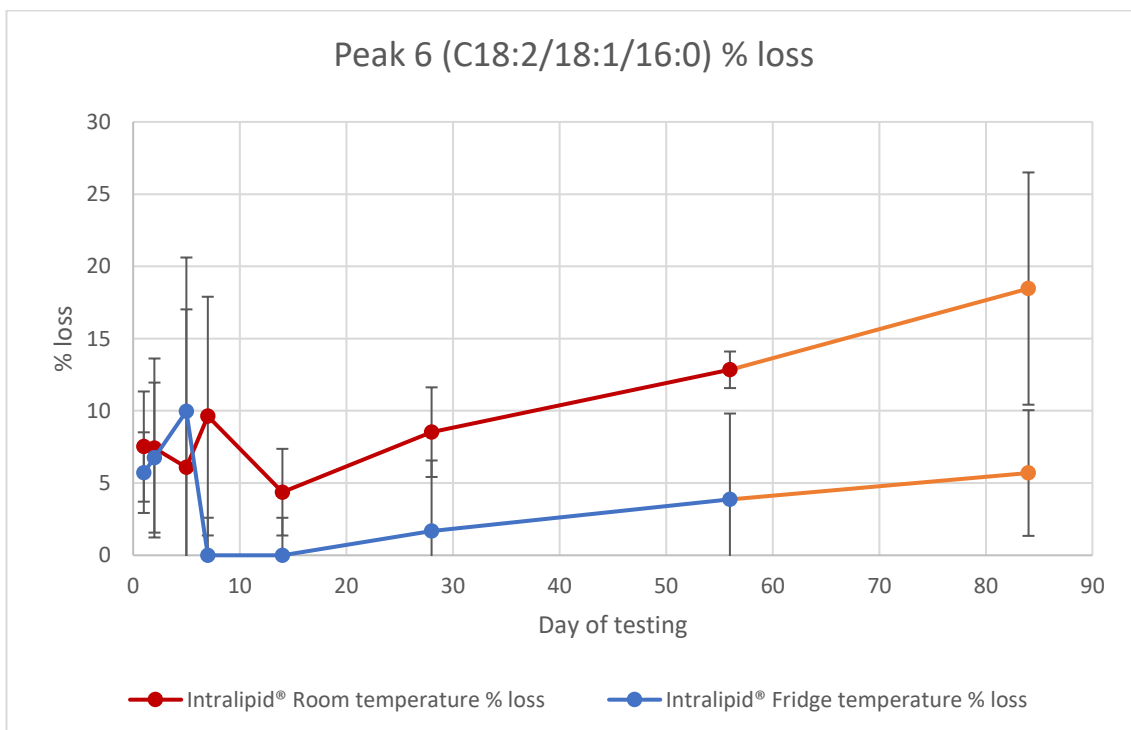*Figure 5.43 HPLC-CAD results for peak 10 (C18:2/18:1/16:0) triglyceride of SMOFlipid® 20 % stored in light protected 50 ml glass vials. Percentage loss of peak shown calculated from day 0 data. Room (Red) and Fridge (Blue) results shown with standard deviation error bars on all points.*
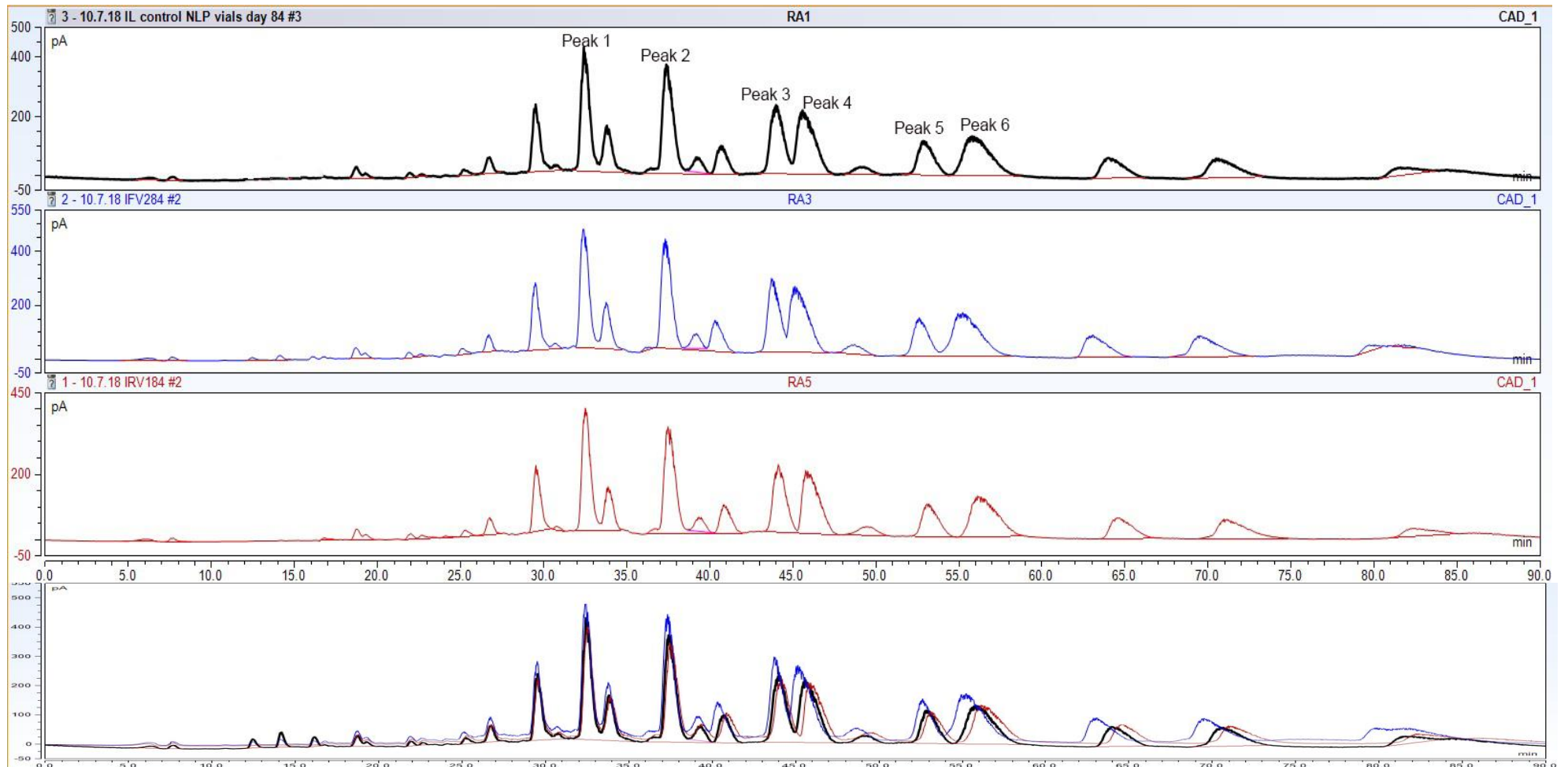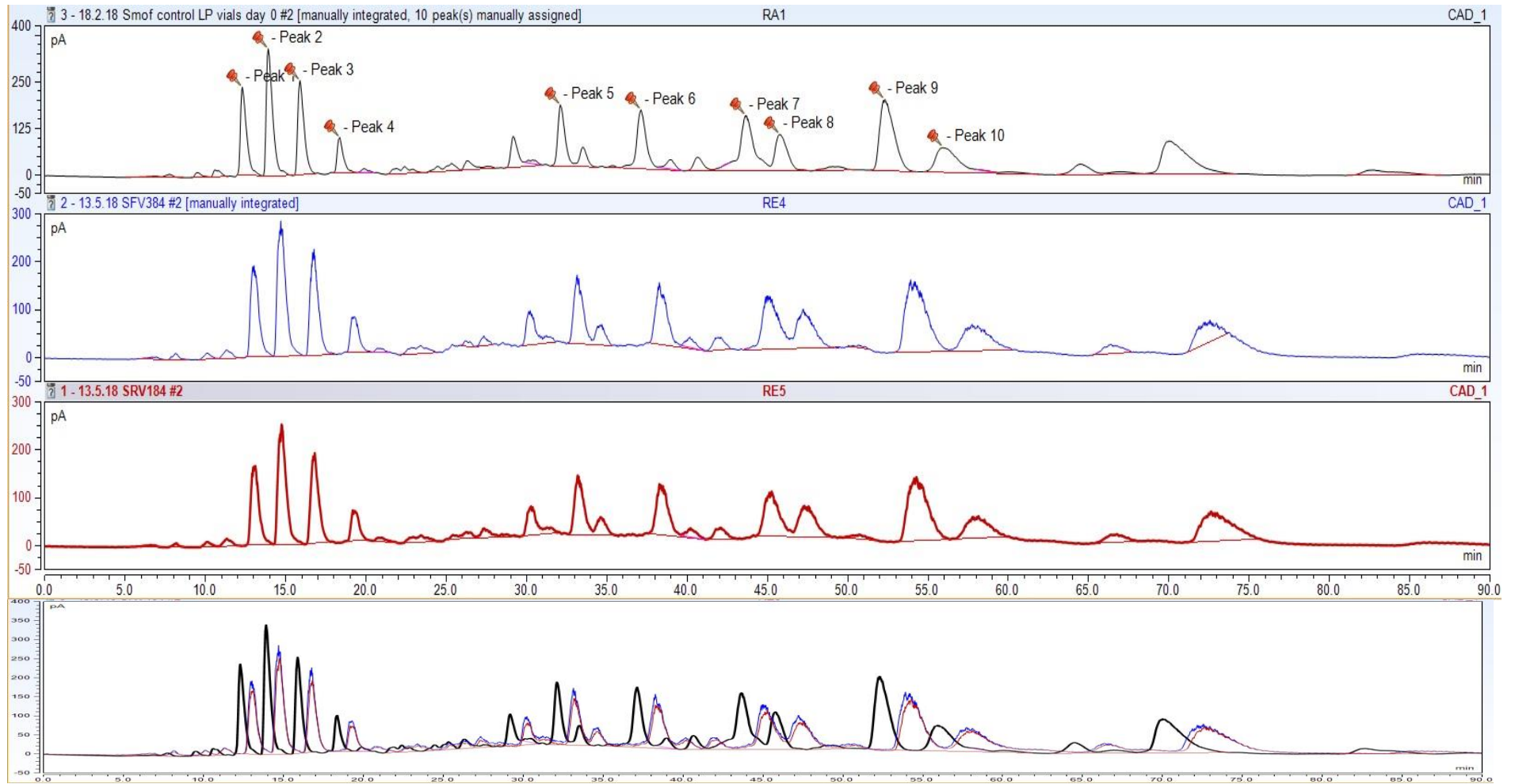
Figure 5.44 HPLC-CAD chromatograms of SMOFlipid® 20% stored in 50 ml glass vials. Day 0 control (black), day 84 fridge temperature chromatogram (blue trace) and day 84 room temperature (red trace). Overlaid chromatogram with signal time offset shows changes in peaks in comparison to control.
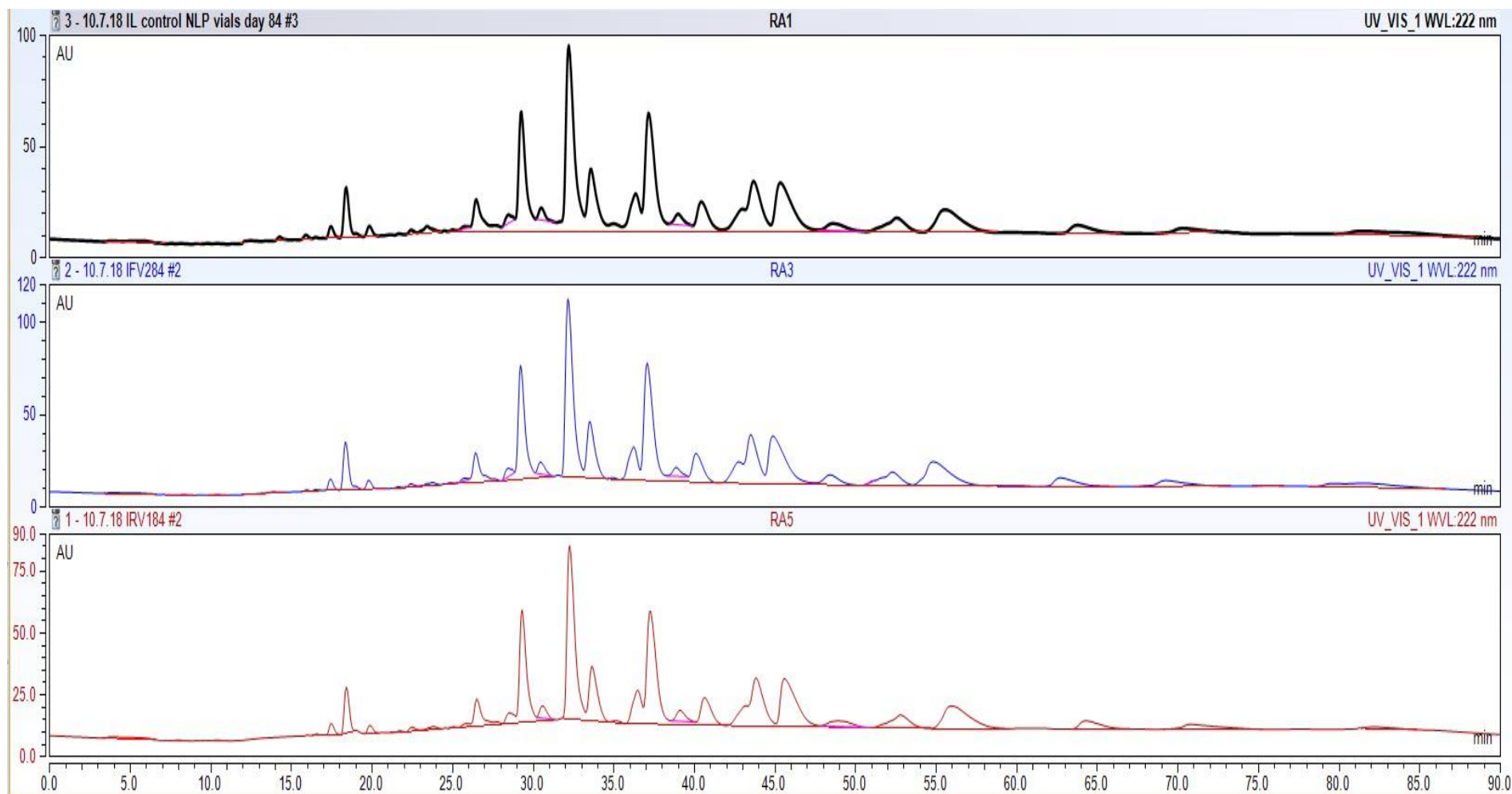
244
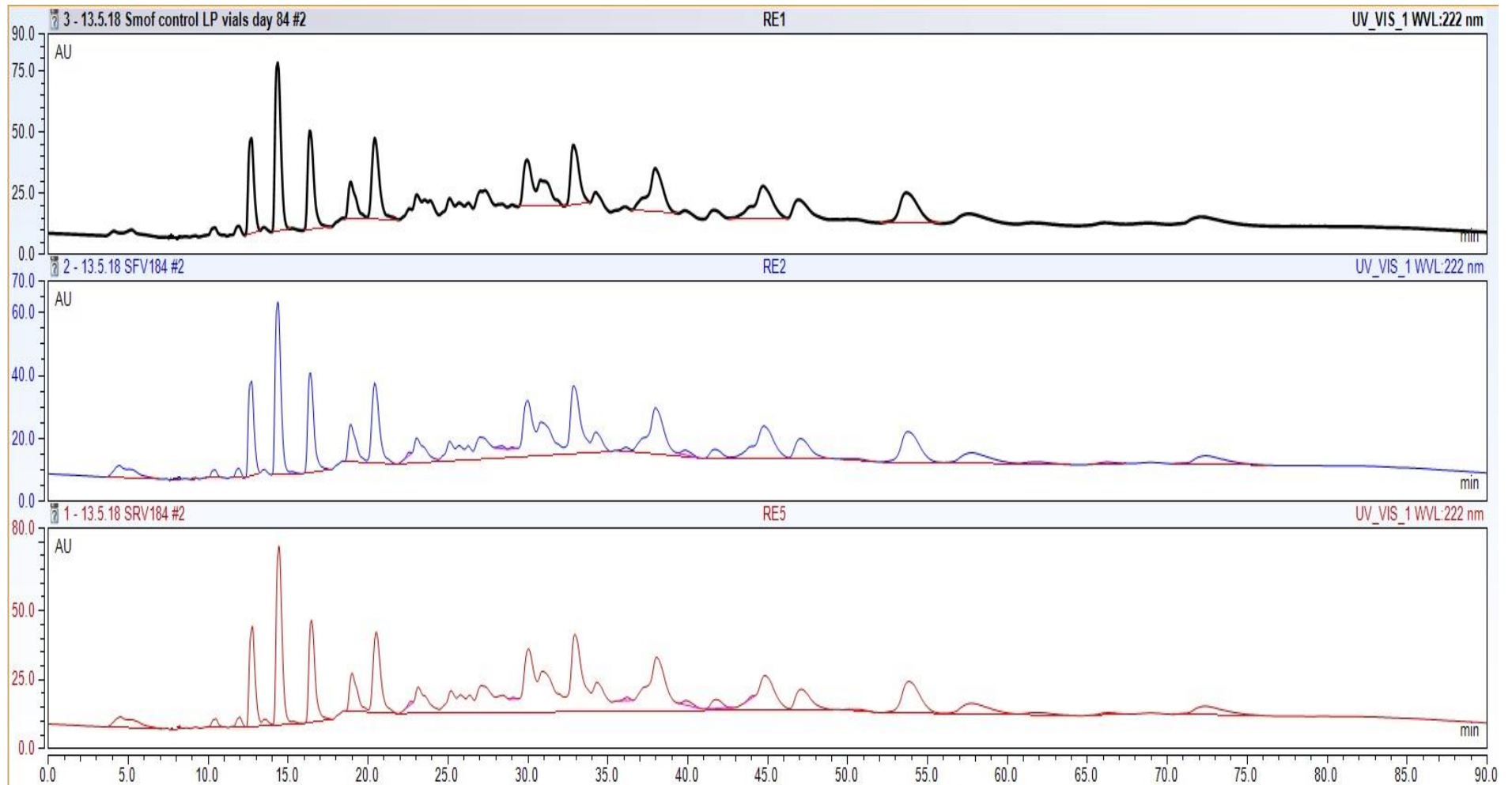
Figure 5.45 HPLC-UV chromatograms of SMOFlipid® 20% stored in 50 ml glass vials. Day 0 chromatogram (black trace), day 84 fridge temperature syringes (blue trace) and day 84 room temperature syringes (red trace). The lack of production of new peaks indicates a lack of degradation products.
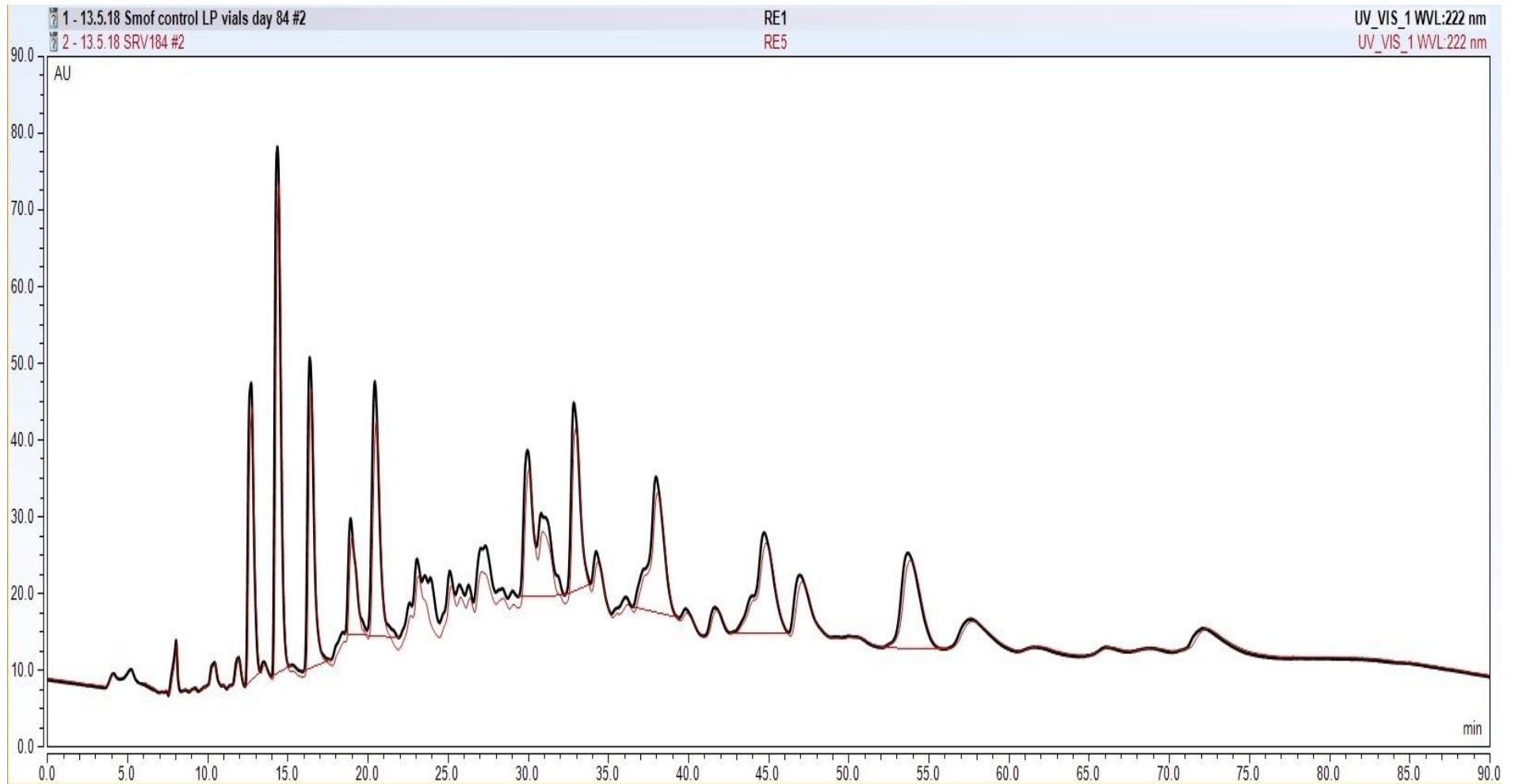
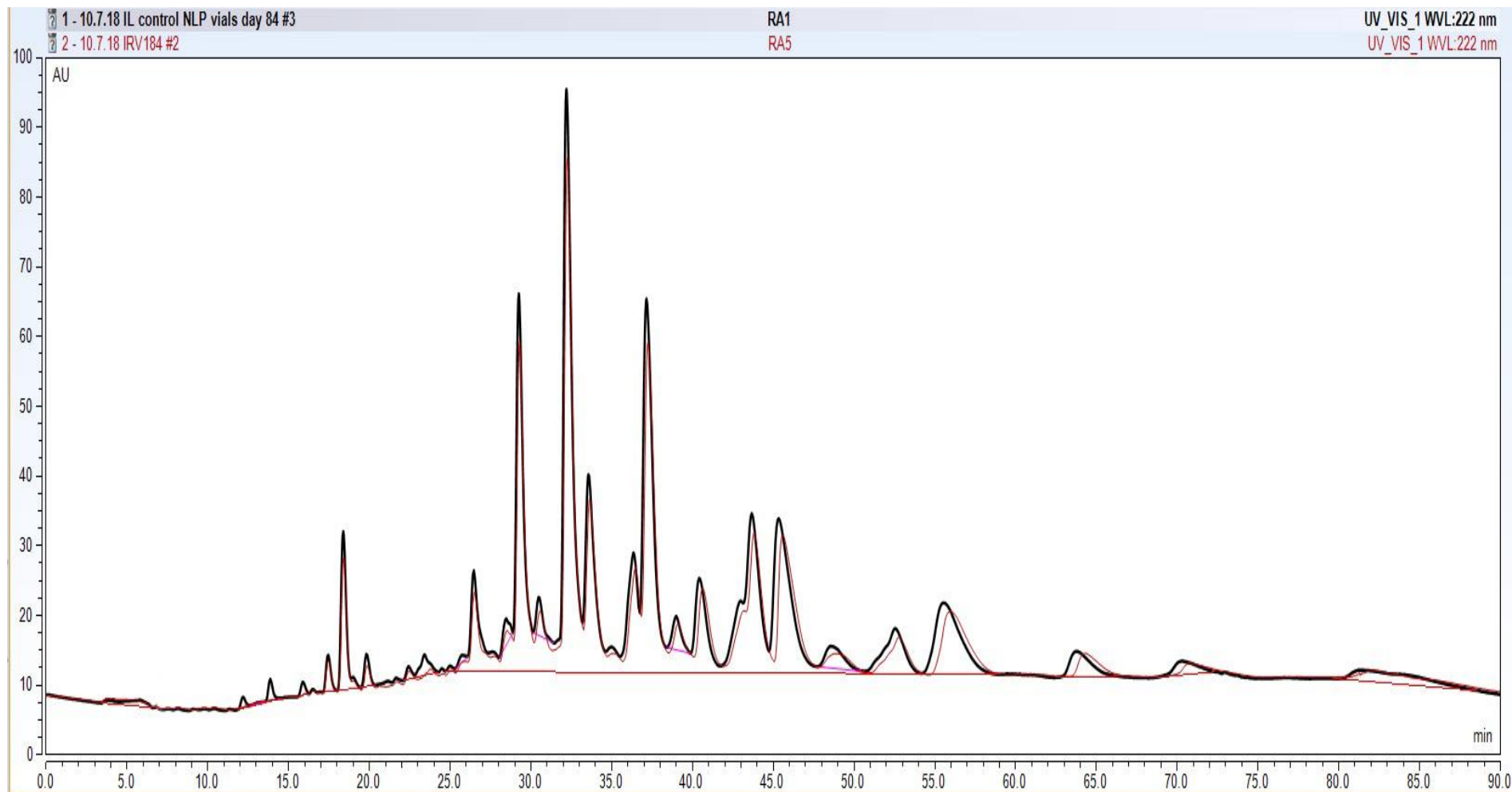*Figure 5.46 Overlaid HPLC-UV chromatograms. Day 0 (back trace) and day 84 room temperature (red trace) SMOFlipid® stored in 50 ml glass vials. The presence of no new peaks indicates a lack of degradation/peroxidation products seen at 222 nm wavelength.*

246

5.7. Discussion of SMOFlipid® light protected results

5.7.1. Triglyceride loss

TAG losses occurred in all containers at fridge and room temperatures over 84 days of storage. Table 5.3 shows the statistical significance in the differences between containers and temperatures. All data was analysed by ANOVA using SPSS (IBM version 25) with Tukey post-hoc analysis (appendix 3 shows data). Statistical significance was achieved with a $P<0.05$. Room temperature PN bags showed the greatest level of TAG loss for all peaks at day 56. Temperature had a significant effect on PN bag results but little effect on syringes or glass vials. Figure 5.49 shows the level of TAG losses seen for all containers at both temperatures at 56 days. Day 84 data is excluded from the comparison between containers as PN bag data showed high control RSD's on day 84.

PN bags showed maximal losses of >40 % at room temperature with fridge temperature reducing the level of TAG loss observed. During the formulation of PN bags lipid is removed from its original container (flexible infusion bag) using a 50 ml BD Plastipak syringe and needle. The lipid is then injected into the 250 ml PN bag and as much air as possible removed. During this production process, the act of pulling lipid into a syringe could introduce air and therefore oxygen into the lipid in the form of dissolved oxygen that cannot be removed. Once in the PN bag, whilst all possible air is removed, small amounts remain. In clinical practise an amount less than the area of a 50 pence piece is deemed acceptable upon formulation. The oxygen present in the PN bags tested could initiate the peroxidation process, accounting for the large TAG losses observed. Fridge temperature storage will inhibit the peroxidation process occurring as temperature acts to reduce the number of collisions occurring between molecules, thus physically reducing the ability of lipid radicals to interact with another lipid molecule and propagate the peroxidation cycle (Steger and Mühlebach 1997; Seppanen and Saari Csallany 2002). When considering each TAG monitored, PN bags showed greatest losses in peaks 5,8,9 and 10, TAGs containing polyunsaturated and monounsaturated fatty acids prone to peroxidation. There were however significant losses in peaks 1 to 4 which is of note as these peaks contain only saturated fatty acids, discussed further in section 5.7.2.

When considering the syringe results, TAG losses were greatest in peaks 5 to 10 (<20 %) at day 56, with minimal losses in TAGs 1 to 4. This is suggestive of

peroxidation, as expected, occurring primarily in polyunsaturated and monounsaturated fatty acids. No significant difference was shown between fridge and room temperatures. Both the rate and extent of peroxidation was significantly lower in all syringes than PN bags. Figure 5.47 shows the day 7 data for all containers and allows a comparison into the rate of peroxidation. Syringes when formulated have all visible air removed and at each testing time point all air again is expelled before storage. This minimises oxygen presence, though as discussed in chapter 4.7.1.1, oxygen can leech into syringes bypassing the rubber seals on the plunger and barrel over time. This is reflected when looking at the figures shown in section 5.4 for each TAG where the greatest losses occur over the last 28 days of storage, indicating the initiation of peroxidation as oxygen becomes present in the system.

As predicted, all glass vials showed little (<10 %) losses during the first 28 days of storage with exception of peak 1 at room temperature where oxygen is minimised within the system due to the presence of nitrogen. However, as the data at day 56 shows (figure 5.49) TAG losses increased after day 28 up to 30 %. All peaks 1 to 10 suffered similar amounts of loss over 56 days. The loss of TAGs from day 28 onwards suggests ingress of oxygen into the system and the initiation of peroxidation. Whilst every effort was made to prevent the presence of oxygen, the repetitive piercing of the rubber vial septum could have weakened the seal to the point where oxygen could leech into the system. To try and prevent this in future testing at every testing point a different section of the rubber bung was pierced to try and prevent a weak area occurring. It is again worth noting that TAG losses were recorded in peaks 1 to 4, TAGs made of saturated fatty acids which should not be susceptible to peroxidation however the TAG losses suggest the breakdown of these TAGs (discussed further in section 5.7.2).
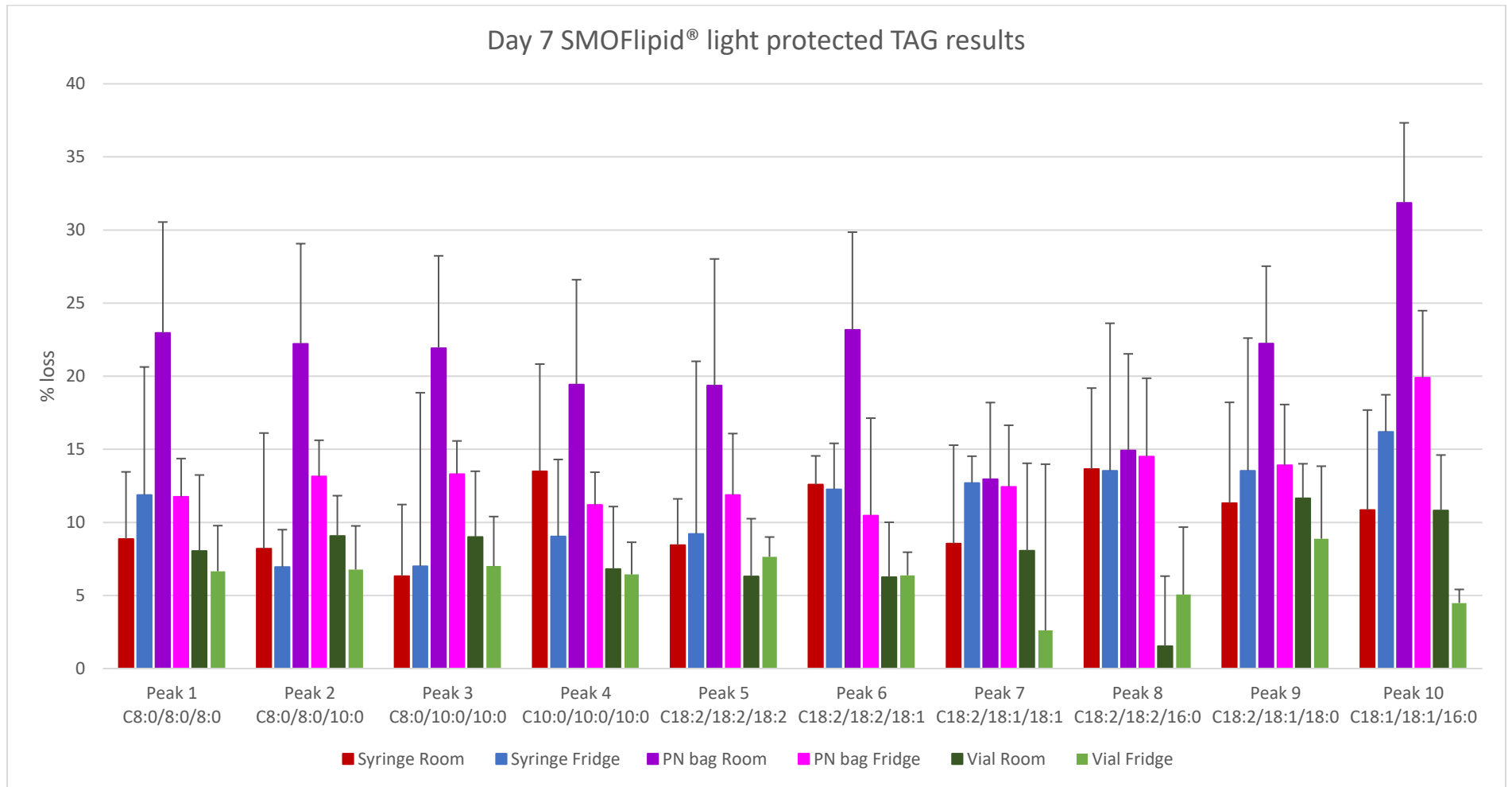
Figure 5.47 Triglyceride loss at 7 days storage for SMOFlipid® stored in syringes, PN bags and glass vials.
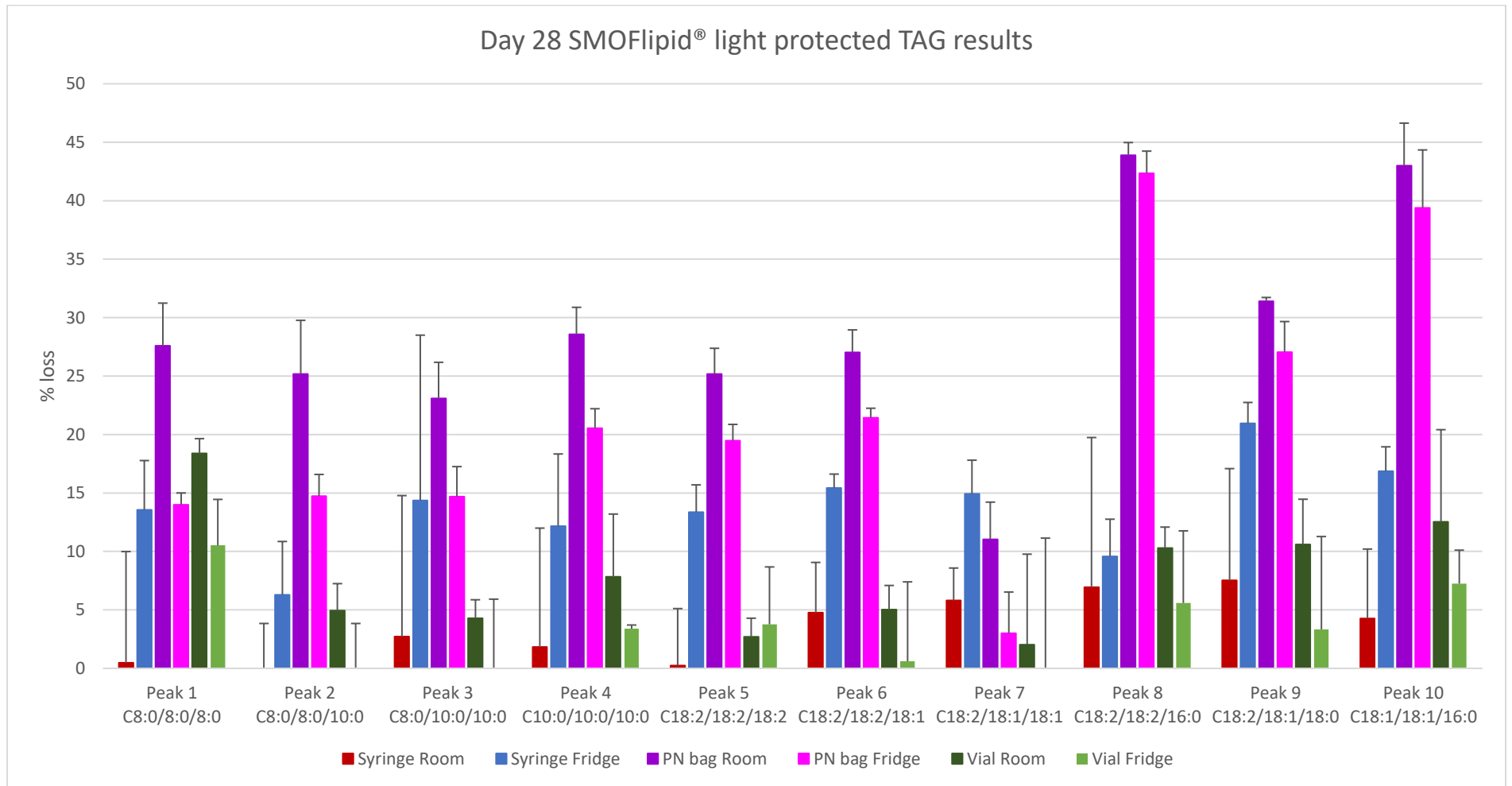
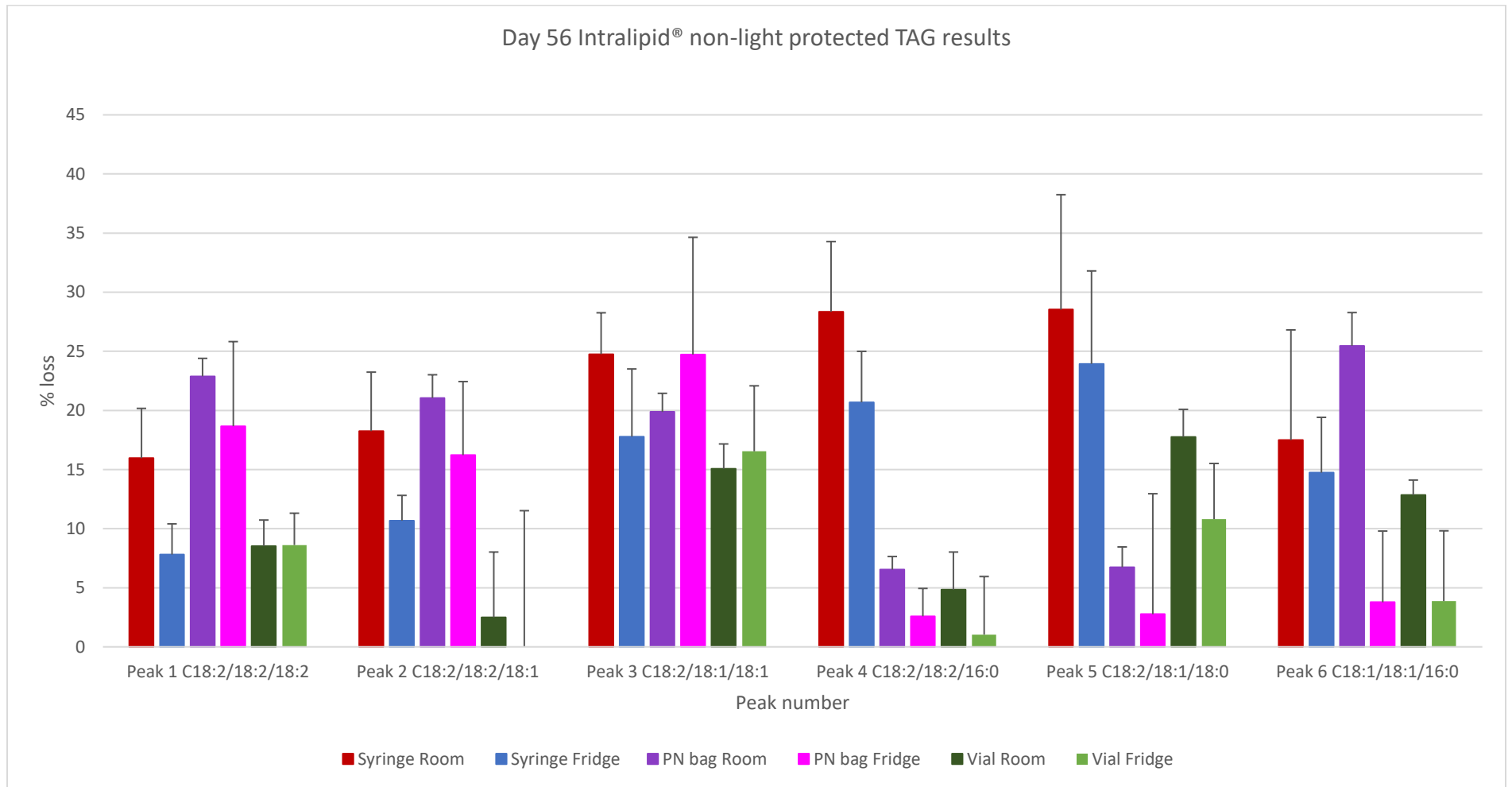*Figure 5.48 Triglyceride loss at 28 days storage for SMOFlipid® stored in syringes, PN bags and glass vials.*
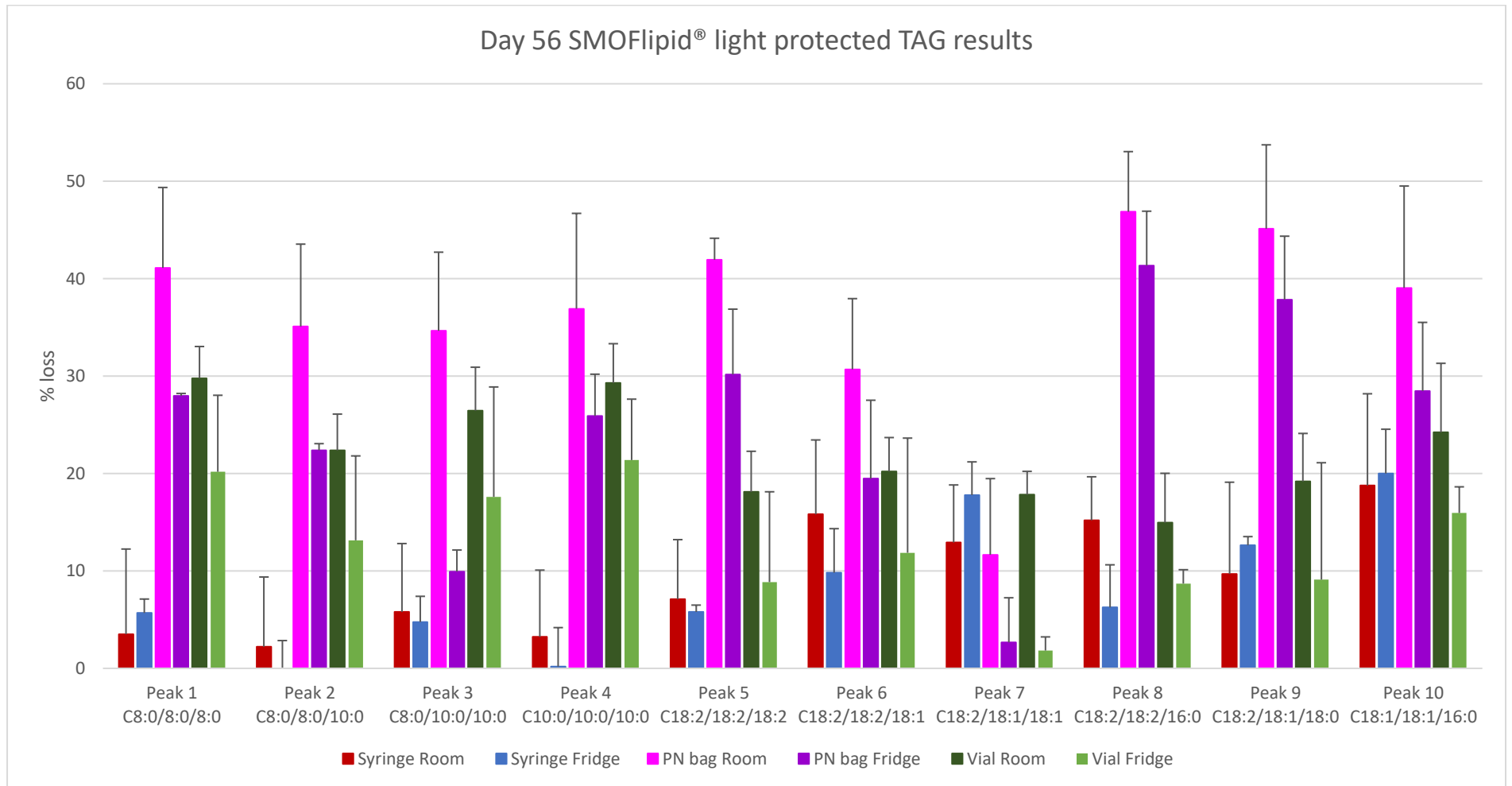
Figure 5.49 Triglyceride loss at 56 days storage for SMOFlipid® stored in syringes, PN bags and glass vials.

Table 5.3 Light protected SMOFlipid® in all containers at all temperatures for each of the ten peaks monitored. * indicates significant differences between results as calculated through ANOVA analysis with post hock Tukey analysis between each container type. (significant defined as P<0.05).

Peak 1	Room syringe	Room Bag	Room Vial	Fridge Syringe	Fridge Bag	Fridge Vial
Room Syringe		*			*	
Room Bag	*				*	*
Room Vial						
Fridge Syringe						
Fridge Bag		*				
Fridge Vial		*				

Peak 5	Room syringe	Room Bag	Room Vial	Fridge Syringe	Fridge Bag	Fridge Vial
Room Syringe			*			
Room Bag						*
Room Vial	*					
Fridge Syringe						
Fridge Bag						*
Fridge Vial		*				

Peak 2	Room syringe	Room Bag	Room Vial	Fridge Syringe	Fridge Bag	Fridge Vial
Room Syringe		*				
Room Bag	*			*		*
Room Vial						
Fridge Syringe		*			*	
Fridge Bag				*		
Fridge Vial		*				

Peak 6	Room syringe	Room Bag	Room Vial	Fridge Syringe	Fridge Bag	Fridge Vial
Room Syringe					*	
Room Bag					*	
Room Vial					*	*
Fridge Syringe					*	
Fridge Bag	*	*	*	*		
Fridge Vial			*			

Peak 9	Room syringe	Room Bag	Room Vial	Fridge Syringe	Fridge Bag	Fridge Vial
Room Syringe		*			*	*
Room Bag	*		*	*	*	*
Room Vial		*				*
Fridge Syringe		*				*
Fridge Bag	*					*
Fridge Vial	*	*	*	*	*	

Peak 3	Room syringe	Room Bag	Room Vial	Fridge Syringe	Fridge Bag	Fridge Vial
Room Syringe						
Room Bag						
Room Vial						
Fridge Syringe						
Fridge Bag						
Fridge Vial						

Peak 7	Room syringe	Room Bag	Room Vial	Fridge Syringe	Fridge Bag	Fridge Vial
Room Syringe			*			
Room Bag			*			
Room Vial	*	*			*	
Fridge Syringe			*			
Fridge Bag						
Fridge Vial						

Peak 10	Room syringe	Room Bag	Room Vial	Fridge Syringe	Fridge Bag	Fridge Vial
Room Syringe		*	*			
Room Bag	*				*	*
Room Vial	*				*	*
Fridge Syringe		*	*			
Fridge Bag						*
Fridge Vial		*	*		*	

Peak 4	Room syringe	Room Bag	Room Vial	Fridge Syringe	Fridge Bag	Fridge Vial
Room Syringe		*				
Room Bag	*		*	*		*
Room Vial		*				*
Fridge Syringe		*				
Fridge Bag						*
Fridge Vial		*	*		*	

Peak 8	Room syringe	Room Bag	Room Vial	Fridge Syringe	Fridge Bag	Fridge Vial
Room Syringe		*			*	*
Room Bag	*		*			*
Room Vial		*			*	*
Fridge Syringe		*				
Fridge Bag	*		*	*		*
Fridge Vial	*	*	*		*	

5.7.2. Saturated TAG losses

As figure 5.49 shows apart from SMOFlipid® stored in 50 ml syringes, PN bags and to a lesser extent glass vials showed significant losses in peaks 1 to 4 over 56 days of storage at all temperatures. As shown in chapter 2 through mass spectrometry peaks 1 to 4 were identified as TAGs with saturated fatty acids. Each TAG (1 to 4) is formed from medium chain (8 to 10 carbons) caprylic and capric fatty acids chemically synthesised from coconut oil. As discussed in section 5.2 these saturated TAGs were chosen to be monitored due to their expected lack of susceptibility to peroxidation and therefore loss. Therefore, the results showing a drop in these TAGs are not predicted. To ensure the results were precise, as for all testing control samples of SMOFlipid® in its original container was tested at all time points. As discussed through the results in this chapter all RSDs were monitored and found to be within acceptable limits (<12). As such the results obtained were deemed reliable and therefore the loss of saturated TAGs indicates that processes other than peroxidation of unsaturated lipids may have occurred. When considering the overall levels of TAG losses occurring the loss in saturated TAGs only occurs when overall TAG losses are high. From this it can be postulated that saturated TAG loss only appears when high levels of peroxidation is present.

Considering other research, little work can be found on the potential breakdown of saturated TAGs within emulsions. Endres and Kummerow's (1962) research showed the breakdown of saturated TAGs occurring with thermal oxidation at high temperatures through hydrolysis of the ester linkage between the fatty acid and the glycerol backbone. Applying this breakdown process to the saturated TAGs in SMOFlipid® the expected results would show a loss of each TAG peak (1 to 4) as fatty acids were cleaved from each TAG resulting in free fatty acids, mono and diacylglycerides. Whilst SMOFlipid® testing was not carried out under high temperatures (room and fridge only), the saturated TAG losses occurred only in lipids where excess peroxidation was seen and as such in lipids where high levels of reactive oxygen species, lipid radicals and highly reactive lipid hydroperoxides will be present. The presence of water and oxygen within these emulsions also would theoretically permit hydrolysis to occur. The CAD detector used would be unable to detect the free fatty acids formed due to their relative volatility. As the assay is monitoring only the 10 TAGs identified, the breakdown of these saturated TAGs into mono and diacylglycerides would be indicated by peak loss as seen. Whilst this process acts as a hypothesis for the saturated TAG losses seen, further

work beyond the scope of this thesis could confirm the processes occurring. The lipid could be subjected to HPLC-UV designed to specifically look for the free fatty acids present from the TAG breakdown, or mass spectrometry could be employed to identify the fatty acid methyl esters, mono and diacylglycerides formed.

5.7.3. HNE, HUE and TAG remnant production

Contrary to TAG losses which were greatest in PN bags, the only recorded occurrences of HNE and HUE were found in syringes. Whilst the level of HNE recorded was under the level of quantitation (LOQ), significant HUE was seen in room temperature syringes at day 14 onwards and in fridge temperature syringes from day 56. Considering HUE production, looking at the TAG losses in PN bags at day 56 all peaks monitored showed significant losses except for peak 7 (C18:2/18:1/18:1) which showed minimal (~ 10 % room and <5 % fridge) loss. As discussed in chapter 3 (section 3.8.3) figure 5.50 shows the potential pathway for the production of HUE from the peak 7 triglyceride. The lack of HUE seen in PN bags would be predicted if the lack of loss of peak 7 was used as a predictor for its formation. This pathway of HUE production is supported when considering the production of HUE in room temperature syringes. Figure 5.49 shows the 56-day results for all peaks. The greatest TAG losses observed for syringes were seen for peaks 6,7 and 10 corresponding to TAGs C18:2/18:2/18:1, C18:2/18:1/18:1 and C18:2/18:1/16:0). It would be expected that both HUE and HNE would be formed from the peroxidation of these TAGs, only HUE is shown in the data (HNE present but below LOQ). The results do however substantiate the production of HUE from TAGs containing oleic acid (C18:1).

TAG remnant production was observed in syringes from day 28 onwards and in PN bags from day 14 onwards at room temperatures only. The proposed schematic for the production of the TAG remnant from peak 7 is suggested in chapter 3 and summarised again below in figure 5.50.

C18:1/18:1/18:2 (OLEIC/OLEIC/LINOLEIC)

+H$_2$O

13' HYDROPEROXIDE

OLEIC RADICALS +OH$^\cdot$

HUE

HUE

HNE

Triglyceride 'remnant'
m/z: 495.35
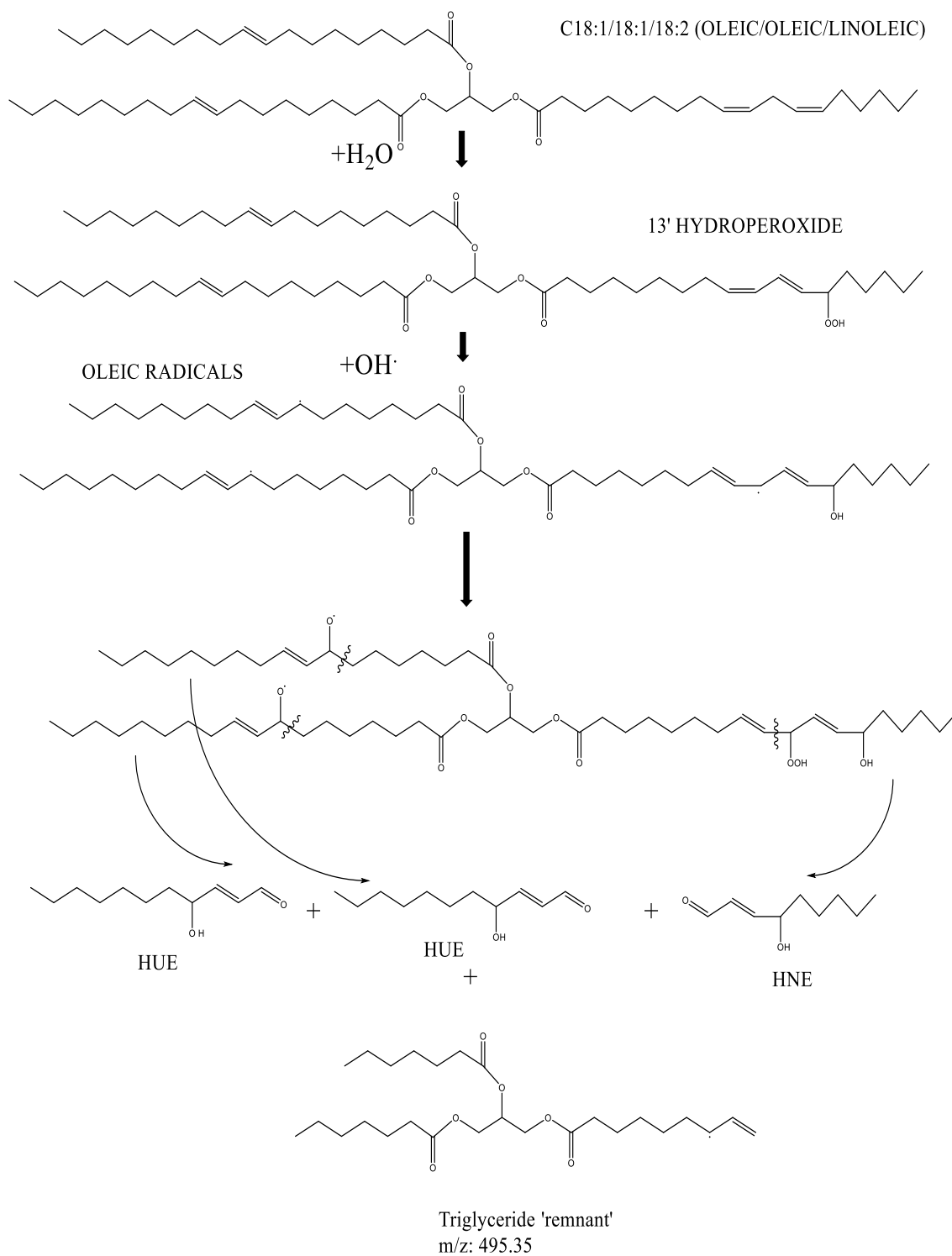
Figure 5.50 As shown in chapter 3 schematic of the potential chemical breakdown of peak 7 TAG with the production of HUE and HNE.

255

TAG remnant production is temperature dependant as shown by the data recorded. Both syringes and bags as discussed above have HUE present at day 56 but not HNE. This questions the validity of the schematic shown in figure 5.50 due to the lack of HNE from the proposed pathway of peroxidation. One possible explanation however is the peroxidation of the linoleic acid is occurring at either the other double bond or at the same bond as the schematic indicates but at the other end, leading to a different positional isomer being creating. This would create a different positional hydroperoxide as a primary product and ultimately a secondary peroxidation product, potentially not visualised through the UV chromatogram at the wavelength of 222 nm. Figure 5.51 Shows the potential peroxidation of linoleic acid, the positional isomers and products created. Of interest within this schematic is the production of a possible 11-hydroperoxide only found in peroxidation in the presence of an antioxidant. SMOFlipid® unlike Intralipid® contains tocopherols with the ambition to quench free radicals and inhibit peroxidation. Its effectiveness however is questioned as discussed in section 5.2.1. Schneider's (2009) work that shows the occurrence of an 11-hydroperoxide in the presence of tocopherols provides a potential pathway where other peroxidation products (not HNE/HUE) would be formed and subsequently not identified through this assay.
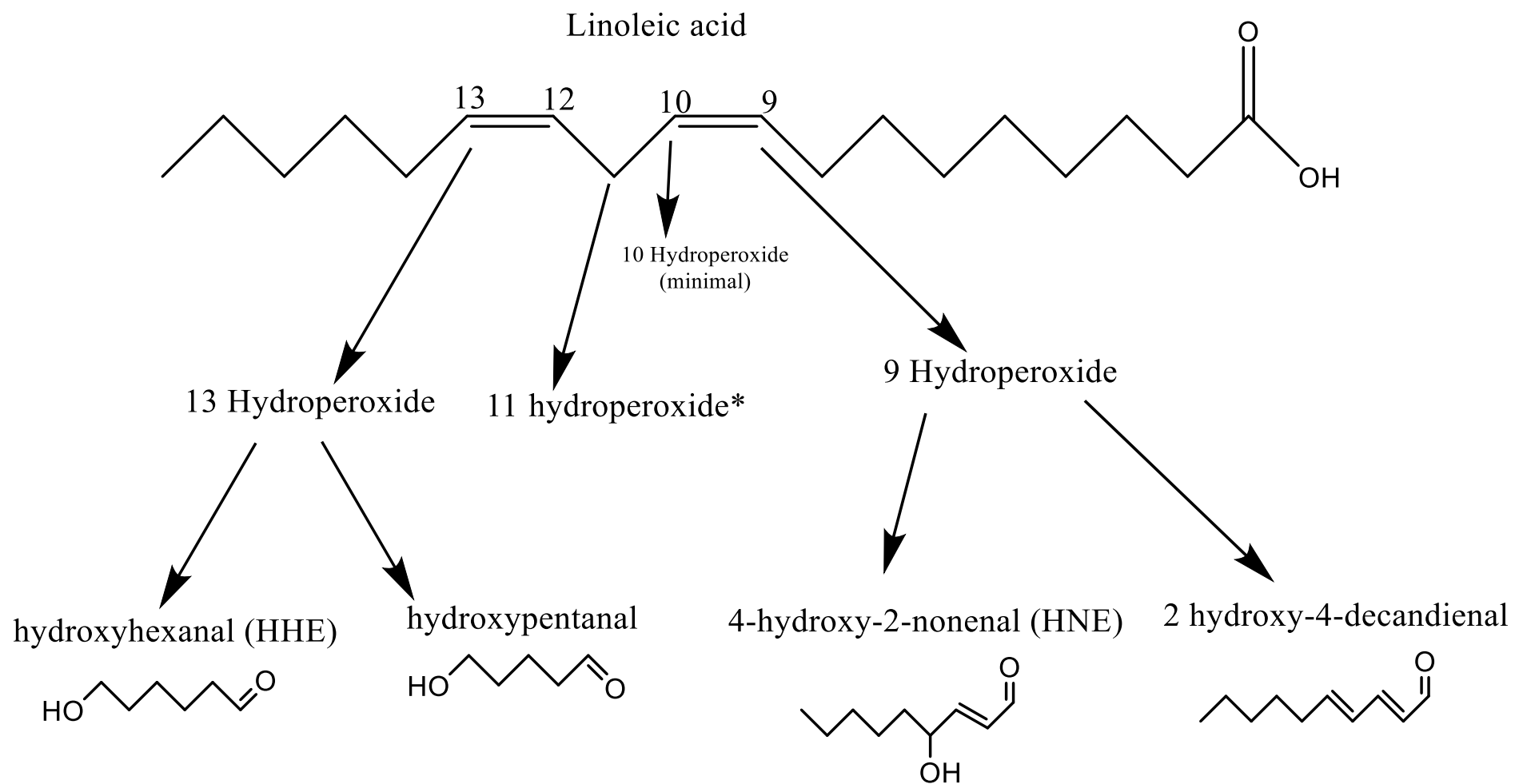
Figure 5.51 Potential products of Linoleic acid peroxidation. *bis-allylic 11-Hydroperoxide, formed only in the presence of an antioxidant such as vitamin E (tocopherols) (Schneider 2009).

SMOFlipid® Non-light Protected Syringes, Bags and Vials

6.1. Introduction to non-light protected SMOFlipid® testing

As discussed for Intralipid® non-light protected testing in chapter 4 (section 4.1), light induced peroxidation (photo-oxidation) is an alternative pathway for lipid radical formation and breakdown to occur. This chapter of testing subjects SMOFlipid® to controlled light exposure with the aim to provide an insight into the importance of light protection of PN. Light radical formation is discussed in section 4.1.1.

6.2. Light control

To enable a comparative set of data to be established an identical testing protocol to all previous chapters was employed. In summary, 50 ml syringes, 250ml ML PN bags and 50 ml glass vials (vials filled with nitrogen) were filled with 50 ml SMOFlipid® and all possible air removed. Fridge temperature samples were held in a refrigerator and as such light exposure was limited. Room temperature containers were exposed to controlled light through storage in a stability chamber as discussed in section 4.2.1. Light intensity was set as 5/10 as per the manufacturer's recommendations providing a mimic for natural light (Weiss Gallenkamp, 2006). Humidity was controlled to 60 % and temperature to 22°C, reflecting light protected room temperature storage.

6.3. Testing schedule

As all previous chapters 6 samples of each container were formulated, 3 refrigerated and 3 stored at room temperature, all exposed to light as discussed above. 1 ml of lipid was removed at each timepoint and placed into amber HPLC vials for testing. All possible air was removed from each container at each timepoint and nitrogen replaced in glass vials as per protocol in section 3.8. Samples were tested at days 0, 1, 2, 7, 14, 28, 56 and 84. All samples were subjected to the HPLC method as described in chapter 2. A control sample of SMOFlipid® in its original packaging was tested at all timepoints, its RSD monitored for method precision. Between each sample a blank of 30 minutes was run as described in chapter 2 to ensure column cleaning and effective re-equilibration. For each of the 10 peaks monitored for SMOFlipid® TAG loss was recorded as peak area and presented as a

% loss from day 0. The production of secondary peroxidation products HNE, HUE and the TAG remnant were monitored through UV detection and presented as peak area. All chromatograms were integrated using Chromeleon software (Thermo Scientific) and all samples tested in triplicate. Standard deviations and RSD's were calculated for all results.

6.4. SMOFlipid® non-light protected syringe results.

Figures 6.1 to 6.10 show the TAG loss results for non-light protected syringes through 84 days. However, the RSD's of the control samples for peaks 1, 2, 3, 4, 5, 9 and 10 at days 56 and 84 fell out of the acceptable range of <12. As shown on each of the peaks graphs, presented as % TAG loss from day 0, day 56 and 84 results are marked in orange to indicate the high RSD's. Maximal peak loss at 84 days was observed for peak 9 at room temperature of 50 %. However, when considering only up to the day 28 results due to the RSD drift in control samples (discussed in section 6.7.2), minimal TAG loss was seen across all peaks with peak 10 at room temperature showing the highest level of ~12 %. As shown in the figures for the syringe results, the majority of TAG losses visualised occurred during later storage times (56 to 84 days). The high RSD's of the control samples at these timepoints do however make the results questionable and are discussed further in section 6.7. The peak areas recorded for the control samples were ~ 50 % greater than all other control readings. As an approximation if adjusted for this within the day 84 results of the affected peaks, maximal TAG loss would be estimated to be around 25 %. Temperature had little effect on early storage, however at 84 days (when considering adjusted values) there was a statistically significant (ANOVA one-way with Tukey post-hoc) difference in room and fridge temperature recordings for peaks 1 to 5, 9 and 10 as summarised in table 6.1 (section 6.7) with room temperature syringes showing greater % TAG losses.

Figure 6.11 shows the production of minimal levels of HNE detected through the UV assay. The maximum peak area observed was 4.423 (AU) for room temperature syringes and 3.584 for fridge temperature samples. Using the calibration equation from the validation of HNE (y = 0.2476x + 1.0452) the recorded areas equate to 13.642 µM and 10.253 µM of HNE which is above the limit of quantification (LOQ) for the assay. The results are however significant in terms of concentrations at day 84. Levels of HNE recorded are only quantifiable from day 14 onwards when they

exceed the LOQ for the assay. As shown temperature effects the production of HNE but both temperatures tested produced quantifiable levels over 84 days.

When considering the production of the other peroxidation products identified in chapter 3 and monitored, HUE was observed in SMOFlipid® non-light protected syringes at room temperature from day 14 onwards and in fridge temperature syringes from day 56 as shown in figure 6.12 The amounts observed cannot be quantified as discussed in previous chapters due to the lack of validation of the assay for HUE detection. The differences in peak areas observed between containers and lipids is however comparable and discussed in chapter 7.

Figure 6.13 shows the production of the TAG remnant peroxidation product monitored through UV detection. This peak was present in room temperature syringes only from day 14 onwards. Again, whilst not quantifiable due to a lack of a standard for validation, the comparison between lipids and containers can be undertaken and is discussed in chapter 7. The production of this TAG remnant between non-light protected containers of SMOFlipid® is compared in section 6.7.
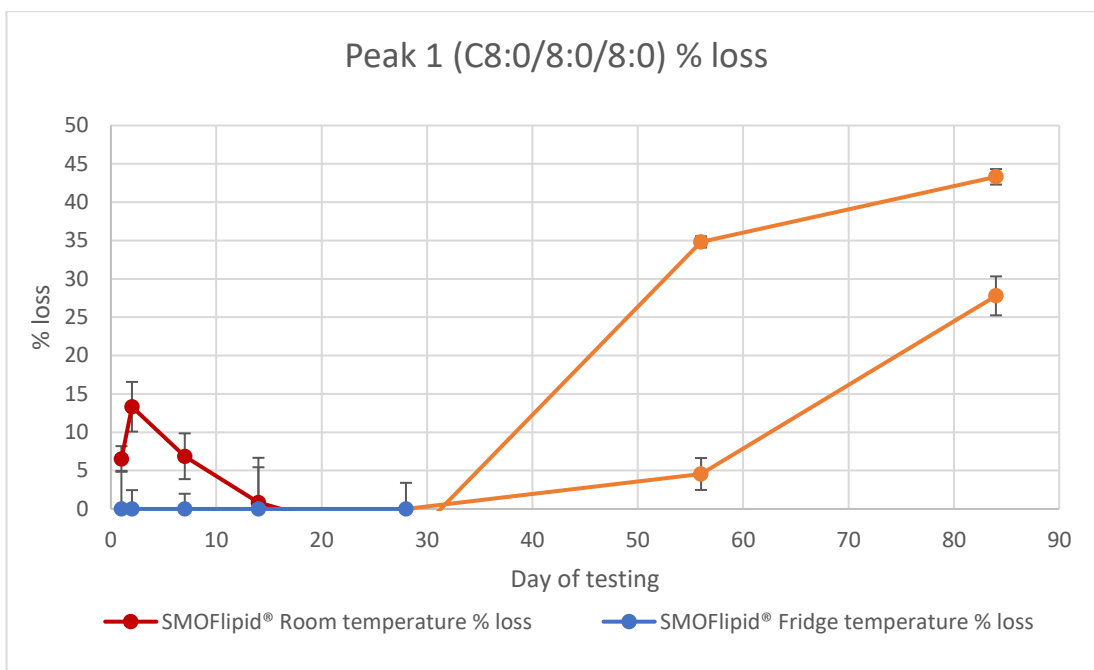
Figure 6.1 HPLC-CAD results for peak 1 (C8:0/8:0/8:0) triglyceride of SMOFlipid® 20 % stored in non-light protected 50 ml syringes. Percentage loss of peak shown calculated from day 0 data. Room (Red) and Fridge (Blue) results shown with standard deviation error bars on all points. Orange points indicate readings where RSD of control samples exceeded acceptable levels.
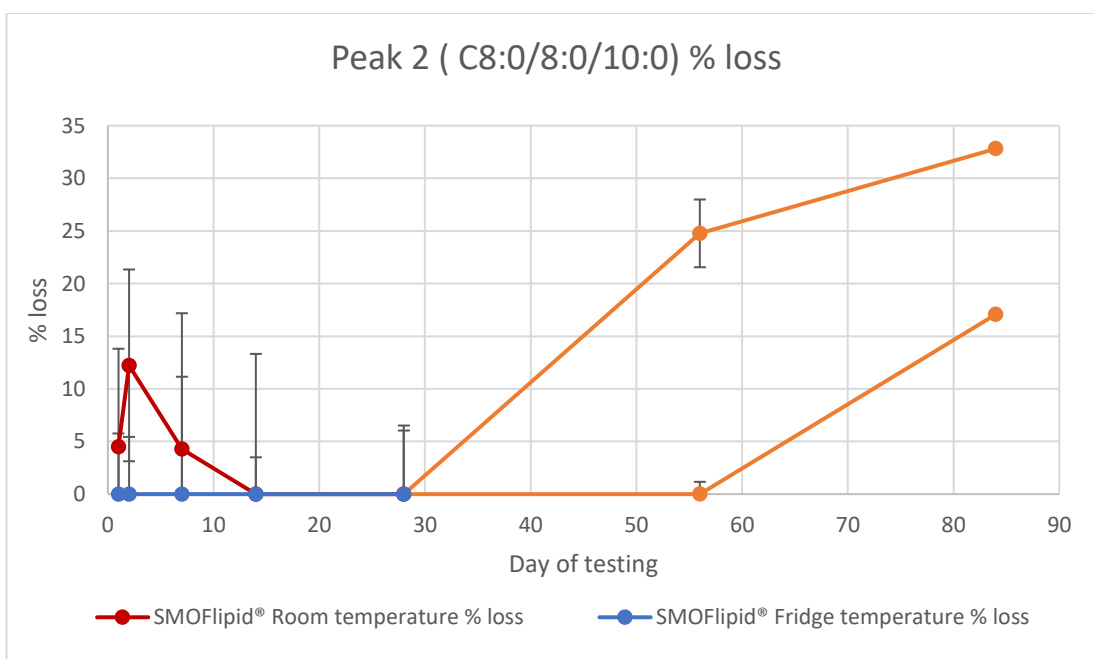
Figure 6.2 HPLC-CAD results for peak 2 (C8:0/8:0/10:0) triglyceride of SMOFlipid® 20 % stored in non-light protected 50 ml syringes. Percentage loss of peak shown calculated from day 0 data. Room (Red) and Fridge (Blue) results shown with standard deviation error bars on all points. Orange points indicate readings where RSD of control samples exceeded acceptable levels.

262
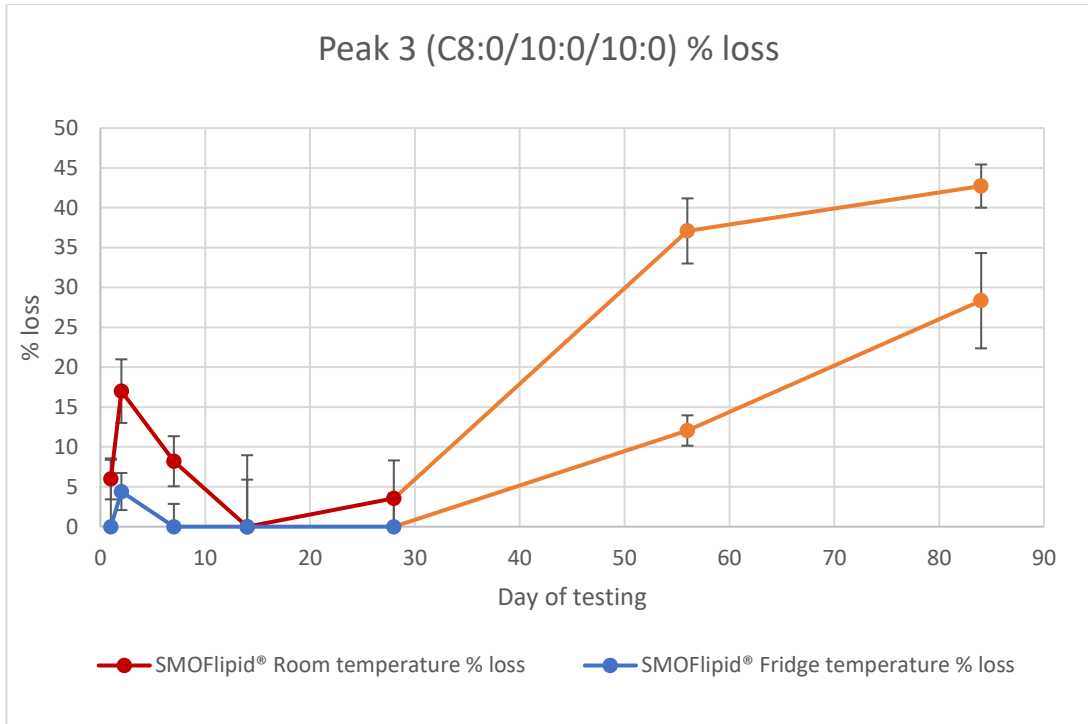
Figure 6.3 HPLC-CAD results for peak 3 (C8:0/10:0/10:0) triglyceride of SMOFlipid® 20 % stored in non-light protected 50 ml syringes. Percentage loss of peak shown calculated from day 0 data. Room (Red) and Fridge (Blue) results shown with standard deviation error bars on all points. Orange points indicate readings where RSD of control samples exceeded acceptable levels.
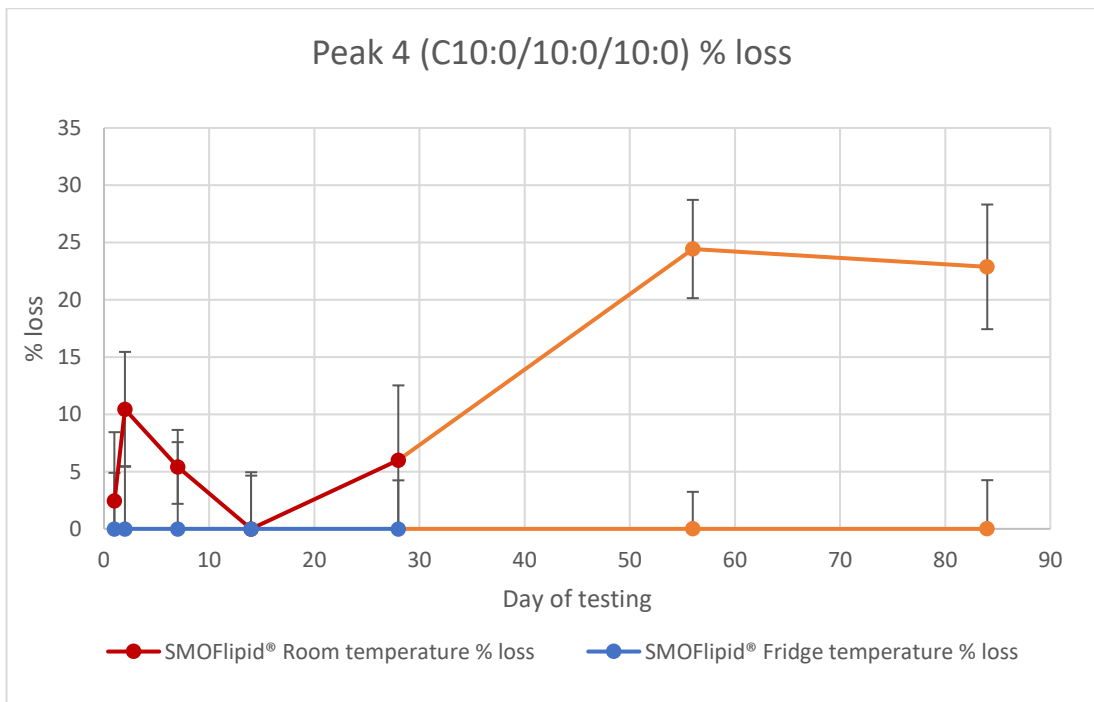
Figure 6.4 HPLC-CAD results for peak 4 (C10:0/10:0/10:0) triglyceride of SMOFlipid® 20 % stored in non-light protected 50 ml syringes. Percentage loss of peak shown calculated from day 0 data. Room (Red) and Fridge (Blue) results shown with standard deviation error bars on all points. Orange points indicate readings where RSD of control samples exceeded acceptable levels.

263
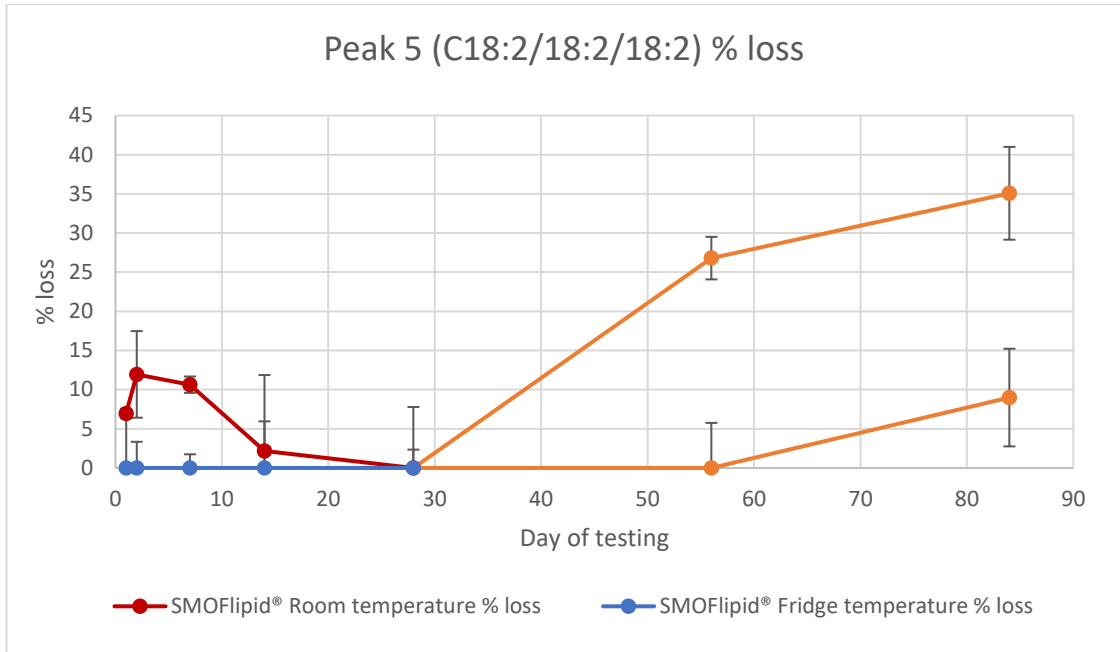
Figure 6.5 HPLC-CAD results for peak 5 (C18:2/18:2/18:2) triglyceride of SMOFlipid® 20 % stored in non-light protected 50 ml syringes. Percentage loss of peak shown calculated from day 0 data. Room (Red) and Fridge (Blue) results shown with standard deviation error bars on all points. Orange points indicate readings where RSD of control samples exceeded acceptable levels.
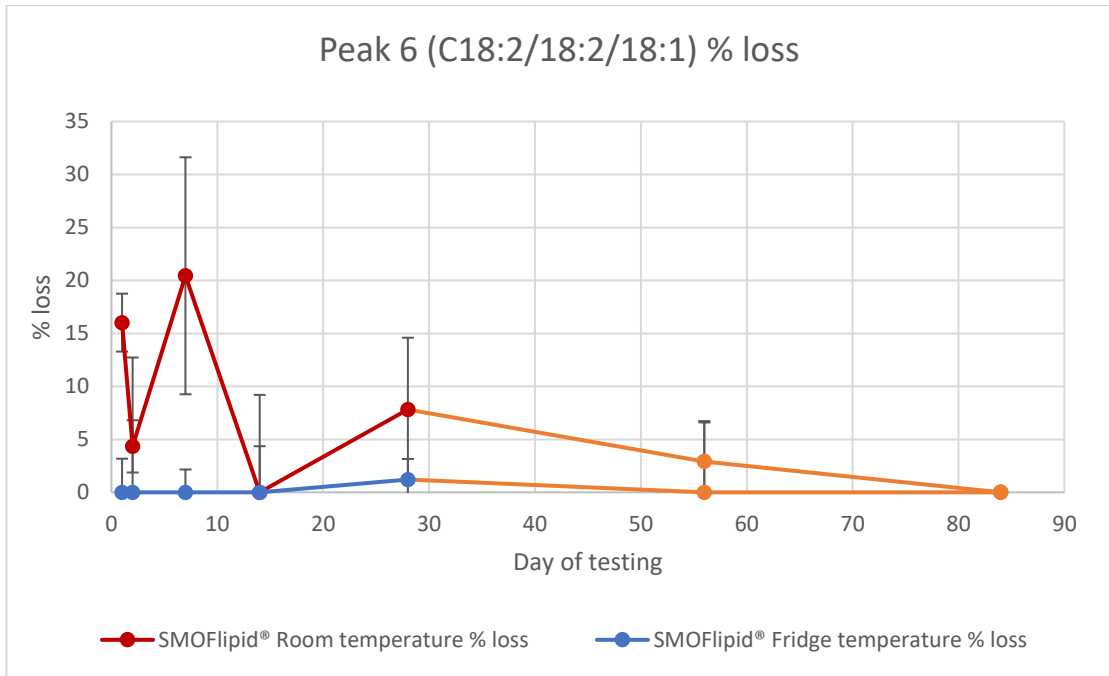
Figure 6.6 HPLC-CAD results for peak 6 (C18:2/18:2/18:1) triglyceride of SMOFlipid® 20 % stored in non-light protected 50 ml syringes. Percentage loss of peak shown calculated from day 0 data. Room (Red) and Fridge (Blue) results shown with standard deviation error bars on all points.
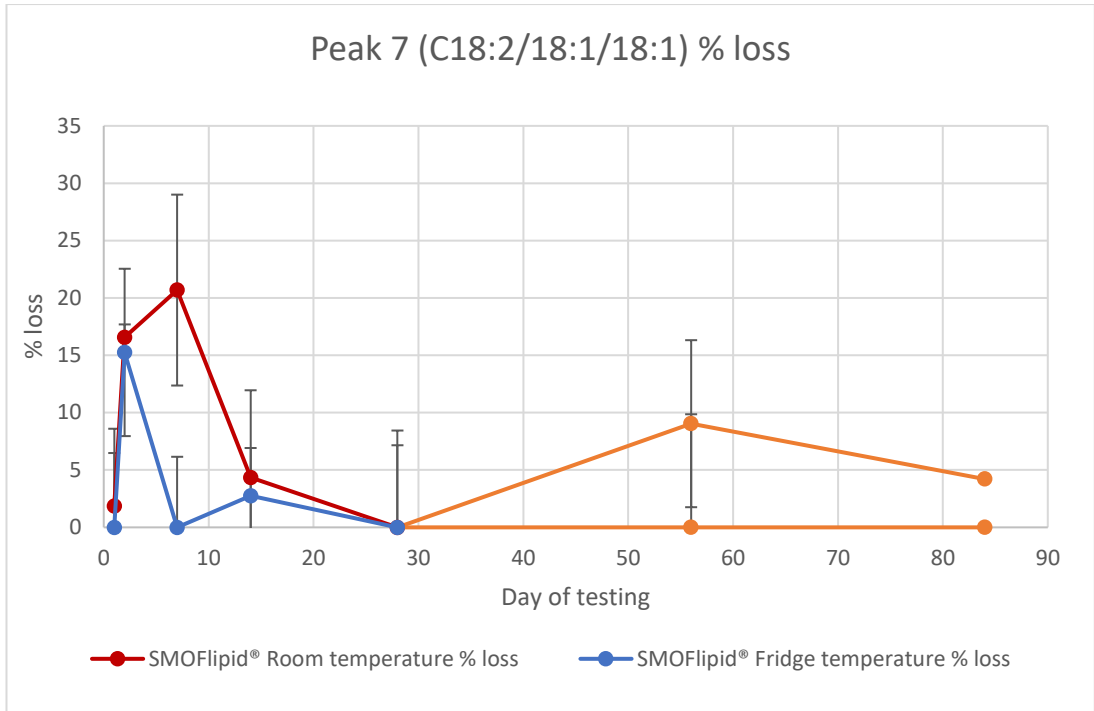
Figure 6.7 HPLC-CAD results for peak 7 (C18:2/18:1/18:1) triglyceride of SMOFlipid® 20 % stored in non-light protected 50 ml syringes. Percentage loss of peak shown calculated from day 0 data. Room (Red) and Fridge (Blue) results shown with standard deviation error bars on all points.
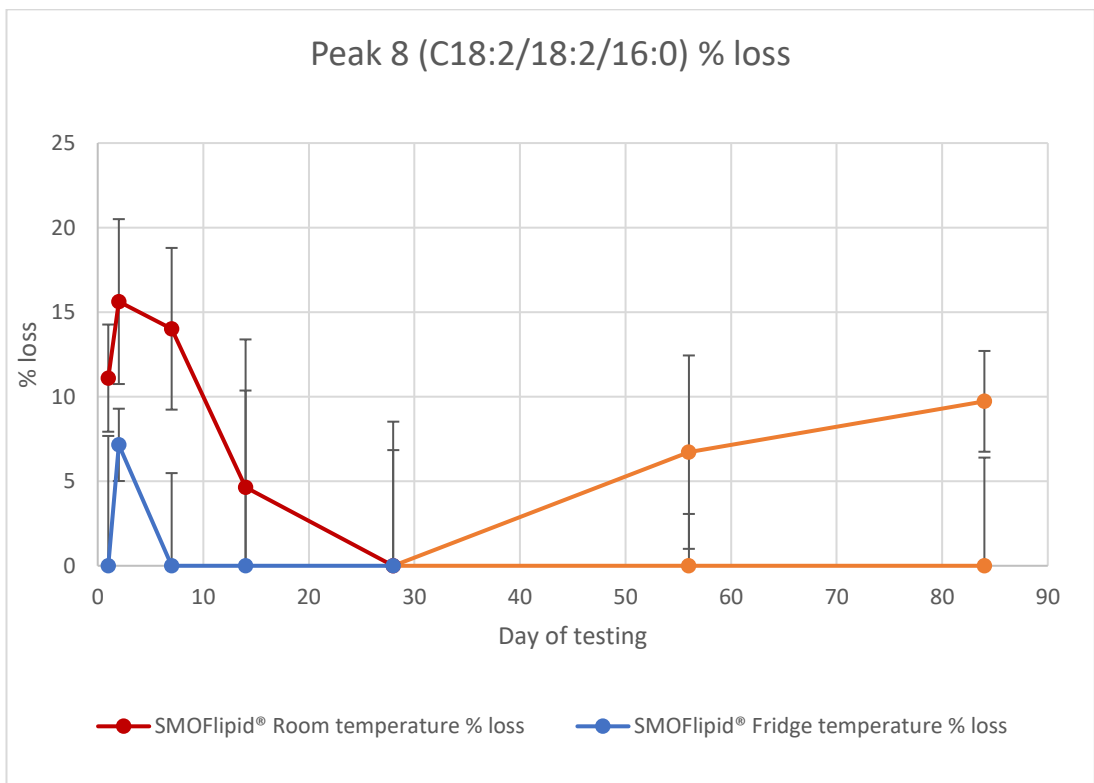
Figure 6.8 HPLC-CAD results for peak 8 (C18:2/18:2/16:0) triglyceride of SMOFlipid® 20 % stored in non-light protected 50 ml syringes. Percentage loss of peak shown calculated from day 0 data. Room (Red) and Fridge (Blue) results shown with standard deviation error bars on all points.
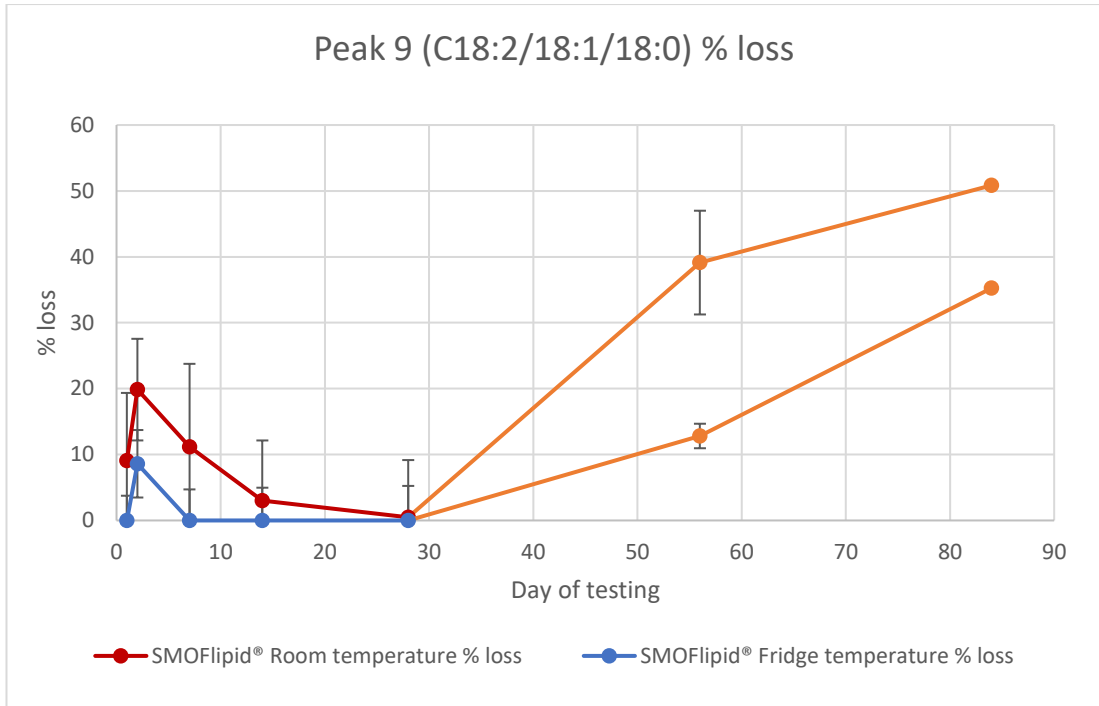
Figure 6.9 HPLC-CAD results for peak 9 (C18:2/18:1/18:0) triglyceride of SMOFlipid® 20 % stored in non-light protected 50 ml syringes. Percentage loss of peak shown calculated from day 0 data. Room (Red) and Fridge (Blue) results shown with standard deviation error bars on all points. Orange points indicate readings where RSD of control samples exceeded acceptable levels.
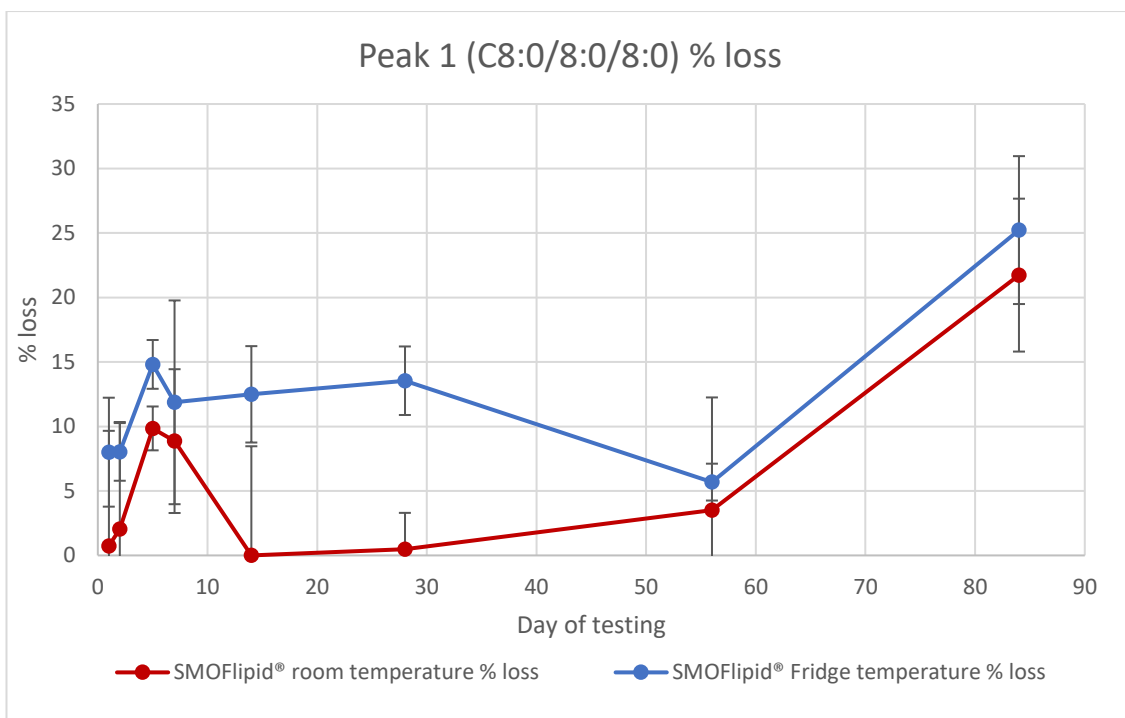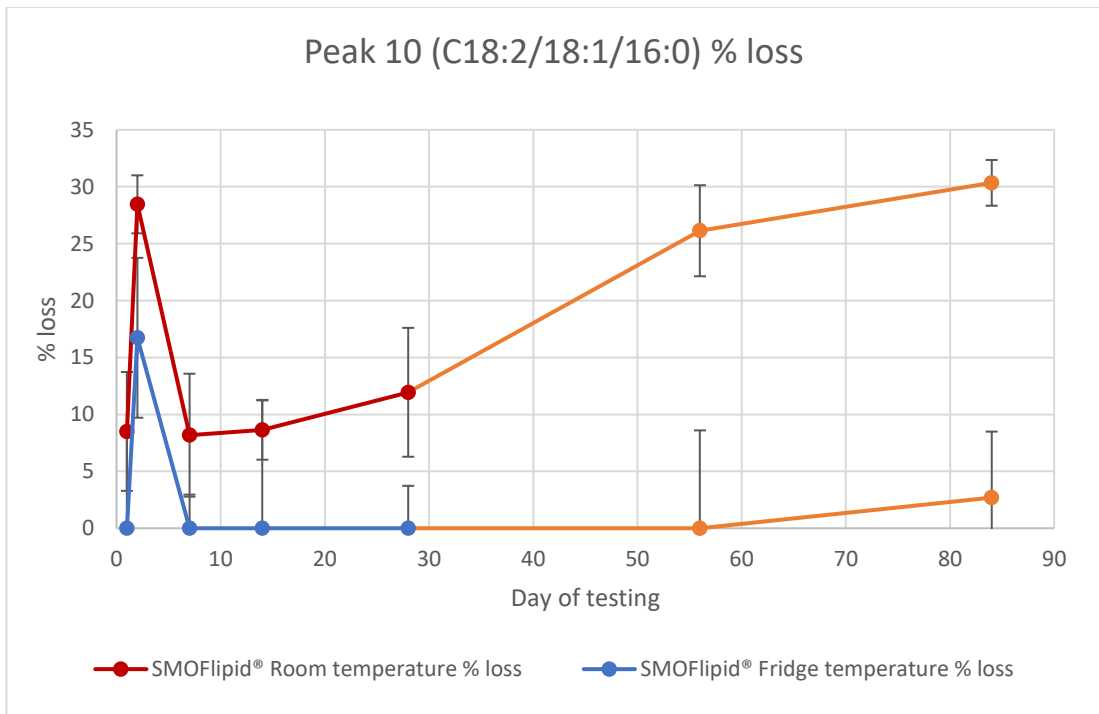

Figure 6.10 HPLC-CAD results for peak 10 (C18:2/18:1/16:0) triglyceride of SMOFlipid® 20 % stored in non-light protected 50 ml syringes. Percentage loss of peak shown calculated from day 0 data. Room (Red) and Fridge (Blue) results shown with standard deviation error bars on all points. Orange points indicate readings where RSD of control samples exceeded acceptable levels.
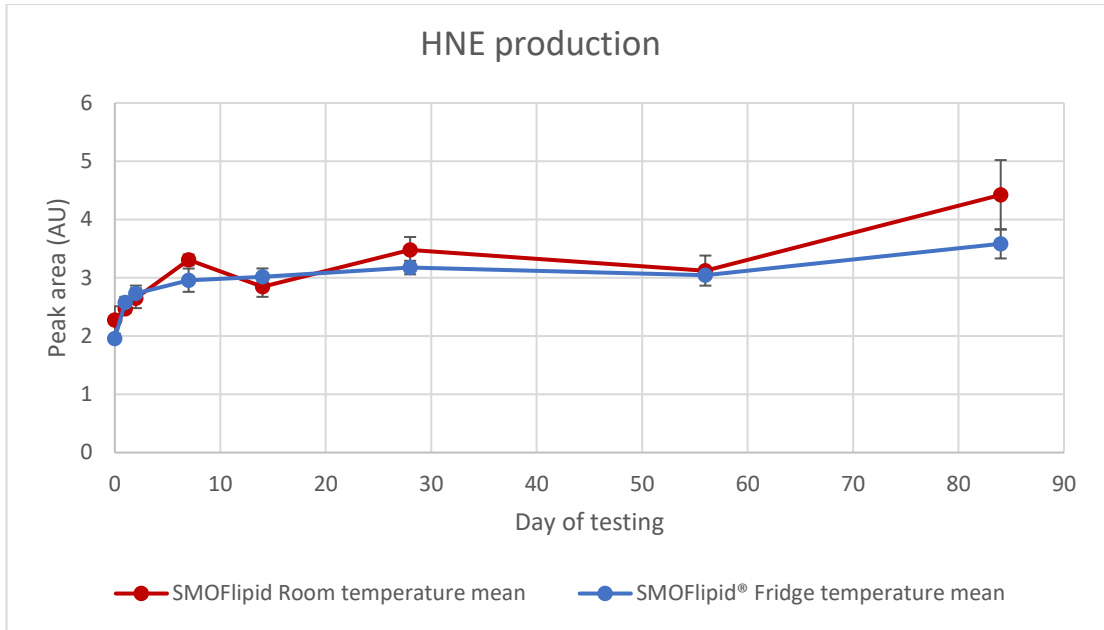
Figure 6.11 HPLC-UV data showing the minimal production of 4-Hydroxynonenal in SMOFlipid® 20 % over 84-day storage and both room (red) and fridge (blue) temperatures in 50 ml non-light protected syringes.
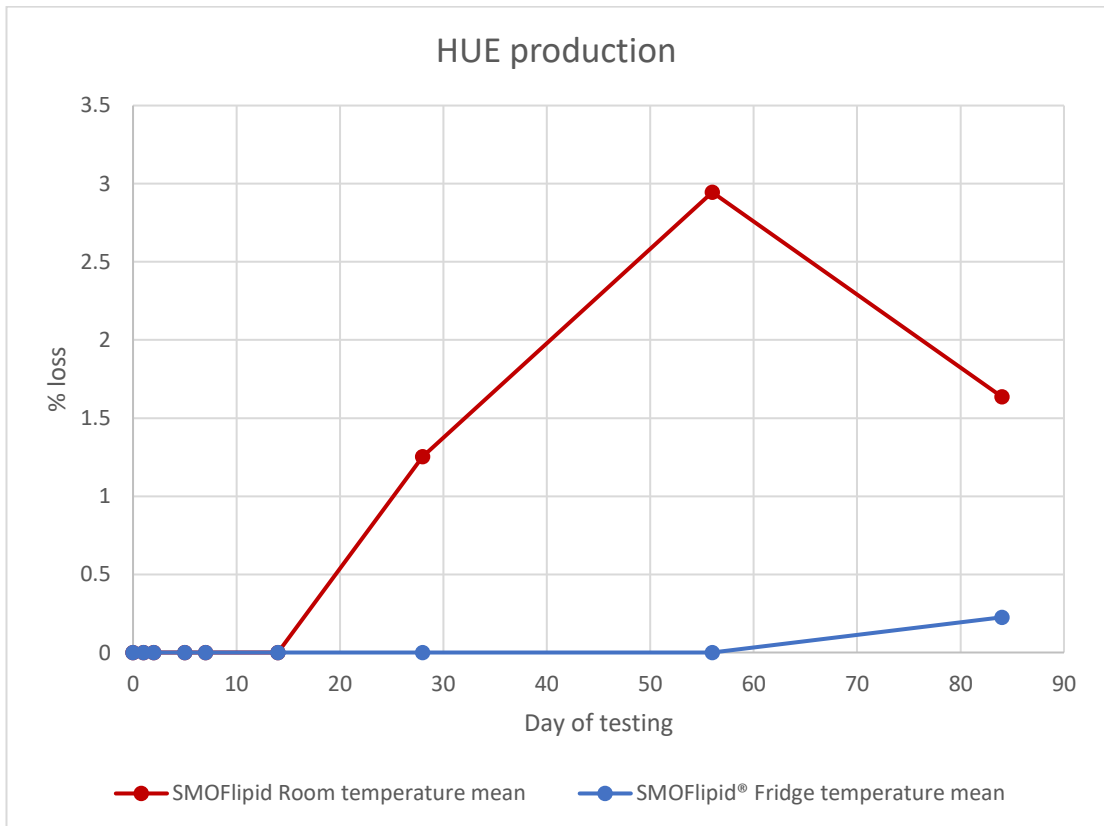
Figure 6.12 HUE production in 50 ml SMOFlipid® non-light protected syringes over 84 days of storage. Room temperature (red trace) and fridge temperature (blue trace).
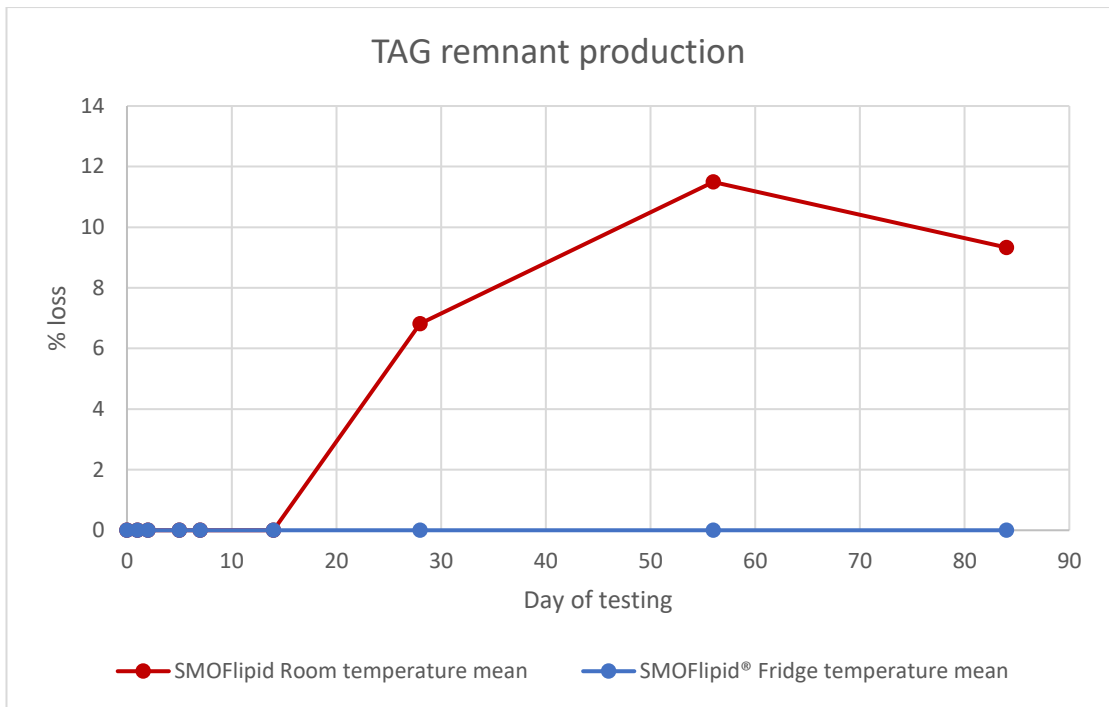
Figure 6.13 HPLC-UV of TAG remnant production in 50 ml SMOFlipid® non-light protected syringes over 84 days storage. Room temperature (red trace) showing production from day 28, no fridge temperature production (blue trace).
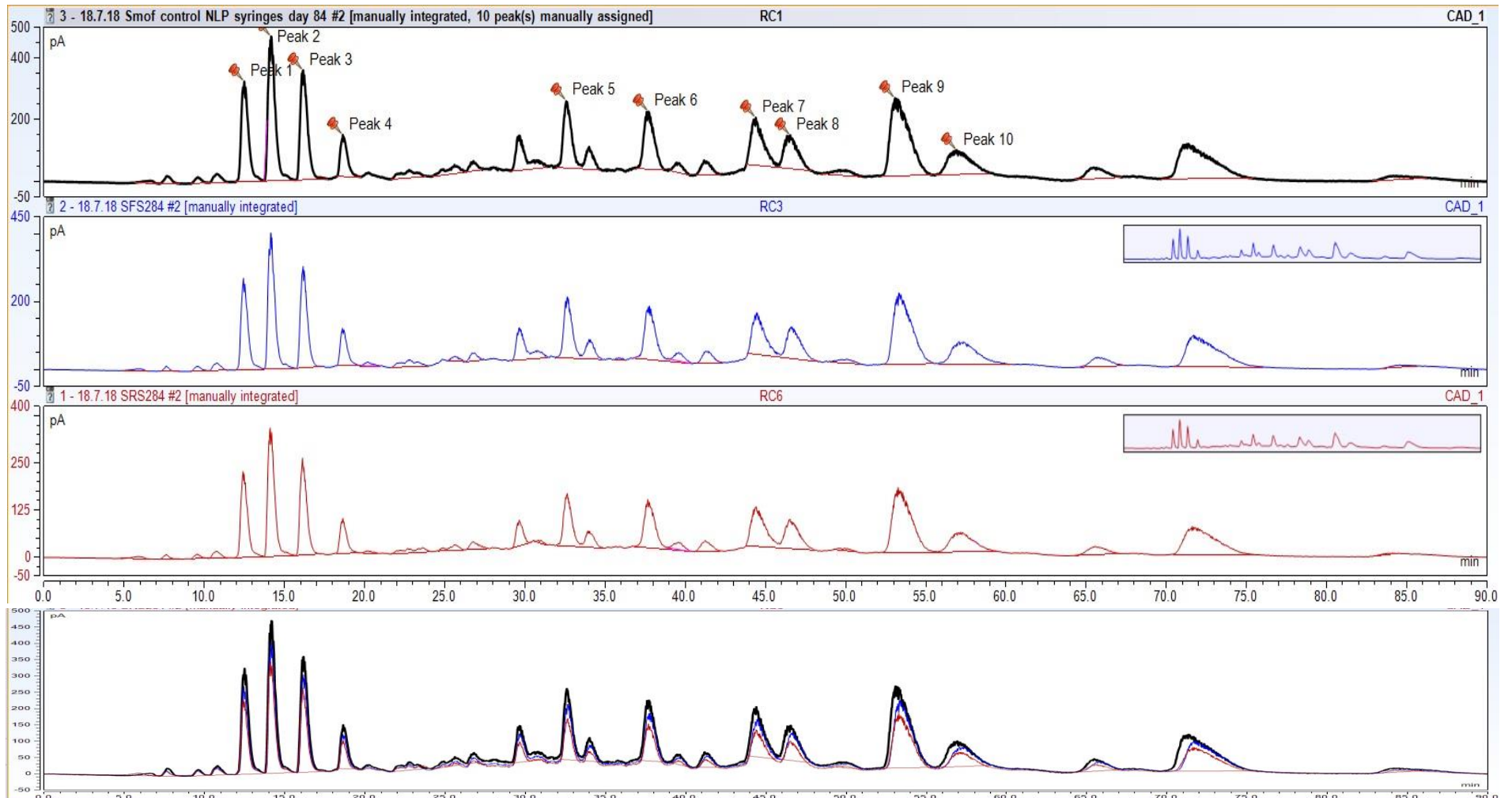
Figure 6.14 HPLC-CAD chromatograms of SMOFlipid® 20% stored in non-light protected 50 ml syringes. Day 0 control (black), day 84 fridge temperature (blue trace) and day 84 room temperature (red trace). Overlaid chromatogram with signal time offset shows changes in peaks in comparison to control.
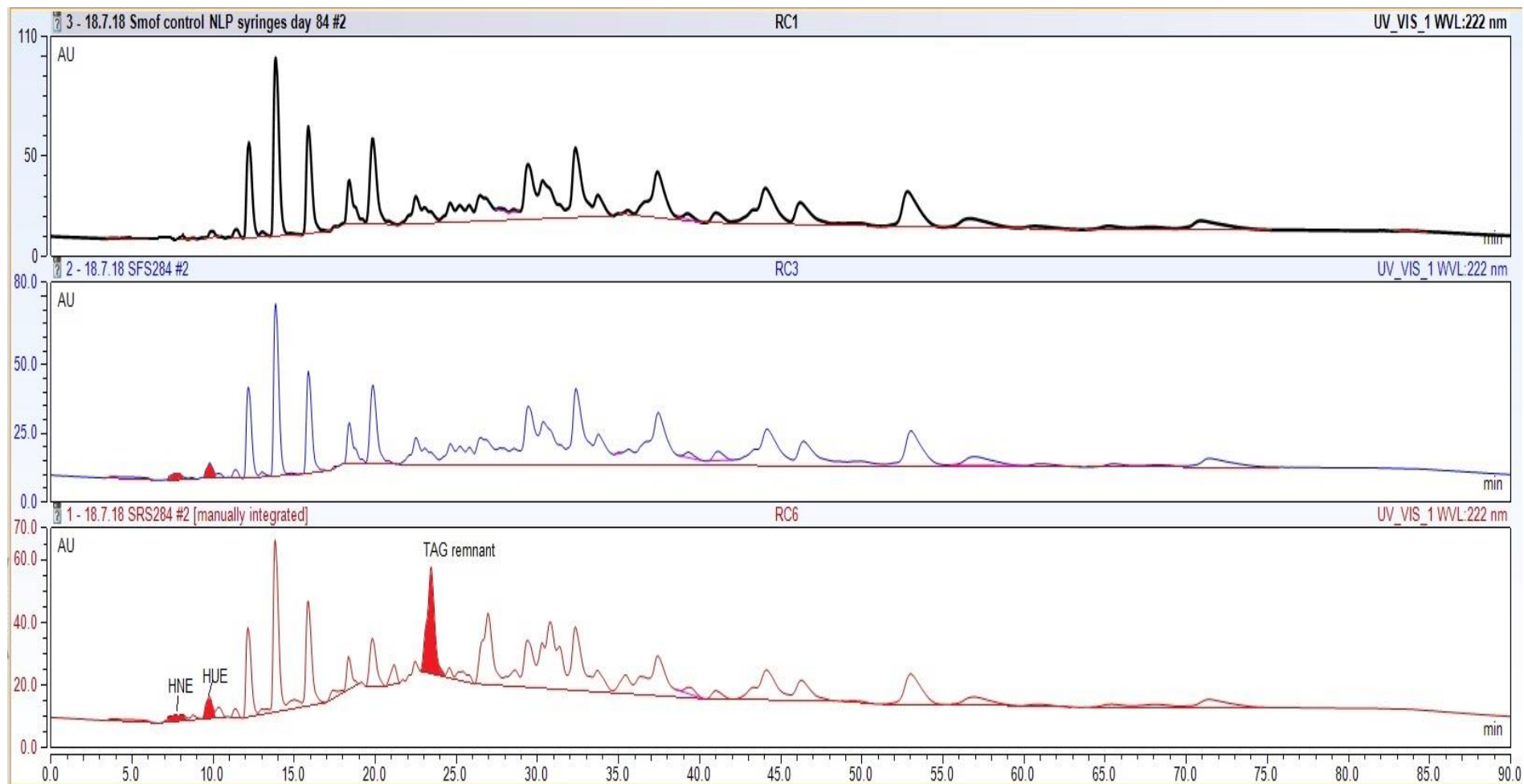
Figure 6.15 HPLC-UV chromatograms of SMOFlipid® 20% stored in non-light protected 50 ml syringes. Day 0 chromatogram (black trace), day 84 fridge temperature syringes (blue trace) and day 84 room temperature syringes (red trace). The production of HNE, HUE and TAG remnant in room and fridge temperature syringes can be seen and is indicated on the chromatogram.
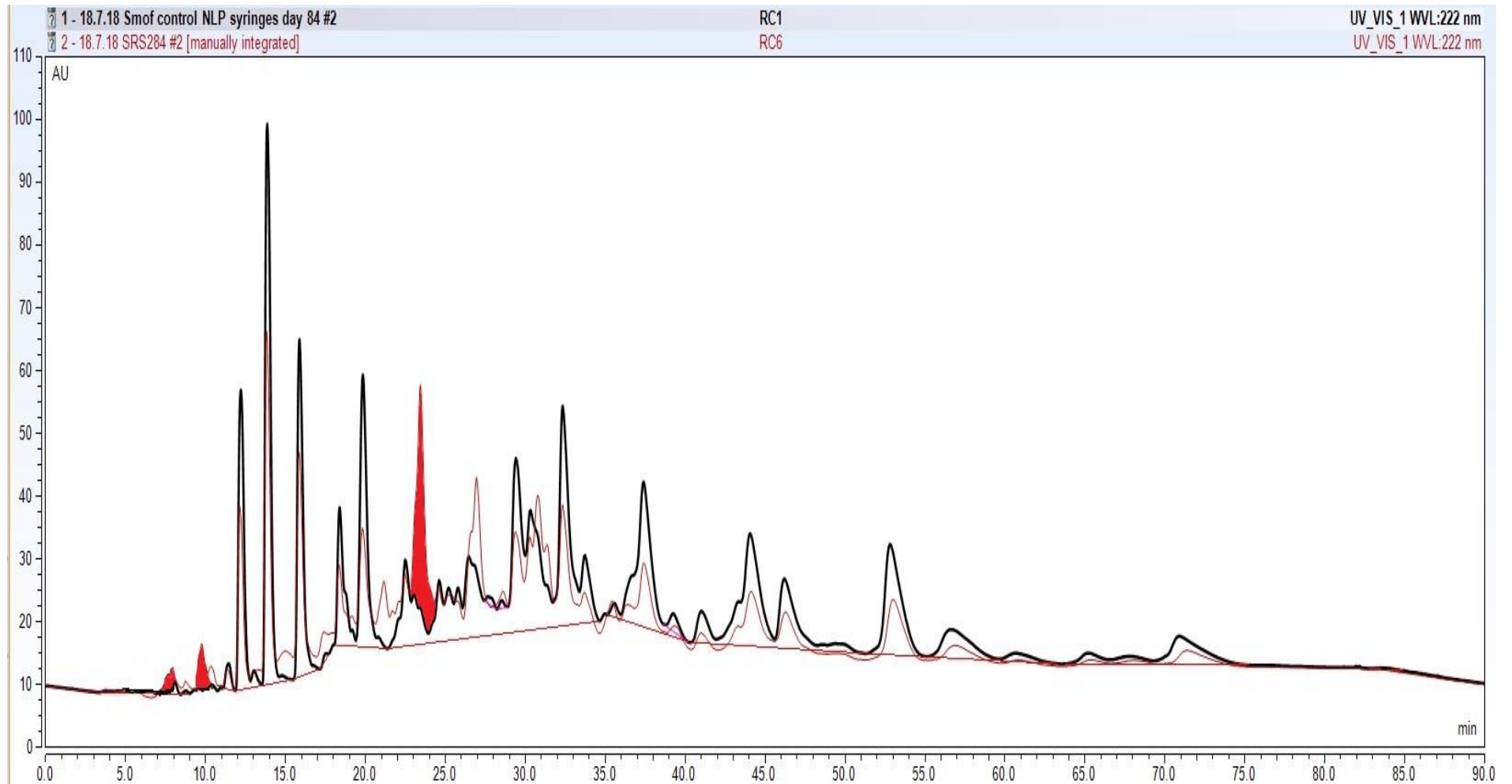
Figure 6.16 Overlaid HPLC-UV chromatograms of day 0 (black trace) and day 84 room temperature (red trace) SMOFlipid® 20 % stored in non-light protected 50 ml syringes. Peaks on the 84-day chromatogram highlighted in red show HNE, HUE and TAG remnant.

6.5. SMOFlipid® non-light protected PN bag results.

Formulation of each PN bag sample was done according to testing protocols (section 6.2.3) with 1ml of lipid removed at each testing timepoint and all possible air removed. As discussed previously small volumes of air remain within each bag as reflected in clinical practise. Control samples of lipid were tested at all timepoints and RSD's monitored for method precision. All chromatograms were integrated, and peak areas recorded.

Figures 6.17 to 6.26 show the % TAG losses recorded for all 10 peaks compared to day 0. RSD's for peaks 1, 2, 3, 5, 8 and 9 were above the acceptable levels at day 28 testing. Therefore, for these peaks day 28 results were identified as outliers as shown on each figure and excluded from analysis. For peaks 6, 7 and 8 day-84 control RSD's fell out of acceptable ranges. As such results are identified on each figure in orange and excluded from analysis. Although the RSD's of the control samples above fell outside the acceptable level of 12, maximal RSD's recorded were 16 and as such consideration is given to these results when comparing containers (section 6.7). At day 56 where all RSD's were within acceptable limits maximal TAG losses recorded were ~20 % for peak 7 (C18:2/18:1/18:1) and peak 5 (C18:2/18:2/18:2) both at fridge temperatures. Both TAGs were predicted to be the most liable to peroxidation and breakdown due to the high levels of unsaturation present. No statistical difference was seen between temperatures of storage (table 6.1 section 6.7). TAG losses were observed in peaks 1 to 4 though minimal at day 56 (less than 10 %) levels rise significantly at day 84 (~ 25 %). All four saturated peaks have acceptable control RSD's for day 84 samples, so the results can be considered accurate. The loss of saturated TAGs is discussed further with all results in section 6.7.

No detectable levels of HNE were observed in all PN bags across 84 days of storage. With regards to HUE production, only a very small peak area was recorded in fridge temperature bags at day 84 (figure 6.27), however the amount present is not quantifiable due to the lack of assay validation for HUE as discussed in chapter 7. The production of the TAG remnant is seen in significant quantities from day 7 onwards in room temperature PN bags (figures 6.28, 6.29, 6.30). Comparison between containers is shown in section 6.7.
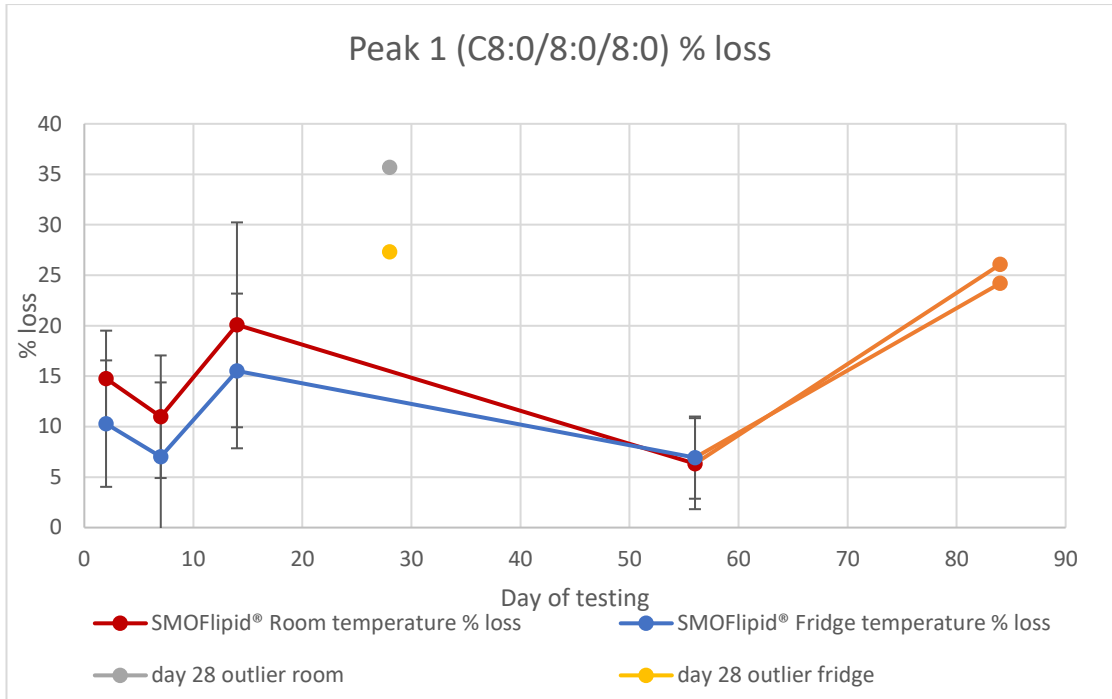
Figure 6.17 HPLC-CAD results for peak 1 (C8:0/8:0/8:0) triglyceride of 50 ml SMOFlipid® 20 % stored in non-light protected 250 ml PN bags. Percentage loss of peak shown calculated from day 0 data. Room (Red) and Fridge (Blue) results shown with standard deviation error bars on all points. Day 28 outliers excluded from analysis.
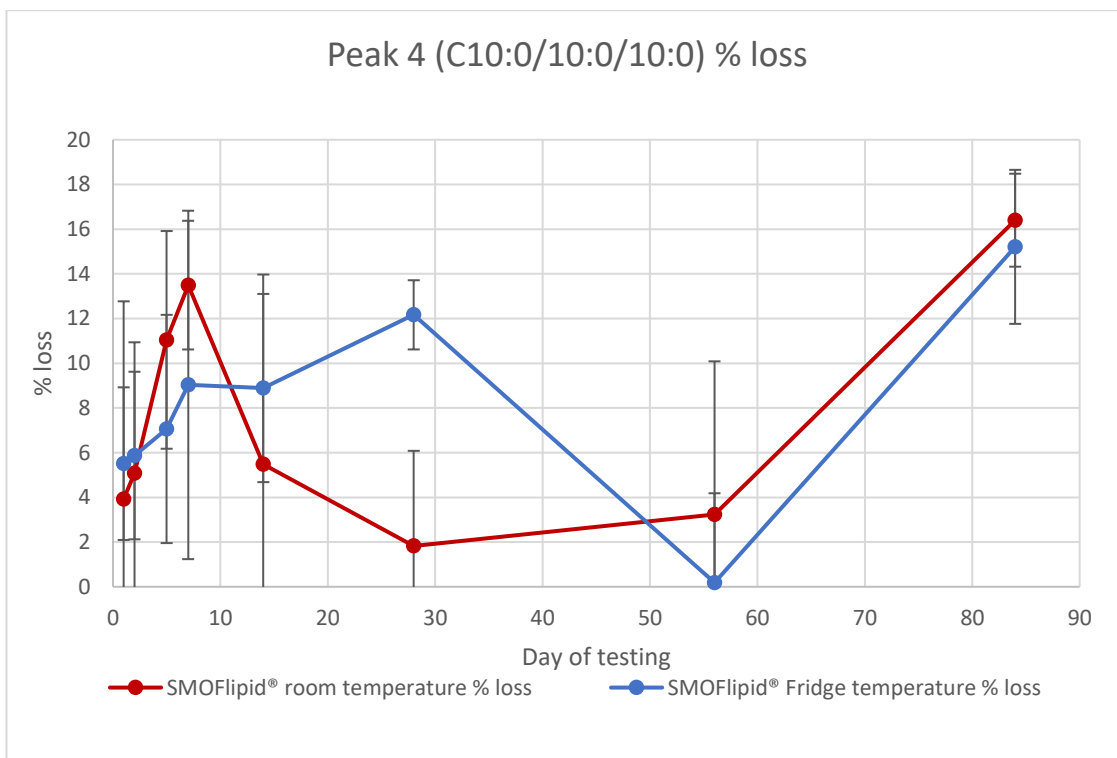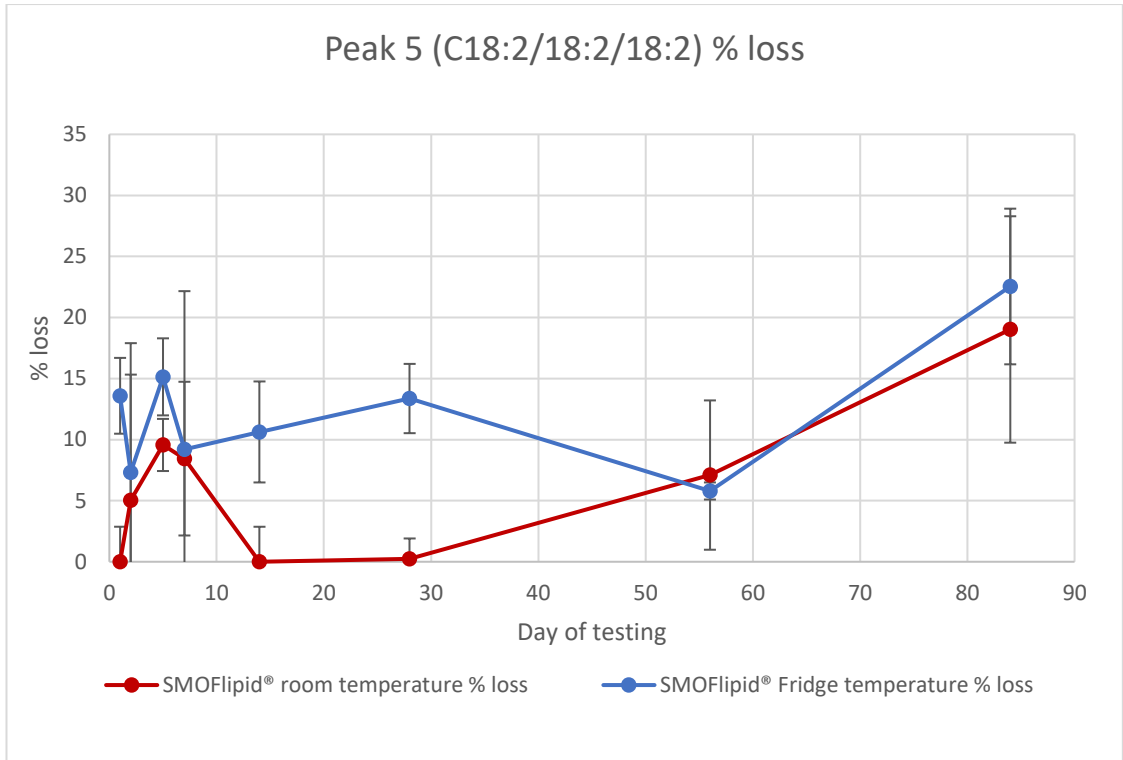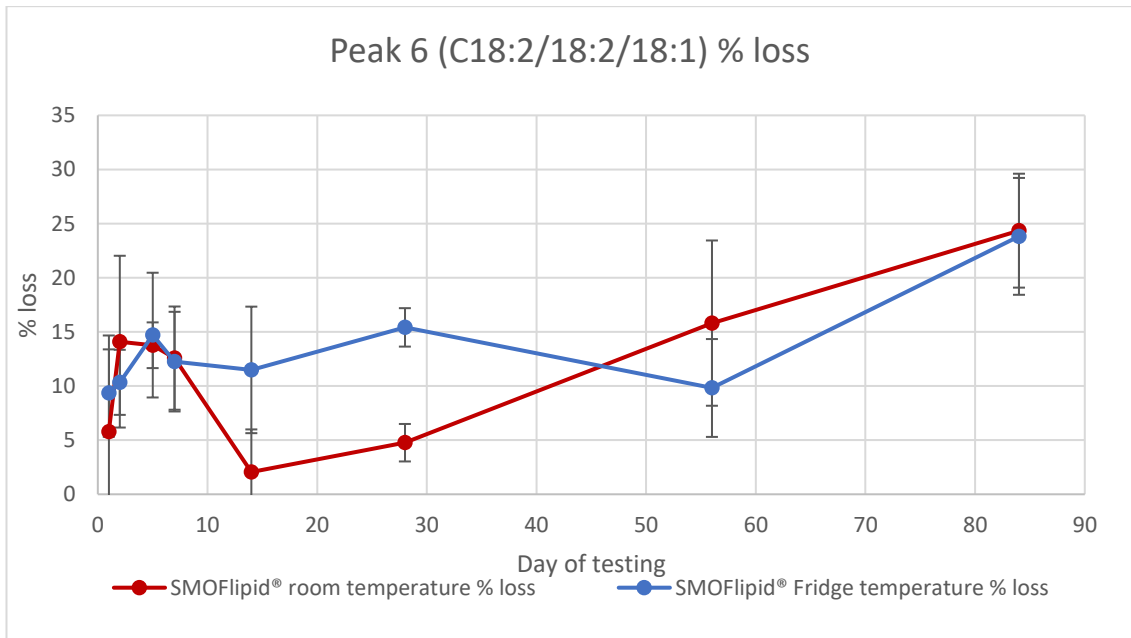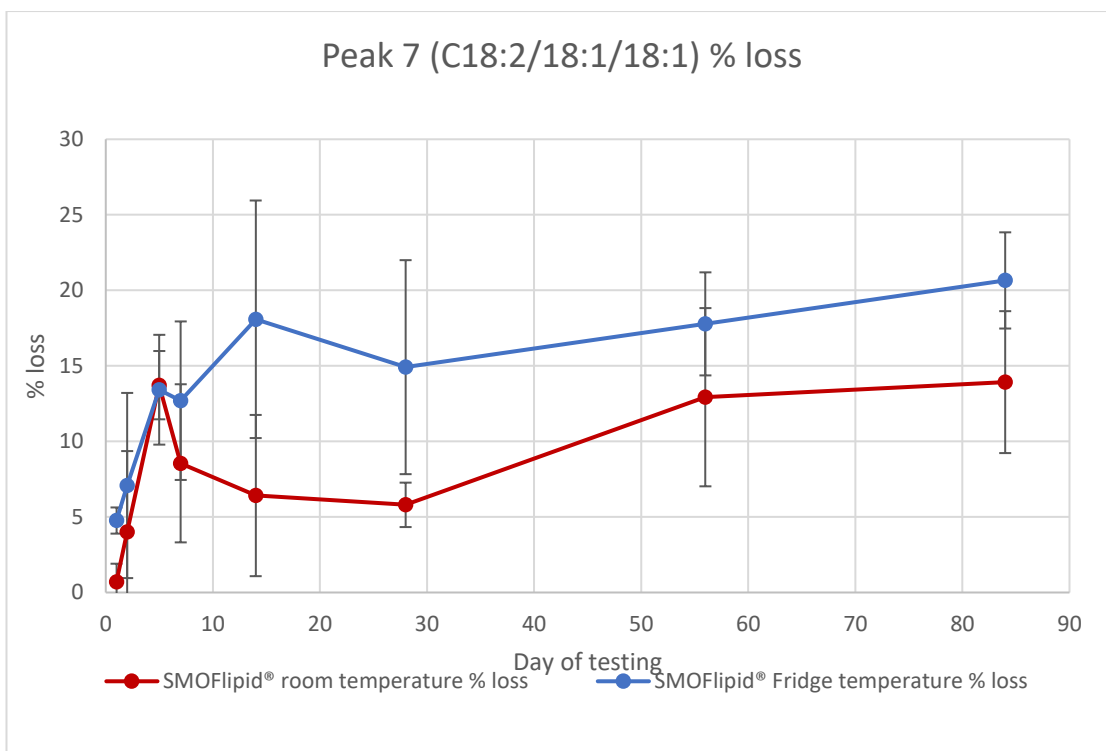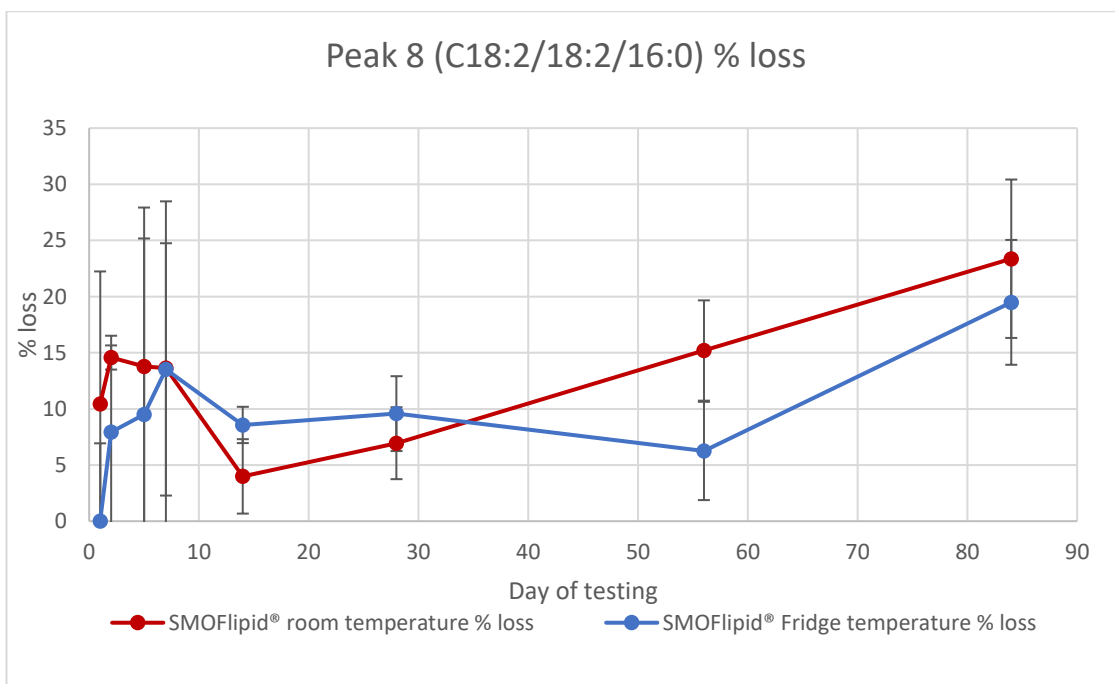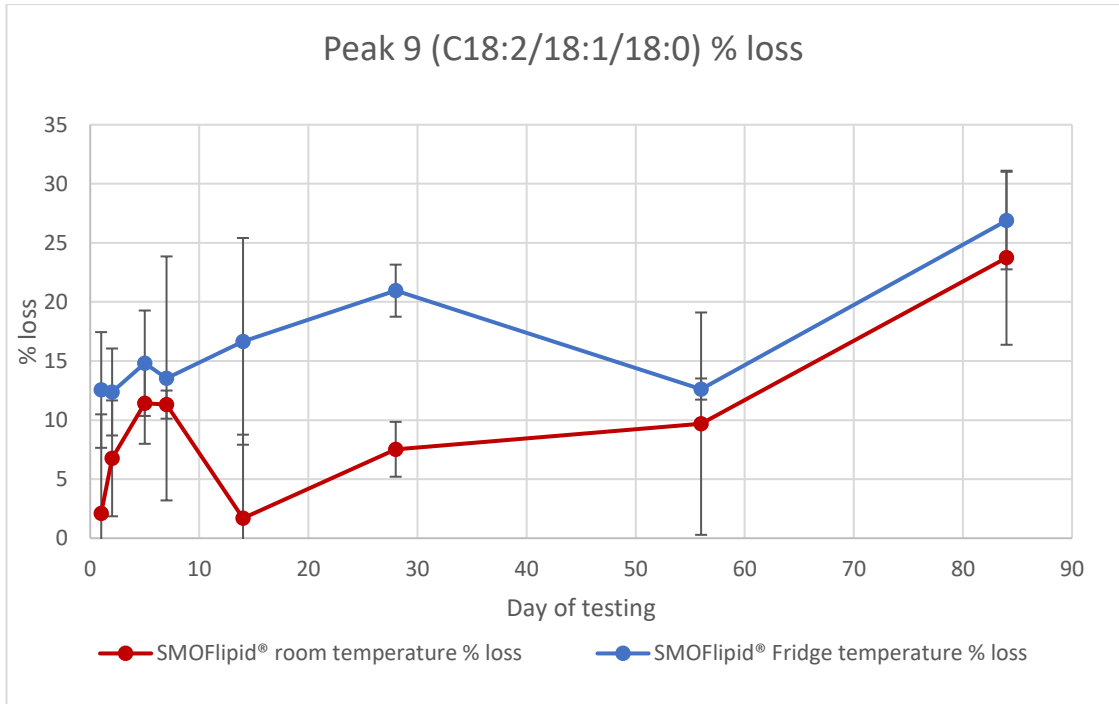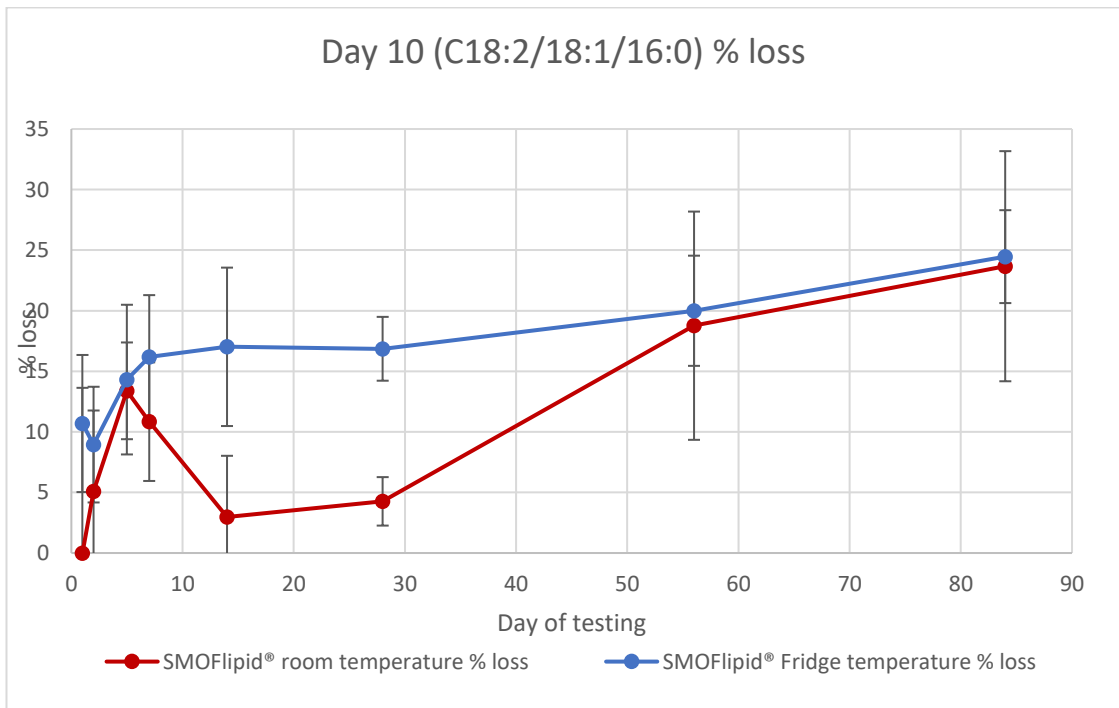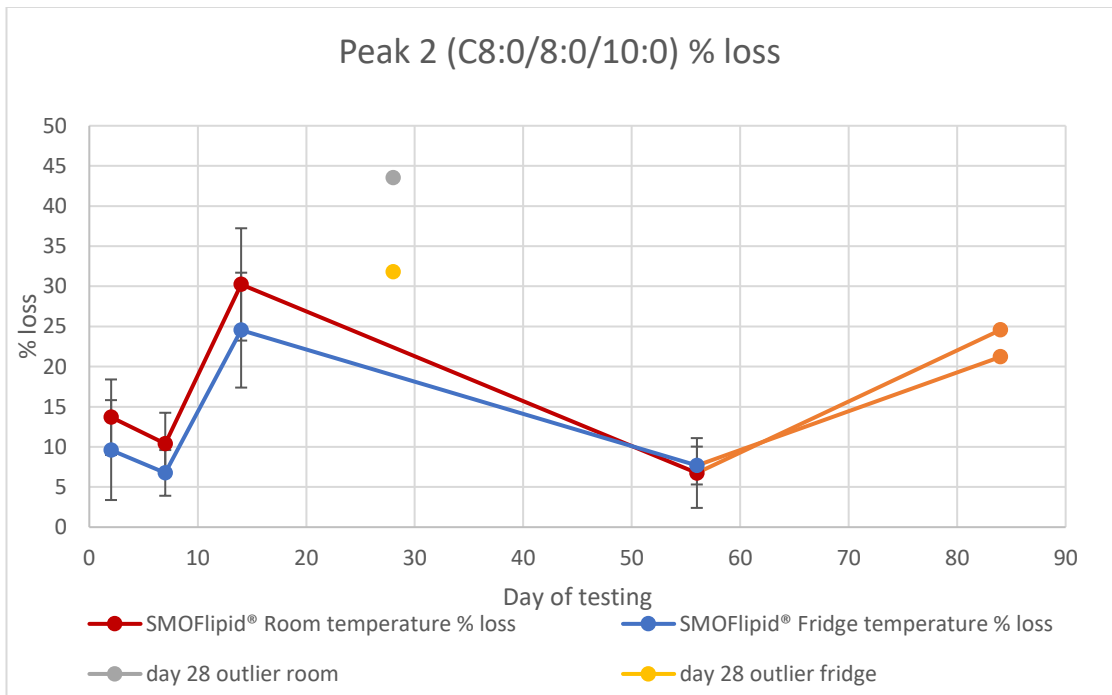

Figure 6.18 HPLC-CAD results for peak 2 (C8:0/8:0/10:0) triglyceride of 50 ml SMOFlipid® 20 % stored in non-light protected 250 ml PN bags. Percentage loss of peak shown calculated from day 0 data. Room (Red) and Fridge (Blue) results shown with standard deviation error bars on all points. Day 28 outliers excluded from analysis.
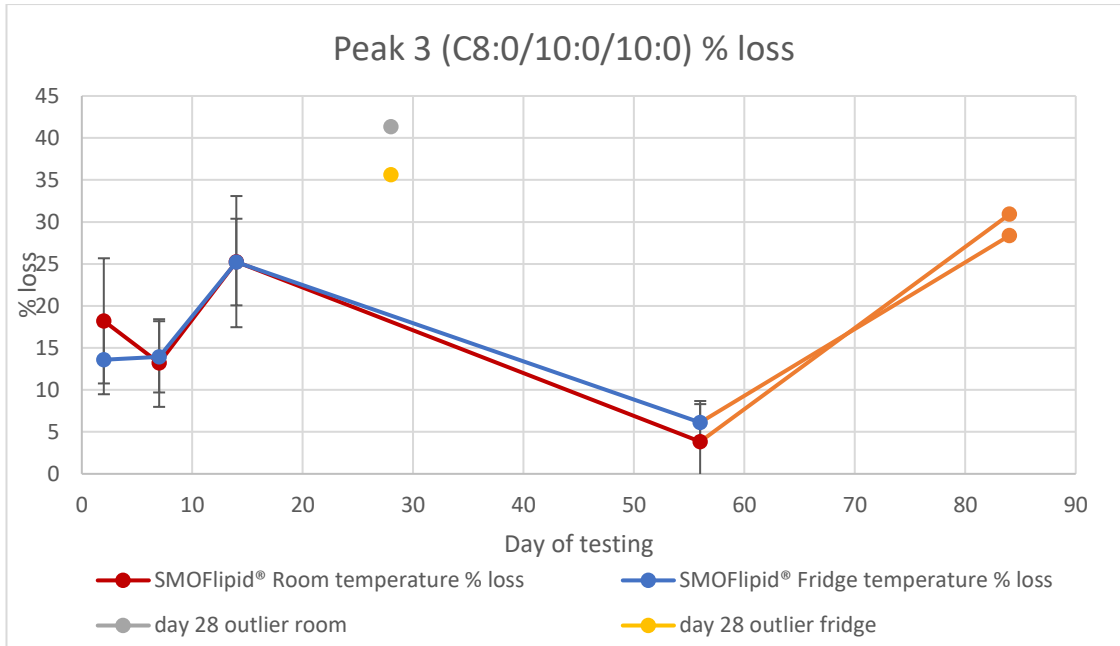
Figure 6.19 HPLC-CAD results for peak 3 (C8:0/10:0/10:0) triglyceride of 50 ml SMOFlipid® 20 % stored in non-light protected 250 ml PN bags. Percentage loss of peak shown calculated from day 0 data. Room (Red) and Fridge (Blue) results shown with standard deviation error bars on all points. Day 28 outliers excluded from analysis.
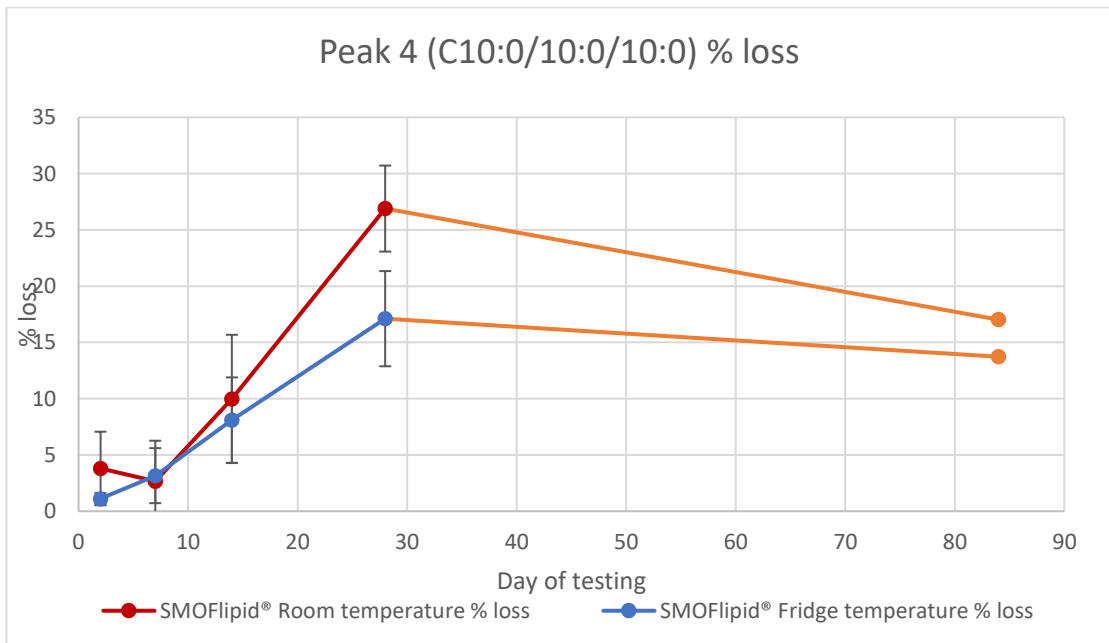
Figure 6.20 HPLC-CAD results for peak 4 (C10:0/10:0/10:0) triglyceride of 50 ml SMOFlipid® 20 % stored in non-light protected 250 ml PN bags. Percentage loss of peak shown calculated from day 0 data. Room (Red) and Fridge (Blue) results shown with standard deviation error bars on all points.

274
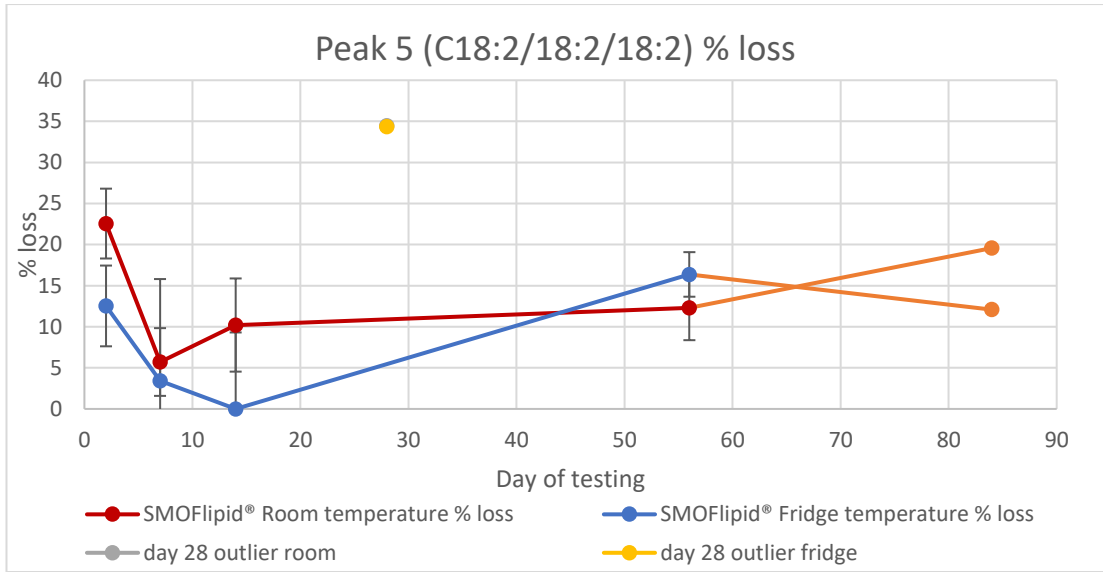
Figure 6.21 HPLC-CAD results for peak 5 (C18:2/18:2/18:2) triglyceride of 50 ml SMOFlipid® 20 % stored in 250ml non-light protected PN bags. Percentage loss of peak shown calculated from day 0 data. Room (Red) and Fridge (Blue) results shown with standard deviation error bars on all points. Day 28 outliers excluded from analysis.
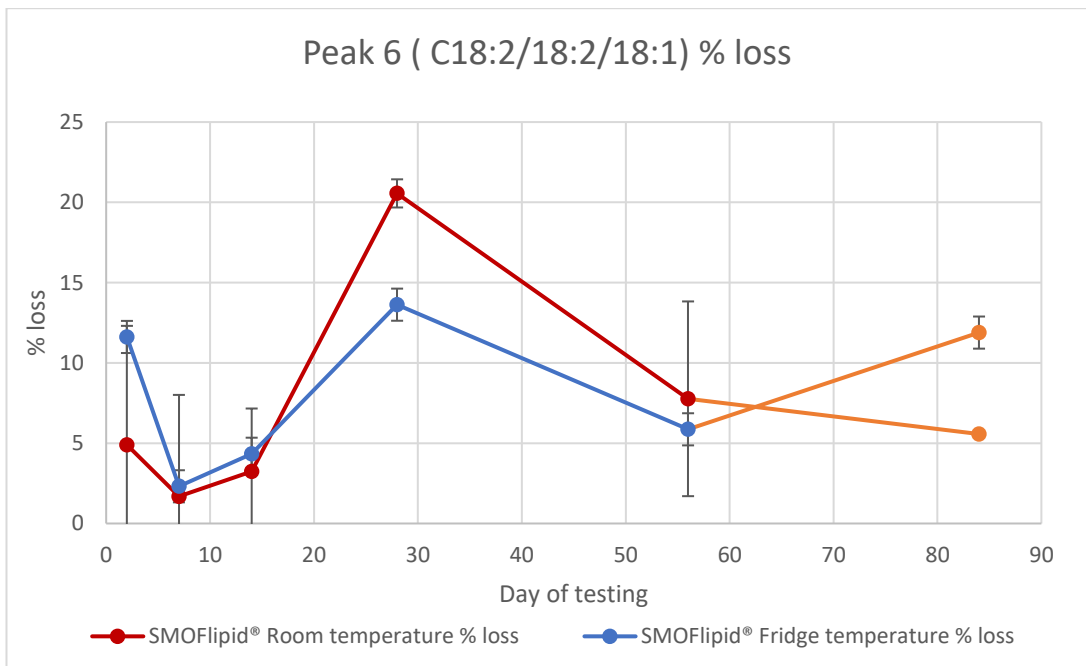
Figure 6.22 HPLC-CAD results for peak 6 (C18:2/18:2/18:1) triglyceride of 50ml SMOFlipid® 20 % stored in non-light protected 250 ml PN bags. Percentage loss of peak shown calculated from day 0 data. Room (Red) and Fridge (Blue) results shown with standard deviation error bars on all points. Orange data from day 84 excluded from further analysis due to high RSD.
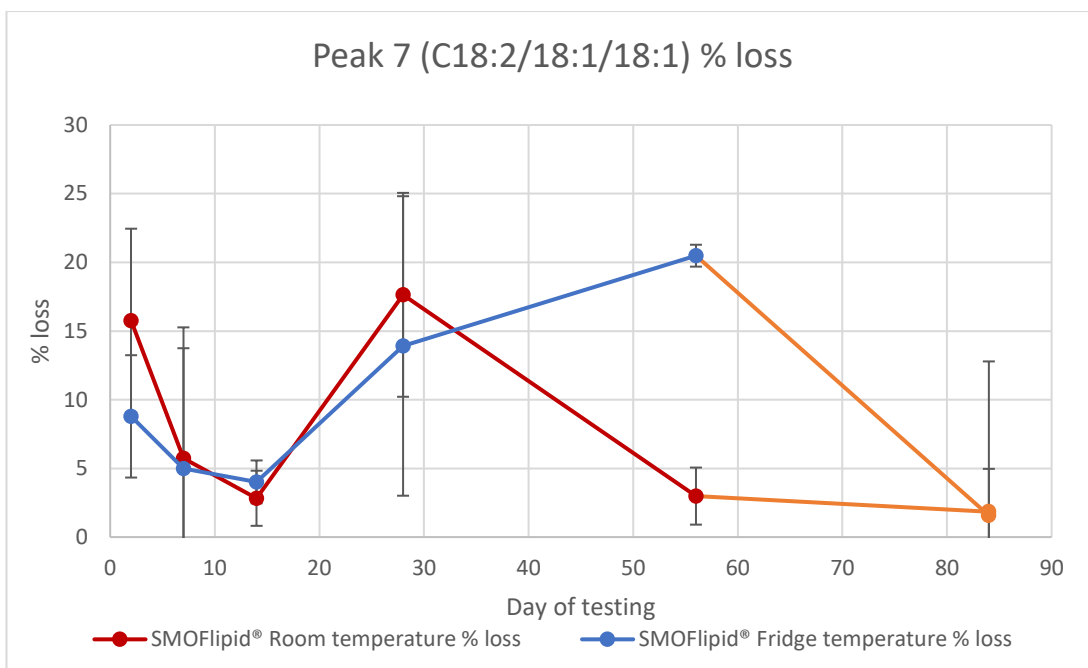
Figure 6.23 HPLC-CAD results for peak 7 (C18:2/18:1/18:1) triglyceride of 50 ml SMOFlipid® 20 % stored in non-light protected 250 ml PN bags. Percentage loss of peak shown calculated from day 0 data. Room (Red) and Fridge (Blue) results shown with standard deviation error bars on all points. Orange data from day 84 excluded from further analysis due to high RSD.
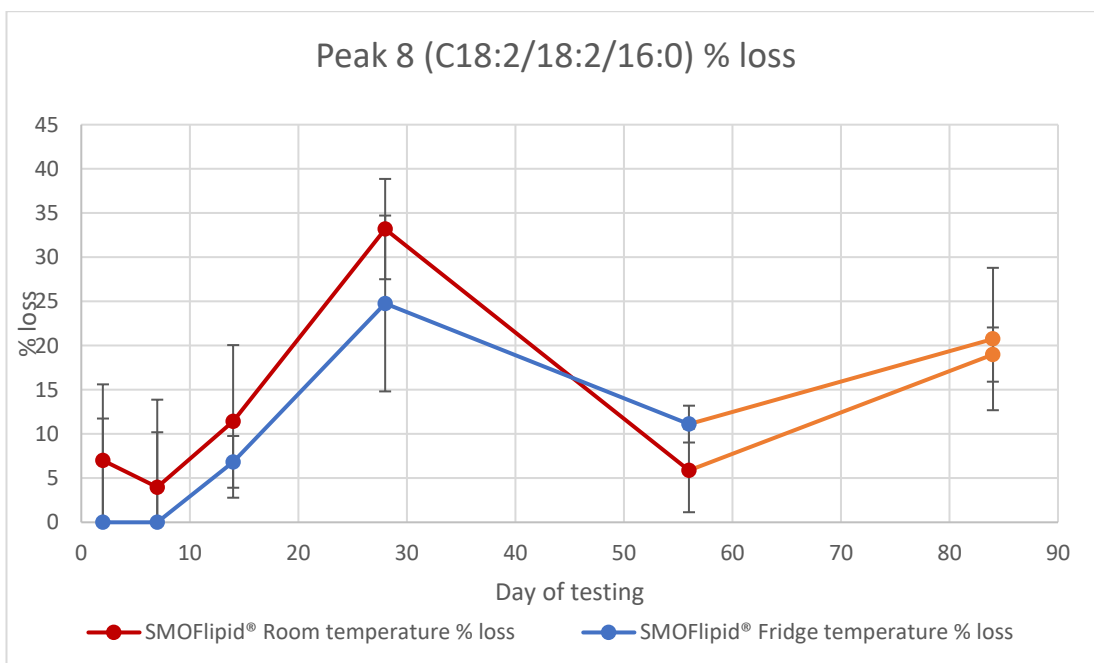
Figure 6.24 HPLC-CAD results for peak 8 (C18:2/18:2/16:0) triglyceride of 50 ml SMOFlipid® 20 % stored in non-light protected 250 ml PN bags. Percentage loss of peak shown calculated from day 0 data. Room (Red) and Fridge (Blue) results shown with standard deviation error bars on all points. Orange data from day 84 excluded from further analysis due to high RSD.
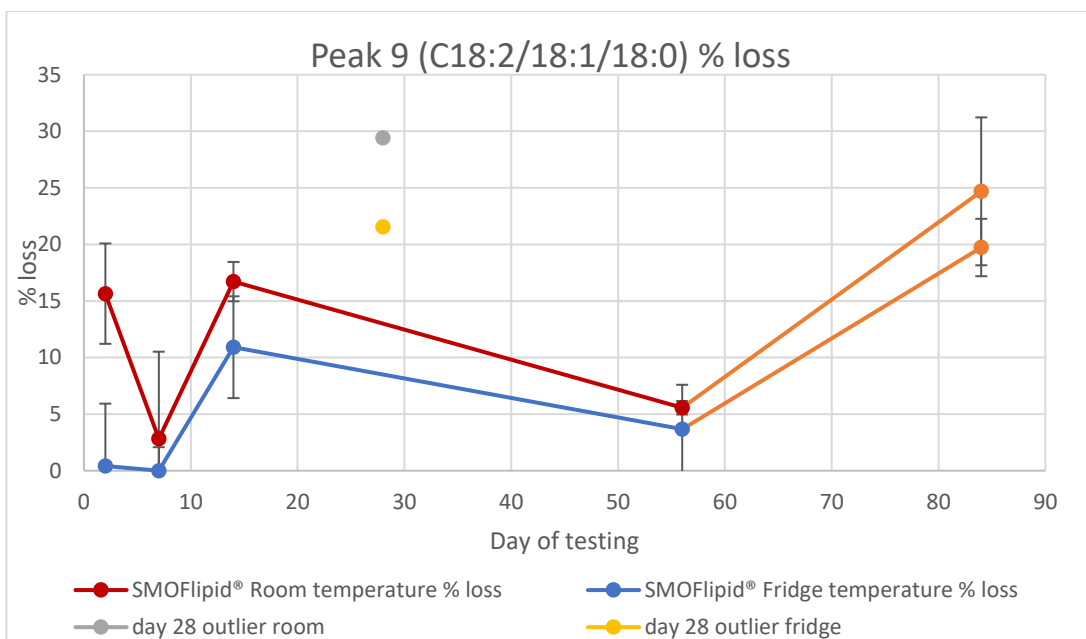
Figure 6.25 HPLC-CAD results for peak 9 (C18:2/18:1/18:0) triglyceride of 50 ml SMOFlipid® 20 % stored in non-light protected 250 ml PN bags. Percentage loss of peak shown calculated from day 0 data. Room (Red) and Fridge (Blue) results shown with standard deviation error bars on all points. Day 28 outlier excluded from analysis.
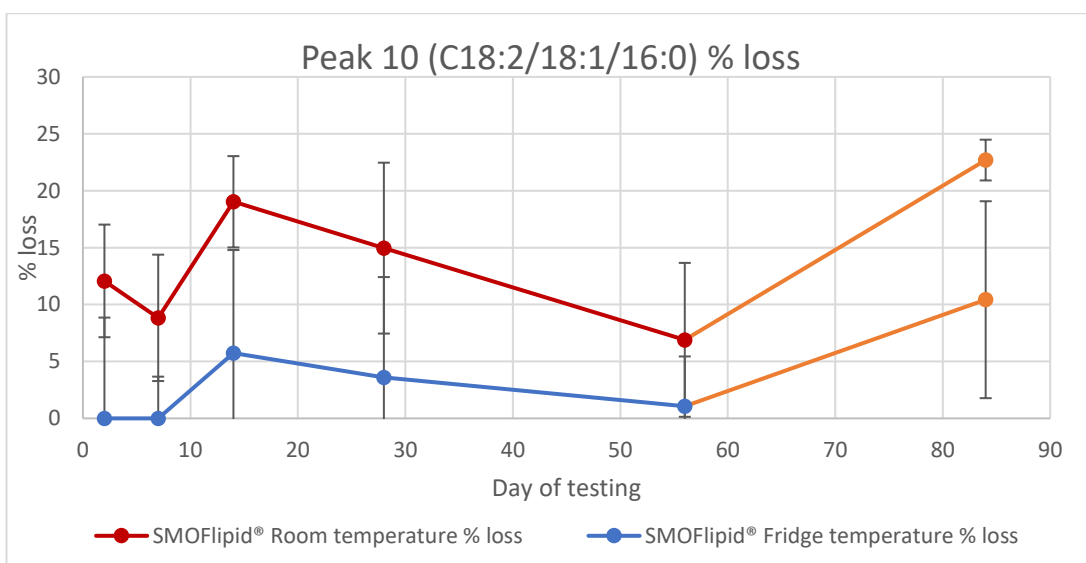
Figure 6.26 HPLC-CAD results for peak 10 (C18:2/18:1/16:0) triglyceride of 50 ml SMOFlipid® 20 % stored in non-light protected 250 ml PN bags. Percentage loss of peak shown calculated from day 0 data. Room (Red) and Fridge (Blue) results shown with standard deviation error bars on all points
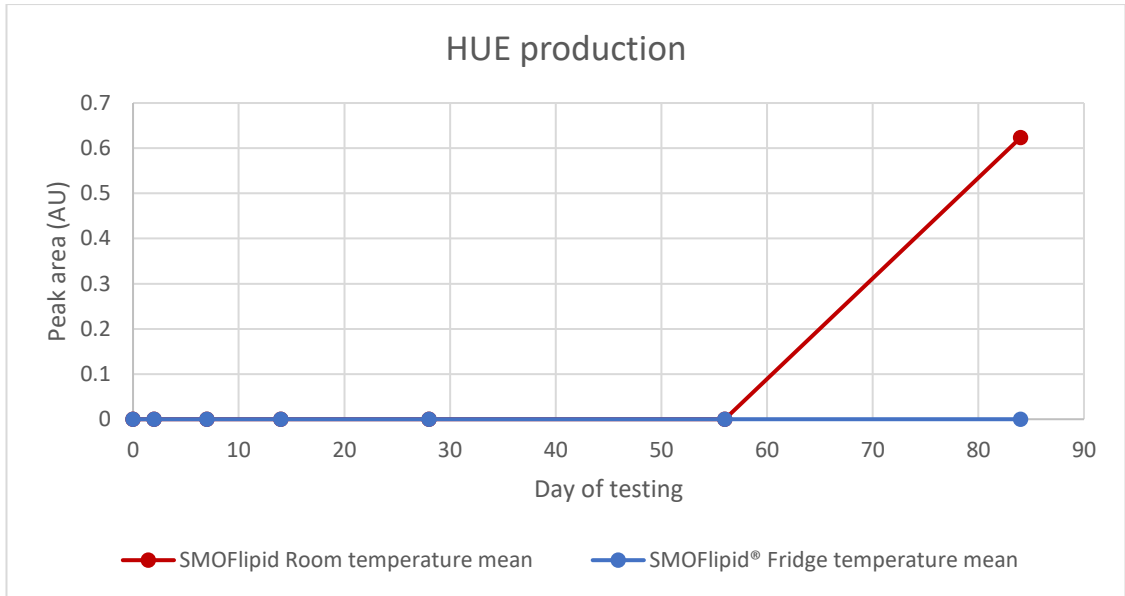
Figure 6.27 HUE production in 50 ml SMOFlipid® stored in non-light protected 250 ml PN bags over 84 days of storage. Room temperature (red trace) and fridge temperature (blue trace).
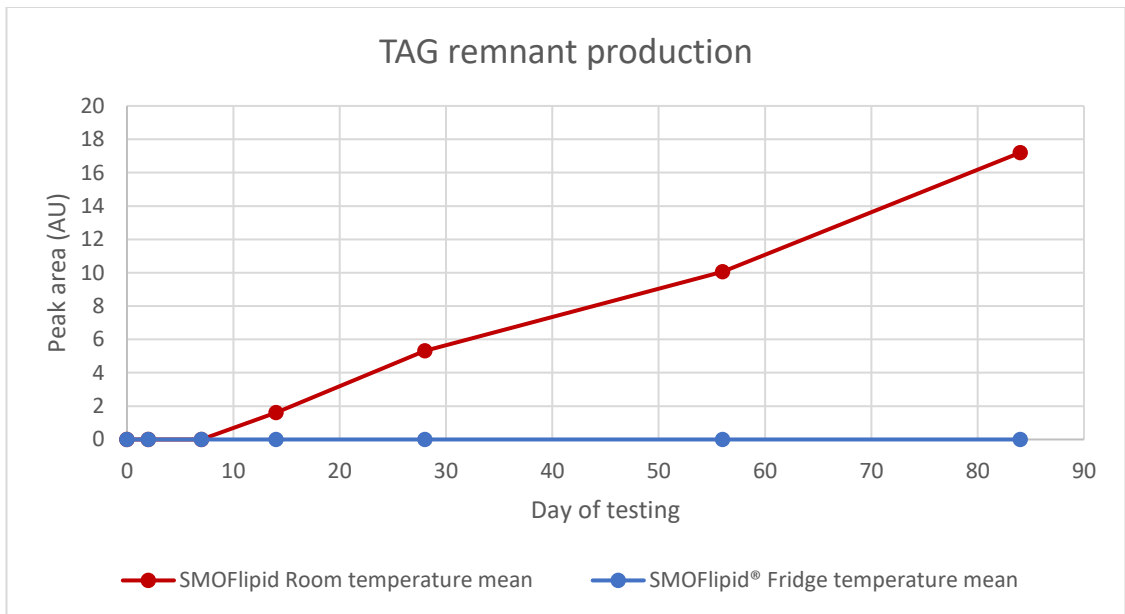
Figure 6.28 HPLC-UV of TAG remnant production in 50 ml SMOFlipid® non-light protected 250 ml PN bags over 84 days storage. Room temperature (red trace) showing production from day 7, no fridge temperature production (blue trace).
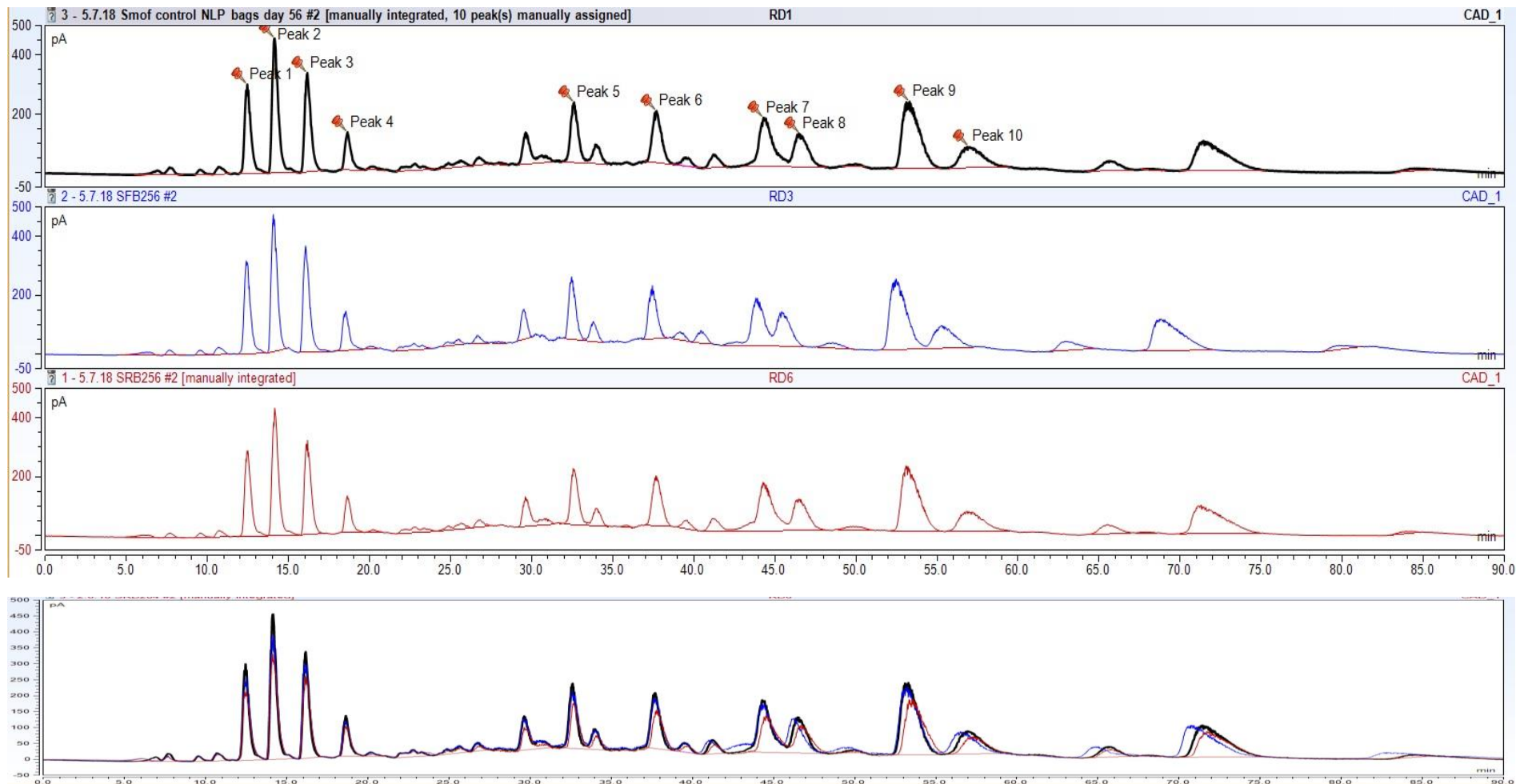
Figure 6.29 HPLC-CAD chromatograms of 50 ml SMOFlipid® 20% stored in 250 ml non-light protected PN bags. Day 0 control (black), day 84 fridge temperature chromatogram (blue trace) and day 84 room temperature (red trace). Overlaid chromatogram with signal time offset shows changes in peaks in comparison to control.
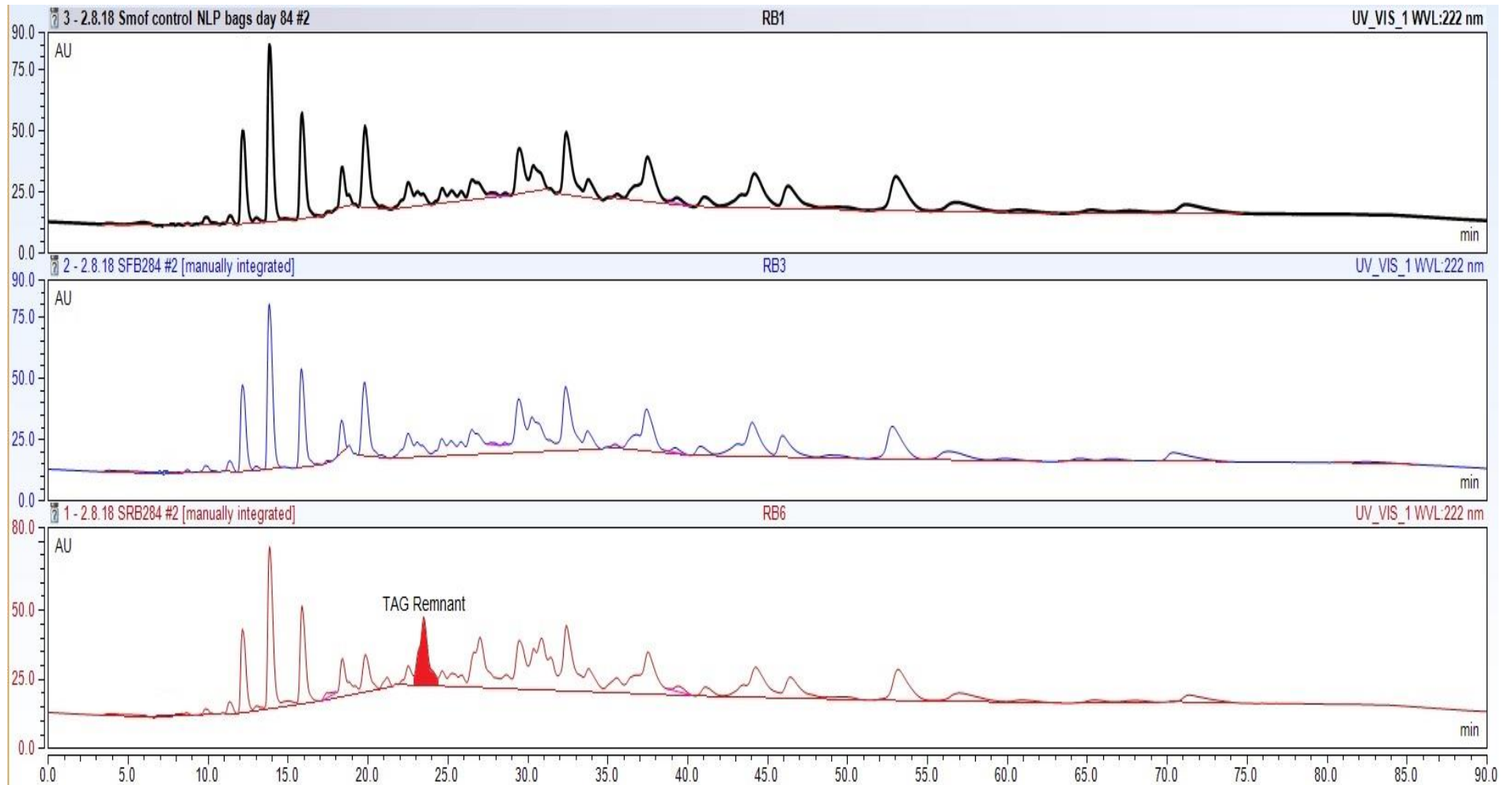
Figure 6.30 HPLC-UV chromatograms of 50 ml SMOFlipid® 20% stored in non-light protected 250 ml PN bags. Day 0 chromatogram (black trace), day 84 fridge temperature bags (blue trace) and day 84 room temperature syringes (red trace). TAG remnant production is indicated in room temperature PN bags.
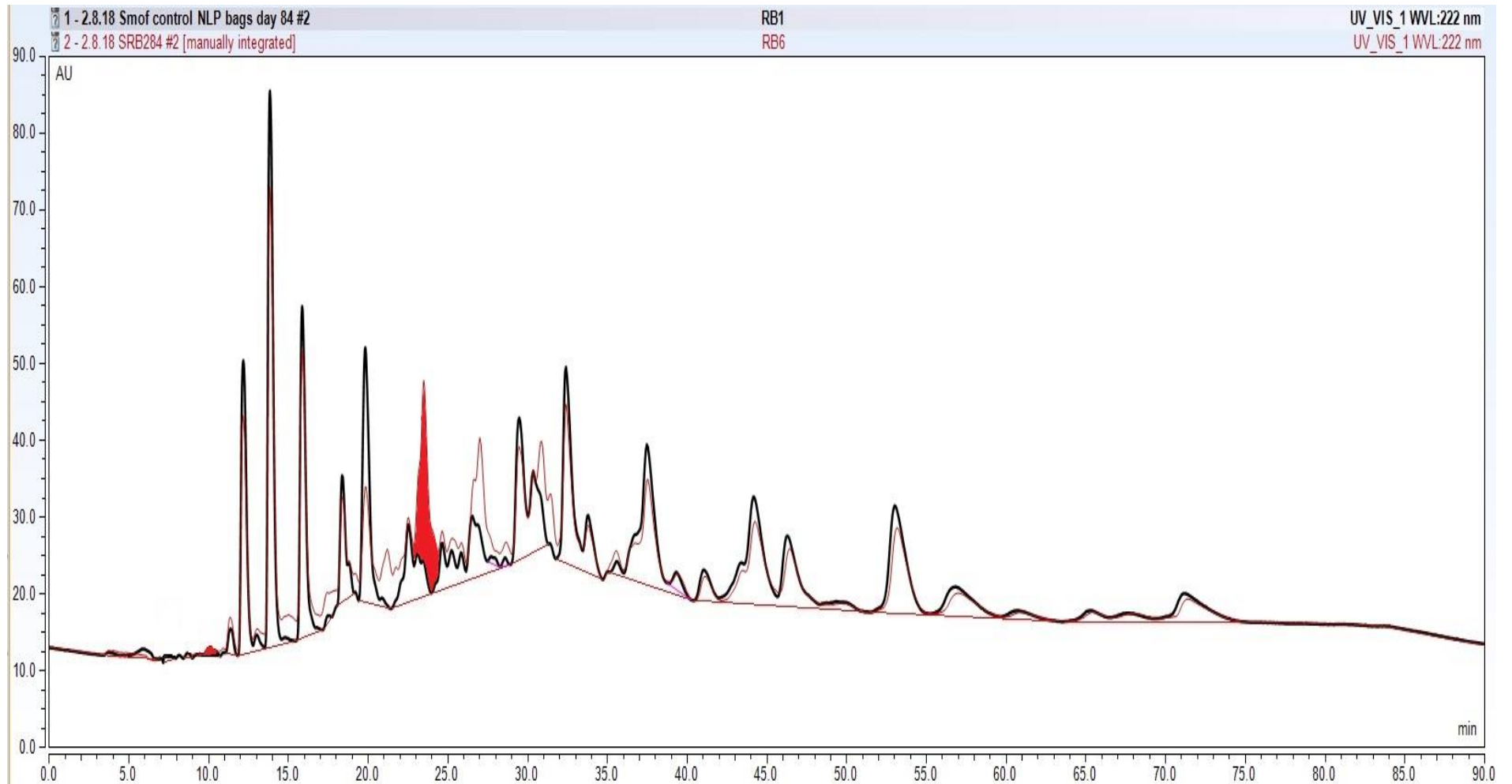
Figure 6.31 Overlaid HPLC-UV chromatograms of day 0 (black trace) and day 84 room temperature (red trace) SMOFlipid® 20 % stored in non-light protected 250 ml PN bags. Peak on the 84 day chromatogram highlighted in red shows the TAG remnant produced.

281

6.6. SMOFlipid® non-light protected vials results.

All 50 ml glass vials were filled as per protocol in section 3.4 and all possible atmospheric air removed through purging with nitrogen bubbled through the lipid and headspace. Air was further purged with nitrogen at all testing points to maintain an oxygen free environment through storage. Removal of lipid for testing was performed with a needle and syringe and at each timepoint the rubber septum was pierced in a different place to try and minimise air seeping into the vial. The purpose of the inclusion of glass vials within the study was to create a data set that indicated the importance of oxygen within the system with regards to TAG loss and peroxidation. All samples were tested in triplicate with standard deviations and relative standard deviations calculated. A control sample of lipid in its original container was tested at each timepoint and RSD's monitored for method precision. All chromatograms were integrated using Chromeleon software and peak areas recorded.

TAG results are presented as % loss from day 0 testing. All ten TAGs monitored showed minimal TAG losses over 84 days of storage. This is significant, as shown in previous chapters all lipids within vials had shown TAG losses later during storage due to hypothesised air leakage into the vial thereby initiating peroxidation. The method of vial testing (moving testing sites at each sampling time, re-purging with nitrogen) was modified after each set of testing, thereby ultimately creating a testing protocol where minimal TAG losses were shown, creating a positive set for comparison of lipid stored in an air-free testing environment. The results in this data set as presented in figures 6.32 to 6.41 show the very minimal TAG losses (maximum of ~ 7 %) over 84 days, with the majority of TAGs showing no loss. With respect to the control sample RSD's over 84 days the set of samples taken at day 2 exceeded the acceptable RSD level of 12 for peaks 2, 5, 6, 7,8 and 10 and as such results for day 2 were excluded from analysis (all results at this time point were 0).

Reinforcing the results shown in the TAG loss figured discussed above no detectable HNE, HUE or TAG remnant were seen throughout storage at either temperature of storage as shown in figured 6.42, 6.43 and 6.44. The results when considered collectively indicate a lack of peroxidation and TAG breakdown occurring, suggesting that a lack of oxygen within a storage system inhibits loss occurring. These results compound the evidence that oxygen presence is vital for the occurrence of peroxidation within SMOFlipid® and indicated that peroxidation is

the mechanism resulting in the observed TAG losses in other containers. Results are discussed further in section 6.7.
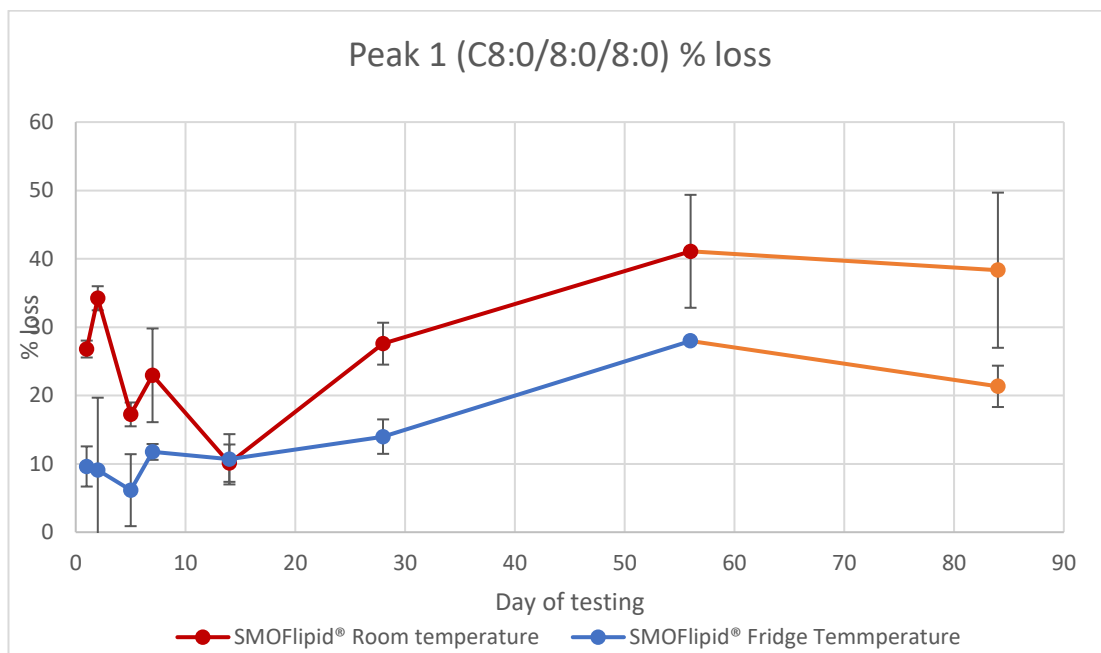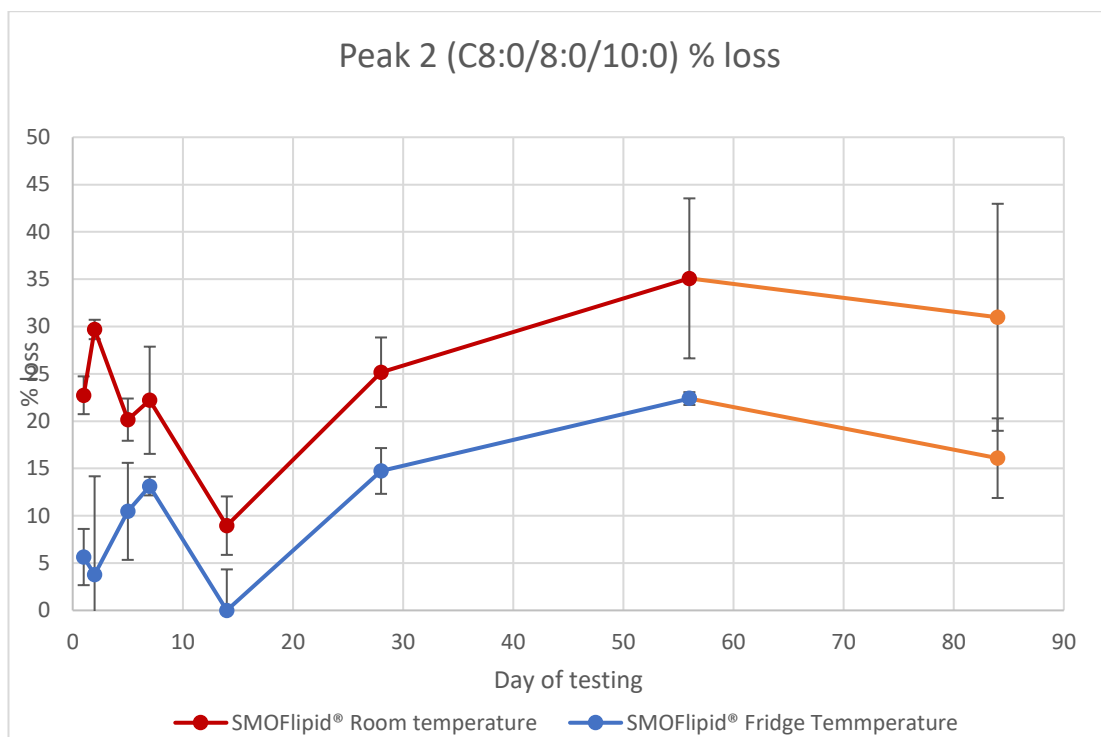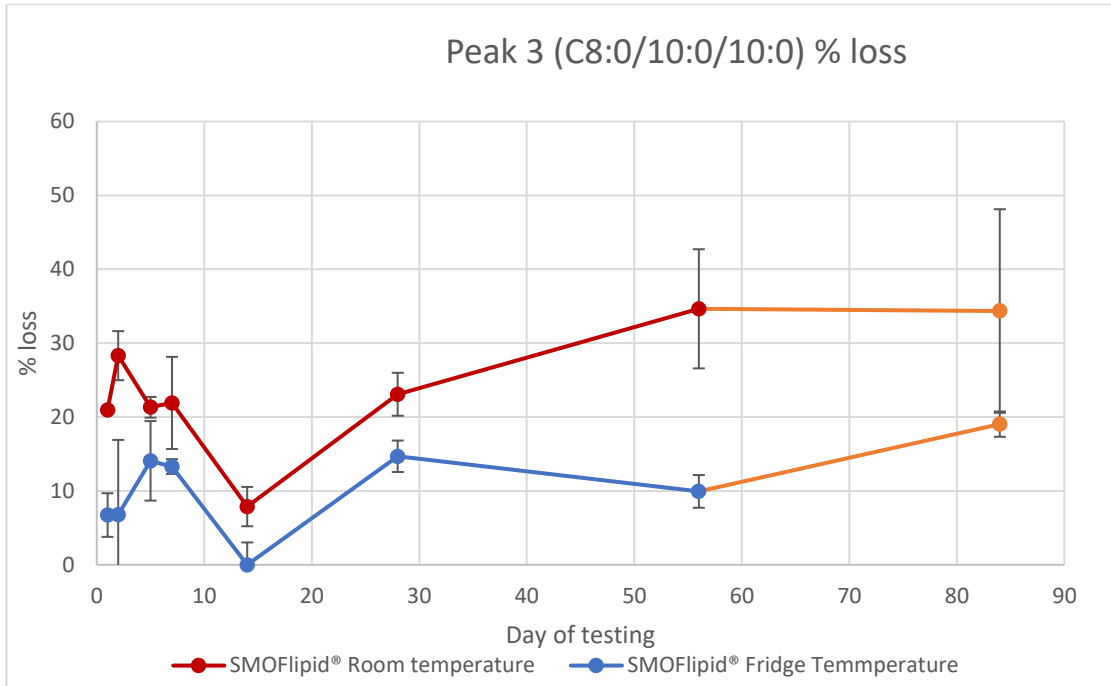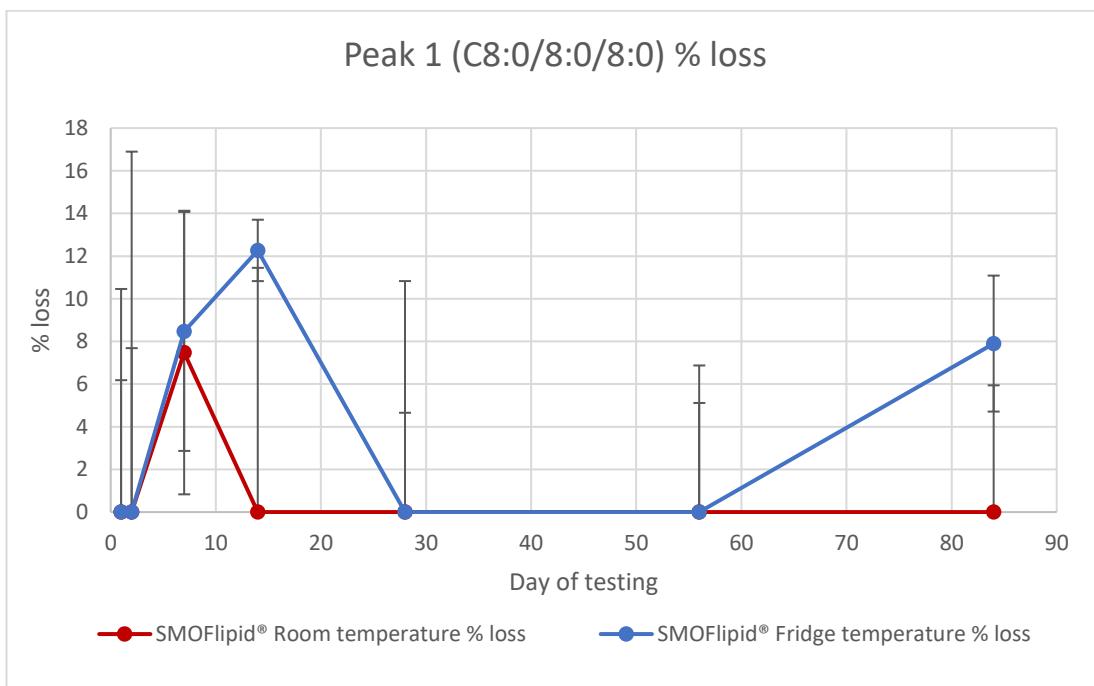

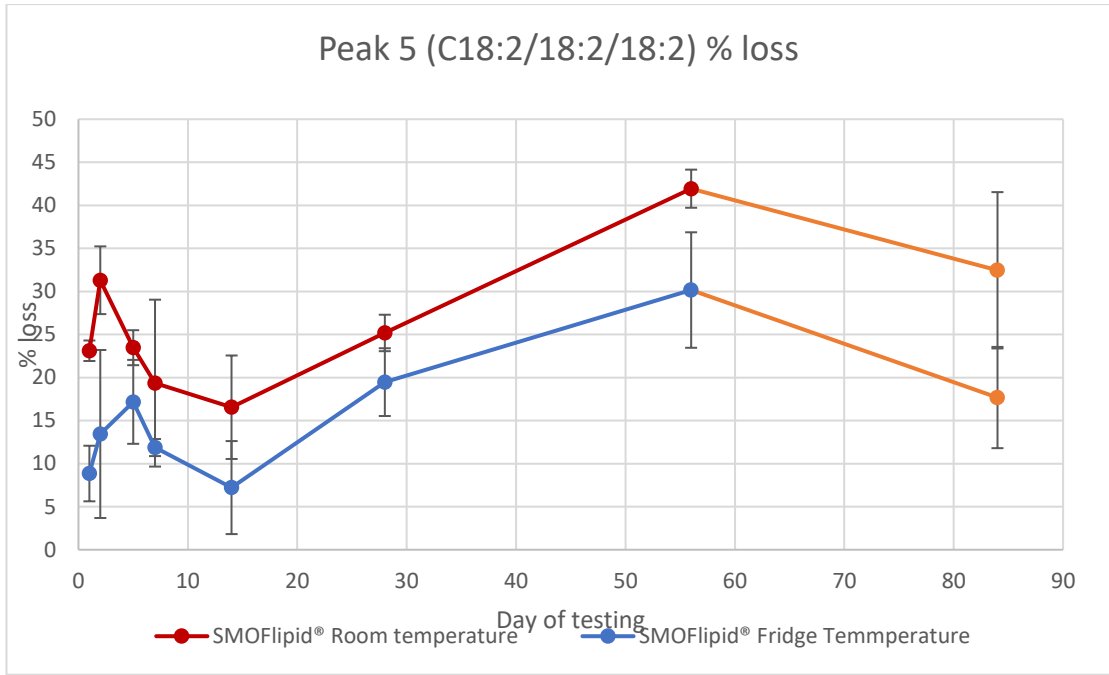*Figure 6.32 HPLC-CAD results for peak 1 (C8:0/8:0/8:0) triglyceride of SMOFlipid® 20 % stored in 50ml non-light protected glass vials. Percentage loss of peak shown calculated from day 0 data. Room (Red) and Fridge (Blue) results shown with standard deviation error bars on all points.*
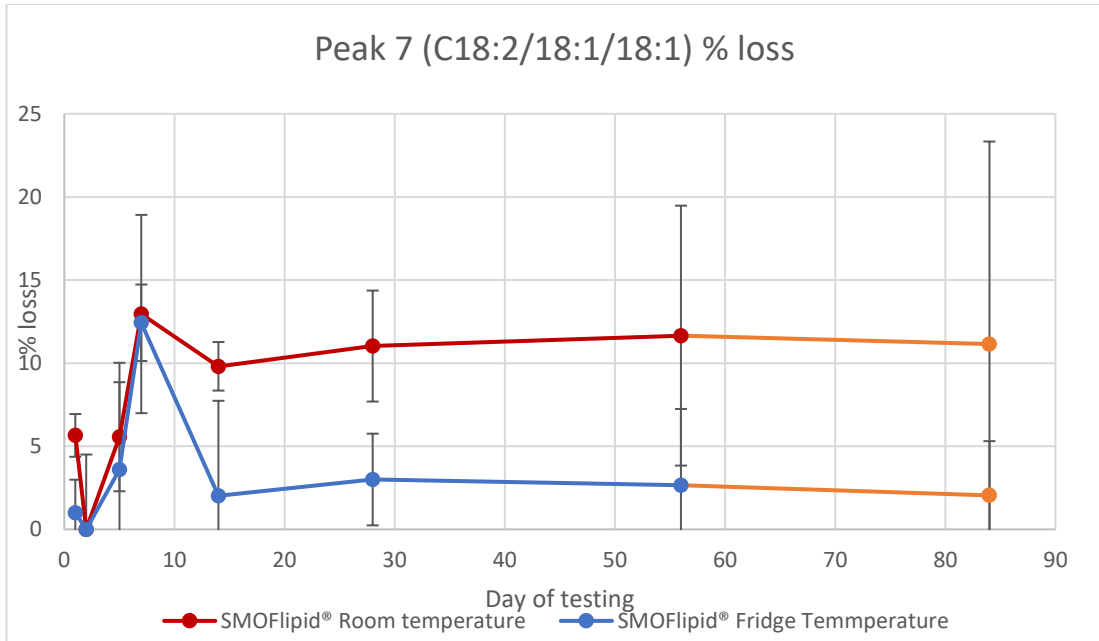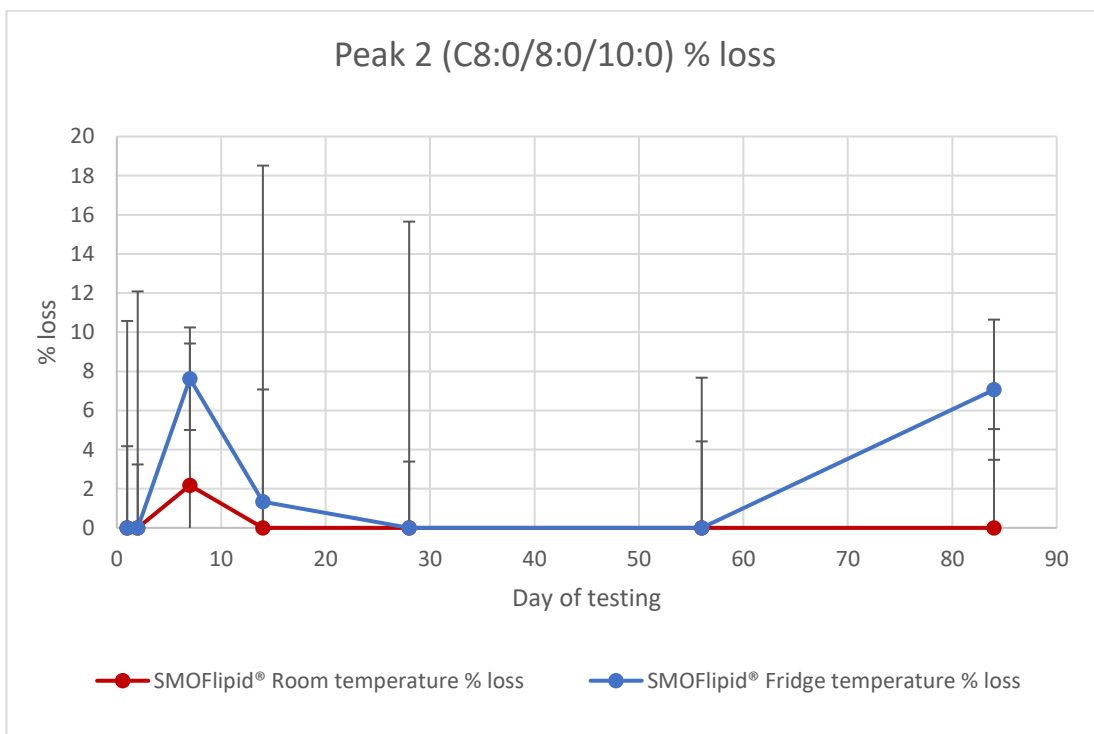

Figure 6.33 HPLC-CAD results for peak 2 (C8:0/8:0/10:0) triglyceride of SMOFlipid® 20 % stored in non-light protected 50 ml glass vials. Percentage loss of peak shown calculated from day 0 data. Room (Red) and Fridge (Blue) results shown with standard deviation error bars on all points.
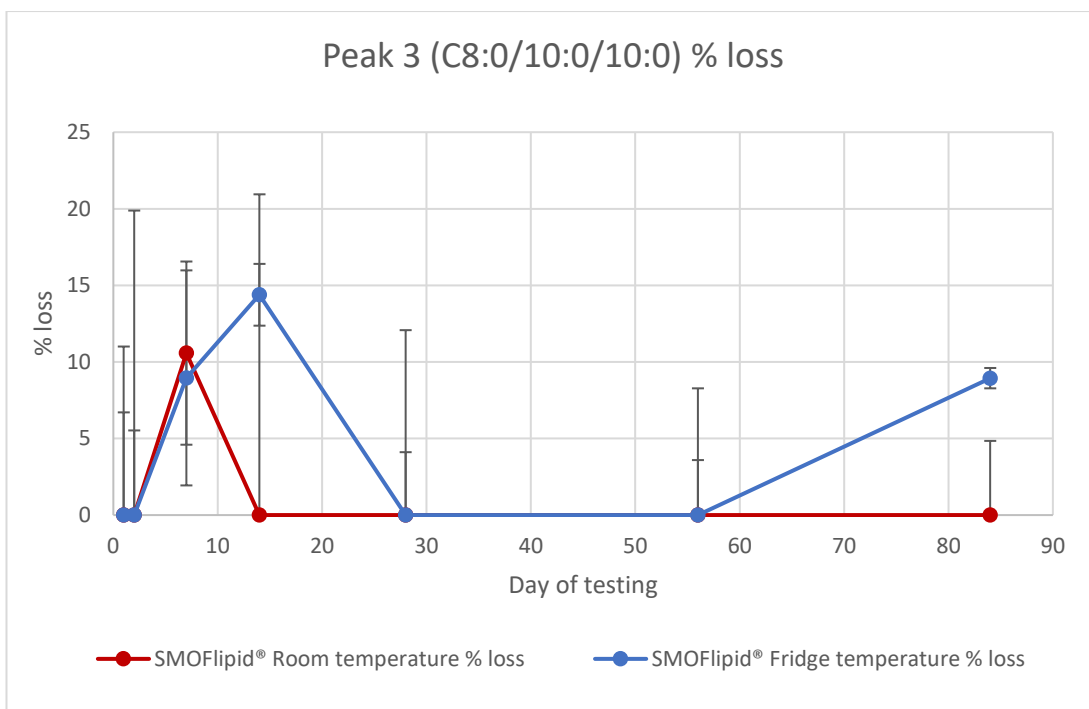
Figure 6.34 HPLC-CAD results for peak 3 (C8:0/10:0/10:0) triglyceride of SMOFlipid® 20 % stored in 50ml non-light protected glass vials. Percentage loss of peak shown calculated from day 0 data. Room (Red) and Fridge (Blue) results shown with standard deviation error bars on all points.
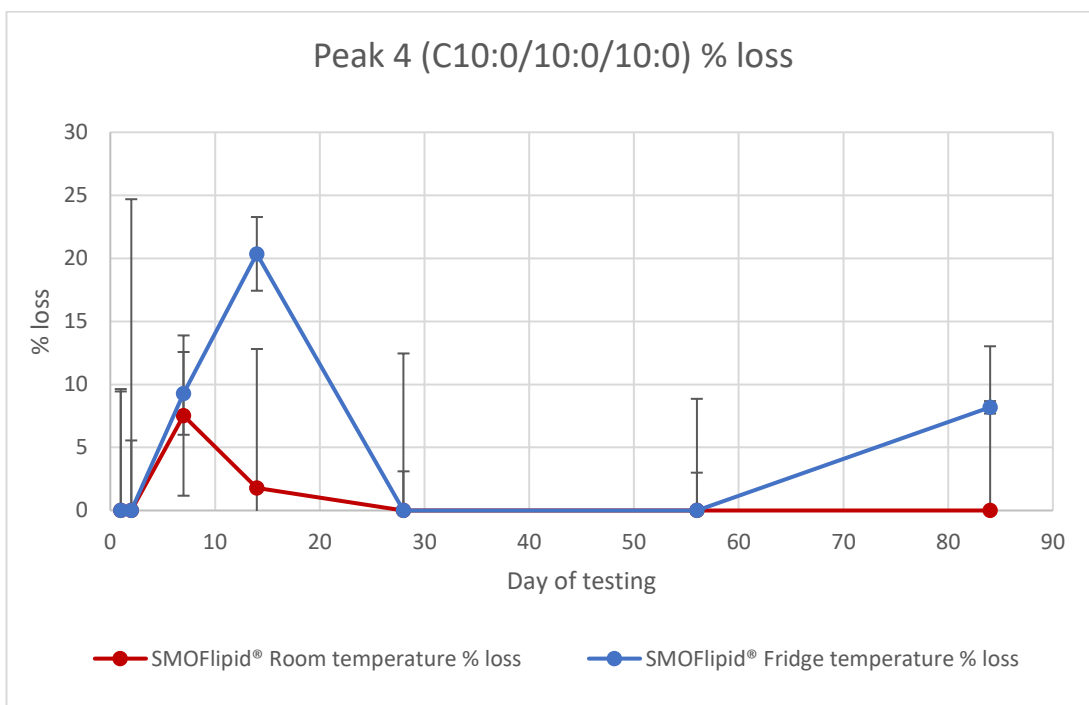
Figure 6.35 HPLC-CAD results for peak 4 (C10:0/10:0/10:0) triglyceride of SMOFlipid® 20 % stored in 50ml non-light protected glass vials. Percentage loss of peak shown calculated from day 0 data. Room (Red) and Fridge (Blue) results shown with standard deviation error bars on all points.
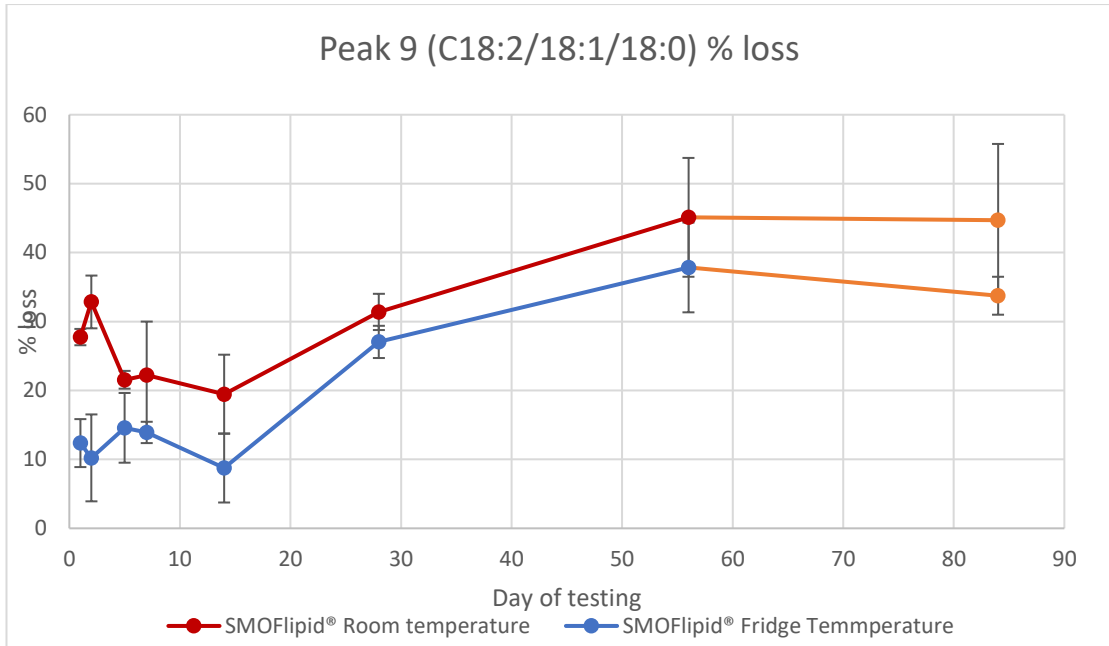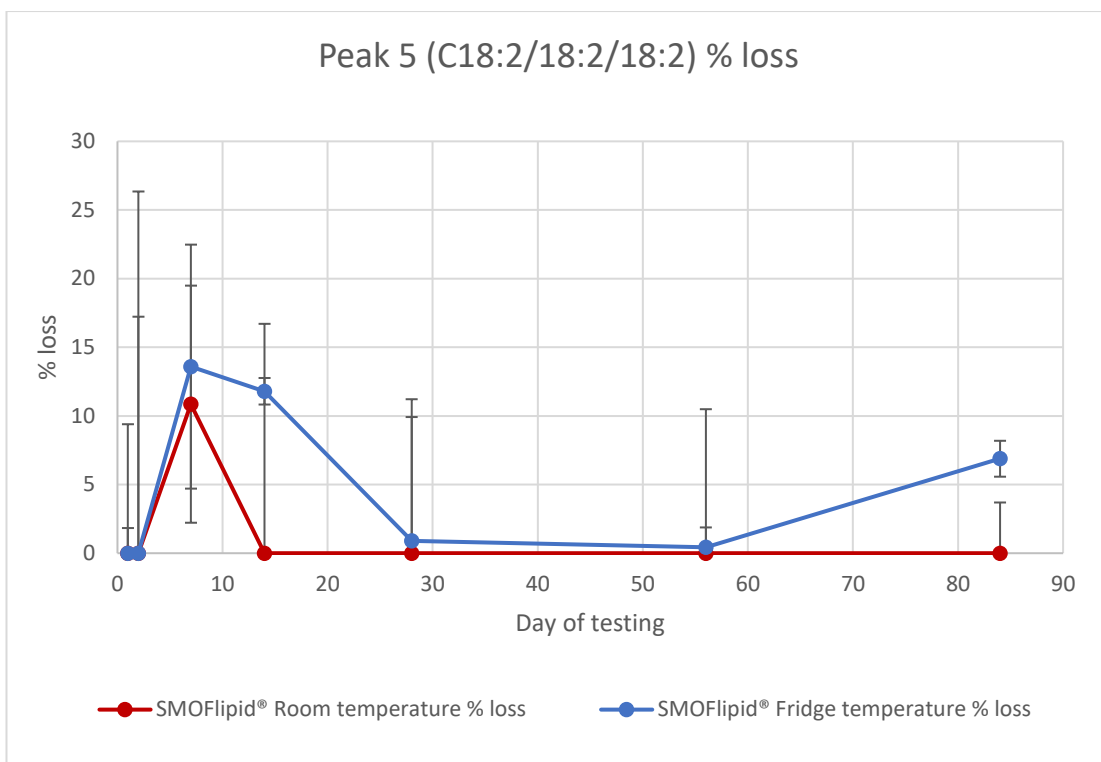
Figure 6.36 HPLC-CAD results for peak 5 (C18:2/18:2/18:2) triglyceride of SMOFlipid® 20 % stored in 50ml non-light protected glass vials. Percentage loss of peak shown calculated from day 0 data. Room (Red) and Fridge (Blue) results shown with standard deviation error bars on all points.
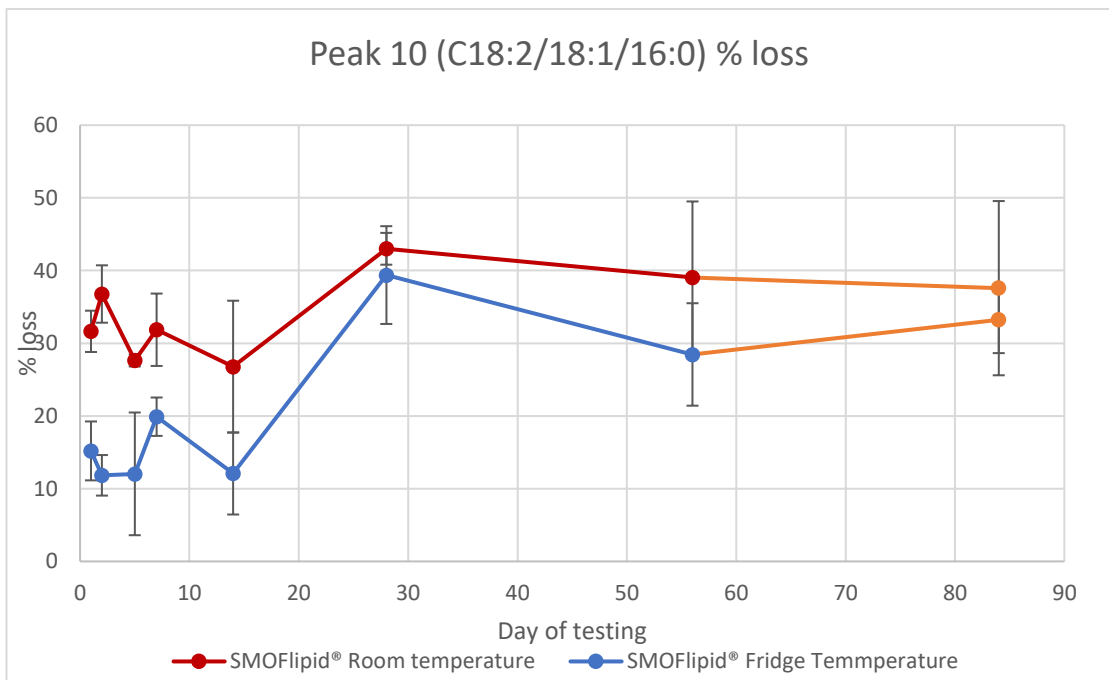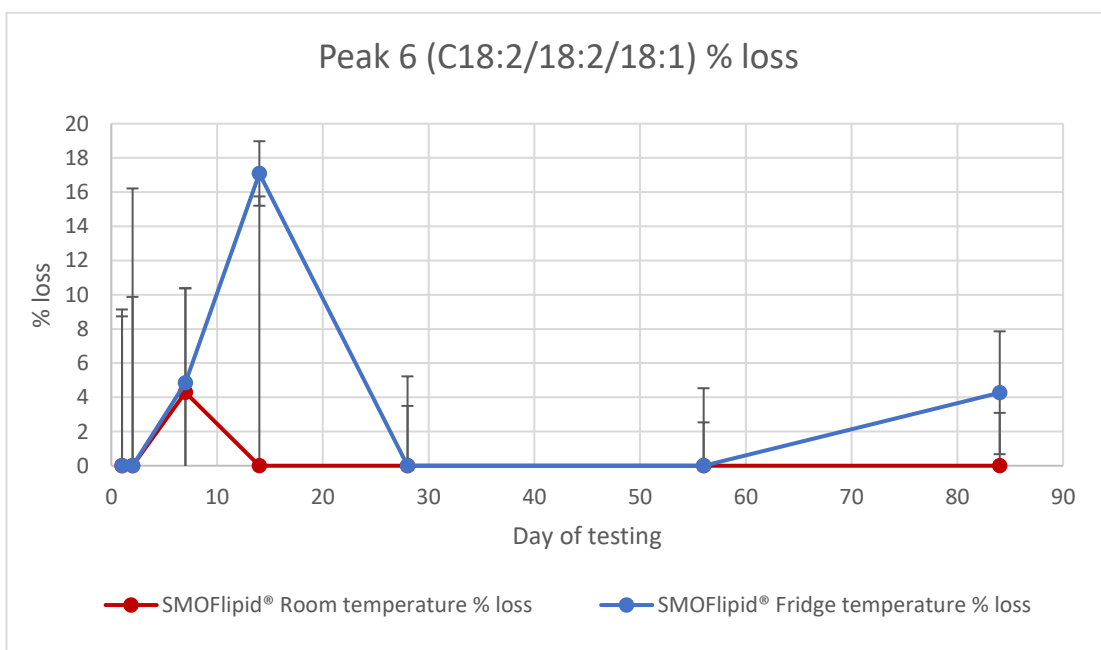

Figure 6.37 HPLC-CAD results for peak 6 (C18:2/18:2/18:1) triglyceride of SMOFlipid® 20 % stored in non-light protected 50 ml glass vials. Percentage loss of peak shown calculated from day 0 data. Room (Red) and Fridge (Blue) results shown with standard deviation error bars on all points.
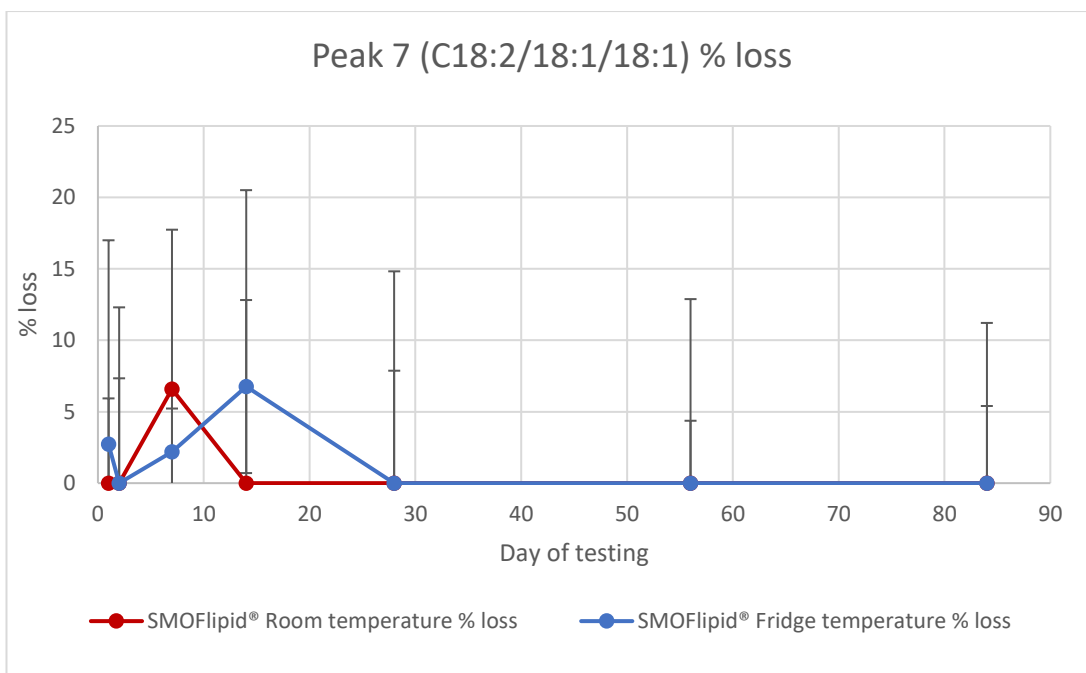
Figure 6.38 HPLC-CAD results for peak 7 (C18:2/18:1/18:1) triglyceride of SMOFlipid® 20 % stored in non-light protected 50 ml glass vials. Percentage loss of peak shown calculated from day 0 data. Room (Red) and Fridge (Blue) results shown with standard deviation error bars on all points.
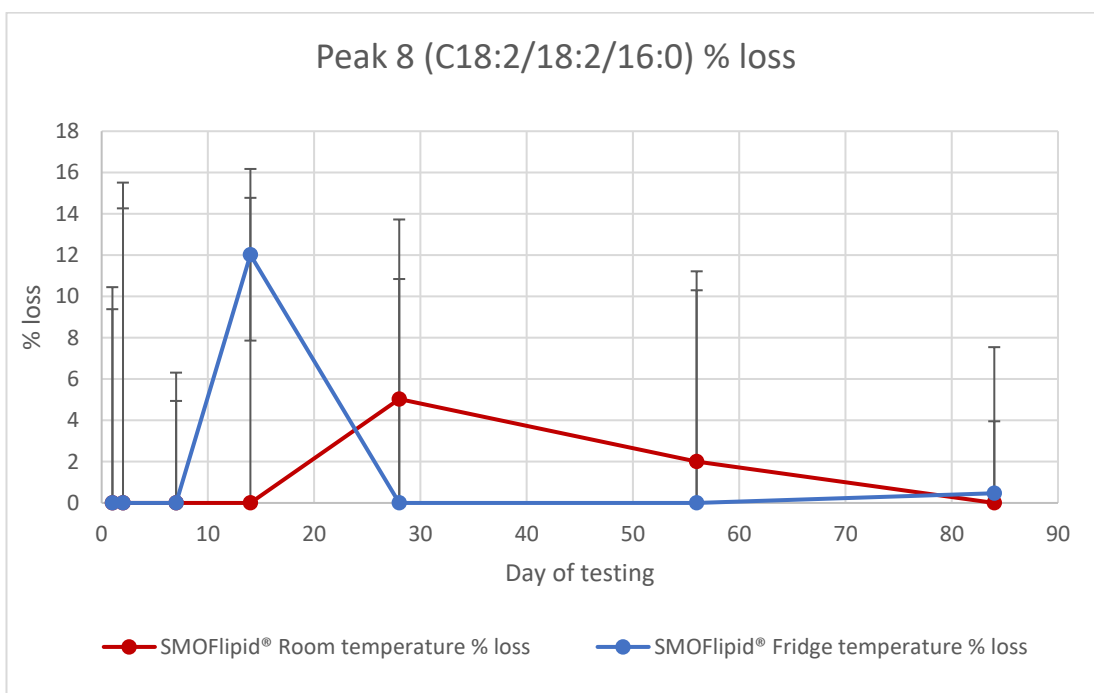

Figure 6.39 HPLC-CAD results for peak 8 (C18:2/18:2/16:0) triglyceride of SMOFlipid® 20 % stored in non-light protected 50 ml glass vials. Percentage loss of peak shown calculated from day 0 data. Room (Red) and Fridge (Blue) results shown with standard deviation error bars on all points.
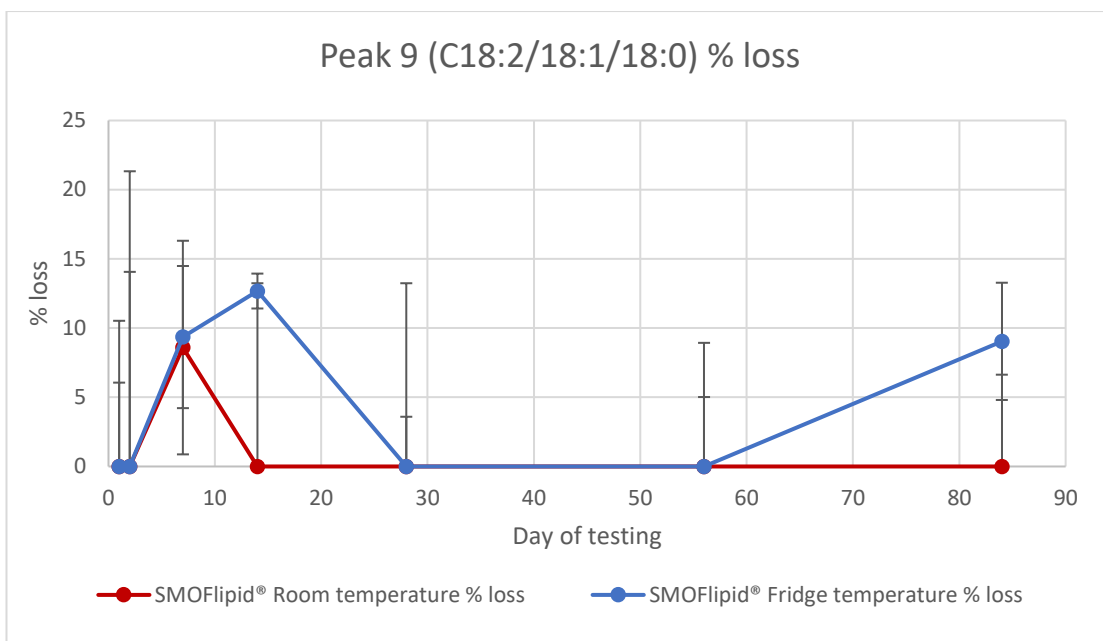
Figure 6.40 HPLC-CAD results for peak 9 (C18:2/18:1/18:0) triglyceride of SMOFlipid® 20 % stored in non-light protected 50 ml glass vials. Percentage loss of peak shown calculated from day 0 data. Room (Red) and Fridge (Blue) results shown with standard deviation error bars on all points.
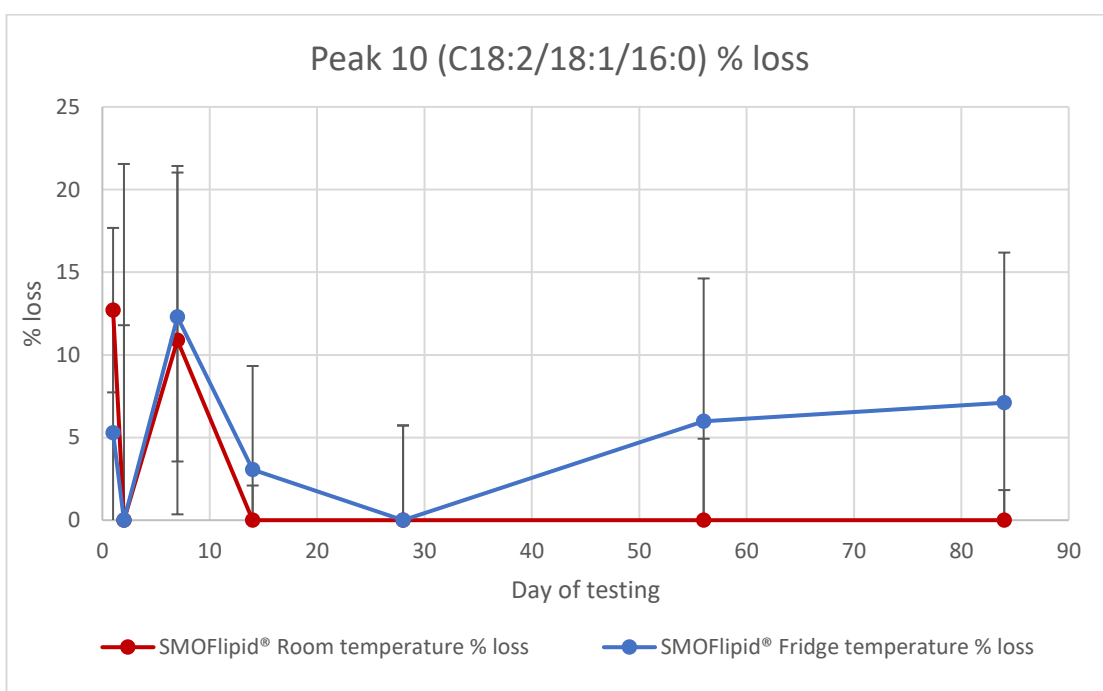
Figure 6.41HPLC-CAD results for peak 10 (C18:2/18:1/16:0) triglyceride of SMOFlipid® 20 % stored in non-light protected 50 ml glass vials. Percentage loss of peak shown calculated from day 0 data. Room (Red) and Fridge (Blue) results shown with standard deviation error bars on all points.
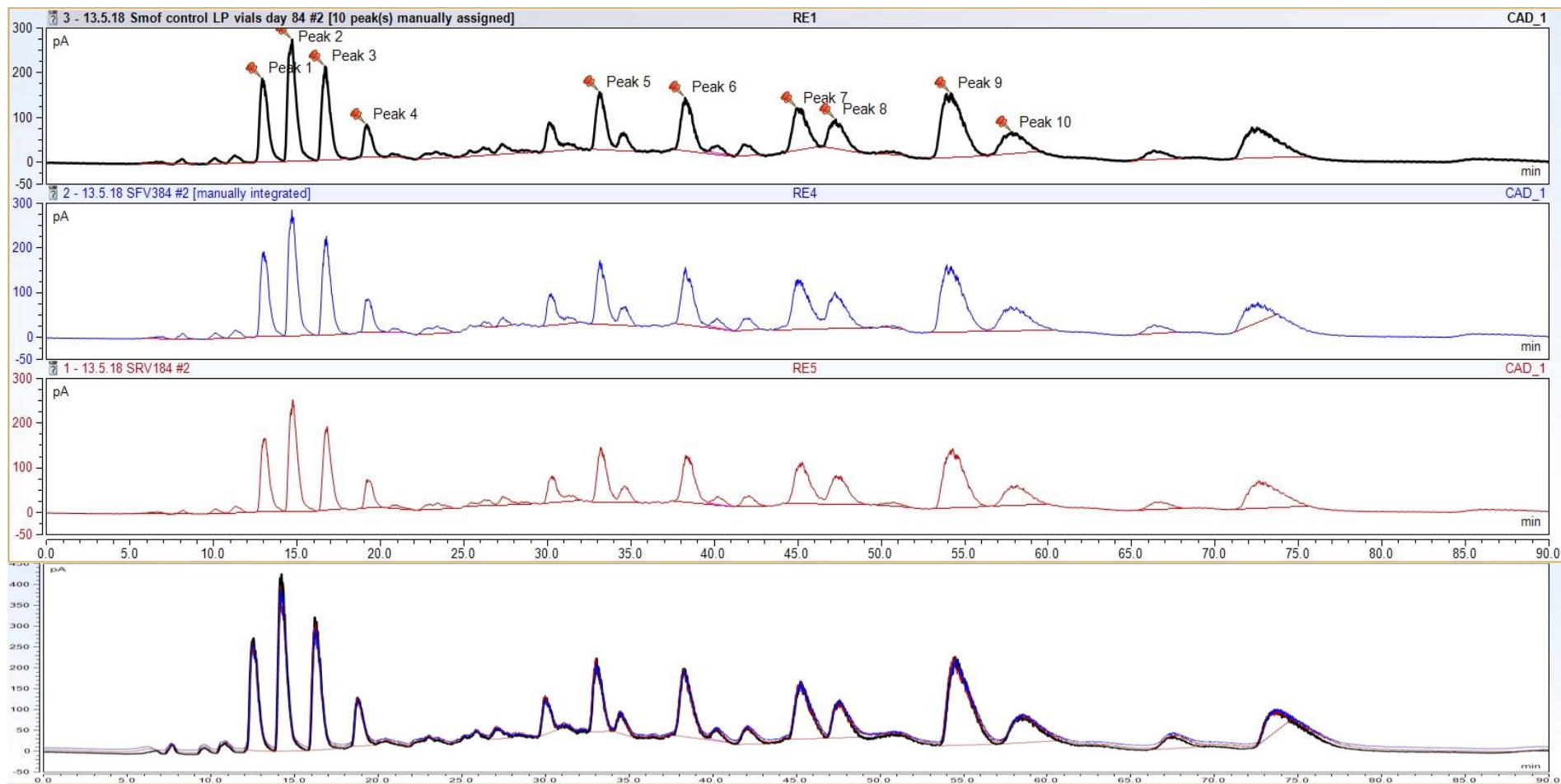
Figure 6.42 HPLC-CAD chromatograms of SMOFlipid® 20% stored in 50 ml non-light protected glass vials. Day 0 control (black), day 84 fridge temperature chromatogram (blue trace) and day 84 room temperature (red trace). Right hand axis (peak area) gives an indication of the lack of loss in peak area across 84 days compared to control. Overlaid chromatogram with signal time offset shows changes in peaks in comparison to control.

288
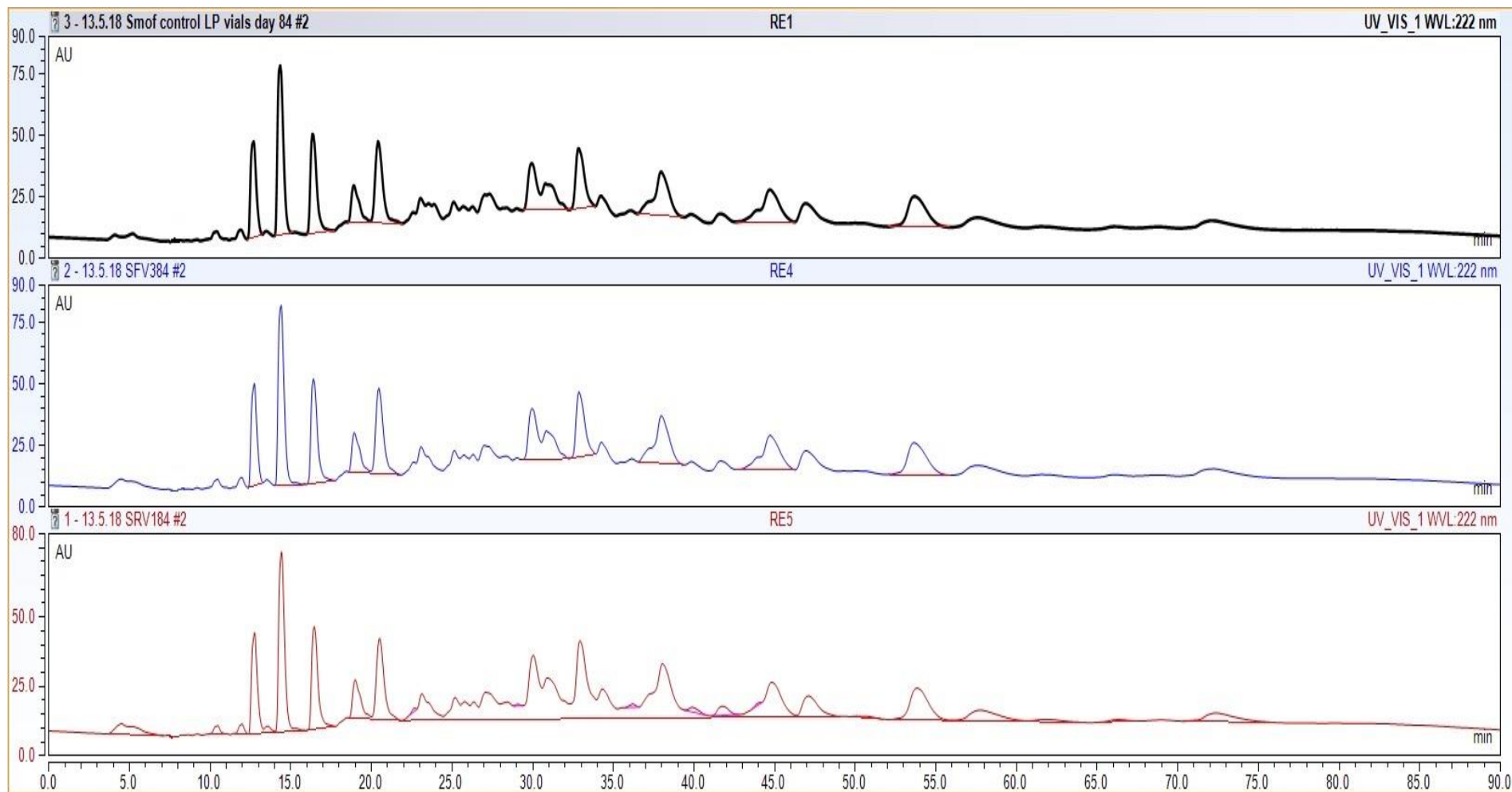
Figure 6.43 HPLC-UV chromatograms of SMOFlipid® 20% stored in 50 ml non-light protected glass vials. Day 0 chromatogram (black trace), day 84 fridge temperature syringes (blue trace) and day 84 room temperature syringes (red trace). The lack of production of new peaks indicates a lack of degradation products.
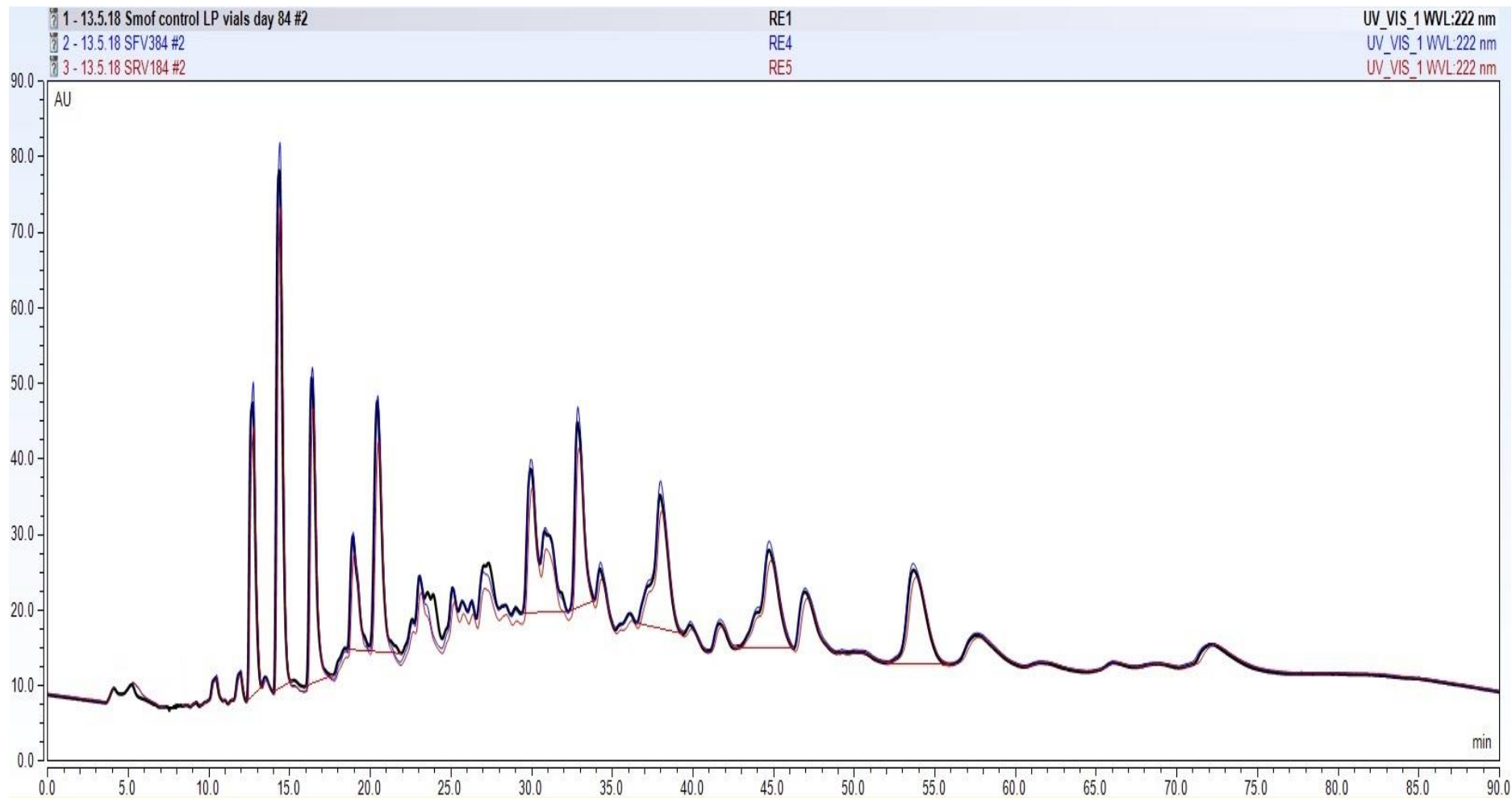
Figure 6.44 Overlaid HPLC-UV chromatograms. Day 0 (back trace) and day 84 room temperature (red trace) and fridge temperature (blue) SMOFlipid® stored in non-light protected 50 ml glass vials. The presence of no new peaks indicates a lack of degradation/peroxidation products seen at 222 nm wavelength.

6.7. Discussion of SMOFlipid® non-light protected results.

6.7.1. Triglyceride loss

When considering the TAG losses between different containers of SMOFlipid® when not-light protected, the RSD drift observed in day 56 and 84 syringes and day 28 PN bag results make comparison difficult. However, figures 6.46 and 6.45 show the TAG losses at day 7 and day 84 for all containers with standard deviation. The day 84 results for syringes were recorded as markedly higher however the RSD of the control samples at this timepoint (~ 22) was nearly double that of the acceptable variation in precision. Whilst not considered precise due to the variation in control samples the TAG losses in syringes for day 84 as shown in 6.45 have been corrected by the same amount as the variation in the control sample. This enables the day 84 results to be broadly compared between containers. PN bags showed maximal losses at all peaks except peak 7 (C18:2/18:1/18:1) where minimal losses (>5 %) were recorded across all containers. Unsaturated peaks (5, 8, 9 and 10) showed significant losses in PN bags at all temperatures. These peaks correspond to TAGs containing C18:2 and 18:1 fatty acids and present TAG losses of between 20 to 25 % as discussed in previous results sections. The smallest levels of TAG losses through all containers was observed in peak 6 (C18:2/18:2/18:1) and peak 7 (C18:2/18:1/18:1) which is markedly different to the results observed in other chapters and discussed further in chapter 7.

When considering the effect of temperature on the level of TAG losses observed, table 6.1 shows results that are statistically significant ($P<0.05$) between containers at fridge and room temperatures as tested by ANOVA one-way analysis with Tukey post hoc testing. Significant differences are recorded between temperatures in syringes for peaks 1, 2, 3, 4, 5, 9 and 10, corresponding to the four saturated TAGs monitored (peaks 1 to 4), peak 5 (C18:2/18:2/18:2), peak 9 (C18:2/18:1/18:0) and peak 10 (C18:2/18:1/16:0). No statistically significant differences were observed in PN bags at different temperatures and glass vials showed a single significant result for peak 3 (C8:0/10:0/10:0). Results indicate that temperature has the largest effect on TAG loss in syringes. One can postulate that a raised temperature acts by increasing the collisions between TAG molecules thus increasing TAG loss both through peroxidation and hydrolysis. Whilst table 6.1 shows statistical significance between non-light protected containers at two temperatures, trends exist between

the data created in all previous chapters and as such all are discussed further in chapter 7.

Loss of saturated TAGs occurred both in PN bags (up to ~30 %) and in syringes (~17 %). In both containers, loss occurred at 84 days when there was significant unsaturated peroxidation (peaks 5 (C18:2/18:2/18:2), 8 (C18:2/18:2/16:0), 9 (C18:2/18:1/18:0) and 10 (C18:2/18:1/16:0). This, as discussed in chapter 5 (section 5.7.2) indicates saturated TAG losses occurring at high energy levels through processes other than peroxidation. It is postulated that hydrolysis reactions leading to cleavage of fatty acids from the saturated TAG backbone result in the TAG losses observed. When looking at figure 6.45 showing the TAG losses occurring at day 7, saturated TAG losses are observed in all containers up to ~15 % (room temperature PN bags). Levels of losses in unsaturated TAGs at this timepoint are only raised in room temperature syringes and glass vials whilst PN bag unsaturated losses are < 5 %. This is of interest as previous data only show saturated TAG losses occurring when high levels of unsaturated TAG loss and perceived peroxidation is recorded. The data suggests the breakdown of saturated TAGs through hydrolysis occurred in relatively low energy systems where little other peroxidation was observed. As such the postulated hydrolysis reactions and the availability of water within the emulsion must be considered and is discussed further in chapter 7.

6.7.2. RSD variation

As indicated throughout the testing in this chapter, both syringe and PN bags at days 56 and 84 and day 28 respectively recorded control sample results that resulted in RSD values above an acceptable level, up to a maximum of ~22. All testing was undertaken over a tight testing schedule and as such was carried out over a period of around 4.5 weeks where raised temperatures within the laboratory were experienced. This was due to the unusually hot weather at the time and was unavoidable. Whilst every effort was made to reduce temperatures within the laboratory environment, the raised temperatures resulted in the RSD and result variations seen within this time period. This affected results at different timepoints across all lipids and containers tested and is discussed further in chapter 7.
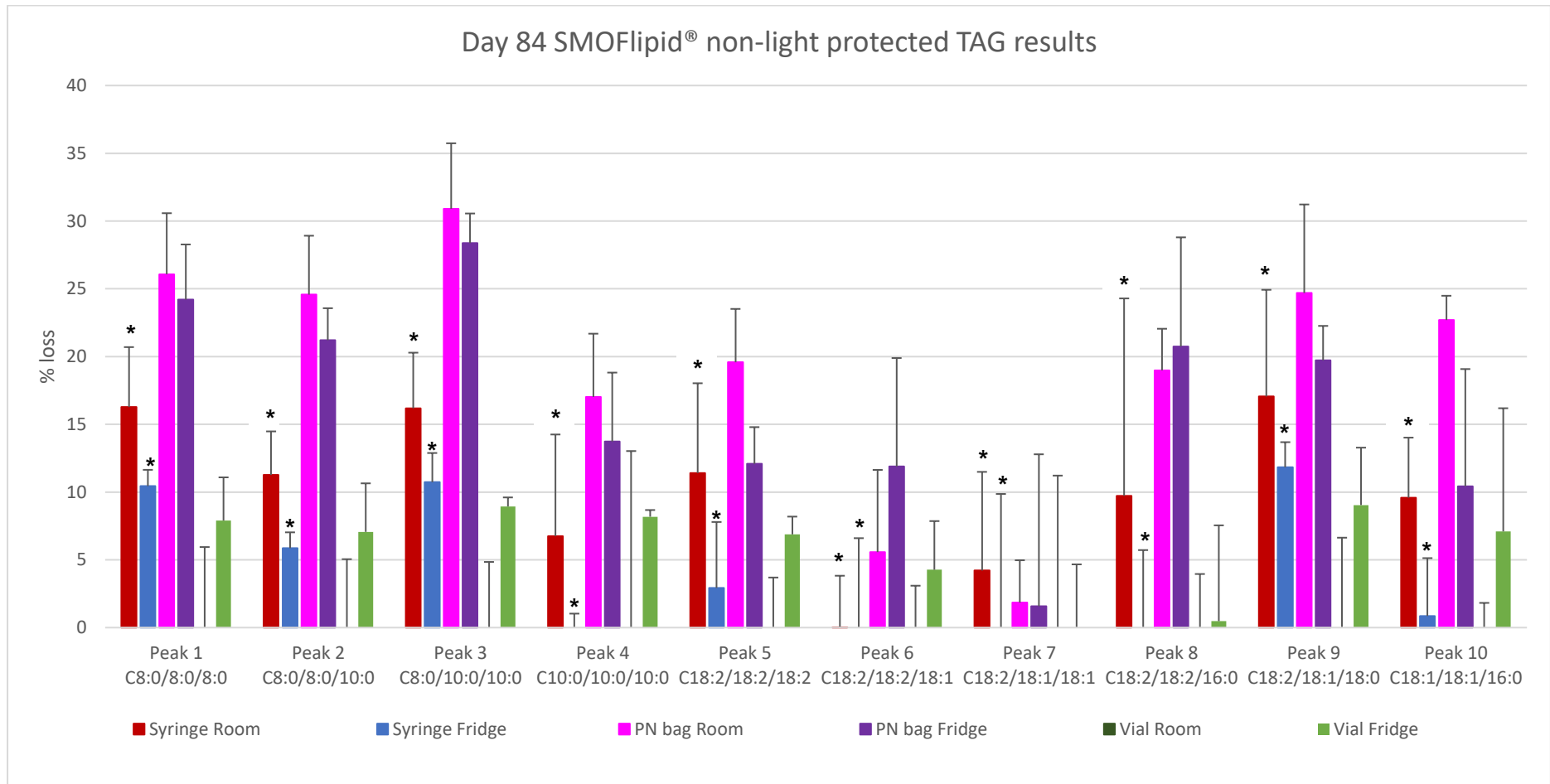
*Figure 6.45 Triglyceride loss at 84 days storage for SMOFlipid® stored in non-light protected syringes, PN bags and glass vials. * Denotes syringe results adjusted according to level of RSD drift of control sample as discussed in section 6.7.1.*
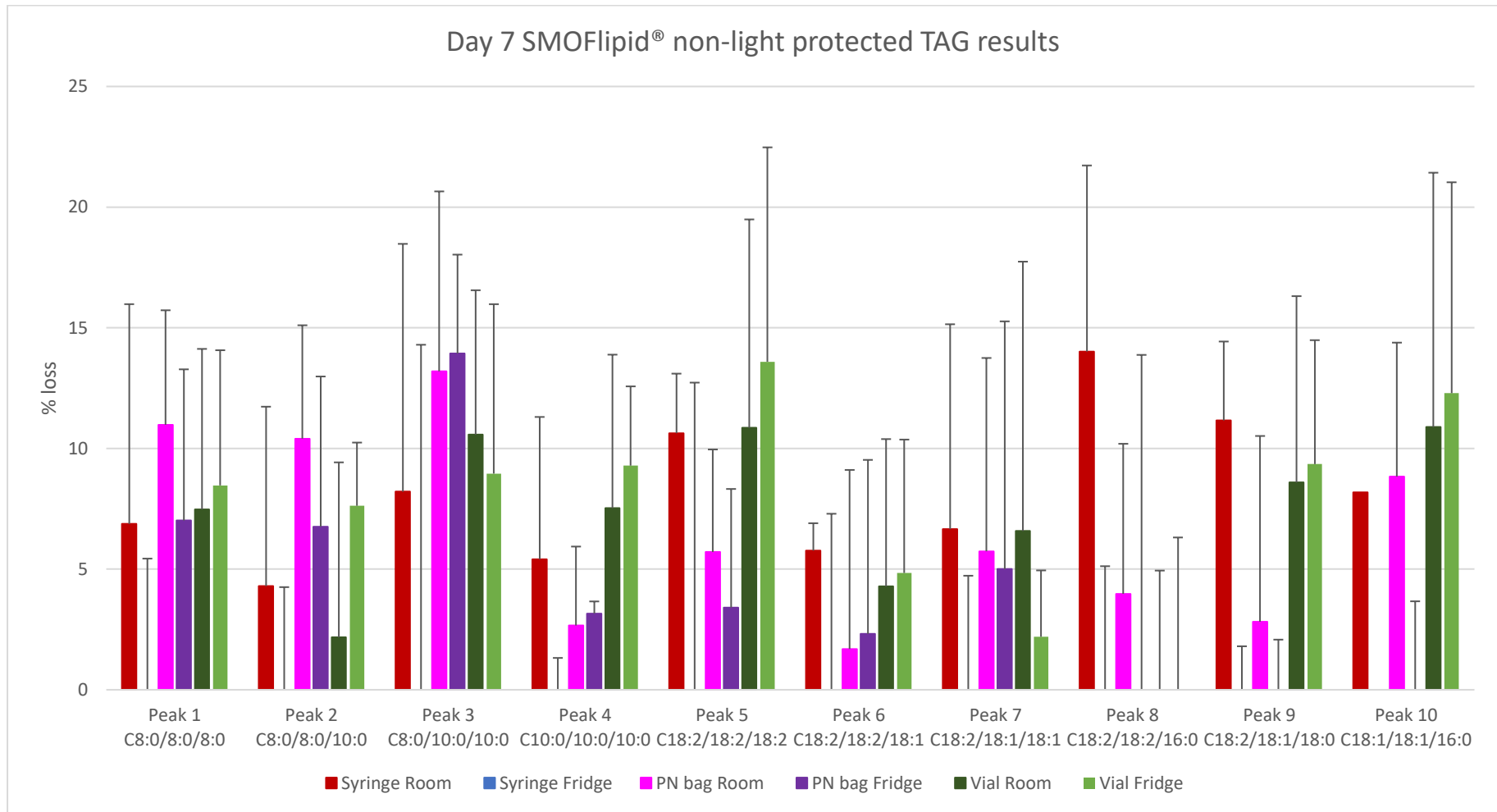
Figure 6.46 Triglyceride loss at 7 days storage for SMOFlipid® stored in non-light protected syringes, PN bags and glass vials.

Table 6.1 Non-light protected SMOFlipid® in all containers at all temperatures for each of the ten peaks monitored. * indicates significant differences between results as calculated through ANOVA analysis with post hock Tukey analysis between each container type. (significant defined as P<0.05).

Peak 1

Peak 1	Room syringe	Room Bag	Room Vial	Fridge Syringe	Fridge Bag	Fridge Vial
Room Syringe	▨	*	*	*	*	*
Room Bag	*	▨	*			*
Room Vial	*	*	▨	*	*	
Fridge Syringe	*		*	▨		*
Fridge Bag	*		*		▨	*
Fridge Vial	*	*		*	*	▨

Peak 5

Peak 5	Room syringe	Room Bag	Room Vial	Fridge Syringe	Fridge Bag	Fridge Vial
Room Syringe	▨	*	*	*		
Room Bag	*	▨	*			*
Room Vial	*	*	▨			
Fridge Syringe	*			▨	*	
Fridge Bag	*				▨	
Fridge Vial	*	*			*	▨

Peak 2

Peak 2	Room syringe	Room Bag	Room Vial	Fridge Syringe	Fridge Bag	Fridge Vial
Room Syringe	▨	*	*	*	*	*
Room Bag	*	▨	*			*
Room Vial	*	*	▨	*	*	
Fridge Syringe	*		*	▨		*
Fridge Bag	*		*		▨	
Fridge Vial	*	*		*	*	▨

Peak 6

Peak 6	Room syringe	Room Bag	Room Vial	Fridge Syringe	Fridge Bag	Fridge Vial
Room Syringe	▨					
Room Bag		▨				
Room Vial			▨	*		
Fridge Syringe				▨	*	
Fridge Bag			*	*	▨	
Fridge Vial						▨

Peak 9

Peak 9	Room syringe	Room Bag	Room Vial	Fridge Syringe	Fridge Bag	Fridge Vial
Room Syringe	▨	*	*	*	*	*
Room Bag	*	▨				*
Room Vial	*		▨		*	*
Fridge Syringe	*			▨	*	*
Fridge Bag	*		*	*	▨	
Fridge Vial	*	*		*		▨

Peak 3

Peak 3	Room syringe	Room Bag	Room Vial	Fridge Syringe	Fridge Bag	Fridge Vial
Room Syringe	▨	*	*	*	*	*
Room Bag	*	▨	*			*
Room Vial	*	*	▨	*	*	*
Fridge Syringe	*		*	▨		*
Fridge Bag	*		*		▨	*
Fridge Vial	*	*	*	*	*	▨

Peak 7

Peak 7	Room syringe	Room Bag	Room Vial	Fridge Syringe	Fridge Bag	Fridge Vial
Room Syringe	▨					
Room Bag		▨				
Room Vial			▨		*	
Fridge Syringe				▨	*	
Fridge Bag			*	*	▨	
Fridge Vial						▨

Peak 10

Peak 10	Room syringe	Room Bag	Room Vial	Fridge Syringe	Fridge Bag	Fridge Vial
Room Syringe	▨		*	*	*	*
Room Bag		▨	*	*		
Room Vial	*	*	▨			
Fridge Syringe	*	*		▨		
Fridge Bag	*				▨	
Fridge Vial	*					▨

Peak 4

Peak 4	Room syringe	Room Bag	Room Vial	Fridge Syringe	Fridge Bag	Fridge Vial
Room Syringe	▨		*	*		*
Room Bag		▨	*	*		
Room Vial	*	*	▨			
Fridge Syringe	*	*		▨	*	
Fridge Bag				*	▨	
Fridge Vial	*					▨

Peak 8

Peak 8	Room syringe	Room Bag	Room Vial	Fridge Syringe	Fridge Bag	Fridge Vial
Room Syringe	▨					
Room Bag		▨				
Room Vial			▨		*	
Fridge Syringe				▨	*	
Fridge Bag			*	*	▨	
Fridge Vial						▨

6.7.3. HNE, HUE and TAG remnant production.

As discussed in section 6.4, HNE was only detected in non-light protected syringes (13.6 µM at room temperature and 10.2 µM at fridge temperature). The formation of HNE as one of the secondary products of the peroxidation of linoleic acid was predicted to occur where TAGs with C18:2 fatty acids underwent large losses. As figure 6.45 shows, peaks 5 (C18:2/18:2/18:2), 6 (C18:2/18:2/18:1), 7 (C18:2/18:1/18:1), 8 (C18:2/18:2/16:0) and 9 (C18:2/18:1/18:0) all showed maximal losses in PN bags as opposed to syringes. Room temperature syringes where HNE was maximal experienced TAG losses of peak 5, 8 and 9 however all were less than PN bags. As such it can be postulated that peroxidation occurring in syringes resulted in different products being formed vs PN bags. As previously discussed in chapter 5 there are multiple potential sites for the peroxidation of linoleic acid, resulting in four potential hydroperoxides. From these primary products HNE is only one of multiple secondary products that can be formed. The lack of HNE in PN bags indicates a lack of peroxidation occurring at the 9' position of the linoleic acid backbone. The relatively large TAG losses occurring in such bags indicate peroxidation or breakdown of TAGs **is** occurring. Therefore, the peroxidation of linoleic acid containing TAGs within PN bags is resulting either in other secondary peroxidation products being formed or the loss of whole fatty acids from the glycerol backbone of the triglyceride through hydrolysis. The presence of a large proportion of water within the SMOFlipid® emulsion needs to be considered in the losses of all TAGs both saturated and unsaturated that are observed. Whilst this is discussed in detail in chapter 7, it is important to note that hydrolysis alone cannot be attributed to the TAG losses observed in all containers. This is substantiated by the detection of the secondary peroxidation product HUE in room temperature syringes and room temperature PN bags. Figure 6.47 shows the production of HUE in both bags and syringes. As indicated maximal HUE is formed within room temperature syringes. Whilst as previously discussed the concentration of HUE present cannot be calculated due to a lack of available standard for validation, both the peak heights observed for room temperature syringes and PN bags give a signal to noise ratio of >3 and are therefore detectable. Temperature has an effect on HUE formation with fridge storage inhibiting its formation (discussed further in chapter 7).

Figure 6.48 shows the TAG remnant formation in both room temperature syringes and PN bags. Maximal amounts were recorded in PN bags, corresponding to the higher levels of TAG losses observed. As previously postulated the TAG remnant

m/z corresponds to the breakdown of peak 7 (C18:2/18:1/18:1). The results shown in figure 6.45 indicate minimal losses to this peak 7 and therefore the production of relatively large quantities of TAG remnant (see chapter 7 for comparisons) is of interest. The m/z of the TAG remnant as identified through mass spectrometry was 495.40 (496.4 [M-H]$^+$) and postulated to be from the peroxidation of peak 7 creating HNE and HUE and the TAG remnant. The lack of apparent peak 7 peroxidation and the presence of water within the emulsions results in the conclusion that the TAG remnant could also be due to a different peak/TAG breakdown. A combination of peroxidation and hydrolysis of different TAG peaks resulting in a TAG remnant with the same m/z ratio as identified, offers a potential explanation for the presence of the TAG remnant and lack of HUE and HNE seen in PN bags. The specific TAGs liable to breakdown and the chemical processes resulting in the TAG remnant formation are discussed further in chapter 7.
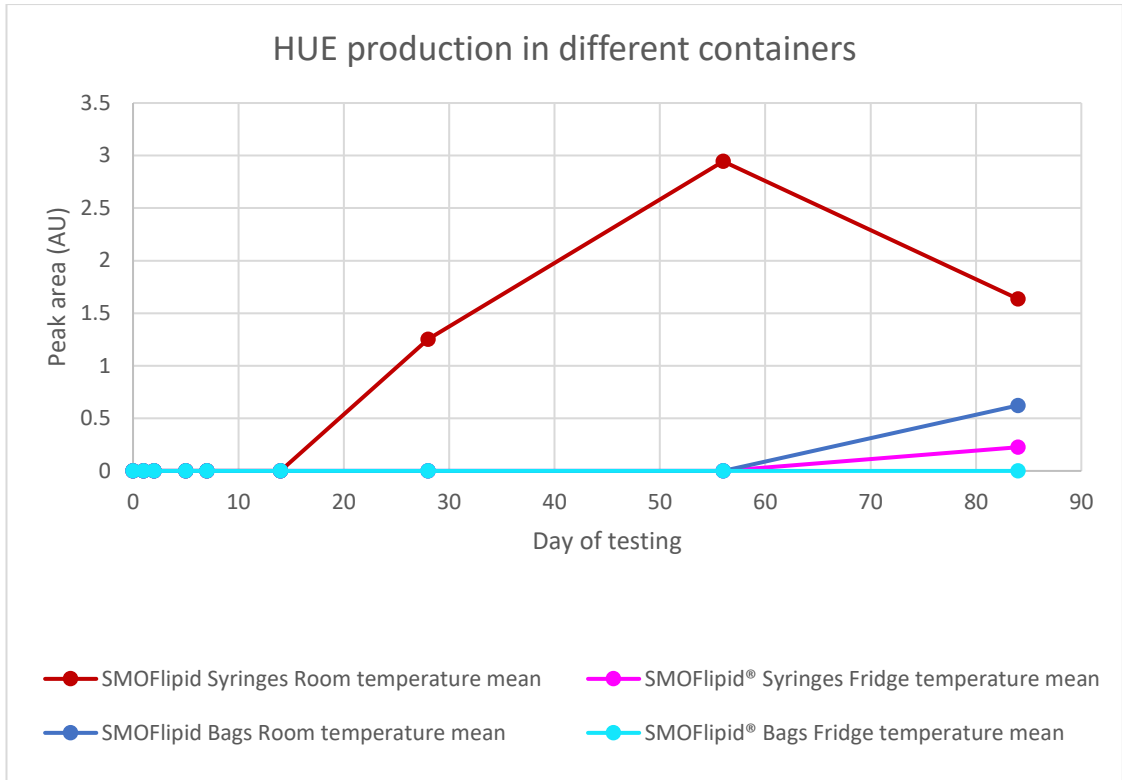
Figure 6.47 Production of HUE in non-light protected syringes and PN bags with 50 ml of SMOFlipid® over 84 days storage.
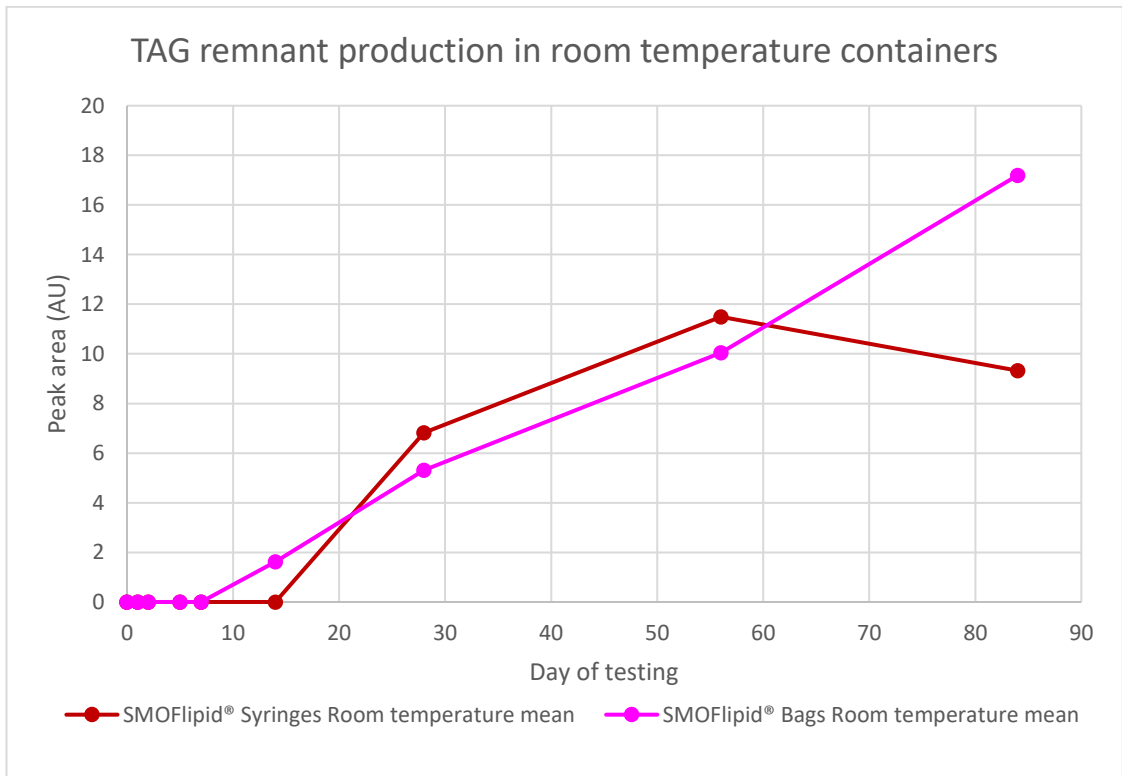
Figure 6.48 TAG remnant production in non-light protected SMOFlipid® room temperature syringes and PN bags over 84 days storage.

Chapter 7

Lipid Formulation Comparisons, Discussion and Conclusions

The following chapter is divided into two main sections, initially the comparison of SMOFLipid® and Intralipid® results in the four previous chapters followed by discussion of the results and conclusions from this thesis.

7.1. Introduction to SMOFlipid® and Intralipid® comparisons

Due to the large amount of data presented in the previous chapters, comparisons between each of the two lipid formulations tested is presented in the following text by dividing results into the following sections;

- Peroxidation products monitored (HNE, HUE and TAG remnant).
- Unsaturated TAGs monitored (peaks 5 to 10) are compared considering light protected and non-light protected results and differences between temperatures of storage
- Saturated TAG losses only seen in SMOFlipid® are discussed with comparisons between light and non-light protection and temperature.
- All of the monitored TAGs (1 to 10) comparisons are presented split into each container type followed by comparison between containers for each lipid.

7.2. Peroxidation product comparisons

7.2.1. 4-Hydroxynonenal (HNE)

HNE was detected in syringes of both lipid formulations at both temperatures (room 22°C and fridge, 4°C). Figure 7.1 presents this data showing Intralipid® and SMOFlipid® in light protected and non-light protected syringes at room and fridge temperatures. Maximal HNE was found in non-light protected SMOFlipid® room temperature syringes at a concentration of 13.65 µM. As previously discussed in the method validation section for HNE (chapter 2), the limit of quantification (LOQ) was established as 8.974 µM and is shown on the graph. As indicated, results at day 84 for all syringes except SMOFlipid® and Intralipid® fridge temperature (2 to 8°C) fall above the LOQ and can therefore be considered accurate. The maximal concentrations at day 84 for each syringe are shown in table 7.1. Temperature has a minimal effect on the amount of HNE produced for all lipids, producing an average of 1.76 µM difference between temperatures.
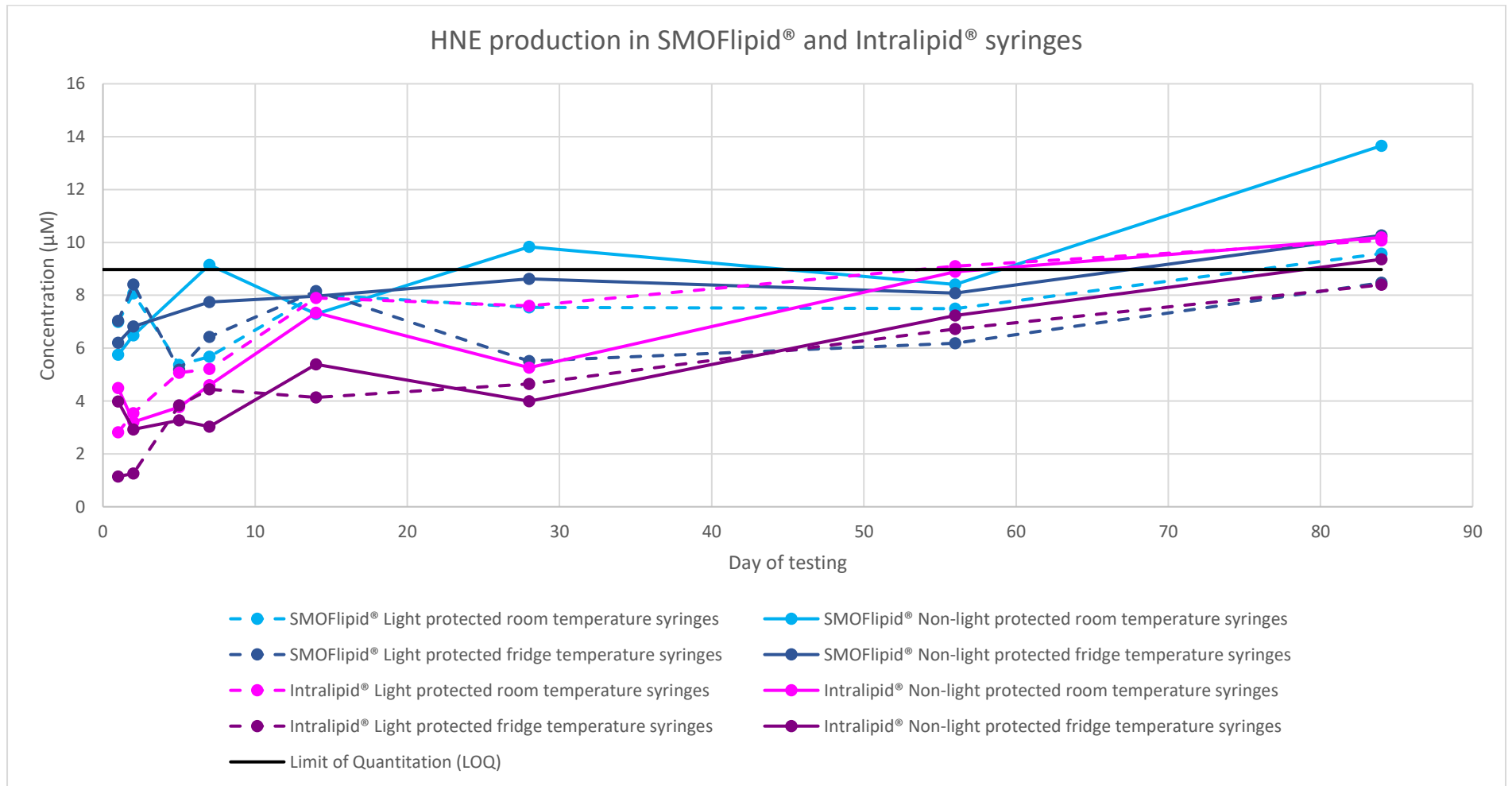
Figure 7.1 HNE production in SMOFlipid® and Intralipid® syringes.

Table 7.1 Maximal concentrations of HNE produced in lipid syringes.

Lipid type	Room or Fridge Temperature	Light (LP) or Non-light (NLP) protection	Concentration at day 84 (µM)
SMOFlipid®	**Room**	**NLP**	**13.655**
SMOFlipid®	Fridge	NLP	10.20
SMOFlipid®	Room	LP	9.57
SMOFlipid®	Fridge	LP	8.47 (under LOQ)
Intralipid®	**Room**	**NLP**	**10.18**
Intralipid®	Fridge	NLP	9.36
Intralipid®	Room	LP	10.07
Intralipid®	Fridge	LP	8.39 (under LOQ)

Light protection for SMOFlipid® syringes had a positive effect in reducing the level of HNE produced by 4.08 µM (approximately a third). It was predicted that non-light protected syringes would produce more HNE than light protected syringes due to the potential for light-initiated peroxidation (photo-oxidation) to occur in addition to 'standard' peroxidation and TAG breakdown. This is as shown in SMOFlipid®, however little difference (<1 µM) is observed in Intralipid® syringes indicating that minimal HNE is produced by photo-oxidation.

HNE as discussed in chapter 1 is produced through the peroxidation and breakdown of linoleic acid (C18:2) through production of a primary hydroperoxide at the 9' position (denoted from the free methyl end) of the fatty acid as shown in figure 5.51 (chapter 5) and subsequent cleavage producing HNE and a fatty acid remnant attached to the TAG backbone. Linoleic acid is found in relatively high concentrations in SMOFlipid® (14 to 25%) but in significantly greater amounts in Intralipid® (44 to 62%) (Eriksson 2001; Kabi 2018) and as such it would be predicted that under the same conditions, Intralipid® should create more HNE than SMOFlipid®. Results contradict this however, with SMOFlipid® NLP room temperature syringes producing ~4 µM more HNE than Intralipid® under the same conditions. One explanation for the results observed is that more overall peroxidation (and thus many different oxidation products) is occurring in SMOFlipid® than Intralipid® due to the presence of multiple poly-unsaturated TAGs in SMOFlipid® from both soybean (C18:3, C18:2 and C18:1) and fish oil (C20:5, C22:6). Whilst minimal and as such not monitored with the assay used in this work, the multiple double bonds in fish oil are liable to peroxidation, creating more lipid radicals than found in Intralipid®. As discussed in chapter 1, lipid peroxidation and breakdown is a self-propagating cyclical reaction and therefore the greater number of lipid radicals present, the greater the rate and amount of peroxidative breakdown,

ultimately leading to the largest amounts of secondary products created. Thus, this breakdown does not necessarily resulting in a single product formation, i.e. HNE.

As discussed in previous results chapters and shown in figure 5.51 (chapter 5) the peroxidation of linoleic acid can lead to multiple secondary peroxidation products, HNE being only one of them. The assay developed and used only detects HNE, HUE and a TAG remnant. All syringes tested in both lipids undergo significant TAG losses as shown in subsequent sections except NLP SMOFlipid® room temperature syringes which conversely show the highest levels of HNE. Whilst the multiple levels of unsaturation present in fish oils when in combination with other oils within an emulsion could increase the levels of peroxidation present *in vitro*, when considering the important fact that this work deals with IVLE's for infusion to patients, *in vivo* fish oils have been shown to reduce the levels of HNE formed within cells (Ishikado et al. 2013).

When considering the relevance of the detection of HNE within syringes, all produced a concentration of ~ 10 µM or above upon storage. Esterbauer, Schaur and Zollner's work (1991) on the toxicity of HNE provides an extensive review on the in vivo toxicity of HNE. The review states "HNE concentrations in the range of 1 to 20 µM can inhibit DNA and protein synthesis, stimulate phospholipase A_2 and inhibit c-myc expression." All the syringes tested other than the light protected fridge samples produced HNE at concentrations within this range and as such can be considered to be within toxic levels. It is noteworthy however that whilst this concentration of HNE is present within the lipids tested and therefore have the potential to be infused into the patient, this level of lipid would then be dispersed throughout a patient's blood volume, reducing the systemic concentration of HNE compared to that found within the syringes. The levels produced however are significant and important in the clinical development of future lipid emulsions and storage containers.

As discussed in chapter 1, many recent works exist implicating HNE in multiple disease pathologies including cancer, colorectal inflammation, metabolic and neurological disorders (Esterbauer et al. 1991; Chen et al. 2006; Castro et al. 2016; Rossin et al. 2016; Zarkovic et al. 2016). With specific regards to PN patients, plasma adducts of protein-HNE was shown to be raised in long term home PN patients albeit in a small sample population (41) indicating the delivery of HNE within PN correlates to an increase in plasma levels (Massorenti et al. 2004). The results obtained are therefore clinically relevant and of importance when considering

the delivery of lipids to neonatal patients. The work within this thesis was designed to test lipid emulsions in 50 ml quantities replicating the amount and storage of lipids administered to neonatal patients. The detection of HNE within syringes is important as current clinical practise involves the storage and delivery of neonatal PN lipids in 50 ml syringes. Recent clinical safety concerns have been raised over the inappropriateness of syringes as storage devices due to the permeability of oxygen and the potential for leachables to enter stored components. As such there is a drive to move small volume lipids from syringes to small volume PN bags. With regards to the HNE data acquired during this work, the results substantiate this recommendation as HNE was only detected in syringes and not in PN bags.

7.2.2. Hydroxy-undecanal (HUE)

HUE was identified through mass spectrometry as shown in chapter 3 section 3.8.3.1 and formed from the peroxidation of omega-9 TAGs containing oleic acid (C18:1). Oleic acid peroxidation requires much greater bond dissociation energy (approx. 10kcal/mol) to abstract a hydrogen than in the case of linoleic or linolenic acids (C18:2 & C18:3) due to the singular double bond and therefore relatively 'stable' electron pairs. As such the identification of HUE within lipids confers high levels of energy within a system and therefore the potential for extensive peroxidation to be present. As the assay was developed to detect HNE and validated accordingly and due to the lack of an available standard of HUE for validation purposes, results are presented as peak area rather than concentration. Limits of detection and quantification cannot be established in terms of concentration again due to a lack of validation, however a signal to noise ratio for the HUE peak could be established. From this a LOD and LOQ using a signal to noise ratio of >3 and >10 respectively (Synder et al. 1997) could be used to monitor each HUE peak recorded to ensure some precision within the results presented. All results had a signal to noise ratio above 10. Both SMOFlipid® and Intralipid® created HUE through storage in syringes and in PN bags. Results were significantly higher in syringes than PN bags for both lipids. Room temperature Intralipid® and SMOFlipid® light protected syringes produced maximum levels of HUE over 84 days. All light protected containers for both lipids produced significantly more HUE than non-light protected containers. This is of interest as non-light protected containers were predicted to produce more HUE due to light exposure and photo-oxidation potential. Results indicate a lack of photo-oxidation processes occurring with both lipids tested. The light protection employed aluminium foil wraps and it can

be postulated that this could cause an insulation effect on the container, increasing temperature of the lipid leading to the results observed. It is again worth noting that the assay developed and used was designed to detect HNE and as such monitors a specific wavelength of 222 nm. Therefore, results shown cannot conclusively determine if other secondary peroxidation products other than HNE and HUE are being created and not visualised at this specific wavelength. Further work beyond the scope of this thesis using a variable wavelength or diode array detector could determine the presence of further peroxidation products and establish an overall picture on the levels of secondary or end products of peroxidation present within samples.

Figures 7.2, 7.3 and 7.4 graphically show the data recorded for each container where HUE was detected. As shown, all light protected syringes produced significantly more HUE than non-light protected containers as discussed above. Temperature of storage influenced HUE production as predicted with room temperature syringes and PN bags producing more HUE than fridge storage. PN storage within a clinical setting is always within fridge temperatures and results substantiate the necessity for this to continue. With regards to the rate of HUE production, all room temperature syringes created HUE at a relatively steady rate as shown within the graphical figures from within the first week of storage. This is significant as current practise limits small volume lipids for neonatal patients to less than 7 days storage. The presence of HUE within the initial days of testing is of clinical importance when considering the infusion of such lipids into neonatal premature patients who will already be under high levels of oxidative stress. Whilst HUE confers less toxicity than HNE (Eckl et al. 1993) its presence in infused lipids could potentially cause harm to a patient if there innate antioxidant systems are already stressed. The results for PN bags differ from syringes in their capacity to limit HUE formation during initial storage. Only room temperature PN bags produced detectable levels of HUE and only from day 14 onwards, indicating that with respect to secondary peroxidation products PN bag storage is superior to syringe storage of lipids. A caveat to this however is that the assay and work is detecting secondary peroxidation products, i.e. end stage peroxidation products. Whilst the results indicate greater levels of peroxidation in syringes than PN bags, consideration must be given to the primary products of peroxidation, namely lipid hydroperoxides.

Whilst results above indicate PN bag storage is superior to syringe storage, TAG losses occurring the PN bags is far higher than within syringe indicating higher levels of peroxidation or TAG breakdown in bags. One explanation for these results

that seem to contradict each other is the possibility of peroxidation within PN bags is occurring but at testing products present are primary products namely lipid hydroperoxides. As such this would be indicated by TAG losses with an apparent lack of secondary peroxidation products as shown in the data. PN bags are impermeable to oxygen whereas syringes permit oxygen to leak into the storage system over time. One can postulate that this increase in oxygen is catalysing the cleavage of short chain aldehydes from lipid hydroperoxides resulting in the raised levels of secondary products seen within syringes. The limited supply of oxygen within impermeable PN bags however is being used for initiation and propagation of peroxidation and resulting in the formation of hydroperoxides that are then held in 'stasis' and therefore a lack of secondary products is recorded. Beyond the scope of this work, further studies detecting the presence and levels of hydroperoxides, whilst complicated and often not accurate, would prove the presence of hydroperoxides within PN bags.
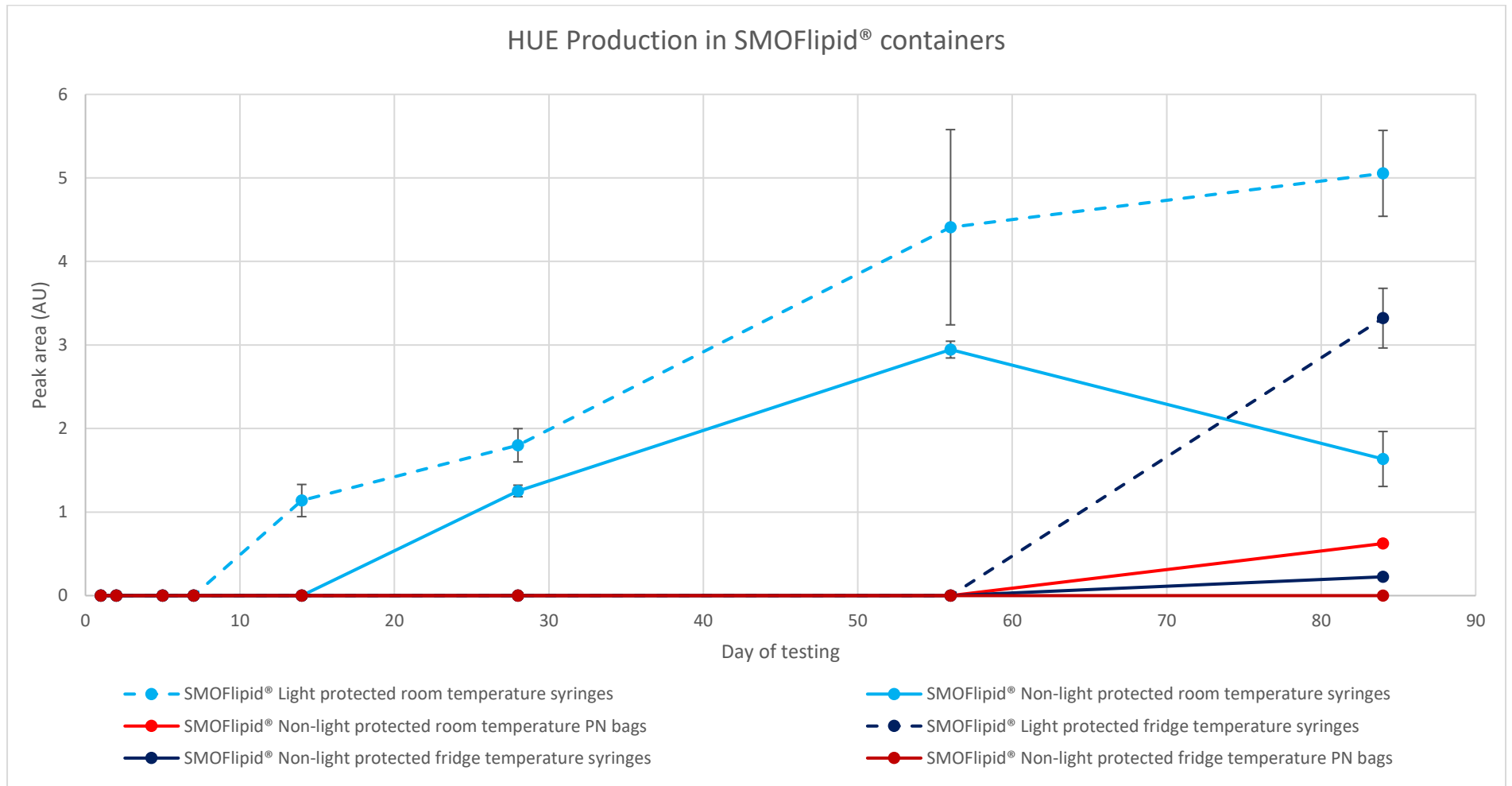
Figure 7.2 HUE production in SMOFlipid® containers Standard deviation error bars indicated on results.
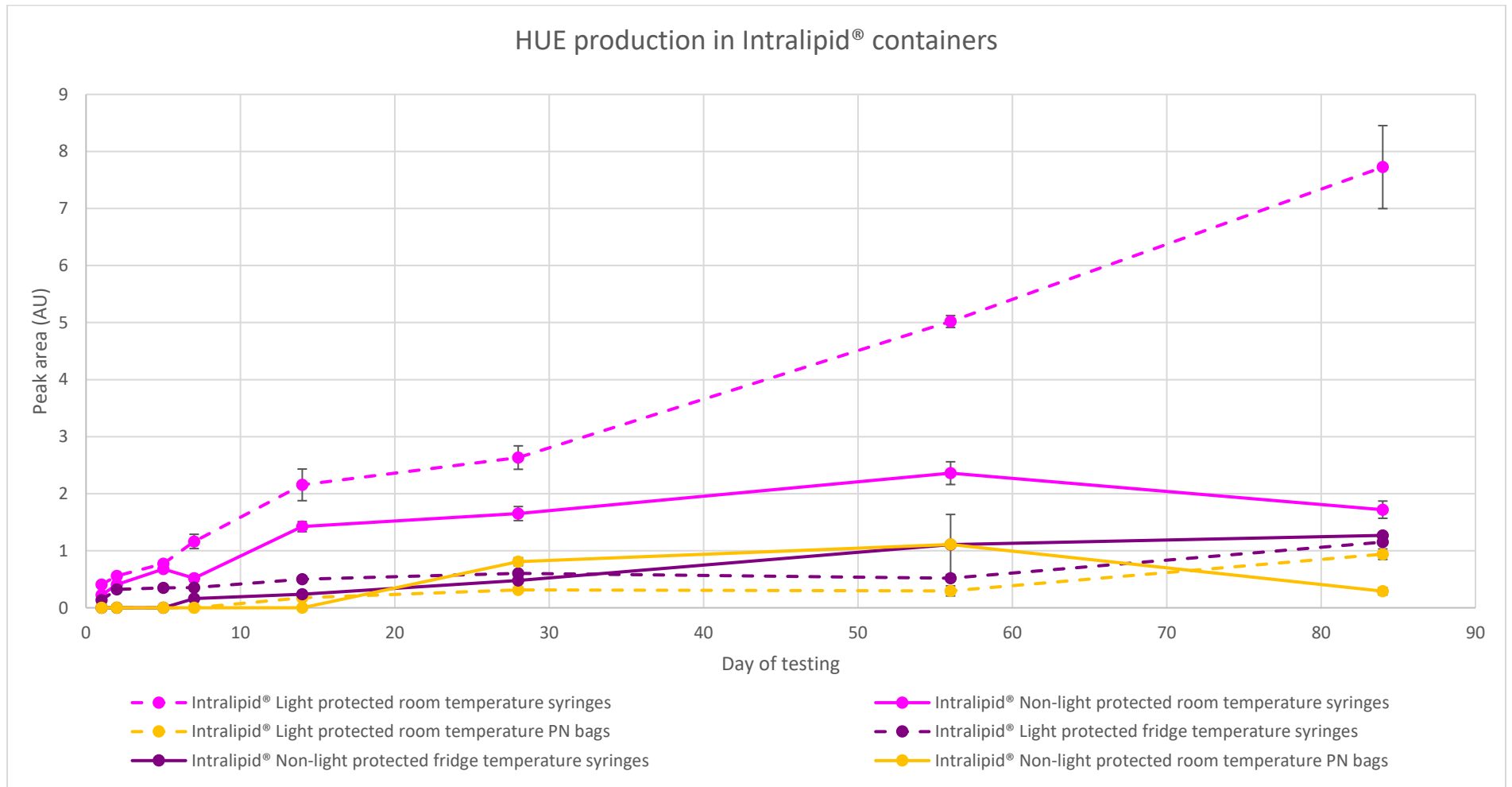
Figure 7.3 HUE production in Intralipid® containers. Standard deviation error bars indicated on results.
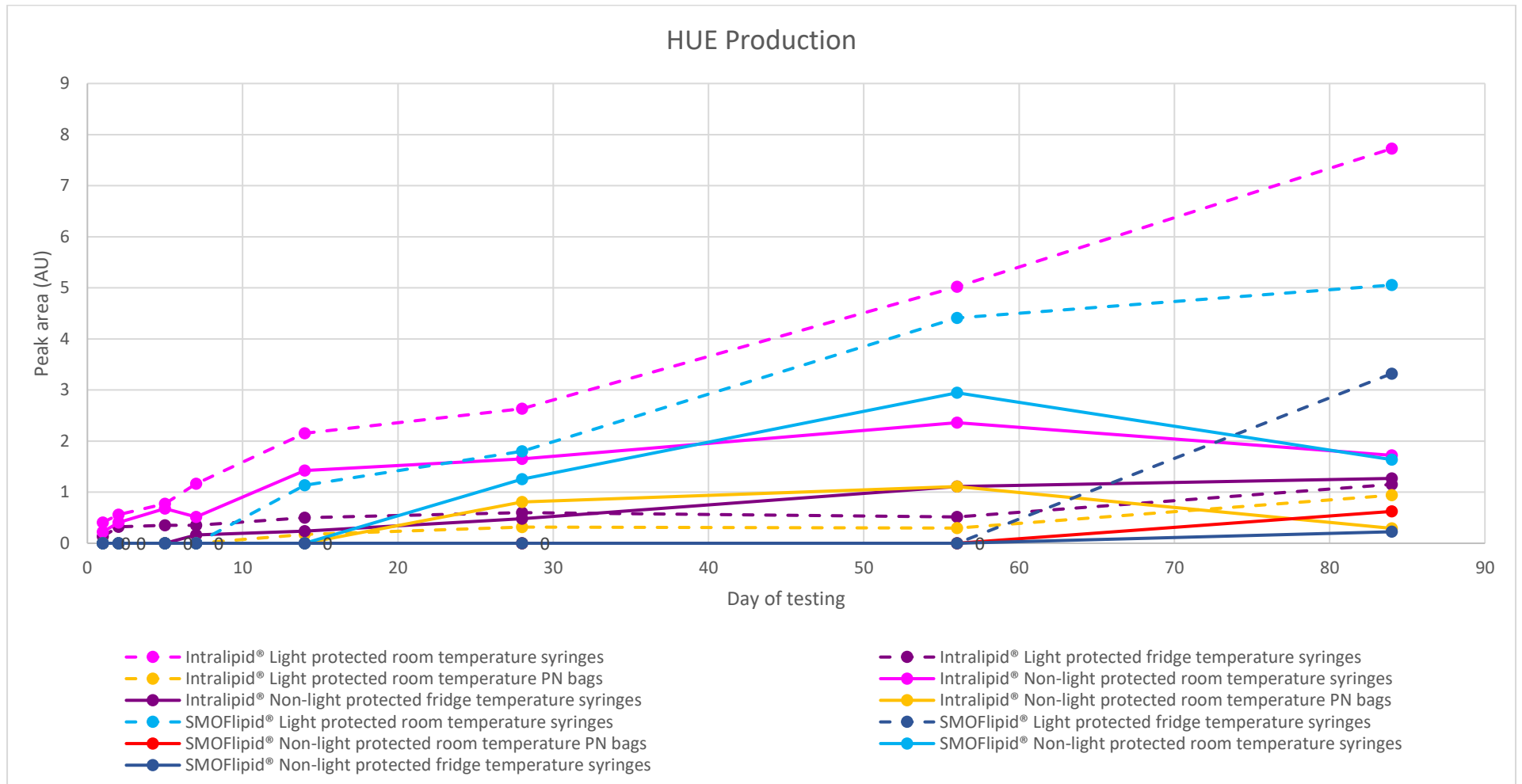
Figure 7.4 HUE production across all containers of SMOFlipid® and Intralipid® both light and non-light protected at fridge and room temperatures.

As predicted, removal of oxygen from the storage system results in an apparent lack of peroxidation when considering the detection of secondary peroxidation products. No HUE or HNE was detected in any of the glass vials tested that were purged with nitrogen to remove atmospheric air. The results substantiate the necessity of oxygen in the production of secondary products within the lipid emulsions tested.

7.2.3. TAG remnant

The TAG 'remnant' was identified through mass spectrometry in chapter 3 section 3.8.3.2. The proposed production of this remnant at the stage of initial identification was from the cleavage of HUE (x2) and HNE (x1) from peak 7 TAG (C18:1/18:1/18:2). As shown schematically in figure 7.5 the TAG remnant with a m/z of 495.4 could also be from the breakdown of peak 5 (c18:2/18:2/18:2) or peak 10 (18:2/18:1/16:0) as well as peak 7 (C18:1/18:1/18:2). The level of TAG loss of each of these peaks is discussed section 7.4, but broadly all undergo TAG loss during storage in both lipid formulations. As shown the production of a remnant with the m/z of 495 from peak 5 (C18:2/18:2/18:2) involves a loss of one HNE molecule and a process different than the typical peroxidative cleavage of an aldehyde from the end of one of the other linoleic acid chains. Hydrolysis of the ester bond between the fatty acid and the glycerol backbone of the TAG is instead the process that leads to the production of a diacylglyceride remnant that has a m/z ratio of 495. Whist considered unlikely within an oil, the presence of extensive water within a lipid emulsion and therefore the interaction between water and TAGs at the oil-to-water interface makes hydrolysis of TAGs within emulsions a possibility. The extensive losses of the saturated TAGs found in SMOFlipid® and discussed in section 7.3 substantiate this. The production of the remnant from peak 10 (C18:2/18:1/16:0) also involves the hydrolytic cleavage of the saturated palmitic acid chain from the glycerol backbone. Whilst the work cannot definitively ascertain which peak's breakdown is responsible for the production of the TAG remnant seen, peroxidation is more likely than hydrolysis. This is due to the limited amounts of appropriate TAGs that would be at the oil-water interface to undergo hydrolysis and the presence of both HNE and relatively high levels of HUE within the results as discussed above and as such the production of the remnant from Peak 7 (C18:1/18:1/18:2) is probable.

As discussed above in HUE results an analytical standard for the TAG remnant molecule was not obtainable and therefore results cannot be validated. LOD's and

LOQ's were calculated as signal to noise ratios as with HUE and all results were above 10 conferring a level of reliability. Results are therefore presented as peak area rather than concentration.

Figure 7.5 Chemical reaction schematic of hydrolysis of fatty acid from TAG backbone and cleavage of HNE from TAG 5 (C18:2/18:2/18:2) producing TAG remnant.

312

Both lipid formulations results show the formation of the TAG remnant only at room temperature storage. All non-light protected containers produce substantially more remnant than light protected for both lipids. Differences are apparent between Intralipid® and SMOFlipid® when looking at the highest levels of remnant formation in each container type. All TAG remnant results are shown in figures 7.6, 7.7 and 7.8. In SMOFlipid® maximal results were recorded in non-light protected PN bags. This is similar to the extensive TAG losses observed in PN. The Intralipid® results were highest in non-light protected syringes which also produced maximal levels of TAG losses for each of the six peaks monitored. This indicates that the highest levels of peroxidation are occurring in room temperature PN bags and syringes for SMOFlipid® and Intralipid® respectively.

It was predicted that non-light protected containers would result in the highest levels of peroxidation as discussed in chapter 1 due to the potential for photo-oxidation to occur as well as the 'standard' initiation pathways for peroxidation. Results substantiate this in respect to levels of TAG remnant seen. HUE production as discussed above is higher in light protected containers, however significant amounts are also produced in non-light protected lipids, whilst conversely HNE is higher in non-light protected SMOFlipid® syringes. When considering which pathways of peroxidation are responsible for the products detected, from the results obtained it is not possible to definitively ascertain the level of photo-oxidation occurring in any containers. The TAG remnant and HNE results indicate a definite increase in peroxidation occurring in non-light protected containers and as such it can be postulated that light exposure is a catalyst for peroxidation suggesting the presence of a level of photo-oxidation within SMOFlipid® PN bags and Intralipid syringes.

The lack of TAG remnant seen in fridge temperature containers is of interest, though it is noteworthy that whilst non-light protection was employed, when placed within a refrigerator, containers are stored in the dark and as such only experience limited light exposure upon their removal for sampling. This is a definite limitation to the fridge temperature work with respect to non-light protection, however within a clinical setting all containers are refrigerated and as such the results between light and non-light protected containers held at such temperatures is relevant and discussed in subsequent sections.
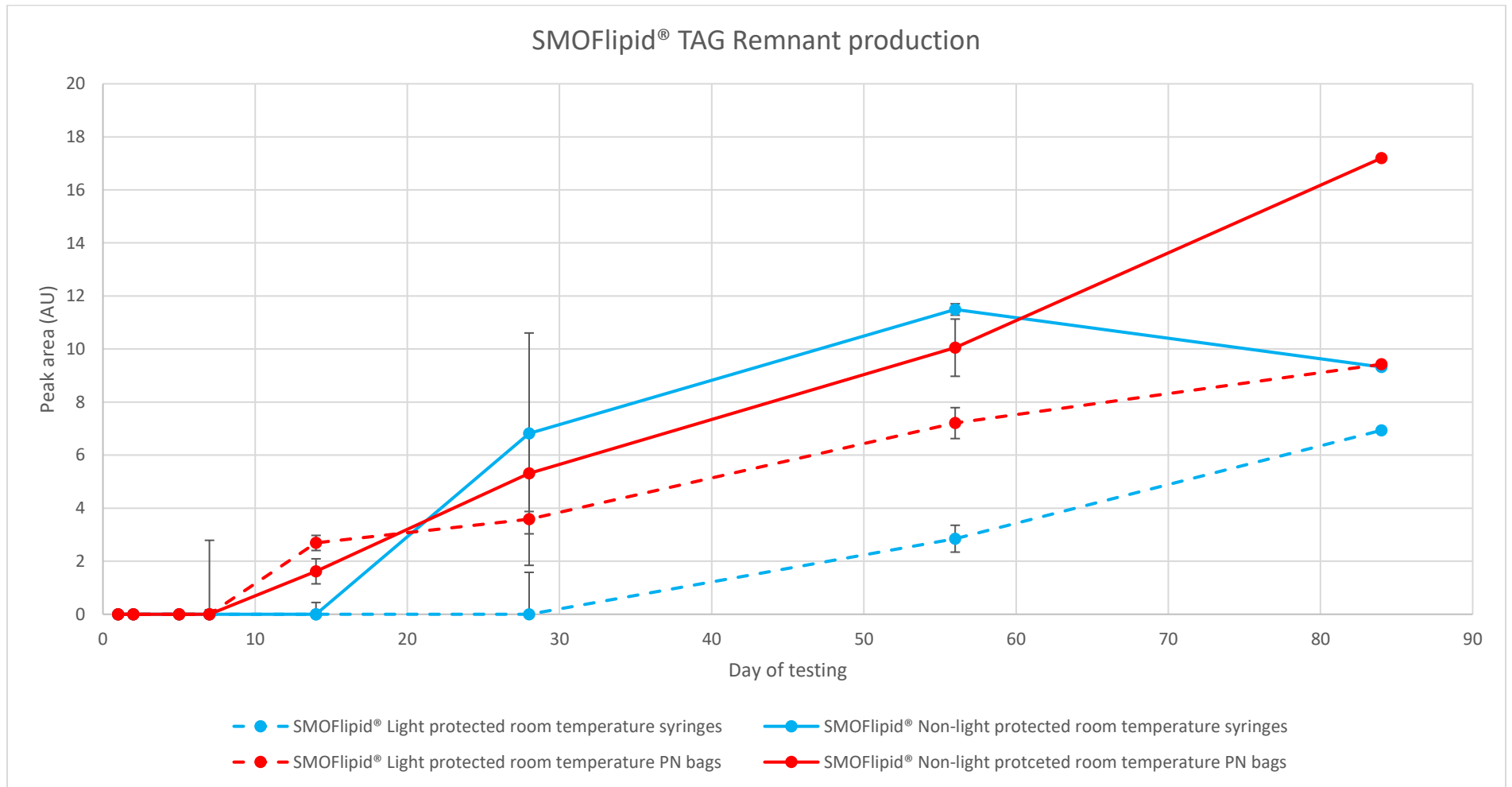
Figure 7.6 TAG remnant production within SMOFlipid® room temperature containers. Standard deviation error bars indicated on results.
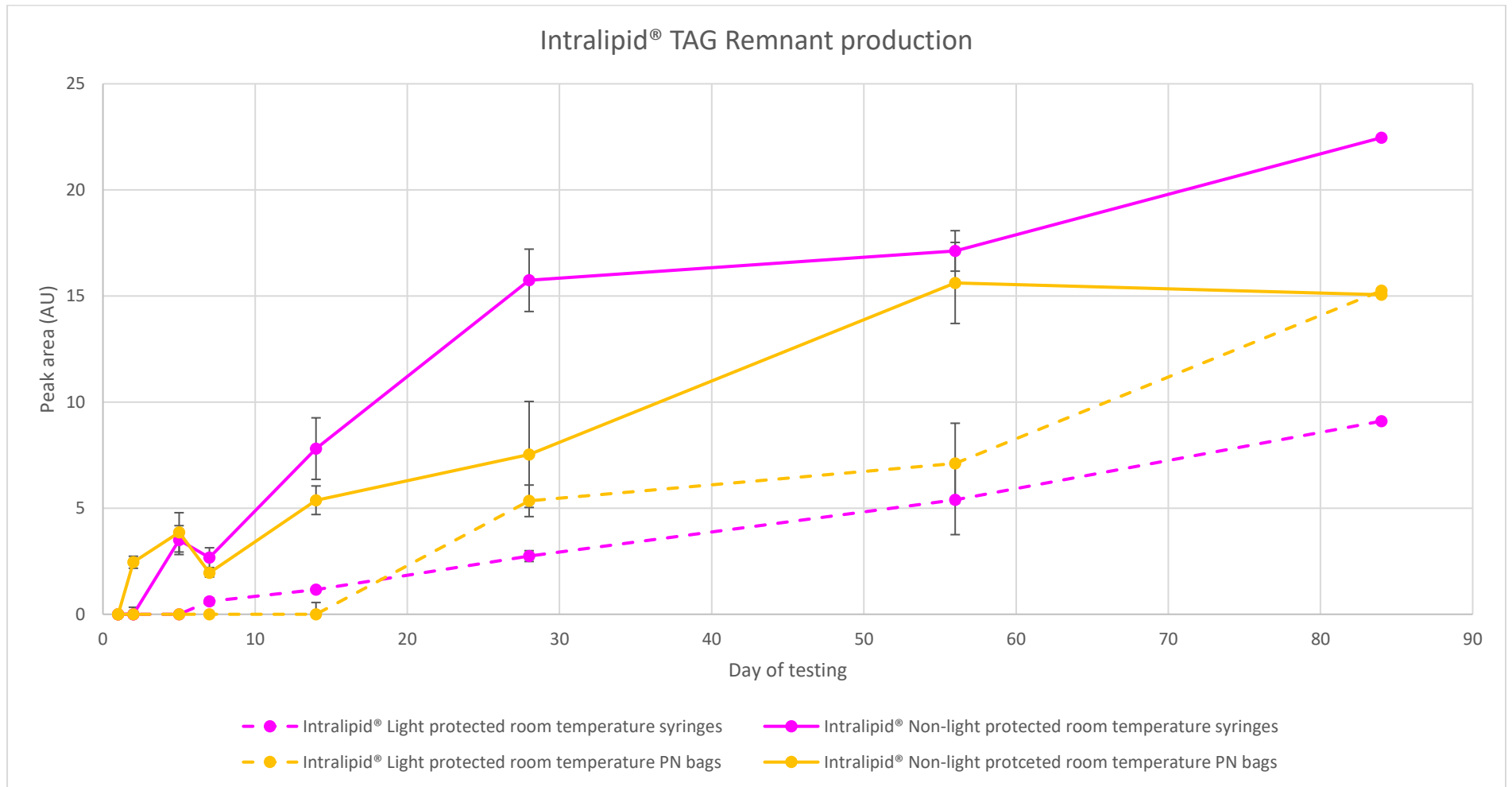
Figure 7.7 TAG remnant production in Intralipid® room temperature containers. Standard deviation error bars indicated on results.
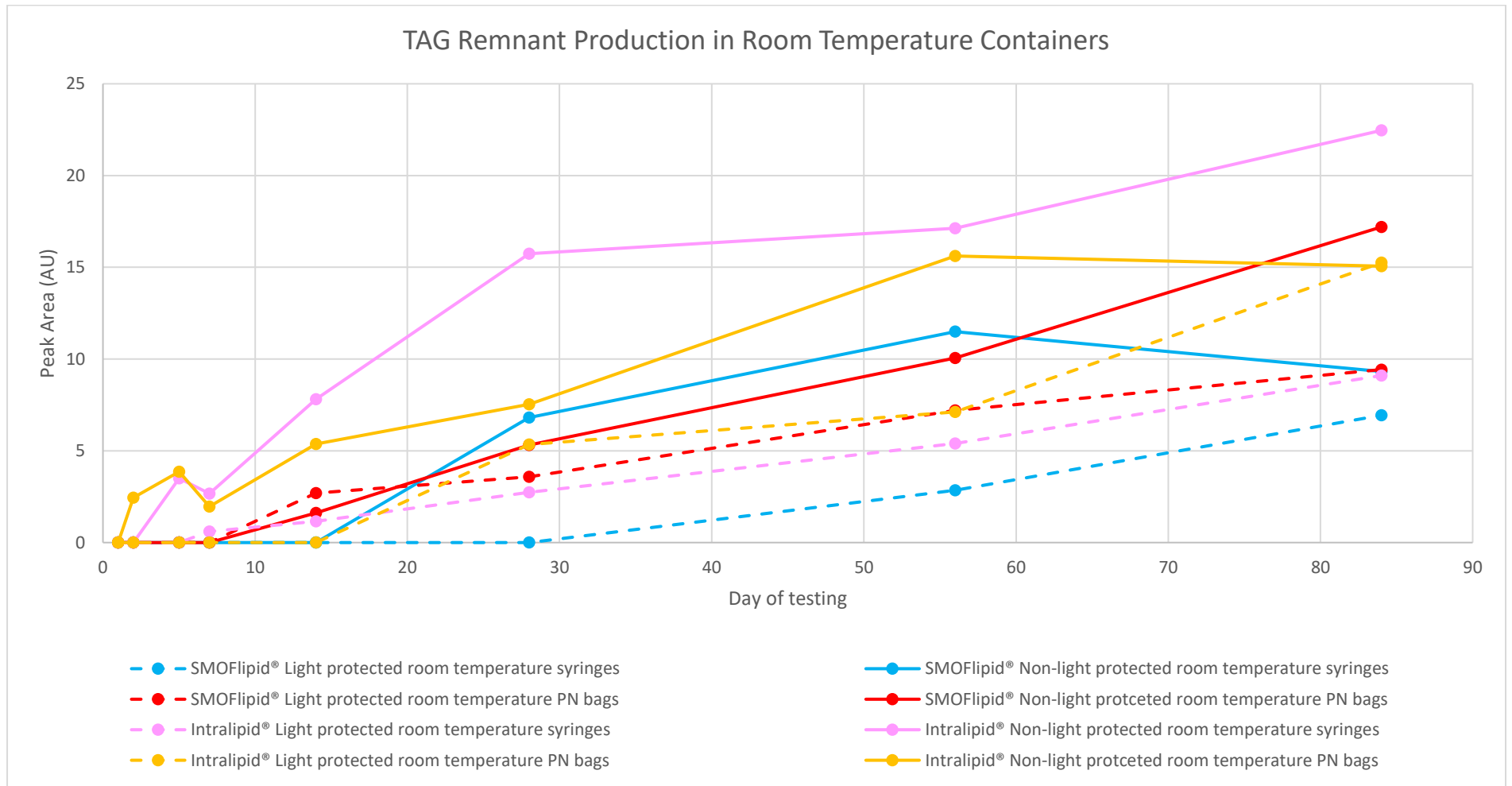
Figure 7.8 TAG remnant production in all containers of SMOFlipid® and Intralipid®.

Collectively the terminal products detected and monitored within this work (HNE, HUE, TAG remnant) show the presence of peroxidation within all PN bags and syringes. Whilst a lack of TAG remnant was seen in all fridge temperature containers, and results show a significant reduction in terminal products within refrigerated containers, quantifiable levels were still detected and whilst only HNE concentrations can be definitively determined, even at fridge temperatures up to ~10 µM concentrations were detected within both SMOFlipid® and Intralipid® syringes. This is critically important as this work was designed to give an initial set of data that explored the potential for chemical breakdown of lipids to occur during storage as per common clinical practise before delivery to the patient. The identification of secondary peroxidation products from as little as two days onwards in fridge temperature containers is clinically relevant and suggests that an update to clinical protocols may be required. This is discussed further in section 7.8.

7.3. Saturated TAG losses in SMOFlipid®

The following sections deal with the comparison between containers, non-light and light protection and temperatures of storage of SMOFlipid®. Saturated peaks 1 to 4 (C8:0/8:0/8:0, C8:0/8:0/10:0, C8:0/10:0/10:0 and C10:0/10:0/10:0) are present only within SMOFlipid® from chemically synthesised fatty acids derived from coconut oil. Each peaks' results are presented in the following subsections. As previously discussed in chapters 5 and 6, such saturated TAGs should be resistant to peroxidative breakdown due to the lack of unsaturation. The losses observed are therefore due to a different chemical degeneration postulated to be hydrolysis and cleavage of fatty acids from the TAG glycerol backbone. The presence of relatively high levels of water within SMOFlipid® emulsions and the potential for an lipid hydroperoxides to be present (R-COO/R-COOH) from peroxidation of unsaturated TAGs create conditions where hydrolytic cleavage at the ester linkage of the fatty acid can occur, creating the results discussed below.

7.3.1. Peak 1 (C8:0/8:0/8:0)

Figure 7.9 shows the % losses of peak 1 observed in all SMOFlipid® containers. As shown, light protected PN bags both room and fridge showed maximal losses of over 40 % and ~ 27 % respectively at day 56. Data within the graph for each container is only included up to the point where RSD's for control samples were within acceptable limits (<12). The light protected glass vials recorded the second

highest TAG losses seen. As discussed in chapter 5, the high levels of TAG losses observed in glass vials from day 28 onwards for all peaks was potentially due to ingress of oxygen within the system during sampling resulting in the initiation of peroxidation. The lack of secondary products within these vials suggests that peroxidation may be in the propagation phase and be in the form of hydroperoxides. Such lipid primary products would result in a lowering of pH favouring hydrolytic reactions and producing the cleavage of fatty acids from the TAG as shown in the graph for peak 1.

Whilst light protected results showed significant losses for all containers, non-light protected also produced losses, particularly within PN bags suggesting that light protection was not a dependant factor in limiting peroxidative hydrolysis from occurring. Both syringe results are of interest as little TAG 1 losses are observed in non-light protected samples but up to ~ 25 % of loss in light protected syringes. As discussed in subsequent unsaturated sections non-light protected syringes showed minimal losses throughout all peaks monitored whereas light protected syringes produced significant loss again substantiating the lack of importance of light protection of syringes when considering this pathway of degradation.

Temperature of storage does have a significant effect on light protected storage with greater losses observed in room temperature syringes, PN bags and vials. Non-light protected results for this peak across all containers are not affected by temperature of storage. Higher temperatures of storage would be predicted to catalyse hydrolysis reactions occurring and result in higher TAG losses. This whilst observed in light protected results is contradicted by the non-light protected containers. The results when considered separately suggest that temperature of storage influences PN bags to a greater extent than syringes, a trend that is seen across all peaks/TAGs monitored in SMOFlipid®. The oxygen availability within each container must be considered as an overarching factor limiting the occurrence of peroxidation and subsequent hydrolysis and can explain the losses observed in different containers. This is discussed in detail in section 7.8.
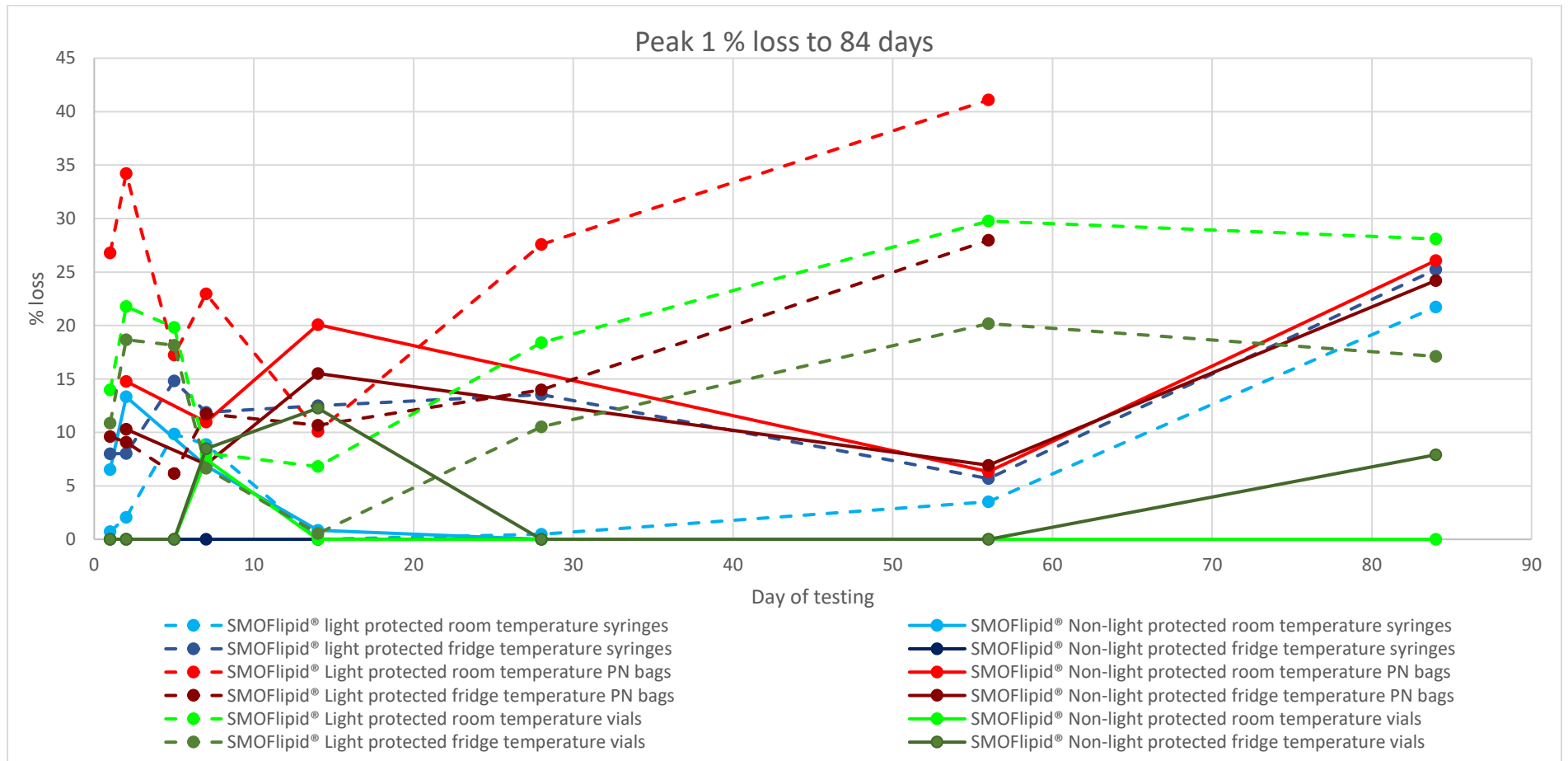
Figure 7.9 Peak 1 (C8:0/8:0/8:0) losses in SMOFlipid® containers at room and fridge temperatures.

7.3.2. Peak 2 (C8:0/8:0/10:0)

Results for peak 2 as shown in figure 7.10 show similar trends as for the peak 1 results discussed above. Light protected results for all containers show significantly more loss than non-light protected results. PN bags give maximal losses of 35 % at room temperature at 56 days. Light protected glass vials also show significant loss suggesting oxygen ingress as discussed above. Within syringes, minimal loss is observed in non-light protected samples however light protected syringes do show significant loss of ~ 20 % over 84 days. This substantiates the results seen in peak 1 and suggest that non-light protection and as such photo-oxidation is not present in significant quantities within SMOFlipid® containers.

The initial rate of saturated loss observed is greater in PN bags than within syringes. Light protected syringes only show evidence of hydrolysis and peak 2 loss from day 28 and significant loss (more than ~ 5 %) from day 56 onwards. Conversely PN bags show significant TAG loss by day 14. The availability of oxygen within syringes and bags must be considered when looking at the levels of TAG loss observed. PN bags are formulated with a small but finite volume of air left in them and as such oxygen is present both within this air bubble and dissolved within the lipid from the manufacturing process which utilises a syringe to draw lipid from its raw material container, a process which can result in dissolved oxygen forming within the lipid. It is postulated that this available oxygen from day 0 of storage within PN bags results in the rapid onset of peroxidation and hydrolysis seen and therefore the higher initial TAG losses observed. Syringes however have minimal levels of air and oxygen present initially as all non-dissolved air is completely removed at manufacturing. Therefore, peroxidation, hydrolysis and TAG losses are only observed upon air ingress into the syringe due to leakage into the system over time between the barrel of the syringe and the rubber plunger resulting in the slower rates of saturated TAG losses observed. As discussed in pervious sections, hydrolysis and subsequent TAG loss appeared to only occur when significant unsaturated peroxidation was detected, i.e. when high levels of radicals, hydroperoxides and secondary products are present (high levels of energy).
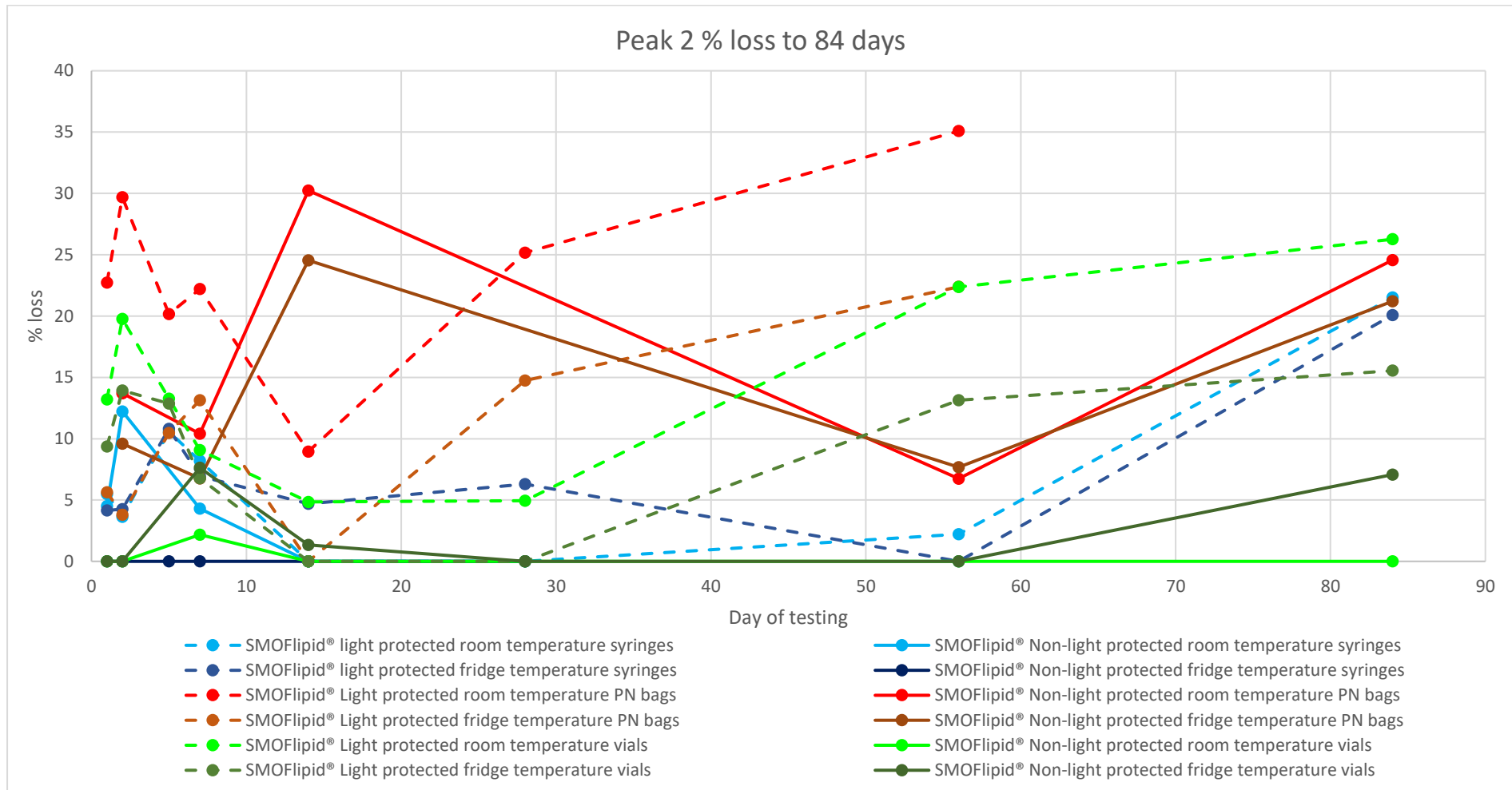
Figure 7.10 Peak 2 (C8:0/8:0/10:0) TAG loss observed in SMOFlipid® in all containers at room and fridge temperatures.

Temperature has a similar effect to peak 1 results and is implicated in the level of hydrolysis occurring within PN bags and glass vials. To a lesser extent, light protected syringes only show a ~2 % variation between temperatures. When considering peak 1 and 2 collectively it was predicted that levels of loss should be similar between peaks due to the lack of selectiveness of hydrolytic cleavage of saturated fatty acids. This is substantiated in the results with less than a 5 % difference observed between peaks for each container subset of results.

7.3.3. Peak 3 (C8:0/10:0/10:0)

As figure 7.11 displays, the results for peak 3 follow the same trends as recorded for peaks 1 and 2. Temperature had a much larger effect in light protected containers than non-light protected ones particularly for PN bags and glass vials. Syringes again show less of a difference than with non-light protected results showing minimal (< 5 %) TAG losses for both temperatures and ~3 % difference between light protected syringes. It can be postulated that the combination of oxygen availability and temperature are limiting factors on the rate and extent of peroxidation and hydrolysis. PN bags where oxygen is available from day 0 suffer greater losses which are limited by fridge temperature storage. Syringes where oxygen in only available over prolonged storage times show less TAG loss and as such temperature has less of an effect on loss occurring.

The results for all saturated peaks as shown in figures 7.9 to 7.12 show the TAG losses occurring in all SMOFlipid® containers over up to 84 days. Of interest is the fluctuations observed in results over time. It was predicted that losses occurring should increase over time and whist this is the case in the majority of results and represents an overall trend, results appear to reduce in % loss at certain data points (e.g. Day 56 Non-light protected PN bag results). Whilst no definitive explanation can be formed from this work and the results obtained, several potential reasons for the fluctuation in results can be postulated. For minor deviations from the above trend, variation in control samples below the acceptable RSD level of 12 will create minor deviations in the results obtained for the tested samples including the reduction in results observed. The large deviations in results as shown in the PN bag day 56 results show the potential for condensation reactions to occur between cleaved and therefore 'free' fatty acids and the OH of the glycerol backbone, reforming saturated TAGs and resulting in the reductions observed in TAG loss. It can be postulated that the availability of water within the emulsion and the presence

of TAGs at the water-oil interface will govern the losses or reformations of TAGs observed.
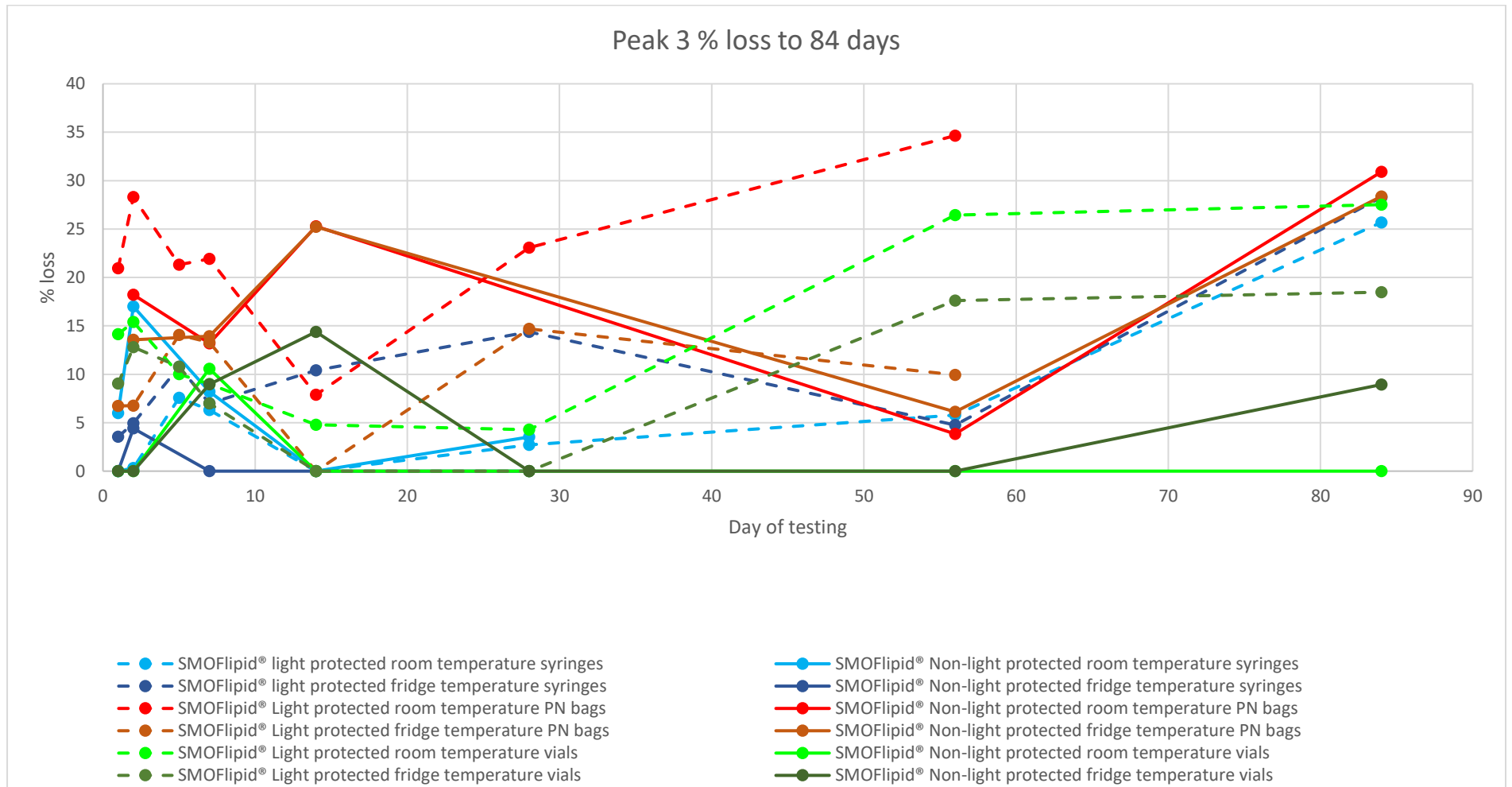
Figure 7.11 Peak 3 (C8:0/10:0/10:0) TAG losses in all containers at room and fridge temperatures.

7.3.4. Peak 4 (C10:0/10:0/10:0)

Figure 7.12 shows the results for all SMOFlipid® containers and follows similar trends in loss to those discussed in all the previous peaks (1 to 3). Peak 4 light protected PN bags held at room temperature produced the maximum loss observed (37%). Lower temperature had a significant effect on light protected containers, reducing % loss in each by up to 15 % (light protected glass vials). Within syringes minimal loss was observed throughout 84 days in non-light protected results and up to 56 days in light protected samples, suggesting the initiation of peroxidation only upon oxygen ingress during extended storage times. The conclusions drawn above for the previous 3 peaks and all saturated TAGs (C8:0/8:0/8:0, C8:0/8:0/10:0, C8:0/10:0/10:0, C10:0/10:0/10:0) are applicable to all peaks 1 to 4 and show that when considering saturated TAG loss and hydrolysis occurring chain length (C8 to C10) does not affect levels of cleavage and loss.
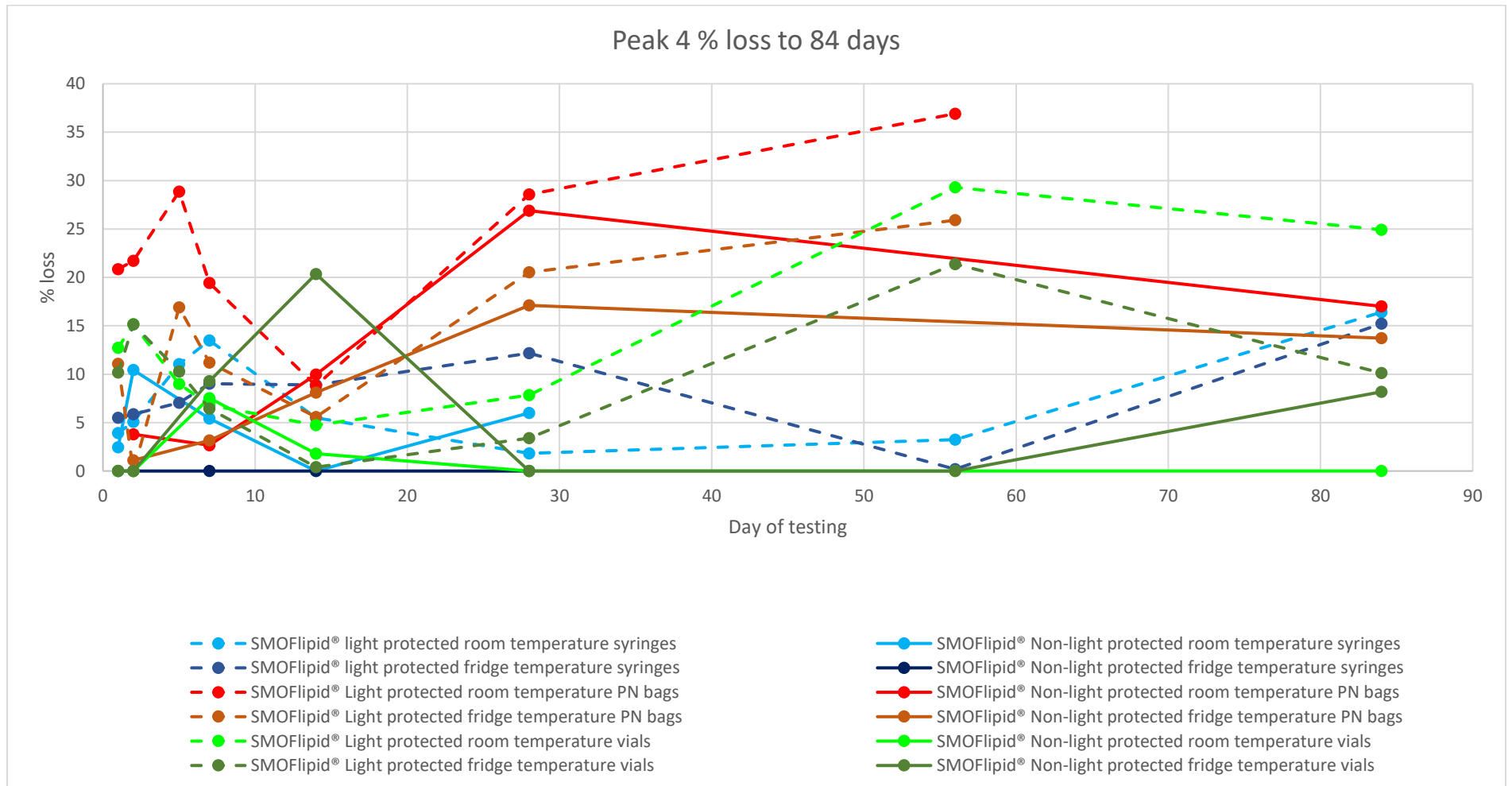
Figure 7.12 Peak 4 (C10:0/10:0/10:0) % losses in all SMOFlipid® containers at room and fridge temperatures.

7.4. Unsaturated TAG losses in Intralipid® and SMOFlipid®

The following comparisons between each lipid, container and mode of storage are presented in graphical form. Each lipid is compared in each container both light protected and non-light protected. The large amount of data present prevents graphical representation of all results together and therefore they are split as described above (section 7.1) to enable comparisons to be drawn. Each peak (5 to 10) are discussed in the following subsections. All results displayed are those where control sample RSD's were below 12 and therefore considered reliable. Therefore, whilst all available data is plotted (up to day 84), day 28 results for syringes and day 56 results for PN bags and vials serve as the points at which main comparisons are drawn as this timepoint is the latest at which all tested containers have reliable results.

As discussed within the assay validation section in chapter 2, limits of detection (LOD) and limits of quantification (LOQ) for TAG losses were unable to be calculated from the validation protocols due to the lack of available standards for calibration. Using a signal to noise ratio for each peak, an LOD and LOQ were however established as a minimum % TAG remaining. All of the following results for peaks 5 to 10 show results that were recorded to be well below the maximum loss that would result in being under the LOQ for each peak. Therefore, all results displayed in the following sections were deemed quantifiable.

7.4.1. Peak 5 (C18:2/18:2/18:2)

7.4.1.1. Syringes

Figure 7.13 shows peak 5 results for both lipids in each container in light protected and non-light protected samples. In syringes Intralipid® both light and non-light protected show larger losses than SMOFlipid® syringes. Room temperature non-light protected Intralipid® syringes show maximal losses of 25 % at 28 days storage. Light protected Intralipid® results were ~10 % lower than non-light protected samples and indicate that within Intralipid®, light exposure had an effect on peroxidation and TAG loss occurring. Peak 5 contains three linoleic fatty acids (C18:2) which were predicted to be highly susceptible to peroxidation due to their level of unsaturation. The TAG losses observed substantiate this as does this TAG

loss when HUE and TAG remnant productions are also collectively considered. Both HUE production and TAG remnant formation were high in Intralipid® room temperature non-light protected results, however HUE formation was increased in light protected syringes. The results with the TAG losses observed for Intralipid® indicate high levels of peroxidation, and it can be postulated that a level of photo-oxidation is occurring within syringes. The process of photo-oxidation favours the formation of different hydro-peroxides (Porter et al. 1995). As discussed in section 5.7.3 (chapter 5), four potential hydroperoxides are formed from the peroxidation of linoleic acid, however auto-oxidation ('standard' peroxidation) favours the formation of two hydroperoxides at the 9' and 13' positions. Photo-oxidation has the ability to form all four hydroperoxides and whilst beyond the scope of this work, detection of these four hydroperoxides within the lipids tested would provide confirmation of the occurrence of photo-oxidation of linoleic acid.

SMOFlipid® syringes showed markedly less peroxidation and % loss of peak 5 in both light and non-light protected samples except for fridge temperature light protected results that gave a maximum of ~15 % loss at 28 days. All other SMOFlipid® syringes gave no detectable levels of loss at 28 days suggesting a lack of peroxidation. It is postulated that the lack of initial available oxygen within the syringe system inhibits the initiation of peroxidation. The extensive loss seen in Intralipid® at the same timepoint however contradicts this and as such the large difference in loss between the two lipids tested needs to be further considered. The addition of vitamin E within SMOFlipid® and its absence in Intralipid® provides a possible explanation for the lack of peroxidation shown however when considering loss of the same peak in PN bags, SMOFlipid® showed the greatest losses. Therefore, the anti-oxidant activity of the added tocopherols does not provide an adequate explanation for the syringe losses observed.

It can be postulated that the vulnerability of each lipid emulsion to photo-oxidation may be different due to the higher numbers of different TAGs observed within SMOFlipid® and the lower concentration of linoleic acid containing TAGs compared to Intralipid®. The light exposure and surface area of exposure in all syringes tested was constant, however when considering the TAGs present at the edge of each oil globule within an emulsion, i.e. the TAGs that would have physical exposure to light, the increase in TAGs present within SMOFlipid® of which four do not contain linoleic acid, would lead to less numbers of peak 5 (C18:2/18:2/18:2) physically exposed to light and could explain the apparent lack of TAG loss observed. When considering the result within SMOFlipid® and the HNE, HUE and TAG remnant production

collectively, positive production of all the secondary products suggests peroxidation is occurring within syringes. The lack of losses observed at day 28 for both light protected and non-light protected samples suggests a delay in peroxidation. Beyond 28 days, the RSD's of control samples for days 56 and 84 for non-light protected SMOFlipid® syringes fell outside of acceptable levels and were therefore excluded from analysis. The day 56 and 84 results for light protected SMOFlipid® syringes are however recorded and deemed precise and show peak 5 TAG loss occurring up to ~ 20 % at both temperatures. As such it is postulated that TAG losses and subsequent production of secondary products is delayed but present in all SMOFlipid® syringes.

Temperature had a significant effect (~ 15 %) in Intralipid® non-light protected syringes, however little difference is observed in light protected results in both lipids. As such this suggests that the potential for photo-oxidation is inhibited by fridge temperature storage.
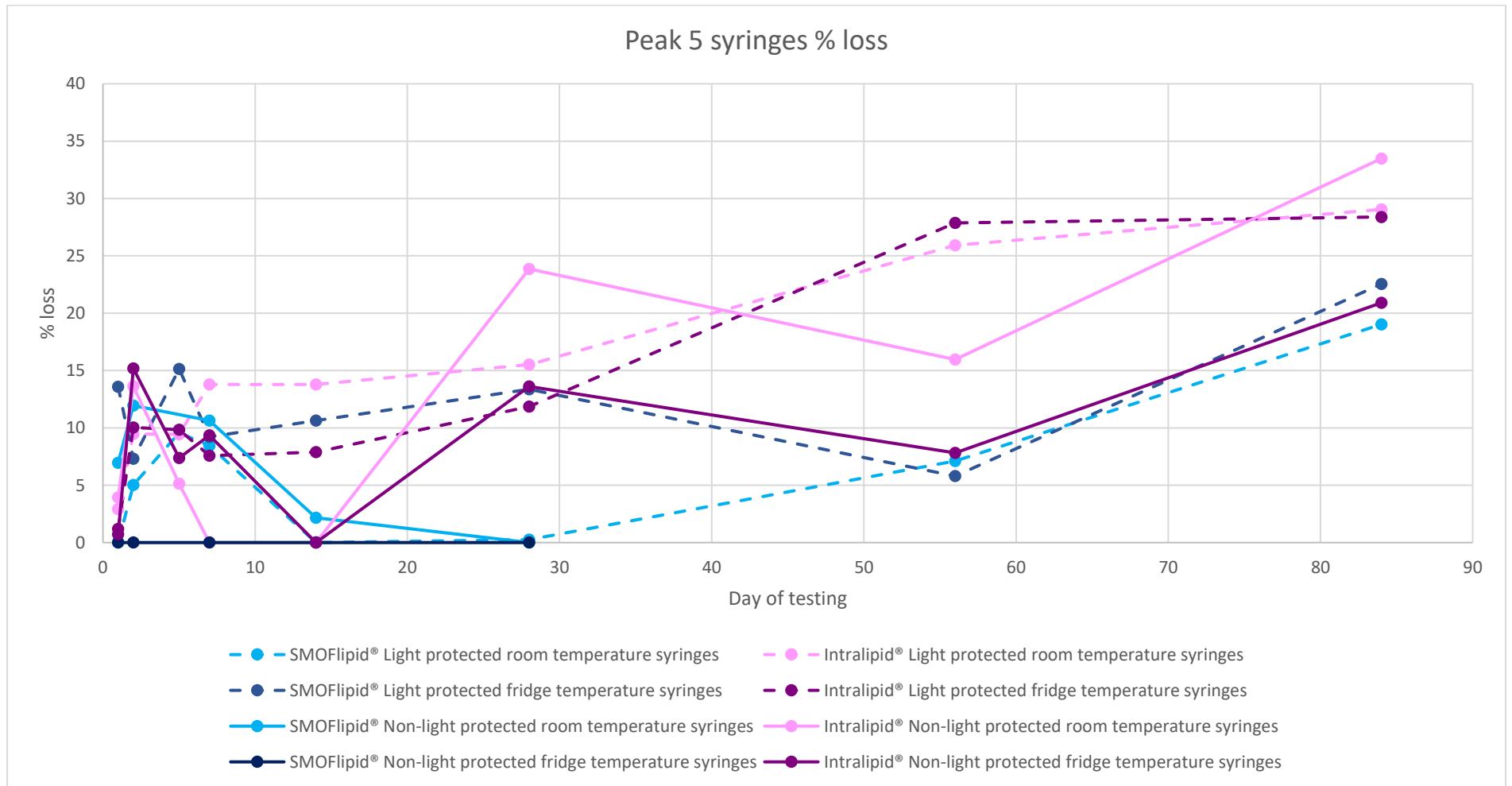
Figure 7.13 Peak 5 (C18:2/18:2/18:2) TAG losses occurring in 50 ml syringes of SMOFlipid® (blue traces) and Intralipid® (pink/purple traces).

RSD's of control samples for both lipids for PN bag results were within acceptable levels for all results up to and including day 56. As such, day 56 is considered as a point of comparison between PN bags, however day 28 results are also considered to enable comparison between syringes and bags.

As shown in figure 7.14 within PN bags light protected results for both lipids gave maximal losses of 40 % for SMOFlipid® and ~28 % for Intralipid® both at room temperature, in contrast to syringe results where non-light protected results were maximal. Total losses observed for PN bags were similar to syringes at day 28, with extensive losses occurring in later storage periods (55 and 84). Within PN bags all light protected samples suffered greater losses than non-light protected results suggesting that photo-oxidation within PN bags is not an extensive mechanism of peroxidation.

Temperature of storage had a significant (7 to ~15 %) effect on limiting peak 5 (C18:2/18:2/18:2) TAG loss in SMOFlipid® containers both light and non-light protected, however results show little effect in inhibition of loss within all Intralipid® bags at day 84. As discussed above with syringes, both temperature and oxygen availability were predicted to be limiting factors on the occurrence of peroxidation and subsequent TAG loss.

Within PN bags of both lipids a limited finite amount of atmospheric air is left within each container upon manufacturing. The presence of such oxygen from day 0 and raised temperatures are postulated to cause the initiation of and catalyse peroxidation creating TAG losses observed. When considering the peak 5 TAG loss within PN bags collectively with the secondary peroxidation products discussed in previous sections, only the TAG remnant was detected within PN bags of SMOFlipid®, whilst the TAG remnant and minimal levels of HUE were shown within Intralipid®. These results when considered collectively with the greater TAG losses in SMOFlipid® with lower levels of secondary products suggest that within SMOFlipid® the stage of peroxidation may differ to that within Intralipid® at each time-point of testing. The initial primary peroxidation products of lipid hydroperoxides are as previously discussed not detected through this assay. As such, it is postulated that within PN bags SMOFlipid® peroxidation when tested through 84 days produced primary hydroperoxides, with lower amounts of secondary cleavages occurring than within Intralipid®. Whilst this explains the

apparent TAG loss in SMOFlipid® PN bags observed with the lack of HUE or HNE, the substantial production of the TAG remnant as shown in figure 7.6 is of interest. As previously postulated, the TAG remnant within Intralipid® and until now within SMOFlipid® was formed from the cleavage of secondary peroxidation products from peak 7 (C18:2/18:1/18:1). The results within PN bags however contradict this due to the presence of large amounts of the TAG remnant within SMOFlipid® but an absence of HUE or HNE. As such, it can be postulated that within such PN bags, which as shown in the saturated TAG loss figures 7.9 to 7.12 show the largest levels of hydrolysis, that the TAG remnant seen within these containers may be resultant from the cleavage of a fatty acid from peak 10 (C18:2/18:1/16:0) through hydrolysis. As discussed within the TAG remnant section above (7.2.3) further identification of the chemical structure of the TAG remnant beyond that carried out was not possible within this work, however future studies using a sensitive mass spectrometer and fragmentation analysis of this remnant would give a definitive answer to the TAG remnant composition.

Figure 7.14 Peak 5 (C18:2/18:2/18:2) TAG loss in SMOFlipid® and Intralipid® PN 250 ml PN bags filled with 50 ml of lipid.

RSD's of control samples for all glass vials were acceptable up to and including day 56 results and therefore are used for comparisons. As discussed through previous chapters glass vial results were designed to provide a comparative set of data to PN bags and syringes. Each vial was purged with nitrogen during production to remove atmospheric air and therefore exclude oxygen from the system during storage. This was designed to indicate the vital nature of oxygen within the peroxidation pathway and TAG losses observed within each lipid. As established previously, oxygen ingress at sampling times was observed within these vials and extensive TAG losses were therefore observed in both Intralipid® and SMOFlipid® light protected results. Light protected testing occurred prior to initiation of non-light protected testing and as such modification of the method occurred with nitrogen being passed through all vials at each sampling point. In response, a minimal level of peak 5 TAG loss is observed in all non-light protected results. Figure 7.15 shows the TAG losses for peak 5 (C18:2/18:2/18:2) in both lipids. As shown, SMOFlipid® light protected vials and Intralipid® light protected vials recorded maximal losses. Whilst due to the ingress of oxygen, the higher levels of loss in SMOFlipid® is postulated to be caused by a level of hydrolysis occurring as previously discussed. Such hydrolysis appears to be lacking within Intralipid® where peroxidation is the driving lipid breakdown pathway.
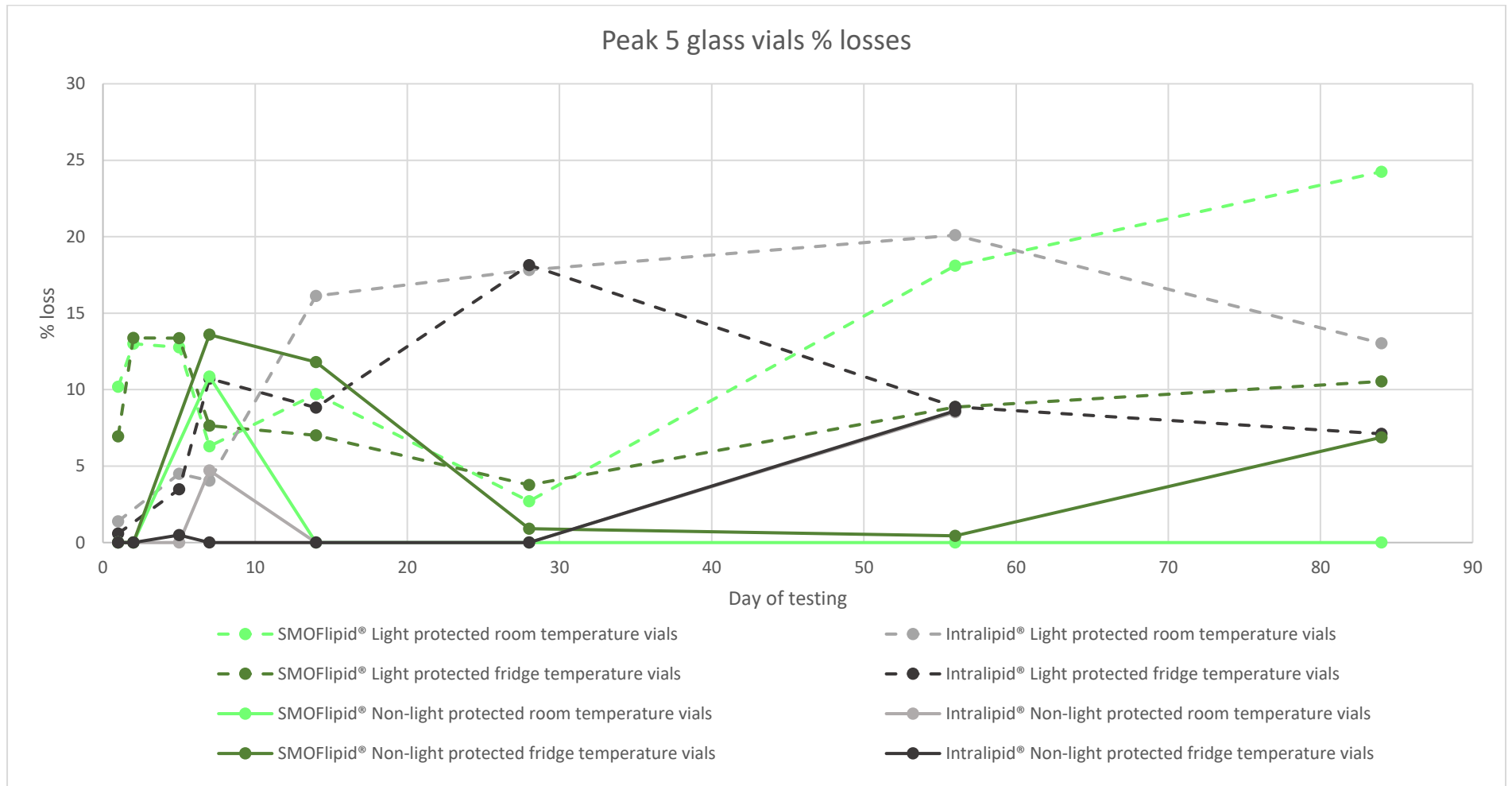
Figure 7.15 Peak 5 (C18:2/18:2/18:2) TAG loss occurring in SMOFlipid® and Intralipid® 50 ml glass vials.

Maximal TAG loss was observed in light protected SMOFlipid® PN bags (> 40 %) followed by Intralipid® non-light protected syringes (< 35 %). Temperature influenced non-light protected syringes, non-light and light protected PN bags of both lipids and fridge storage effectively reduced TAG loss occurring. Peak 5 TAG loss occurred in all containers at all temperatures of storage except non-light protected SMOFlipid® syringes although these results are only shown up to day 28 due to control sample RSD drift. Hydrolysis reactions within peak 5 appear to occur within SMOFlipid® but not within Intralipid® and explain the large losses observed within SMOFlipid® PN bags and glass vials with the absence of recorded secondary peroxidation products other than the TAG remnant. It is postulated that the stage of peroxidation occurring within 84-day storage of SMOFlipid® is different (hydroperoxides) to that within Intralipid® where terminal peroxidation products are detected.

7.4.2. Peak 6 (C18:2/18:2/18:1)

7.4.2.1. Syringes

As discussed in peak 5 comparisons RSD's were acceptable within syringes until day 28 and as such this day of testing was used for comparisons. All light protected results within both lipids showed maximal losses recorded, suggesting a lack of photo-oxidation occurring within this TAG. Figure 7.16 shows the TAG loss observed within both lipids in syringes. At day 28, all syringes tested recorded a level of TAG loss, with temperature having a significant effect on loss observed, fridge temperatures inhibiting loss and therefore peroxidation occurring. Peroxidation and therefore TAG losses increase in all results except light protected SMOFlipid® fridge samples from day 14 onwards, substantiating previous conclusions that oxygen presence is vital in the initiation and propagation of peroxidation. As such syringe losses are limited initially as oxygen ingress is at a minimal rate due to leaking between the syringe barrel and plunger. Peroxidation of peak 6 (C18:2/18:2/18:1) is predicted to cleave each of the fatty acid chains, resulting in one molecule of HUE from oleic acid and the formation of secondary aldehydic products from linoleic acid, one of which being HNE. When considering the peak 6 syringe results collectively with the HNE and HUE, formation of HUE was highest in light protected Intralipid® and SMOFlipid® room temperature syringes,

which recorded ~35 % and ~20 % of peak 6 TAG loss, showing as predicted the peroxidation of oleic acid from peak 6. The production of HNE was however highest in SMOFlipid® non-light protected syringes, which showed little loss within peak 6 and suggests that HNE production is from another TAG within the lipid.
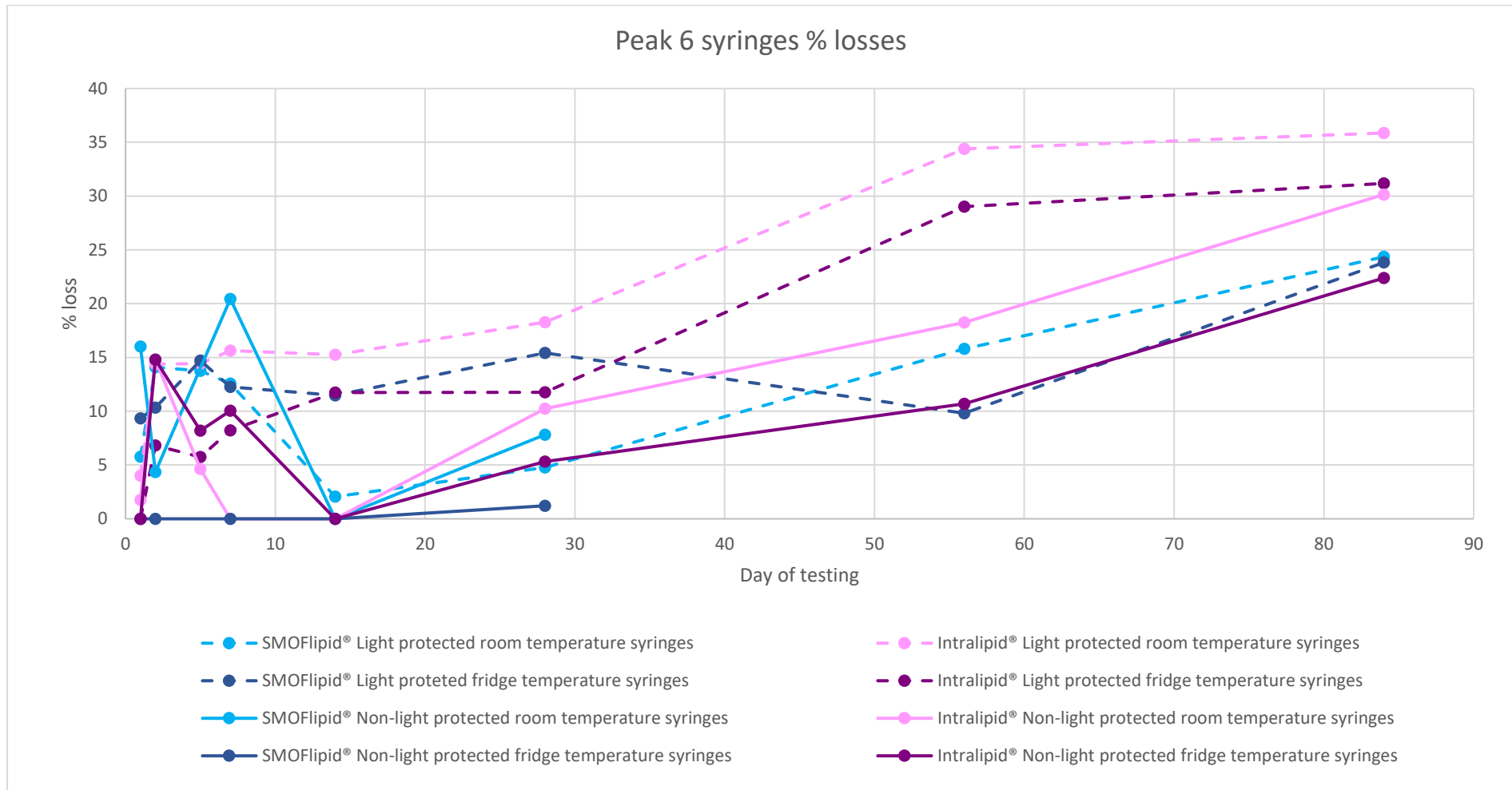
Figure 7.16 Peak 6 (C18:2/18:2/18:1) TAG losses in SMOFlipid® and Intralipid® 50 ml syringes at room and fridge temperatures.

Within PN bags SMOFlipid® light protected results showed maximal peak 6 loss of >30 %. All light protected results for both lipids produced larger losses than non-light protected results as shown in figure 7.17, suggesting a lack of photo-oxidation occurring. Rates of TAG loss and peroxidation unlike syringes was rapid initially and reduced over prolonged storage which, as postulated in peak 5 results, was due to the oxygen availability within the PN bags. The finite amount of air present within PN bags at the point of manufacturing leads to initial rapid peroxidation and TAG loss, with a tapering of the rate as oxygen is exhausted and the termination of peroxidation occurs.

Whilst SMOFlipid® showed maximal loss, Intralipid® PN bags also showed extensive losses of >25 %. The breakdown of Peak 6 TAG (C18:2/18:2/18:1) would be predicted to formulate HUE and potentially HNE as discussed within syringe results. However, results obtained for PN bags showed no HNE formation within PN bags and minimal HUE production over 84 days, suggesting that losses observed within PN bags could be resultant from the peroxidation of the linoleic acid chains within the TAG at a position where the secondary product produced is not HNE but another secondary aldehyde and as such not detected through the assay. This explains the extensive losses observed with little HNE or HUE detected.

7.4.2.3. Glass vials

Glass vial results for peak 6 (C18:2/18:2/18:1) follow identical trends to peak 5 losses. SMOFlipid® light protected vials show maximal losses followed by Intralipid® light protected vials which as discussed previously were tested first and as such the method of sampling used left the potential for ingress of oxygen within the vial, resulting in peroxidation and the TAG losses observed. All vials where nitrogen was used to purge air at all testing points showed minimal TAG loss over 84 days. As with peak 5 the higher TAG loss in SMOFlipid® was postulated to be due to an element of hydrolysis and peroxidation occurring. Figure 7.18 shows all peak 6 (C18:2/18:2/18:1) TAG losses in glass vial samples tested.
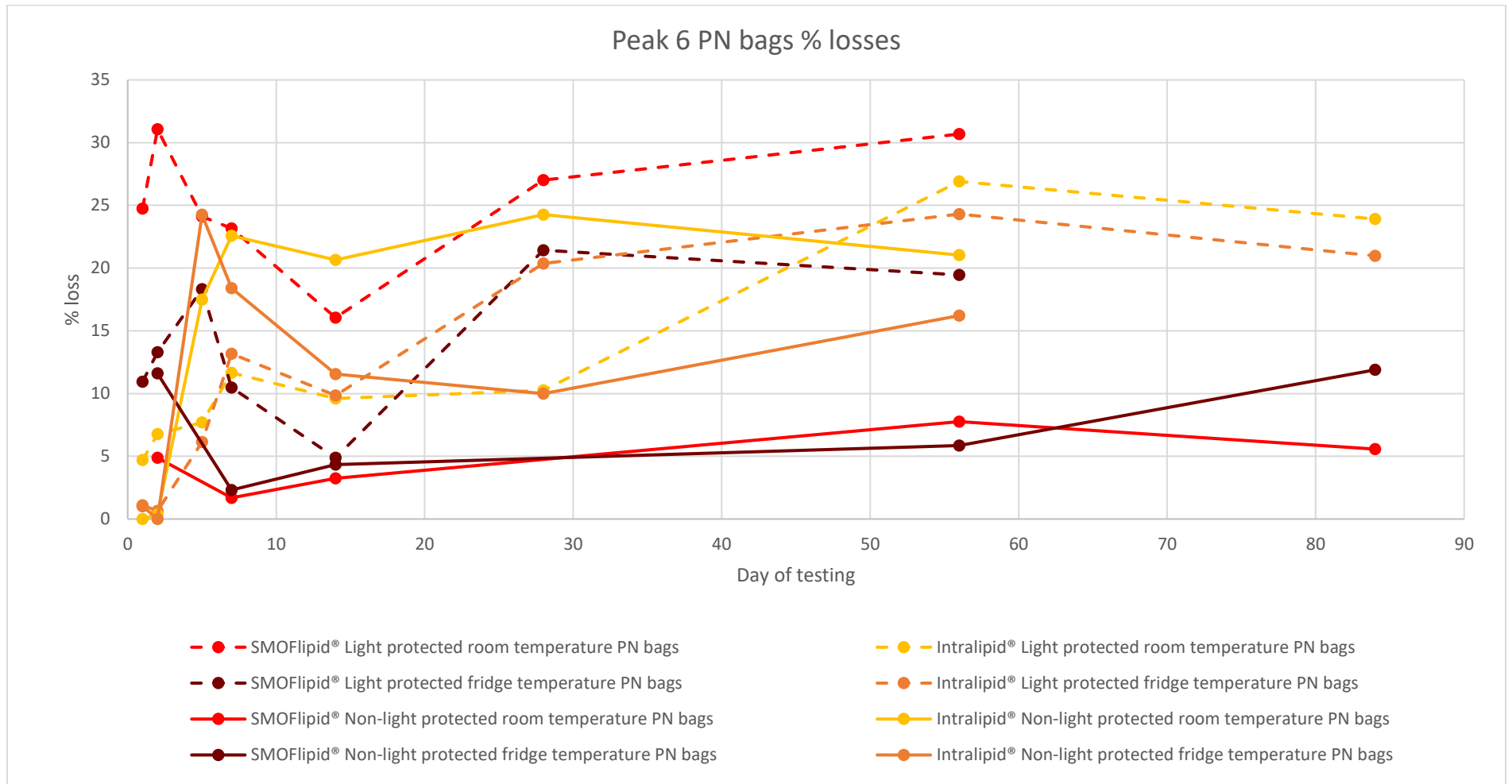
Figure 7.17 Peak 6 (C18:2/18:2/18:1) TAG loss in SMOFlipid® and Intralipid® PN bags at room and fridge temperatures.
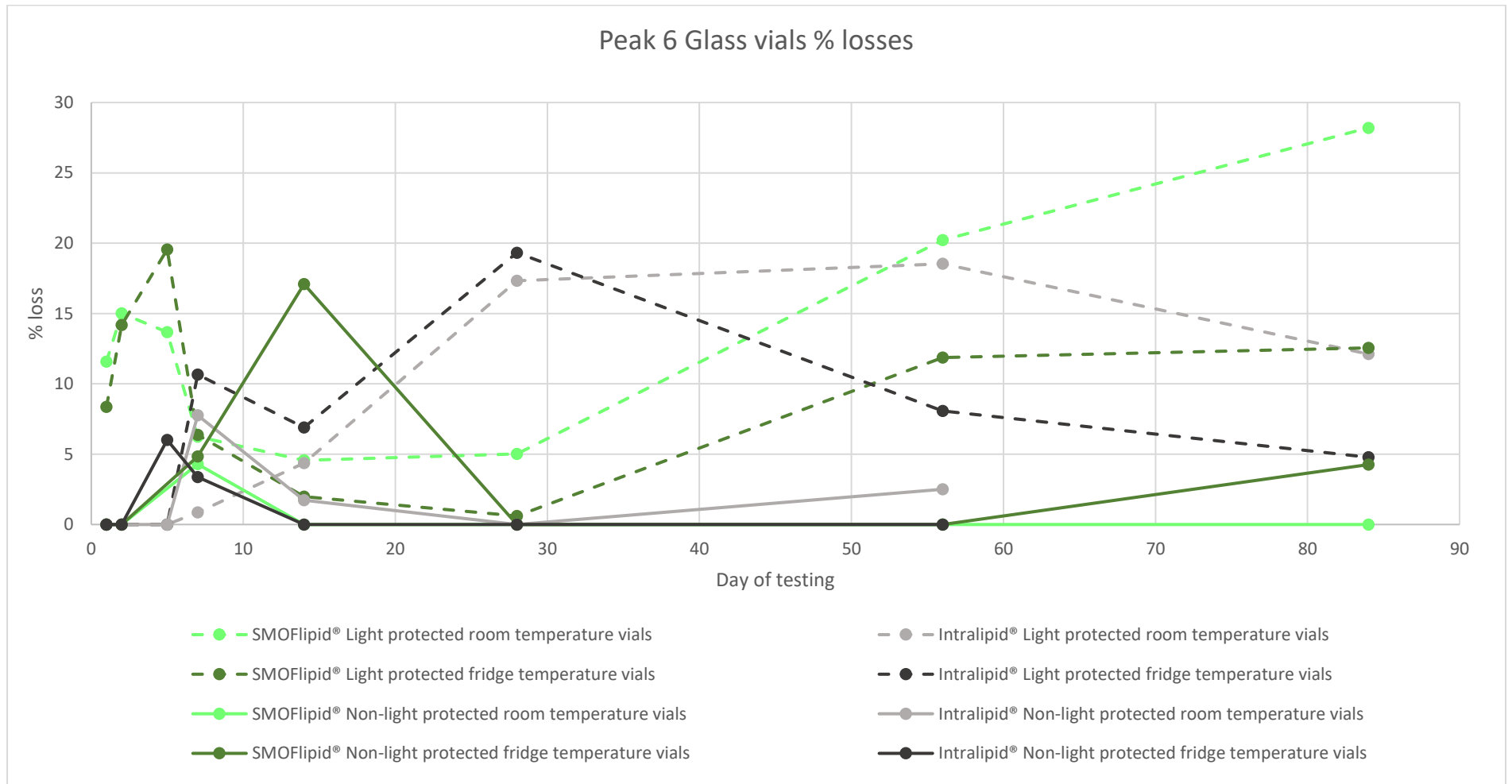
Figure 7.18 Peak 6 (C18:2/18:2/18:1) TAG losses in SMOFlipid® and Intralipid® 50 ml glass vials at room and fridge temperatures.

341

7.4.2.4. Peak 6 conclusions

Following similar trends as seen with peak 5 TAG losses, peak 6 loss was maximal in light protected SMOFlipid® PN bags followed by light protected Intralipid® syringes both at room temperatures. HUE formation within syringes suggests peak 6 TAG loss through oleic acid peroxidation. The lack of HNE and minimal HUE within SMOFlipid® PN bags suggests a level of hydrolysis is responsible for the TAG losses observed. Maximal losses observed within peak 6 are similar to the levels of loss observed in peak 5 across all containers tested. Light protected results in all containers showed maximal peak 6 (C18:2/18:2/18:1) TAG losses and a lack of photo-oxidation is concluded from these results.

7.4.3. Peak 7 (C18:2/18:1/18:1)

Peak 7 results are of particular interest as it is postulated that the TAG remnant formed is from the peroxidation of this TAG and the loss of HNE and HUE. As with all previous peaks container results are shown with comparisons between lipid formulations and levels of light protection drawn.

7.4.3.1. Syringes

As shown in figure 7.19 syringe results for peak 7 show maximal TAG losses occurring in non-light protected Intralipid® (~ 38 %) and light protected Intralipid® (~ 34 %) syringes at room temperature, though fridge temperature also showed significant losses greater than all SMOFlipid® syringes tested. At day 28, SMOFlipid® light protected syringes showed peak 7 loss however non-light protected syringes showed no losses. This indicates the potential for the presence of a level of photo-oxidation to be present within Intralipid® and an apparent lack within SMOFlipid® syringes. Both lipids showed a significant effect when temperature of storage is considered, with fridge storage prohibiting loss occurring within Intralipid®. Within SMOFlipid® light protected results however recorded fridge temperature losses significantly greater than room temperature syringes. This indicates within these samples' peroxidation was not inhibited by refrigeration.

When considering the results collectively with secondary peroxidation product results, Intralipid® light protected syringes show high levels of HUE as does light protected SMOFlipid® syringes which, whilst smaller also show peak 7 TAG loss (15

– 20 %). The peroxidative breakdown of peak 7 to create the TAG remnant observed requires the cleavage of two molecules of HUE and one molecule of HNE. TAG remnant results show highest levels of production in Intralipid® non-light protected syringes (room temperature) which show the largest levels of peak 7 loss. HNE production of ~ 10 µM was also observed within these syringes which when considered collectively indicate the peroxidation of TAG 7, the cleavage of HNE and HUE and the formation of the TAG remnant within Intralipid® as previously predicted. Within SMOFlipid syringes, HNE production is maximal (non-light protected), a level of HUE production is observed (light protected) and TAG remnant production is present but minimal. The TAG losses observed within these syringes for peak 7 is minimal in light protected syringes and very low (< 1%) in non-light protected results suggesting that the production of the secondary products seen is due to minimal peak 7 peroxidation and due to other TAG breakdown.

7.4.3.2. PN Bags

PN bag results for peak 7 (C18:2/18:1/18:1) show markedly different trends to those observed in previous peaks (5 & 6). At day 56 Intralipid® light protected and non-light protected bags showed maximal loss (25 %) with no significant difference between temperatures of storage. SMOFlipid® PN bags in comparison to previous peaks discussed show significantly less loss for peak 7. Light protected results of (3 – 12 %) for SMOFlipid® and (~3 to 20 %) for non-light protected PN bags at day 56 show significant differences between temperatures of storage. All results for peak 7 PN bags are presented in figure 7.20.

When considered with the secondary product results discussed above, within PN bags the lack of HNE and minimal HUE detected suggests that the peroxidation within this TAG is unlikely to be due to cleavage of HNE and HUE as shown previously in syringes. There is however a level of TAG remnant produced within both SMOFlipid® and Intralipid® PN bags. This is of interest and suggests that the TAG remnant structure within these bags may be different to that observed within syringes and potentially be formed from the breakdown of a different TAG. The presence of significant losses within Intralipid® and the lack of HNE or HUE observed provides evidence for the presence of hydrolysis occurring within PN bags. Cleavage of one or more of the fatty acids from the TAG backbone of peak 7 would result in the loss observed within PN bags and correspond to the lack of presence of secondary products.
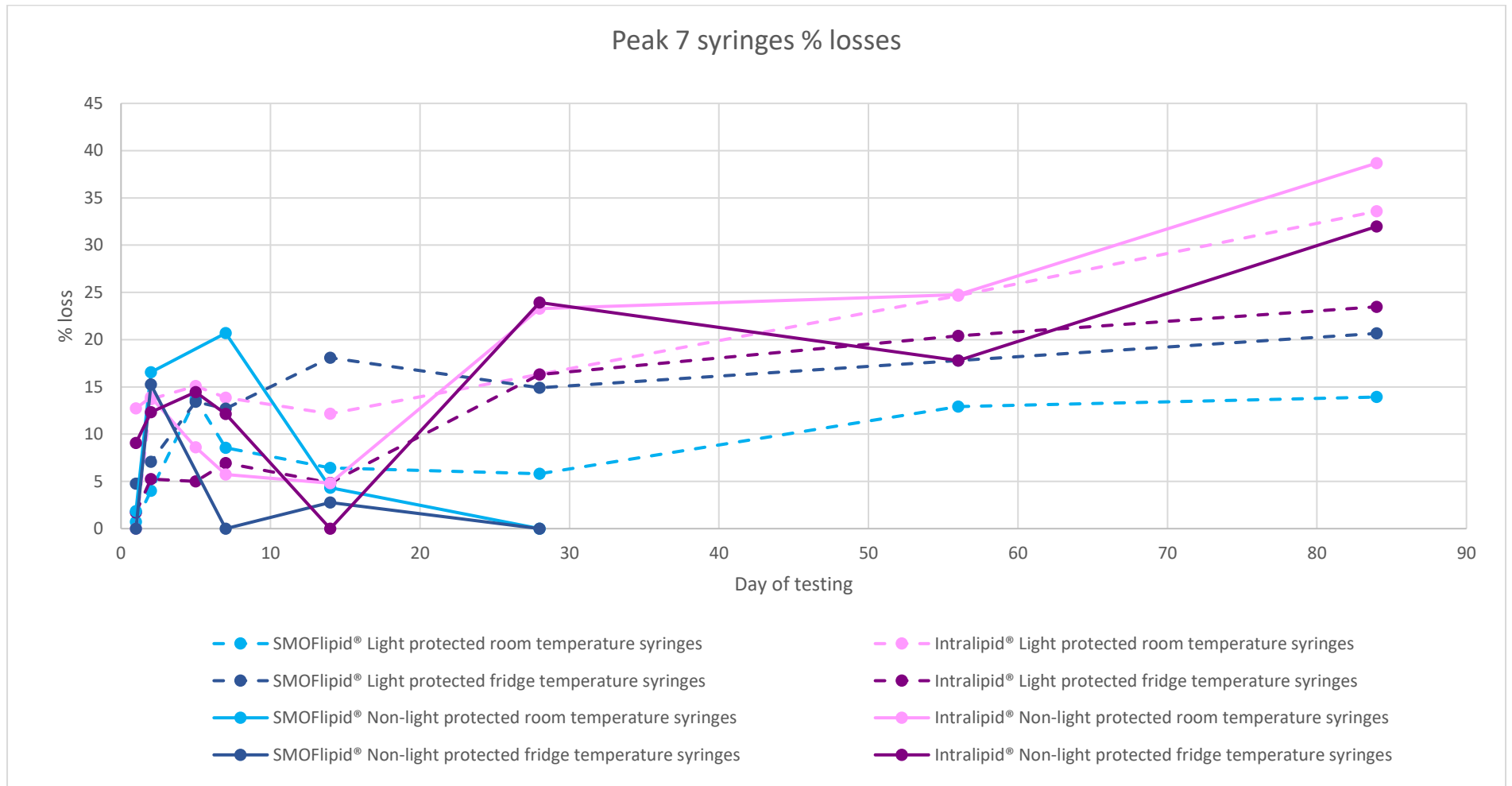
Figure 7.1 Peak 7 (C18:2/18:1/18:1) TAG losses in 50 ml syringes of SMOFlipid® and Intralipid® at room and fridge temperatures.

344
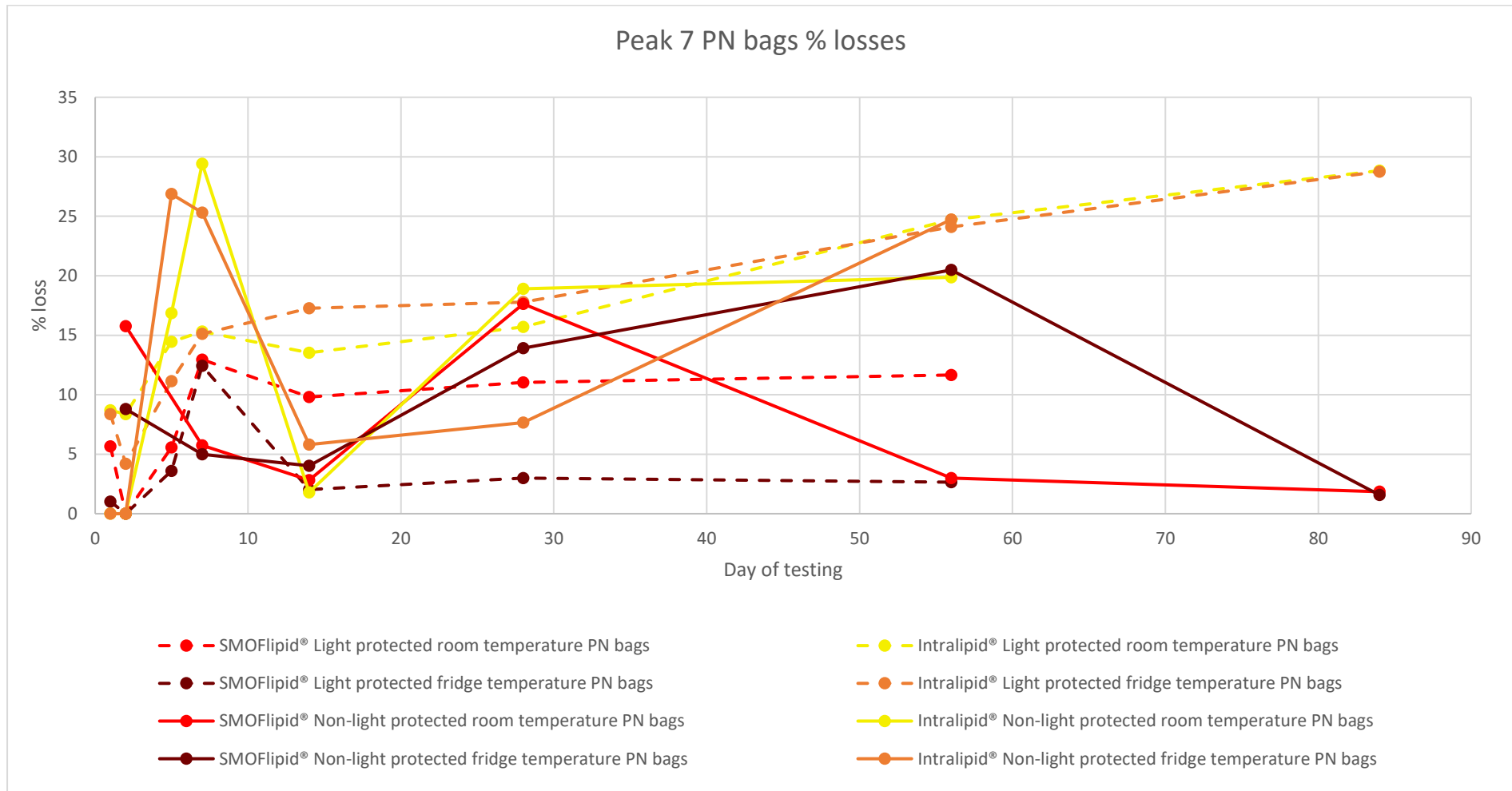
Figure 1.2 Peak 7 (C18:2/18:1/18:1) TAG losses in PN bags of SMOFlipid® and Intralipid® at room and fridge temperatures.

As with previous peaks 5 and 6, peak 7 (C18:2/18:1/18:1) show similar trends in losses observed. Both lipids light protected results show maximal losses as postulated due to oxygen ingress into the system. The lack of all secondary products indicates that the losses seen are due either to hydrolysis of fatty acids from the TAG backbone, peroxidation resulting in different secondary products not detected or that peroxidation present is limited and as such primary products (lipid hydroperoxides) are present and not detected. Confirmation of the type of losses observed could be carried out in future studies through detection and identification of free fatty acids as methyl esters through mass spectrometry. Figure 7.21 shows all glass vial results recorded for all temperatures. As indicated in non-light protected results when vials were purged with nitrogen at each sampling point peroxidation was minimal to zero again substantiating the vital nature of oxygen presence for peroxidation and TAG loss.

7.4.3.4. Peak 7 conclusions

Results within syringes show the positive peroxidation of peak 7 with the production of HNE and HUE and indicate that the TAG remnant observed is resultant from peak 7 breakdown within syringes. PN bag results differ from syringes and indicate a minimal loss of peak 7 through production of the TAG remnant and it is postulated that either hydrolysis or cleavage of different secondary products from linoleic acid is the cause of the TAG loss observed. Intralipid® results for both PN bags and syringes are significantly higher than SMOFlipid® though TAG loss occurs in both lipids. Light protection had a positive effect in syringes but less in PN bags suggesting that temperature has an effect on the initial trends of TAG loss observed when oxygen presence is minimal (syringes). It can be postulated that within syringes high temperatures creates plastic and rubber weakening which increases the leakage of oxygen into the system leading to the superior levels of TAG loss observed at room temperatures.
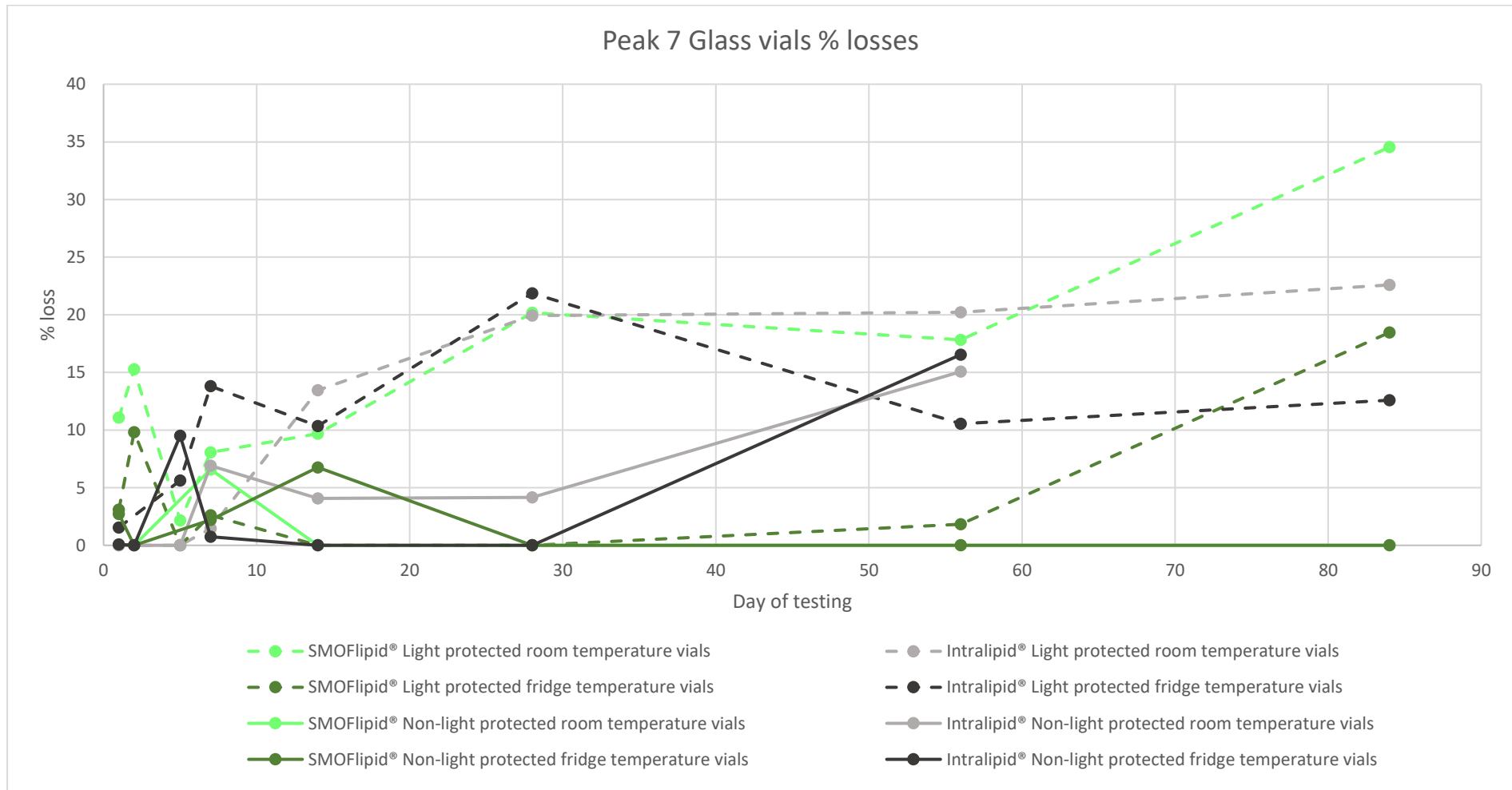
Figure 1.3 Peak 7 (C18:2/18:1/18:1) TAG losses in 50 ml glass vials of SMOFlipid® and Intralipid® at room and fridge temperatures.

7.4.4. Peak 8 (C18:2/18:2/16:0)

7.4.4.1. Syringes

Peak 8 syringes follow similar to trends in results to peaks 5 and 6 with all Intralipid® results surpassing SMOFlipid® losses. Non-light protected results are maximal in Intralipid® (~ 30 % at day 28) with zero levels recorded in SMOFlipid® at the same time point. Temperature has a negative effect in all results where loss was recorded suggesting an inhibition of TAG loss at fridge temperatures. When considering results for peak 8 in combination with HNE, HUE and TAG remnant production, HNE would be the only secondary product potentially detected due to the TAGs chemical structure. Losses within Intralipid® syringes are substantial and could therefore contribute to the HNE detected within these containers. Figure 7.22 shows the peak 8 TAG losses observed in both lipids in syringes.

7.4.4.2. PN bags

PN bag results follow the same trends as peaks 5 and 6 with SMOFlipid® light protected bags creating maximal losses of > 45 %. This is the highest loss observed in all unsaturated peaks (5 to 10) and suggests extensive TAG breakdown is occurring. Light protected Intralipid® results also show extensive loss (~ 30%). A lack of HNE is observed within PN bags of both lipids suggesting that the peroxidation occurring within this TAG is either at a different site within the linoleic acid chain or through a different degradation process. Figure 7.23 shows the PN bag results for peak 8 TAG in both lipids at room and fridge temperatures.

As previously discussed in chapter 5, linoleic acid is predicted to peroxidise readily where available oxygen is present. The products created however are dependent on the double bond targeted and the positional hydroperoxide created. It can therefore be postulated that peroxidation occurring is resulting in a different aldehydic product, one that is not detected at 222nm through UV detection. It is also of note however that as shown in peaks 1 to 4 in SMOFlipid®, hydrolytic reactions appear to occur within the emulsions. Peak 8 contains a palmitic acid chain which can be postulated to also be prone to hydrolysis.
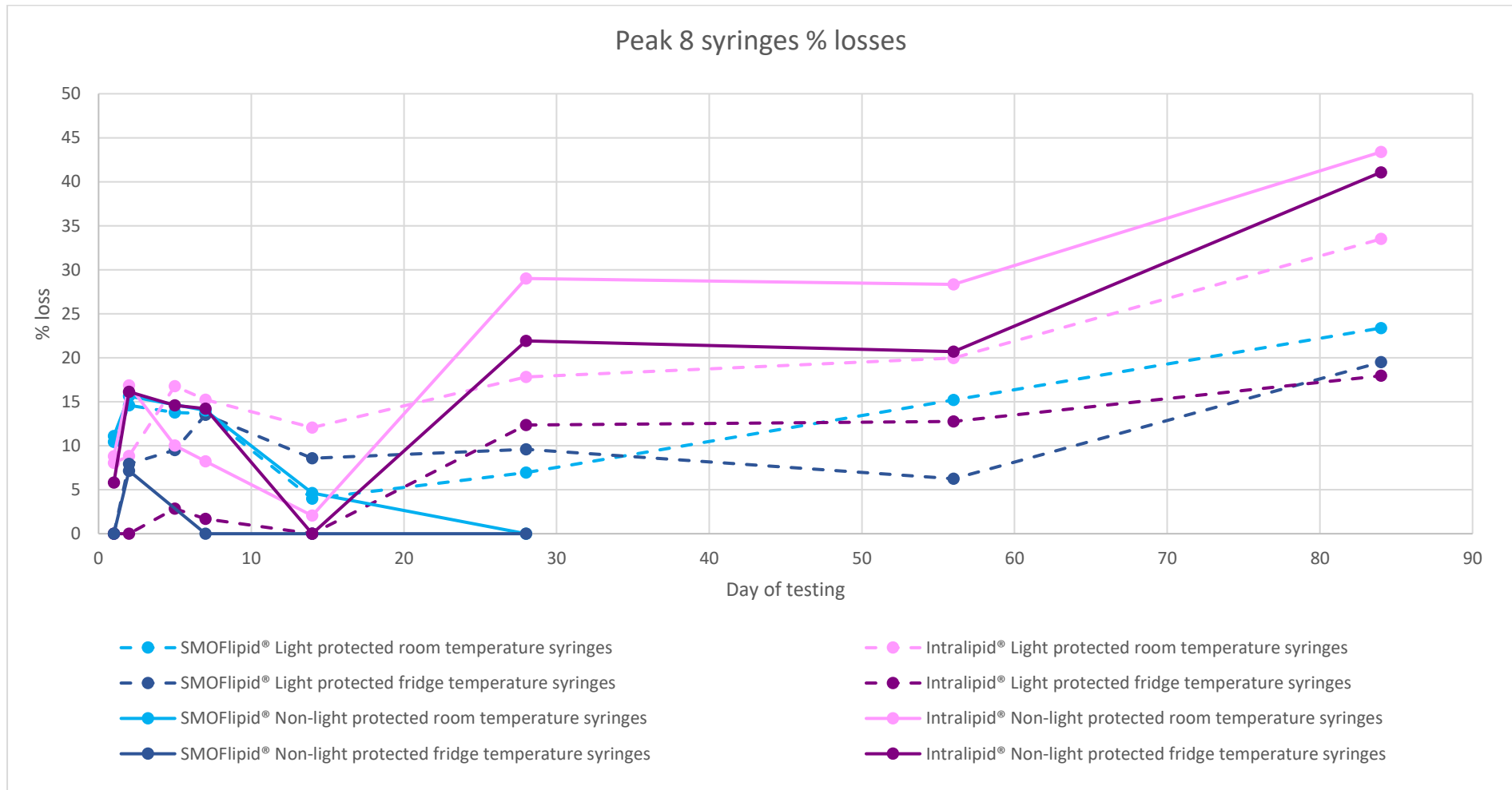
Figure 1.4 Peak 8 (C18:2/18:2/16:0) TAG losses in 50 ml syringes of SMOFlipid® and Intralipid® at room and fridge temperatures.
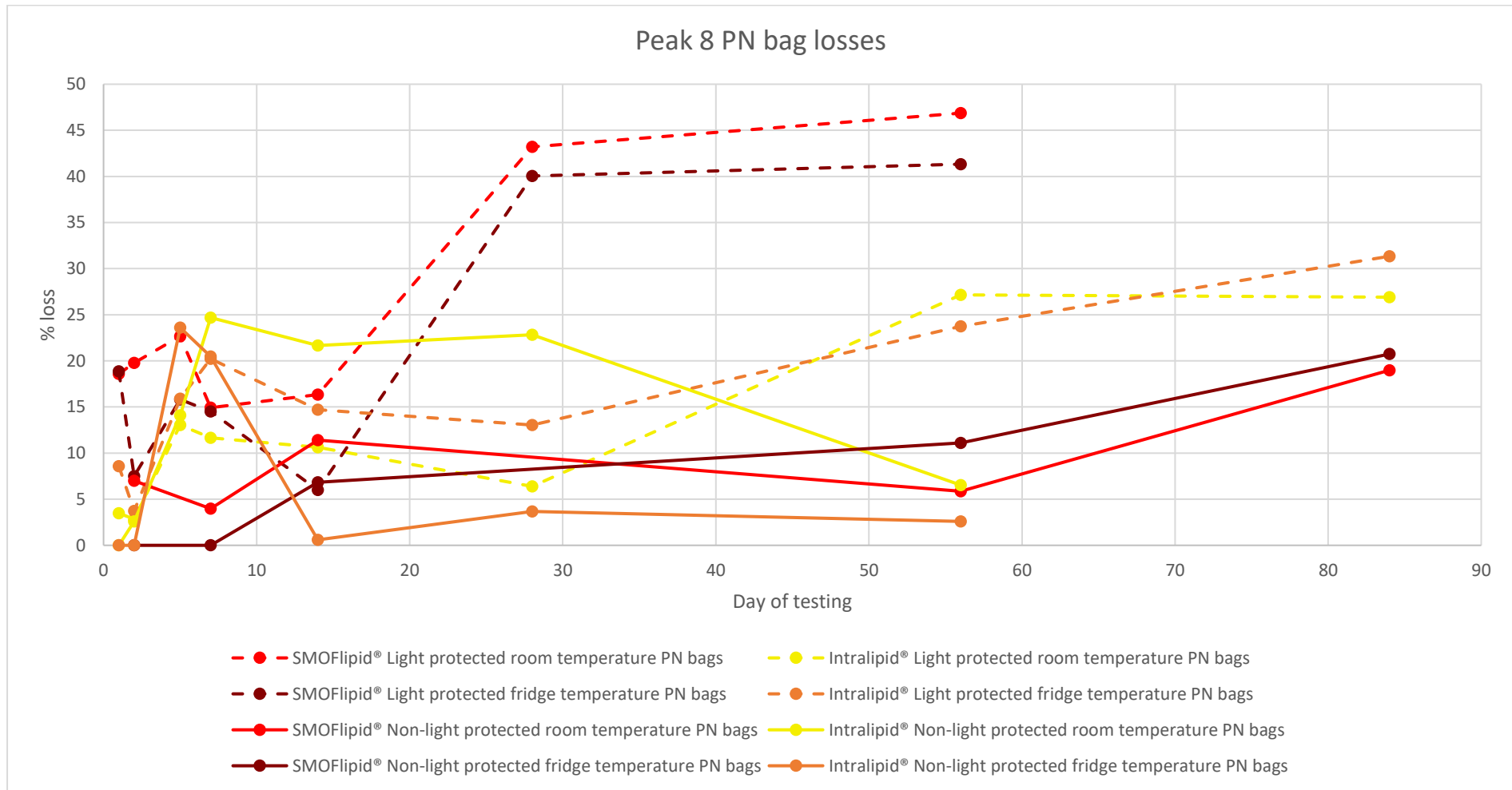
Figure 1.5 Peak 8 (C18:2/18:2/16:0) TAG losses in PN bags of SMOFlipid® and Intralipid® at room and fridge temperatures.

7.4.4.3. Glass vials

Glass vials show under 25 % loss in all containers with light protected results maximal for both SMOFlipid® and Intralipid® in line with previous peaks results and due to ingress of oxygen into the vial. Non-light protected results where nitrogen was purged at all testing points showed minimal (near zero) losses and suggest that the lack of oxygen within the system prohibits peroxidation occurring. The lack of TAG losses within glass vials also indicates a lack of hydrolysis occurring. Whilst hydrolysis of the ester bonds between the fatty acid chain and the glycerol backbone does not require oxygen, it is postulated that the hydrolysis reactions only occur where the emulsion system is under a state of high energy, i.e. where high levels of peroxidation and reactive oxygen/radicals are present. Figure 7.24 shows the peak 8 TAG losses recorded in all glass vials.

7.4.4.4. Peak 8 conclusions

Peak 8 losses were similar to those shown in peaks 5 and 6 and indicate maximal losses in Intralipid® within syringes and SMOFlipid® in PN bags. Peak 8 (C18:2/18:2/16:0) results showed evidence of hydrolysis of fatty acids from the TAG backbone contributing to the losses observed and the postulated presence of secondary peroxidation products other than HNE that were therefore not detected through the assay.
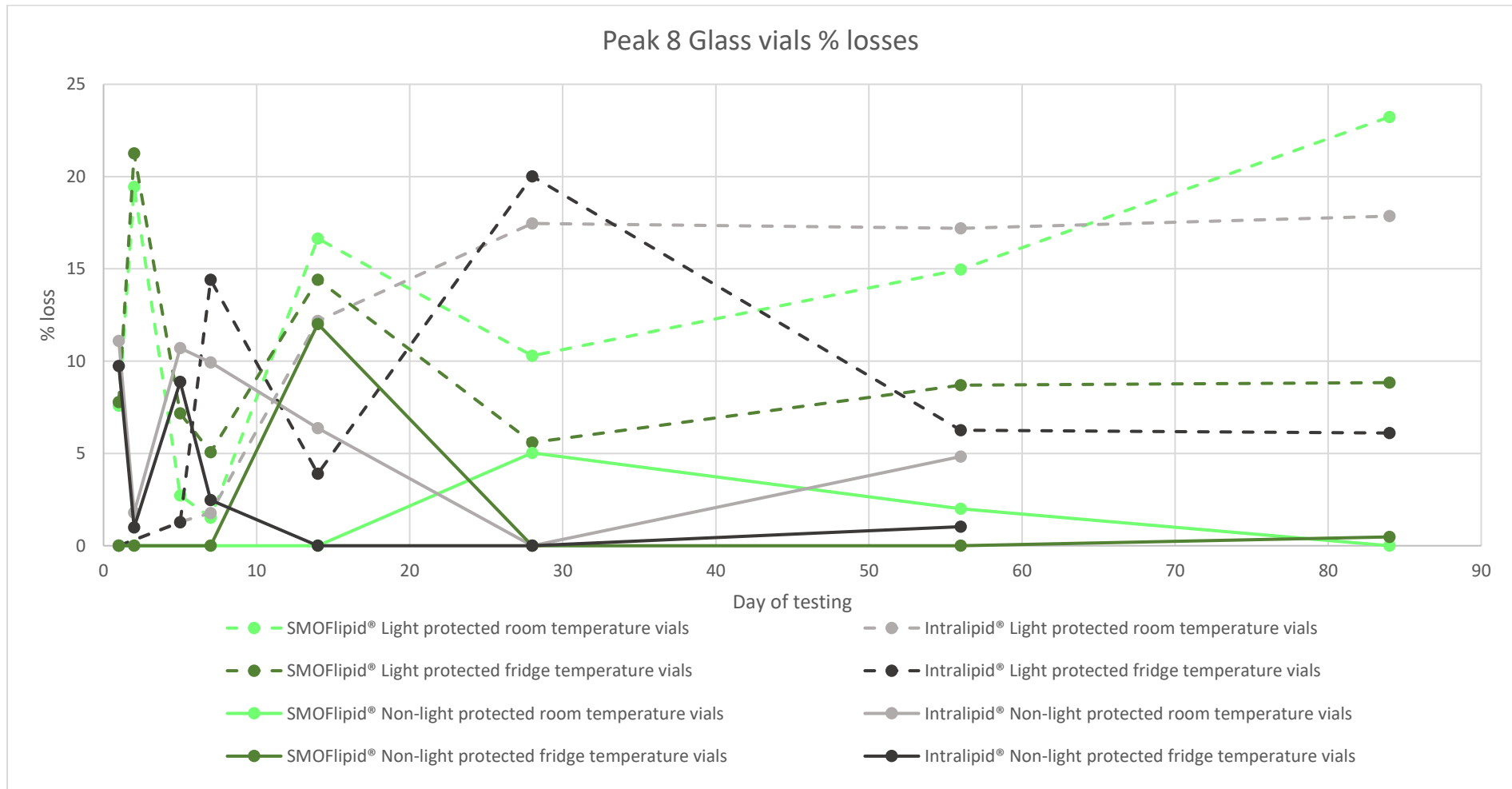
Figure 1.6 Peak 8 (C18:2/18:2/16:0) TAG losses in 50 ml glass vials of SMOFlipid® and Intralipid® at room and fridge temperatures.

7.4.5. Peak 9 (C18:1/18:1/18:1)

It is postulated that within each lipid, higher peak 9 TAG losses would be observed within SMOFlipid® than Intralipid® due to increased quantities of oleic acid present within SMOFlipid® as previously discussed in chapter 5 (section 5.1). Oleic acid peroxidation is predicted to create HUE as a secondary aldehydic product and as such SMOFlipid® was postulated to make higher levels of loss.

7.4.5.1. Syringes

Intralipid® non-light protected syringes created maximal losses of > 45% followed by SMOFlipid® light protected results of >25 %. SMOFlipid® non-light protected syringes at day 28 showed no TAG loss, however RSD's of control samples beyond 28 days of testing exclude further results from analysis so later TAG loss in these syringes cannot be excluded. When considering HUE production collectively with C18:1/18:1/18:1 TAG loss observed Intralipid® and SMOFlipid® light protected and non-light protected results all show a level of production of HUE within syringes and when considered with the peak 9 TAG losses indicates peroxidation of oleic acid chains resulting in HUE production and losses observed.

Figure 7.25 shows the peak 9 TAG losses recorded in all syringes tested. As with pervious peaks 5, 6 and 8 temperature had a significant effect on all results except non-light protected SMOFlipid® with Intralipid® loss being inhibited as predicted by fridge storage. SMOFlipid® light protected results as with previous peaks are of interest as fridge temperature results recorded higher losses than those stored at room temperature. This result when considered with the zero losses recorded in non-light protected SMOFlipid® syringes at day 28 show little peroxidation within room temperature syringes. The presence of vitamin E within this emulsion offers a potential explanation for this when considering the syringe results alone, however as previously seen extensive TAG losses are observed in PN bags and as such vitamin E appears ineffective as an antioxidant. Hydrolysis of a fatty acid from peak 9 TAG within SMOFlipid® is postulated to be unaffected by temperature and could therefore create the greater loss observed within fridge temperature results.
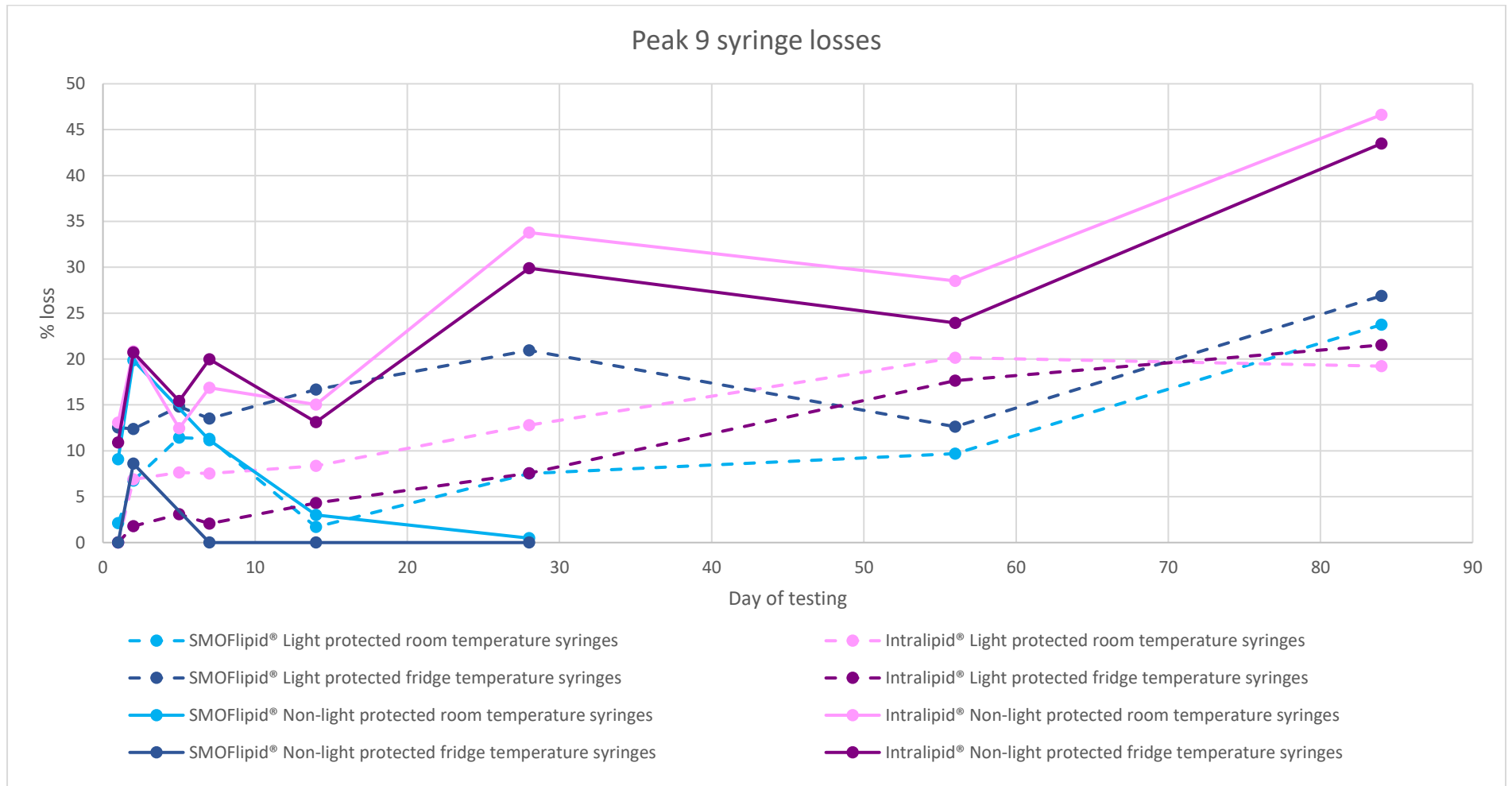
Figure 1.7. Peak 9 (C18:1/18:1/18:1) TAG losses within 50 ml syringes of SMOFlipid® and Intralipid® at room and fridge temperatures.

As with syringe results above, PN bag data for peak 9 (C18:1/18:1/18:1) follow the same trends as peaks 5,6 and 8 with SMOFlipid® light protected PN bags recording maximal losses of 45 % at room temperature. All light protected bags showed greater losses than non-light protected samples indicating a lack of photooxidation occurring. The minimal HUE detected within PN bags suggests that the extensive losses observed within this TAG are due to hydrolysis and cleavage of fatty acid(s) from the TAG backbone. This TAG (C18:1/18:1/18:1) is particularly important when considering the large loss observed within SMOFlipid® as it substantiates the evidence of hydrolytic TAG breakdown occurring. The only two secondary aldehydic products formed from oleic acid due to its single double bond is that of HUE (C11) and hydroxydecenal (HDE C10) as discussed in chapter 3 (peak B identification). Therefore, the minimal HUE observed and the lack of other unknown new peaks within the UV chromatogram seen from SMOFlipid® PN bags suggests that hydrolysis is the only breakdown occurring.

Within all PN bag results for peak 9 temperature had a predicted effect on storage where fridge temperatures reduced TAG losses. Figure 7.26 shows peak 9 losses within both lipids.

7.4.5.3. Glass vials

As shown in figure 7.27 both peak 9 SMOFlipid® and Intralipid® light protected glass vials recorded similar losses and trends of results to previous peaks where oxygen ingress into the testing system occurred at sampling. Intralipid® non-light protected results were higher than in previous peaks, but under 20 % at day 56 (day 84 result excluded due to high control RSDs). The level of control of oxygen within all samples appeared to directly relate to the levels of TAG loss observed.

7.4.5.4. Peak 9 conclusions

The peak 9 results are of interest as significant losses are observed in both lipid formulations in different storage containers. SMOFlipid® PN bags and Intralipid® syringes, both light protected showed maximal losses with the formation of HUE in Intralipid® syringes indicating peroxidation of this TAG into terminal secondary products. Large PN bag SMOFlipid® losses with minimal detection of secondary

peroxidation products suggest extensive hydrolysis occurring or peroxidation in early stages (lipid hydroperoxides).
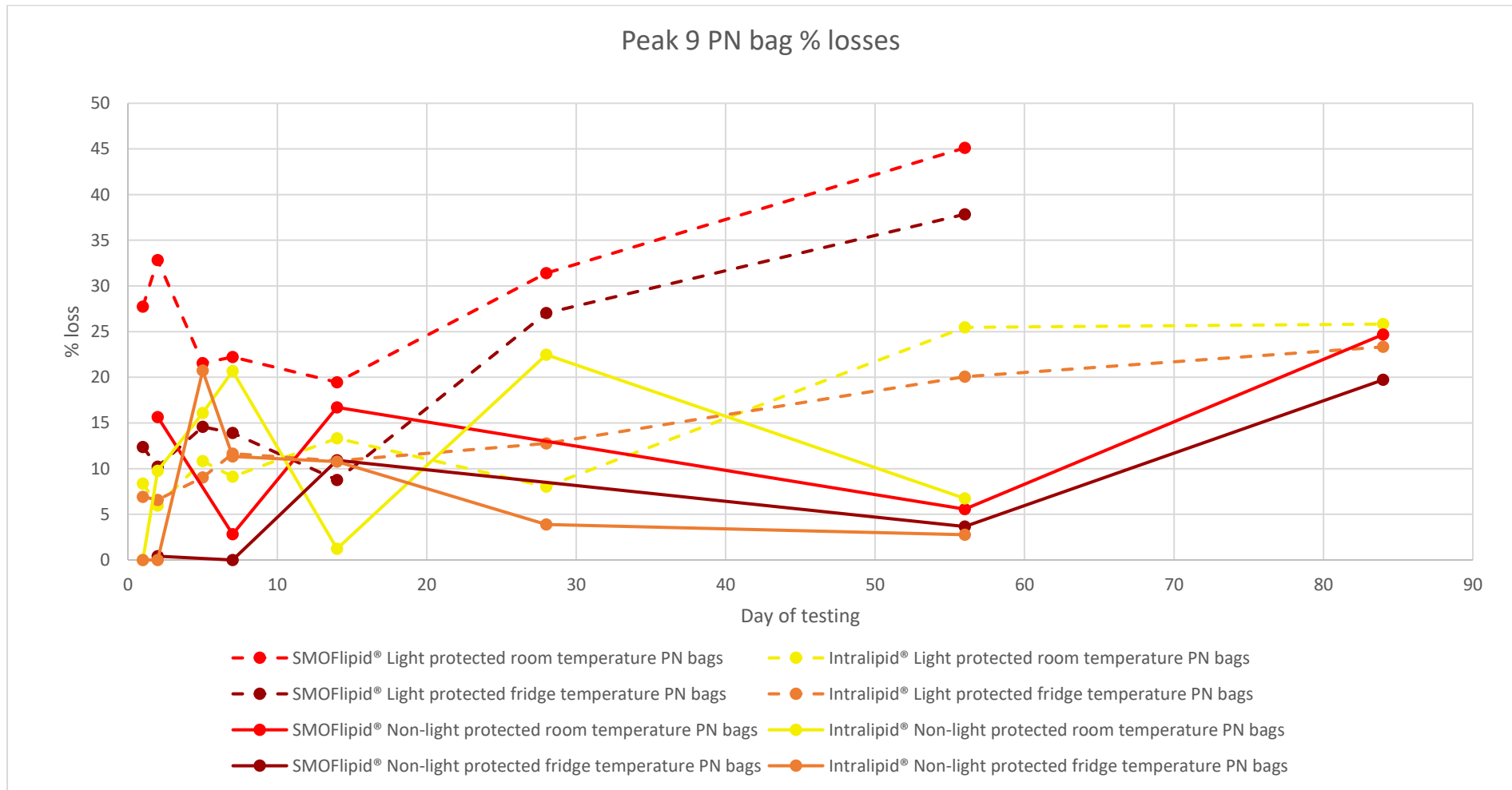
Figure 1.8 Peak 9 (C18:1/18:1/18:1) TAG losses in PN bags of SMOFlipid® and Intralipid® at room and fridge temperatures.
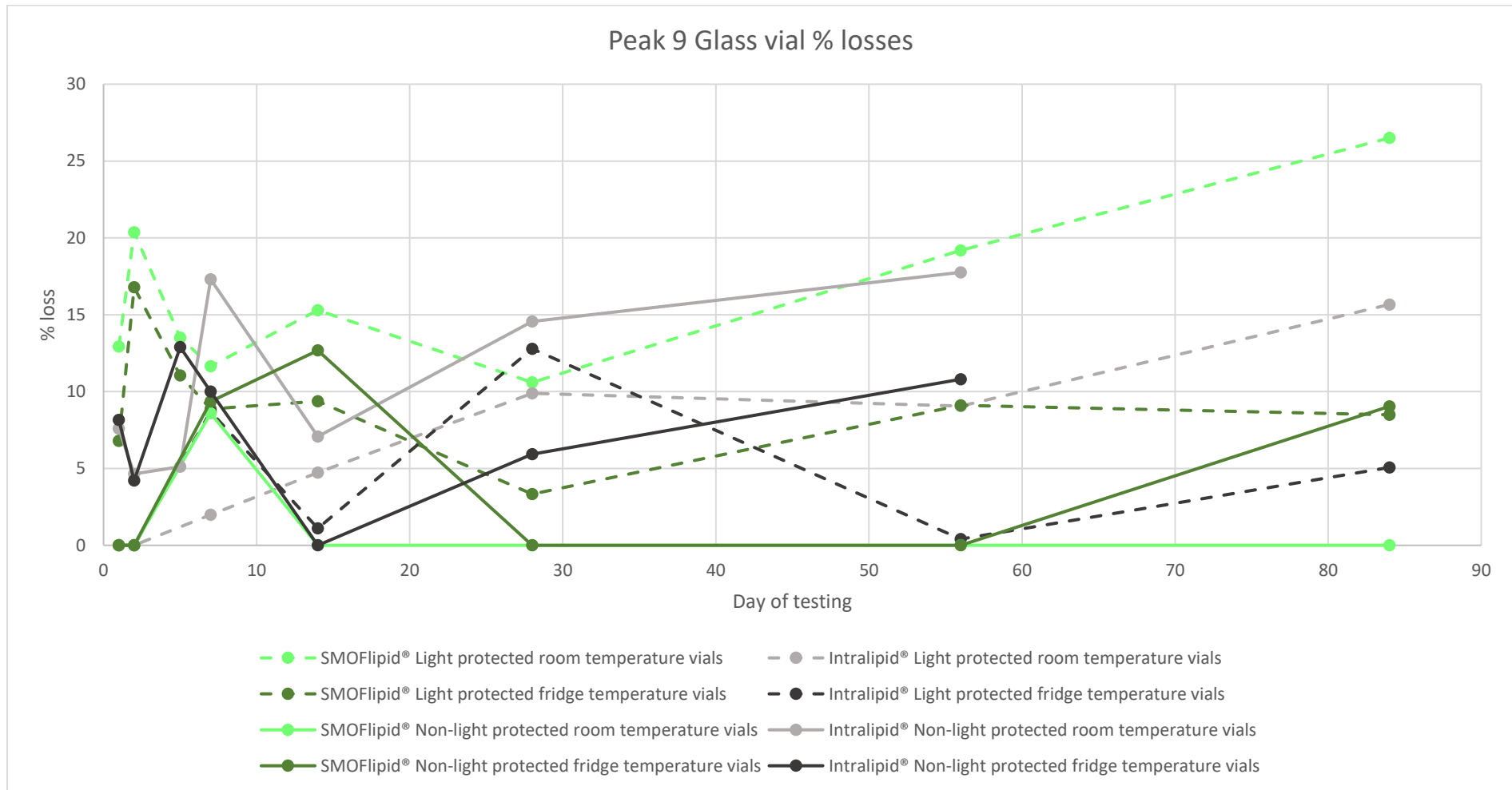
Figure 1.9 Peak 9 (C18:1/18:1/18:1) TAG losses in 50 ml glass vials of SMOFlipid® and Intralipid® at room and fridge temperatures.

7.4.6. Peak 10 (C18:2/18:1/16:0)

Peak 10 losses follow trends as discussed above for peaks 5, 6, 8 and 9. The breakdown of peak 10 was previously postulated to form a TAG remnant matching the m/z of the TAG remnant monitored. This would be formulated from a hydrolysis of the C16:0 fatty acid from the glycerol backbone of the TAG. Results indicating this would be expected to show a large % TAG loss and a lack of apparent HNE or HUE formation.

7.4.6.1. Syringes

Intralipid® syringes both light and non-light protected show maximal losses of peak 10 of >40 % and >30 % respectively at room temperatures. At day 28 SMOFlipid® syringes show losses in all conditions except in fridge temperature non-light protected samples. The presence of non-light protected room temperature peroxidation at day 28 is of interest as this TAG is the only result at 28 days for SMOFlipid® that shows any TAG loss in non-light protected syringes. This result when coupled with the finding of the highest (>13 µM) concentration of HNE in all syringes suggests that peak 10 peroxidation within syringes is responsible for the HNE formation within SMOFlipid®.

Figure 7.28 shows the peak 10 TAG loss occurring in all syringes of both lipids. Whilst previous results showed a large effect on loss by temperature of storage, only non-light protected SMOFlipid® syringes showed a large variation of results between temperatures. As such for this particular TAG, temperature of storage has little effect on the peroxidation and TAG losses occurring within syringes.

7.4.6.2. PN bags

SMOFlipid® light protected PN bags showed maximal losses of ~ 40 % at day 56 followed by light protected and non-light protected Intralipid® PN bags. All of these PN bags show minimal levels of HUE production and a lack of HNE production indicating a lack of terminal peroxidation product formation. When considering the TAG remnant formation seen in PN bags both Intralipid® and SMOFlipid® non-light protected samples show significant TAG remnant production. This finding however when compared to the minimal peak 10 TAG losses observed in these PN bags

indicates that peak 10 peroxidation within PN bags is not responsible for the TAG remnant formation observed.

Figure 7.29 shows the peak 10 TAG losses for both lipids within PN bags. As predicted for all results within PN bags temperature of storage had an effect on TAG loss seen with fridge temperatures inhibiting TAG loss observed.
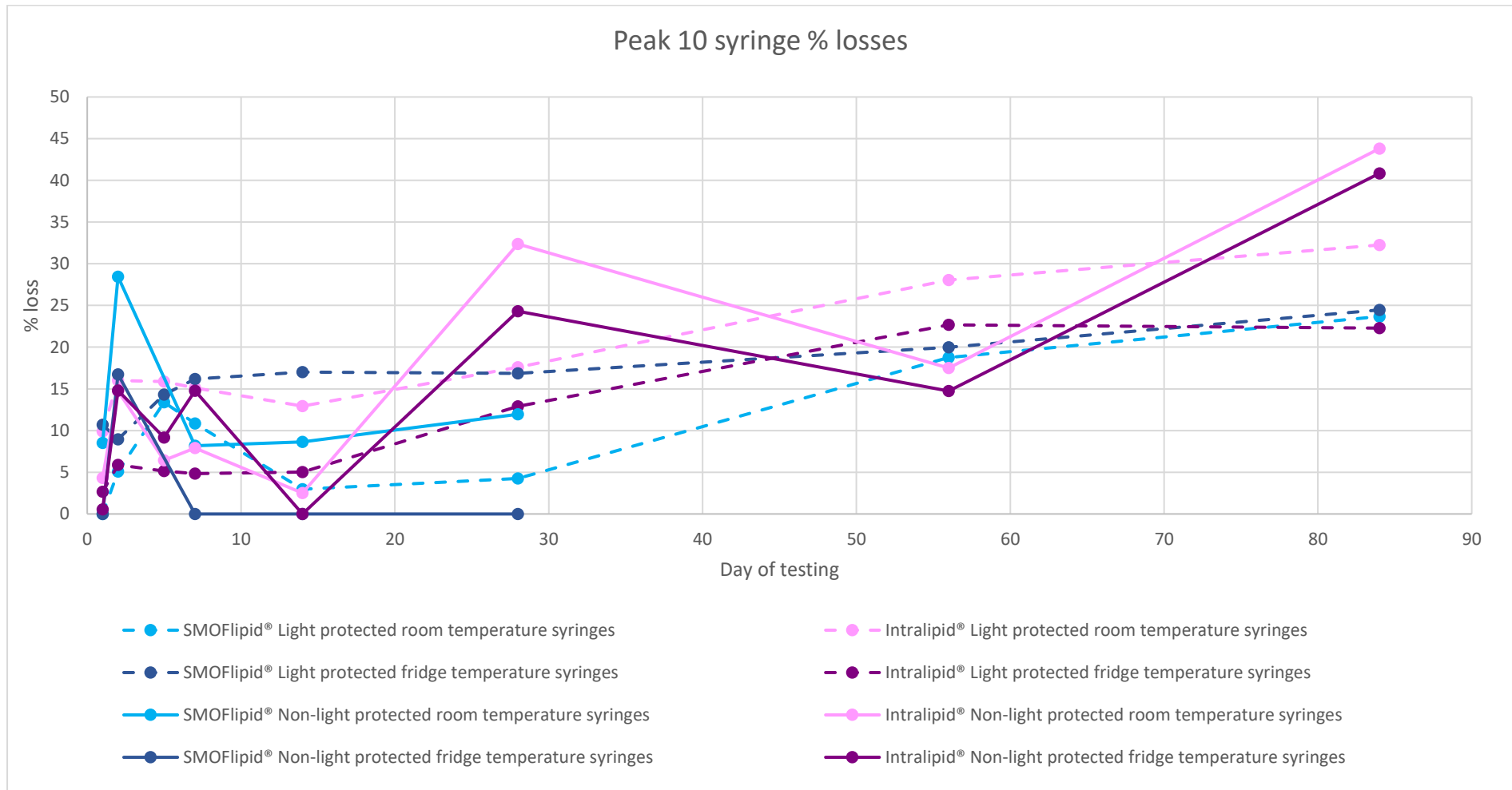
Figure 1.10. Peak 10 (C18:2/18:1/16:0) TAG losses in 50 ml syringes of SMOFlipid® and Intralipid® at room and fridge temperatures.
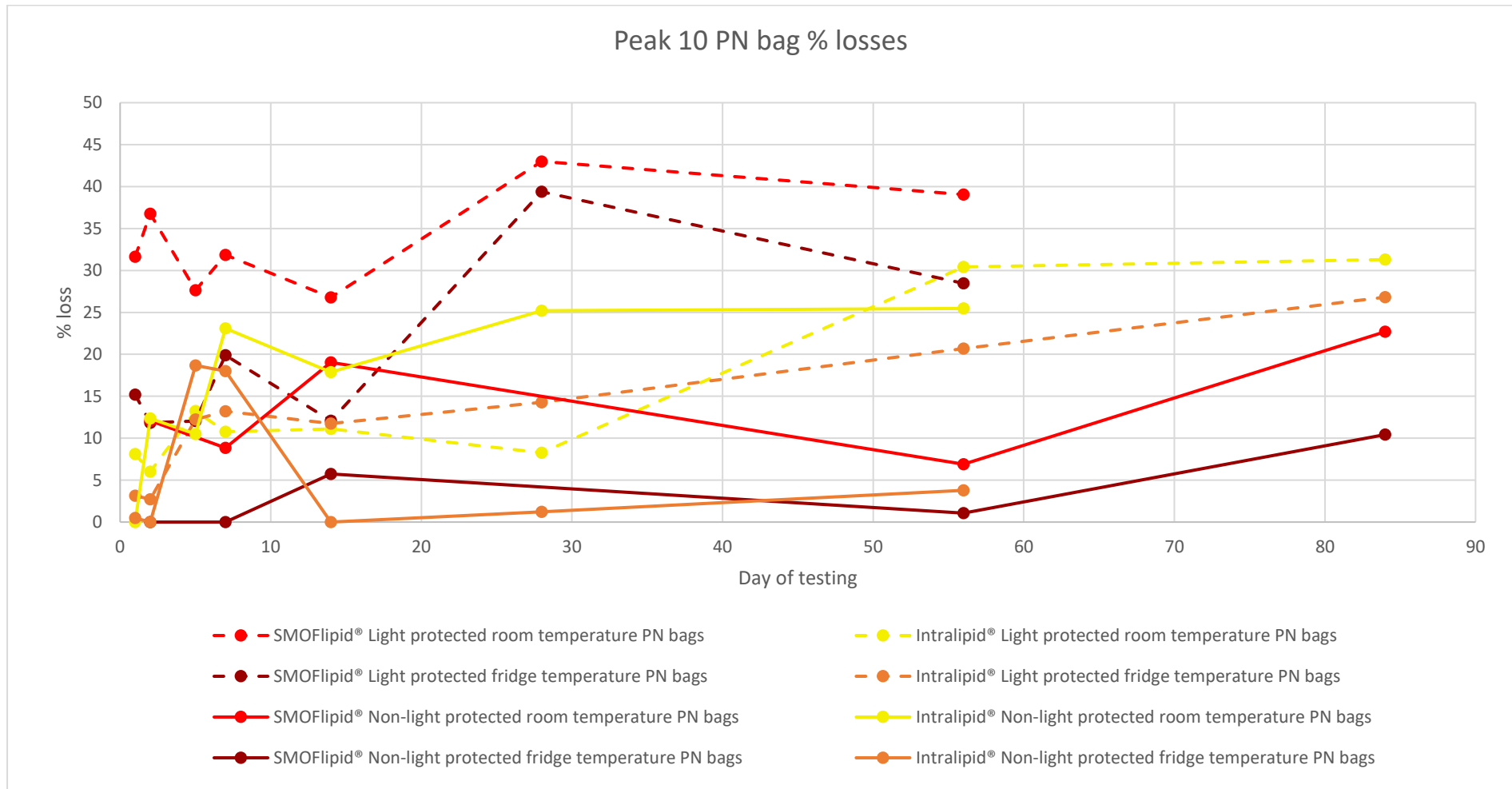
Figure 1.11 Peak 10 (C18:2/18:1/16:0) TAG losses in PN bags of SMOFlipid® and Intralipid® at room and fridge temperatures.

362

As shown in figure 7.30 glass vial results follow the same trends as peaks 5,6 and 8 with SMOFlipid® and Intralipid® light protected vials showing maximal losses due to early testing without nitrogen purging and subsequent oxygen ingress into the system leading to TAG breakdown. Both lipid non-light protected sample sets showed minimal to no loss of peak 10 throughout storage and confirm the lack of TAG breakdown when oxygen is removed from the storage system. Temperature of storage for light protected results where losses were observed affected TAG breakdown significantly. The lack of any secondary peroxidation products or TAG remnant within these vials however suggest either peroxidative breakdown is resulting in secondary products not detected through the assay, that peroxidation is in an earlier stage (propagation) or that hydrolysis is responsible for the TAG losses observed.

7.4.6.4. Peak 10 conclusions

When considered collectively peak 10 results indicate extensive losses are occurring within PN bags and syringes of both lipids. Syringe results indicate that peak 10 is responsible for the production of HNE within SMOFlipid® non-light protected syringes through cleavage of the C18:2 chain. In contrast to this SMOFlipid® and Intralipid® within PN bags shows extensive peak 10 loss but a lack of detected secondary products suggesting PN peak 10 breakdown could be creating undetected secondary products. The lack of loss in non-light protected SMOFlipid® PN bags indicates that peak 10 is not undergoing hydrolysis of the C16:0 chain and production of the TAG remnant observed.
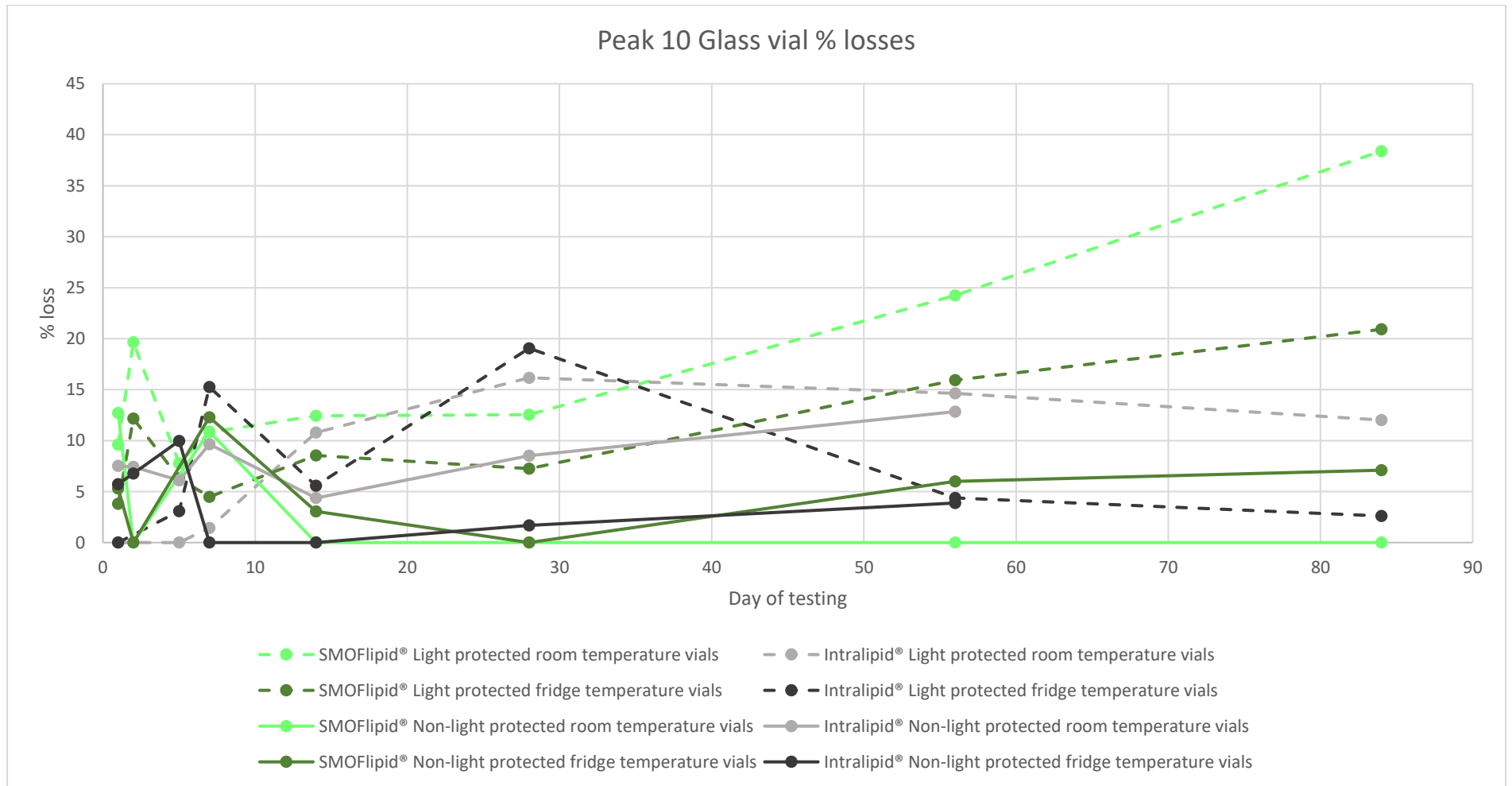
Figure 1.12 Peak 10 (C18:2/18:1/16:0) TAG loss in 50 ml glass vials of SMOFlipid® and Intralipid® at room and fridge temperatures.

7.5. Statistical trends between chapters

As shown in table 7.2 combination of the statistical analysis done in each result chapter for each lipid by ANOVA one-way analysis with Tukey post-hoc testing indicates the statistical significance for each peak between lipid formulations.

Peaks 1 to 4 only occur within SMOFlipid® and whilst multiple significant results are indicated, there is a lack of trends observed. Peaks 5 to 10 occur within both SMOFlipid® and Intralipid® and multiple significant results occur within both lipids in light and non-light protected results. The highlighted results indicate where results were significant across both lipids in either light protected, or non-light protected containers. Only 5 results were significant across all samples in both light states, however multiple results were significant between each light state as highlighted within the table. This is significant as the highlighted peaks indicate a trend within either light protected or non-light protected results and these specific results (peak, container and temperature) could be used to monitor further lipids tested depending on the light state used.

Table 7.2 Statistical significance between SMOFlipid® and Intralipid® both non-light and light protected. Yellow highlights non-light protected results of both lipids. Orange highlights light protected results of both lipids. Analysis by ANOVA one-way analysis and Tukey post hoc testing. Significance set as $p<0.05$.

Legend:

Colour	Meaning
* SMOFlipid® NLP (red)	
* SMOFlipid® LP (green)	
* Intralipid® LP (blue)	
* Intralipid® NLP (magenta)	
Orange	LP both lipids
Yellow	NLP both lipids

Peak 1

	Room syringe	Room Bag	Room Vial	Fridge Syringe	Fridge Bag	Fridge Vial
Room Syringe		**	*	*	**	*
Room Bag	**		*		*	**
Room Vial	*	*		*	*	
Fridge Syringe	*		*			*
Fridge Bag	*	*	*			*
Fridge Vial	*	**		*		

Peak 2

	Room syringe	Room Bag	Room Vial	Fridge Syringe	Fridge Bag	Fridge Vial
Room Syringe		**	*	*	*	*
Room Bag	**		*	*		**
Room Vial	*	*		*	*	
Fridge Syringe	*	*	*		*	*
Fridge Bag	*		*	*		*
Fridge Vial	*	**		*	*	

Peak 3

	Room syringe	Room Bag	Room Vial	Fridge Syringe	Fridge Bag	Fridge Vial
Room Syringe		*	*	*	*	*
Room Bag	*		*			*
Room Vial	*	*		*	*	*
Fridge Syringe	*		*			*
Fridge Bag	*		*	*		*
Fridge Vial	*	*	*	*	*	

Peak 4

	Room syringe	Room Bag	Room Vial	Fridge Syringe	Fridge Bag	Fridge Vial
Room Syringe		*	*	*		*
Room Bag	*		**	**		*
Room Vial	*	**				*
Fridge Syringe	*	**			*	
Fridge Bag		*		*		*
Fridge Vial	*	*	*			

Peak 5

	Room syringe	Room Bag	Room Vial	Fridge Syringe	Fridge Bag	Fridge Vial
Room Syringe		**	***	*		**
Room Bag	**		***	*		***
Room Vial	***	***		*	*	*
Fridge Syringe	*	*	*		**	**
Fridge Bag	*		*	*		***
Fridge Vial	***	***	**	**	****	

Peak 6

	Room syringe	Room Bag	Room Vial	Fridge Syringe	Fridge Bag	Fridge Vial
Room Syringe			*		*	*
Room Bag					**	*
Room Vial	**			*	***	*
Fridge Syringe	*				***	**
Fridge Bag	*	**	***	***		**
Fridge Vial	*	*	*	**	**	

Peak 7

	Room syringe	Room Bag	Room Vial	Fridge Syringe	Fridge Bag	Fridge Vial
Room Syringe		*	*			**
Room Bag			**	*		*
Room Vial	*	**			*	*
Fridge Syringe		*	*			*
Fridge Bag						**
Fridge Vial	**	*	*	*	**	

Peak 8

	Room syringe	Room Bag	Room Vial	Fridge Syringe	Fridge Bag	Fridge Vial
Room Syringe		**	**	*	*	***
Room Bag	**		**	***	*	**
Room Vial	*	**			**	***
Fridge Syringe	*	**			***	*
Fridge Bag	*	*	**	**		***
Fridge Vial	***	**	***	*	***	

Peak 9

	Room syringe	Room Bag	Room Vial	Fridge Syringe	Fridge Bag	Fridge Vial
Room Syringe		***	**	*	**	****
Room Bag	***		***	**	**	***
Room Vial	**	***		*	*	***
Fridge Syringe	*	**	*		*	****
Fridge Bag	**	*	*	*		***
Fridge Vial	****	***	***	****	***	

Peak 10

	Room syringe	Room Bag	Room Vial	Fridge Syringe	Fridge Bag	Fridge Vial
Room Syringe		**	***	**	*	***
Room Bag	**		***	***	*	**
Room Vial	***	***		*	*	**
Fridge Syringe	**	***	*			**
Fridge Bag	*	*	*	*		***
Fridge Vial	***	**	**	**	***	

7.6. RSD variation in control samples

Within each chapter and each graph plotted, results were highlighted as outliers where the RSD of the control sample run at that testing timepoint exceeded an acceptable level (>12% as previously discussed). The drift in RSD beyond this level was an indication of a loss of reliability of the assay and as such the results were excluded from comparisons between chapters. The results where the RSD's were excessive for control samples were either days 28, 56 or 84 of testing. Due to the testing schedule and the method used, each sample set tested (one sample set was one lipid in one container at both temperatures either light or non-light protected) took a total of 22 hours to complete and therefore only one set was tested on each day. The large amount of data collected and the testing time for each set meant a tight schedule over 10+ months was used to enable all results to be obtained. When considering the dates when the containers were tested that resulted in excessive RSD's of control samples, these were over a period of ~ 8 weeks during the summer months. During this time the laboratory where the HPLC equipment was placed regularly exceeded 30ºC ambient temperature. The rise in room temperature was linked to the high RSD's observed and whilst the column temperature was maintained at 5ºC and the autosampler at 8ºC, no temperature control was possible over the solvents used until they were drawn into the system from the HPLC bottle. The HPLC system whilst managing to maintain the column and autosampler settings did struggle to maintain these temperatures at times and as such the ambient temperature was concluded to be responsible for the high RSD's observed. This was substantiated by the return of control RSDs to within acceptable levels when the ambient temperature of the laboratory returned to normal. Future studies ideally would be within a laboratory with ambient temperature control to exclude the problem reoccurring.

7.7. Conclusions between lipids.

As shown within the comparisons between chapters made in section 7.4 the TAG losses observed and the extent of peroxidation recorded varies between lipids and different containers. Intralipid® showed maximal peroxidation, TAG loss and the production of HNE and HUE within both light protected and non-light protected syringes at room and fridge temperatures. SMOFlipid® conversely showed maximal TAG losses and TAG remnant production in light protected PN bags at both

temperatures, however the production of the secondary peroxidation products HNE and HUE were only observed in syringes. Considering each lipid formulation individually Intralipid® results within syringes indicate the presence of peroxidation through 'standard' mechanisms (radical initiation, propagation and termination) over extensive testing time. Rate of production of products and TAG losses was slow initially and increased during storage, suggesting oxygen availability is a crucial factor in peroxidation occurring. The leach of air into syringes during storage is the initiating factor in the extensive peroxidation occurring. The presence of HNE, HUE and TAG remnant show peroxidation progressing through to the termination phase and the production of toxic secondary aldehydes. Whilst smaller in percentage, significant (>25 %) losses were also observed in Intralipid® PN bags however only the TAG remnant and minimal HUE were recorded suggesting a lower amount of terminal peroxidation occurring. The TAG losses observed however indicated initiation of peroxidation is occurring and as such it is postulated that within these PN bags peroxidation is either maintained in an earlier stage (hydroperoxides rather than terminal secondary aldehydes) or that hydrolysis reactions are occurring at the water-oil interface of the emulsion and cleaving fatty acids from the glycerol backbone of the TAG. Rates of TAG losses within Intralipid® PN bags are initially higher than within syringes, with a slowing of loss occurring during extended storage. It is concluded that again oxygen availability is a key control in the rate of loss observed. The finite oxygen available within PN bags results in initial rapid TAG loss occurring however as this oxygen supply is exhausted loss rates reduce. This apparent reliance on oxygen within these sets of results indicates the likelihood that the loss within Intralipid® bags is as a result of peroxidation rather than hydrolysis.

When considering the SMOFlipid® results obtained, the stark difference to Intralipid® within both syringes and PN bags is of interest. SMOFlipid® experienced maximal loss in PN bags for all peaks both saturated and unsaturated. All light protected results for SMOFlipid® were worse than non-light protected results. The extensive saturated losses observed within PN bags indicates the presence of hydrolysis within the emulsion. The positive presence of the TAG remnant within these PN bags and the lack of HNE and HUE substantiates the occurrence of hydrolysis both within saturated and unsaturated peaks. Conversely within syringes the presence of HNE and TAG remnant within SMOFlipid® syringes indicates peroxidation is also occurring within unsaturated peaks. The results suggest that a combination of hydrolysis and peroxidation is possible within SMOFlipid® which, when considering its formulation with highly unsaturated fish oils, suggests that the reactive energy

within the system, i.e. the level of peroxidation/radicals likely to be present is higher compared to soybean oil alone as in Intralipid®.

When considering the results in the context of light protection, the highest results in both lipids were observed in light protected samples which is particularly interesting as PN and lipids are always protected from light. Whilst previous work testing the effects of light protection on PN as discussed in chapter 3 showed a positive correlation between light protection and a reduction in mortality of patients receiving PN (Chessex et al. 2007), when considering lipids alone results within this work suggests light protection is less important. The results also indicate a lack of photo-oxidation within lipid emulsions alone. A caveat to these results when applied to PN mixtures however is that light induced peroxidation is proven to be more prominent in the presence of riboflavin and trace elements which are within all-in one mixtures of PN (Allwood and Kearney 1998). As such whilst light protection is not proven to be beneficial within this study it should be continued in PN mixtures used within clinical practise.

Conversely to light protection results, temperature of storage testing gave results as were predicted with fridge temperatures (with the exception of SMOFlipid® light protected syringes) inhibiting or reducing TAG losses and peroxidation products occurring.

When considering SMOFlipid® previous contradicting works has shown the addition of tocopherols to the lipid emulsion to be beneficial in reducing the level of peroxidation occurring (Pironi et al. 2003) and that high concentrations of tocopherols were shown to have a pro-oxidative effect (Steger and Mühlebach 1998). The Pironi et al. (2003) study however used a colorimetric kit to measure the occurrence of lipid peroxides and HPLC of TBA adducts to measure MDA content. Both methods as discussed in chapter 1 can potentially over and under estimate the occurrence of peroxidation. Whilst the data produced within this thesis was testing lipids alone (i.e. not in all-in-one mixtures) the presence of added tocopherols within SMOFlipid® is of interest as the results indicate extensive TAG loss occurring within this lipid. As discussed above, the levels of proven peroxidation within this lipid were however lower than Intralipid® when considering the formation of TAG remnants and HUE. HNE however was highest within SMOFlipid® syringes indicating the presence of lipid peroxidation occurring. The extensive TAG losses seen in PN bags is postulated to be a combination of peroxidation and hydrolysis and as such the

positive presence of HNE within SMOFlipid® syringes suggests that the ability of tocopherols to act as an anti-oxidant within a high energy system is questionable.

When considering how tocopherols quench radicals, the structure of tocopherols are as shown in figure 7.31 These act as chain-breaking anti-oxidants where the radical is transferred from the lipid radical to the tocopherol structure creating a phenoxyl radical which is resonance stabilised and therefore 'contains' the radical until a termination reaction occurs (Burton and Ingold 1986; Niki 1987). For this to occur as described the physical position of the tocopherol molecule needs to be very close to the radical attached to the complex TAG molecule. Whilst theoretically possible due to the lipid soluble nature of tocopherols, the relatively large size of each TAG molecule is postulated to cause physical hindrance to the anti-oxidant ability of tocopherols. As such, the extensive peroxidation and lack of inhibition by addition of tocopherols within SMOFlipid® is explained.

Tocopherol	R_5	R_7
α	CH_3	CH_3
β	CH_3	H
γ	H	CH_3
δ	H	H
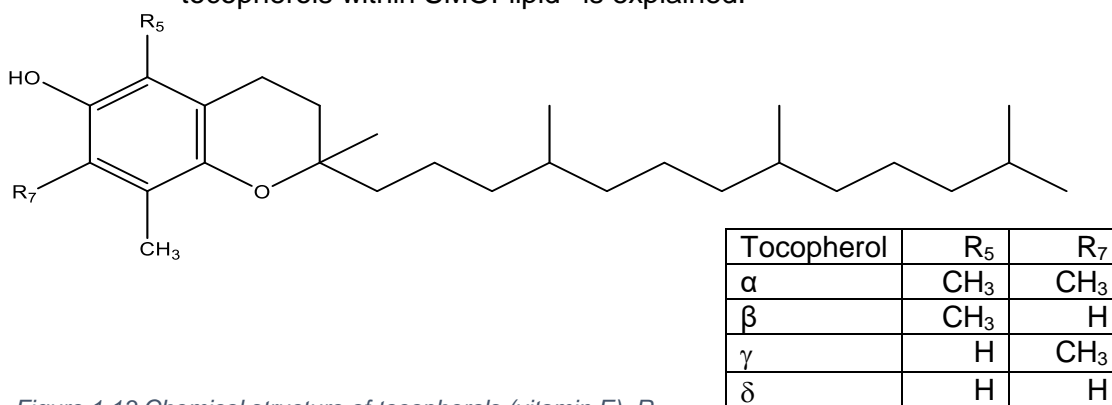
Figure 1.13 Chemical structure of tocopherols (vitamin E). R groups denotes differences in structure dependant on form as shown in table.

7.8. Clinical relevance of study

As presented in the objectives and introduction this study was designed to create an initial set of data looking into the TAG loss and peroxidation occurrence within two lipid emulsions. Its aim was to develop and employ an assay that was reliable and repeatable and enable the chemical stability of an established lipid emulsion and a newer lipid emulsion to be tested. As discussed above the results for both lipid formulations show extensive TAG losses throughout storage over 84 days at both fridge and room temperatures and the production of HNE, HUE and a TAG remnant that serve as confirmation of the occurrence of peroxidation.

When considering current clinical practise adult PN is often delivered in an all-in-one mixture of aqueous and lipid components, making chemical testing difficult due to

the inherent complexities of the formulation. Common physical stability testing done for such regimes are carried out over 84 days and used to provide storage limits and conditions. Whilst the data within the studies carried out in this work is with lipid alone, the combination of lipid with aqueous components, vitamins and trace elements has been proven to enhance instability within the formulation when considering physical stability (Allwood and Kearney 1998; Driscoll et al. 2007b; Ferguson et al. 2014). When considering chemical stability, the presence of trace elements and vitamins are known to catalyse the rate of peroxidation occurring within all-in-one PN. Work by Grand et al. (2011) measured the levels of MDA present within all-in-one PN mixtures with vitamins, iron and trace elements and concluded that all additions resulted in higher levels of MDA observed. Therefore, in relation to the work compiled within this thesis it can be postulated that the peroxidation and TAG loss observed within all-in-one mixtures would be greater than the results and extensive losses observed within lipid emulsions alone. As such, the data produced is of great clinical significance to both lipid only PN (neonatal) and adult all-in-one PN.

Current storage of neonatal PN lipids is within 50 ml syringes, stored light protected and at fridge temperature. Typical delivery is over 24 hours via syringe driver at temperatures up to 30^0C and as such the room temperature data collected is relevant. The presence of HNE and HUE within both room and fridge temperature syringes is important as delivery of any concentration of these toxic peroxidation products to a neonatal patient whose innate anti-oxidant system is already stressed is potentially catastrophic. The data suggests that limiting the storage of this neonatal lipid PN to a maximum of 24 hours and maintaining fridge storage throughout would limit the peroxidation occurring, however the storage device should be reviewed for future delivery. Whilst 250 ml PN bags were tested within this study due to a lack of availability of 50 ml bags, ideally 50 ml PN bags would be employed as a substitute for 50 ml syringes for neonatal lipids. The data produced showed extensive TAG losses within these bags, but a lack of HNE and minimal HUE suggesting the occurrence of hydrolytic TAG breakdown as opposed to peroxidation. Whilst not optimal for delivery to the neonate, the lack of peroxidation products would be favourable when compared to lipids stored within syringes. Further in-depth testing of 50 ml PN bags over an initial 48-hour period would confirm the safety of this device with respect to lipid peroxidation and chemical stability.

When considering the two lipids together, SMOFlipid® showed greater levels of TAG losses within PN bags and showed maximal HNE production in syringes, however Intralipid® produced more consistent TAG losses and HNE, HUE and TAG remnant production within all containers. As such it can be concluded that with regards to lipid peroxidation alone, SMOFlipid® is superior to Intralipid® though both lipid formulations are not optimal when considering the actual lipid amount delivered to a patient vs the amount of lipid prescribed. Future research and development into a lipid emulsion formulated to optimise chemical stability is a recommendation made from the conclusions within this work. Whilst lipids are typically formulated to match research into optimal patient nutrition this body of work suggests that patients may not be receiving the prescribed amount or chemical composition of lipid as previously thought. As such, the development of a chemically stable lipid emulsion that provides a finite amount of lipid to the patient in un-peroxidised form would lead to optimal safe delivery of nutrition to the patient.

Clinical recommendations from the work within this study include moving small volume lipid PN from syringes to PN bags, light protecting all containers and delivery lines (though only relevant in limiting TAG remnant production and HNE formation), limiting storage of lipids to 24 hours prior to delivery to the neonatal patient and storing all lipids at fridge temperatures. With respect to adult all-in-one PN the work suggests that the extensive storage limits placed on home PN (limits formed from physical stability testing) may not be appropriate in delivering a lipid containing PN that is stable to the patient. As such storage limits should be reviewed on lipid containing PN.

7.9. Study limitations and future work

As discussed in section 7.8 PN bags tested were as small as possible but in practise ideally 50 ml bags would be used for the storage of lipid portions of PN. Therefore, whilst the data collected is relevant as it is the first chemical stability data collected with respect to TAG loss and peroxidation, ideally the study should be repeated using 50 ml PN bags to provide an accurate overview.

With regards to SMOFlipid® and the perceived relatively high levels of hydrolysis observed and with respect to further identification of the TAG remnant structure detected, identification of fatty acids methyl esters through mass spectrometry could be employed to provided confirmation on the presence and type of free fatty acids and as such the position of hydrolysis occurring within TAGs monitored. The

presence of earlier stages of peroxidation ie. the presence of primary peroxidation products (hydroperoxides) is also postulated to be responsible for some of the data observed and as such, whilst hydroperoxide testing is often not accurate (see introduction chapter), detection of hydroperoxides in combination with the assay used within this work or the addition of reducing agents would confirm their presence or lack of within each lipid formulation tested.

The presence of oxygen within the storage system was proven through the studies to be of vital importance in the extent of peroxidation and TAG losses observed. The testing protocol within glass vials where oxygen was replaced with nitrogen was designed to act as a control to show the removal of oxygen led to the inhibition of TAG losses and peroxidation occurring. Whilst the protocol was updated through the testing to try and ensure a lack of oxygen ingress into the container at each testing point, TAG losses were still observed which were postulated to be from either oxygen ingress into the system (though a lack of peroxidation products were detected) or through hydrolysis. As such glass vial results whilst still of interest did not act as controls per se. Future work to confirm hydrolysis as the cause of the TAG loss observed would aid to substantiate the data collected that shows the vital presence of oxygen for peroxidation to occur.

This study was designed to look at lipid emulsions alone, with no other additives present. Within a clinical setting this work is directly relevant to lipid delivery to neonatal patients however adults commonly have all-in-one PN. The additions of other required elements to lipids for all-in-one PN is postulated to have a further destabilising effect on lipids and catalyse peroxidation occurring. Whilst the study results reported stand alone as a vitally important piece of research that should influence PN storage, future work testing lipids within all-in-one mixtures would be ideal to formulate stability data that is directly transferable to the clinic. There are however inherent challenges when considering lipid testing within all-in-one PN. For example, HNE is known to readily bond with amino acids, particularly cysteine residues as supplied within the amino acid portion of all-in-one PN. As such the detection of free HNE as presented within the assay developed would not be appropriate for all-in-one PN and further assay modifications would be required to detect such bound HNE. It is postulated that a lipid extraction stage would be required prior to lipid analysis with this assay for all-in-one PN, enabling the lipid portion to be analysed without the HPLC chromatograms being altered by other non-lipid components. The non-aqueous nature of the HPLC assay would also be

incompatible with aqueous portions of a PN mixture making lipid extraction necessary.

At the time of writing to my knowledge this is the first chemical stability study undertaken on the two lipid emulsions using the assay developed and presented within this work looking at both TAG losses and peroxidation products occurring. Future work as discussed above would act to extend the stability testing carried out to include all-in-one PN mixtures. The testing of other lipid emulsions could also be possible using the same assay if it was validated for each lipid used. Whilst the data and conclusions drawn from this work show the occurrence of extensive TAG loss and peroxidation within both lipids that are currently used within PN delivery it is important to recognise that PN delivery to a patient is only undertaken in critical illness. As such, PN provides life sustaining nutrition and thus this work should serve to limit the storage time placed on current PN and drive research into the development of more stable lipids and not prohibit the delivery of currently available lipids in clinical practise.

REFERENCES

Adams, L.K. et al. 1999. Effects of the Lipid Peroxidation Products 4-Hydroxy-2-Nonenal and Malondialdehyde on the Proliferation and Morphogenetic Development of in vitro Plant Cells. *Journal of Plant Physiology* 155(3), pp. 376–386.

Allwood, M.C. 2000. Light protection during parenteral nutrition infusion: Is it really necessary? *Nutrition* 16(3), pp. 234–235.

Allwood, M.C. and Kearney, M.C.J. 1998. Compatibility and Stability of Additives in Parenteral Nutrition Admixtures. *Nutrition* 14(9), pp. 697–706.

Balet, A. et al. 2004. Effects of Multilayered Bags vs Ethylvinyl-acetate Bags on Oxidation of Parenteral Nutrition. *Journal of Parenteral and Enteral Nutrition* 28(2), pp. 85–91.

Barr, L. et al. 1981. Essential Fatty Acid Deficiency During Total Parenteral Nutrition. *Annals Of Surgery* 193(3), pp. 304–311.

Basu, R. et al. 1999a. Free Radical Formation in Infants: The Effect of Critical Illness, Parenteral Nutrition, and Enteral Feeding. *Journal of Pediatric Surgery* 34(7), pp. 1091–1095.

Basu, R. et al. 1999b. Lipid peroxidation can be reduced in infants on total parenteral nutrition by promoting fat utilisation. *Journal of Pediatric Surgery* 34(2), pp. 255–259.

BD Medical 2015. TECHNICAL DATA SHEET BD Plastipak TM Syringe without needle Sterile , Single use , Latex Free., pp. 1–10.

Beisel, W. 1975. Metabolic Response to Infection. *Annual Review of Medicine* 26, pp. 9–20.

Benedetti, A. et al. 1980. Identification of 4-Hydroxynonenal as a Cytotoxic Product Originating from the Peroxidation of Liver Microsomal Lipids. *Biochimica et Biophysica Acta* 620, pp. 281–296.

Benedetti, A. et al. 1986. 4-Hydroxynonenal and other aldehydes produced in the liver in vivo after bromobenzene intoxication. *Toxicol Pathol* 14(4), pp. 457–461.

Burrin, D.G. et al. 2014. Impact of New-Generation Lipid Emulsions on Cellular Mechanisms of Parenteral Nutrition – Associated Liver Disease. *Advances in Nutrition* 5, pp. 82–91.

Burton, G.W. and Ingold, K.U. 1986. Vitamin E : Application of the Principles of Physical Organic Chemistry to the Exploration of Its Structure and Function1. *Accounts of chemical research* 2(25976), pp. 194–201.

Byrdwell, W.C. et al. 1996. Quantitative analysis of triglycerides using atmospheric pressure chemical ionization-mass spectrometry. *Lipids* 31(9), pp. 919–935.

Calder, P. et al. 2015. *Intravenous Lipid Emulsions*. New York: Karger.

Castro, J.P. et al. 2016. 4-Hydroxynonenal (HNE) modified proteins in metabolic diseases. *Free Radical Biology and Medicine* 111(October 2016), pp. 309–315.

Chen, Z. et al. 2006. Is There An Answer ? 4-Hydroxynonenal (4-HNE) has been Widely Accepted as an Inducer of Oxidative Stress . Is this the Whole Truth about it or can 4-HNE also exert Protective Effects ?*. 58(June), pp. 372–373.

Chessex, P. et al. 2007. In Preterm Neonates , is the Risk of Developing Bronchopulmonary Dysplasia Influenced by the Failure to Protect Total Parenteral Nutrition from Exposure to Ambient Light ? *J Pediatr* 151, pp. 213–214.

Chessex, P. et al. 2015. Shielding Parenteral Nutrition From Light Improves Survival Rate in Premature Infants : A Meta-Analysis. *Journal of Parenteral and Enteral Nutrition* 20, pp. 1–6.

Christie, W. 2003. *Lipid Analysis*. The Oily Press.

Chromacademy, L.G. 1999. Reversed Phase Chromatography. Available at: www.chromacademy.com [Accessed: 2 February 2017].

Crafts, C. et al. 2011. *Validating analytical methods with charged aerosol detection.*

Csala, M. et al. 2015. On the role of 4-hydroxynonenal in health and disease. *Biochimica et Biophysica Acta - Molecular Basis of Disease* 1852(5), pp. 826–838.

Cutler, M. and Schneider, R. 1974. Tumours and hormonal changes produced in rats by subcutaneous injections of linoleic acid hydroperoxide. *Food and Cosmetics Toxicology* 12, pp. 451–459.

Dorival-García, N. et al. 2017. Non-volatile extractable analysis of prefilled syringes for parenteral administration of drug products. *Journal of Pharmaceutical and Biomedical Analysis* 142(2017), pp. 337–342.

Driscoll, D.F. et al. 2007a. Physical stability of 20% lipid injectable emulsions via simulated syringe infusion: Effects of glass vs plastic product packaging. *Journal of Parenteral and Enteral Nutrition* 31(2), pp. 148–153. doi: 10.1177/0148607107031002148.

Driscoll, D.F. et al. 2007b. Stability of total nutrient admixtures with lipid injectable emulsions in glass versus plastic packaging. *American Journal of Health-System Pharmacy* 64(4), pp. 396–403. doi: 10.2146/ajhp060062.

Driscoll, D.F. et al. 2008. Pharmaceutical and clinical aspects of parenteral lipid emulsions in neonatology. *Clinical Nutrition* 27(4), pp. 497–503. doi: 10.1016/j.clnu.2008.05.003.

Dudrick, S.J. 2003. Early developments and clinical applications of total parenteral nutrition. *Journal of Parenteral and Enteral Nutrition* 27(4), pp. 291–299.

Dudrick, S.J. 2009. History of parenteral nutrition. *Journal of the American College of Nutrition* 28(3), pp. 243–251.

Van Dyck, S. 2010. The impact of singlet oxygen on lipid oxidation in foods. *Oxidation in Foods and Beverages and Antioxidant Applications: Understanding Mechanisms of Oxidation and Antioxidant Activity* 19(12), pp. 57–75.

Eckl, P.M. et al. 1993. Genotoxic properties of 4-hydroxyalkenals and analogous aldehydes. *Mutation Research - Fundamental and Molecular Mechanisms of Mutagenesis* 290(2), pp. 183–192. doi: 10.1016/0027-5107(93)90158-C.

Emerit, I. et al. 1991. Hydroxynonenal a Component of Clastogenic Factors? *Free Radical Biology and Medicine* 10, pp. 371–377.

Endres, I.G. and Kummerow, F.A. 1962. *Thermal Oxidation of Synthetic Triglycerides I . Composition of Oxidized Triglycerides*.

Eriksson, J. 2001. Intralipid ® 20 % Pharmacy Bulk Package Container.

Esterbauer, H. et al. 1991. Chemistry and Biochemistry of 4-hydroxynonenal, malonaldehyde and related aldehydes. *Free Radical Biology and Medicine* 11(1), pp. 81–128.

Esterbauer, H. 1993. Cytotoxicity and genotoxicity of lipid-oxidation. *American Journal of Clinical Nursing* 57, p. 779S–786S.

Esterbauer, H. and Zollern, H. 1989. Methods for determination of aldehydic lipid peroxidation products. *Free Radical Biology and Medicine* 7, pp. 197–203. doi: 10.1016/0891-5849(89)90015-4.

Fahy, E. et al. 2007. Lipid maps online tools for lipid research. *Nucleic acids Research* 35, pp. W606-12.

Ferguson, T.I. et al. 2014. A review of stability issues associated with vitamins in parenteral nutrition. *e-SPEN Journal* 9(2), pp. e49–e53.

Fox, C.B. et al. 2013. Charged aerosol detection to characterize components of dispersed-phase formulations. *Advances in Colloid and Interface Science* 199–200, pp. 59–65.

Gamache, P. 2018. *Charged aerosol detection for liquid chromatography and related separation techniques.* wiley.

Gibson, P.R. 2012. Advances in nutrition. *Gastroenterology & Hepatology* 8(1), pp. 39–41.

Gonyon, T. et al. 2013. Interactions between Parenteral Lipid Emulsions and Container Surfaces. *PDA J Pharm Sci Technol* 67(3), pp. 247–254.

Grand, A. et al. 2011. Influence of vitamins, trace elements, and iron on lipid peroxidation reactions in all-in-one admixtures for neonatal parenteral nutrition. *Journal of Parenteral and Enteral Nutrition* 35(4), pp. 505–510.

Gura, K.M. et al. 2005. Use of a fish oil-based lipid emulsion to treat essential fatty acid deficiency in a soy allergic patient receiving parenteral nutrition. *Clinical Nutrition* 24(5), pp. 839–847.

Gura, K.M. et al. 2006. Reversal of Parenteral Nutrition-Associated Liver Disease in Two Infants With Short Bowel Syndrome Using Parenteral Fish Oil: Implications for Future Management. *Pediatrics* 118(1), pp. e197–e201.

Halliwell, B. and Chirico, S. 1993. Lipid peroxidation : its mechanism, measurement, and significance. *The American Journal of Clinical Nutrition* 57, p. 715S–725S.

Hamilton, C. et al. 2006. Essential fatty acid deficiency in human adults during parenteral nutrition. *Nutrition in Clinical Practise* 21(4), pp. 387–394.

Hamilton, R. and Hamilton, S. 1992. *Lipid analysis - A practical approach.* New York: Oxford University Press.

Hardy, G. et al. 2009. Trace element supplementation in parenteral nutrition: Pharmacy, posology, and monitoring guidance. *Nutrition* 25(11–12), pp. 1073–1084.

Hardy, G. and Puzovic, M. 2009. Formulation, stability, and administration of parenteral nutrition with new lipid emulsions. *Nutrition in Clinical Practice* 24(5), pp. 616–625.

Harmonisation, I.C. for 2018. Harmonisation for better health. Available at:

http://www.ich.org/about/mission.html [Accessed: 27 July 2018].

Harmonisation, I.C.F. 1996. *Stability Testing: Photostability Testing of New Drug Substances and Products Q1B*. doi: 10.1136/bmj.333.7574.873-a.

Hauck, A.K. and Bernlohr, D.A. 2016. Oxidative Stress and Lipotoxicity. *Journal of Lipid Research* , pp. 1–37.

Helbock, H.J. et al. 1993. Toxic hydroperoxides in intravenous lipid emulsions used in preterm infants. *Pediatrics* 91(1), pp. 83–7.

Hippalgaonkar, K. et al. 2010. Injectable lipid emulsions-advancements, opportunities and challenges. *AAPS PharmSciTech* 11(4), pp. 1526–1540.

Hmida, D. et al. 2015. Comparison of iso-eluotropic mobile phases at different temperatures for the separation of triacylglycerols in Non-Aqueous Reversed Phase Liquid Chromatography. *Journal of Chromatography B: Analytical Technologies in the Biomedical and Life Sciences* 990, pp. 45–51.

Ho, C.S. et al. 2003. Electrospray ionisation mass spectrometry: principles and clinical applications. *The Clinical biochemist* 24(1), pp. 3–12.

Hoff, D.S. and Michaelson, A.S. 2009. Effects of Light Exposure on Total Parenteral Nutrition and its implications in the neonatal population. *The Journal of Pediatric Pharmacology and Therapeutics* 14(3), pp. 132–143.

ICH 2005. *ICH Topic Q2 (R1) Validation of Analytical Procedures : Text and Methodology.*

Ilko, D. et al. 2014. Fatty acid composition analysis in polysorbate 80 with high performance liquid chromatography coupled to charged aerosol detection. *European Journal of Pharmaceutics and Biopharmaceutics* 94, pp. 569–574.

Ishikado, A. et al. 2013. 4-Hydroxy Hexenal Derived from Docosahexaenoic Acid Protects Endothelial Cells via Nrf2 Activation. *PLoS ONE* 8(7), pp. 1–13.

Kabi, F. 2009. *Intralipid 10% Summary of Product Characteristics*.

Kabi, F. 2018. *SMOFlipid SUMMARY OF PRODUCT CHARACTERISTICS*.

Kamal-Eldin, A. 2003. *Lipid Oxidation Pathways*. 1st ed. AOCS.

Kamal-Eldin, A. and Min, D. 2008. *Lipid Oxidation Pathways - Volume 2*. AOCS.

Karatas, F. et al. 2002. Determination of free malondialdehyde in human serum by high-

performance liquid chromatography. *Analytical Biochemistry* 311(1), pp. 76–79.

Karen, M. and Winterbourn, C.C. 2001. Lipid Peroxide and Hydrogen Peroxide Formation in Parenteral. *Journal of Parenteral and Enteral Nutrition* 25(1), pp. 14–17.

Khanum, R. and Thevanayagam, H. 2017. Lipid Peroxidation: Its Effects on the Formulation and Use of Pharmaceutical Emulsions. *Asian Journal of Pharmaceutical Sciences* 12(5), pp. 401–411.

Laborie, S. et al. 1999. Protecting solutions of parenteral nutrition from peroxidation. *Journal of Parenteral and Enteral Nutrition* 23(2), pp. 104–108.

Lang, J. et al. 1985. Quantitative determination of the lipid peroxidation product 4-Hydroxynonenal by High-Performance Liquid Chromatography. *Analytical Biochemistry* 150, pp. 369–378.

Lavoie, J.-C. et al. 2018. Impact of SMOFLipid on Pulmonary Alveolar Development in Newborn Guinea Pigs. *Journal of Parenteral and Enteral Nutrition* 00(0), pp. 1–8.

Lavoie, J.C. et al. 1997. Admixture of a multivitamin preparation to parenteral nutrition: the major contributor to in vitro generation of peroxides. *Pediatrics* 99(3), p. E6.

Leray, C. 2016. Lipid peroxidation. Available at: http://www.cyberlipid.org/cyberlip/home0001.htm [Accessed: 4 April 2016].

Li, M. et al. 2014. Comprehensive quantification of triacylglycerols in soybean seeds by electrospray ionization mass spectrometry with multiple neutral loss scans. *Scientific reports* 4, p. 6581.

Ligor, M. et al. 2015. The chromatographic assay of 4-hydroxynonenal as a biomarker of diseases by means of MEPS and HPLC technique. *Biomedical chromatography : BMC* 29(4), pp. 584–9.

Lin, J.T. et al. 1997. Non-aqueous reversed-phase high-performance liquid chromatography of synthetic triacylglycerols and diacylglycerols. *Journal of Chromatography A* 782(1), pp. 41–48.

Lin, J.T. and McKeon, T.A. 2005. *HPLC of Acyl Lipids*. HNB publishing.

Lísa, M. et al. 2007. Quantitation of triacylglycerols from plant oils using charged aerosol detection with gradient compensation. *Journal of Chromatography A* 1176, pp. 135–142.

List, G.R. et al. 2000. Hydrogenation of soybean oil triglycerides: Effect of pressure on selectivity. *Journal of the American Oil Chemists' Society* 77(3), pp. 311–314.

Liu, X. et al. 2014. Use of C30 as a General-Purpose Stationary Phase for a Broad Range of Applications. *Thermo Application Note* , pp. 1–4.

Loidl-Stahlhofen, A. et al. 1995. Gas chromatographic-electron impact mass spectrometric screening procedure for unknown hydroxyaldehydic lipid peroxidation products after pentafluorobenzyloxime derivatization. *Journal of Chromatography B: Biomedical Sciences and Applications* 673(1), pp. 1–14.

Lovell, M. 2003. Analysis of aldehydic markers of lipid peroxidation in biological tissues by HPLC with fluorescence detection. *Methods in Biological Oxidative Stress* (2), pp. 17–23.

Machmon, P. et al. 1990. Calcium and Phosphorus Solubility in Neonatal Intravenous-Feeding Solutions. *Archives of Disease in Childhood* 65(4), pp. 352–353.

Makahleh, A. et al. 2010. Determination of underivatized long chain fatty acids using RP-HPLC with capacitively coupled contactless conductivity detection. *Talanta* 81(1–2), pp. 20–24.

Manuel-y-Keenoy, B. et al. 2016. Effects of intravenous supplementation with a -tocopherol in patients receiving total parenteral nutrition containing medium- and long-chain triglycerides. *European Journal of Clinical Nutrition* 56(March 2002), pp. 121–128.

Márquez-Sillero, I. et al. 2013. Determination of water-soluble vitamins in infant milk and dietary supplement using a liquid chromatography on-line coupled to a corona-charged aerosol detector. *Journal of Chromatography A* 1313, pp. 253–258.

Marrow, J. 2010. Looking for Lipid Peroxidation in Vitro and in Vivo : Is Seeing Believing ? Available at: http://www.sfrbm.org/frs/Morrow2002.pdf [Accessed: 3 November 2015].

Maruyama, H. et al. 2018. Maximization of calcium and phosphate in neonatal total parenteral nutrition. *Pediatrics International* 60(7), pp. 634–638.

Massorenti, P. et al. 2004. 4-Hydroxynonenal is Markedly Higher in Patients on a Standard Long-term Home Parenteral Nutrition. *Free Radical Research* 38(1), pp. 73–80.

Miller, E.R.I. et al. 2005. Review Meta-Analysis : High-Dosage Vitamin E Supplementation May Increase all Cause Mortality. *Ann Intern Med* 142, pp. 37–46. doi: 1.

Miloudi, K. et al. 2012. The mode of administration of total parenteral nutrition and nature

of lipid content influence the generation of peroxides and aldehydes. *Clinical Nutrition* 31(4), pp. 526–34.

Mlakar, A. and Spiteller, G. 1996. Distinction between enzymic and nonenzymic lipid peroxidation. *Journal of Chromatography A* 743(2), pp. 293–300.

Moreau, R. a. 2009. Lipid analysis via HPLC with a charged aerosol detector. *Lipid Technology* 21(8), pp. 191–194.

Muhlebach, S. 2015. Peroxidation of Intravenous Lipid Emulsions. Available at: www.espen.org/presfile/Muhlebach-010824-web.doc [Accessed: 11 November 2015].

Mühlebach, S. and Steger, P.J. 1998. Lipid peroxidation of intravenous fat emulsions: a pharmaceutical issue with clinical impact? *Nutrition* 14(9), pp. 720–1.

Murphy, R. 2017. RCM lipid Calculator. Available at: www.pharmacology.ucdenver.edu/lipidcalc/Defailt.aspx [Accessed: 3 April 2017].

Niki, E. 1987. ANtioxidants in relation to lipid peroxidation. *Chemistry and physics of lipids* 44, pp. 227–253.

Nonneman, L. et al. 2002. Effects of intravenous supplementation with a - tocopherol in patients receiving total parenteral nutrition containing medium- and long-chain triglycerides. *European Journal of Clinical Nutrition* 56, pp. 121–128.

Nourooz-Zadeh, J. et al. 1995. Measurement of Hydroperoxides in Edible Oils Using the Ferrous Oxidation in Xylenol Orange Assay. *Journal of Agricultural and Food Chemistry* 43(1), pp. 17–21.

Ozcan, A. and Ogun, M. 2015. Biochemistry of Reactive Oxygen and Nitrogen Species. In: *Basic Principles and Clinical Significance of Oxidative Stress*., pp. 37–58.

Paltrinieri, A.L. et al. 2016. Parenteral nutrition is not a fluid ! *Archives of Disease in Childhood* 0, pp. 1–6.

Pereira, A.D.S. et al. 2000. Gas chromatography problem solving and troubleshooting. *Journal of Chromatographic Science* 38(6), pp. 309–310.

Picaud, J. et al. 2004. Lipid peroxidation assessment by malondialdehyde measurement in parenteral nutrition solutions for newborn infants: a pilot study. *Acta Paediatrica* 93(2), pp. 241–245.

Pironi, L. et al. 2003. Peroxidation potential of lipid emulsions after compounding in all-in-one solutions. *Nutrition* 19(9), pp. 784–788.

Pitkanen, O. et al. 1991. Generation of free radicals in lipid emulsion used in parenteral nutrition. *Pediatric Research* 29(1), pp. 56–59.

Pittiruti, M. et al. 2009. ESPEN Guidelines on Parenteral Nutrition: Central Venous Catheters (access, care, diagnosis and therapy of complications). *Clinical Nutrition* 28(4), pp. 365–377.

Plante, M. et al. 2011. Analysis of Lipids by HPLC-CAD. *Dionex Company*

Plante, M. et al. 2013. Determination of Olive Oil Adulteration by Principal Component Analysis with HPLC – Charged Aerosol Detector Data. *Thermo Application Note*

Plattner, R.D. 1989. High-Performance liquid chromatography of Triglycerides. *Methods in Enzymology* 72, pp. 21–34.

Porter, N.A. et al. 1980. Autoxidation of polyunsaturated lipids. Factors controlling the stereochemistry of product hydroperoxides. *Journal of the American Chemical Society* 102(17), pp. 5597–5601.

Porter, N.A. et al. 1995. Mechanisms of Free Radical Oxidation of Unsaturated Lipids. *Lipids* 30(4), pp. 277–290.

Porter, N.A. 2013. A Perspective on Free Radical Autoxidation: The Physical Organic Chemistry of Polyunsaturated Fatty Acid and Sterol Peroxidation. *Journal of Organic Chemistry* 78(8), pp. 3511–3524.

Repetto, M. et al. 2012. Lipid Peroxidation. *Lipid Peroxidation* , pp. 3–30.

Rossin, D. et al. 2016. HNE and cholesterol oxidation products in colorectal inflammation and carcinogenesis. *Free Radical Biology and Medicine* 111(November 2016), pp. 186–195.

Sala-Vila, A. et al. 2007. Olive oil in parenteral nutrition. *Current Opinion in Clinical Nutrition and Metabolic Care* 10(2), pp. 165–74.

Schaur, R. et al. 2015. *4-Hydroxy-nonenal: A Bioactive Lipid Peroxidation Product*.

Schneider, C. et al. 2001. Two distinct pathways of formation of 4-hydroxynonenal. Mechanisms of nonenzymatic transformation of the 9- and 13-hydroperoxides of linoleic acid to 4-hydroxyalkenals. *Journal of Biological Chemistry* 276(24), pp. 20831–20838.

Schneider, C. et al. 2008. Routes to 4-hydroxynonenal: Fundamental issues in the mechanisms of lipid peroxidation. *Journal of Biological Chemistry* 283(23), pp. 15539–15543.

Schneider, C. 2009. An update on products and mechanisms of lipid peroxidation. *Molecular nutrition and food research* 53(3), pp. 315–321.

Schönherr, C. et al. 2009. Simple and precise detection of lipid compounds present within liposomal formulations using a charged aerosol detector. *Journal of Chromatography A* 1216(5), pp. 781–786.

Scientific, T. 2003. Acclaim ® 120 HPLC Columns.

Scientific, T. 2011. Acclaim C30 Column.

Seppanen, C.M. and Saari Csallany, A. 2002. Formation of 4-hydroxynonenal, a toxic aldehyde, in soybean oil at frying temperature. *Journal of the American Oil Chemists' Society* 79(10), pp. 1033–1038.

Sewell, P.A. 1992. Non-aqueous reversed-phase separation of triacylglycerols. In: *Lipid Analysis- a practical approach*. Oxford University Press, pp. 187–191.

Shabir, B.Y.G. 2004. Step-by-step analytical methods validation and protocol in the quality system compliance industry. *Journal of Validation Technology* 10, pp. 210–218.

Shintani, H. 2013. Lipid Peroxides. *Pharmaceutica Analytica Acta* 04(05), pp. 4–5.

Silvers, K.M. et al. 2001. Limiting light-induced lipid peroxidation and vitamin loss in infant parenteral nutrition by adding multivitamin preparations to Intralipid. *Acta Paediatrica* 90(3), pp. 242–249.

Skouroliakou, M. et al. 2012. Physicochemical stability assessment of all-in-one parenteral emulsion for neonates containing SMOFlipid. *European Journal of Hospital Pharmacy: Science and Practice* 19(6), pp. 514–518.

Smith, T. et al. 2011. Annual BANS Report 2011. Available at: http://www.bapen.org.uk/pdfs/bans_reports/bans_report_11.pdf.

Smith, T. and Naghibi, M. 2016. *BANS Report 2016 Artificial Nutrition Support in the UK 2005-2015*.

Sodergren, E. 2000. *Lipid peroxidation in vivo*.

Sousa, B.C. et al. 2017. Chemistry and analysis of HNE and other prominent carbonyl-containing lipid oxidation compounds. *Free Radical Biology and Medicine*

Steger, P.J.K. and Mühlebach, S.F. 1997. In vitro oxidation of IV lipid emulsions in different all-in-one admixture bags assessed by an iodometric assay and gas-liquid chromatography. *Nutrition* 13(2), pp. 133–140. doi: 10.1016/S0899-9007(96)00387-5.

Steger, P.J.K. and Mühlebach, S.F. 1998. Lipid peroxidation of IV lipid emolsions in TPN bags: The influence of tocopherols. *Nutrition* 14(2), pp. 179–185.

Steghens, J.-P. et al. 2001. Diaminonaphtalene, a new highly specific regent for HPLC-UV measurement of total and free malondialdehyde in human plasma or serum. *Free Radical Biology and Medicine* 31(2), pp. 242–249.

Swe, P.Z. et al. 1996. Improved NARP-HPLC method for separating triglycerides of palm olein and its solid fractions obtained at low temperature storage. *Food Chemistry* 56(2), pp. 181–186.

Synder, L. et al. 1997. *Practical HPLC method development*. second. Wiley-interscience.

Tashiro, T. et al. 1992. Intravenous intralipid 10% vs 20%, hyperlipidemia, and increase in lipoprotein X in humans. *Nutrition* 8(3), pp. 155–160.

United States Pharmacopeia and National Formulary (USP38 - NF 33) 2016a. 〈 401 〉 Fats and Fixed Oils. In: *United States Pharmacopeia*., pp. 276–289.

United States Pharmacopeia and National Formulary (USP38 - NF 33) 2016b. Chapter 729. Globule size distribution in lipid injectable emulsions. In: *United States Pharmacopeia*., pp. 504–506.

Wabel, C. 1998. *Influence of Lecithin on structure and stability of parenteral fat emulsions.* Available at: http://www2.chemie.uni-erlangen.de/services/dissonline/data/dissertation/Christoph_Wabel/html/Chapter3.html.

Waitzberg, D.L. et al. 2015. New parenteral lipid emulsions for clinical use. *Journal of parenteral and enteral nutrition* 30(4), pp. 351–367.

Waters 2018. Solvents and Caveats for LC/MS. Available at: http://www.waters.com/waters/en_GB/Solvents-and-Caveats-for-LC-MS/nav.htm?cid=10091173&locale=en_GB [Accessed: 25 July 2018].

Weiss Gallenkamp 2006. SERVICE MANUAL PSC 022/ PSC 062 Pharmaceutical stability

chambers.

Wischmeyer, P.E. 2015. Alternative Lipid Emulsions as a New Standard of Care for Total Parenteral Nutrition. *Critical Care Medicine* 43(1), pp. 230–231.

Wu, G.H. et al. 1999. Phagocyte-induced lipid peroxidation of different intravenous fat emulsions and counteractive effect of vitamin E. *Nutrition* 15(5), pp. 359–364.

Yamamoto, Y. and Ames, B.N. 1987. Detection of lipid hydroperoxides and hydrogen peroxide at picomole levels by an HPLC and isoluminol chemiluminescence assay. *Free Radical Biology & Medicine* 3(5), pp. 359–61.

Yamauchi, R. 1997. Vitamin E : Mechanism of Its Antioxidant Activity. *Food Science and Technology International Tokyo* (3), pp. 301–309.

Yuan, J. et al. 2018. Formation of 4-Hydroxy-2-Trans-Nonenal, a Toxic Aldehyde, in Thermally Treated Olive and Sunflower Oils. *JAOCS, Journal of the American Oil Chemists' Society* 95(7), pp. 813–823.

Zarkovic, K. et al. 2016. Contribution of the HNE-immunohistochemistry to modern pathological concepts of major human diseases. *Free Radical Biology and Medicine* 111(October 2016), pp. 110–126.

Zhong, H. and Yin, H. 2015. Role of lipid peroxidation derived 4-hydroxynonenal (4-HNE) in cancer: focusing on mitochondria. *Redox Biology* 4, pp. 193–9.

Contents lists available at ScienceDirect

Clinical Nutrition ESPEN

journal homepage: http://www.clinicalnutritionespen.com

Original article

A HPLC method to monitor the occurrence of lipid peroxidation in intravenous lipid emulsions used in parenteral nutrition using in-line UV and charged aerosol detection

Helen M. King[*], Allan G. Cosslett, Christopher P. Thomas, Rebecca Price-Davies

Cardiff School of Pharmacy and Pharmaceutical Sciences, Cardiff, Wales, CF10 3NB, UK

SUMMARY

Parenteral Nutrition (PN) provides life sustaining support where gastrointestinal nutrition is inadequate due to disease or prematurity. Intravenous lipid emulsions (IVLEs) form a staple part of PN. Whilst the physical stability of IVLE's is relatively well known and quantified, chemical stability is an area where little testing has occurred. We report a new sensitive method for the monitoring of selected triglycerides present within two IVLEs and the detection and quantification of the peroxidation product 4-hydroxynonenal (HNE) using HPLC with in-line UV and charged aerosol detection (CAD). IVLEs used included the soy-bean oil based emulsion Intralipid® 20% and SMOFlipid® 20% (Fresenius Kabi UK), based on soy-bean, olive, fish oil and medium chain triglycerides. Assay validation gave R^2 values of ≥ 0.99 for all selected triglyceride peaks and 4-hydroxynonenal. Inter and intra-day repeatability gave RSD values < 7.2% for CAD detection, achieving a precise and repeatable method. HNE was confirmed through internal standardisation of the HPLC method. Selected triglycerides were identified using ESI-MS with MicroTOF. This novel method permits the chemical stability of IVLEs to be quantified and monitored in respect to lipid peroxidation during storage prior to delivery to the patient, ensuring the optimal safety of IVLEs in a clinical setting.

1. Introduction

Intravenous lipid emulsions (IVLEs) form a staple part of parenteral nutrition (PN). PN provides life sustaining support where gastrointestinal nutrition is either not possible, or inadequate due to disease or prematurity. IVLE's are provided in PN either in combination all-in-one (AIO) mixtures with all other PN components (glucose, amino acids, vitamins, trace elements and electrolytes), or separated, in the case of delivery of PN to neonates [1]. Physical stability of PN is well studied and currently governs the combinations and concentrations of components permissible within a PN admixture for a patient. Lipid globule size, pH, visual inspection for signs of emulsion instability and globule size distribution are commonly tested to confirm physical stability [2—4]. Chemical stability of PN during storage after manufacturing is currently not extensively studied, but is an area which needs to be addressed due to the growing body of knowledge on the harmful effects of breakdown products of lipids due to peroxidation [5—9].

All unsaturated lipids are susceptible to peroxidation, a cyclical process resulting in the production of primary and secondary toxic peroxidation products [7,10]. Primary hydroperoxides are transient making their quantification a challenge. Therefore, secondary peroxidation products are more extensively tested. These include malondialdehyde (MDA), 4-hydroxynonenal (HNE), 4-hydroxyhexanal (HHE) and 4-hydroxundecenal (HUE) which are by far the most extensively studied with regards to there in vitro toxicity [5,11—16].

With regards to PN, Intralipid® 20% (Fresenius Kabi) has been the most extensively used IVLE and is formulated from soy bean oil rich in omega 6 linoleic acid, omega 9 oleic acid and omega 3 α-linolenic acid, proportions of each displayed in Table 1 [17]. All contain levels of unsaturation and therefore are susceptible to

---

Table 1
Fatty acid composition of Intralipid® 20% and SMOFlipid® 20% as shown in summary of product characteristics (Fresenius Kabi). All are subsequently formulated into triglycerides forming stable intravenous lipid emulsions.

Fatty acid	Carbon number: double bond	SMOFlipid® 20%	Intralipid® 20%
Oleic acid	C18:1	23–35%	19–30%
Linoleic acid	C18:2	14–25%	44–62%
Caprylic acid	C8:0	13–24%	–
Palmitic acid	C16:0	7–12%	7–14%
Capric acid	C10:0	5–15%	–
Stearic acid	C18:0	1.5–4%	1.4–5.5%
α-linolenic acid	C18:3	1.5–3.5%	4–11%
EPA	C20:5	1–3.5%	–
DHA	C22:6	1–3.5%	–

peroxidation into HNE, HUE and HHE respectively. SMOFlipid® 20% (FK), a newer generation IVLE contains a mixture of soy bean, olive and fish oils and saturated medium chain triglycerides as shown in Table 1. Whilst the level of saturated fatty acids is higher in SMO-Flipid® than Intralipid®, both contain linoleic, oleic and α-linolenic acids that can peroxidise to the aldehydes mentioned. In an effort to inhibit peroxidation from occurring, SMOFlipid®, which contains the longer polyunsaturated EPA and DHA, contains tocopherols which are proposed potent free radical scavengers [18]. In a clinical setting PN formulations are prepared often on an individual patient basis, manufactured in a hospital pharmacy setting. Formulations may be exposed to air during preparation and are stored in either oxygen permeable syringes for neonatal lipid PN or oxygen impermeable PN bags. Every effort is made to remove as much air as possible after manufacturing, but a level of oxygen remains providing the initial environment for peroxidation to occur.

Current assays available to quantify peroxidation include the TBARs assay [19,20], FOX assay [21] and HPLC assays looking for derivatised aldehydic products of peroxidation [22–24]. Whilst effective in certain conditions both the TBARs and FOX assays are unsuitable as are proven to be relatively inaccurate in their estimations of lipid peroxidation [21]. HPLC with derivatisation for the detection of HNE [25,26] is accurate and quantifiable but the derivatisation is time consuming and unnecessary as free HNE should theoretically be formed within IVLE's. HPLC with UV detection of free HNE has been documented and used successfully by Emerit et al. and Esterbauer et al. [27,28]. Here we present a method that provides accurate detection and monitoring of the triglycerides present within each IVLE via HPLC with charged aerosol detection (CAD) in-line with the UV detection of HNE, aiming to circumvent the limitations with current methods and complement the detection of HNE with a secondary method to monitor the breakdown of lipids occurring.

2. Materials and methods

2.1. Reagents and materials

LC-MS grade isopropanol (IPA) for HPLC analysis, water with 0.1% formic acid, and methanol (MeOH) with 0.1% formic acid for MS analysis were purchased from Fisher Scientific. LC-MS grade acetonitrile for HPLC analysis was purchased from VWR chemicals. 4-Hydroxynonenal standard (1 mg 100 μl [1]) was purchased from Santa-Cruz Biotechnology and used for HPLC method development. Intralipid® 20% and SMOFlipid® 20% IVLE's were kindly donated by Fresenius Kabi UK.

2.2. HPLC-UV-CAD conditions

The analysis of the triglycerides and HNE was performed on a Thermo Scientific Ultimate 3000 HPLC system coupled firstly to a Spectra system UV detector and then to an in-line CAD. Gonyon et al. [29] provides an initial set of chromatographic conditions employing non-aqueous reversed phase HPLC from which the assay was developed. Separations were carried out on an Acclaim C30 column 3.0 mm × 250 mm, 3 μm particle size at a flow rate of 0.2 ml min [1]. The non-aqueous mobile phase consisted of an IPA (phase A) and ACN (phase B) gradient. The gradient program started at 60% phase B, decreased to 40% B over the first 20 min, was held at 40% B for a further 50 min then increased to 60% B over 15 min with a 5-min isocratic hold for re-equilibration at the end of each run. The column temperature was held at 5 °C after optimisation to maximise resolution and the autosampler was held at 8 °C throughout to maintain refrigerated conditions of samples and inhibit further peroxidation from occurring during analysis. Injection volume was 1 μl of lipid and the sample loop was washed with 60% MeOH/water after each injection. Sample preparation was unnecessary due to the ability of the CAD detector to detect triglycerides present within an emulsion without any sample extraction required [29]. The UV detector was set and maintained at 222 nm wavelength [30] with a data collection rate at 1.0 Hz for the detection of HNE. CAD detector settings were maintained at 50 °C evaporating temperature, data collection rate of 10 Hz and a filter of 3.6 s. A 30-min blank run was performed after each set of three repetitions from each sample to ensure optimal column cleaning between samples. This blank ran the same CAD, UV, column and autosampler conditions as above. The flow rate was increased to 0.4 ml min [1] and a 2 μl injection of blank mobile phase was carried out. During this period, mobile phase gradient followed the same pattern as above but was proportionally compressed into 30 min. Chromatography control and integration of chromatograms was completed using Chromeleon (ver 7.2) software (Thermo Scientific).

2.3. MS conditions for triglyceride identification

Identification of selected triglycerides from each IVLE was performed by collection of fragments from the HPLC effluent at point of entry to the CAD at time points corresponding to the 5 main peaks in Intralipid® and the 9 main peaks in SMOFlipid®. These main peaks were selected due to the objective of monitoring the changes in triglyceride levels that occur during storage before delivery to the patient, providing an overview of the lipid changes occurring during storage. Therefore, not all peaks in each chromatogram were identified, just the main primary peaks (5 in Intralipid® and 9 in SMOFlipid®). These collected fragments were then analysed by MS, performed on an Agilent 1100 series autosampler and a Bruker MicroTOF ESI-MS. The mass spectrometer was operated in positive ionisation mode with a full scan mode from 0 to 2000 Da. An isocratic mobile phase consisted of MeOH (0.1% formic acid): water 90:10 at a flow rate of 1 ml min [1]. Source parameters were as follows: capillary voltage 4.5 kV, end plate offset −500 V, nebuliser pressure (N_2) 0.4 Bar, dry gas (N_2) 4 L min [1], dry heater 200 °C.

Sample injection size was 30 μl—60 μl dependant on response. Analysis of MS data was carried on Hystar post acquisition (Bruker Daltonics) software with base peak chromatograms for each sample created from 0 to 1000 Da.

2.4. HPLC-UV-CAD method validation

HNE was quantified by creation of standard curves prepared from a stock solution of HNE standard (10 mg ml^{-1}) in ethanol. This stock solution was further diluted with ethanol to create a 1 mg ml^{-1} solution. Aliquots of 64, 48, 32, 16 and 8 μl of this stock solution were made up to 2 ml with Intralipid 20% creating a set of standards for calibration at 204.83, 153.62, 102.51, 51.21 and 25.60 μM HNE respectively. These standard solutions were then subjected to HPLC and calibration curves created to assess linearity. Calibration of selected triglycerides was carried out using Intralipid® 20% and SMOFlipid® 20% as internal standards of specific triglycerides are unsuitable due to the emulsion nature of the IVLE's. Using individual standards of each triglyceride to create calibration curves was not employed as elution times of triglycerides not formulated within emulsions will be different to those as seen when analysing the selected IVLE's when using the above assay conditions. Therefore, standard solutions of each lipid emulsion were created by adding volumes of each IVLE to water to obtain 12.5, 25, 50, 75 and 100% concentrations for each emulsion. Again, these were then subjected to the HPLC conditions detailed above and calibration curves for each triglyceride peak were created. Selectivity, intra-day and inter-day variability and precision was determined for triglycerides through separate sampling of

1 ml of each IVLE and using the stock solution of HNE in Intralipid® and SMOFlipid® as detailed above. Precision was expressed as a percentage of relative SD (RSD) and tested both inter and intra-day by testing standard samples over separate runs on the same day separated by blank runs and on two separate days on different weeks. All samples were freshly prepared on each required day and stored at 2—8 °C before analysis.

3. Results

3.1. Optimisation of HPLC-UV-CAD method

We have presented what is to our knowledge a novel method for the simultaneous analysis of triglycerides within IVLE's and the detection of HNE. Example chromatograms for both Intralipid® 20% and SMOFlipid® 20% show sufficient resolution for quantification (Figs. 1 and 2). Intralipid® spiked with 16 μg HNE standard (Fig. 3) shows the importance of the initial gradient elution in producing effective separation of HNE from triglyceride peaks. Figs. 4 and 5 show Intralipid® 20% and SMOFlipid® 20% in varying states of degradation, clearly showing the production of HNE in comparison with new fresh samples and samples spiked with HNE standard. Method development and optimisation was carried out initially separately for HNE and triglycerides before placing the UV and CAD detectors in-line with each other creating the final assay conditions. Temperature optimisation of the column was found to be a key governing factor on creating sufficient resolution. Flow rate, CAD conditions and UV data collection rate were all optimised to achieve maximal resolution.
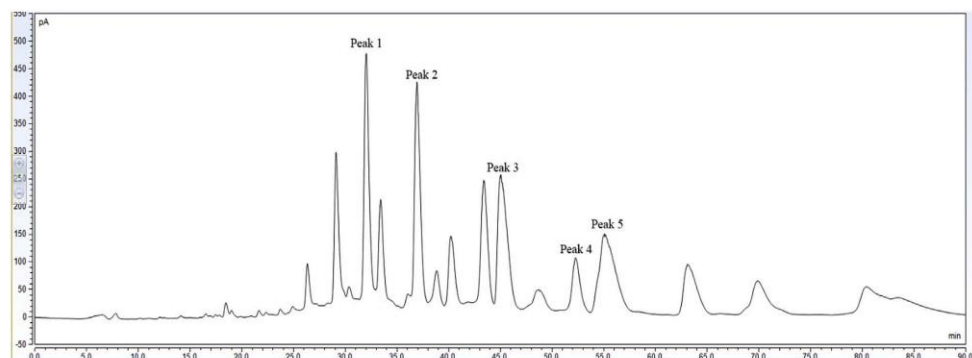
Fig. 1. HPLC-CAD chromatogram of Intralipid® 20% showing selected peaks collected for mass spectrometry and identification.
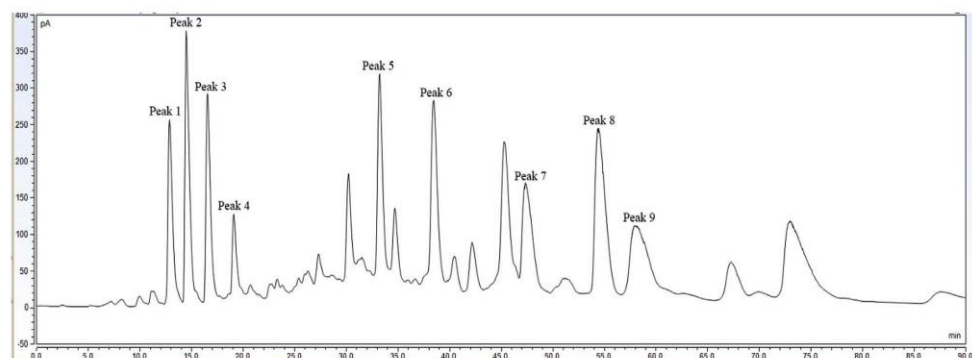
Fig. 2. HPLC-CAD chromatogram of SMOFlipid® 20% showing selected peaks subsequently collected for mass spectrometry identification.
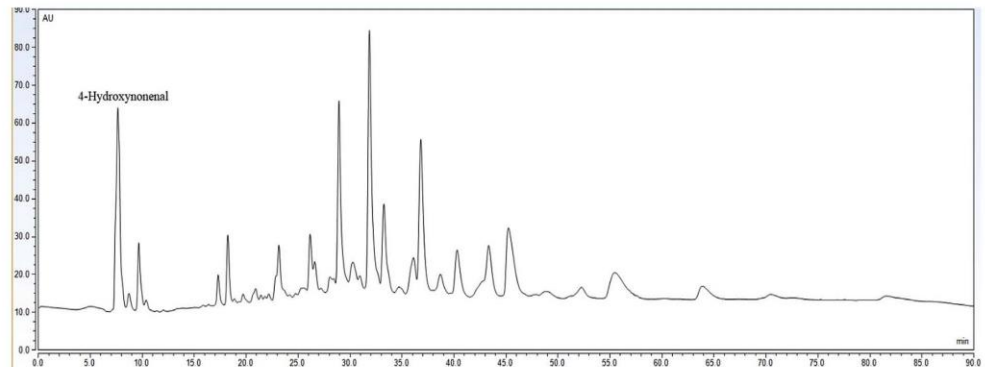
Fig. 3. HPLC-UV chromatogram of degraded (84 days at room temperature in a 50ml oxygen permeable syringe) Intralipid® 20% with additional 16 μg of HNE standard. HNE peak shows clear separation from triglycerides and other peroxidation products that elute early due to their short chain length.
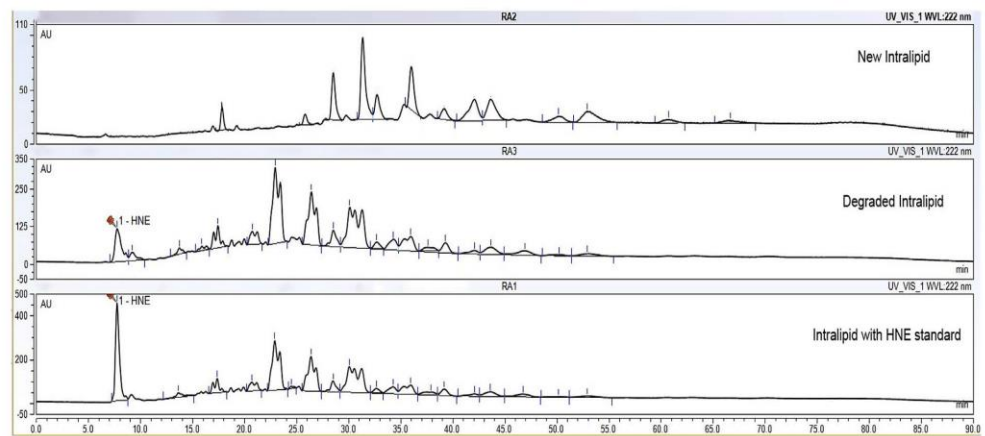
Fig. 4. HPLC-UV chromatograms of fresh Intralipid® 20%, degraded Intralipid® 20% and Intralipid with added HNE standard.
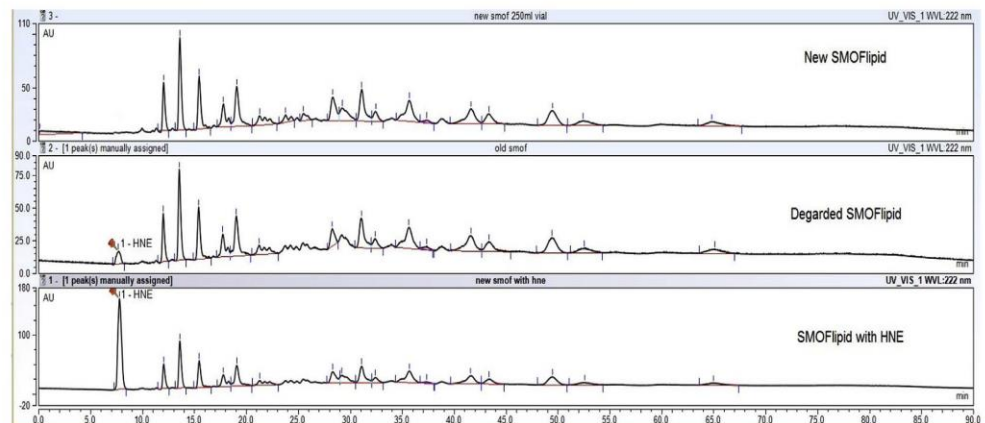
Fig. 5. HPLC-UV chromatogram of new SMOFlipid® 20%, degraded SMOFlipid® 20% and SMOFlipid® with added HNE standard.

3.2. Mass spectrometry for triglyceride analysis

MS was employed to identify the selected peaks in Intralipid® (Fig. 1) and SMOFlipid® (Fig. 2). Due to the emulsion formulations being analysed, internal addition of standards for each triglyceride could not be employed for assay validation and peak identification. Therefore, to circumvent this issue fragments of HPLC effluent were collected corresponding to each selected peak for identification. The CAD detector is destructive in its analysis therefore fragments were collected at the entry point to the detector using time points corresponding to each selected peak of interest and subjected to analysis by MS. Data collected from MS is presented in Tables 2 and 3 for Intralipid® 20% and SMOFlipid® 20% and analysed using RCM's lipid data [31] and Hystar (Bruker) post processing software.

Putative peak identification with the likely fatty acid composition of each triglyceride was carried out. Whilst the sensitivity of the MS used didn't allow runs to distinguish between triglycerides with the same m/z ratio, we can predict the TAG responsible for each peak analysed. Li et al. [32] shows the analysis of TAGs present within soy bean oil by percentage occurrence. This combined with the prevalence of the individual fatty acids as recorded in each IVLE's Summary of Product Characteristics (SPC) shown in Table 1 was used to assign specific TAGs to each selected peak in Intralipid® 20% and peaks 5 to 9 of SMOFlipid® 20%. Peaks 1 to 4 of SMOFlipid® 20% were identified as medium chain saturated fatty acids of C8 to C10 in length.

3.3. Method validation for HNE detection

HNE calibration was performed as described with linear regression analysis giving a R^2 of 0.998 in a concentration range from 25 to 204 μM. The LLOD and LLOQ detailed as the concentration producing signal to noise ratio of 3 and 10 respectively was 3.523 μM and 11.743 μM obtained from injection of standard solutions. Precision was determined as detailed in Table 4 and show high levels of precision for HNE over both low (25 μM) and high (204 μM) both intra and inter-day. At all concentrations accuracy

fell within acceptable ranges (80–120%). Considered collectively the above data show a sensitive, accurate and precise method for the detection of HNE within IVLE's.

3.4. Method validation for IVLE's Intralipid® 20% and SMOFlipid® 20%

SPC data for both IVLEs provides ranges of concentrations for each fatty acid present. This prevents the individual concentrations of specific triglycerides from being calculated due to the variability of fatty acid concentrations in each IVLE. Individual triglyceride standards cannot be used as internal standards due to the formulation properties of the emulsion. Therefore, to overcome these issues concentrations of 12.5, 25, 50, 75 and 100% of each IVLE diluted with water were created to enable calibration curves to be formed. Triglyceride detection was performed using a CAD detector which typically gives a non-linear response when used over a wide concentration range [33,34], therefore calibration curves for each selected peak were plotted using a second order polynomial function with results for all peaks both in SMOFlipid® and Intralipid® showing good correlation ($R^2 > 0.99$). Precision was calculated for Intralipid® and SMOFlipid® peaks both inter ($n = 3$) and intra-day ($n = 6$) with results yielding a maximum of 4.5% RSD (intra-day) and 5.2% RSD (inter-day) for Intralipid® and 5.0% RSD (intra-day) and 4.7% RSD (inter-day) for SMOFlipid®. In combination as detailed in Table 5, this data demonstrates a precise and repeatable assay to quantify the selected triglycerides within these IVLE's.

4. Discussion

This study presents a novel HPLC method utilising in line UV and CAD detectors to monitor triglycerides in Intralipid® and SMOFlipid® IVLE's whilst simultaneously quantifying HNE produced as a result of lipid peroxidation. This aims to address the lack of chemical testing that occurs in such IVLE's during storage, prior to delivery to the patient, by enabling TAG levels to be monitored and HNE levels to be quantified. The method developed has a total chromatographic time of 90 min. Whilst this is relatively long in comparison to the time required to employ less accurate assays (FOX) [35], the assay is designed to be used as a stability indicating method, not as a day to day testing method, therefore run time isn't of vital importance and the extended time allows for higher concentrations of IPA to be employed during mobile phase gradient. As IPA is relatively viscous at the low temperatures that the column is held at, the long run time and low flow rate counterbalance this. When employing non-

Table 2
Mass spectrometry data for selected Intralipid® 20% peaks and subsequent triglycerides attributed to each peak.

Intralipid® Peak number	Mass spectrometry m/z data	Triglyceride attributed
1	879.74 [M+H]+	TG (18:2/18:2/18:2)
2	881.76 [M+H]+	TG (18:2/18:2/18:1)
3	855.74 [M+H]+	TG (18:2/18:2/16:0)
4	885.78 [M+H]+	TG (18:1/18:1/18:1)
5	857.75 [M+H]+	TG (18:2/18:1/16:0)

Table 3
Mass spectrometry data for selected SMOFlipid® 20% peaks and subsequent triglycerides attributed to each peak.

SMOFlipid® Peak number	Mass spectrometry m/z data	Triglyceride attributed
1	493.35 [M+Na]+	TG (8:0/8:0/8:0)
2	521.37 [M+Na]+	TG (8:0/8:0/10:0)
3	549.40 [M+Na]+	TG (8:0/10:0/10:0)
4	577.43 [M+Na]+	TG (10:0/10:0/10:0)
5	879.75 [M+H]+ 901.73 [M+Na]+	TG (18:2/18:2/18:2)
6	881.76 [M+H]+ 903.75 [M+Na]+	TG (18:2/18:2/18:1)
7	855.74 [M+H]+	TG (18:2/18:2/16:0)
8	855.78 [M+H]+ 907.76 [M+Na]+	TG (18:1/18:1/18:1)
9	857.75 [M+H]+ 879.75 [M+Na]+	TG (18:2/18:1/16:0)

Table 4
Assay validation of precision and accuracy for HNE.

HNE concentration (μM)	Precision		Accuracy
	RSD₁ (%)	RSD₂ (%)	(%)
25.6	7.33	1.05	117.50
51.21	3.07	1.70	84.35
102.51	7.19	3.76	96.90
153.62	5.40	4.37	90.14
204.83	5.53	3.75	97.39

RSD₁, intra-day precision ($n = 3$), RSD₂, inter-day precision ($n = 6$).

Table 5
Assay validation data for Intralipid® 20% and SMOFlipid® 20% selected peaks.

	Peak number	R^2	Precision	
			RSD₁	RSD₂
Intralipid® 20%	1	0.996	1.931	1.689
	2	0.992	1.567	3.679
	3	0.997	4.534	2.079
	4	0.995	4.225	5.209
	5	0.998	3.812	0.566
SMOFlipid® 20%	1	0.997	3.264	3.740
	2	0.997	3.090	2.597
	3	0.996	2.719	2.258
	4	0.996	3.750	1.614
	5	0.997	3.520	2.048
	6	0.996	3.463	2.384
	7	0.999	2.598	3.544
	8	0.991	5.081	2.607
	9	0.993	4.757	4.745

RSD₁, inter-day repeatability ($n = 6$), RSD₂, intra-day repeatability ($n = 3$).

aqueous reversed phase (NARP) chromatography, the difference in polarities of each phase and subsequently the strength assigned to each phase is the governing factor over the phases' ability to elute hydrophobic TAGs from the C30 column [36–38]. In the mobile phase mixture used, IPA constitutes the 'strong' eluting solvent. Initially the gradient employs a high concentration (60%) of ACN, optimised to effectively separate HNE from both early eluting TAGS of low carbon number and other short chain aldehydic products (Fig. 3). The isocratic hold of 60% IPA/40% ACN forms the main body of the assay from 20 to 70 min, creating optimal conditions for TAG elution and effective separations and resolutions. With regards to the order of elution of the TAGs in both Intralipid® and SMOFlipid® all identified TAGs, except the medium chain saturated TAGs in SMOFlipid®, followed the general formula $PN = CN - 2DB$ (PN partition number, CN Carbon number, DB double bonds) [36]. As NARP is employed in the assay with a C30 column the level of unsaturation will govern the level of interaction each fatty acid on each TAG will have with the stationary phase. Due to the significant difference in chain length of the saturated fatty acids (C8 to C10) found in SMOFlipid® these TAGs elute early in the run following the elution order of increasing carbon chain length.

The use of the CAD allows accurate quantification of TAGs without the need for derivatisation or argentation, reducing the sample preparation required and ensuring optimal sample recovery. The CAD has a non-linear response over wide concentration ranges, following a second order polynomial function [39]. Throughout calibration RSD's were monitored for both lipid emulsions the maximum being 5.1%, proving an acceptable level of precision and repeatability.

When considering the validation of the CAD section of the assay for the quantification of TAGs, LLOD and LLOQ cannot be calculated due to the limited information given in each of the IVLE's SPC: amounts are given as a range of concentrations of individual fatty acids. Due to this, exact concentrations of each triglyceride attributed to each selected peak cannot be calculated, preventing LLOD and LLOQ from being calculated as a molarity. We can however express LLOD and LLOQ as a percentage concentration from a neat standard (100%) of IVLE. For Intralipid® 20%, the LLOD and LLOQ for the smallest measured peak was 0.64% and 2.32% respectively. SMOFlipid® 20% produced LLOD and LLOQs of 1.57% and 5.57%. For the purposes of the use of the assay, such LLOD's and LLOQ's are sufficient validation as, during storage before delivery to the patient, the amount of TAGs lost will be no more than 50%. The calculation of peak area for each selected peak cannot be translated into a concentration for TAG peaks within these lipid emulsions, therefore data from the assay can be presented as a percentage loss of TAG from an initial day 0 run.

In conclusion, a novel non-aqueous reversed phase HPLC assay has been established that employs in line UV and CAD detection for the accurate quantification of both triglycerides and the peroxidation product 4-hydroxynonenal within lipid emulsions. The combination of two detectors in line permits the detection of both short chain volatile aldehydic molecules and non-volatile complex triglycerides without the need for complex sample preparation or derivatisation. The method is precise and reliable and can be employed in the chemical stability testing of a variety of lipid emulsions.

Declarations of interest

None.

Acknowledgments

References

[1] Deshpande G, Simmer K. Lipids for parenteral nutrition in neonates. Curr Opin Clin Nutr Metab Care 2011;14:145–50. https://doi.org/10.1097/MCO.0b013e3283434562.

[2] Driscoll DF, Silvestri AP, Bistrian BR, Mikrut BA. Stability of total nutrient admixtures with lipid injectable emulsions in glass versus plastic packaging. Am J Heal Pharm 2007;64:396–403. https://doi.org/10.2146/ajhp060062.

[3] Müller RH, Heinemann S. Fat emulsions for parenteral nutrition. I: evaluation of microscopic and laser light scattering methods for the determination of the physical stability. Clin Nutr 1992:223–36.

[4] Pertkiewicz M, Cosslett A, Mühlebach S, Dudrick SJ. Basics in clinical nutrition: stability of parenteral nutrition admixtures. E-SPEN 2009;4:117–9. https://doi.org/10.1016/j.eclnm.2009.01.010.

[5] Esterbauer H. Cytotoxicity and genotoxicity of lipid-oxidation. Am J Clin Nurs 1993;57:779S–86S.

[6] Kaneko t, kazuhiko k. Cytotoxicities of a Linoleic acid hydroperoxide and its related aliphatic aldehydes toward cultured umbilical vein endothelial cells. Chem Biol Interact 1988;67:295–304.

[7] Halliwell B, Chirico S. Lipid peroxidation : its mechanism, measurement, and significance. Am J Clin Nutr 1993;57:715S–25S.

[8] Zarkovic N. 4-Hydroxynonenal as a bioactive marker of pathophysiological processes. Mol Aspects Med 2003;24:281–91. https://doi.org/10.1016/S0098-2997(03)00023-2.

[9] Awasthi YC, Ramana KV, Chaudhary P, Srivastava SK, Awasthi S. Regulatory roles of glutathione-S-transferases and 4-hydroxynonenal in stress-mediated signaling and toxicity. Free Radic Biol Med 2016;111:235–43. https://doi.org/10.1016/j.freeradbiomed.2016.10.493.

[10] Zielinski ZAM, Pratt DA. Lipid peroxidation: kinetics, mechanisms, and products. J Org Chem 2017;82:2817–25. https://doi.org/10.1021/acs.joc.7b00152.

[11] Schaur R, Siems W, Bresgen N, Eckl P. 4-Hydroxy-nonenal: a bioactive lipid peroxidation product. Biomolecules 2015. https://doi.org/10.3390/biom5042247.

[12] Csala M, Kardon T, Legeza B, Lizák B, Mandl J, Margittai É, et al. On the role of 4-hydroxynonenal in health and disease. Biochim Biophys Acta Mol Basis Dis 2015;1852:826–38. https://doi.org/10.1016/j.bbadis.2015.01.015.

[13] Zhong H, Yin H. Role of lipid peroxidation derived 4-hydroxynonenal (4-HNE) in cancer: focusing on mitochondria. Redox Biol 2015;4:193–9. https://doi.org/10.1016/j.redox.2014.12.011.

[14] Basu R, Muller DP, Papp E, Merryweather I, Eaton S, Klein N, et al. Free radical formation in infants: the effect of critical illness, parenteral nutrition, and enteral feeding. J Pediatr Surg 1999;34:1091–5. https://doi.org/10.1016/S0022-3468(99)90573-0.

[15] Esterbauer H, Schaur RJ, Zollner H. Chemistry and Biochemistry of 4-hydroxynonenal, malonaldehyde and related aldehydes. Free Radic Biol Med 1991;11:81–128. https://doi.org/10.1016/0891-5849(91)90192-6.

[16] Spickett CM. The lipid peroxidation product 4-hydroxy-2-nonenal: advances in chemistry and analysis. Redox Biol 2013;1:145–52. https://doi.org/10.1016/j.redox.2013.01.007.

[17] Driscoll DF, Bistrian BR, Demmelmair H, Koletzko B. Pharmaceutical and clinical aspects of parenteral lipid emulsions in neonatology. Clin Nutr 2008;27:497–503. https://doi.org/10.1016/j.clnu.2008.05.003.

[18] Wanten GJA. Parenteral lipid tolerance and adverse Effects : fat chance for Trouble ? J Parenter Enter Nutr 2015:1–6. https://doi.org/10.1177/0148607115595973.

[19] Devasagayam TPA, Boloor KK, Ramasarma T. Methods for estimating lipid peroxidation: an analysis of merits and demerits. Indian J Biochem Biophys 2003;40:300–8.

[20] Sochor J, Ruttkay-Nedecky B, Babula P. Automation of methods for determination of lipid peroxidation. Lipids 2012. https://doi.org/10.5772/2929.

[21] Karen M, Winterbourn CC. Lipid peroxide and hydrogen peroxide formation in parenteral. J Parenter Enter Nutr 2001;25:14–7. https://doi.org/10.1177/0148607101025000114.

[22] Fenaille F, Mottier P, Turesky RJ, Ali S, Guy PA. Comparison of analytical techniques to quantify malondialdehyde in milk powders. J Chromatogr A 2001;921:237–45. https://doi.org/10.1016/S0021-9673(01)00883-4.

[23] Adams LK, Benson EE, Staines HJ, Bremner DH, Millam S, Deighton N. Effects of the lipid peroxidation products 4-hydroxy-2-nonenal and malondialdehyde on the proliferation and morphogenetic development of in vitro plant cells. J Plant Physiol 1999;155:376–86. https://doi.org/10.1016/S0176-1617(99)80120-5.

[24] Gutteridge JM, Halliwell B. The measurement and mechanism of lipid peroxidation in biological systems. Trends Biochem Sci 1990;15:129–35. https://doi.org/10.1016/0968-0004(90)90206-Q.

[25] Chevolleau S, Noguer-Meireles MH, Jouanin I, Naud N, Pierre F, Gueraud F, et al. Development and validation of an ultra high performance liquid chromatography-electrospray tandem mass spectrometry method using selective derivatisation, for the quantification of two reactive aldehydes produced by lipid peroxidation. J Chromatogr B Anal Technol Biomed Life Sci 2018;1083:171–9. https://doi.org/10.1016/j.jchromb.2018.03.002.

[26] Benedetti A, Pompella A, Fulceri R, Romani A, Comporti M. 4-Hydroxynonenal and other aldehydes produced in the liver in vivo after bromobenzene intoxication. Toxicol Pathol 1986;14:457–61.

[27] Emerit I, Khan SH, Esterbauer H. Hydroxynonenal a component of clastogenic factors? Free Radic Biol Med 1991;10:371–7.

[28] Esterbauer H, Zollern H. Methods for determination of aldehydic lipid peroxidation products. Free Radic Biol Med 1989;7:197–203. https://doi.org/10.1016/0891-5849(89)90015-4.

[29] Gonyon T, Tomaso Jr AE, Kotha P, Owen H, Patel D, Carter PW, et al. Interactions between parenteral lipid emulsions and container surfaces. PDA J Pharm Sci Technol 2013;67:247–54. https://doi.org/10.5731/pdajpst.2013.00918.

[30] Benedetti A, Comporti M, Esterbauer H. Identification of 4-hydroxynonenal as a cytotoxic product originating from the peroxidation of liver microsomal lipids. Biochim Biophys Acta 1980;620:281–96. https://doi.org/10.1016/0005-2760(80)90209-X.

[31] Murphy RC. Mass spectrometry of phispholipids: tables of molecular and product ions. Illuminati Press; 2002.

[32] Li M, Butka E, Wang X. Comprehensive quantification of triacylglycerols in soybean seeds by electrospray ionization mass spectrometry with multiple neutral loss scans. Sci Rep 2014;4:6581. https://doi.org/10.1038/srep06581.

[33] Nováková L, Lopéz SA, Solichová D, Šatínský D, Kulichová B, Horna A, et al. Comparison of UV and charged aerosol detection approach in pharmaceutical analysis of statins. Talanta 2009;78:834–9. https://doi.org/10.1016/j.talanta.2008.12.057.

[34] Carlos G, Comiran E, de Oliveira MH, Limberger RP, Bergold AM, Fröehlich PE. Development, validation and comparison of two stability-indicating RP-LC methods using charged aerosol and UV detectors for analysis of lisdex-amfetamine dimesylate in capsules. Arab J Chem 2016;9:S1905–14. https://doi.org/10.1016/j.arabjc.2015.06.001.

[35] Balet A, Cardona D, Jane S, Molins-Pujol AM, Quesada JLS, Gich I, et al. Effects of multilayered bags vs ethylvinyl-acetate bags on oxidation of parenteral nutrition. J Parenter Enter Nutr 2004;28:85–91.

[36] Hmida D, Abderrabba M, Tchapla A, Heron S, Moussa F. Comparison of iso-eluotropic mobile phases at different temperatures for the separation of tri-acylglycerols in Non-Aqueous Reversed Phase Liquid Chromatography. J Chromatogr B Anal Technol Biomed Life Sci 2015;990:45–51. https://doi.org/10.1016/j.jchromb.2015.03.007.

[37] Heidorn M, Liu X, Tracy M, Pohl C. Use of C30 as a general-purpose stationary phase for a broad range of applications. Thermo Appl Note 2014:1–4.

[38] Lísa M, Holčapek M, Sovová H. Comparison of various types of stationary phases in non-aqueous reversed-phase high-performance liquid chromatography-mass spectrometry of glycerolipids in blackcurrant oil and its enzymatic hydrolysis mixture. J Chromatogr A 2009;1216:8371–8. https://doi.org/10.1016/j.chroma.2009.09.060.

[39] Fibigr J, Satíns D, Solich P. A UHPLC method for the rapid separation and quantification of phytosterols using tandem UV/Charged aerosol detection – A comparison of both detection techniques. J Pharm Biomed Anal J Pharm Biomed 2017;140:274–80. https://doi.org/10.1016/j.jpba.2017.03.057.

Appendix 2: Statistical Analysis Data

For all statistical analysis:
Group 1 = Room temperature syringes
Group 2 = Room temperature PN bags
Group 3 = Room temperature vials
Group 4 = Fridge temperature syringes
Group 5 = Fridge temperature PN bags
Group 6 = Fridge temperature vials

Intralipid® light protected containers. Peak 1 (C18:2/18:2/18:20)

ANOVA

data

	Sum of Squares	df	Mean Square	F	Sig.
Between Groups	1581.723	5	316.345	45.340	.000
Within Groups	83.726	12	6.977		
Total	1665.449	17			

Dependent Variable: data

	(I) group	(J) group	Mean Difference (I-J)	Std. Error	Sig.	95% Confidence Interval	
						Lower Bound	Upper Bound
Tukey HSD	1.00	2.00	-2.61947	2.15672	.822	-9.8637	4.6248
		3.00	15.99782*	2.15672	.000	8.7536	23.2421
		4.00	.64976	2.15672	1.000	-6.5945	7.8940
		5.00	.14625	2.15672	1.000	-7.0980	7.3905
		6.00	21.94051*	2.15672	.000	14.6962	29.1848
	2.00	1.00	2.61947	2.15672	.822	-4.6248	9.8637
		3.00	18.61730*	2.15672	.000	11.3730	25.8616
		4.00	3.26923	2.15672	.662	-3.9750	10.5135
		5.00	2.76572	2.15672	.789	-4.4785	10.0100
		6.00	24.55998*	2.15672	.000	17.3157	31.8043
	3.00	1.00	-15.99782*	2.15672	.000	-23.2421	-8.7536
		2.00	-18.61730*	2.15672	.000	-25.8616	-11.3730
		4.00	-15.34807*	2.15672	.000	-22.5923	-8.1038
		5.00	-15.85158*	2.15672	.000	-23.0958	-8.6073
		6.00	5.94269	2.15672	.134	-1.3016	13.1870
	4.00	1.00	-.64976	2.15672	1.000	-7.8940	6.5945
		2.00	-3.26923	2.15672	.662	-10.5135	3.9750

395

		3.00	15.34807*	2.15672	.000	8.1038	22.5923
		5.00	-.50351	2.15672	1.000	-7.7478	6.7408
		6.00	21.29076*	2.15672	.000	14.0465	28.5350
	5.00	1.00	-.14625	2.15672	1.000	-7.3905	7.0980
		2.00	-2.76572	2.15672	.789	-10.0100	4.4785
		3.00	15.85158*	2.15672	.000	8.6073	23.0958
		4.00	.50351	2.15672	1.000	-6.7408	7.7478
		6.00	21.79427*	2.15672	.000	14.5500	29.0385
	6.00	1.00	-21.94051*	2.15672	.000	-29.1848	-14.6962
		2.00	-24.55998*	2.15672	.000	-31.8043	-17.3157
		3.00	-5.94269	2.15672	.134	-13.1870	1.3016
		4.00	-21.29076*	2.15672	.000	-28.5350	-14.0465
		5.00	-21.79427*	2.15672	.000	-29.0385	-14.5500

Peak 2

ANOVA

	Sum of Squares	df	Mean Square	F	Sig.
Between Groups	2024.317	5	404.863	29.936	.000
Within Groups	162.293	12	13.524		
Total	2186.610	17			

Post Hoc Tests

Dependent Variable:

Tukey HSD

		Mean Difference			95% Confidence Interval	
(I) Peak 2	(J) Peak 2	(I-J)	Std. Error	Sig.	Lower Bound	Upper Bound
1.00	2.00	11.96103*	3.00271	.017	1.8752	22.0469
	3.00	23.75384*	3.00271	.000	13.6680	33.8397
	4.00	4.73452	3.00271	.627	-5.3514	14.8204
	5.00	12.84170*	3.00271	.011	2.7558	22.9276
	6.00	31.09713*	3.00271	.000	21.0113	41.1830

2.00	1.00	-11.96103*	3.00271	.017	-22.0469	-1.8752
	3.00	11.79280*	3.00271	.019	1.7069	21.8787
	4.00	-7.22651	3.00271	.228	-17.3124	2.8594
	5.00	.88067	3.00271	1.000	-9.2052	10.9665
	6.00	19.13610*	3.00271	.000	9.0502	29.2220
3.00	1.00	-23.75384*	3.00271	.000	-33.8397	-13.6680
	2.00	-11.79280*	3.00271	.019	-21.8787	-1.7069
	4.00	-19.01931*	3.00271	.000	-29.1052	-8.9334
	5.00	-10.91213*	3.00271	.031	-20.9980	-.8263
	6.00	7.34330	3.00271	.215	-2.7426	17.4292
4.00	1.00	-4.73452	3.00271	.627	-14.8204	5.3514
	2.00	7.22651	3.00271	.228	-2.8594	17.3124
	3.00	19.01931*	3.00271	.000	8.9334	29.1052
	5.00	8.10718	3.00271	.146	-1.9787	18.1931
	6.00	26.36261*	3.00271	.000	16.2767	36.4485
5.00	1.00	-12.84170*	3.00271	.011	-22.9276	-2.7558
	2.00	-.88067	3.00271	1.000	-10.9665	9.2052
	3.00	10.91213*	3.00271	.031	.8263	20.9980
	4.00	-8.10718	3.00271	.146	-18.1931	1.9787
	6.00	18.25543*	3.00271	.001	8.1696	28.3413
6.00	1.00	-31.09713*	3.00271	.000	-41.1830	-21.0113
	2.00	-19.13610*	3.00271	.000	-29.2220	-9.0502
	3.00	-7.34330	3.00271	.215	-17.4292	2.7426
	4.00	-26.36261*	3.00271	.000	-36.4485	-16.2767
	5.00	-18.25543*	3.00271	.001	-28.3413	-8.1696

*. The mean difference is significant at the 0.05 level.

Peak 3

ANOVA

	Sum of Squares	df	Mean Square	F	Sig.
Between Groups	808.313	5	161.663	7.888	.002
Within Groups	245.944	12	20.495		
Total	1054.257	17			

Post Hoc Tests

Dependent Variable:

Tukey HSD

(I) Peak 3	(J) Peak 3	Mean Difference (I-J)	Std. Error	Sig.	95% Confidence Interval	
					Lower Bound	Upper Bound
1.00	2.00	5.26978	3.69642	.713	-7.1462	17.6858
	3.00	11.05002	3.69642	.092	-1.3660	23.4660
	4.00	10.10323	3.69642	.139	-2.3128	22.5192
	5.00	4.89331	3.69642	.768	-7.5227	17.3093
	6.00	21.35050*	3.69642	.001	8.9345	33.7665
2.00	1.00	-5.26978	3.69642	.713	-17.6858	7.1462
	3.00	5.78024	3.69642	.634	-6.6358	18.1962
	4.00	4.83345	3.69642	.776	-7.5825	17.2494
	5.00	-.37648	3.69642	1.000	-12.7925	12.0395
	6.00	16.08072*	3.69642	.009	3.6647	28.4967
3.00	1.00	-11.05002	3.69642	.092	-23.4660	1.3660
	2.00	-5.78024	3.69642	.634	-18.1962	6.6358
	4.00	-.94679	3.69642	1.000	-13.3628	11.4692
	5.00	-6.15672	3.69642	.576	-18.5727	6.2593
	6.00	10.30048	3.69642	.128	-2.1155	22.7165
4.00	1.00	-10.10323	3.69642	.139	-22.5192	2.3128
	2.00	-4.83345	3.69642	.776	-17.2494	7.5825
	3.00	.94679	3.69642	1.000	-11.4692	13.3628
	5.00	-5.20992	3.69642	.722	-17.6259	7.2061
	6.00	11.24727	3.69642	.084	-1.1687	23.6633
5.00	1.00	-4.89331	3.69642	.768	-17.3093	7.5227
	2.00	.37648	3.69642	1.000	-12.0395	12.7925
	3.00	6.15672	3.69642	.576	-6.2593	18.5727
	4.00	5.20992	3.69642	.722	-7.2061	17.6259
	6.00	16.45719*	3.69642	.008	4.0412	28.8732
6.00	1.00	-21.35050*	3.69642	.001	-33.7665	-8.9345
	2.00	-16.08072*	3.69642	.009	-28.4967	-3.6647
	3.00	-10.30048	3.69642	.128	-22.7165	2.1155
	4.00	-11.24727	3.69642	.084	-23.6633	1.1687
	5.00	-16.45719*	3.69642	.008	-28.8732	-4.0412

*. The mean difference is significant at the 0.05 level.

Peak 4
ANOVA

	Sum of Squares	df	Mean Square	F	Sig.
Between Groups	1563.901	5	312.780	11.875	.000
Within Groups	316.074	12	26.339		
Total	1879.974	17			

Post Hoc Tests

Dependent Variable:

Tukey HSD

(I) Peak 4	(J) Peak 4	Mean Difference (I-J)	Std. Error	Sig.	95% Confidence Interval	
					Lower Bound	Upper Bound
1.00	2.00	6.28486	4.19042	.671	-7.7904	20.3602
	3.00	15.29437*	4.19042	.031	1.2191	29.3697
	4.00	15.19651*	4.19042	.032	1.1212	29.2718
	5.00	1.88766	4.19042	.997	-12.1876	15.9630
	6.00	27.09318*	4.19042	.000	13.0179	41.1685
2.00	1.00	-6.28486	4.19042	.671	-20.3602	7.7904
	3.00	9.00951	4.19042	.326	-5.0658	23.0848
	4.00	8.91166	4.19042	.336	-5.1636	22.9870
	5.00	-4.39720	4.19042	.892	-18.4725	9.6781
	6.00	20.80832*	4.19042	.003	6.7330	34.8836
3.00	1.00	-15.29437*	4.19042	.031	-29.3697	-1.2191
	2.00	-9.00951	4.19042	.326	-23.0848	5.0658
	4.00	-.09786	4.19042	1.000	-14.1732	13.9774
	5.00	-13.40671	4.19042	.065	-27.4820	.6686
	6.00	11.79881	4.19042	.122	-2.2765	25.8741
4.00	1.00	-15.19651*	4.19042	.032	-29.2718	-1.1212
	2.00	-8.91166	4.19042	.336	-22.9870	5.1636
	3.00	.09786	4.19042	1.000	-13.9774	14.1732
	5.00	-13.30886	4.19042	.068	-27.3842	.7664
	6.00	11.89667	4.19042	.117	-2.1786	25.9720
5.00	1.00	-1.88766	4.19042	.997	-15.9630	12.1876
	2.00	4.39720	4.19042	.892	-9.6781	18.4725
	3.00	13.40671	4.19042	.065	-.6686	27.4820

	4.00	13.30886	4.19042	.068	-.7664	27.3842
	6.00	25.20552*	4.19042	.001	11.1302	39.2808
6.00	1.00	-27.09318*	4.19042	.000	-41.1685	-13.0179
	2.00	-20.80832*	4.19042	.003	-34.8836	-6.7330
	3.00	-11.79881	4.19042	.122	-25.8741	2.2765
	4.00	-11.89667	4.19042	.117	-25.9720	2.1786
	5.00	-25.20552*	4.19042	.001	-39.2808	-11.1302

The mean difference is significant at the 0.05 level.

Peak 5
ANOVA

	Sum of Squares	df	Mean Square	F	Sig.
Between Groups	842.524	5	168.505	7.651	.003
Within Groups	242.268	11	22.024		
Total	1084.792	16			

Post Hoc Tests

Dependent Variable:

Tukey HSD

(I) Peak 5	(J) Peak 5	Mean Difference (I-J)	Std. Error	Sig.	95% Confidence Interval	
					Lower Bound	Upper Bound
1.00	2.00	-6.16841	4.28412	.705	-20.7788	8.4420
	3.00	3.89072	4.28412	.936	-10.7196	18.5011
	4.00	-2.24418	4.28412	.994	-16.8545	12.3662
	5.00	-3.67204	4.28412	.949	-18.2824	10.9383
	6.00	14.71895*	4.28412	.048	.1086	29.3293
2.00	1.00	6.16841	4.28412	.705	-8.4420	20.7788
	3.00	10.05913	3.83183	.170	-3.0088	23.1270
	4.00	3.92424	3.83183	.900	-9.1437	16.9921
	5.00	2.49638	3.83183	.984	-10.5715	15.5643
	6.00	20.88737*	3.83183	.002	7.8195	33.9553
3.00	1.00	-3.89072	4.28412	.936	-18.5011	10.7196
	2.00	-10.05913	3.83183	.170	-23.1270	3.0088
	4.00	-6.13490	3.83183	.614	-19.2028	6.9330
	5.00	-7.56276	3.83183	.412	-20.6307	5.5052
	6.00	10.82823	3.83183	.126	-2.2397	23.8961
4.00	1.00	2.24418	4.28412	.994	-12.3662	16.8545
	2.00	-3.92424	3.83183	.900	-16.9921	9.1437
	3.00	6.13490	3.83183	.614	-6.9330	19.2028
	5.00	-1.42786	3.83183	.999	-14.4958	11.6400
	6.00	16.96313*	3.83183	.010	3.8952	30.0310
5.00	1.00	3.67204	4.28412	.949	-10.9383	18.2824
	2.00	-2.49638	3.83183	.984	-15.5643	10.5715
	3.00	7.56276	3.83183	.412	-5.5052	20.6307
	4.00	1.42786	3.83183	.999	-11.6400	14.4958
	6.00	18.39099*	3.83183	.006	5.3231	31.4589
6.00	1.00	-14.71895*	4.28412	.048	-29.3293	-.1086
	2.00	-20.88737*	3.83183	.002	-33.9553	-7.8195
	3.00	-10.82823	3.83183	.126	-23.8961	2.2397

Peak 6
ANOVA

	Sum of Squares	df	Mean Square	F	Sig.
Between Groups	2064.022	5	412.804	15.261	.000
Within Groups	324.593	12	27.049		
Total	2388.615	17			

Post Hoc Tests

Dependent Variable:

Tukey HSD

(I) Peak 6	(J) Peak 6	Mean Difference (I-J)	Std. Error	Sig.	95% Confidence Interval Lower Bound	95% Confidence Interval Upper Bound
1.00	2.00	.97716	4.24652	1.000	-13.2866	15.2409
	3.00	20.27470*	4.24652	.005	6.0110	34.5384
	4.00	9.91372	4.24652	.253	-4.3500	24.1775
	5.00	5.58095	4.24652	.773	-8.6828	19.8447
	6.00	29.70878*	4.24652	.000	15.4451	43.9725
2.00	1.00	-.97716	4.24652	1.000	-15.2409	13.2866
	3.00	19.29753*	4.24652	.007	5.0338	33.5613
	4.00	8.93656	4.24652	.346	-5.3272	23.2003
	5.00	4.60379	4.24652	.879	-9.6599	18.8675
	6.00	28.73162*	4.24652	.000	14.4679	42.9954
3.00	1.00	-20.27470*	4.24652	.005	-34.5384	-6.0110
	2.00	-19.29753*	4.24652	.007	-33.5613	-5.0338
	4.00	-10.36098	4.24652	.217	-24.6247	3.9028
	5.00	-14.69375*	4.24652	.042	-28.9575	-.4300
	6.00	9.43409	4.24652	.296	-4.8296	23.6978
4.00	1.00	-9.91372	4.24652	.253	-24.1775	4.3500
	2.00	-8.93656	4.24652	.346	-23.2003	5.3272
	3.00	10.36098	4.24652	.217	-3.9028	24.6247
	5.00	-4.33277	4.24652	.902	-18.5965	9.9310
	6.00	19.79506*	4.24652	.006	5.5313	34.0588
5.00	1.00	-5.58095	4.24652	.773	-19.8447	8.6828
	2.00	-4.60379	4.24652	.879	-18.8675	9.6599
	3.00	14.69375*	4.24652	.042	.4300	28.9575
	4.00	4.33277	4.24652	.902	-9.9310	18.5965
	6.00	24.12784*	4.24652	.001	9.8641	38.3916

6.00	1.00	-29.70878*	4.24652	.000	-43.9725	-15.4451
	2.00	-28.73162*	4.24652	.000	-42.9954	-14.4679
	3.00	-9.43409	4.24652	.296	-23.6978	4.8296
	4.00	-19.79506*	4.24652	.006	-34.0588	-5.5313
	5.00	-24.12784*	4.24652	.001	-38.3916	-9.8641

*. The mean difference is significant at the 0.05 level.

Intralipid® light protected containers.
Peak 1 (C18:2/18:2/18:2)

ANOVA

data

	Sum of Squares	df	Mean Square	F	Sig.
Between Groups	1581.723	5	316.345	45.340	.000
Within Groups	83.726	12	6.977		
Total	1665.449	17			

Dependent Variable: data

	(I) group	(J) group	Mean Difference (I-J)	Std. Error	Sig.	95% Confidence Interval	
						Lower Bound	Upper Bound
Tukey HSD	1.00	2.00	-2.61947	2.15672	.822	-9.8637	4.6248
		3.00	15.99782*	2.15672	.000	8.7536	23.2421
		4.00	.64976	2.15672	1.000	-6.5945	7.8940
		5.00	.14625	2.15672	1.000	-7.0980	7.3905
		6.00	21.94051*	2.15672	.000	14.6962	29.1848
	2.00	1.00	2.61947	2.15672	.822	-4.6248	9.8637
		3.00	18.61730*	2.15672	.000	11.3730	25.8616
		4.00	3.26923	2.15672	.662	-3.9750	10.5135
		5.00	2.76572	2.15672	.789	-4.4785	10.0100
		6.00	24.55998*	2.15672	.000	17.3157	31.8043
	3.00	1.00	-15.99782*	2.15672	.000	-23.2421	-8.7536
		2.00	-18.61730*	2.15672	.000	-25.8616	-11.3730
		4.00	-15.34807*	2.15672	.000	-22.5923	-8.1038
		5.00	-15.85158*	2.15672	.000	-23.0958	-8.6073

		6.00	5.94269	2.15672	.134	-1.3016	13.1870
4.00	1.00		-.64976	2.15672	1.000	-7.8940	6.5945
	2.00		-3.26923	2.15672	.662	-10.5135	3.9750
	3.00		15.34807*	2.15672	.000	8.1038	22.5923
	5.00		-.50351	2.15672	1.000	-7.7478	6.7408
	6.00		21.29076*	2.15672	.000	14.0465	28.5350
5.00	1.00		-.14625	2.15672	1.000	-7.3905	7.0980
	2.00		-2.76572	2.15672	.789	-10.0100	4.4785
	3.00		15.85158*	2.15672	.000	8.6073	23.0958
	4.00		.50351	2.15672	1.000	-6.7408	7.7478
	6.00		21.79427*	2.15672	.000	14.5500	29.0385
6.00	1.00		-21.94051*	2.15672	.000	-29.1848	-14.6962
	2.00		-24.55998*	2.15672	.000	-31.8043	-17.3157
	3.00		-5.94269	2.15672	.134	-13.1870	1.3016
	4.00		-21.29076*	2.15672	.000	-28.5350	-14.0465
	5.00		-21.79427*	2.15672	.000	-29.0385	-14.5500

Peak 2

ANOVA

	Sum of Squares	df	Mean Square	F	Sig.
Between Groups	2024.317	5	404.863	29.936	.000
Within Groups	162.293	12	13.524		
Total	2186.610	17			

Post Hoc Tests

Dependent Variable:

Tukey HSD

(I) Peak 2	(J) Peak 2	Mean Difference (I-J)	Std. Error	Sig.	95% Confidence Interval	
					Lower Bound	Upper Bound
1.00	2.00	11.96103*	3.00271	.017	1.8752	22.0469
	3.00	23.75384*	3.00271	.000	13.6680	33.8397

	4.00	4.73452	3.00271	.627	-5.3514	14.8204
	5.00	12.84170*	3.00271	.011	2.7558	22.9276
	6.00	31.09713*	3.00271	.000	21.0113	41.1830
2.00	1.00	-11.96103*	3.00271	.017	-22.0469	-1.8752
	3.00	11.79280*	3.00271	.019	1.7069	21.8787
	4.00	-7.22651	3.00271	.228	-17.3124	2.8594
	5.00	.88067	3.00271	1.000	-9.2052	10.9665
	6.00	19.13610*	3.00271	.000	9.0502	29.2220
3.00	1.00	-23.75384*	3.00271	.000	-33.8397	-13.6680
	2.00	-11.79280*	3.00271	.019	-21.8787	-1.7069
	4.00	-19.01931*	3.00271	.000	-29.1052	-8.9334
	5.00	-10.91213*	3.00271	.031	-20.9980	-.8263
	6.00	7.34330	3.00271	.215	-2.7426	17.4292
4.00	1.00	-4.73452	3.00271	.627	-14.8204	5.3514
	2.00	7.22651	3.00271	.228	-2.8594	17.3124
	3.00	19.01931*	3.00271	.000	8.9334	29.1052
	5.00	8.10718	3.00271	.146	-1.9787	18.1931
	6.00	26.36261*	3.00271	.000	16.2767	36.4485
5.00	1.00	-12.84170*	3.00271	.011	-22.9276	-2.7558
	2.00	-.88067	3.00271	1.000	-10.9665	9.2052
	3.00	10.91213*	3.00271	.031	.8263	20.9980
	4.00	-8.10718	3.00271	.146	-18.1931	1.9787
	6.00	18.25543*	3.00271	.001	8.1696	28.3413
6.00	1.00	-31.09713*	3.00271	.000	-41.1830	-21.0113
	2.00	-19.13610*	3.00271	.000	-29.2220	-9.0502
	3.00	-7.34330	3.00271	.215	-17.4292	2.7426
	4.00	-26.36261*	3.00271	.000	-36.4485	-16.2767
	5.00	-18.25543*	3.00271	.001	-28.3413	-8.1696

*. The mean difference is significant at the 0.05 level.

Peak 3

ANOVA

	Sum of Squares	df	Mean Square	F	Sig.
Between Groups	808.313	5	161.663	7.888	.002
Within Groups	245.944	12	20.495		

		1054.257	17			
Total						

Post Hoc Tests

Dependent Variable:

Tukey HSD

(I) Peak 3	(J) Peak 3	Mean Difference (I-J)	Std. Error	Sig.	95% Confidence Interval Lower Bound	Upper Bound
1.00	2.00	5.26978	3.69642	.713	-7.1462	17.6858
	3.00	11.05002	3.69642	.092	-1.3660	23.4660
	4.00	10.10323	3.69642	.139	-2.3128	22.5192
	5.00	4.89331	3.69642	.768	-7.5227	17.3093
	6.00	21.35050[*]	3.69642	.001	8.9345	33.7665
2.00	1.00	-5.26978	3.69642	.713	-17.6858	7.1462
	3.00	5.78024	3.69642	.634	-6.6358	18.1962
	4.00	4.83345	3.69642	.776	-7.5825	17.2494
	5.00	-.37648	3.69642	1.000	-12.7925	12.0395
	6.00	16.08072[*]	3.69642	.009	3.6647	28.4967
3.00	1.00	-11.05002	3.69642	.092	-23.4660	1.3660
	2.00	-5.78024	3.69642	.634	-18.1962	6.6358
	4.00	-.94679	3.69642	1.000	-13.3628	11.4692
	5.00	-6.15672	3.69642	.576	-18.5727	6.2593
	6.00	10.30048	3.69642	.128	-2.1155	22.7165
4.00	1.00	-10.10323	3.69642	.139	-22.5192	2.3128
	2.00	-4.83345	3.69642	.776	-17.2494	7.5825
	3.00	.94679	3.69642	1.000	-11.4692	13.3628
	5.00	-5.20992	3.69642	.722	-17.6259	7.2061
	6.00	11.24727	3.69642	.084	-1.1687	23.6633
5.00	1.00	-4.89331	3.69642	.768	-17.3093	7.5227
	2.00	.37648	3.69642	1.000	-12.0395	12.7925
	3.00	6.15672	3.69642	.576	-6.2593	18.5727
	4.00	5.20992	3.69642	.722	-7.2061	17.6259
	6.00	16.45719[*]	3.69642	.008	4.0412	28.8732
6.00	1.00	-21.35050[*]	3.69642	.001	-33.7665	-8.9345
	2.00	-16.08072[*]	3.69642	.009	-28.4967	-3.6647
	3.00	-10.30048	3.69642	.128	-22.7165	2.1155
	4.00	-11.24727	3.69642	.084	-23.6633	1.1687

5.00	-16.45719*	3.69642	.008	-28.8732	-4.0412

*. The mean difference is significant at the 0.05 level.

Peak 4
ANOVA

	Sum of Squares	df	Mean Square	F	Sig.
Between Groups	1563.901	5	312.780	11.875	.000
Within Groups	316.074	12	26.339		
Total	1879.974	17			

Post Hoc Tests

Dependent Variable:

Tukey HSD

(I) Peak 4	(J) Peak 4	Mean Difference (I-J)	Std. Error	Sig.	95% Confidence Interval	
					Lower Bound	Upper Bound
1.00	2.00	6.28486	4.19042	.671	-7.7904	20.3602
	3.00	15.29437*	4.19042	.031	1.2191	29.3697
	4.00	15.19651*	4.19042	.032	1.1212	29.2718
	5.00	1.88766	4.19042	.997	-12.1876	15.9630
	6.00	27.09318*	4.19042	.000	13.0179	41.1685
2.00	1.00	-6.28486	4.19042	.671	-20.3602	7.7904
	3.00	9.00951	4.19042	.326	-5.0658	23.0848
	4.00	8.91166	4.19042	.336	-5.1636	22.9870
	5.00	-4.39720	4.19042	.892	-18.4725	9.6781
	6.00	20.80832*	4.19042	.003	6.7330	34.8836
3.00	1.00	-15.29437*	4.19042	.031	-29.3697	-1.2191
	2.00	-9.00951	4.19042	.326	-23.0848	5.0658
	4.00	-.09786	4.19042	1.000	-14.1732	13.9774
	5.00	-13.40671	4.19042	.065	-27.4820	.6686
	6.00	11.79881	4.19042	.122	-2.2765	25.8741
4.00	1.00	-15.19651*	4.19042	.032	-29.2718	-1.1212
	2.00	-8.91166	4.19042	.336	-22.9870	5.1636
	3.00	.09786	4.19042	1.000	-13.9774	14.1732
	5.00	-13.30886	4.19042	.068	-27.3842	.7664
	6.00	11.89667	4.19042	.117	-2.1786	25.9720

5.00	1.00	-1.88766	4.19042	.997	-15.9630	12.1876
	2.00	4.39720	4.19042	.892	-9.6781	18.4725
	3.00	13.40671	4.19042	.065	-.6686	27.4820
	4.00	13.30886	4.19042	.068	-.7664	27.3842
	6.00	25.20552*	4.19042	.001	11.1302	39.2808
6.00	1.00	-27.09318*	4.19042	.000	-41.1685	-13.0179
	2.00	-20.80832*	4.19042	.003	-34.8836	-6.7330
	3.00	-11.79881	4.19042	.122	-25.8741	2.2765
	4.00	-11.89667	4.19042	.117	-25.9720	2.1786
	5.00	-25.20552*	4.19042	.001	-39.2808	-11.1302

. The mean difference is significant at the 0.05 level.

Peak 5
ANOVA

	Sum of Squares	df	Mean Square	F	Sig.
Between Groups	842.524	5	168.505	7.651	.003
Within Groups	242.268	11	22.024		
Total	1084.792	16			

Post Hoc Tests

Dependent Variable:

Tukey HSD

(I) Peak 5	(J) Peak 5	Mean Difference (I-J)	Std. Error	Sig.	95% Confidence Interval	
					Lower Bound	Upper Bound
1.00	2.00	-6.16841	4.28412	.705	-20.7788	8.4420
	3.00	3.89072	4.28412	.936	-10.7196	18.5011
	4.00	-2.24418	4.28412	.994	-16.8545	12.3662
	5.00	-3.67204	4.28412	.949	-18.2824	10.9383
	6.00	14.71895*	4.28412	.048	.1086	29.3293
2.00	1.00	6.16841	4.28412	.705	-8.4420	20.7788
	3.00	10.05913	3.83183	.170	-3.0088	23.1270
	4.00	3.92424	3.83183	.900	-9.1437	16.9921
	5.00	2.49638	3.83183	.984	-10.5715	15.5643
	6.00	20.88737*	3.83183	.002	7.8195	33.9553
3.00	1.00	-3.89072	4.28412	.936	-18.5011	10.7196
	2.00	-10.05913	3.83183	.170	-23.1270	3.0088
	4.00	-6.13490	3.83183	.614	-19.2028	6.9330
	5.00	-7.56276	3.83183	.412	-20.6307	5.5052
	6.00	10.82823	3.83183	.126	-2.2397	23.8961
4.00	1.00	2.24418	4.28412	.994	-12.3662	16.8545
	2.00	-3.92424	3.83183	.900	-16.9921	9.1437
	3.00	6.13490	3.83183	.614	-6.9330	19.2028
	5.00	-1.42786	3.83183	.999	-14.4958	11.6400
	6.00	16.96313*	3.83183	.010	3.8952	30.0310
5.00	1.00	3.67204	4.28412	.949	-10.9383	18.2824
	2.00	-2.49638	3.83183	.984	-15.5643	10.5715
	3.00	7.56276	3.83183	.412	-5.5052	20.6307
	4.00	1.42786	3.83183	.999	-11.6400	14.4958
	6.00	18.39099*	3.83183	.006	5.3231	31.4589
6.00	1.00	-14.71895*	4.28412	.048	-29.3293	-.1086
	2.00	-20.88737*	3.83183	.002	-33.9553	-7.8195
	3.00	-10.82823	3.83183	.126	-23.8961	2.2397

Peak 6
ANOVA

	Sum of Squares	df	Mean Square	F	Sig.
Between Groups	2064.022	5	412.804	15.261	.000
Within Groups	324.593	12	27.049		
Total	2388.615	17			

Post Hoc Tests

Dependent Variable:

Tukey HSD

(I) Peak 6	(J) Peak 6	Mean Difference (I-J)	Std. Error	Sig.	95% Confidence Interval	
					Lower Bound	Upper Bound
1.00	2.00	.97716	4.24652	1.000	-13.2866	15.2409
	3.00	20.27470*	4.24652	.005	6.0110	34.5384
	4.00	9.91372	4.24652	.253	-4.3500	24.1775
	5.00	5.58095	4.24652	.773	-8.6828	19.8447
	6.00	29.70878*	4.24652	.000	15.4451	43.9725
2.00	1.00	-.97716	4.24652	1.000	-15.2409	13.2866
	3.00	19.29753*	4.24652	.007	5.0338	33.5613
	4.00	8.93656	4.24652	.346	-5.3272	23.2003
	5.00	4.60379	4.24652	.879	-9.6599	18.8675
	6.00	28.73162*	4.24652	.000	14.4679	42.9954
3.00	1.00	-20.27470*	4.24652	.005	-34.5384	-6.0110
	2.00	-19.29753*	4.24652	.007	-33.5613	-5.0338
	4.00	-10.36098	4.24652	.217	-24.6247	3.9028
	5.00	-14.69375*	4.24652	.042	-28.9575	-.4300
	6.00	9.43409	4.24652	.296	-4.8296	23.6978
4.00	1.00	-9.91372	4.24652	.253	-24.1775	4.3500
	2.00	-8.93656	4.24652	.346	-23.2003	5.3272
	3.00	10.36098	4.24652	.217	-3.9028	24.6247
	5.00	-4.33277	4.24652	.902	-18.5965	9.9310
	6.00	19.79506*	4.24652	.006	5.5313	34.0588
5.00	1.00	-5.58095	4.24652	.773	-19.8447	8.6828
	2.00	-4.60379	4.24652	.879	-18.8675	9.6599
	3.00	14.69375*	4.24652	.042	.4300	28.9575
	4.00	4.33277	4.24652	.902	-9.9310	18.5965
	6.00	24.12784*	4.24652	.001	9.8641	38.3916

6.00	1.00	-29.70878*	4.24652	.000	-43.9725	-15.4451
	2.00	-28.73162*	4.24652	.000	-42.9954	-14.4679
	3.00	-9.43409	4.24652	.296	-23.6978	4.8296
	4.00	-19.79506*	4.24652	.006	-34.0588	-5.5313
	5.00	-24.12784*	4.24652	.001	-38.3916	-9.8641

*. The mean difference is significant at the 0.05 level.

SMOFlipid Light Protected stats day 84

Peak 1

ANOVA

data

	Sum of Squares	df	Mean Square	F	Sig.
Between Groups	808.974	5	161.795	5.338	.008
Within Groups	363.723	12	30.310		
Total	1172.697	17			

Multiple Comparisons

Dependent Variable: data

Tukey HSD

(I) factor	(J) factor	Mean Difference (I-J)	Std. Error	Sig.	95% Confidence Interval	
					Lower Bound	Upper Bound
1.00	2.00	-16.54606*	4.49520	.029	-31.6451	-1.4470
	3.00	-6.22767	4.49520	.735	-21.3267	8.8714
	4.00	-3.38638	4.49520	.970	-18.4854	11.7126
	5.00	.33040	4.49520	1.000	-14.7686	15.4294
	6.00	4.56813	4.49520	.904	-10.5309	19.6672
2.00	1.00	16.54606*	4.49520	.029	1.4470	31.6451
	3.00	10.31839	4.49520	.267	-4.7806	25.4174
	4.00	13.15968	4.49520	.102	-1.9393	28.2587
	5.00	16.87646*	4.49520	.026	1.7774	31.9755

	6.00	21.11419*	4.49520	.005	6.0152	36.2132
3.00	1.00	6.22767	4.49520	.735	-8.8714	21.3267
	2.00	-10.31839	4.49520	.267	-25.4174	4.7806
	4.00	2.84130	4.49520	.986	-12.2577	17.9403
	5.00	6.55808	4.49520	.694	-8.5409	21.6571
	6.00	10.79580	4.49520	.229	-4.3032	25.8948
4.00	1.00	3.38638	4.49520	.970	-11.7126	18.4854
	2.00	-13.15968	4.49520	.102	-28.2587	1.9393
	3.00	-2.84130	4.49520	.986	-17.9403	12.2577
	5.00	3.71678	4.49520	.957	-11.3822	18.8158
	6.00	7.95451	4.49520	.517	-7.1445	23.0535
5.00	1.00	-.33040	4.49520	1.000	-15.4294	14.7686
	2.00	-16.87646*	4.49520	.026	-31.9755	-1.7774
	3.00	-6.55808	4.49520	.694	-21.6571	8.5409
	4.00	-3.71678	4.49520	.957	-18.8158	11.3822
	6.00	4.23773	4.49520	.927	-10.8613	19.3368
6.00	1.00	-4.56813	4.49520	.904	-19.6672	10.5309
	2.00	-21.11419*	4.49520	.005	-36.2132	-6.0152
	3.00	-10.79580	4.49520	.229	-25.8948	4.3032
	4.00	-7.95451	4.49520	.517	-23.0535	7.1445
	5.00	-4.23773	4.49520	.927	-19.3368	10.8613

*. The mean difference is significant at the 0.05 level.

Peak 2

ANOVA

data

	Sum of Squares	df	Mean Square	F	Sig.
Between Groups	530.356	5	106.071	2.284	.112
Within Groups	557.177	12	46.431		
Total	1087.533	17			

Multiple Comparisons

Dependent Variable: data

Tukey HSD

(I) factor	(J) factor	Mean Difference (I-J)	Std. Error	Sig.	95% Confidence Interval	
					Lower Bound	Upper Bound
1.00	2.00	-9.60232	5.56366	.541	-28.2902	9.0856
	3.00	-5.02127	5.56366	.939	-23.7092	13.6666
	4.00	1.31459	5.56366	1.000	-17.3733	20.0025
	5.00	5.18139	5.56366	.931	-13.5065	23.8693
	6.00	5.64119	5.56366	.905	-13.0467	24.3291
2.00	1.00	9.60232	5.56366	.541	-9.0856	28.2902
	3.00	4.58105	5.56366	.957	-14.1068	23.2689
	4.00	10.91691	5.56366	.414	-7.7710	29.6048
	5.00	14.78371	5.56366	.156	-3.9042	33.4716
	6.00	15.24351	5.56366	.137	-3.4444	33.9314
3.00	1.00	5.02127	5.56366	.939	-13.6666	23.7092
	2.00	-4.58105	5.56366	.957	-23.2689	14.1068
	4.00	6.33587	5.56366	.856	-12.3520	25.0237
	5.00	10.20266	5.56366	.482	-8.4852	28.8905
	6.00	10.66246	5.56366	.438	-8.0254	29.3503
4.00	1.00	-1.31459	5.56366	1.000	-20.0025	17.3733
	2.00	-10.91691	5.56366	.414	-29.6048	7.7710
	3.00	-6.33587	5.56366	.856	-25.0237	12.3520
	5.00	3.86680	5.56366	.979	-14.8211	22.5547
	6.00	4.32659	5.56366	.966	-14.3613	23.0145
5.00	1.00	-5.18139	5.56366	.931	-23.8693	13.5065
	2.00	-14.78371	5.56366	.156	-33.4716	3.9042
	3.00	-10.20266	5.56366	.482	-28.8905	8.4852
	4.00	-3.86680	5.56366	.979	-22.5547	14.8211
	6.00	.45980	5.56366	1.000	-18.2281	19.1477
6.00	1.00	-5.64119	5.56366	.905	-24.3291	13.0467
	2.00	-15.24351	5.56366	.137	-33.9314	3.4444
	3.00	-10.66246	5.56366	.438	-29.3503	8.0254
	4.00	-4.32659	5.56366	.966	-23.0145	14.3613
	5.00	-.45980	5.56366	1.000	-19.1477	18.2281

Peak 3

ANOVA

data

	Sum of Squares	df	Mean Square	F	Sig.
Between Groups	521.890	5	104.378	2.002	.151
Within Groups	625.725	12	52.144		
Total	1147.615	17			

Multiple Comparisons

Dependent Variable: data

Tukey HSD

(I) factor	(J) factor	Mean Difference (I-J)	Std. Error	Sig.	95% Confidence Interval	
					Lower Bound	Upper Bound
1.00	2.00	-8.59684	5.89597	.694	-28.4009	11.2073
	3.00	-1.80353	5.89597	1.000	-21.6076	18.0006
	4.00	-1.35164	5.89597	1.000	-21.1557	18.4525
	5.00	6.63823	5.89597	.862	-13.1659	26.4423
	6.00	7.18519	5.89597	.820	-12.6189	26.9893
2.00	1.00	8.59684	5.89597	.694	-11.2073	28.4009
	3.00	6.79331	5.89597	.850	-13.0108	26.5974
	4.00	7.24521	5.89597	.815	-12.5589	27.0493
	5.00	15.23508	5.89597	.175	-4.5690	35.0392
	6.00	15.78203	5.89597	.152	-4.0221	35.5861
3.00	1.00	1.80353	5.89597	1.000	-18.0006	21.6076
	2.00	-6.79331	5.89597	.850	-26.5974	13.0108
	4.00	.45190	5.89597	1.000	-19.3522	20.2560
	5.00	8.44176	5.89597	.709	-11.3623	28.2459
	6.00	8.98872	5.89597	.657	-10.8154	28.7928
4.00	1.00	1.35164	5.89597	1.000	-18.4525	21.1557
	2.00	-7.24521	5.89597	.815	-27.0493	12.5589
	3.00	-.45190	5.89597	1.000	-20.2560	19.3522
	5.00	7.98987	5.89597	.751	-11.8142	27.7940
	6.00	8.53682	5.89597	.700	-11.2673	28.3409
5.00	1.00	-6.63823	5.89597	.862	-26.4423	13.1659

	2.00	-15.23508	5.89597	.175	-35.0392	4.5690
	3.00	-8.44176	5.89597	.709	-28.2459	11.3623
	4.00	-7.98987	5.89597	.751	-27.7940	11.8142
	6.00	.54696	5.89597	1.000	-19.2571	20.3511
6.00	1.00	-7.18519	5.89597	.820	-26.9893	12.6189
	2.00	-15.78203	5.89597	.152	-35.5861	4.0221
	3.00	-8.98872	5.89597	.657	-28.7928	10.8154
	4.00	-8.53682	5.89597	.700	-28.3409	11.2673
	5.00	-.54696	5.89597	1.000	-20.3511	19.2571

Peak 4

ANOVA

data

	Sum of Squares	df	Mean Square	F	Sig.
Between Groups	1856.172	5	371.234	10.120	.001
Within Groups	440.220	12	36.685		
Total	2296.392	17			

Multiple Comparisons

Dependent Variable: data

Tukey HSD

(I) factor	(J) factor	Mean Difference (I-J)	Std. Error	Sig.	95% Confidence Interval	
					Lower Bound	Upper Bound
1.00	2.00	-24.53633*	4.94537	.003	-41.1474	-7.9252
	3.00	-8.65009	4.94537	.528	-25.2612	7.9610
	4.00	1.59302	4.94537	.999	-15.0181	18.2041
	5.00	-11.18614	4.94537	.280	-27.7972	5.4250
	6.00	6.14996	4.94537	.808	-10.4611	22.7611
2.00	1.00	24.53633*	4.94537	.003	7.9252	41.1474
	3.00	15.88624	4.94537	.064	-.7249	32.4973
	4.00	26.12935*	4.94537	.002	9.5182	42.7405
	5.00	13.35019	4.94537	.146	-3.2609	29.9613

	6.00	30.68629[*]	4.94537	.001	14.0752	47.2974
3.00	1.00	8.65009	4.94537	.528	-7.9610	25.2612
	2.00	-15.88624	4.94537	.064	-32.4973	.7249
	4.00	10.24311	4.94537	.361	-6.3680	26.8542
	5.00	-2.53605	4.94537	.995	-19.1472	14.0751
	6.00	14.80005	4.94537	.092	-1.8111	31.4112
4.00	1.00	-1.59302	4.94537	.999	-18.2041	15.0181
	2.00	-26.12935[*]	4.94537	.002	-42.7405	-9.5182
	3.00	-10.24311	4.94537	.361	-26.8542	6.3680
	5.00	-12.77916	4.94537	.175	-29.3903	3.8319
	6.00	4.55694	4.94537	.933	-12.0542	21.1680
5.00	1.00	11.18614	4.94537	.280	-5.4250	27.7972
	2.00	-13.35019	4.94537	.146	-29.9613	3.2609
	3.00	2.53605	4.94537	.995	-14.0751	19.1472
	4.00	12.77916	4.94537	.175	-3.8319	29.3903
	6.00	17.33610[*]	4.94537	.039	.7250	33.9472
6.00	1.00	-6.14996	4.94537	.808	-22.7611	10.4611
	2.00	-30.68629[*]	4.94537	.001	-47.2974	-14.0752
	3.00	-14.80005	4.94537	.092	-31.4112	1.8111
	4.00	-4.55694	4.94537	.933	-21.1680	12.0542
	5.00	-17.33610[*]	4.94537	.039	-33.9472	-.7250

*. The mean difference is significant at the 0.05 level.

Peak 5

ANOVA

data

	Sum of Squares	df	Mean Square	F	Sig.
Between Groups	802.503	5	160.501	5.053	.010
Within Groups	381.192	12	31.766		
Total	1183.694	17			

Multiple Comparisons

Dependent Variable: data

Tukey HSD

(I) factor	(J) factor	Mean Difference (I-J)	Std. Error	Sig.	95% Confidence Interval Lower Bound	95% Confidence Interval Upper Bound
1.00	2.00	-13.31572	4.60188	.108	-28.7731	2.1416
	3.00	-5.08835	4.60188	.870	-20.5457	10.3690
	4.00	-3.32274	4.60188	.975	-18.7801	12.1346
	5.00	1.58196	4.60188	.999	-13.8754	17.0393
	6.00	8.55297	4.60188	.468	-6.9044	24.0103
2.00	1.00	13.31572	4.60188	.108	-2.1416	28.7731
	3.00	8.22737	4.60188	.507	-7.2300	23.6847
	4.00	9.99298	4.60188	.317	-5.4644	25.4503
	5.00	14.89768	4.60188	.061	-.5597	30.3550
	6.00	21.86869*	4.60188	.005	6.4113	37.3260
3.00	1.00	5.08835	4.60188	.870	-10.3690	20.5457
	2.00	-8.22737	4.60188	.507	-23.6847	7.2300
	4.00	1.76561	4.60188	.999	-13.6917	17.2230
	5.00	6.67031	4.60188	.699	-8.7870	22.1277
	6.00	13.64131	4.60188	.096	-1.8160	29.0987
4.00	1.00	3.32274	4.60188	.975	-12.1346	18.7801
	2.00	-9.99298	4.60188	.317	-25.4503	5.4644
	3.00	-1.76561	4.60188	.999	-17.2230	13.6917
	5.00	4.90470	4.60188	.886	-10.5527	20.3621
	6.00	11.87571	4.60188	.176	-3.5816	27.3331
5.00	1.00	-1.58196	4.60188	.999	-17.0393	13.8754
	2.00	-14.89768	4.60188	.061	-30.3550	.5597
	3.00	-6.67031	4.60188	.699	-22.1277	8.7870
	4.00	-4.90470	4.60188	.886	-20.3621	10.5527
	6.00	6.97101	4.60188	.662	-8.4863	22.4284
6.00	1.00	-8.55297	4.60188	.468	-24.0103	6.9044
	2.00	-21.86869*	4.60188	.005	-37.3260	-6.4113
	3.00	-13.64131	4.60188	.096	-29.0987	1.8160
	4.00	-11.87571	4.60188	.176	-27.3331	3.5816
	5.00	-6.97101	4.60188	.662	-22.4284	8.4863

*. The mean difference is significant at the 0.05 level.

Peak 6

ANOVA

data

	Sum of Squares	df	Mean Square	F	Sig.
Between Groups	1042.843	5	208.569	7.407	.002
Within Groups	337.878	12	28.157		
Total	1380.722	17			

Multiple Comparisons

Dependent Variable: data

Tukey HSD

(I) factor	(J) factor	Mean Difference (I-J)	Std. Error	Sig.	95% Confidence Interval Lower Bound	95% Confidence Interval Upper Bound
1.00	2.00	.91972	4.33255	1.000	-13.6330	15.4724
	3.00	-3.83048	4.33255	.943	-18.3832	10.7222
	4.00	.52397	4.33255	1.000	-14.0287	15.0767
	5.00	17.73514*	4.33255	.014	3.1824	32.2878
	6.00	11.86061	4.33255	.138	-2.6921	26.4133
2.00	1.00	-.91972	4.33255	1.000	-15.4724	13.6330
	3.00	-4.75020	4.33255	.874	-19.3029	9.8025
	4.00	-.39575	4.33255	1.000	-14.9485	14.1570
	5.00	16.81542*	4.33255	.021	2.2627	31.3681
	6.00	10.94089	4.33255	.191	-3.6118	25.4936
3.00	1.00	3.83048	4.33255	.943	-10.7222	18.3832
	2.00	4.75020	4.33255	.874	-9.8025	19.3029
	4.00	4.35445	4.33255	.908	-10.1983	18.9072
	5.00	21.56563*	4.33255	.003	7.0129	36.1183
	6.00	15.69110*	4.33255	.032	1.1384	30.2438
4.00	1.00	-.52397	4.33255	1.000	-15.0767	14.0287
	2.00	.39575	4.33255	1.000	-14.1570	14.9485
	3.00	-4.35445	4.33255	.908	-18.9072	10.1983
	5.00	17.21117*	4.33255	.018	2.6585	31.7639
	6.00	11.33664	4.33255	.166	-3.2161	25.8893
5.00	1.00	-17.73514*	4.33255	.014	-32.2878	-3.1824

	2.00	-16.81542*	4.33255	.021	-31.3681	-2.2627
	3.00	-21.56563*	4.33255	.003	-36.1183	-7.0129
	4.00	-17.21117*	4.33255	.018	-31.7639	-2.6585
	6.00	-5.87453	4.33255	.751	-20.4272	8.6782
6.00	1.00	-11.86061	4.33255	.138	-26.4133	2.6921
	2.00	-10.94089	4.33255	.191	-25.4936	3.6118
	3.00	-15.69110*	4.33255	.032	-30.2438	-1.1384
	4.00	-11.33664	4.33255	.166	-25.8893	3.2161
	5.00	5.87453	4.33255	.751	-8.6782	20.4272

*. The mean difference is significant at the 0.05 level.

Peak 7

ANOVA

data

	Sum of Squares	Df	Mean Square	F	Sig.
Between Groups	1768.098	5	353.620	6.612	.004
Within Groups	641.760	12	53.480		
Total	2409.857	17			

Multiple Comparisons

Dependent Variable: data

Tukey HSD

		Mean Difference			95% Confidence Interval	
(I) factor	(J) factor	(I-J)	Std. Error	Sig.	Lower Bound	Upper Bound
1.00	2.00	2.71994	5.97104	.997	-17.3363	22.7762
	3.00	-20.66453*	5.97104	.042	-40.7208	-.6083
	4.00	-6.53251	5.97104	.875	-26.5888	13.5237
	5.00	11.90738	5.97104	.398	-8.1489	31.9636
	6.00	-4.09578	5.97104	.980	-24.1520	15.9605
2.00	1.00	-2.71994	5.97104	.997	-22.7762	17.3363
	3.00	-23.38447*	5.97104	.020	-43.4407	-3.3282
	4.00	-9.25245	5.97104	.642	-29.3087	10.8038
	5.00	9.18744	5.97104	.649	-10.8688	29.2437
	6.00	-6.81572	5.97104	.855	-26.8720	13.2405
3.00	1.00	20.66453*	5.97104	.042	.6083	40.7208
	2.00	23.38447*	5.97104	.020	3.3282	43.4407

	4.00	14.13202	5.97104	.241	-5.9242	34.1883
	5.00	32.57191*	5.97104	.002	12.5157	52.6282
	6.00	16.56875	5.97104	.130	-3.4875	36.6250
4.00	1.00	6.53251	5.97104	.875	-13.5237	26.5888
	2.00	9.25245	5.97104	.642	-10.8038	29.3087
	3.00	-14.13202	5.97104	.241	-34.1883	5.9242
	5.00	18.43989	5.97104	.078	-1.6164	38.4961
	6.00	2.43673	5.97104	.998	-17.6195	22.4930
5.00	1.00	-11.90738	5.97104	.398	-31.9636	8.1489
	2.00	-9.18744	5.97104	.649	-29.2437	10.8688
	3.00	-32.57191*	5.97104	.002	-52.6282	-12.5157
	4.00	-18.43989	5.97104	.078	-38.4961	1.6164
	6.00	-16.00317	5.97104	.151	-36.0594	4.0531
6.00	1.00	4.09578	5.97104	.980	-15.9605	24.1520
	2.00	6.81572	5.97104	.855	-13.2405	26.8720
	3.00	-16.56875	5.97104	.130	-36.6250	3.4875
	4.00	-2.43673	5.97104	.998	-22.4930	17.6195
	5.00	16.00317	5.97104	.151	-4.0531	36.0594

*. The mean difference is significant at the 0.05 level.

Peak 8

ANOVA

data

	Sum of Squares	df	Mean Square	F	Sig.
Between Groups	6556.672	5	1311.334	67.623	.000
Within Groups	232.703	12	19.392		
Total	6789.375	17			

Multiple Comparisons

Dependent Variable: data

Tukey HSD

		Mean Difference			95% Confidence Interval	
(I) factor	(J) factor	(I-J)	Std. Error	Sig.	Lower Bound	Upper Bound
1.00	2.00	-38.09953*	3.59555	.000	-50.1767	-26.0224
	3.00	-.02888	3.59555	1.000	-12.1060	12.0483
	4.00	3.61324	3.59555	.908	-8.4639	15.6904

	5.00	-30.76121*	3.59555	.000	-42.8384	-18.6841
	6.00	14.37192*	3.59555	.017	2.2948	26.4491
2.00	1.00	38.09953*	3.59555	.000	26.0224	50.1767
	3.00	38.07065*	3.59555	.000	25.9935	50.1478
	4.00	41.71277*	3.59555	.000	29.6356	53.7899
	5.00	7.33832	3.59555	.376	-4.7388	19.4155
	6.00	52.47145*	3.59555	.000	40.3943	64.5486
3.00	1.00	.02888	3.59555	1.000	-12.0483	12.1060
	2.00	-38.07065*	3.59555	.000	-50.1478	-25.9935
	4.00	3.64212	3.59555	.905	-8.4350	15.7193
	5.00	-30.73233*	3.59555	.000	-42.8095	-18.6552
	6.00	14.40080*	3.59555	.017	2.3236	26.4780
4.00	1.00	-3.61324	3.59555	.908	-15.6904	8.4639
	2.00	-41.71277*	3.59555	.000	-53.7899	-29.6356
	3.00	-3.64212	3.59555	.905	-15.7193	8.4350
	5.00	-34.37445*	3.59555	.000	-46.4516	-22.2973
	6.00	10.75868	3.59555	.092	-1.3185	22.8358
5.00	1.00	30.76121*	3.59555	.000	18.6841	42.8384
	2.00	-7.33832	3.59555	.376	-19.4155	4.7388
	3.00	30.73233*	3.59555	.000	18.6552	42.8095
	4.00	34.37445*	3.59555	.000	22.2973	46.4516
	6.00	45.13313*	3.59555	.000	33.0560	57.2103
6.00	1.00	-14.37192*	3.59555	.017	-26.4491	-2.2948
	2.00	-52.47145*	3.59555	.000	-64.5486	-40.3943
	3.00	-14.40080*	3.59555	.017	-26.4780	-2.3236
	4.00	-10.75868	3.59555	.092	-22.8358	1.3185
	5.00	-45.13313*	3.59555	.000	-57.2103	-33.0560

*. The mean difference is significant at the 0.05 level.

Peak 9

ANOVA

data

	Sum of Squares	df	Mean Square	F	Sig.
Between Groups	2144.027	5	428.805	45.584	.000
Within Groups	112.884	12	9.407		
Total	2256.910	17			

421

Multiple Comparisons

Dependent Variable: data

Tukey HSD

(I) factor	(J) factor	Mean Difference (I-J)	Std. Error	Sig.	95% Confidence Interval Lower Bound	95% Confidence Interval Upper Bound
1.00	2.00	-21.11967*	2.50426	.000	-29.5313	-12.7081
	3.00	-2.86925	2.50426	.853	-11.2809	5.5424
	4.00	-3.21955	2.50426	.787	-11.6312	5.1921
	5.00	-10.04204*	2.50426	.017	-18.4537	-1.6304
	6.00	15.17858*	2.50426	.001	6.7670	23.5902
2.00	1.00	21.11967*	2.50426	.000	12.7081	29.5313
	3.00	18.25042*	2.50426	.000	9.8388	26.6620
	4.00	17.90012*	2.50426	.000	9.4885	26.3117
	5.00	11.07763*	2.50426	.008	2.6660	19.4892
	6.00	36.29825*	2.50426	.000	27.8866	44.7099
3.00	1.00	2.86925	2.50426	.853	-5.5424	11.2809
	2.00	-18.25042*	2.50426	.000	-26.6620	-9.8388
	4.00	-.35030	2.50426	1.000	-8.7619	8.0613
	5.00	-7.17279	2.50426	.113	-15.5844	1.2388
	6.00	18.04783*	2.50426	.000	9.6362	26.4594
4.00	1.00	3.21955	2.50426	.787	-5.1921	11.6312
	2.00	-17.90012*	2.50426	.000	-26.3117	-9.4885
	3.00	.35030	2.50426	1.000	-8.0613	8.7619
	5.00	-6.82249	2.50426	.141	-15.2341	1.5891
	6.00	18.39813*	2.50426	.000	9.9865	26.8097
5.00	1.00	10.04204*	2.50426	.017	1.6304	18.4537
	2.00	-11.07763*	2.50426	.008	-19.4892	-2.6660
	3.00	7.17279	2.50426	.113	-1.2388	15.5844
	4.00	6.82249	2.50426	.141	-1.5891	15.2341
	6.00	25.22063*	2.50426	.000	16.8090	33.6322
6.00	1.00	-15.17858*	2.50426	.001	-23.5902	-6.7670
	2.00	-36.29825*	2.50426	.000	-44.7099	-27.8866
	3.00	-18.04783*	2.50426	.000	-26.4594	-9.6362
	4.00	-18.39813*	2.50426	.000	-26.8097	-9.9865
	5.00	-25.22063*	2.50426	.000	-33.6322	-16.8090

*. The mean difference is significant at the 0.05 level.

Peak 10

ANOVA

data

	Sum of Squares	df	Mean Square	F	Sig.
Between Groups	867.569	5	173.514	11.064	.000
Within Groups	188.196	12	15.683		
Total	1055.765	17			

Multiple Comparisons

Dependent Variable: data

Tukey HSD

(I) factor	(J) factor	Mean Difference (I-J)	Std. Error	Sig.	95% Confidence Interval	
					Lower Bound	Upper Bound
1.00	2.00	-13.89003*	3.23347	.010	-24.7510	-3.0291
	3.00	-14.49756*	3.23347	.008	-25.3585	-3.6366
	4.00	-.69651	3.23347	1.000	-11.5575	10.1645
	5.00	-9.36269	3.23347	.107	-20.2237	1.4983
	6.00	2.90669	3.23347	.939	-7.9543	13.7677
2.00	1.00	13.89003*	3.23347	.010	3.0291	24.7510
	3.00	-.60752	3.23347	1.000	-11.4685	10.2534
	4.00	13.19352*	3.23347	.015	2.3326	24.0545
	5.00	4.52734	3.23347	.727	-6.3336	15.3883
	6.00	16.79673*	3.23347	.002	5.9358	27.6577
3.00	1.00	14.49756*	3.23347	.008	3.6366	25.3585
	2.00	.60752	3.23347	1.000	-10.2534	11.4685
	4.00	13.80105*	3.23347	.011	2.9401	24.6620
	5.00	5.13486	3.23347	.620	-5.7261	15.9958
	6.00	17.40425*	3.23347	.002	6.5433	28.2652
4.00	1.00	.69651	3.23347	1.000	-10.1645	11.5575
	2.00	-13.19352*	3.23347	.015	-24.0545	-2.3326
	3.00	-13.80105*	3.23347	.011	-24.6620	-2.9401
	5.00	-8.66618	3.23347	.151	-19.5271	2.1948

(I) group	(J) group	Mean Difference (I-J)	Std. Error	Sig.	Lower Bound	Upper Bound
	6.00	3.60320	3.23347	.866	-7.2578	14.4642
5.00	1.00	9.36269	3.23347	.107	-1.4983	20.2237
	2.00	-4.52734	3.23347	.727	-15.3883	6.3336
	3.00	-5.13486	3.23347	.620	-15.9958	5.7261
	4.00	8.66618	3.23347	.151	-2.1948	19.5271
	6.00	12.26939*	3.23347	.024	1.4084	23.1304
6.00	1.00	-2.90669	3.23347	.939	-13.7677	7.9543
	2.00	-16.79673*	3.23347	.002	-27.6577	-5.9358
	3.00	-17.40425*	3.23347	.002	-28.2652	-6.5433
	4.00	-3.60320	3.23347	.866	-14.4642	7.2578
	5.00	-12.26939*	3.23347	.024	-23.1304	-1.4084

*. The mean difference is significant at the 0.05 level.

SMOFlipid® Non-light Protected Stats

Peak 1

ANOVA

data

	Sum of Squares	df	Mean Square	F	Sig.
Between Groups	3060.438	5	612.088	49.414	.000
Within Groups	136.256	11	12.387		
Total	3196.693	16			

Multiple Comparisons

Dependent Variable: data

Tukey HSD

(I) group	(J) group	Mean Difference (I-J)	Std. Error	Sig.	95% Confidence Interval	
					Lower Bound	Upper Bound
1.00	2.00	17.24114*	2.87366	.001	7.4409	27.0413
	3.00	43.09015*	3.21285	.000	32.1332	54.0471
	4.00	15.52526*	2.87366	.002	5.7251	25.3255
	5.00	19.11033*	2.87366	.000	9.3101	28.9105
	6.00	35.41277*	2.87366	.000	25.6126	45.2130
2.00	1.00	-17.24114*	2.87366	.001	-27.0413	-7.4409
	3.00	25.84901*	3.21285	.000	14.8920	36.8060
	4.00	-1.71588	2.87366	.989	-11.5161	8.0843

(I) group	(J) group	Mean Difference (I-J)	Std. Error	Sig.	Lower Bound	Upper Bound
	5.00	1.86920	2.87366	.984	-7.9310	11.6694
	6.00	18.17163*	2.87366	.001	8.3714	27.9718
3.00	1.00	-43.09015*	3.21285	.000	-54.0471	-32.1332
	2.00	-25.84901*	3.21285	.000	-36.8060	-14.8920
	4.00	-27.56489*	3.21285	.000	-38.5219	-16.6079
	5.00	-23.97982*	3.21285	.000	-34.9368	-13.0228
	6.00	-7.67738	3.21285	.239	-18.6343	3.2796
4.00	1.00	-15.52526*	2.87366	.002	-25.3255	-5.7251
	2.00	1.71588	2.87366	.989	-8.0843	11.5161
	3.00	27.56489*	3.21285	.000	16.6079	38.5219
	5.00	3.58507	2.87366	.806	-6.2151	13.3853
	6.00	19.88751*	2.87366	.000	10.0873	29.6877
5.00	1.00	-19.11033*	2.87366	.000	-28.9105	-9.3101
	2.00	-1.86920	2.87366	.984	-11.6694	7.9310
	3.00	23.97982*	3.21285	.000	13.0228	34.9368
	4.00	-3.58507	2.87366	.806	-13.3853	6.2151
	6.00	16.30244*	2.87366	.002	6.5022	26.1026
6.00	1.00	-35.41277*	2.87366	.000	-45.2130	-25.6126
	2.00	-18.17163*	2.87366	.001	-27.9718	-8.3714
	3.00	7.67738	3.21285	.239	-3.2796	18.6343
	4.00	-19.88751*	2.87366	.000	-29.6877	-10.0873
	5.00	-16.30244*	2.87366	.002	-26.1026	-6.5022

*. The mean difference is significant at the 0.05 level.

Peak 2

ANOVA

data

	Sum of Squares	df	Mean Square	F	Sig.
Between Groups	2137.546	5	427.509	52.318	.000
Within Groups	98.057	12	8.171		
Total	2235.603	17			

Multiple Comparisons

Dependent Variable: data

Tukey HSD

(I) group	(J) group	Mean Difference (I-J)	Std. Error	Sig.	95% Confidence Interval	
					Lower Bound	Upper Bound

1.00	2.00	8.23816*	2.33401	.038	.3984	16.0779
	3.00	32.80617*	2.33401	.000	24.9664	40.6459
	4.00	15.73291*	2.33401	.000	7.8931	23.5727
	5.00	11.59816*	2.33401	.003	3.7584	19.4379
	6.00	25.74490*	2.33401	.000	17.9051	33.5847
2.00	1.00	-8.23816*	2.33401	.038	-16.0779	-.3984
	3.00	24.56801*	2.33401	.000	16.7282	32.4078
	4.00	7.49474	2.33401	.064	-.3450	15.3345
	5.00	3.36000	2.33401	.705	-4.4798	11.1998
	6.00	17.50673*	2.33401	.000	9.6670	25.3465
3.00	1.00	-32.80617*	2.33401	.000	-40.6459	-24.9664
	2.00	-24.56801*	2.33401	.000	-32.4078	-16.7282
	4.00	-17.07327*	2.33401	.000	-24.9130	-9.2335
	5.00	-21.20801*	2.33401	.000	-29.0478	-13.3682
	6.00	-7.06128	2.33401	.087	-14.9010	.7785
4.00	1.00	-15.73291*	2.33401	.000	-23.5727	-7.8931
	2.00	-7.49474	2.33401	.064	-15.3345	.3450
	3.00	17.07327*	2.33401	.000	9.2335	24.9130
	5.00	-4.13475	2.33401	.516	-11.9745	3.7050
	6.00	10.01199*	2.33401	.010	2.1722	17.8518
5.00	1.00	-11.59816*	2.33401	.003	-19.4379	-3.7584
	2.00	-3.36000	2.33401	.705	-11.1998	4.4798
	3.00	21.20801*	2.33401	.000	13.3682	29.0478
	4.00	4.13475	2.33401	.516	-3.7050	11.9745
	6.00	14.14674*	2.33401	.001	6.3070	21.9865
6.00	1.00	-25.74490*	2.33401	.000	-33.5847	-17.9051
	2.00	-17.50673*	2.33401	.000	-25.3465	-9.6670
	3.00	7.06128	2.33401	.087	-.7785	14.9010
	4.00	-10.01199*	2.33401	.010	-17.8518	-2.1722
	5.00	-14.14674*	2.33401	.001	-21.9865	-6.3070

*. The mean difference is significant at the 0.05 level.

Peak 3

ANOVA

data

	Sum of Squares	df	Mean Square	F	Sig.
Between Groups	3642.549	5	728.510	86.193	.000

Within Groups	101.425	12	8.452			
Total	3743.975	17				

Multiple Comparisons

Dependent Variable: data

Tukey HSD

(I) group	(J) group	Mean Difference (I-J)	Std. Error	Sig.	95% Confidence Interval Lower Bound	95% Confidence Interval Upper Bound
1.00	2.00	11.81551*	2.37376	.003	3.8422	19.7888
	3.00	42.26333*	2.37376	.000	34.2900	50.2366
	4.00	14.37392*	2.37376	.001	6.4006	22.3472
	5.00	14.34605*	2.37376	.001	6.3728	22.3193
	6.00	33.77944*	2.37376	.000	25.8062	41.7527
2.00	1.00	-11.81551*	2.37376	.003	-19.7888	-3.8422
	3.00	30.44781*	2.37376	.000	22.4745	38.4211
	4.00	2.55840	2.37376	.881	-5.4149	10.5317
	5.00	2.53054	2.37376	.886	-5.4427	10.5038
	6.00	21.96393*	2.37376	.000	13.9907	29.9372
3.00	1.00	-42.26333*	2.37376	.000	-50.2366	-34.2900
	2.00	-30.44781*	2.37376	.000	-38.4211	-22.4745
	4.00	-27.88941*	2.37376	.000	-35.8627	-19.9161
	5.00	-27.91727*	2.37376	.000	-35.8906	-19.9440
	6.00	-8.48388*	2.37376	.035	-16.4572	-.5106
4.00	1.00	-14.37392*	2.37376	.001	-22.3472	-6.4006
	2.00	-2.55840	2.37376	.881	-10.5317	5.4149
	3.00	27.88941*	2.37376	.000	19.9161	35.8627
	5.00	-.02787	2.37376	1.000	-8.0011	7.9454
	6.00	19.40553*	2.37376	.000	11.4322	27.3788
5.00	1.00	-14.34605*	2.37376	.001	-22.3193	-6.3728
	2.00	-2.53054	2.37376	.886	-10.5038	5.4427
	3.00	27.91727*	2.37376	.000	19.9440	35.8906
	4.00	.02787	2.37376	1.000	-7.9454	8.0011
	6.00	19.43339*	2.37376	.000	11.4601	27.4067
6.00	1.00	-33.77944*	2.37376	.000	-41.7527	-25.8062
	2.00	-21.96393*	2.37376	.000	-29.9372	-13.9907
	3.00	8.48388*	2.37376	.035	.5106	16.4572
	4.00	-19.40553*	2.37376	.000	-27.3788	-11.4322
	5.00	-19.43339*	2.37376	.000	-27.4067	-11.4601

*. The mean difference is significant at the 0.05 level.

Peak 4

ANOVA

data

	Sum of Squares	df	Mean Square	F	Sig.
Between Groups	1160.618	5	232.124	11.454	.000
Within Groups	243.189	12	20.266		
Total	1403.807	17			

Multiple Comparisons

Dependent Variable: data

Tukey HSD

(I) group	(J) group	Mean Difference (I-J)	Std. Error	Sig.	95% Confidence Interval	
					Lower Bound	Upper Bound
1.00	2.00	5.85486	3.67566	.618	-6.4914	18.2011
	3.00	20.46599*	3.67566	.001	8.1197	32.8122
	4.00	22.87239*	3.67566	.000	10.5261	35.2186
	5.00	9.14353	3.67566	.202	-3.2027	21.4898
	6.00	14.69164*	3.67566	.017	2.3454	27.0379
2.00	1.00	-5.85486	3.67566	.618	-18.2011	6.4914
	3.00	14.61113*	3.67566	.018	2.2649	26.9574
	4.00	17.01753*	3.67566	.006	4.6713	29.3638
	5.00	3.28867	3.67566	.941	-9.0576	15.6349
	6.00	8.83678	3.67566	.229	-3.5095	21.1830
3.00	1.00	-20.46599*	3.67566	.001	-32.8122	-8.1197
	2.00	-14.61113*	3.67566	.018	-26.9574	-2.2649
	4.00	2.40641	3.67566	.984	-9.9398	14.7527
	5.00	-11.32246	3.67566	.079	-23.6687	1.0238
	6.00	-5.77435	3.67566	.630	-18.1206	6.5719
4.00	1.00	-22.87239*	3.67566	.000	-35.2186	-10.5261
	2.00	-17.01753*	3.67566	.006	-29.3638	-4.6713
	3.00	-2.40641	3.67566	.984	-14.7527	9.9398
	5.00	-13.72887*	3.67566	.027	-26.0751	-1.3826
	6.00	-8.18075	3.67566	.294	-20.5270	4.1655
5.00	1.00	-9.14353	3.67566	.202	-21.4898	3.2027

	2.00	-3.28867	3.67566	.941	-15.6349	9.0576
	3.00	11.32246	3.67566	.079	-1.0238	23.6687
	4.00	13.72887*	3.67566	.027	1.3826	26.0751
	6.00	5.54811	3.67566	.665	-6.7981	17.8944
6.00	1.00	-14.69164*	3.67566	.017	-27.0379	-2.3454
	2.00	-8.83678	3.67566	.229	-21.1830	3.5095
	3.00	5.77435	3.67566	.630	-6.5719	18.1206
	4.00	8.18075	3.67566	.294	-4.1655	20.5270
	5.00	-5.54811	3.67566	.665	-17.8944	6.7981

*. The mean difference is significant at the 0.05 level.

Peak 5

ANOVA

data

	Sum of Squares	df	Mean Square	F	Sig.
Between Groups	2250.812	5	450.162	29.273	.000
Within Groups	184.538	12	15.378		
Total	2435.351	17			

Multiple Comparisons

Dependent Variable: data

Tukey HSD

		Mean Difference			95% Confidence Interval	
(I) group	(J) group	(I-J)	Std. Error	Sig.	Lower Bound	Upper Bound
1.00	2.00	15.49333*	3.20190	.004	4.7384	26.2482
	3.00	35.07140*	3.20190	.000	24.3165	45.8263
	4.00	26.08252*	3.20190	.000	15.3276	36.8374
	5.00	22.99089*	3.20190	.000	12.2360	33.7458
	6.00	28.19060*	3.20190	.000	17.4357	38.9455
2.00	1.00	-15.49333*	3.20190	.004	-26.2482	-4.7384
	3.00	19.57806*	3.20190	.001	8.8231	30.3330
	4.00	10.58919	3.20190	.055	-.1657	21.3441
	5.00	7.49756	3.20190	.250	-3.2574	18.2525
	6.00	12.69727*	3.20190	.018	1.9424	23.4522
3.00	1.00	-35.07140*	3.20190	.000	-45.8263	-24.3165
	2.00	-19.57806*	3.20190	.001	-30.3330	-8.8231
	4.00	-8.98887	3.20190	.123	-19.7438	1.7660

	5.00	-12.08051*	3.20190	.025	-22.8354	-1.3256
	6.00	-6.88079	3.20190	.326	-17.6357	3.8741
4.00	1.00	-26.08252*	3.20190	.000	-36.8374	-15.3276
	2.00	-10.58919	3.20190	.055	-21.3441	.1657
	3.00	8.98887	3.20190	.123	-1.7660	19.7438
	5.00	-3.09164	3.20190	.920	-13.8466	7.6633
	6.00	2.10808	3.20190	.983	-8.6468	12.8630
5.00	1.00	-22.99089*	3.20190	.000	-33.7458	-12.2360
	2.00	-7.49756	3.20190	.250	-18.2525	3.2574
	3.00	12.08051*	3.20190	.025	1.3256	22.8354
	4.00	3.09164	3.20190	.920	-7.6633	13.8466
	6.00	5.19972	3.20190	.600	-5.5552	15.9546
6.00	1.00	-28.19060*	3.20190	.000	-38.9455	-17.4357
	2.00	-12.69727*	3.20190	.018	-23.4522	-1.9424
	3.00	6.88079	3.20190	.326	-3.8741	17.6357
	4.00	-2.10808	3.20190	.983	-12.8630	8.6468
	5.00	-5.19972	3.20190	.600	-15.9546	5.5552

*. The mean difference is significant at the 0.05 level.

Peak 6

ANOVA

data

	Sum of Squares	df	Mean Square	F	Sig.
Between Groups	317.391	5	63.478	3.492	.035
Within Groups	218.157	12	18.180		
Total	535.548	17			

Multiple Comparisons

Dependent Variable: data

Tukey HSD

(I) group	(J) group	Mean Difference (I-J)	Std. Error	Sig.	95% Confidence Interval Lower Bound	95% Confidence Interval Upper Bound
1.00	2.00	-4.75567	3.48136	.745	-16.4493	6.9379
	3.00	1.29015	3.48136	.999	-10.4034	12.9837
	4.00	1.29015	3.48136	.999	-10.4034	12.9837
	5.00	-10.59906	3.48136	.084	-22.2927	1.0945
	6.00	-2.97735	3.48136	.950	-14.6710	8.7162
2.00	1.00	4.75567	3.48136	.745	-6.9379	16.4493
	3.00	6.04582	3.48136	.535	-5.6478	17.7394
	4.00	6.04582	3.48136	.535	-5.6478	17.7394
	5.00	-5.84339	3.48136	.568	-17.5370	5.8502
	6.00	1.77831	3.48136	.995	-9.9153	13.4719
3.00	1.00	-1.29015	3.48136	.999	-12.9837	10.4034
	2.00	-6.04582	3.48136	.535	-17.7394	5.6478
	4.00	.00000	3.48136	1.000	-11.6936	11.6936
	5.00	-11.88921[*]	3.48136	.046	-23.5828	-.1956
	6.00	-4.26751	3.48136	.817	-15.9611	7.4261
4.00	1.00	-1.29015	3.48136	.999	-12.9837	10.4034
	2.00	-6.04582	3.48136	.535	-17.7394	5.6478
	3.00	.00000	3.48136	1.000	-11.6936	11.6936
	5.00	-11.88921[*]	3.48136	.046	-23.5828	-.1956
	6.00	-4.26751	3.48136	.817	-15.9611	7.4261
5.00	1.00	10.59906	3.48136	.084	-1.0945	22.2927
	2.00	5.84339	3.48136	.568	-5.8502	17.5370
	3.00	11.88921[*]	3.48136	.046	.1956	23.5828
	4.00	11.88921[*]	3.48136	.046	.1956	23.5828
	6.00	7.62170	3.48136	.309	-4.0719	19.3153
6.00	1.00	2.97735	3.48136	.950	-8.7162	14.6710
	2.00	-1.77831	3.48136	.995	-13.4719	9.9153
	3.00	4.26751	3.48136	.817	-7.4261	15.9611
	4.00	4.26751	3.48136	.817	-7.4261	15.9611
	5.00	-7.62170	3.48136	.309	-19.3153	4.0719

*. The mean difference is significant at the 0.05 level.

Peak 7

ANOVA

data

	Sum of Squares	df	Mean Square	F	Sig.
Between Groups	65.062	5	13.012	1.180	.374
Within Groups	132.342	12	11.029		
Total	197.404	17			

Multiple Comparisons

Dependent Variable: data

Tukey HSD

(I) group	(J) group	Mean Difference (I-J)	Std. Error	Sig.	95% Confidence Interval Lower Bound	95% Confidence Interval Upper Bound
1.00	2.00	4.84717	2.71152	.507	-4.2606	13.9550
	3.00	4.97836	2.71152	.480	-4.1294	14.0861
	4.00	4.97836	2.71152	.480	-4.1294	14.0861
	5.00	2.36611	2.71152	.946	-6.7417	11.4739
	6.00	4.97836	2.71152	.480	-4.1294	14.0861
2.00	1.00	-4.84717	2.71152	.507	-13.9550	4.2606
	3.00	.13119	2.71152	1.000	-8.9766	9.2390
	4.00	.13119	2.71152	1.000	-8.9766	9.2390
	5.00	-2.48105	2.71152	.935	-11.5888	6.6267
	6.00	.13119	2.71152	1.000	-8.9766	9.2390
3.00	1.00	-4.97836	2.71152	.480	-14.0861	4.1294
	2.00	-.13119	2.71152	1.000	-9.2390	8.9766
	4.00	.00000	2.71152	1.000	-9.1078	9.1078
	5.00	-2.61224	2.71152	.921	-11.7200	6.4955
	6.00	.00000	2.71152	1.000	-9.1078	9.1078
4.00	1.00	-4.97836	2.71152	.480	-14.0861	4.1294
	2.00	-.13119	2.71152	1.000	-9.2390	8.9766
	3.00	.00000	2.71152	1.000	-9.1078	9.1078
	5.00	-2.61224	2.71152	.921	-11.7200	6.4955
	6.00	.00000	2.71152	1.000	-9.1078	9.1078
5.00	1.00	-2.36611	2.71152	.946	-11.4739	6.7417
	2.00	2.48105	2.71152	.935	-6.6267	11.5888

	3.00	2.61224	2.71152	.921	-6.4955	11.7200
	4.00	2.61224	2.71152	.921	-6.4955	11.7200
	6.00	2.61224	2.71152	.921	-6.4955	11.7200
6.00	1.00	-4.97836	2.71152	.480	-14.0861	4.1294
	2.00	-.13119	2.71152	1.000	-9.2390	8.9766
	3.00	.00000	2.71152	1.000	-9.1078	9.1078
	4.00	.00000	2.71152	1.000	-9.1078	9.1078
	5.00	-2.61224	2.71152	.921	-11.7200	6.4955

Peak 8

ANOVA

data

	Sum of Squares	df	Mean Square	F	Sig.
Between Groups	1312.543	5	262.509	5.259	.009
Within Groups	599.050	12	49.921		
Total	1911.593	17			

Multiple Comparisons

Dependent Variable: data

Tukey HSD

(I) group	(J) group	Mean Difference (I-J)	Std. Error	Sig.	95% Confidence Interval	
					Lower Bound	Upper Bound
1.00	2.00	-9.25770	5.76893	.611	-28.6351	10.1197
	3.00	9.72563	5.76893	.564	-9.6518	29.1030
	4.00	9.72563	5.76893	.564	-9.6518	29.1030
	5.00	-11.01537	5.76893	.441	-30.3927	8.3620
	6.00	6.88664	5.76893	.832	-12.4907	26.2640
2.00	1.00	9.25770	5.76893	.611	-10.1197	28.6351
	3.00	18.98332	5.76893	.056	-.3941	38.3607
	4.00	18.98332	5.76893	.056	-.3941	38.3607
	5.00	-1.75767	5.76893	1.000	-21.1351	17.6197
	6.00	16.14433	5.76893	.125	-3.2330	35.5217
3.00	1.00	-9.72563	5.76893	.564	-29.1030	9.6518
	2.00	-18.98332	5.76893	.056	-38.3607	.3941
	4.00	.00000	5.76893	1.000	-19.3774	19.3774
	5.00	-20.74100*	5.76893	.034	-40.1184	-1.3636
	6.00	-2.83899	5.76893	.996	-22.2164	16.5384

4.00	1.00	-9.72563	5.76893	.564	-29.1030	9.6518
	2.00	-18.98332	5.76893	.056	-38.3607	.3941
	3.00	.00000	5.76893	1.000	-19.3774	19.3774
	5.00	-20.74100*	5.76893	.034	-40.1184	-1.3636
	6.00	-2.83899	5.76893	.996	-22.2164	16.5384
5.00	1.00	11.01537	5.76893	.441	-8.3620	30.3927
	2.00	1.75767	5.76893	1.000	-17.6197	21.1351
	3.00	20.74100*	5.76893	.034	1.3636	40.1184
	4.00	20.74100*	5.76893	.034	1.3636	40.1184
	6.00	17.90201	5.76893	.076	-1.4754	37.2794
6.00	1.00	-6.88664	5.76893	.832	-26.2640	12.4907
	2.00	-16.14433	5.76893	.125	-35.5217	3.2330
	3.00	2.83899	5.76893	.996	-16.5384	22.2164
	4.00	2.83899	5.76893	.996	-16.5384	22.2164
	5.00	-17.90201	5.76893	.076	-37.2794	1.4754

*. The mean difference is significant at the 0.05 level.

Peak 9

ANOVA

data

	Sum of Squares	df	Mean Square	F	Sig.
Between Groups	5143.157	5	1028.631	43.631	.000
Within Groups	282.910	12	23.576		
Total	5426.067	17			

Multiple Comparisons

Dependent Variable: data

Tukey HSD

(I) group	(J) group	Mean Difference (I-J)	Std. Error	Sig.	95% Confidence Interval	
					Lower Bound	Upper Bound
1.00	2.00	26.16098*	3.96450	.000	12.8446	39.4774
	3.00	51.93696*	3.96450	.000	38.6205	65.2534
	4.00	15.59392*	3.96450	.019	2.2775	28.9104
	5.00	31.12492*	3.96450	.000	17.8085	44.4414
	6.00	41.80813*	3.96450	.000	28.4917	55.1246
2.00	1.00	-26.16098*	3.96450	.000	-39.4774	-12.8446

	3.00	25.77598*	3.96450	.000	12.4596	39.0924
	4.00	-10.56706	3.96450	.154	-23.8835	2.7494
	5.00	4.96394	3.96450	.804	-8.3525	18.2804
	6.00	15.64715*	3.96450	.019	2.3307	28.9636
3.00	1.00	-51.93696*	3.96450	.000	-65.2534	-38.6205
	2.00	-25.77598*	3.96450	.000	-39.0924	-12.4596
	4.00	-36.34304*	3.96450	.000	-49.6595	-23.0266
	5.00	-20.81204*	3.96450	.002	-34.1285	-7.4956
	6.00	-10.12883	3.96450	.183	-23.4453	3.1876
4.00	1.00	-15.59392*	3.96450	.019	-28.9104	-2.2775
	2.00	10.56706	3.96450	.154	-2.7494	23.8835
	3.00	36.34304*	3.96450	.000	23.0266	49.6595
	5.00	15.53100*	3.96450	.019	2.2146	28.8474
	6.00	26.21421*	3.96450	.000	12.8978	39.5306
5.00	1.00	-31.12492*	3.96450	.000	-44.4414	-17.8085
	2.00	-4.96394	3.96450	.804	-18.2804	8.3525
	3.00	20.81204*	3.96450	.002	7.4956	34.1285
	4.00	-15.53100*	3.96450	.019	-28.8474	-2.2146
	6.00	10.68321	3.96450	.147	-2.6332	23.9996
6.00	1.00	-41.80813*	3.96450	.000	-55.1246	-28.4917
	2.00	-15.64715*	3.96450	.019	-28.9636	-2.3307
	3.00	10.12883	3.96450	.183	-3.1876	23.4453
	4.00	-26.21421*	3.96450	.000	-39.5306	-12.8978
	5.00	-10.68321	3.96450	.147	-23.9996	2.6332

*. The mean difference is significant at the 0.05 level.

Peak 10

ANOVA

data

	Sum of Squares	df	Mean Square	F	Sig.
Between Groups	2090.489	5	418.098	13.451	.000
Within Groups	372.986	12	31.082		
Total	2463.476	17			

Multiple Comparisons

Dependent Variable: data

Tukey HSD

(I) group	(J) group	Mean Difference (I-J)	Std. Error	Sig.	95% Confidence Interval Lower Bound	Upper Bound
1.00	2.00	7.64932	4.55208	.567	-7.6408	22.9394
	3.00	30.34354*	4.55208	.000	15.0535	45.6336
	4.00	27.26062*	4.55208	.001	11.9705	42.5507
	5.00	19.87551*	4.55208	.009	4.5854	35.1656
	6.00	22.90446*	4.55208	.003	7.6144	38.1945
2.00	1.00	-7.64932	4.55208	.567	-22.9394	7.6408
	3.00	22.69422*	4.55208	.003	7.4041	37.9843
	4.00	19.61130*	4.55208	.010	4.3212	34.9014
	5.00	12.22619	4.55208	.149	-3.0639	27.5163
	6.00	15.25514	4.55208	.051	-.0349	30.5452
3.00	1.00	-30.34354*	4.55208	.000	-45.6336	-15.0535
	2.00	-22.69422*	4.55208	.003	-37.9843	-7.4041
	4.00	-3.08292	4.55208	.981	-18.3730	12.2072
	5.00	-10.46803	4.55208	.266	-25.7581	4.8221
	6.00	-7.43908	4.55208	.594	-22.7292	7.8510
4.00	1.00	-27.26062*	4.55208	.001	-42.5507	-11.9705
	2.00	-19.61130*	4.55208	.010	-34.9014	-4.3212
	3.00	3.08292	4.55208	.981	-12.2072	18.3730
	5.00	-7.38511	4.55208	.601	-22.6752	7.9050
	6.00	-4.35616	4.55208	.923	-19.6462	10.9339
5.00	1.00	-19.87551*	4.55208	.009	-35.1656	-4.5854
	2.00	-12.22619	4.55208	.149	-27.5163	3.0639
	3.00	10.46803	4.55208	.266	-4.8221	25.7581
	4.00	7.38511	4.55208	.601	-7.9050	22.6752
	6.00	3.02895	4.55208	.983	-12.2611	18.3190
6.00	1.00	-22.90446*	4.55208	.003	-38.1945	-7.6144
	2.00	-15.25514	4.55208	.051	-30.5452	.0349
	3.00	7.43908	4.55208	.594	-7.8510	22.7292
	4.00	4.35616	4.55208	.923	-10.9339	19.6462
	5.00	-3.02895	4.55208	.983	-18.3190	12.2611

*. The mean difference is significant at the 0.05 level.